

**Phytochemical Investigation of a
Traditional West African Ethnomedicinal Plant, *Icacina trichantha***

BY

Brian C Guo

B.S., Northwestern University, 2010

M.S., Northwestern University, 2012

DISSERTATION

Submitted as partial fulfillment of the requirements
for the degree of Doctor of Philosophy in Pharmacognosy
in the Graduate College of the
University of Illinois at Chicago, 2020

Chicago, Illinois

Defense Committee:

Dr. Chun-Tao Che, Chair and Advisor

Dr. Joanna E. Burdette

Dr. Jeremy J. Johnson, Pharmacy Practice

Dr. Gail B. Mahady

Dr. Brian T. Murphy

Dr. Duncan Wardrop, Chemistry

DEDICATION

I dedicate this to Chicago, the city that has meant so much to me.

The city where my father came to continue his work in Traditional Chinese Medicine.

The city where my immigrant parents met in a new country.

The city where they settled and raised our family.

The city where I fell in love with my best friend.

The city that will always be with me.

ACKNOWLEDGEMENTS

My first acknowledgement is to my advisor and mentor, Dr. Chun-Tao Che. His guidance and support made me a better student of the world and the natural power that it holds. Under his tutelage, I have grown as a research scientist. Thanks to him, I can proudly consider myself a pharmacognosist.

I would also like to thank my dissertation and preliminary examination committee members. Dr. Jeremy Johnson was a helpful advisor and always willing with his time to help my biological experiments. I am also thankful to him for accepting me as a rotational research student. Dr. Brian Murphy and Dr. Joanna Burdette were very passionate instructors and gave me much needed support early in my career. I would also like to thank Dr. Gail Mahady and Dr. Duncan Wardrop for kindly giving their time and advice towards this dissertation.

I am particularly grateful to Dr. Alec Krunic for helpful guidance and support in my NMR experiments, as well as being a good friend. I would like to thank Dr. Ben Ramirez and Dr. David Lankin for their assistance with NMR acquisition and interpretation as well. Dr. Dejan Nikolic was a great teacher and friend who was incredibly helpful in mass spectrometry analysis. I would like to express my gratitude to the fellow members of the CT Che research group past and present. I am especially grateful to Dr. Monday M. Onakpa for establishing this international collaboration and without whom none of this work would be possible. I am also particularly grateful to Dr. Ming Zhao who was instrumental for teaching me the skills and techniques needed to study natural products. Dr. Karina Szymulanska-Ramamurthy was a great mentor and friend in my first years as a student. I am thankful to Dr. Zhenlong Wu for his assistance in ECD calculations and Dr. Junfei Zhou, a talented pharmacognosist who provided very helpful advice

ACKNOWLEDGEMENTS (continued)

and guidance. My other fellow lab members were amazing colleagues and friends, including, Dr. Jordan Gunn, Dr. Joshua Henkin, Dr. Bamisaye Oyawaluja, Dr. Xia Wu, Meng Sun, Isoo Youn, Aleksandra Gurgul, Dr. Sharna-kay Daley, Steven Lane, Tomasz Karwas, Samiya Papa, Kevin He, Isheng Hou, Nathan Brown, and Meghna Gill. I would like to thank Dr. Laura Sanchez for allowing access to her lab and mass spectrometry instruments and Valya Petukhova for assisting with training. I am also thankful to Dr. Guido Pauli and Dr. Jonathan Bisson for access and training to the Pauli lab's resources. I am also grateful to all my fellow classmates and friends that made UIC such a welcoming place to work and study.

I would like to thank the many members of the Department of Pharmaceutical Sciences and those associated with the Department for their help and assistance with this work, especially those that contributed their time and resources. I am appreciative for the organizational and logistical help readily given by Elizabeth Ryan. The collaboration with Dr. Katherine Warpeha and her group including Tiffany Wong and Kyo Wakasa was very productive and insightful into the potential of natural products as pesticides and herbicides in agriculture. I am thankful for the members of the Joanna Burdette lab for assisting with cytotoxicity assays including Wei-Lun Chen, Austin Czarnecki, and Brenna Kirkpatrick. I am also thankful to Jeremy Johnson lab member Bhaskar Vemu for assisting with colorectal and prostate cancer cytotoxicity assays. I am very grateful to Dr. Bernie Santarsiero for his assistance in acquiring and analyzing x-ray crystallographic data.

Finally, I am thankful to my family and friends for their love and support through the years. The memories and experiences outside of the lab made the work and effort presented here that much more rewarding.

ACKNOWLEDGEMENTS (continued)

My research was supported by the Office of the Director, National Institutes of Health (OD) and National Center for Complementary and Integrative Health (NCCIH) (5T32AT007533) through a T32 pre-doctoral training fellowship and a Oscar Robert Oldberg Prize in Pharmaceutical Chemistry from the Department of Pharmaceutical Sciences in the College of Pharmacy at UIC. I would also like to thank the Pharmacology Industry Internships for PhD Students (PIIPS) Program for supporting my internship with Sirenas MD in San Diego, California.

CONTRIBUTION OF AUTHORS

Chapter 1 is an original work by Brian Guo with editing provided by Dr. Chun-Tao Che.

Chapter 2 is composed of a published manuscript (Guo, B., *et al. J. Nat. Prod.* **2016**, 79 (7), 1815–1821) of which I am first author. Dr. Monday M. Onakpa assisted with plant material collection and identification. Dr. Ming Zhao and I carried out NMR acquisition and interpretation and writing of the manuscript. Drs. Xiao-Jun Huang and Xiao-Qi Zhang assisted with ECD calculations. Dr. Bernard D. Santarsiero assisted with acquiring and interpreting x-ray crystallographic data. Drs. Wei-Lun Chen, Steven M. Swanson, and Joanna E. Burdette assisted with antiproliferative assays against cancer cell lines. My mentor Dr. Chun-Tao Che assisted with revising of the final manuscript. Chapter 2 is also composed of a published manuscript (Guo, B. *et al. Fitoterapia* 104612 (**2020**), 144, 104612) for which I am first author as well and the primary generator of content. Dr. Ming Zhao assisted with NMR interpretation. Dr. Zhenlong Wu assisted with ECD calculations. Dr. Monday M. Onakpa assisted with plant material collection and identification. Dr. Joanna E. Burdette assisted with antiproliferative assays against cancer cell lines. My mentor Dr. Chun-Tao Che assisted with revising of the manuscript. Chapter 3 is composed of a published manuscript (Zhao, M.; Guo, B., *et al. J. Nat. Prod.* **2017**, 80 (12), 3314–3318) of which I am a co-author. Tiffany Wong, Kyo Wakasa, and Dr. Katherine Warpeha assisted with anti-germination assays. The chapter is also composed of cytotoxicity data from a published manuscript (Guo, B., *et al. J. Nat. Prod.* **2016**, 79 (7), 1815–1821) and unpublished biological activity data. Drs. Bhaskar Vemu and Jeremy J. Johnson assisted with antiproliferative assays against cancer cell lines. Chapter 4 is an original work by Brian Guo with editing provided by Dr. Chun-Tao Che.

TABLE OF CONTENTS

<u>CHAPTER</u>	<u>PAGE</u>
1. Introduction to Natural Products and <i>Icacina</i>	1
1.1 Background	2
1.1.1 Pharmacognosy & Phytochemistry.....	2
1.1.2 Medicinal Plants and Botanicals for Drug Discovery.....	3
1.1.3 African Traditional Medicine (TM).....	7
1.2 Literature Review	10
1.2.1 Taxonomy of <i>Icacina</i> genus	10
1.2.2 Morphological description of <i>Icacina trichantha</i>	11
1.2.3 Ethnomedicinal use of <i>Icacina</i> species	14
1.2.4 Summary of scientific investigations.....	20
1.2.5 Chemical constituents	20
1.2.6 Biological activities of <i>Icacina</i> genus.....	32
1.3 Objectives.....	45
2. Structure Elucidation of Pimarane Diterpenoids	48
2.1 Introduction	49
2.2 Materials and Methods.....	50
2.2.1 General Experimental Procedures.	50
2.2.2 Plant Material.....	51
2.2.3 Extraction and Isolation.	51
2.2.4 Single Crystal X-Ray Structure Determination.....	55
2.2.5 Computational Section for ECD Calculation.....	57
2.3 Chemical Investigation	58
2.3.1 Dereplication Library Generation Workflow	58
2.3.2 Isolation and Structure Elucidation of 9 β H-pimarane diterpenoids	61
2.3.3 Isolation and Structure Elucidation of 9 β H-17- <i>nor</i> -pimarane diterpenoids.....	71
2.3.4 Isolation and Structure Elucidation of 17- <i>nor</i> -pimarane diterpenoids	78
2.3.5 Isolation and Structure Elucidation of 19- <i>nor</i> -pimarane diterpenoids	91
2.3.6 Isolation and Structure Elucidation of Di- <i>nor</i> -pimaranes	107

TABLE OF CONTENTS (continued)

<u>CHAPTER</u>	<u>PAGE</u>
2.3.7 Other compounds.....	113
2.4 Conclusion.....	120
3. Biological Activity of Select Pimaranes.....	121
3.1 Introduction.....	122
3.2 Anti-germination Materials and Methods.....	124
3.2.1 General Experimental Procedures.	124
3.2.2 Plant Material.....	125
3.2.3 Extraction and Isolation.	125
3.2.4 Plant Growth Response Screening Materials.....	126
3.2.5 Assays for Growth Responses.	126
3.2.6 Vertical Growth Assays of <i>Arabidopsis</i>	127
3.2.7 Germination and Phenotyping.	127
3.2.8 Vegetative Assessment.....	128
3.2.9 Statistical Analysis.	128
3.3 Anti-germination Results and Discussion.....	128
3.4 Cytotoxicity Materials and Methods.....	132
3.4.1 General Experimental Procedures.	132
3.4.2 Plant Material.....	132
3.4.3 Extraction and Isolation.	133
3.4.4 Cytotoxicity Assays.....	133
3.5 Cytotoxicity Results and Discussion.....	134
3.6 Conclusion.....	139
4. Conclusions and Perspectives.....	140
References.....	148
Appendices.....	163
Appendix A. Spectroscopic Data and Figures.....	163
Appendix B. Permissions to use Copyrighted Material.....	340
Vitae.....	342

LIST OF TABLES

<u>TABLE</u>	<u>PAGE</u>
TABLE I. ETHNOBOTANICAL USES FOR <i>ICACINA</i> GENUS	17
TABLE II. SUMMARY OF COMPOUNDS REPORTED FROM <i>I. TRICHANTHA</i>	22
TABLE III. GC-MS ANALYSIS OF <i>I. TRICHANTHA</i> LEAF EXTRACT.....	31
TABLE IV. SUMMARY OF CYTOTOXIC ACTIVITY FOR SELECT COMPOUNDS FROM <i>I. TRICHANTHA</i>	33
TABLE V. ¹ H (400 MHz) AND ¹³ C NMR (100 MHz) OF COMPOUNDS 1 AND 2	65
TABLE VI. ¹ H (400 MHz) AND ¹³ C NMR (100 MHz) OF COMPOUNDS 4 AND 5.....	69
TABLE VII. ¹ H (400 MHz) AND ¹³ C (100 MHz) NMR SPECTROSCOPIC DATA	74
TABLE VIII. ¹ H (400 MHz) NMR SPECTROSCOPIC DATA FOR COMPOUNDS 9 AND 11-14.....	82
TABLE IX. ¹³ C (100 MHz) NMR SPECTROSCOPIC DATA FOR COMPOUNDS 9 AND 11-14.....	83
TABLE X. ¹ H (400 MHz) NMR SPECTROSCOPIC DATA OF COMPOUNDS 17-20.....	93
TABLE XI. ¹³ C (100 MHz) NMR SPECTROSCOPIC DATA OF COMPOUNDS 17-20	94
TABLE XII. ¹ H (400 MHz) AND ¹³ C (100 MHz) NMR OF COMPOUND 21 AND 22.....	109
TABLE XIII. ¹ H (900 MHz) AND ¹³ C (226 MHz) NMR OF COMPOUND 24	119
TABLE XIV. CYTOTOXIC ACTIVITY OF ISOLATED NOVEL COMPOUNDS	136
TABLE XV. CYTOTOXIC ACTIVITY OF ICACINOL, HUMIRIANTHOL, AND ICACINLACTONE E	137
TABLE XVI. X-RAY CRYSTAL STRUCTURE DETERMINATION FOR COMPOUND 5	329
TABLE XVII. X-RAY CRYSTAL STRUCTURE DETERMINATION FOR COMPOUND 11	330
TABLE XVIII. CARTESIAN COORDINATE OF PREDOMINANT CONFORMER OF COMPOUND 17.....	331
TABLE XIX. CARTESIAN COORDINATE OF PREDOMINANT CONFORMER OF COMPOUND 18.....	332
TABLE XX. CARTESIAN COORDINATE OF PREDOMINANT CONFORMER OF COMPOUND 19.....	333
TABLE XXI. CARTESIAN COORDINATE OF PREDOMINANT CONFORMERS OF COMPOUND 20.....	335

LIST OF TABLES (continued)

<u>TABLE</u>	<u>PAGE</u>
TABLE XXII. ECD CALCULATIONS FOR COMPOUND 21	336
TABLE XXIII. ECD CALCULATIONS FOR COMPOUND 22	338

LIST OF FIGURES

<u>FIGURE</u>	<u>PAGE</u>
Figure 1. Botanical IND applications submitted to the FDA from 2002 to 2016	6
Figure 2. Aerial parts of <i>I. trichantha</i> in Nigeria.	13
Figure 3. Herbarium specimen of <i>I. trichantha</i> leaves, stem, and fruits collected by C. Barter in Nigeria in 1858.	13
Figure 4. Geographic distribution of <i>I. trichantha</i>	16
Figure 5. Structures of Compounds Reported from <i>Icacina trichantha</i>	23
Figure 6. Icachine and its acetyl-derivative from <i>I. guessfeldtii</i>	25
Figure 7. Icaceine and de-N-methylicaceine from <i>I. guessfeldtii</i>	26
Figure 8. Glucosides isolated from <i>I. oliviformis</i>	26
Figure 9. Diterpenes isolated from <i>I. oliviformis</i>	27
Figure 10. Flavone-C-glycosides and <i>trans</i> -(S, E)-(-) clovamide from <i>I. oliviformis</i>	28
Figure 11. Pimaranes and pimarane glycosides isolated from <i>I. oliviformis</i>	29
Figure 12. Further diterpenoids isolated from <i>I. oliviformis</i>	30
Figure 13. Isolated 9 β H-pimarane diterpenoids from <i>I. trichantha</i>	61
Figure 14. UV chromatograms of HPLC separation of compounds 1 and 2	63
Figure 15. ORTEP representation of 14-hydroxyicacinlactone I	71
Figure 16. Isolated 9 β H-17- <i>nor</i> -pimarane diterpenoids from <i>I. trichantha</i>	71
Figure 17. ¹ H- ¹ H COSY and selective HMBC correlations for compounds 6 and 7	75
Figure 18. Key NOESY correlations for compounds 6 and 7	75
Figure 19. ORTEP representations of compound 6	75
Figure 20. Isolated 17- <i>nor</i> -pimarane diterpenoids from <i>I. trichantha</i>	78
Figure 21. ¹ H- ¹ H COSY and selective HMBC for compounds 9 and 11-14	80
Figure 22. Key NOESY correlations for compounds 9 and 11-14	81
Figure 23. ORTEP representation of compound 11	85
Figure 24. Isolated 19- <i>nor</i> -pimarane diterpenoids from <i>I. trichantha</i>	91
Figure 25. ¹ H- ¹ H COSY and selective HMBC for compounds 17-20	96
Figure 26. Key NOESY correlations for compounds 17-20	97

LIST OF FIGURES (continued)

<u>FIGURE</u>	<u>PAGE</u>
Figure 27. Experimental and calculated ECD spectra for 17-20, and their enantiomers.....	98
Figure 28. Proposed biogenesis for compound 17 via Scheme 1 and Scheme 2.....	105
Figure 29. Isolated di- <i>nor</i> -pimaranes from <i>I. trichantha</i>	107
Figure 30. ¹ H– ¹ H COSY and selective HMBC correlations for compounds 21 and 22.....	110
Figure 31. Key NOESY correlations for compounds 21 and 22	110
Figure 32. ORTEP representation of compound 21.....	110
Figure 33. Experimental and calculated ECD spectra for 21 and 22, and their enantiomers.....	111
Figure 34. Artifact of humirianthenolide C structural analogue.....	115
Figure 35. Key COSY and HMBC correlations for compound 24.....	116
Figure 36. Proposed biogenesis of compound 24	118
Figure 37. <i>Ikacina trichantha</i> fractions and icacinol (1) effects on seed germination.	129
Figure 38. <i>I. tricantha</i> EtOAc-extract and icacinol (1) impact on vegetative growth.	130
Figure 39. <i>Ikacina trichantha</i> extract and icacinol (1) impacts on longer term vegetative growth	131
Figure 40. Related pimarane diterpenoids screened against PC-3 cancer cells.....	138
Figure 41. ¹ H spectrum (400 MHz, DMSO- <i>d</i> ₆) of icacinol	163
Figure 42. ¹ H NMR (400 MHz, DMSO- <i>d</i> ₆) spectra of compound 1 and icacinol standard	164
Figure 43. ¹³ C spectrum (100 MHz, DMSO- <i>d</i> ₆) of icacinol	165
Figure 44. DEPT-135 spectrum (100 MHz, DMSO- <i>d</i> ₆) of icacinol	166
Figure 45. LC-MS library similarity search for icacinol.....	167
Figure 46. HRESIMS (positive mode) for icacinol	167
Figure 47. ¹ H spectrum (400 MHz, DMSO- <i>d</i> ₆) of humirianthol	168
Figure 48. ¹ H NMR (400 MHz, DMSO- <i>d</i> ₆) spectra of isolated compound and humirianthol standard	169
Figure 49. ¹³ C spectrum (100 MHz, DMSO- <i>d</i> ₆) of humirianthol	170
Figure 50. DEPT-135 spectrum (100 MHz, DMSO- <i>d</i> ₆) of humirianthol.....	171
Figure 51. LC-MS library similarity search for humirianthol	172
Figure 52. HRESIMS (positive mode) for humirianthol.....	172
Figure 53. LC-MS library similarity search for 14- α OCH ₃ -humirianthol	173
Figure 54. ¹ H spectrum (400 MHz, CD ₃ OD) of 14- α -methoxy-humirianthol	174

LIST OF FIGURES (continued)

<u>FIGURE</u>	<u>PAGE</u>
Figure 55. ¹ H NMR (400 MHz, CD ₃ OD) spectra of isolated compound and 14- α -methoxy-humirianthol standard.....	175
Figure 56. DEPTQ spectrum (100 MHz, CD ₃ OD) of 14- α -methoxy-humirianthol.....	176
Figure 57. HSQC spectrum (400 MHz, CD ₃ OD) of 14- α - methoxy-humirianthol.....	177
Figure 58. COSY spectrum (400 MHz, CD ₃ OD) of 14- α -methoxy-humirianthol.....	178
Figure 59. HMBC spectrum (400 MHz, CD ₃ OD) of 14- α -methoxy-humirianthol.....	179
Figure 60. HRESIMS (negative mode) for icacinlactone I.....	180
Figure 61. ¹ H spectrum (400 MHz, CD ₃ OD) of icacinlactone I.....	181
Figure 62. ¹ H NMR (400 MHz, CD ₃ OD) spectra of isolated compound and icacinlactone I standard	182
Figure 63. ¹³ C spectrum (100 MHz, CD ₃ OD) of icacinlactone I.....	183
Figure 64. DEPT-135 spectrum (100 MHz, CD ₃ OD) of icacinlactone I.....	184
Figure 65. HSQC spectrum (400 MHz, CD ₃ OD) of icacinlactone I	185
Figure 66. COSY spectrum (400 MHz, CD ₃ OD) of icacinlactone I	186
Figure 67. HMBC spectrum (400 MHz, CD ₃ OD) of icacinlactone I	187
Figure 68. HRESIMS (positive mode) for 14-hydroxy-icacinlactone I.....	188
Figure 69. ¹ H spectrum (400 MHz, CD ₃ OD) of 14-hydroxy-icacinlactone I	189
Figure 70. ¹³ C spectrum (100 MHz, CD ₃ OD) of 14-hydroxy-icacinlactone I	190
Figure 71. DEPT-135 spectrum (100 MHz, CD ₃ OD) of 14-hydroxy-icacinlactone I.....	191
Figure 72. HSQC spectrum (400 MHz, CD ₃ OD) of 14-hydroxy-icacinlactone I	192
Figure 73. COSY spectrum (400 MHz, CD ₃ OD) of 14-hydroxy-icacinlactone I	193
Figure 74. HMBC spectrum (400 MHz, CD ₃ OD) of 14-hydroxy-icacinlactone I	194
Figure 75. NOESY spectrum (400 MHz, CD ₃ OD) of 14-hydroxy-icacinlactone I.....	195
Figure 76. IR spectrum of 14-hydroxy-icacinlactone I.....	196
Figure 77. ¹ H spectrum (400 MHz, CD ₃ OD) of 7 α -hydroxyicacenone.....	197
Figure 78. ¹³ C spectrum (100 MHz, CD ₃ OD) of 7 α -hydroxyicacenone.....	198
Figure 79. ¹ H- ¹ H COSY (400 MHz, CD ₃ OD) of 7 α -hydroxyicacenone	199
Figure 80. HSQC (400 MHz, CD ₃ OD) of 7 α -hydroxyicacenone.....	200
Figure 81. HMBC (400 MHz, CD ₃ OD) of 7 α -hydroxyicacenone.....	201

LIST OF FIGURES (continued)

<u>FIGURE</u>	<u>PAGE</u>
Figure 82. NOESY (400 MHz, CD ₃ OD) of 7 α -hydroxyicacenone	202
Figure 83. IR Spectrum of 7 α -hydroxyicacenone.....	203
Figure 84. ¹ H spectrum (400 MHz, CD ₃ OD) of 2 β -hydroxyhumirianthenolide C	204
Figure 85. ¹³ C spectrum (100 MHz, CD ₃ OD) of 2 β -hydroxyhumirianthenolide C	205
Figure 86. ¹ H- ¹ H COSY spectrum (400 MHz, CD ₃ OD) of 2 β -hydroxyhumirianthenolide C	206
Figure 87. HSQC spectrum (400 MHz, CD ₃ OD) of 2 β -hydroxyhumirianthenolide C	207
Figure 88. HMBC spectrum (400 MHz, CD ₃ OD) of 2 β -hydroxyhumirianthenolide C	208
Figure 89. NOESY spectrum (400 MHz, CD ₃ OD) of 2 β -hydroxyhumirianthenolide C.....	209
Figure 90. IR spectrum of 2 β -hydroxyhumirianthenolide C	210
Figure 91. HRESIMS (positive mode) for icacinlactone E.....	210
Figure 92. ¹ H spectrum (400 MHz, CD ₃ OD) of icacinlactone E.....	211
Figure 93. ¹ H NMR (400 MHz, CD ₃ OD) spectra of compound 8 and icacinlactone E standard	212
Figure 94. ¹³ C spectrum (100 MHz, CD ₃ OD) of icacinlactone E.....	213
Figure 95. DEPT-135 spectrum (100 MHz, CD ₃ OD) of icacinlactone E	214
Figure 96. HSQC spectrum (400 MHz, CD ₃ OD) of icacinlactone E	215
Figure 97. HMBC spectrum (400 MHz, CD ₃ OD) of icacinlactone E	216
Figure 98. NOESY spectrum (400 MHz, CD ₃ OD) of icacinlactone E.....	217
Figure 99. LC-MS library similarity search for icacinlactone E	218
Figure 100. ¹ H spectrum (400 MHz, CD ₃ OD) of 7 α -hydroxyicacinlactone B	219
Figure 101. ¹³ C spectrum (100 MHz, CD ₃ OD) of 7 α -hydroxyicacinlactone B	220
Figure 102. ¹ H- ¹ H COSY spectrum (400 MHz, CD ₃ OD) of 7 α -hydroxyicacinlactone B.....	221
Figure 103. HSQC spectrum (400 MHz, CD ₃ OD) of 7 α -hydroxyicacinlactone B	222
Figure 104. HMBC spectrum (400 MHz, CD ₃ OD) of 7 α -hydroxyicacinlactone B	223
Figure 105. NOESY spectrum (400 MHz, CD ₃ OD) of 7 α -hydroxyicacinlactone B.....	224
Figure 106. IR spectrum of 7 α -hydroxyicacinlactone B.....	225
Figure 107. ¹ H NMR (400 MHz, CD ₃ OD) spectrum of 7 β -hydroxyicacinlactone B.....	226
Figure 108. ¹ H NMR (400 MHz, CD ₃ OD) spectra of compound 10 and 7 β -hydroxyicacinlactone B standard.....	227
Figure 109. ¹ H NMR (400 MHz, CDCl ₃ - <i>d</i>) spectrum of 7-oxo-icacinlactone B	228
Figure 110. ¹³ C (100 MHz, CDCl ₃ - <i>d</i>) spectrum of 7-oxo-icacinlactone B	229

LIST OF FIGURES (continued)

<u>FIGURE</u>	<u>PAGE</u>
Figure 111. ^1H (400 MHz, CD_3OD) spectrum of 7-oxo-icacinlactone B	230
Figure 112. ^{13}C (100 MHz, CD_3OD) spectrum of 7-oxo-icacinlactone B	231
Figure 113. HSQC (400 MHz, CDCl_3 - <i>d</i>) spectrum of 7-oxo-icacinlactone B.....	232
Figure 114. ^1H - ^1H COSY (400 MHz, CDCl_3 - <i>d</i>) spectrum of 7-oxo-icacinlactone B	233
Figure 115. HMBC (400 MHz, CDCl_3 - <i>d</i>) spectrum of 7-oxo-icacinlactone B.....	234
Figure 116. NOESY (400 MHz, CDCl_3 - <i>d</i>) spectrum of 7-oxo-icacinlactone B	235
Figure 117. HRESIMS (+) spectrum of 7-oxo-icacinlactone B	236
Figure 118. IR spectrum of 7-oxo-icacinlactone B.....	236
Figure 119. ^1H (400 MHz, CD_3OD) spectrum of 3-dehydroxy-icacinlactone B.....	237
Figure 120. ^{13}C (100 MHz, CD_3OD) spectrum of 3-dehydroxy-icacinlactone B	238
Figure 121. DEPTQ (100 MHz, CD_3OD) spectrum of 3-dehydroxy-icacinlactone B	239
Figure 122. HSQC (400 MHz, CD_3OD) spectrum of 3-dehydroxy-icacinlactone B	240
Figure 123. ^1H - ^1H (400 MHz, CD_3OD) spectrum of 3-dehydroxy-icacinlactone B	241
Figure 124. HMBC (400 MHz, CD_3OD) spectrum of 3-dehydroxy-icacinlactone B	242
Figure 125. NOESY (400 MHz, CD_3OD) spectrum of 3-dehydroxy-icacinlactone B.....	243
Figure 126. HRESIMS (+) spectrum of 3-dehydroxy-icacinlactone B	244
Figure 127. IR spectrum of 3-dehydroxy-icacinlactone B.....	244
Figure 128. ^1H (400 MHz, CD_3OD) spectrum of 3-dehydroxy-icacinlactone A	245
Figure 129. ^{13}C (100 MHz, CD_3OD) spectrum of 3-dehydroxy-icacinlactone A	246
Figure 130. DEPTQ (100 MHz, CD_3OD) spectrum of 3-dehydroxy-icacinlactone A.....	247
Figure 131. HSQC (400 MHz, CD_3OD) spectrum of 3-dehydroxy-icacinlactone A	248
Figure 132. ^1H - ^1H COSY (400 MHz, CD_3OD) spectrum of 3-dehydroxy-icacinlactone A.....	249
Figure 133. HMBC (400 MHz, CD_3OD) spectrum of 3-dehydroxy-icacinlactone A	250
Figure 134. NOESY (400 MHz, CD_3OD) spectrum of 3-dehydroxy-icacinlactone A.....	251
Figure 135. HRESIMS (+) spectrum of 3-dehydroxy-icacinlactone A	252
Figure 136. ^1H (400 MHz, CD_3OD) spectrum of icacinlactone L.....	253
Figure 137. ^{13}C (100 MHz, CD_3OD) spectrum of icacinlactone L.....	254
Figure 138. HSQC (400 MHz, CD_3OD) spectrum of icacinlactone L	255
Figure 139. ^1H - ^1H (400 MHz, CD_3OD) spectrum of icacinlactone L	256
Figure 140. HMBC (400 MHz, CD_3OD) spectrum of icacinlactone L	257

LIST OF FIGURES (continued)

<u>FIGURE</u>	<u>PAGE</u>
Figure 141. NOESY (400 MHz, CD ₃ OD) spectrum of icacinlactone L	258
Figure 142. IR spectrum of icacinlactone L	259
Figure 143. ¹ H NMR (400 MHz, CD ₃ OD) spectrum of icacinlactone D.....	260
Figure 144. ¹ H NMR (400 MHz, CD ₃ OD) spectra of compound 15 and icacinlactone D standard	261
Figure 145. LC-MS library similarity search for icacinlactone D	262
Figure 146. ¹ H NMR (400 MHz, CD ₃ OD) spectrum of icacinlactone H.....	263
Figure 147. ¹ H NMR (400 MHz) spectra of compound 15 and icacinlactone H standard	264
Figure 148. LC-MS library similarity search for icacinlactone H.....	265
Figure 149. ¹ H NMR (400 MHz, CD ₃ OD) spectrum of icatrichanone.....	266
Figure 150. ¹³ C NMR (100 MHz, CD ₃ OD) spectrum of icatrichanone.....	267
Figure 151. DEPTQ (100 MHz, CD ₃ OD) spectrum of icatrichanone	268
Figure 152. HSQC NMR (400 MHz, CD ₃ OD) spectrum of icatrichanone.....	269
Figure 153. ¹ H- ¹ H COSY NMR (400 MHz, CD ₃ OD) spectrum of icatrichanone	270
Figure 154. HMBC NMR (400 MHz, CD ₃ OD) spectrum of icatrichanone.....	271
Figure 155. NOESY NMR (400 MHz, CD ₃ OD) spectrum of icatrichanone	272
Figure 156. IR spectrum of icatrichanone	273
Figure 157. HRESIMS (+) spectrum of icatrichanone.....	274
Figure 158. ¹ H NMR (400 MHz, CD ₃ OD) spectrum of 14-hydroxyicatrichanone.....	275
Figure 159. ¹³ C NMR (100 MHz, CD ₃ OD) spectrum of 14-hydroxyicatrichanone.....	276
Figure 160. DEPTQ NMR (100 MHz, CD ₃ OD) spectrum of 14-hydroxyicatrichanone.....	277
Figure 161. HSQC NMR (400 MHz, CD ₃ OD) spectrum of 14-hydroxyicatrichanone.....	278
Figure 162. ¹ H- ¹ H NMR (400 MHz, CD ₃ OD) spectrum of 14-hydroxyicatrichanone.....	279
Figure 163. HMBC NMR (400 MHz, CD ₃ OD) spectrum of 14-hydroxyicatrichanone.....	280
Figure 164. NOESY NMR (400 MHz, CD ₃ OD) spectrum of 14-hydroxyicatrichanone	281
Figure 165. IR spectrum of 14-hydroxyicatrichanone	282
Figure 166. HRESIMS (+) spectrum of 14-hydroxyicatrichanone.....	283
Figure 167. ¹ H NMR (400 MHz, CD ₃ OD) spectrum of 3-methoxyicatrichanone	284
Figure 168. ¹³ C (100 MHz, CD ₃ OD) spectrum of 3-methoxyicatrichanone	285
Figure 169. DEPTQ (100 MHz, CD ₃ OD) spectrum of 3-methoxyicatrichanone	286

LIST OF FIGURES (continued)

<u>FIGURE</u>	<u>PAGE</u>
Figure 170. HSQC (400 MHz, CD ₃ OD) spectrum of 3-methoxyicatrichanone.....	287
Figure 171. ¹ H- ¹ H COSY (400 MHz, CD ₃ OD) spectrum of 3-methoxyicatrichanone	288
Figure 172. HMBC (400 MHz, CD ₃ OD) spectrum of 3-methoxyicatrichanone.....	289
Figure 173. NOESY (400 MHz, CD ₃ OD) spectrum of 3-methoxyicatrichanone	290
Figure 174. IR spectrum of 3-methoxyicatrichanone	291
Figure 175. HRESIMS (+) spectrum of 3-methoxyicatrichanone.....	291
Figure 176. ¹ H (400 MHz, chloroform- <i>d</i>) spectrum of 3-methoxy-14-hydroxy-icatrichanone ..	292
Figure 177. ¹³ C (100 MHz, chloroform- <i>d</i>) spectrum of 3-methoxy-14-hydroxy-icatrichanone .	293
Figure 178. DEPT135 (100 MHz, chloroform- <i>d</i>) spectrum of 3-methoxy-14-hydroxy- icatrichanone.....	294
Figure 179. HSQC (400 MHz, chloroform- <i>d</i>) spectrum of 3-methoxy-14-hydroxy-icatrichanone	295
Figure 180. ¹ H- ¹ H COSY (400 MHz, chloroform- <i>d</i>) spectrum of 3-methoxy-14-hydroxy- icatrichanone.....	296
Figure 181. HMBC (400 MHz, chloroform- <i>d</i>) spectrum of 3-methoxy-14-hydroxy-icatrichanone	297
Figure 182. NOESY (400 MHz, chloroform- <i>d</i>) spectrum of 3-methoxy-14-hydroxy- icatrichanone.....	298
Figure 183. IR spectrum of 3-methoxy-14-hydroxy-icatrichanone.....	299
Figure 184. HRESIMS (+) spectrum of 3-methoxy-14-hydroxy-icatrichanone	299
Figure 185. ¹ H (400 MHz, CD ₃ OD) spectrum of icacinlactone K.....	300
Figure 186. ¹³ C (100 MHz, CD ₃ OD) spectrum of icacinlactone K	301
Figure 187. HSQC (400 MHz, CD ₃ OD) spectrum of icacinlactone K.....	302
Figure 188. ¹ H- ¹ H COSY (400 MHz, CD ₃ OD) spectrum of icacinlactone K.....	303
Figure 189. HMBC (400 MHz, CD ₃ OD) spectrum of icacinlactone K.....	304
Figure 190. NOESY (400 MHz, CD ₃ OD) spectrum of icacinlactone K	305
Figure 191. IR spectrum of icacinlactone K.....	306
Figure 192. ¹ H (400 MHz, CD ₃ OD) spectrum of icacintrichanone.....	307
Figure 193. ¹³ C (100 MHz, CD ₃ OD) spectrum of icacintrichanone.....	308
Figure 194. HSQC (400 MHz, CD ₃ OD) spectrum of icacintrichanone.....	309
Figure 195. ¹ H- ¹ H COSY (400 MHz, CD ₃ OD) spectrum of icacintrichanone	310

LIST OF FIGURES (continued)

<u>FIGURE</u>	<u>PAGE</u>
Figure 196. HMBC (400 MHz, CD ₃ OD) spectrum of icacintrichanone.....	311
Figure 197. NOESY (400 MHz, CD ₃ OD) spectrum of icacintrichanone	312
Figure 198. IR spectrum of icacintrichanone	313
Figure 199. ¹ H (400 MHz, CD ₃ OD) spectrum of (+)-pinoresinol	314
Figure 200. ¹³ C (100 MHz, CD ₃ OD) spectrum of (+)-pinoresinol	315
Figure 201. DEPTQ (100 MHz, CD ₃ OD) spectrum of (+)-pinoresinol.....	316
Figure 202. HSQC (400 MHz, CD ₃ OD) spectrum of (+)-pinoresinol.....	317
Figure 203. ¹ H- ¹ H COSY (400 MHz, CD ₃ OD) spectrum of (+)-pinoresinol	318
Figure 204. HMBC (400 MHz, CD ₃ OD) spectrum of (+)-pinoresinol.....	319
Figure 205. NOESY (400 MHz, CD ₃ OD) spectrum of (+)-pinoresinol	320
Figure 206. IR spectrum of (+)-pinoeresinol.....	321
Figure 207. ¹ H NMR (400 MHz) spectra of compound 24 and humirianthenolide C standard..	322
Figure 208. ¹ H (900 MHz, CD ₃ OD) spectrum of compound 24	323
Figure 209. DEPTQ (226 MHz, CD ₃ OD) spectrum of compound 24.....	324
Figure 210. HSQC (900 MHz, CD ₃ OD) spectrum of compound 24.....	325
Figure 211. ¹ H- ¹ H COSY (900 MHz, CD ₃ OD) spectrum of compound 24.....	326
Figure 212. HMBC (900 MHz, CD ₃ OD) spectrum of compound 24.....	327
Figure 213. NOESY (900 MHz, CD ₃ OD) spectrum of compound 24	328

LIST OF ABBREVIATIONS

22Rv1	Human prostate carcinoma cell line
ABRC	Arabidopsis Biological Resource Center
ACN	Acetonitrile
ALP	Alkaline phosphatase
ALT	Alanine transaminase
AR	Androgen receptor
AST	Aspartate transaminase
ATCC	American Type Culture Collection
AU	Absorbance units
BDCP	Bioresources Development and Conservation Programme (Nigeria)
BuOH	Butanol
calcd	Calculated
C ₈	Octyl carbon chain-bonded silica
C ₁₈	Octadecyl carbon chain-bonded silica
CCD	Charge-couple device
CCDC	The Cambridge Crystallographic Data Centre
CD	Circular dichroism spectroscopy
CHCl ₃	Chloroform
COSY	Correlation spectroscopy
CYP	Cytochrome P450
DCM	Dichloromethane (methylene chloride)
DEPT	Distortionless enhancement by polarization transfer
DEPTQ	Distortionless enhancement by polarization transfer with quaternaries
DMSO	Dimethyl sulfoxide
DNA	Deoxyribonucleic acid
DPPH	2,2-diphenyl-1-picrylhydrazyl
ECD	Electronic circular dichroism
ESI	Electrospray ionization

LIST OF ABBREVIATIONS (continued)

EtOAc	Ethyl acetate
EtOH	Ethanol
FBS	Fetal bovine serum
FDA	Food and Drug Administration (USA)
FRAP	Ferric reducing antioxidant power
HCT-116	Human colorectal carcinoma cell line
HDL	High-density lipoprotein
HMBC	Heteronuclear multiple bond correlation spectroscopy
HPLC	High-performance liquid chromatography
HRESIMS	High resolution electrospray ionization mass spectrometry
HRMS	High resolution mass spectrometry
HSQC	Heteronuclear single quantum coherence spectroscopy
HT-29	Human colorectal adenocarcinoma cell line
IC ₅₀	Half maximal inhibitory concentration
IND	Investigational new drug
IPA	Isopropyl alcohol
IR	Infrared spectroscopy/ vibrational spectroscopy
IT-TOF	Ion-trap-time-of-flight
LC	Liquid chromatography
LDL	Low-density lipoprotein
M	Molarity
MBC	Minimum bactericidal concentration
MDA	Malondialdehyde
MDA-MB-231	Human breast adenocarcinoma cell line
MDA-MB-435	Human melanoma cell line
MeOH	Methanol
MIC	Minimum inhibition concentration
MM2	Molecular mechanics force field
MOA	Mechanism of action
mPCE	Micronucleated polychromatic erythrocytes
MS	Mass spectrometry

LIST OF ABBREVIATIONS (continued)

m/z	Mass to charge ratio
NCCIH	National Center for Complementary and Integrative Health
NCI	National Cancer Institute
NDA	New drug application
NIH	National Institutes of Health
NMR	Nuclear magnetic resonance
NOESY	Nuclear Overhauser spectroscopy
OVCAR	Human ovarian carcinoma cell line
PC	Prostate cancer
PC-3	Human prostate adenocarcinoma cell line
PDA	Photodiode array detector
qTOF	Quadrupole-time-of-flight
RB1	Retinoblastoma protein
RP	Reversed phase
SAR	Structure-activity relationship
SB-C ₁₈	StableBond octadecyl carbon chain-bonded silica
SOD	Superoxide dismutase
TAIR	The Arabidopsis Information Resource
TCM	Traditional Chinese Medicine
TDDFT	Time-dependent density functional theory
TFA	Trifluoroacetic acid
TM	Traditional medicine
TLC	Thin layer chromatography
TOF	Time-of-flight
UV	Ultraviolet
VLC	Vacuum liquid chromatography
vol	Volume
WHO	World Health Organization
WT	Wild type

SUMMARY

A phytochemical analysis was undertaken of an ethnomedicinal plant with reported traditional use endemic to West Africa identified as *Icacina trichantha*. Chapter 1 reviews the history of natural products as source for drug discovery and the advantage of targeting medicinal plants and herbs utilized in traditional medicine systems. The taxonomy and ethnomedicinal background of *I. trichantha* is discussed in addition to a current survey of the scientific literature assessing its chemical and biological profile. Chapter 2 discusses the results of a bioassay-guided fractionation of *I. trichantha* tuber extract. Through the application of analytical chemistry methods and spectroscopic acquisition, fourteen novel compounds are presented along with their structural descriptions. Previously reported compounds were also identified and enriched for further biological activity experiments. Chapter 3 describes the biological experiments conducted to assess the validity of reported traditional use of the ethnobotanical as well as other possible biological applications. Cytotoxicity assays were conducted in several different human cancer cell lines *in vitro*. Anti-germination experiments were also conducted to assess potential of icacinol as a potential naturally derived herbicide. Chapter 4 provides an overview of this work, and perspectives for future directions of this ethnomedicinal plant species and the field of pharmacognosy.

1. INTRODUCTION TO NATURAL PRODUCTS AND *ICACINA*

1.1 **Background**

1.1.1 **Pharmacognosy & Phytochemistry**

Since the earliest humans, new treatments have been sought for illness and disease. The field of pharmacy is a vital tool that concentrates on the science of drugs for the treatment of ailments. Today, pharmacy encompasses a vast and complex field that utilizes modern technology to synthesize, formulate, and standardize chemical compounds and biological agents for use in medicine.¹ Until the recent development of synthetic drugs and biologics, pharmacists relied on the natural resources around them as a source for remedies. Therefore, it can be said that the history of pharmacognosy can be traced to early human history.

Pharmacognosy was first introduced in the early 19th century by J.A. Schmidt and C.A. Seydler to describe the medicinal use of crude drugs.² The etymology of the word is based on the Greek words *pharmakon*, meaning “drug”, and *gnosis*, meaning “knowledge.” Since that time, the term has expanded to encompass the study of natural products within a multidisciplinary field that includes chemistry, biology, genetics, and pharmacology. The field seeks to understand the properties of natural products for their medical, pharmaceutical, and other practical properties. Natural products, also known as secondary metabolites, come from a variety of biological life, such as plants, animals, and bacteria, that often produce these unique chemical entities for specialized purposes.

Pharmacognosy also includes the field of phytochemistry, which seeks to discover and identify new chemicals from plants, and ethnobotany, the study of traditional medicinal uses of botanicals. Combining these two elements makes for an interesting field that seeks to identify and analyze medicinal plants that are promising candidates for drug discovery of new lead compounds. The phytochemistry side utilizes analytical chemistry techniques such as

chromatography and spectroscopy to separate and isolate secondary metabolites produced from higher plants. These chemicals are then analyzed with spectroscopic methods such as mass spectrometry and nuclear magnetic resonance (NMR) to elucidate their structures. A complete chemical characterization of novel compounds is essential to the drug discovery process, in addition to the analysis of biological activity and the subsequent clinical research necessary in the drug development process. The ethnobotanical aspect relies on anthropological and medical information to understand and discover traditional medicine methods and materials used by various civilizations. This is often composed of *Materia Medica* texts listing medicinal herbs and recorded clinical observations of treatments. Modern medicine can take advantage of this privileged knowledge, which can be thousands of years old, to provide a more targeted and promising lead for the discovery of new drug therapies.

1.1.2 Medicinal Plants and Botanicals for Drug Discovery

The history of humans using botanicals for medicinal purposes can be traced back 60,000 years to the Paleolithic period. The discovery of a Neanderthal burial site in Iraq uncovered a tomb that contained several species of flowers with reported pharmaceutical use, including *Muscari*, *Ephedra*, *Althaea*, and *Achillea*. The presumption is these early humans held these plants in high regard, and possibly knew of their medicinal properties.³ Over time, disparate civilizations developed their own organized systems of medicine. Systems such as Traditional Chinese Medicine (TCM),⁴ Ayurveda,⁵ and Unani⁶ differ in their philosophies and approaches, but the utilization of plants and herbs is a common trait. Another important mutual aspect is the documentation of their respective medicinal knowledge in texts that date back hundreds and even thousands of years.^{4,7} Similarly, the ancient Greeks and Romans kept records of medicinal herbs and formulas.⁸ Fortunately, the preservation of this collective knowledge and the continued

prevalence of some of these systems allowed for modern scientists and pharmacists to interrogate this information to better understand and develop new therapeutics.

Natural products are a vital part of the current global medical system. Traditional medicine remains prevalent throughout the globe, especially herbal medicine. In many developing regions and countries, primarily Africa, South America, and Asia, up to 80% of the population consider traditional medicine their primary form of healthcare due to a combination of economics, accessibility, and cultural beliefs.^{9,10} On the other hand, in developed countries, an increasing number of people are using “complementary and alternative medicine” (CAM) therapies to address health concerns, such as acupuncture, yoga, and herbs.¹¹ In the past 20 years, the reported usage of herbal medicines has increased, coinciding with additional government regulation, expanded registration of pharmacopeias, and increasing sales of natural product therapies. The WHO reports that as of 2019, 57% of member states’ populations use some type of herbal medicine treatment.¹² In the United States, the total sales of herbal supplements has increased every year since 2003. In 2018, the total amount spent was \$8.842 billion, a 9.4% increase from the previous year.¹³ Additionally, secondary metabolites from plants, fungi, bacteria, and marine organisms directly or indirectly influence the development of most approved drugs.¹⁴ A survey of small molecule drugs approved by the U.S. FDA from 1981 to 2014 show that nearly two-thirds are directly or indirectly derived from natural products.¹⁵ Even though an increasing percentage of drug discovery leads now focus on microbial sources,¹⁶ botanicals remain an important source for new drugs. In addition, the pharmaceutical industry remains interested in these new botanical-based traditional therapies evidenced by the consistent number of IND applications to the FDA (Figure 1). An important turning point was in 2004 when the FDA established guidelines for “botanical drugs,” pharmaceuticals that are mixtures of

botanical extracts. The guidelines provided an update on the FDA regulatory requirements for botanical drugs and the results were soon obvious. Following the establishment of these new regulations, there was an increase in IND submissions and the number of botanical drugs approved for Phase II clinical trials.¹⁷ The annual application numbers remain steady. In 2016, there were 48 IND applications for botanical drugs to the FDA.¹⁸ Since the guidelines were issued, two NDAs under this designation have been approved for the U.S. market. In 2006, green tea-derived (*Camellia sinensis* Kuntze) Veregen® was approved for the treatment of genital warts.¹⁹ The other, Fulyzaq®, was approved for treatment of HIV-associated diarrhea. The drug is derived from the latex of the South American croton tree (*Croton lechlerii* Mull Arg.).²⁰ In addition to these two prescription botanical drugs, there are several botanical ingredients approved by the FDA for over-the-counter (OTC) use. There are several botanicals approved as OTC drug products, including senna and witch hazel.^{21,22} Taken together, these trends indicate a strong demand for botanical medicines in regions where traditional medicine is widely accepted and by the pharmaceutical industry in developed nations.

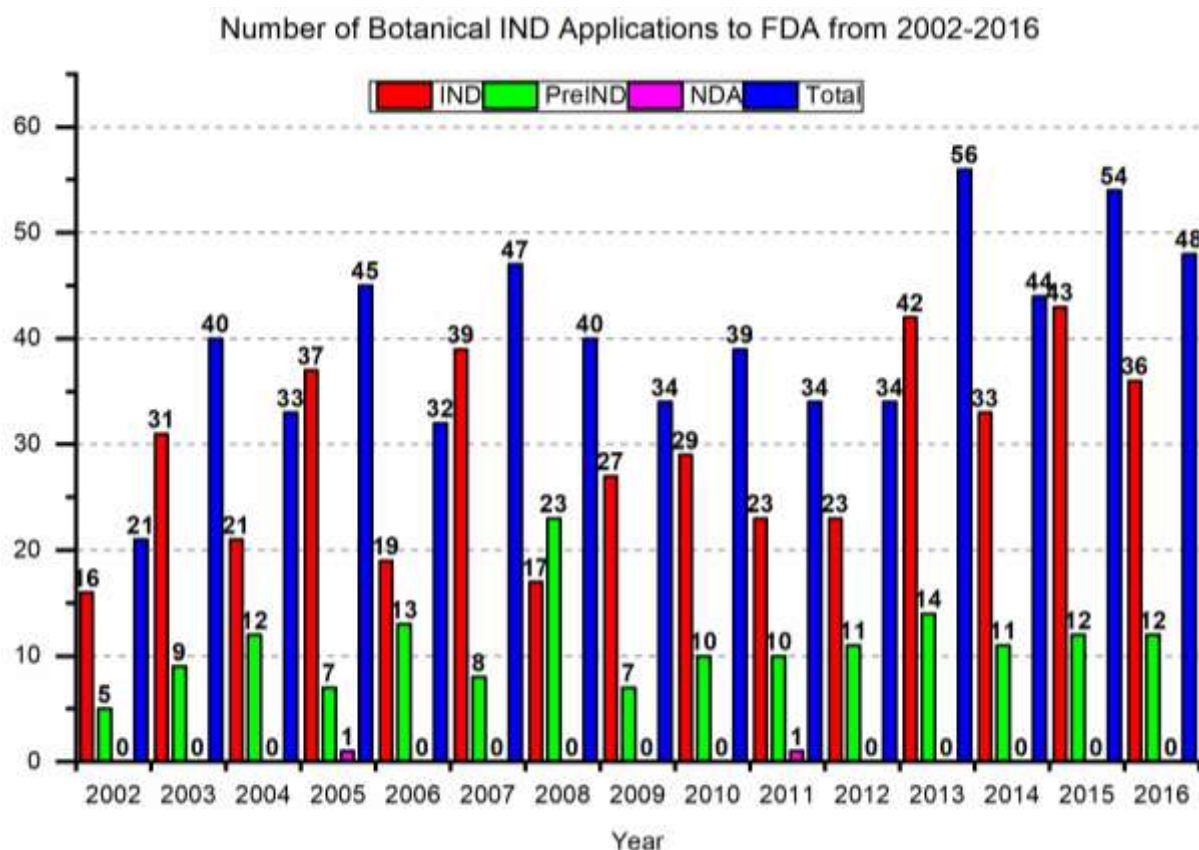


Figure 1. Botanical IND applications submitted to the FDA from 2002 to 2016¹⁸

One approach to develop new pharmaceutical drugs is to study the use of herbal medicines in traditional medicine systems. It stands to reason that focusing on plants with a long record of clinical observation in traditional medicine offers a more reasonable starting point for drug discovery.^{23,24} In general, there is a high correlation between traditional medicine claims for a plant shown to be legitimate and supported in ensuing phytochemical and biological analyses. A 1985 survey of approved drugs derived from plants showed that 80% matched or were related to the reported ethnomedicinal purpose of the source.²⁴ This can also extend to the study of taxonomically similar species which can yield different and potentially more effective drug candidates. Prominent examples of successful drugs derived from a targeted ethnomedical approach include quinine from *Cinchona* for malaria, galegine from *Galega* for diabetes (which

led to the development of metformin), morphine from *Papaver* for pain,^{2,8} and artemisinin from *Artemisia* for malaria. Artemisinin deserves attention in no small part due to the shared Nobel Prize in Medicine awarded to the work of Tu Youyou in 2015. The clinical observations of *A. annua* L. for the treatment of malaria from TCM records was supported by *in vivo* anti-plasmodial activity. However, identification of an active principal was elusive until Tu developed a different chemical extraction method inspired by a TCM text from the 4th century.¹⁶ The identification of artemisinin led to a new class of anti-malarial drugs, discovery of a novel mechanism of action for inhibiting *Plasmodium* parasite, and greatly impacted global health.²⁵ Today, the pursuit of traditional medicine knowledge continues to develop potential drug discovery leads, and also to help standardize, regulate, and organize this important and still relevant cultural resource.

1.1.3 African Traditional Medicine (TM)

Traditional medicine was relied upon as the primary form of healthcare throughout Africa, from ancient Egyptians to tribal healers in South Africa. The common practice of TM might have changed in some areas due to colonization that introduced European medical systems and, in some cases, banned the practice and teaching of TM.²⁶ However, the prevalence of TM among the various indigenous populations remains strong throughout the continent. In post-colonialism Africa, the research of traditional medicine has increased across the continent along with interest in standardization and regulation of medicinal plants to properly incorporate TM into national healthcare systems. The majority of the research output comes from a few countries including Nigeria, Ghana, South Africa, Kenya, and Sierra Leone.²⁷ These countries have demonstrated solid infrastructures to support clinical and pharmaceutical research focused on natural products. These efforts are primarily supported by respective governments that have implemented

initiatives to preserve cultural knowledge and improve health outcomes. Recent measures include documenting TM practices, integrating that knowledge into current healthcare systems, and supporting educational programs focused on TM.²⁸

African TM generally uses a holistic approach to healing both physical and spiritual aspects of a person's health. Spiritual disconnect or possession is sometimes attributed to the onset of illness. Therefore, treatments involve addressing physical health in addition to balancing the patient's spiritual well-being. African traditional doctors commonly utilize objects from nature, such as rocks or animal bones, that possess desirable properties to address physical symptoms and spiritual maladies. Medicinal plants are only part of the treatment process and can have a spiritual cleansing aspect, but seems to be relied upon primarily as prescribed herbal medicine.^{29,30} From a pharmacognosy aspect, the physical action of the botanical herbs prescribed for treatment is of more interest rather than the spiritual aspects. Ongoing research to organize and catalogue the African *materia medica* in the hopes of continued analysis and study by phytochemists, pharmacists, and clinicians.^{31,32} This has led to increased clinical data generation and acceptance of many African plants known to have beneficial health effects such as rooibos (*Aspalathus linearis*). Rooibos tea is widely consumed for its potential benefits and activity, including antioxidant and chemopreventive properties. There has also been drug development success from African botanicals, most notably anticancer alkaloids vincristine and vinblastine. These compounds were isolated from Madagascan periwinkle (*Catharanthus roseus*), a well-known medicinal plant that has been reported to be used in the TM systems of many countries outside of Africa, including China, India, and the Caribbean. Hot water extracts of the plant are commonly cited to be used to treat a variety of ailments, including diabetes and cancer.^{33,34}

The majority of the biodiversity from nature remains unexplored for scientific purposes.³⁵ Concurrently, the prevalence of traditional medicine use throughout Africa combined with the increased interest in exploring its merits provides a unique research opportunity. A pharmacognosy approach to the analysis of African ethnobotanicals can expand the knowledge of medicinal plants to improve their safety and efficacy of use. Africa contains over 45,000 plant species, mostly concentrated in the West African coast and the Southern tip.³⁶ Over 5,000 of those species are reported to be used in TM, but less than 10% have been pursued and developed for commercial consumption, such as *Aloe vera*.³⁷ These medicinal plant species represent a reservoir of chemical diversity and potential therapeutic value.^{38,39} There has been an increased effort into documenting and cataloging the plants used in African TM,⁴⁰⁻⁴² with the vast majority of published research on African ethnobotanicals generated since the turn of the century.³⁷ However, it is imperative to move beyond the basic screening of crude extracts and focus more on the clinical development of identified active phytochemicals as potential drug leads. Taking advantage of this opportunity is even more important with African environmental biodiversity under threat.^{43,44}

Analysis of West African ethnobotanicals show a diversity of phytochemical classes and biodiversity as seen in the rest of Africa.⁴⁵⁻⁴⁷ In Burkill's seminal work "The Useful Flora of West Africa"⁴⁸ several species of the *Icacina* genus were recorded, including their reported traditional medicine uses. Currently, there are five officially recognized species of *Icacina*, according to The Plant List Database.⁴⁹ However, there has been little published research on this genus. In a 2014 analysis of published scientific literature covering the flora of West Africa, the Icacinaceae family was not among the top 15 plant families from which isolated natural products have been reported.⁴⁵ This indicates an opportunity to study *Icacina* further.

1.2 Literature Review

1.2.1 Taxonomy of *Icacina* genus

The genus of *Icacina* was first created by Adrien Henri Laurent de Jussieu in 1823 with the report of species *Icacina senegalensis*,⁵⁰ which is now a synonym. *I. senegalensis* was properly reassigned as *Icacina oliviformis* in 1975.⁵¹ Ten additional species have been reported since, though only five are officially recognized according to “The Plant List”⁴⁹: *I. oliviformis* (Poir.) J. Raynal, *I. claessensii* (De Wild.), *I. guessfeldtii* (Asch.), *I. mannii* (Oliv.), and *I. trichantha* (Oliv.). Other species include *I. dubia* (Macfad.), *I. grandifolia* (Miers), *I. macrocarpa* (Oliv.), *I. mauritiana* (Miers), and *I. poeppigiana* (Baill.) Valetton.⁵² The genus is grouped with angiosperm dicots and falls under the following classification:

Class - Equisetopsida (C. Agardh);

Subclass - Magnoliidae (Novák ex Takht.);

Superorder - Asteranae (Takht.);

Order - Icacinales (Tiegh. ex Tiegh.);

Family – Icacinaceae (Miers);

Genus - *Icacina* (A. Juss.).⁵²

The Icacinaceae family is a diverse plant family that is geographically associated with tropical regions in South America and Africa.⁵³ As an angiosperm, the family was grouped in the euasterids II order.⁵⁴ The family was later moved to euasterids I based on the phylogenetic analysis and DNA sequencing of Icacinaceae members.⁵⁵ Though some other genera were reassigned to other family within euasterids II.⁵⁶

The genus *Icacina* is described morphologically as follows: “Calyx 5-toothed or -partite. Petals 5, valvate, usually hirsute or pubescent externally and bearded within (glabrous in *I. macrocarpa*). Stamens 5, alternate with the petals, free, often inserted beneath a small hypogynous disk. Anthers ovoid or oblong, dorsally affixed. Ovary 1-celled, usually narrowed into the style and more or less pilose or hirsute; stigma minute or slightly peltate-dilated; ovules 2 pendulous. Fruit indehiscent, 1-celled, 1-seeded; pericarp crustaceous or outer layer fleshy with a thin woody or bony putamen. Seed pendulous; embryo shorter than the fleshy uniform albumen, with thin foliaceous cotyledons and a short radicle. — Shrubs sometimes scrambling or scandent. Leaves alternate, entire, penniveined. Flowers in axillary or terminal panicles or glomerate in short simple or branched axillary spikes or racemes.”⁵⁷

1.2.2 Morphological description of *Icacina trichantha*

I. trichantha was first reported by Dr. Daniel Oliver collected from “Upper Guinea” which encompasses the western coastal region of Africa from Senegal to the equator. Today, *I. trichantha* is considered endemic to Nigeria. Collections were made Mr. Charles Barter in 1857-1859. It belongs to the order Icacinales,⁵⁸ Icacinaceae family. The species was reported in *Flora of Tropic Africa Vol. I* 1868 as follows:

“Scandent. Extremities terete, rusty- or cinnamon-tomentose-pubescent. Leaves ample, membranous, oblong-elliptical or broadly elliptical, cuspidate or shortly acuminate, rounded, sometimes broadly, pressed-hispid beneath, 6 – 9 in. long, 2 – 5 in. broad; petiole 1 – 3 lines or leaves sessile. Flowers densely and rather softly silky-hirsute, crowded in very short simple or slightly branched racemes or spikes; pedicels very equalling (sic) the petals. Petals barbate within. Anthers ovate-oblong. Ovary hirsute, narrowed into the style. Fruit an ellipsoidal drupe, with a thin strongly 2-keeled and slightly reticulate. Seed solitary; embryo often oblique or

transverse, shorter than the albumen, with thin foliaceous cotyledons. Testa thinly membranous.”⁵⁷ An image of the leaves and stems of *I. trichantha* is shown in Figure 2 and Figure 3.



Figure 2. Aerial parts of *I. trichantha* in Nigeria.



© copyright of the Board of Trustees of the Royal Botanic Gardens, Kew.

Figure 3. Herbarium specimen of *I. trichantha* leaves, stem, and fruits collected by C. Barter in Nigeria in 1858.⁵⁹

1.2.3 Ethnomedicinal use of *Ipomoea* species

The *Ipomoea* genus contains several different species, though *I. pes-caprae* is arguably the most well-known. It is found throughout western Africa, including Nigeria, Ghana, Senegal, and Guinea, and shares many traits with the other species. The scandent shrubs are found in both forested and cleared areas and can be considered a weed by locals. A common morphological trait is the large root tubers. Due to its pervasive distribution, the tubers are commonly used as food sources during famines after careful treatment. The different species also have a variety of medicinal uses, particularly the emetic effect of the tubers after consumption. A summary of the reported ethnobotanical uses of the *Ipomoea* genus is listed in TABLE I. This list of reported uses was compiled from peer-reviewed literature and encyclopedia collections covering West African medicinal plants. However, nearly every source only reports the purported ethnomedicinal use and does not comment on the effectiveness. Also, these reports often come from the local population including traditional healers, herbalists, and the general population. However, in some cases, the source of information is unclear or not given. Only the literature reported uses for *I. trichantha* will be discussed further.

Ipomoea trichantha is common in the southern areas of Nigeria and is found in the jungles and forested areas. A map of the distribution for this species is shown in Figure 4. The root is large and similar in appearance to a yam. The root is reported to be consumed after cooking during famine periods. Common names include “urumbia,” “eriagbo,” (induces vomiting when eaten, in Ibo language) and “gbegbe” (to carry away in the Yoruba language). The primary ethnomedicinal use of the root is for purgative effects by inducing emesis. This activity is induced by consuming alcoholic extracts of the tuber. Ailments treated include poisoning, constipation, and malaria. There are also reports of the plant being used on soft tumors. Reports

indicate rural households commonly keep alcoholic tinctures of the roots on hand for self-treatment.⁴⁸

In 2010 a report on the biodiversity of flora found in the Niger Delta region and a survey of ethnobotanical uses by R. Ubom⁶⁰, *I. trichantha* was one of only two reported species from Icacinaceae in an eight year survey period from 2002 to 2010. The findings were consistent with previous ethnomedicinal information: The species is not cultivated for agriculture but found in forested areas. Only the tuber is used for medicinal purposes as a decoction or lotion. Ubom only reports treatment for mumps but lists *I. trichantha* as one of the most widely known and used medicinal plants in the region.

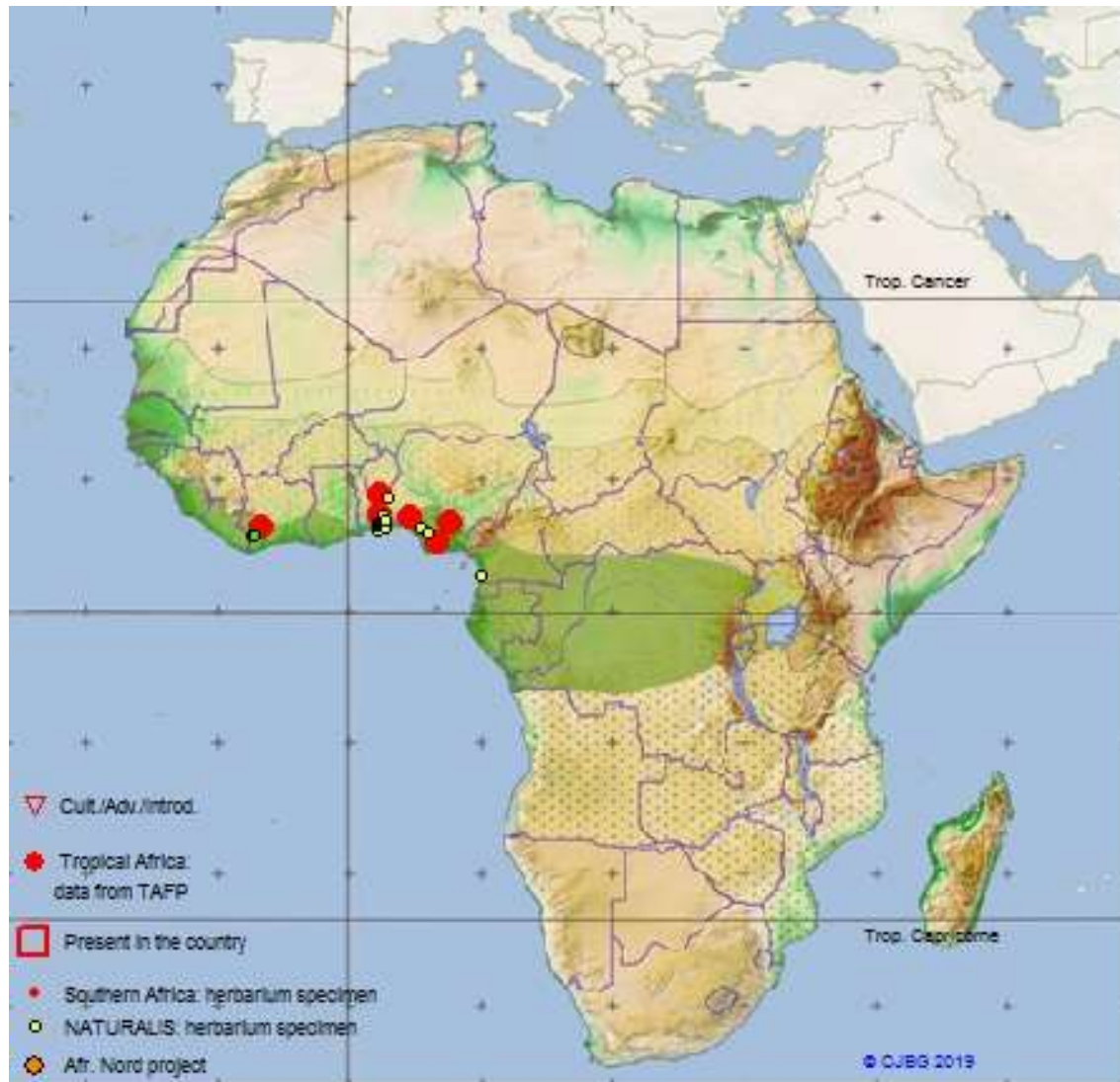


Figure 4. Geographic distribution of *I. trichantha*.⁶¹

TABLE I. ETHNOBOTANICAL USES FOR *ICACINA* GENUS

Reported Use	Species	Plant Part	Source
<i>Cytotoxicity</i>			
Soft tumors	<i>I. trichantha</i>	Unknown	62
Fibrous tumors	<i>I. mannii</i>	Root	63
<i>Analgesic</i>			
Sickle cell disorder	<i>I. trichantha</i>	Leaf	64
Costochondritis	<i>I. mannii</i>	Leaf sap	62
Headache	<i>I. oliviformis</i>	Root	62
Analgesic	<i>I. oliviformis</i>	Leaf	62
Back Pain	<i>I. oliviformis</i>	Leaf	65
Snake bite	<i>I. oliviformis</i>	Leaf	65
<i>Antiseptic</i>			
Eye infections	<i>I. oliviformis</i>	Leaf sap	62
Chest infection, cough	<i>I. oliviformis</i>	Leafy twig	62
	<i>I. trichantha</i>	Leaves	66
Bronchial infections, coughs	<i>I. mannii</i>	Leaves	67
	<i>I. oliviformis</i>	Root, Leaf	68
<i>Digestive</i>			
Dysentery, gastrointestinal disorders	<i>I. mannii</i>	Root	67
Swollen stomach	<i>I. oliviformis</i>	Root	65
Constipation	<i>I. trichantha</i>	Root	62
<i>Anti-inflammatory</i>			
Fever	<i>I. oliviformis</i>	Leafy twig	62
Wounds	<i>I. mannii</i>	Leaf sap	67
Oral infection	<i>I. oliviformis</i>	Root	68
Dermatitis	<i>I. oliviformis</i>	Root	62

TABLE I. ETHNOBOTANICAL USES FOR *ICACINA* GENUS

Reported Use	Species	Plant Part	Source
<i>Sexual Health</i>			
Aphrodisiac, male impotency	<i>I. trichantha</i>	unknown	29,62
Uterine pain	<i>I. trichantha</i>	unknown	69
Female sterility	<i>I. mannii</i>	unknown	62
Impotence	<i>I. oliviformis</i>	Root	62
<i>Other</i>			
Heart issues	<i>I. trichantha</i>	Leaf	70
Edema	<i>I. mannii</i>	unknown	62
Pediatric rickets	<i>I. oliviformis</i>	Root	71
General weakness	<i>I. oliviformis</i>	Root	71
General panacea	<i>I. oliviformis</i>	Leaf	62
Internal hemorrhage	<i>I. oliviformis</i>	Leafy twig	62
Kidney Issues	<i>I. oliviformis</i>	Root	62
Anti-convulsant	<i>I. claussensii</i>	Root	72
	<i>I. guessfeldtii</i>		
Tooth decay	<i>I. oliviformis</i>	Root	62
Mumps	<i>I. trichantha</i>	Root	60

An ethnobotanical survey of Akwa Ibom State in southern coastal Nigeria from 2000 – 2002 found that the indigenous population used the leaves and seeds of *I. trichantha* for treatment of hypertension and asthma.⁷³ According to the authors, the plant is “crushed and macerated in local gin” for internal use daily for up to five days. Another survey also in Akwa Ibom State focused on plants used for pediatric ailments, but the time period was not reported. Local herbalists and health care workers were interviewed regarding treatments for children from 1 week to 5 years old. The only reported entry of *Icacina* species was *I. trichantha* for treatment of measles. The whole plant or just the leaves are macerated, suspended in water for an unknown amount of time, and then filtered. Alternatively, the tubers would be cut into pieces, boiled in water, and filtered. There were several different methods of administration reported and it was unclear how they were differently applied. Extracts could be administered as an enema (150 mL), orally consumed as a tea twice a day for 2 weeks (50 mL), or mixed with clay and applied as an ointment.⁷⁴

Another survey of traditional medicinal use was conducted in southern Oyo state from 2008 to 2012 focusing on the treatment of circulatory and nervous system ailments.⁷⁰ The survey reports that leaves of *I. trichantha* are boiled and then squeezed into cold water for treatment of “heart problems”. This concoction is consumed daily. A 2016 survey of traditional healers and herb traders across Southern Nigeria collected reported plant species used to treat pain associated with Sickle cell disorder. The leaves of *Icacina trichantha* and the roots of *Rhaphiostylis beninensis* (Hook. f. ex Planch.) also in the Icacinaceae family were recorded.⁶⁴

In summary, the reported ethnomedicinal uses for *Icacina trichantha* and the *Icacina* genus in general, as listed in Table 1, is diverse. Drawing upon the history of medicinal plants and phytochemistry research, it is highly unlikely the species produces natural products that are

effective for every disease it is reported to be used for. As previously discussed, plants possess chemically diverse secondary metabolites that have been developed into effective drugs. For medicinal plants used in traditional medicine, there is a high correlation between reported use and confirmed biological activity.^{23,24} Therefore, we should expect a phytochemical analysis of *Icacina trichantha* to yield compounds that are active in at least one related traditional use.

1.2.4 Summary of scientific investigations

The *Icacina* genus has been known for some time, especially its ethnobotanical profile. However, most scientific studies and analyses of these claims were published since the year 2000. Curiously, the first species studied were the lesser known *I. claessensii*, *I. guessfeldtii*, and *I. mannii*. These reports focused on phytochemical analysis and resulted in the only reported alkaloids from the species in addition to the first of many pimarane diterpenes. No further work on these species could be found in the literature. Research focus then shifted to the two more prominent species, *I. trichantha* and *I. oliviformis*. The first pharmacological profile of *I. trichantha* focused on verifying the ethnomedicinal claims was conducted by Asuzu and colleagues⁷⁵ in 1990. Subsequent investigations began to explore other bioactivities related to reported ethnomedicinal uses, including anti-inflammatory, antimalarial, and antimicrobial activity both *in vitro* and *in vivo*. Then in 2014, Onakpa and colleagues at the University of Illinois at Chicago conducted the first phytochemical analysis of an *Icacina* species after nearly 25 years. This began a series of studies that not only isolated novel compounds in the pimarane class but also examined other biological activities, mainly cytotoxicity.

1.2.5 Chemical constituents

The first phytochemical analysis of *I. trichantha* was carried out by Onakpa and coworkers at the University of Illinois at Chicago in 2014.⁷⁶ Since that time, a total of 19

compounds have been reported, novel and previously reported from other plant species. All the compounds are diterpenoids in the pimarane subclass. Most possess a bicyclic ether ring and lactone moiety (TABLE II, Figure 5). All compounds with a number label will be discussed further in Chapters 2 and 3. The remaining compounds are included for reference.

TABLE II. SUMMARY OF COMPOUNDS REPORTED FROM *I. TRICHANTHA*

Name	Type	Source
Icacinol (1)	(9 β -H)-pimarane	76
Humirianthol (2)	(9 β -H)-pimarane	76
14 α -Methoxyhumirianthol (3)	(9 β -H)-pimarane	77
Icacinlactone I (4)	(9 β -H)-pimarane	77
Icacinlactone E (8)	17-nor-(9 β -H)-pimarane	78
7 β -Hydroxyicacinlactone B (10)	17-nor-pimarane	77
Icacinlactone D (15)	17-nor-pimarane	78
2 β -Hydroxyicacinlactone B (Icacinlactone H, 16)	17-nor-pimarane	79
Icacinlactone A	17-nor-pimarane	78
12-Hydroxyicacinlactone A	17-nor-pimarane	77
Icacinlactone B	17-nor-pimarane	78
Icacinlactone C	17-nor-pimarane	78
Icacinlactone F	17-nor-(9 β -H)-pimarane	78
Icacinlactone G	17-nor-(9 β -H)-pimarane	78
Icacinlactone J	17-nor-(9 β -H)-pimarane	77
Humirianthenolide C	17-nor-(9 β -H)-pimarane	76
Icacintrichantholide	rearranged 17-nor-pimarane	79
17-Hydroxyicacinol	(9 β -H)-pimarane	76
Icacenone	17-nor-(9 β -H)-pimarane	76

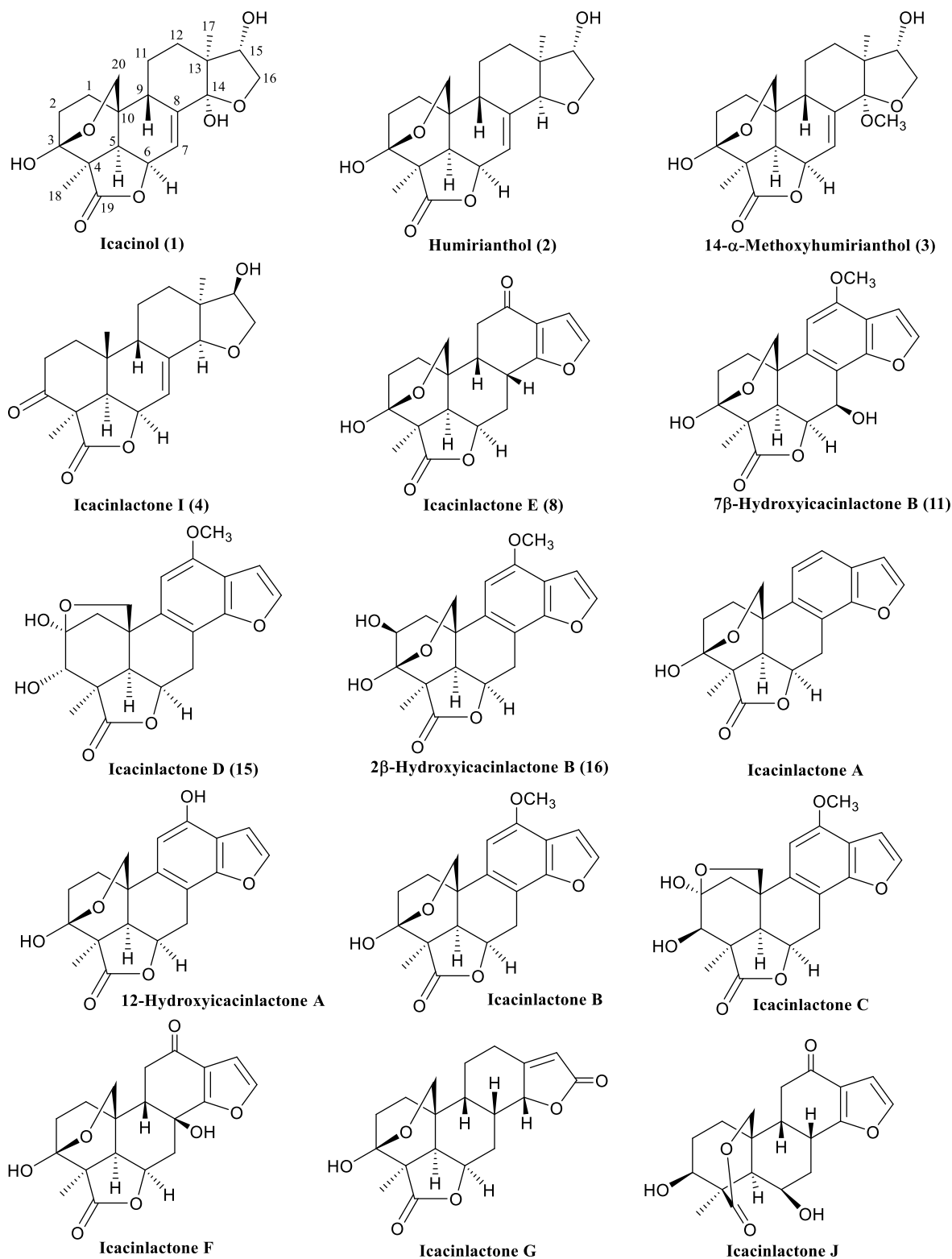


Figure 5. Structures of Compounds Reported from *Icacina trichantha*

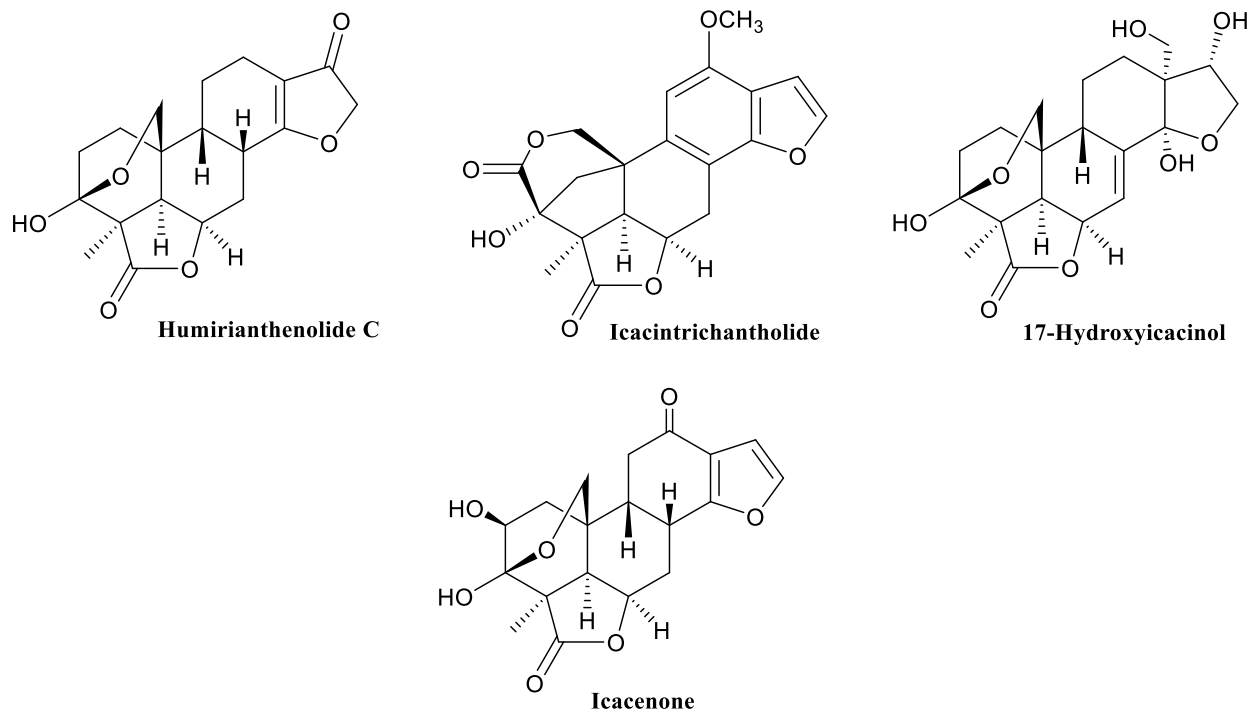


Figure 5. Structures of Compounds Reported from *Icacina trichantha*

Brief phytochemical analyses were also carried out on *I. guessfeldtii*, *I. mannii*, and *I. claessensii*. In fact, based on literature searches, the first phytochemical analysis of the *Icacina* genus was carried out by Penge On'Okoko and coworkers.⁸⁰ They reported the novel alkaloid diterpene icacine and its acetyl-derivative (Figure 6) from *I. guessfeldtii*, without specifying from which part of the plant the compounds were isolated. Icacine possesses many shared traits with the diterpenoids that were subsequently isolated from *I. trichantha*: a bicyclic A-ring with 3,20-ether bridge, γ -lactone moiety, and furan ring. The x-ray crystallography data also verifies similar absolute configurations of chiral centers corresponding to those determined in *I. trichantha* in TABLE II. The original reports for icacine or acetyl-icacine did not include biological activity data and no later published data could be found in the literature.

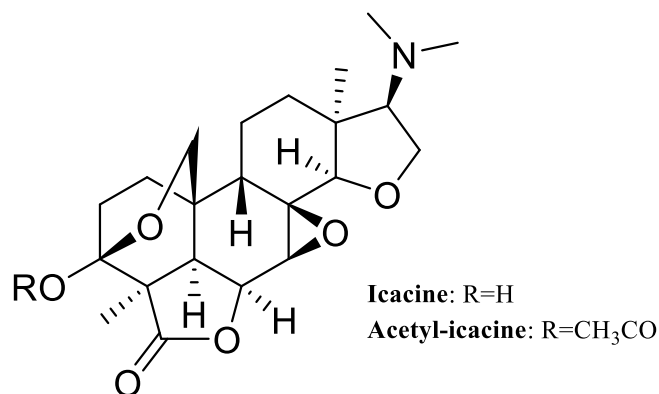


Figure 6. Icachine and its acetyl-derivative from *I. guessfeldtii*

Follow up of *I. guessfeldtii* by On'Okoko and Vanhaelen⁸¹ identified two additional alkaloid diterpenoids: icachine and de-N-methylicachine (Figure 7). The absolute configuration of these two alkaloids was not determined. Analysis and comparison of the alkaloid content of *I. guessfeldtii* showed that icachine is the main constituent (0.25% for icachine and 0.056% for de-N-methylicachine of dried material) and the leaves contain more total alkaloids (0.218%) compared with the roots (0.091%). Icachine, icachine, and de-N-methylicachine are unique as the only nitrogen-possessing metabolites from this genus reported thus far. However, the nitrogen atom exists as an amine or amide group at the C-15 position and not incorporated into the carbon skeleton, which is still very similar to other isolated compounds. Many of the other pimaranes from *Icacina* are oxygenated at C-15 as well, suggesting these uncommon alkaloids should be considered part of the diterpenoids and not a unique subclass of alkaloids.

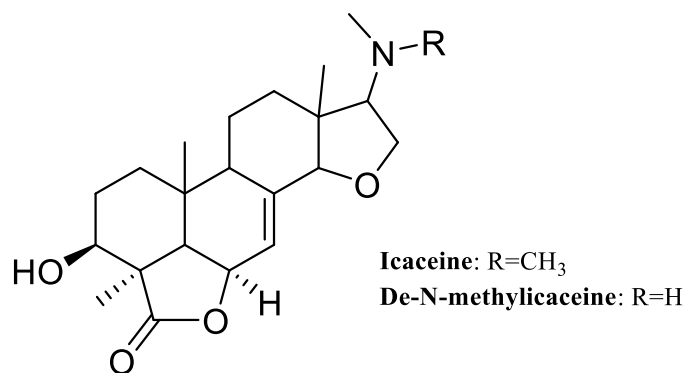


Figure 7. Icaceine and de-N-methylicaceine from *I. guessfeldtii*

The chemical study of *I. claessensii* also isolated icacine, icaceine, and de-N-methylicaceine and resulted in the first report of icacinol (**1**).⁷² Work on *I. mannii* isolated icacenone, the first report for that compound.⁶³ These two species and their respective phytochemicals have not been analyzed further by the original authors or other researchers. Work on *Icacina* then moved to *I. oliviformis*. Initial work isolated glucosides sitosterol 3-O- β -D-glucopyranoside and stigmasterol 3-O- β -D-glucopyranoside in addition to icacinol (**1**) and icacenone (Figure 8).⁸²

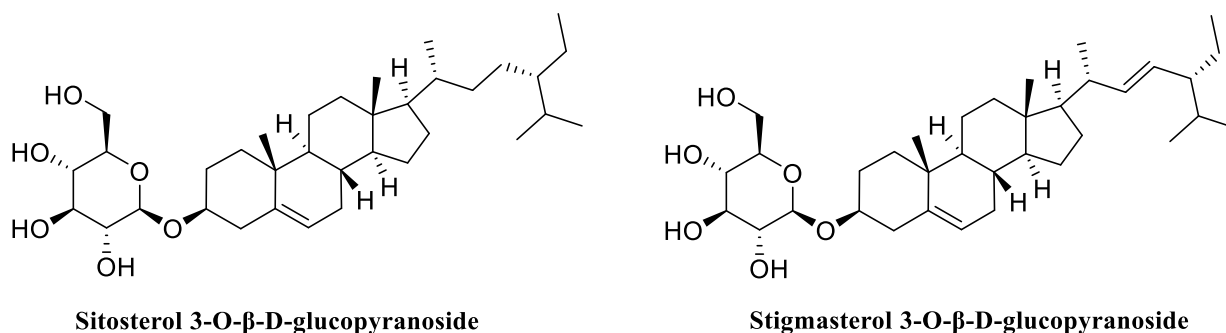
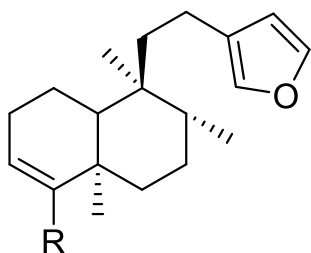


Figure 8. Glucosides isolated from *I. oliviformis*

Further studies on nonpolar fractions of tuber from *I. oliviformis* resulted in the isolation of a group of related diterpenes (Figure 9).⁸³ The only novel compound is the linoleate derivative of hardwickiol. The remaining compounds are clerodane diterpenoids.



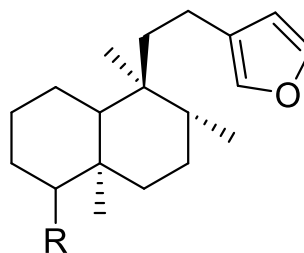
Hardwickiol linoleate: $\text{CH}_2\text{COO-C}_{17}\text{H}_{32}$

Annonene: CH_3

Hardwickiic acid methyl ester: COOCH_3

1-Naphthalenecarboxaldehyde: CHO

Hardwickiol: CH_2OH



1-Naphthalenecarboxylic acid, methyl ester: COOCH_3

1-Naphthalenemethanol: CH_2OH

1-Naphthalenecarboxylic acid: COOH

Figure 9. Diterpenes isolated from *I. oliviformis*

The leaves of *I. oliviformis* were subjected to solvent partitioning and further fractionation by chromatography and HPLC. The ethanol partition yielded two new flavone-C-glycosides and previously reported *trans*(-) clovamide (Figure 10).⁸⁴

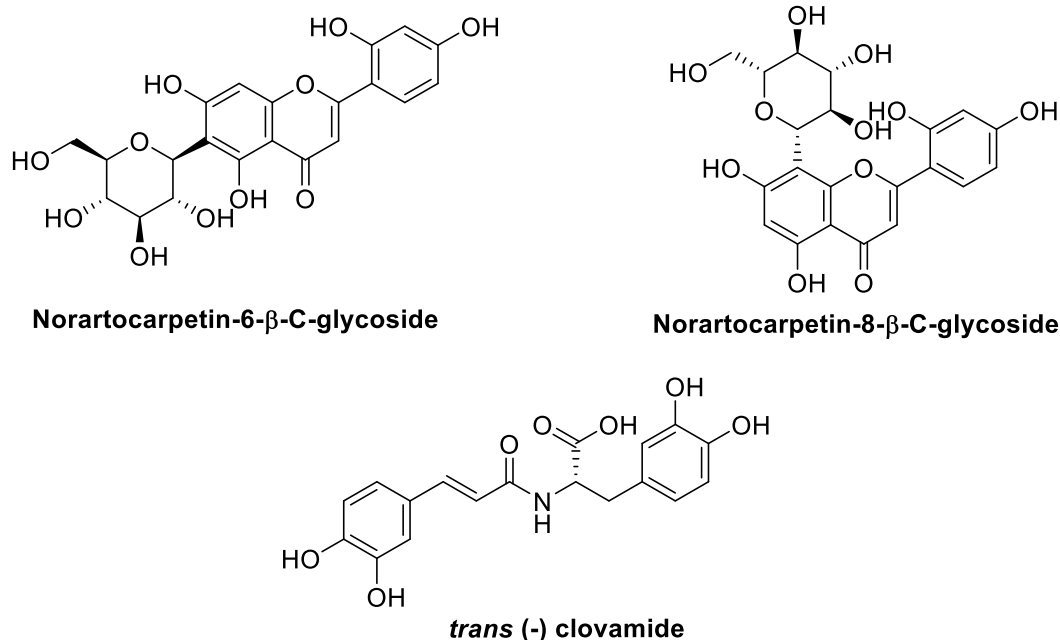


Figure 10. Flavone-C-glycosides and *trans*-(S, E)-(-) clovamide from *I. oliviformis*

More recently, we at the University of Illinois at Chicago conducted phytochemical studies focusing on polar fractions of extract from tuber of *I. oliviformis*. A new pimarane diterpenoid (icacinlactone M) and two glycosides were isolated (Figure 11).⁸⁵ Though both glycosides have glucose as the sugar, the aglycone for one is the previously reported 2β-hydroxyicacinlactone B/ icacinlactone H (**16**) and the aglycone for the other is a novel diterpenoid structure (icacinlactone N) with a γ-lactone group between C-4 and C-10 instead of C-4 and C-6 as observed in most other *Ikacina* pimaranes. In addition to previously reported compounds 14α-methoxyhumirianthol (**3**), icacinol (**1**), icacinlactone A, 12-hydroxyicacinlactone A, icacinlactone B, 2β-hydroxyicacinlactone B/ icacinlactone H (**16**), the known compound annonalide was reported for the first time from *Ikacina*.

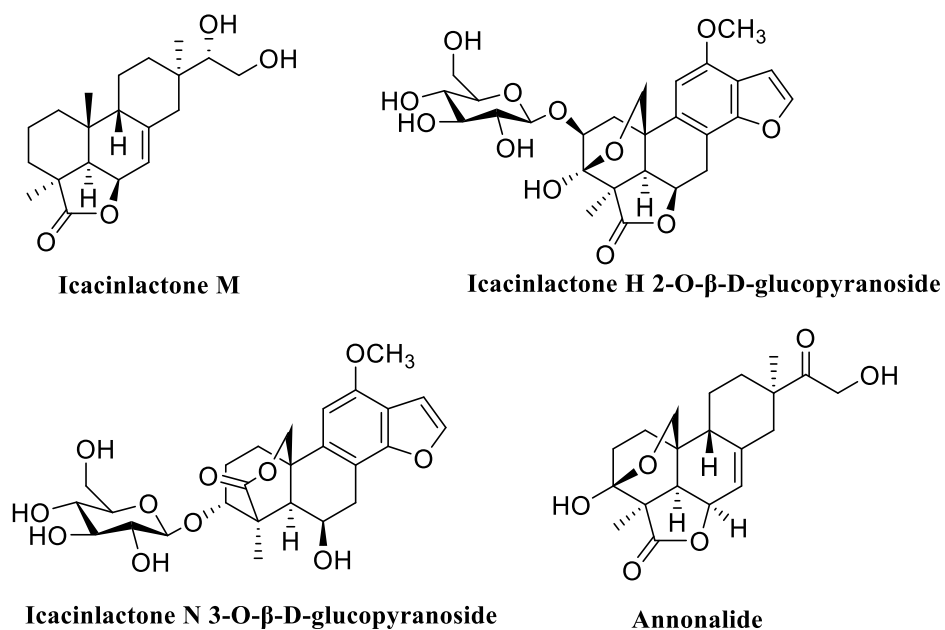
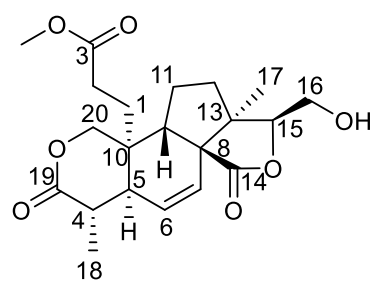


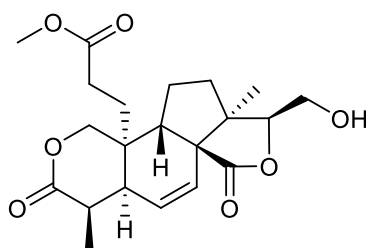
Figure 11. Pimaranes and pimarane glycosides isolated from *I. oliviformis*

Finally, a reexamination of *I. oliviformis* tuber was conducted and resulted in the isolation of seven new diterpenoids (Figure 12). Three of the compounds are structural analogues of humirianthol (**2**). However, four of these compounds, oliviformislactone A, oliviformislactone B, secopimaranolactone A, and secoleisthanthanolactone A are the first reported examples of 3,4-*seco*-pimaranes and 3,4-*seco*-cleistanthane from *Icacina*.⁸⁶

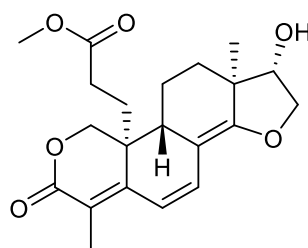
In a slightly different approach, leaves of *I. trichantha* extracted with n-hexane and ethyl acetate have been analyzed by GC-MS to identify chemical constituents. Various fatty acids were reported, which are summarized in TABLE III.⁸⁷



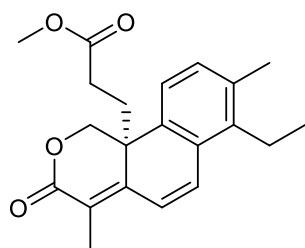
Oliviformislactone A



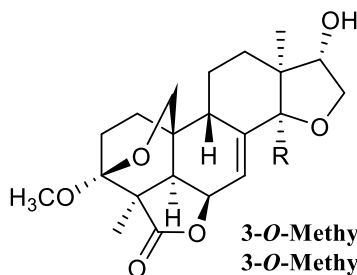
Oliviformislactone B



Secopimaranolactone A



Secoleisthanthanlactone A



3-*O*-Methylhumirianthol: H
 3-*O*-Methyl-14-hydroxyhumirianthol: OH
 3-*O*-Methyl-14-methoxyhumirianthol: OCH₃

Figure 12. Further diterpenoids isolated from *I. oliviformis*

TABLE III. GC-MS ANALYSIS OF *I. TRICHANTHA* LEAF EXTRACT⁸⁷

Compound	Yield (%)	Extract
Oleic acid	36.04	<i>I. trichantha</i> leaf EtOAc
9,12-octadecadienyl chloride	32.48	<i>I. trichantha</i> leaf EtOAc
Stearolic acid	30.74	<i>I. trichantha</i> leaf n-hexane
Palmitic acid	27.74	<i>I. trichantha</i> leaf n-hexane
	11.33	<i>I. trichantha</i> leaf EtOAc
Stearic acid	11.31	<i>I. trichantha</i> leaf n-hexane
	5.08	<i>I. trichantha</i> leaf EtOAc
Lauric acid ethyl ester	6.57	<i>I. trichantha</i> leaf EtOAc
9,12-octadecadienoic acid	6.08	<i>I. trichantha</i> leaf n-hexane
3,3-dimethyl-2-hexanone	4.22	<i>I. trichantha</i> leaf n-hexane
9,17-octadecadienal	3.56	<i>I. trichantha</i> leaf n-hexane
Undecane	3.22	<i>I. trichantha</i> leaf n-hexane
Palmitic acid ethyl ester	3.14	<i>I. trichantha</i> leaf EtOAc
9,12-decadienoic acid methyl ester	3.08	<i>I. trichantha</i> leaf EtOAc
Eicosanoic acid	1.39	<i>I. trichantha</i> leaf n-hexane
1,2-ethanediol monoacetate	0.85	<i>I. trichantha</i> leaf EtOAc
5-octadecenoic acid methyl ester	0.68	<i>I. trichantha</i> leaf n-hexane
4-tetradecene	0.56	<i>I. trichantha</i> leaf EtOAc
1-tetradecane	0.45	<i>I. trichantha</i> leaf EtOAc
1,2,3-propanetriol monoacetate	0.42	<i>I. trichantha</i> leaf EtOAc

1.2.6 Biological activities of *Icacina* genus

1.2.6.1 In vitro activity

1.2.6.1.1 Cytotoxic activity

In a cytotoxicity screen of an aqueous ethanolic extract of leaves of *I. trichantha*, the n-hexane, chloroform, and EtOAc fractions were tested against *Artemia salina* in a brine shrimp lethality assay. The results showed the detannified aqueous fraction and the crude extract were most active with reported LC₅₀ values of 66.08 and 185.68 µg/mL, respectively, after a 24-hour treatment period. Only the detannified aqueous fraction was chosen for testing against estrogen receptor-positive human breast cancer cell line MCF-7. Cells were treated for 48 hours at a concentration five-fold lower than the recorded LC₅₀ value. Gene expression analysis showed an upregulation of retinoblastoma tumor suppressor gene (RB1) that the authors reported was statistically significant ($P<0.05$) though the expression levels were not given.⁸⁸

Several isolated compounds have been screened against human cancer cell lines. A summary of IC₅₀ values is given in TABLE IV. Screened cell lines include human melanoma (MDA-MB-435), human colorectal (HT-29), human breast (MDA-MB-231), and human ovarian (OVCAR3). Humirianthenolide C was consistently the most active against all cell lines followed by icacinol (**1**), humirianthol (**2**), and icacenone. Vinblastine was used as a positive control in three of the cell lines.^{76,78} These four compounds are structurally similar pimaranes with a characteristic H-9 in β -orientation. In contrast, other pimaranes from *I. trichantha* that lack H-9 due to conjugation of the C-ring were screened against the same cancer cells and showed little to no activity.^{77,78,89} These results led to the hypothesis that the presence of 9 β H plays a role in anticancer activity.

TABLE IV. SUMMARY OF CYTOTOXIC ACTIVITY FOR SELECT COMPOUNDS FROM *I. TRICHANTHA*^{76,78}

Compounds	IC ₅₀ (μM)			
	MDA-MB-435	MDA-MD-231	OVCAR3	HT-29
Humirianthenolide C	0.66	0.67	1.05	3.00
Icacinol (1)	1.25	7.30	7.55	4.23
Humirianthol (2)	1.65	3.74	4.12	4.94
Icacenone	6.44	10.85	18.71	13.25
Icacinlactone F	6.16	8.94	10.50	
Vinblastine	0.49 nM	8.78 nM	1.82 nM	

1.2.6.1.2 Cytotoxicity and Genotoxicity

An *Allium cepa* bioassay model was used to assess the cytotoxic and genotoxic activity of an aqueous extract of *I. trichantha* leaves. Onion bulbs were suspended in solution of the extracted material at different concentrations from 0 – 100%. A dose-dependent reduction in root growth was observed, but a statistically significant change occurred at the 25% concentration level. Effects on cell division and chromosomal changes were also recorded for root tip cells. The authors noted a decrease in the number of dividing cells and an increase in chromosomal aberrations in a dose-dependent manner.⁹⁰

1.2.6.1.3 Antioxidant activity

Free radical scavenging and reducing power of leaves from *I. trichantha* was studied by Sofidiya and colleagues.⁹¹ The group used a methanolic extract to assess antioxidant activity by measuring inhibition of DPPH and correlating with total phenolic content. The authors concluded mild activity, $30.9 \pm 0.004\%$ DPPH inhibition at 0.025 mg/mL extract concentration, and moderate phenolic content (5 mg/g of gallic acid equivalent) when compared with other Nigerian medicinal plants.

Otun and coworkers also measured the antioxidant activity of *I. trichantha* leaves using the DPPH assay. The n-hexane extract was most active with an IC₅₀ value of 0.210 µg/mL. The EtOAc and ethanol extracts reported IC₅₀ values were 3.917 and 4.812 µg/mL, respectively. A positive control was not reported.⁸⁷

The tubers of *I. trichantha* were analyzed for antioxidant activity by Onakpa and colleagues. An 80% aqueous methanolic extract was screened in the DPPH assay as well as the FRAP assay. At 400 µg/mL, the plant extract displayed 67.3% antioxidant activity in the DPPH assay compared with the ascorbic acid control value of 80.3%. Similar antioxidant activity was observed in the FRAP assay in a dose-dependent manner, with the highest tested concentration (800 µg/mL) FRAP value at 6.7 µM. The previously reported FRAP value of ascorbic acid was 2.0 µM at 1000 µg/mL concentration.⁹²

Another study of *I. trichantha* antioxidant activity carried out by Alawode and coworkers compared extracts from both leaves and tuber plant material extracted successively with hexane, EtOAc, and methanol. In the DPPH assay, the methanolic extracts from the tuber and leaves had the strongest IC₅₀ values (0.343 and 0.332 mg/mL respectively) compared with the ascorbic acid positive control (0.017 mg/mL). The methanolic tuber extract also had the highest antioxidant activity in the FRAP assay (76.784 mg ascorbic acid equivalence / g of sample) compared with all other extracts.⁹³

1.2.6.1.4 Anti-inflammatory activity

The same *I. trichantha* extracts from Alawode and coworkers were tested for anti-inflammatory activity using red blood cells. Erythrocyte membrane stability was measured after 30 minutes of treatment with each extract and reported as mean percentage. Both the EtOAc and

methanol extracts from the leaves performed best compared with the indomethacin positive control.⁹³

1.2.6.1.5 Antimicrobial activity

Timothy and Idu⁹⁴ tested the antimicrobial properties of *I. trichantha* leaf extract. Both methanolic and aqueous extracts were tested against *Staphylococcus aureus*, *Escherichia coli*, *Bacillus subtilis*, and *Pseudomonas aeruginosa*. The methanol fraction was more potent than the water fraction against all strains. The lowest reported minimum inhibitory concentration (MIC) by the methanolic partition was 3.125 mg/mL against *E. coli* and *P. aeruginosa*. In addition, neither fraction displayed fungicidal activity. No controls were reported in these assays. Zone of inhibition was also measured against the four bacterial strains for both extracts at concentrations of 5, 10, 15, and 20 mg/mL. The measured inhibition zones of the methanol extract at 20 mg/mL were most similar to the pefloxacin and gentamycin positive controls. However, the control concentrations were not reported.

These findings were supported by a study from Shagal and Kubmarawa.⁹⁵ The ethanol and water extracts of *I. trichantha* leaves were screened against four bacteria strains and one fungal species. The ethanolic extract was more potent than the aqueous extract against *E. coli* and *S. aureus*. Both water and ethanol extracts performed similarly against *Streptococcus spp.* and *Klebsiella pneumonia*. There was little inhibitory effect against *Candida albicans*. Gentamycin was used as a positive control, but concentrations of treatments were not reported.

Antimicrobial activity was assessed again with n-hexane and EtOAc extracts of *I. trichantha* leaves. Zone of inhibition was measured against *E. coli*, *P. aeruginosa*, and *Klebsiella oxytoca*. The hexane extract resulted in inhibition zones of 22.50, 9.75, and 12.95 mm against *E. coli*, *P. aeruginosa*, and *K. oxytoca*, respectively. The EtOAc extract inhibition zones were

27.00, 10.25, and 10.75 mm, respectively. Extract concentration levels and experimental controls were not reported.⁸⁷

I. oliviformis was screened with many other medicinal herbs from Senegal against *B. subtilis*, *S. aureas*, and *Aspergillus niger*. The ethanol extract of the tuber showed moderate activity at 50 mg/mL against *S. aureas*. The extract was among the most potent of the 33 species tested in the *B. subtilis* screen as well. The authors reported a zone of inhibition of over 15 mm after 24-hour exposure to 5 mg/mL of extract. The zone of inhibition for 10 mg/mL of streptomycin was 35 mm as a positive control.⁹⁶

Further antimicrobial screens were conducted by David-Oku and colleagues with *I. oliviformis* tuber extracted with methanol and water. The authors found that the aqueous extract had stronger overall activity. The reported MBC for the aqueous extract was 5.63 µg/mL against *S. aureus*. The methanol extract performed best against *Shigella dysenteriae* with a MBC of 12.5 µg/mL.⁹⁷

1.2.6.1.6 Anti-plasmodial activity

In the first scientific analysis of *I. oliviformis* as a potential anti-malarial therapeutic, collected leaves were extracted with aqueous methanol, followed by solvent partitioning with pentane, DCM, and water successively. The extract, DCM fraction, and water fraction were screened *in vitro* against the 3D7 strain (chloroquine-sensitive) and 7G8 strain (chloroquine-resistant) of *Plasmodium falciparum*. The DCM fraction was the most active with IC₅₀ values of 0.9 ± 0.2 µg/mL and 4.1 ± 0.1 µg/mL against 3D7 and 7G8, respectively. Chloroquine was used as a control with IC₅₀ values of 44 ± 1.0 nM and 658 ± 14 nM against 3D7 and 7G8, respectively.⁹⁸

1.2.6.2 In vivo Activity

1.2.6.2.1 Emetic Activity

In the first pharmacological analysis of *I. trichantha*, Asuzu and colleagues reported inducement of emesis in mouse models after administering the aqueous extract of *I. trichantha*. This purgative action was also confirmed by observed dose-dependent response of diarrhea from the test animals. The mechanism of purgation was not determined but was suspected to not effect intestinal muscles as the extract did not induce convulsions in isolated guinea pig ileum tissue. The aqueous extract of *I. trichantha* potentiated pentobarbitone sleeping time, suggesting an effect on the central nervous system.⁷⁵

In a later study, methanolic extracts of *I. trichantha* tuber were orally administered to guinea pigs to analyze the emetic activity. The authors found that retching was induced at 400 mg/kg concentration almost immediately. The frequency of retching action increased as the concentration increased as well. The emetic activity could be reversed with administration of hyoscine butylbromide (Buscopan®) and promethazine teoclate (Avomine®), reducing the number of retches per hour to 7.3 and 7.7, respectively, after oral administration of 600 mg/kg extract. The negative control group given just the extract averaged 25.0 retches per hour.⁹⁹

1.2.6.2.2 Molluscicidal Activity

In a screen of Nigerian botanicals to treat schistosomiasis, the methanolic extract of leaves from *I. trichantha* were tested. Snails (*Bulinus globosus*) were exposed to extract prepared to 100 ppm in 200 mL of water for 24 hours. The authors reported a 40% mortality rate, which did not meet their WHO-established activity threshold to warrant further investigation.¹⁰⁰

1.2.6.2.3 Insecticidal Activity

Collected tubers of *I. trichantha* were dried, extracted with water, filtered, and applied directly to worker termites (*Odontotermes obesus*) on petri dishes. Insecticide activity was measured by termite mortality after exposure. At the lowest concentration of 5 mg/L mortality was 76.67% after 70 minutes. The insecticidal activity increased in a dose-dependent manner up to the highest tested concentration of 25 mg/L, with a mortality rate of 100% after 50 minutes. The negative control group survived for 4 days.¹⁰¹

1.2.6.2.4 Antidiabetic Activity

Ezeigbo¹⁰² reported potential antidiabetic activity from the leaves of *I. trichantha*. Type II diabetes-induced mice blood glucose levels were measured shortly after oral treatment with a methanol extract of plant material. The results showed a dose-dependent response in lowering of glucose in the animals. The blood glucose levels were 1.23 ± 0.96 , 4.45 ± 0.96 , and 3.32 ± 1.02 mmol/L 12 hours after treatment with 200, 300, and 450 mg/kg of plant material extract, respectively. The blood glucose levels for the negative control group given only distilled water was 9.23 ± 4.21 mmol/L and the positive control group treated with 2 mg/kg of glibenclamide was 3.00 ± 0.22 mmol/L after the same treatment period.

The antidiabetic effect of *I. trichantha* tuber methanol extract was also tested in alloxan-induced diabetic rats over the course of 21 days. The results again indicated a dose-dependent decrease in blood glucose levels in the test groups throughout the treatment period. Statistically significant ($P < 0.01$) reduction was observed at day 21 after daily treatment level of 400 mg/kg and 600 mg/kg of extract, resulting in glucose levels of 2.70 ± 0.55 and 2.00 ± 0.10 mmol/L, respectively. The negative control group was 16.10 ± 1.42 mmol/L and the positive control group treated with glibenclamide was 2.60 ± 0.34 mmol/L. Compared with the control group,

similar significant reduction was observed in serum triglyceride, HDL, and LDL levels, suggesting an antihyperlipidemic effect. Reduction in liver enzymes AST, ALP, and ALT indicated hepatoprotective traits as well. Histological analysis of pancreatic tissue demonstrated the restoration of islets of Langerhans cells in treatment groups. Comparable to the dose-dependent blood glucose response, increase in plant extract treatment levels resulted in improved restoration of β -cells.¹⁰³

A similar study of antidiabetic activity was conducted with an aqueous extract of *I. oliviformis* tuber. Alloxan-induced rats were treated with 100, 200, or 400 mg/kg of extract for 14 days. The authors noted statistically significant antihyperglycemic, antihyperlipidemic, and renal protective activity in all treatment groups in a dose-dependent manner. After 14 days, the highest treatment group had an average blood glucose level of 108.00 ± 0.86 mg/dL, cholesterol level of 158.50 ± 2.84 mg/dL, and urea level of 3.50 ± 0.22 mmol/L. The same results for the positive control group treated with 10 mg/kg of glibenclamide were 105.00 ± 1.00 mg/dL, 153.17 ± 2.33 mg/dL, and 4.00 ± 0.26 mmol/L, respectively.¹⁰⁴

1.2.6.2.5 Toxicity and Safety

In 2011, the leaves of *I. trichantha* were assessed for hepatotoxicity using Wistar rats treated with methanolic extract from the leaves. Treatment groups were orally administered 100 mg/kg of plant extract for 7 days, after which all subjects were sacrificed for analysis of blood serum and bone marrow tissue. Significant increase in alanine transaminase (ALT) and aspartate transaminase (AST) serum levels were reported for the methanolic extract treatment group at 53.78 and 15.04 units/L, respectively. Treatment groups given an injection of sodium arsenite at the end of the treatment period showed a 3.9x and 1.4x increase in ALT and AST levels, respectively. The authors suggest the hepatotoxic effects of *I. trichantha* methanol extract is

cumulative with arsenic. The study also recorded the formation of mPCEs in bone marrow cells. There was no significant change in the experimental treatment group. However, there was a slight reduction in mPCE levels in the group also injected with sodium arsenite. This result suggests a possible anti-cytogenic activity of the plant extract.¹⁰⁵

A study of an aqueous extract of *I. trichantha* leaves in male and female Wistar rats produced several interesting findings. Experimental treatment groups were observed over 28 days with daily oral treatment of plant extract at 100, 500, or 1000 mg/kg. At the end of the treatment period, various biological markers were measured and compared with the negative control group given 4 mL/kg distilled water daily. First, the authors suggest an LD₅₀ of over 8,000 mg/kg, suggesting a very low risk of acute toxicity. Second, with few exceptions, there were no significant changes in blood markers, liver function, or organ health at all treatment levels. A statistically significant reduction in platelet count at 100 and 500 mg/kg was reversed in the 1,000 mg/kg group. Only ALP levels were affected in all treatment groups while AST, ALT, albumin, and bilirubin levels showed no significant change. Histological examination of heart, lung, spleen, and kidney tissue showed only minor physiological changes at the highest treatment level.¹⁰⁶

1.2.6.2.6 Analgesic Activity

Asuzu and colleagues analyzed rats given a 50% methanolic *I. trichantha* tuber extract to determine toxicity and nervous system effects. The LD₅₀ was determined to be 671 mg/kg, suggesting the extract is relatively non-toxic. The methanolic extract also decreased hind limb grip action, increased muscle relaxation, and reduced convulsions in pentylenetetrazole-induced rats.¹⁰⁷

The chloroform extract of *I. trichantha* was tested *in vivo* in mice. The results suggested the extract possessed a more potent analgesic effect compared with a subsequent 50% methanol partition and a crude 50% methanol extract.¹⁰⁸ The chloroform extract also showed greater effect on central nervous system activity, such as increased pentobarbitone-induced sleeping time, reduced motor coordination, and more protection from leptazole-induced convulsions.

The ethanol extract of *I. oliviformis* tuber was assessed for analgesic activity in albino mice with an acetic acid-induced writhing assay that counted abdominal constrictions and a mouse tail immersion assay measuring time for the mouse to remove its tail from a hot water bath. Randomly assigned experimental groups were treated with 50, 100, and 200 mg/kg of extract via oral administration. Analgesic activity was observed in a dose dependent manner in both assays. The contraction inhibition rate for the 200 mg/kg treatment group was 85% compared with 89% inhibition for positive control group given 150 mg/kg of aspirin. The tail withdrawal time increased from 8.30 sec at time of treatment to 16.10 sec 90 minutes after treatment. The positive control group given 10 mg/kg of morphine displayed tail latency time increase from 7.86 sec to 21.40 sec.¹⁰⁹

1.2.6.2.7 Anti-inflammatory Activity

Asuzu and coworkers¹¹⁰ also explored the potential anti-inflammatory properties of *I. trichantha* tuber. The researchers found that after extraction and partitioning of plant material, the chloroform partition was most active in anti-inflammatory assays compared with the hexane, EtOAc, methanol, and water fractions. The authors reported a dose-dependent response in reducing Croton-oil induced edema in the ears of mice after topical administration of the chloroform fraction with an ID₅₀ value of 107 µg/cm². The ID₅₀ for positive control indomethacin was 93 µg/cm². The chloroform fraction also induced a dose-dependent response

in rats after oral administration in inhibiting carrageenin-induced edema. At 200 mg/kg concentration, global edema was reduced by 34%. The indomethacin positive control at 10 mg/kg had 40% reduction.

David-Oku and colleagues tested the anti-inflammatory activity of an ethanol extract of *I. oliviformis* tuber in mice with egg albumin- and carrageenan-induced edema. The measured edema volume was reduced in a dose-dependent manner for both assays. One hour after inflammation inducement in the egg albumin assay, the measured edema volume was 1.55 mL, 1.36 mL, and 2.29 mL for the 50 mg/kg treatment group, the 150 mg/kg aspirin treatment positive control, and the negative control group respectively. In the carrageenan-inducement assay, the edema volumes were 1.55 mL, 1.38 mL, and 2.24 mL for the same experimental scheme.¹⁰⁹

1.2.6.2.8 Antipyretic Activity

David-Oku and colleagues also tested the antipyretic activity of *I. oliviformis* tuber ethanol extract in mice. In the first experiment, pyrexia was induced with yeast for 24 hours followed by oral administration of the tuber extract. After five hours, the mean internal temperature was reduced from 37.99° C (control group) to 35.98° for the 50 mg/kg treatment group. The positive control group was treated with 150 mg/kg of aspirin and resulted in an average temperature of 35.63°. Similar results were observed with amphetamine-induced fever mice. The mean internal temperatures for the 50 mg/kg treatment group and the aspirin control group were 35.58° and 35.46°, respectively. The negative control group average internal temperature was 37.00°.¹⁰⁹

1.2.6.2.9 Antioxidant Activity

Onakpa and colleagues studied the antioxidant activity of methanolic extract of *I. trichantha* tuber in Wistar rats over 90 days. Superoxide dismutase (SOD) and malondialdehyde (MDA) blood levels were measured at 30-day intervals over 90 days for groups treated with 250, 500, and 1000 mg/kg of extract in the animal feed. By day 60, significant changes were observed for both markers in the 500 and 1000 mg/kg treatment groups compared with the negative control group. At the end of the study, the average SOD activity was 50.6 ± 4 IU/L and the MDA level was 4.8 ± 2 nM/dL for the highest concentration treatment group. The negative control group results were 28.6 ± 3 IU/L and 15.6 ± 0.5 nM/dL for the SOD and MDA assay, respectively.⁹²

1.2.6.2.10 Uterine Contractility Activity

A methanolic extract of powdered leaf material from *I. trichantha* was prepared and tested in non-pregnant albino rat for its effect on uterus contractions. Both oxytocin- and acetylcholine-induced contractions were reduced in a dose-dependent manner. The inhibitory effect was significant at concentrations of 10 and 20 mg/mL. The statistical significance was similar for salbutamol and atropine controls.⁶⁹

1.2.6.2.11 Anti-plasmodial Activity

David-Oku and Obiajunwa-Otteh examined the anti-malarial activity of methanolic extracts of *I. oliviformis* tuber or a combination of both tuber and leaves. Mice infected with *P. berghei* clone were orally given plant extract at concentrations of 25, 50, or 100 mg/kg for 4 days. The combined tuber and leaf extract at 100 mg/kg was the most potent. The calculated parasitemia suppression was 87% four days after the start of treatment. The positive control group given 10mg/kg of chloroquine had 92% suppression. Both results were statistically

significant compared with the negative control group. The results were similar for 30-day test groups as well. The combined extract group resulted in *P. berghei* levels suppressed by 81% with a mean survival time of 29.50 days. The chloroquine treatment group suppression level was 94% with a mean survival time of 30.00 days. The negative control average survival time was 13.17 days.¹¹¹

1.2.6.2.12 Nutritional and Agricultural Analysis

There have been several recent publications that focus on the potential agricultural and nutritional benefits of *Icacina*. The plant is prevalent in forests near residential areas but has very few uses besides medicinal applications. Reports indicate herders actively avoid the plant from affecting grazing livestock.¹¹² However, due to its relative ubiquity and robustness, *Icacina* species, specifically *I. oliviformis* and *I. trichantha*, have been considered potential low-cost alternatives for animal feed and human consumption.

Icacina species have been analyzed for its nutritional value and thus as a potential reliable food source.^{113,114} Overall, analysis shows that the nutritional traits are sufficient for human consumption. However, in order to remove harmful substances, such as oxalate and phytates, processing through heating or extraction with water will also affect the nutritional content.^{115,116}

I. oliviformis tubers were used to partially substitute the regular feed for female broiler chickens (Cobb 50 strain). The tubers were dried and milled into flour from either raw material, replacing 50 g/kg of normal feed, or after soaking in distilled water for 12 days, replacing 150 g/kg. The study found that feed replacement with raw tuber had no significant change in bird health or growth performance compared with the negative control group. However, the soaked

tuber group demonstrated lower growth rate than both the control and the raw tuber treatment group despite a higher rate of feed consumption.¹¹⁷

Another studied assessed the viability of *I. trichantha* tuber as an alternative for livestock feed using albino rats for observation. Three treatment groups had their food replaced with *I. trichantha* tuber prepared by oven-drying, air-drying, or parboiling followed by air-drying. Test animals were treated for 4 weeks before blood and serum analysis. The authors reported significant changes compared to the control group for several hematological markers including hemoglobin, red blood cell counts, white blood cell counts, and platelets. However, no clear trend or relationship to preparation method was obvious. Additionally, serum levels for albumin, urea, globulin, and creatinine were generally similar with the control group. The study authors suggested processed tuber could be a suitable livestock feed substitute regardless of preparation method.¹¹⁸

Okosun and colleagues examined the substitution of food supply for rabbits with dried and processed *I. trichantha* tuber. Animals were randomly assigned to treatment groups with 0, 25, 50, 75, or 100% of normal feed was replaced with powdered tuber for 7 weeks. The 50% treatment group performed best compared to the control group for weight gain over the test period. In economic terms, this group reduced the cost of production per rabbit from ₦85.20 to ₦53.10. The authors proposed *I. trichantha* tuber as a tool to make agricultural livestock production more cost effective.¹¹⁹

1.3 **Objectives**

As stated previously, higher plants are an important source for natural products to serve as a basis for drug discovery and other beneficial applications. The long history of medicinal plants

to treat various ailments provides current researchers with a vast traditional medicinal knowledge base from which to begin a rational phytochemical analysis. Starting the drug discovery process focusing on these plants can increase the chance of success. Using the knowledge of traditional medicine systems can provide a step in the right direction toward identifying and isolating novel therapeutic phytochemicals based upon the reported traditional use.

Ethnomedicinal reports and biological screen assays of *I. trichantha* extract indicate the presence of active phytochemicals. Previous research indicates the chemotaxonomic profile of the plant produces a variety of phytochemicals, primarily unique pimarane diterpenoids. Terpenes are the largest chemical class of natural products due to the fact they have been found to be synthesized in many species of plants, fungi, and bacteria. They are biogenetically derived from five-carbon isopentenyl pyrophosphate building blocks.¹²⁰ Diterpenoids are composed of four isoprene units which lends itself to chemical diversity, which can be taken further through various biogenetic modifications. This class of natural products has demonstrated a variety of biological targets, including anti-tuberculosis, antioxidant, and cytotoxicity. The diterpenoids include the taxane subclass, which has led to the development of paclitaxel (Taxol®, Bristol-Myers Squibb) and docetaxel (Taxotere®, Rhone-Poulenc Rhoer) as highly effective antimicrotubule chemotherapy drugs.^{121–127} The variation of structural chemistry found in diterpenes and the proven success in drug development make this class of natural products a viable target area to continue drug discovery research.

Bioassay-guided fractionation of botanicals is an accepted method to efficiently identify and analyze compounds most likely responsible for bioactivity. Using new plant material provided by our collaborators Dr. Asuzu at the University of Nigeria and Dr. Onakpa at the University of Abuja, bioactive fractions obtained from *I. trichantha* were profiled and purified to

yield active compounds, along with inactive components. Bioactivity testing of fractions was conducted in collaboration with the Dr. Burdette lab at UIC by measuring cytotoxicity with human cancer lines, including MDA-MB-235, MDA-MB-435, and OVCAR3 cells. This process would also provide additional quantities of active phytochemicals to be used in further biological testing beyond the initial screenings. Research interests focused on the continued study of cytotoxic activity, especially to determine cancer cell specificity and molecular targets. We were also interested in anti-germination activity as means of protecting crops from harmful pests and weeds. Experiments to test the potential of isolated compounds as herbicidal agents was completed in collaboration with Dr. Warpeha of UIC.

The additional plant material also provided an opportunity to continue the isolation and purification of novel active compounds. For the isolation, we relied upon column chromatography and semi-prep HPLC techniques. The most active fractions identified from the plant extract were further fractionated to yield as many purified peaks that can be collected. Dereplication will be a necessary process to quickly identify previously isolated compounds to focus efforts on novel targets. This step relied upon the compound library established by our group in previous studies on *I. trichantha* and the spectroscopic data obtained. Spectroscopic techniques, primarily UV-Vis, NMR, and MS, were used to characterize isolated compounds,. Pure novel compounds were studied to determine the chemical structure, including the absolute configuration if possible, and tested in biological activity assays to determine activity and drug lead potential.

2. STRUCTURE ELUCIDATION OF PIMARANE DITERPENOIDS

This chapter is reproduced in part with permissions from Guo, B.; Onakpa, M. M.; Huang, X.-J.; Santarsiero, B. D.; Chen, W.-L.; Zhao, M.; Zhang, X.-Q.; Swanson, S. M.; Burdette, J. E.; Che, C.-T. Di -nor - and 17- nor -Pimaranes from *Icacina Trichantha*. *J. Nat. Prod.* **2016**, 79 (7), 1815–1821, DOI: 10.1021/acs.jnatprod.6b00289. Copyright 2016 American Chemical Society. Reprinted from Guo, B.; Zhao, M.; Wu, Z.; Onakpa, M. M.; Burdette, J. E.; Che, C.-T. 19-nor-Pimaranes from *Icacina Trichantha*. *Fitoterapia* **2020**, DOI: 10.1016/j.fitote.2020.104612, Copyright 2020, (Forthcoming) with permission from Elsevier.

2.1 Introduction

Icacina trichantha (Icacinaceae, Oliv.) is a flowering shrub native to forested vegetation areas of southern Nigeria.¹²⁸ Its large tuber is well known among the local population and traditional medicine practitioners for its nutritional and medicinal applications. In rural areas, tinctures of the tuber are often kept in households as a readily available remedy for treating common ailments and wounds such as fever and snake bite.⁷⁵ One of its vernacular names, ‘unumbia’ (meaning ‘induce emesis’), conveys its seemingly primary physiological action.⁶² The plant is also reportedly used to treat food poisoning and constipation,¹⁰⁷ in addition to chronic conditions such as hypertension¹²⁹ and soft tumors.⁶²

Following reports that demonstrated the emetic activity and other bioactivities of this plant,^{107,108,110} our group has conducted a series of phytochemical studies, leading to the isolation and identification of a number of pimarane diterpenes, in particular, the uncommon 9β H type.^{76–79,89} This interesting class of compounds has demonstrated cytotoxic,¹³⁰ antibacterial,¹²⁵ and antifungal¹³¹ activities. In addition, we have reported the potential herbicidal activity of one of its ingredients, icacinol, which demonstrated selective germination inhibitory activity in *Arabidopsis*.¹³²

In a continuing effort to explore ethnobotanicals for novel and bioactive substances, we have further studied the extract of *I. trichantha* tuber. The tuber of *I. trichantha* was extracted with 80% aqueous MeOH by percolation, followed by solvent partition into petroleum ether-soluble, EtOAc-soluble, and *n*-BuOH-soluble fractions, successively. Another set of tuber plant material was extracted with 80% aqueous acetone by percolation, followed by solvent partition into EtOAc-soluble and *n*-BuOH-soluble fractions, successively. The altered extraction protocol was carried out in an effort to isolate chemically different compounds.

Several novel and previously reported compounds were successfully isolated and elucidated from the plant material, including unusual *nor*-pimarane-type diterpenes. The structures were elucidated primarily based on NMR spectroscopic and HRMS analysis. The absolute configurations were determined by electronic circular dichroism and x-ray crystallography. All isolated compounds, including previously reported, are presented along with the structure identification analysis and results.

2.2 Materials and Methods

2.2.1 General Experimental Procedures.

The melting points were measured on a Thomas-Hoover capillary melting point apparatus (Arthur H. Thomas Company, Philadelphia, PA., U.S.A.). Optical rotations at the sodium D line were measured with a Perkin-Elmer 241 digital polarimeter using a quartz cell with a path length of 100 mm at room temperature. Concentrations (*c*) are given in g/100 mL. IR spectra were measured on a Nicolet 380 Fourier Transform Infrared Spectrometer and analyzed with OMNIC software. UV spectra were collected on a Shimadzu UFLC system with a PDA detector. The ECD spectra were obtained on a JASCO J-810 spectrometer. NMR spectra were recorded on a Bruker AV-400HD spectrometer. All chemical shifts were quoted on the δ scale in ppm using residual solvent as the internal standard (methanol: δ_{H} 3.31 for ^1H NMR, δ_{C} 49.00 for ^{13}C NMR; chloroform: δ_{H} 7.26 for ^1H NMR, δ_{C} 77.16 for ^{13}C NMR; DMSO: δ_{H} 2.50 for ^1H NMR, δ_{C} 39.52 for ^{13}C NMR). Coupling constants (*J*) are reported in Hz. For HPLC purification, C₈ semi-preparative HPLC columns (Agilent C₈ column, 250 × 9.4 mm, 5 μm), C₁₈ semi-preparative HPLC columns (Phenomenex C₁₈ column, 250 × 10 mm, 5 μm)

and Agilent SB-C₁₈ column, 250 × 9.4 mm, 5 μm) and biphenyl semi-preparative HPLC columns (Phenomenex biphenyl column, 250 × 10 mm, 5 μm) and a Shimadzu UFLC system were used. HPLC column stationary phases were chosen based on analysis of fractions for semi-preparative isolation method development. HRESIMS were measured on a Waters SYNAPT hybrid quadrupole/time of flight spectroscopy using positive electrospray ionization and a Shimadzu ion trap/time of flight hybrid mass spectrometer using positive and negative electrospray ionization.

2.2.2 Plant Material.

Tubers of *Ipomoea trichantha* Oliv. were collected in June 2011 from the Orba village in Nsukka of the Enugu State, Nigeria, and authenticated by Prof. B.O. Olorede of the Botany Department, University of Abuja, Nigeria, and Mr. A. Ozioko, botanist at the BDCP Laboratories, Nsukka, Nigeria. A voucher specimen (UNN/FVM 456) was deposited in the pharmacology laboratory at the University of Nigeria, Nsukka, Nigeria.

2.2.3 Extraction and Isolation.

The first batch of tubers of *I. trichantha* (1.5 kg) were milled and extracted with 80% aqueous MeOH by percolation to yield 166 g of crude extract. The crude extract was partitioned into petroleum ether-soluble (11 g), EtOAc-soluble (17 g), *n*-BuOH-soluble (15 g), and H₂O-soluble (128 g) fractions. The EtOAc fraction (17 g) was separated into 88 sub-fractions on a silica gel column (5 × 60 cm) eluted with gradient petroleum ether and EtOAc mixtures (from 100:0 to 0:100, v/v; 600 mL each). The combined sub-fractions 29–32 was chromatographed by semipreparative HPLC eluted with MeOH–H₂O (C₁₈, 48:52 v/v; 3.5 mL/min) to afford icacinlactone L (**14**, 2.9 mg, *t_R* = 18.4 min, soluble in MeOH). 7α-Hydroxyicacinlactone B (**9**, 1.8 mg, *t_R* = 7.6 min, soluble in

MeOH) and icacinlactone K (**21**, 1.5 mg, $t_R = 16.0$ min, soluble in MeOH) were purified from subfractions 33–35 by semipreparative HPLC (C_{18} , MeOH–H₂O, 60:40 v/v; 3.5 mL/min). The combined sub-fractions 36–42 was further separated into five fractions using Sephadex LH-20 column chromatography (1 × 80 cm, eluted with MeOH). The 2nd and 3rd fractions were purified by HPLC (C_{18} , MeOH–H₂O, 55:45 v/v; 3.5 mL/min) to afford icacintrichanone (**22**, 2.1 mg, $t_R = 10.7$ min, soluble in MeOH). The *n*-BuOH-soluble fraction (19 g) was passed through a macroporous resin column (4 × 30 cm) eluted with aqueous MeOH (from 5 to 80%, 800 mL each). The fractions obtained from 20–30% aqueous MeOH were combined and further separated into 30 sub-fractions using MCI CHP20P resin column chromatography (2.5 × 20 cm; eluted by aqueous MeOH, from 10 to 50%). The 3rd and 4th fractions were applied to semipreparative HPLC (C_{18} , MeCN–H₂O, 8:92 v/v; 3.5 mL/min) to afford 7 α -hydroxyicacenone (**6**, 2.3 mg, $t_R = 18.7$ min, soluble in MeOH). In a similar manner, 2 β -hydroxyhumirianthenolide C (**7**, 0.8 mg, $t_R = 16.0$ min, soluble in MeOH) was purified from the 6th and 7th fractions by HPLC (C_{18} , MeCN–H₂O, 12:88 v/v; 3.5 mL/min).

A second batch of the dried tubers of *I. trichantha* (5.0 kg) were milled and extracted with 80% aqueous acetone by percolation to yield 483 g of crude extract. The crude extract was partitioned into EtOAc-soluble (98 g), *n*-BuOH-soluble (109 g), and H₂O-soluble (276 g) fractions. The EtOAc fraction (98 g) was separated into 40 sub-fractions on a silica gel column (10 × 60 cm) eluted with gradient hexane and acetone mixtures (from 100:0 to 0:100, v/v; 700 mL each). The combined sub-fractions 20–24 was further separated into 32 fractions on a silica gel column (3 × 35 cm) with gradient DCM and acetone mixtures (from 100:0 to 50:50, v/v, 100 mL each). Fractions 21, 22, and 23

were combined and further separated using MCI Gel[®] CHP20P column chromatography (2.5 x 30 cm) with gradient MeOH-H₂O mixtures (from 10:90 to 100:0, v/v, 100 mL each) into 17 fractions. The 7th and 8th fractions were purified by semi-preparative HPLC (SB- C₁₈, MeOH-H₂O, 33:67, v/v, 3.0 mL/min) to afford icatrichanone (**17**, 12.9 mg, t_R = 25.3 min, soluble in MeOH and CHCl₃) and 14-hydroxyicatrichanone (**18**, 13.0 mg, t_R = 29.5 min, soluble in MeOH and CHCl₃).

The combined sub-fractions 25-27 and 28-32 resulted in formation of precipitate directly from solution of MeOH at room temperature. The precipitate was purified by semi-preparative HPLC (C₈, MeCN-H₂O, 20:80 v/v, 4.0 mL/min) to afford icacinol (**1**, 576.8 mg, t_R = 8.2 min, soluble in MeOH and DMSO) and humirianthol (**2**, 138.4 mg, t_R = 9.5 min, soluble in MeOH and DMSO).

The mother liquid from combined sub-fractions 25–27 from the EtOAc fraction was further separated into 67 fractions on a silica gel column (2.5 x 30 cm) eluted with gradient DCM and acetone mixtures (from 100:0 to 3:7, v/v, 150 mL each). Sub-fractions 14-17 were combined and further separated into 20 fractions using Sephadex LH-20 resin column chromatography (2.5 x 30 cm) eluted with MeOH. Combined sub-fractions 7-9 were combined and purified by semi-preparative HPLC (Biphenyl, MeOH-H₂O, 60:40 to 95:5 v/v, 3.75 mL/min) to afford 7-oxo-icacinlactone B (**11**, 0.8 mg, t_R = 18.7 min, soluble in MeOH and CHCl₃) and (+)-pinoresinol (**23**, 1.4 mg, t_R = 20.5 min, soluble in MeOH). Sub-fractions 18-24 from the combined EtOAc 25-27 sub-fractions were combined and further separated into 20 fractions using Sephadex LH-20 resin column chromatography (3 x 35 cm) eluted with MeOH. Combined sub-fractions 4-6 were further separated into 20 fractions on a silica gel column (1.0 x 30 cm) eluted with gradient hexane and ethyl

acetate mixtures (from 80:20 to 30:70, v/v, 100 mL each). Sub-fractions 15-16 were combined and purified by semi-preparative HPLC (SB- C₁₈, MeOH-H₂O, 50:50 v/v, 3.5 mL/min) to afford (**24**, 0.6 mg, t_R = 16.1 min, soluble in MeOH).

Combined sub-fractions 9-12 were purified by semi-preparative HPLC (C₁₈, MeOH-H₂O, 37:63 v/v, 4.0 mL/min) to afford 7 β -hydroxyicacinlactone B (**10**, 0.8 mg, t_R = 15.9 min, soluble in MeOH). Combined sub-fractions 13-17 were purified by semi-preparative HPLC (C₁₈, ACN-H₂O, 38:62 v/v, 3.0 mL/min) to afford icacinlactone H (**16**, 13.9 mg, t_R = 11.3 min, soluble in MeOH). Sub-fraction 25 from the EtOAc 25-27 sub-fractions was further separated into 35 fractions using MCI Gel[®] CHP20P column chromatography (2.5 x 30 cm) with gradient MeOH-H₂O mixtures (from 10:90 to 100:0, v/v, 150 mL each). Combined sub-fractions 16-22 were purified by semi-preparative HPLC (SB-C₁₈, MeOH-H₂O, 33:67 v/v, 4.0 mL/min) to afford icacinlactone E (**8**, 9.6 mg, t_R = 12.7 min, soluble in MeOH), 14-hydroxyicacinlactone I (**5**, 1.4 mg, t_R = 16.3 min, soluble in MeOH), 14-methoxyhumirianthol (**3**, 1.1 mg, t_R = 18.5 min, soluble in MeOH), and icacinlactone I (**4**, 1.6 mg, t_R = 28.3 min, soluble in MeOH). Sub-fractions 28-31 from the EtOAc 25-27 sub-fractions were combined and further separated into 25 fractions using Sephadex LH-20 resin column chromatography (2.5 x 30 cm) eluted with MeOH. Combined sub-fractions 10-12 were purified by semi-preparative HPLC (SB-C₁₈, MeOH-H₂O, 55:45 to 100:0 v/v, 4.0 mL/min) to afford 3-dehydroxyicacinlactone B (**12**, 1.8 mg, t_R = 10.7 min, soluble in MeOH), 3-dehydroxyicacinlactone A (**13**, 0.6 mg, t_R = 9.8 min, soluble in MeOH), and icacinlactone D (**15**, 4.0 mg, t_R = 12.8 min, soluble in MeOH). Sub-fractions 40-44 from the EtOAc 25-27 sub-fractions were combined and further separated into 56 fractions using MCI Gel CHP20P column chromatography (2.5 x 30

cm) with gradient MeOH-H₂O mixtures (from 5:95 to 100:0, v/v, 150 mL each).

Combined sub-fractions 23-34 were purified by semi-preparative HPLC (SB-C₁₈, MeOH-H₂O, 38:62 v/v, 4.0 mL/min) to afford 3-*O*-methyl-icatrichanone (**19**, 1.3 mg, t_R = 15.3 min, soluble in MeOH and CHCl₃) and 3-*O*-methyl-14-hydroxyicatrichanone (**20**, 2.4 mg, t_R = 16.1 min, soluble in MeOH and CHCl₃). The spectroscopic data of all novel compounds are given in their respective section.

2.2.4 Single Crystal X-Ray Structure Determination

X-Ray diffraction intensity data were collected at the Advanced Photon Source, Argonne National Laboratory, at LS-CAT (beamline 21-ID-D), with a 50 μ m x-ray beam, at a distance of 100 mm and temperature of 100K, using a MAR CCD 300 mm area detector. For compound **21**, a needle-like crystal, roughly 10 \times 10 \times 50 μ m, was used for data collection. The space group was determined to be P2₁2₁2₁ (No. 19) by identification of the systematic absences. The absolute configuration of the structure was inferred from an analysis of the Bijvoet differences, with a Flack parameter of 0.1(4) (1.1 for the inverted structure), Parsons z parameter = 0.19(16), and a Bayesian Bijvoet probability of P2(true) = 0.999. For compound **6**, a needle-like crystal, roughly 10 \times 10 \times 50 μ m, was used for data collection. The space group was determined to be P2₁ (No. 4) by the systematic absences. The absolute configuration of the structure was inferred from an analysis of Bijvoet differences, with the Flack parameter of 0.10(19) (1.1 for the inverted structure), and a probability of P2(true) = 1.000. Structures for compounds **6** and **21** were solved by SHELXS and refined with SHELX-2014.

Colorless needles of compound **5** were obtained by recrystallization in methanol at room temperature. A crystal measuring roughly 10 \times 10 \times 50 μ m was selected for data collection. It

was encased in silicone oil, transferred to a nylon loop, and cooled to 100K. Data collection was carried out at beamline 21-ID-D, LS-CAT, Advanced Photon Source, Argonne National Laboratory, using an Eiger9M detector at a wavelength of 0.68876Å, crystal-to-detector distance of 100mm, and 0.5° rotation wedges. The data was processed with XDS¹³³ in a triclinic unit cell (space group P1) with three molecules in the asymmetric unit. Integration of the data with XDS resulted in a total of 17303 accepted observations and an averaged set of 8760 unique reflections to a resolution of 0.80Å. The unit cell was identified as triclinic, space group P1 (No. 1), with three molecules in the asymmetric unit. The R(merge) to 0.80Å was 4.0%, and 82% complete with an overall $I/\sigma(I) = 16.9$. The structure was solved using SHELXS and refined with SHELXL¹³⁴ to a $R1 = 0.0631$ for the 9887 reflections with $F_o > 4\sigma(F_o)$, and 0.0644 for all data (9993 reflections) with a goodness-of-fit = 1.05. Bijvoet probability analysis assigns the absolute configuration: $P2(\text{true}) = 1.000$, $P3(\text{false}) = 5 \times 10^{-19}$, Hooft $y = -.40(15)$; the inverted structure yields $P2(t) = 1 \times 10^{-19}$, $P3(f) = 1.000$, Hooft $y = 1.39(15)$, with C3(R), C8(R), C10(R), C11(R), C14(S), C17(S), C19(S), and C21(S) for all three molecules. Additional information is provided in Appendix A.

Colorless needles of compound **11** were obtained by recrystallization in methanol at room temperature. A crystal measuring roughly 10 x 10 x 50 μm was selected for data collection. It was encased in silicone oil, transferred to a nylon loop, and cooled to 100K. Data collection was carried out at beamline 21-ID-D, LS-CAT, Advanced Photon Source, Argonne National Laboratory, using an Eiger9M detector at a wavelength of 0.68877Å, crystal-to-detector distance of 100mm, and 2° rotation wedges. The data was processed with XDS¹³³ in a monoclinic unit cell (space group C2) with one molecule in the asymmetric unit. Integration of the data with XDS resulted in a total of 10835 accepted observations and an averaged set of 3225 unique

reflections to a resolution of 0.80Å. The unit cell was identified as monoclinic, space group C2 (No. 5), with one molecule in the asymmetric unit. The R(merge) to 0.80Å was 5.0%, and 96% complete with an overall $I/\sigma(I) = 18.3$. The structure was solved using SHELXS and refined with SHELXL¹³⁴ to a $R1 = 0.0642$ for the 3068 reflections with $F_o > 4\sigma(F_o)$, and 0.0686 for all data (3225 reflections) with a goodness-of-fit = 1.13. Bijvoet probability analysis assigns the absolute configuration: $P2(\text{true}) = 0.948$, $P3(\text{false}) = 0.033$, Hooft $y = -0.1(4)$; the inverted structure yields $P2(\text{t}) = 0.054$, $P3(\text{f}) = 0.587$, Hooft $y = 0.9(4)$, with C3(S), C4(R), C5(R), C6(S), and C10(R). Additional information is provided in Appendix A.

The data for X-ray diffraction analyses of compounds **5**, **6**, **11**, and **21** have been deposited at the Cambridge Crystallographic Data Centre. CCDC 1998434 (for **5**), 1424347 (for **6**), 1998435 (for **11**), and 1424346 (for **21**) contain the supplementary crystallographic data. These data can be obtained free of charge via <http://www.ccdc.cam.ac.uk/conts/retrieving.html> (or from the CCDC, 12 Union Road, Cambridge CB2 1EZ, UK; Fax: +44 1223 336033; E-mail: deposit@ccdc.cam.ac.uk).

2.2.5 Computational Section for ECD Calculation.

Conformational analysis was performed for the enantiomers of **21** and **22** by the Sybyl 8.1 program using Random Searching together with the MMFF94s molecular mechanics force field charged with MMFF94. Two and six conformers for **21** and **22** were obtained, respectively. Optimization followed by ECD calculation of the resulted conformers were performed over the Gaussian09 software at B3LYP/6-31+G(d,p)//B3LYP/6-31G(d) level in the gas phase.

The systematic random conformational analyses were performed in the SYBYL-X-2.1 program by using MMFF94s molecular force field, with an energy cutoff of 10 kcal/mol to the

global minima. All of the obtained conformers were further optimized using DFT at the b3lyp/6-31+g(d) level in gas phase by using Gaussian09 software.¹³⁵ The optimized stable conformers were used for ECD calculations at the cam-b3lyp/6-31+g(d) level with the PCM solvation model of methanol, with the consideration of the first 30 excitations. The overall ECD curves were all weighted by Boltzmann distribution. The calculated ECD spectra were subsequently compared with the experimental ones. The ECD spectra were produced by SpecDis 1.71 software with the UV correction of +5 nm (**18** and **19**), +10 nm (**17**), and +8 nm (**20**), respectively.^{136,137}

2.3 Chemical Investigation

2.3.1 Dereplication Library Generation Workflow

During the isolation and purification of compounds from bioactive fractions, a dereplication process was sought to improve the efficiency of the process. However, there were a few obstacles that needed to be addressed. First, previously isolated compounds from *I. trichantha*^{76–79} from our group were stored in DMSO solution and kept at -4° C, and not all compounds were available due to limited availability following bioassays. After an initial LC-MS analysis of the available compounds, several did not seem to match the reported molecular weight or the results were unclear, either due to mislabeling, degradation, contamination, or a combination. A decision was made to not use those compounds as standards, so a simple dereplication process using MS could not be implemented immediately.

All compounds had also been analyzed by HPLC-UV using the same parameters and HPLC column to record UV spectra and retention times, which could also potentially be used as data for dereplication. However, UV spectra were only useful for identifying the different subclasses of diterpenoids (i.e. 9 β H-pimaranes vs 17-*nor*-pimaranes) and could not distinguish

between individual compounds. Due to the structural similarity between the diterpenoids, retention times could be within the margin of error for some compounds. In addition, performance of HPLC columns gradually change over time, affecting recorded retention times for the same compound. After some initial trials, it was determined the HPLC data available for the compound library would not be sufficient for dereplication .

Fortunately, previous phytochemistry work provided incredibly useful NMR results for all compounds, including some data that was unpublished. There are several benefits of ^1H NMR spectra in structural analysis including high specificity of spectrum characteristics to their respective compound, sensitivity of data collection, and relatively simple and cost-effective structural data.¹³⁸ For our purposes, it was determined each diterpenoid possess specific chemical shifts and couplings for each signal, making every ^1H spectra unique. However, it would be highly inefficient to obtain NMR data for every isolated compound. That is why MS and specifically LC-MS is the preferred method for the rapid dereplication of natural product extracts.^{139–142}

Mass spectrometry-based dereplication methods rely on the sensitivity and accuracy of high-resolution detectors in addition to the specificity of tandem MS. However, preliminary HR-MS/MS experiments conducted with Dr. Dejan Nolic of UIC provided limited additional structural insight. There was no obvious model or characteristic fractionation pattern from these pimaranes in an initial screen of a few available compounds on a q-TOF detector using standard detection settings. In addition, the base peaks did always correspond with the protonated molecular ion. The inherent chemical characteristics of these molecules required more testing and troubleshooting to find a suitable MS-based protocol for dereplication purposes, however we were limited in time and access to the necessary resources. Therefore, a dereplication process

was developed specific for *I. trichantha* isolates that combined ^1H NMR with LC-MS results that took advantage of the low-resolution single quadrupole detector in our possession tied with Shimadzu LabSolutions detection and analysis software. The hope was to first rebuild the compound library to then return to HR-LC-MS/MS analysis for eventual dereplication from complex fractions from the plant. This would be especially helpful in distinguishing the several known constitutional isomers reported from *I. trichantha*.

The first step in the workflow required the acquisition of ^1H NMR data of isolated compounds. Methanol- d_4 NMR solvent was used because every previously reported compound's ^1H spectrum was obtained in at least deuterated methanol. Simultaneously, low-resolution molecular weight data was acquired using the previously described Shimadzu instrument with a standard LC gradient method and the same UHPLC column. Interpretation of the results helped to narrow potential hits. Direct comparison of acquired ^1H spectra with the library of likely matches was used to visually determine a hit. Once a compound was identified, its MS spectrum and retention time results were added to the LabSolutions software library. This process was repeated for each isolated peak until the digital library grew enough so that hits from the MS analysis were sufficient for high confidence, removing the need for repeated NMR experiments. These results are briefly described in following sections for previously reported compounds and relevant spectra are given in Appendix A.

2.3.2 Isolation and Structure Elucidation of 9 β H-pimarane diterpenoids

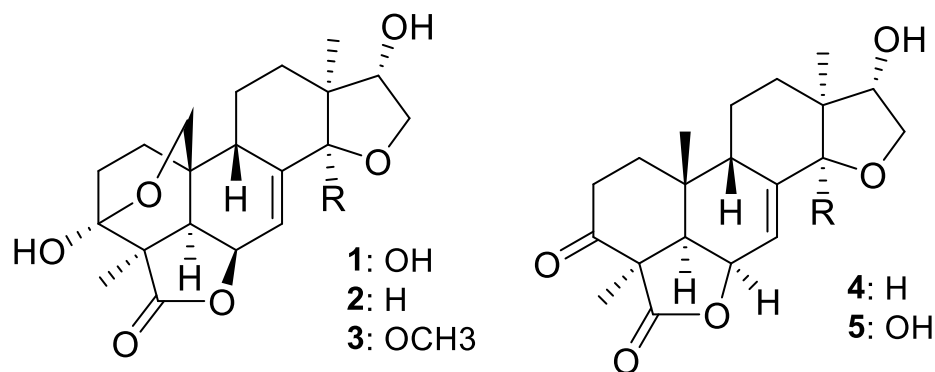


Figure 13. Isolated 9 β H-pimarane diterpenoids from *I. trichantha*

2.3.2.1 Icacinol (1)

Compound **1** was obtained as white amorphous crystal. The isolated sample was identified and dereplicated by obtaining MS, ^1H , and ^{13}C NMR data and comparing with previously reported results. A molecular formula of $\text{C}_{20}\text{H}_{26}\text{O}_6$ with 8 degrees of unsaturation was suggested by HRESIMS (m/z 379.1794 $[\text{M} + \text{H}]^+$; calcd for $\text{C}_{20}\text{H}_{27}\text{O}_6^+$ 379.1751).

Interpretation of the ^1H spectrum confirmed the presence of one olefinic proton at δ_{H} 6.02 (dd, $J = 5.0, 1.3$ Hz, H-7) and two methyls at δ_{H} 0.85 (s, CH_3 -17) and δ_{H} 1.27 (s, CH_3 -18). The ^{13}C spectrum displayed 20 resonances including two methyls, six methylenes, five methines, two dioxxygenated secondary carbons, a carbonyl, and four quaternary carbons (TABLE V). The ^1H NMR spectrum was directly compared with previously obtained spectrum that was used to elucidate **1**, and the two spectra are essentially identical (Figure 42, Appendix A). The δ_{C} chemical shifts were also compared with previous results used to identify icacinol.^{72,76}

Subsequent collected material was dereplicated as icacinol using retention time and low-resolution MS data from HPLC-MS analysis. The low resolution ESIMS resulted in m/z 379 in positive mode, which corresponds to the protonated molecular ion ($[\text{M} + \text{H}]^+$) and m/z 423 in

negative mode, corresponding to the formic acid adduct of the deprotonated molecular ion ($[M-H+HCOOH]^-$). The experimental mass spectrum was compared with the library spectrum of icacinol using Shimadzu LabSolutions software and resulted in a similarity score of 96/100. Altogether, this suggests compound **1** is icacinol (Figure 13).

A semi-prep HPLC method was developed to improve isolation efficiency and purity from precipitate material collected from fractionated plant extract. The goal was to be able to obtain high purity icacinol and humirianthol in significant quantities to carry out additional biological experiments, such as *in vitro* and *in vivo* assays, and material for medicinal chemistry modifications. Though the precipitate contained primarily icacinol and humirianthol, minor impurities were present in UV chromatograms. In addition, the two compounds are structurally similar, differing by a single hydroxyl group substitution, making them likely to behave similarly in an LC system. Therefore, an efficient but effective purification process was needed. A series of method development experiments were carried out to determine the optimum parameters for a reverse phase HPLC separation method. The HPLC solvent system was established by determining aqueous ACN resolved the two target peaks better than aqueous methanol. This also resulted in a lower cost for solvent due to the higher aqueous solvent content. Next, an isocratic method was compared with a gradient method, followed by optimization of flow rate and solvent ratios. Finally, different column stationary phases were assessed by comparing C₁₈, C₈, and biphenyl phases. The C₈ column was determined to result in slightly better peak resolution resulting in the final HPLC method (C₈, ACN-H₂O, 20:80 v/v, 4.0 mL/min) that required 10 minutes per collection. A chromatogram representative of the described method resulting in the resolution of icacinol and humirianthol is shown in Figure 14a. Initial tests of the separation method used HPLC-UV to determine the purity of both compounds.

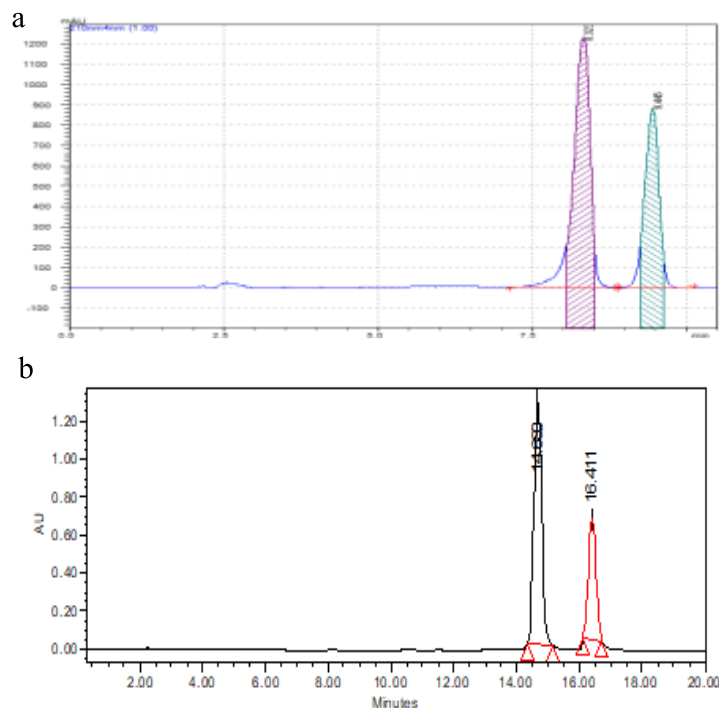


Figure 14. UV chromatograms of HPLC separation of compounds 1 (left peak) and 2 (right peak) for a) semi-prep method using C₈ and b) prep method using C₁₈.

Methanol solubilized the precipitate the best the RP-LC compatible solvents, resulting in an approximate solubility of 5 mg/mL. After optimizing the injection volume to maintain peak resolution, about 15 mg of dissolved precipitate sample could be separated into icacinol and humirianthol in an approximate 4:1 ratio by mass over 8 hours with a loss of 10-15% of sample. Over 500 mg of icacinol has been purified using this method. Later, a Waters prep HPLC system and prep C18 column become available so a method transfer was tested to increase the sample load per injection and improve collection efficiency. Due to pressure limitations of the Waters system, the method was adjusted to ACN-H₂O, 25:75 v/v, 7.0 mL/min that required 18 minutes per collection to maintain a sufficient peak resolution. A representative chromatogram is shown in Figure 14b. Though the sample

load was doubled, the adjusted prep method required four times the volume of organic solvent in addition to eight additional minutes per collection. Therefore, the original semi-prep method was preferred. However, a prep HPLC with higher pressure limitations would be capable of a more efficient separation and collection of the two compounds.

TABLE V. ^1H (400 MHz) AND ^{13}C NMR (100 MHz) OF COMPOUNDS 1 AND 2 (δ in ppm)

position	1^a		2^a	
	δ_{C}	δ_{H} (J in Hz)	δ_{C}	δ_{H} (J in Hz)
1	28.5, CH ₂	1.63, m ^b 1.58, m ^b	28.4, CH ₂	1.64, m ^b 1.60, m ^b
2	28.0, CH ₂	1.99, ddt (J = 12.0, 4.7, 2.2) 1.70, m ^b	28.0, CH ₂	1.99, ddd (J = 13.3, 11.2, 5.5) 1.70, td (J = 13.2, 12.1, 4.5)
3	96.2, C	-	96.2, C	-
4	49.8, C	-	49.9, C	-
5	43.4, CH	2.26, dd (J = 7.0, 1.9)	43.9, CH	2.29, dd (J = 7.1, 2.0)
6	71.4, CH	5.02, dd (J = 6.9, 4.9)	71.5, CH	4.94, dd (J = 6.9, 4.7)
7	115.7, CH	6.02, dd (J = 5.0, 1.3)	116.4, CH	5.85, d (J = 4.7)
8	145.9, C	-	145.6, C	-
9	38.2, CH	1.80, m ^b	36.2, CH	1.82, dd (J = 12.6, 2.7)
10	29.9, C	-	29.7, C	-
11	25.0, CH ₂	1.53, m ^b 1.18, m ^b	29.7, CH ₂	1.54, m ^b 1.14, m ^b
12	34.0, CH ₂	1.35, m ^b 1.12, m ^b	24.9, CH ₂	1.29, m ^b
13	51.9, C	-	48.8, C	-
14	105.2, C	-	85.3, CH	3.85, s
15	77.4, CH	3.70, m ^b	77.4, CH	3.67, t (J = 4.4)
16	74.3, CH ₂	4.32, dd (J = 9.7, 5.4) 3.75, dd (J = 9.8, 1.2)	75.1, CH ₂	4.24, dd (J = 9.7, 4.7) 3.52, d (J = 9.7)
17	13.6, CH ₃	0.85, s	15.1, CH ₃	0.82, s
18	18.4, CH ₃	1.27, s	18.4, CH ₃	1.26, s
19	178.1, C	-	178.2, C	-
20	71.5, CH ₂	3.71, m ^b 3.41, dd (J = 8.8, 2.0)	71.4, CH ₂	3.74, dd (J = 9.0, 2.8) 3.42, dd (J = 8.7, 2.0)
3-OH		5.38, s		5.39, s
14-OH		5.63, s		-
15-OH		4.84, d (J = 6.7)		5.00, d (J = 4.3)

^aData were measured in DMSO-*d*₆. For CH₂, the deshielded signal was assigned as H_a, and the shielded signal as H_b.

^bSignal was partially obscured.

2.3.2.2 Humirianthol (2)

Compound **2** was obtained as a white amorphous crystal. The isolated sample was identified and dereplicated by obtaining MS, ^1H , and ^{13}C NMR data. A molecular formula of $\text{C}_{20}\text{H}_{26}\text{O}_6$ with 8 indices of hydrogen deficiency was suggested by HRESIMS (m/z 363.1792 [$\text{M} + \text{H}$] $^+$; calcd for $\text{C}_{20}\text{H}_{27}\text{O}_6^+$, 363.1802). The ^1H spectrum was compared with **1** and was found to be very similar with the major exception of the appearance of a methine signal at δ_{H} 3.85 (s, H-14). The ^{13}C NMR spectrum was collected and displayed 20 carbon signals. The chemical shifts were found to be similar to icacinol with the exception of C-14, which was more shielded at δ_{C} 85.3 from 105.2 (TABLE V). These results strongly indicated that the compound was a C-14 dehydroxy analogue of icacinol. Comparison of the ^1H NMR spectrum with previously acquired NMR resulted in near identical spectra (Figure 48, Appendix A) confirming this conclusion.^{76,143}

The isolated peak was dereplicated as humirianthol using retention time and low-resolution MS data from HPLC-MS analysis. The low resolution ESIMS resulted in m/z 363 in positive mode, which corresponds to the protonated molecular ion ($[\text{M} + \text{H}]^+$) and m/z 407 in negative mode, corresponding to formic acid adduct of the deprotonated molecular ion ($[\text{M} - \text{H} + \text{HCOOH}]^-$). These two results strongly imply a molecular formula of $\text{C}_{20}\text{H}_{26}\text{O}_6$. Shimadzu LabSolutions software was used to compare experimental results with a standard library as was done with icacinol. The similarity score was 80/100.

Altogether, these results convincingly suggest compound **2** is humirianthol (Figure 13). Subsequent collected material of humirianthol was isolated using the same semi-prep HPLC method mentioned in section 2.2.1.1. This has resulted in over 100 mg of purified humirianthol.

2.3.2.3 14- α -Methoxyhumirianthol (3)

Compound **3** was obtained as a colorless, amorphous powder. The sample was dereplicated and identified via LC-MS and NMR analysis. The sample was analyzed by LC-MS on a low-resolution single quadrupole mass spectrometer. The positive-mode MS resulted in a base peak of m/z 393, suggesting a molecular weight of 392 that corresponds with $C_{21}H_{28}O_7$. These results were compared with a library of previously isolated compounds using retention time and low-resolution MS in positive and negative mode. Using Shimadzu LabSolutions software to compare with a library of compounds, 14- α -methoxyhumirianthol was the closest match with a similarity score of 98/100.

The 1H NMR spectrum was obtained for dereplication. The spectrum demonstrated similarities with humirianthol upon comparison. The primary difference is the addition of a methoxy signal at δ_H 3.28 and loss of the H-14 methine signal. The spectrum was also compared with previously acquired 1H spectrum for 14- α -methoxy-humirianthol and found to be identical (Figure 55, Appendix A). Interpretation of DEPTQ, COSY, HSQC, and HMBC NMR data (Appendix A) further confirmed the identity of the sample.⁷⁷

2.3.2.4 Icacinlactone I (4)

Compound **4** was obtained as a white amorphous powder. A molecular formula of $C_{20}H_{26}O_5$ with eight indices of hydrogen deficiency was suggested by HRESIMS (m/z 391.1742 $[M-H+HCOOH]^-$, calcd for $C_{21}H_{27}O_7^-$, 391.1762) with the aid of ^{13}C NMR spectroscopic data. In the 1H NMR spectrum, signals for one olefinic proton at δ_H 5.97 (H-7) and three methyls at δ_H 0.97 (CH_3 -17), 1.50 (CH_3 -18) and 0.91 (CH_3 -20) were observed (TABLE VI). Twenty resonances were displayed in the ^{13}C NMR spectrum which include three methyls, five methylenes, six methines, two carbonyls, and four

quaternary carbons (TABLE VI). Along with ^1H – ^1H COSY, HSQC, and HMBC analyses, the NMR results correlated with the previously reported structure for icacinlactone I.⁷⁷ Direct comparison of the collected ^1H spectrum with previously acquired data indicated the two spectra are identical (Figure 62, Appendix A).

TABLE VI. ^1H (400 MHz) AND ^{13}C NMR (100 MHz) OF COMPOUNDS 4 AND 5 (δ in ppm)

position	4		5	
	δ_{C}	δ_{H} (J in Hz)	δ_{C}	δ_{H} (J in Hz)
1	31.8, CH ₂	2.03, dt ($J = 13.1, 9.3$) 1.60, ddd ($J = 13.1, 8.0, 2.4$)	32.0, CH ₂	2.03, dt ($J = 12.5, 9.4$) 1.59, ddd ($J = 13.0, 8.0, 2.3$)
2	35.7, CH ₂	2.51 – 2.67, m ^b	35.8, CH ₂	2.51 – 2.67, m ^b
3	208.1, C		208.2, C	
4	54.9, C		54.9, C	
5	47.4, CH	2.58, d ($J = 5.1$)	47.0, CH	2.56, d ($J = 5.1$)
6	74.5, CH	4.96, t ($J = 5.1$)	74.3, CH	5.03, t ($J = 5.1$)
7	117.9, CH	5.97, dd ($J = 4.9, 1.3$)	117.0, CH	6.22, dd ($J = 5.1, 1.3$)
8	149.0, C		149.4, C	
9	43.6, CH	2.28, dd ($J = 12.2, 3.4$)	36.2, CH	2.26, dd ($J = 11.6, 2.3$)
10	33.4, C	-	33.5, C	
11	25.6, CH ₂	1.75, dt ($J = 10.2, 3.3$) 1.45, m ^b	25.6, CH ₂	1.75, dd ($J = 9.8, 4.9, \text{H}_a$) 1.45, m ^b
12	33.6, CH ₂	1.38 – 1.48, m ^b	35.4, CH ₂	1.36 – 1.49, m ^b
13	50.7, C		50.7, C	
14	87.4, CH	2.16, s	107.2, C	
15	79.8, CH	3.82, dd ($J = 4.8, 1.2$)	79.7, CH	3.82, dd ($J = 5.4, 1.4$)
16	76.5, CH ₂	4.42, dd ($J = 10.0, 4.8$) 3.73, dd ($J = 10.0, 1.2$)	75.9, CH ₂	4.47, dd ($J = 10.1, 5.4, \text{H}_a$) 3.96, dd ($J = 10.0, 1.4, \text{H}_b$)
17	15.5, CH ₃	0.97, s	14.0, CH ₃	1.01, s
18	21.7, CH ₃	1.50, s	21.7, CH ₃	1.51, s
19	177.0, C	-	177.1, C	
20	21.6, CH ₃	0.91, s	21.6, CH ₃	0.89, s

^aData were measured in methanol-*d*4. For CH₂, the deshielded signal was assigned as H_a, and the shielded signal as H_b.

^bSignal was partially obscured.

2.3.2.5 14-Hydroxyicacinlactone I (5)

14-Hydroxyicacinlactone I (5): $[\alpha]_D^{20} = -42$ (*c* 0.1, MeOH); IR (film) ν_{\max} 3355, 2936, 1771, 1516, 1456, 1271, 1236, 1158, 1125, 1034 cm^{-1} ; ^1H NMR (methanol- d_4 , 400 MHz) and ^{13}C NMR (methanol- d_4 , 100 MHz), see TABLE VI; (+)-HRESIMS m/z 363.1793 [$\text{M} + \text{H}$] $^+$ (calcd for $\text{C}_{20}\text{H}_{27}\text{O}_6^+$, 363.1802).

Compound **5** was obtained as a colorless needle-like crystal. A molecular formula of $\text{C}_{20}\text{H}_{26}\text{O}_6$ with eight indices of hydrogen deficiency was suggested by HRESIMS (m/z 363.1793 [$\text{M} + \text{H}$] $^+$; calcd for $\text{C}_{20}\text{H}_{27}\text{O}_6^+$, 363.1802). Structure elucidation of this new 9 β H-pimarane was greatly simplified by comparison of NMR results with the library of previously isolated compounds. When contrasted with compound **4**, the only significant change between the ^1H spectra is the absence of a singlet proton signal that corresponded to H-14.⁷⁷ Comparison of δ_{C} chemical shifts also suggested structural similarity except for C-14 (TABLE VI). The deshielding in chemical shift from δ_{C} 87.4 to 107.2 suggested some type of oxygenation. Based upon the molecular formula, hydroxylation at C-14 is mostly likely. After interpretation of HSQC, COSY, and HMBC NMR spectra (Figure 72-69, Appendix A), the structure was confirmed to be the 14-hydroxy derivative of icacinlactone I. The relative configuration was determined to be H-9 and CH₃-10 in the β -orientation, and CH₃-4, H-5, H-6, CH₃-13, and H-15 in the α -orientation through a NOESY experiment (Figure 75, Appendix A), which is similar to the configuration determined for compound **4**.⁷⁷ The previous report of compound **4** determined H-14 was in α -orientation. However, the orientation of the 14-hydroxy group was unclear through NOESY due to the use of deuterated methanol as the NMR solvent. Fortunately, crystal samples of the compound were able to be analyzed by x-ray diffraction (Figure 15). The absolute configuration of the molecule was determined to be 4*R*, 10*R*, 13*S*, 14*S*, and 15*S*. The compound

was determined to be (4*R*, 10*R*, 13*S*, 14*S*, 15*S*)-3-oxo-14 β ,16-epoxy-14 α ,15 β -dihydroxy-(9 β H)-pimar-7-en-19,6 β -olide and given the trivial name 14-hydroxyicacinlactone I.

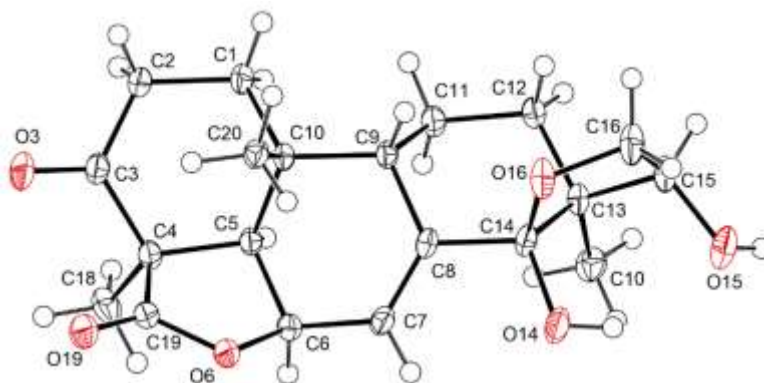


Figure 15. ORTEP representation of 14-hydroxyicacinlactone I

2.3.3 Isolation and Structure Elucidation of 9 β H-17-nor-pimarane diterpenoids

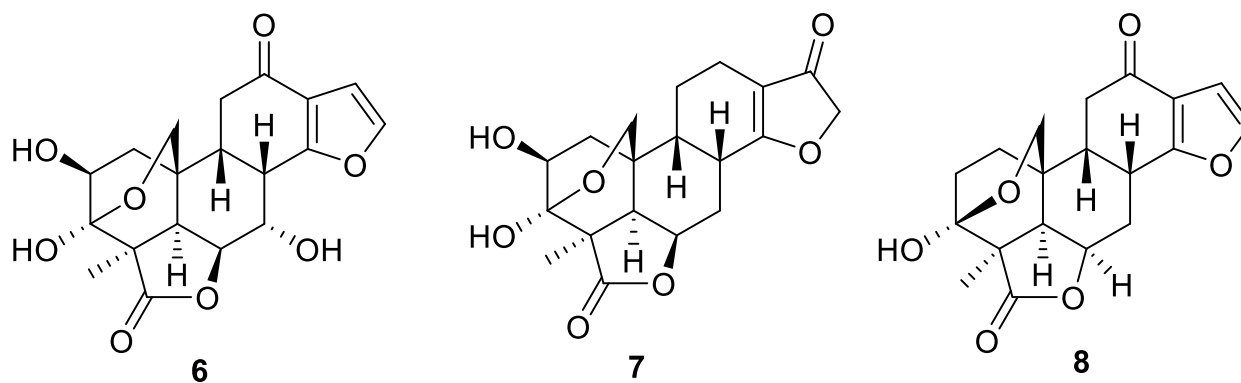


Figure 16. Isolated 9 β H-17-nor-pimarane diterpenoids from *I. trichantha*

2.3.3.1 7 α -Hydroxyicacenone (6)

7 α -Hydroxyicacenone (6): needle-like crystal; mp 244–245 °C; $[\alpha]_D^{20} = -3$ (*c* 0.2, MeOH); IR (film) ν_{\max} 3409, 2916, 1771, 1660, 1452, 1390, 1239, 1194, 1126, 1072, 1003 cm^{-1} ; UV $_{\max}$: 266 nm; ^1H NMR (methanol-*d*₄, 400 MHz) and ^{13}C NMR (methanol-*d*₄, 100 MHz), see TABLE VII; (+)-HRESIMS m/z 377.1232 $[\text{M} + \text{H}]^+$ (calcd for $\text{C}_{19}\text{H}_{21}\text{O}_8^+$, 377.1231).

Compound **6** was obtained as a needle-like crystal. A molecule formula of $\text{C}_{19}\text{H}_{20}\text{O}_8$ with 10 indices of hydrogen deficiency was deduced from HRESIMS (m/z 377.1232 $[\text{M} + \text{H}]^+$; calcd for $\text{C}_{19}\text{H}_{21}\text{O}_8^+$, 377.1231) and the ^{13}C NMR data. The IR spectrum showed two strong absorptions at 1771 and 1660 cm^{-1} , corresponding to γ -lactone and conjugated carbonyl functionalities, respectively. The ^1H NMR spectrum displayed two olefinic protons at δ_{H} 7.54 (d, $J = 2.0$ Hz, H-16) and 6.67 (d, $J = 2.0$ Hz, H-15), and a methyl group at δ_{H} 1.37 (s, CH_3 -18) (TABLE VII). The ^{13}C NMR spectrum exhibited resonances for 19 carbons (TABLE VII). Compound **6** was determined to be the 7-hydroxy derivative of icacenone (Figure 16)⁷⁶ based upon the comparison of the ^{13}C NMR data of **6** with those of icacenone, as well as interpretation of the 2D NMR data (Figure 17). In the NOESY spectrum, the following correlations were observed: between CH_3 -18 and H-1a (δ_{H} 2.41), H-2 (δ_{H} 3.99), H-5 (δ_{H} 2.52), and H-6 (δ_{H} 4.64); between H-20b (δ_{H} 3.63) and H-1b (δ_{H} 1.46) and H-9 (δ_{H} 2.19); between H-8 (δ_{H} 3.29–3.33) and H-20a (δ_{H} 4.31); and between H-8 and H-9. The orientations of 2 α -H, 5 α -H, 6 α -H, 4 α - CH_3 , as well as 8 β -H, 9 β -H, and 3 β ,20-epoxy were thus proposed (Figure 18). However, the orientation of H-7 could not be unambiguously determined from the NOESY data. Finally, single crystal X-ray diffraction was used to establish the absolute configuration as

(2*S*, 3*R*, 4*R*, 5*R*, 6*S*, 7*S*, 8*S*, 9*R*), and 10*S* (Figure 19). The structure of 7 α -hydroxyicacenone was thus defined as (2*S*,3*R*,4*R*,5*R*,6*S*,7*S*,8*S*,9*R*,10*S*)-3 β ,20:14,16-diepox-2 β ,3 α ,7 α -trihydroxy-12-oxo-17-*nor*-(9 β -H)-pimar-13(14),15-dien-19,6 β -olide.

**TABLE VII. ^1H (400 MHz) AND ^{13}C (100 MHz) NMR SPECTROSCOPIC DATA
FOR COMPOUNDS 6 AND 7 (δ in ppm)**

position	6^a	δ_{H} (J in Hz)	7^a	δ_{H} (J in Hz)
	δ_{C} , type		δ_{C} , type	
1	41.7, CH ₂	2.41, ddd (3.1, 10.2, 13.2) 1.46, dd (4.8, 13.1)	41.9, CH ₂	2.45, dd (3.5, 13.2) ^b 1.41, dd (4.8, 13.2)
2	67.1, CH	3.99, dd (4.8, 9.9)	67.2, CH	3.96, dd (4.8, 10.0)
3	97.9, C		98.0, C	
4	51.6, C		52.0, C	
5	43.5, CH	2.52, br d (5.3)	45.5, CH	2.27, br d (4.5)
6	80.2, CH	4.64, dd (2.1, 5.4)	75.4, CH	4.75, ddd/br t-like (0.6, 5.3, 5.4)
7	66.3, CH	4.38, dd (2.1, 3.6)	27.2, CH ₂	2.51, br dd (5.2, 15.8) ^b 1.90, ddd (5.2, 12.8, 16.0) ^b
8	34.8, CH	3.29–3.33 ^b	30.6, CH	2.79, m
9	38.4, CH	2.19, ddd/dt-like (4.7, 4.7, 13.6)	38.4, CH	1.66, m/br d-like
10	34.2, C		33.8, C	
11	38.2, CH ₂	2.68, dd (13.6, 16.8) 2.35, dd (4.7, 16.8)	17.9, CH ₂	1.84, br dd (5.0, 12.8) ^b 1.49, ddd (5.8, 12.9, 12.9)
12	196.8, C		18.7, CH ₂	2.34, ddd (1.1, 4.6, 16.1) 2.07, ddd (6.1, 11.5, 16.1)
13	124.1, C		112.8, C	
14	168.8, C		194.4, C	
15	107.2, CH	6.67, d (2.0)	204.1, C	
16	145.0, CH	7.54, d (2.0)	76.6, CH ₂	4.57, d (4.7)
18	17.1, CH ₃	1.37, s	17.2, CH ₃	1.33, s
19	179.5, C		180.2, C	
20	73.8, CH ₂	4.31, dd (3.5, 9.7) 3.63, dd (1.4, 9.7)	73.8, CH ₂	4.31, dd (3.5, 9.6) 3.62, dd (1.2, 9.6)

^aData were measured in methanol-*d*₄. ^bSignal was partially obscured.

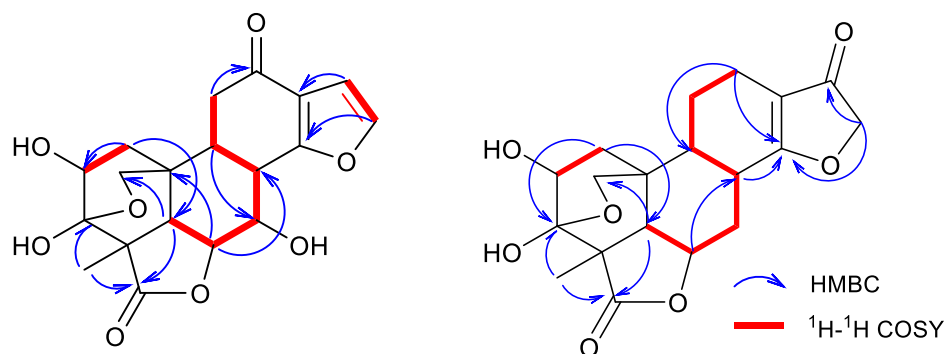


Figure 17. ^1H - ^1H COSY and select HMBC correlations for compounds 6 and 7

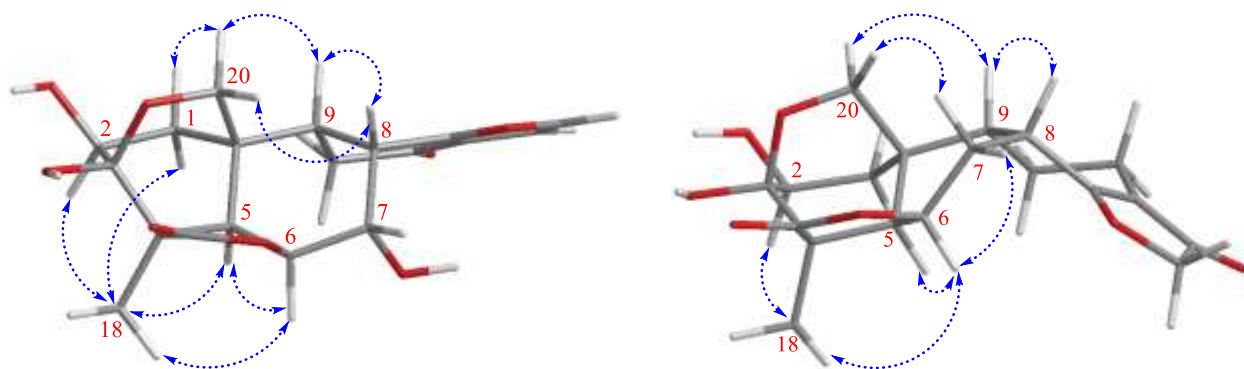


Figure 18. Key NOESY correlations for compounds 6 and 7

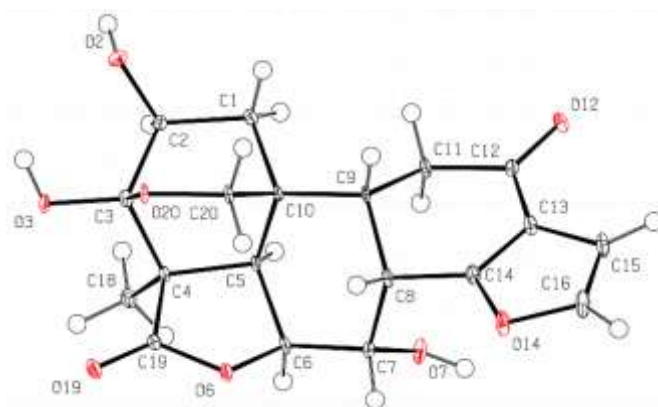


Figure 19. ORTEP representations of compound 6

2.3.3.2 2 β -Hydroxyhumirianthenolide C (7)

2 β -Hydroxyhumirianthenolide C (7): Colorless amorphous powder; $[\alpha]_D^{20} = +8$ (c 0.1, MeOH); IR (film) ν_{\max} 3427, 2919, 1767, 1691, 1605, 1434, 1357, 1296, 1232, 1174, 1066, 1048, 998, 907 cm^{-1} ; UV $_{\max}$: 270 nm; ^1H NMR (methanol- d_4 , 400 MHz) and ^{13}C NMR (methanol- d_4 , 100 MHz), see TABLE VII; (+)–HRESIMS m/z 363.1466 $[\text{M} + \text{H}]^+$ (calcd for $\text{C}_{19}\text{H}_{23}\text{O}_7^+$, 363.1438).

Compound **7** was obtained as a colorless amorphous powder. The HRESIMS data suggested a molecular formula of $\text{C}_{19}\text{H}_{22}\text{O}_7$ with nine indices of hydrogen deficiency (m/z 363.1466 $[\text{M} + \text{H}]^+$; calcd for $\text{C}_{19}\text{H}_{23}\text{O}_7^+$, 363.1438). Two strong IR absorption bands at 1767 and 1691 cm^{-1} suggested the presence of γ -lactone and conjugated carbonyl functionalities, respectively. All ^1H NMR signals were readily assignable to their attached carbons using HSQC data (TABLE VII). The ^{13}C NMR spectrum displayed 19 carbon resonances (TABLE VII) including one methyl, six methylenes, five methines, one dioxygenated secondary carbon, one oxygenated tertiary carbon, two carbonyls, and three quaternary carbons. The ^1H – ^1H COSY spectrum revealed two coupled spin systems: H-1/H-2 and H-5/H-6/H-7/H-8/H-9/H-11/H-12 (Figure 17). On the basis of HMBC results (Figure 17), compound **7** was shown to be the 2-hydroxy derivative of humirianthenolide C.⁷⁶ In the NOESY spectrum (Figure 18), H-2 (δ_{H} 3.96) correlated with CH_3 -18 (δ_{H} 1.33), suggesting the presence of a 2 β -hydroxy group. The remaining relative configurations were confirmed by the observation of the following NOESY correlations: H-6 (δ_{H} 4.75) with H-5 (δ_{H} 2.27), CH_3 -18, and H-7b (δ_{H} 1.90); H-8 (δ_{H} 2.79) with H-7a (δ_{H} 2.51) and H-9 (δ_{H} 1.66); H-20b (δ_{H} 3.62) with H-1b (δ_{H} 1.41) and H-9; H-8 with H-20a (δ_{H} 4.31); and H-1a (δ_{H} 2.45) with H-2 (δ_{H} 3.96) (Figure 18). The structure of 2 β -

hydroxyhumirianthenolide C was thus defined as 3 β ,20:14,16-diepoxy-2 β ,3 α -dihydroxy-15-oxo-17-*nor*-(9 β -H)-pimar-13(14)-en-19,6 β -olide.

2.3.3.3 **Icacinlactone E (8)**

Compound **8** was isolated as a white amorphous powder. HRESIMS analysis and ^{13}C NMR suggested a molecular formula of $\text{C}_{19}\text{H}_{20}\text{O}_6$ (m/z 345.1334 $[\text{M}+\text{H}]^+$, calculated for $\text{C}_{19}\text{H}_{21}\text{O}_6^+$, 345.1333), indicating 10 degrees of unsaturation. The ^1H NMR spectrum demonstrated a singlet methyl signal at δ_{H} 1.37 (CH_3 -18) and two doublet olefinic protons at δ_{H} 7.53 (d , $J = 2.1$, H-16) and 6.66 (dd , $J = 2.1, 0.5$, H-15). The ^{13}C spectrum displayed 19 carbon resonances. DEPT and HSQC NMR experiments aided to assign the signals as one methyl, five methylenes, six methines, one dioxygenated secondary carbon, one oxygenated tertiary carbon, two carbonyls, and three quaternary carbons. The collective data was contrasted with the previously reported results for icacinlactone E and found to be nearly identical (Figure 93, Appendix A). This determination was further confirmed after analysis of HSQC, COSY, and HMBC NMR data. Further, the relative configuration was consistent with previously reported results from a NOESY experiment.⁷⁸ This sample and subsequent isolated compounds suspected of also being icacinlactone E were analyzed by LC-MS and compared with a library of previously reported compounds. Based on retention time and low-resolution MS analysis, the isolated sample and subsequent purified material was analyzed by Shimadzu LabSolutions software and identified as icacinlactone E based on a similarity score of at least 80/100.

2.3.4 Isolation and Structure Elucidation of 17-nor-pimarane diterpenoids

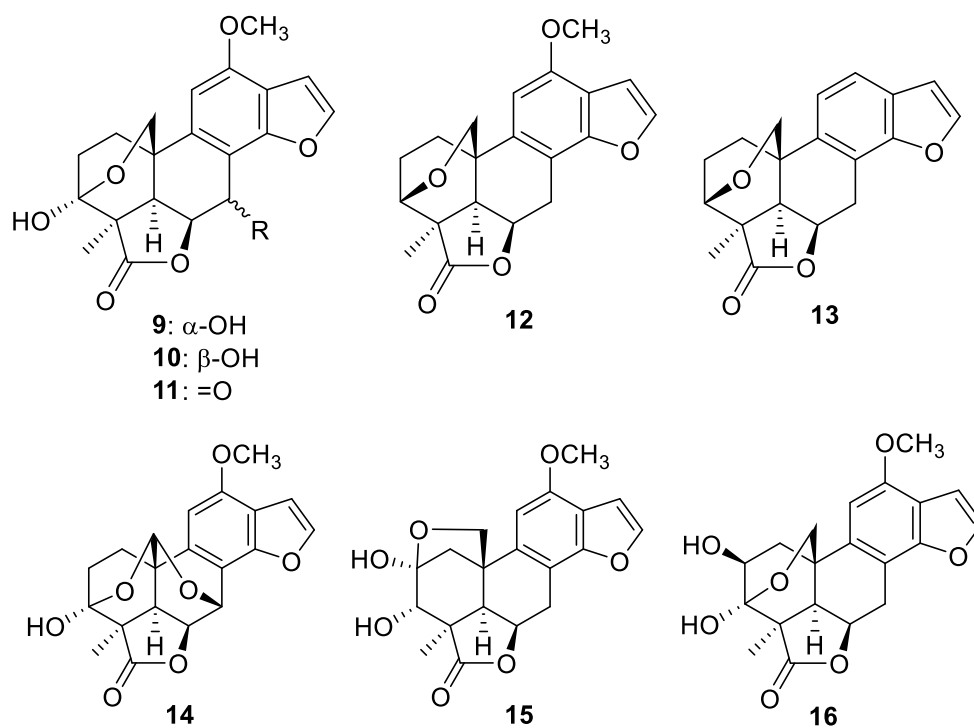


Figure 20. Isolated 17-nor-pimarane diterpenoids from *I. trichantha*

2.3.4.1 7 α -Hydroxyvicacinlactone B (9)

7 α -Hydroxyvicacinlactone B (9): Colorless amorphous powder; $[\alpha]_{\text{D}}^{20} = -2$ (*c* 0.1, MeOH); IR (film) ν_{max} 3470, 2916, 2849, 1729, 1609, 1464, 1378, 1330, 1293, 1224, 1102, 1047 cm^{-1} ; UV_{max}: 218, 252, 262 nm; ^1H NMR (methanol- d_4 , 400 MHz), see TABLE VIII; ^{13}C NMR (methanol- d_4 , 100 MHz), see TABLE IX; (+)-HRESIMS m/z 355.1204 $[\text{M} + \text{H} - \text{H}_2\text{O}]^+$ (calcd for $\text{C}_{20}\text{H}_{19}\text{O}_6^+$, 355.1176).

Compound **9** was obtained as a colorless amorphous powder. A molecular formula of $\text{C}_{20}\text{H}_{20}\text{O}_7$ with 11 indices of hydrogen deficiency was deduced from HRESIMS (m/z 355.1204 $[\text{M} + \text{H} - \text{H}_2\text{O}]^+$; calcd for $\text{C}_{20}\text{H}_{19}\text{O}_6^+$, 355.1176) and ^{13}C NMR spectroscopic data. The IR

absorption at 1729 cm^{-1} indicated the presence of a γ -lactone moiety. The ^1H NMR spectrum displayed resonances for three olefinic protons at δ_{H} 7.69 (d, $J = 2.2\text{ Hz}$, H-16), δ_{H} 6.85 (d, $J = 2.2\text{ Hz}$, H-15), 6.71 (s, H-11), a methyl group at δ_{H} 1.46 (s, CH_3 -18), and a methoxy group at δ_{H} 3.94 (s, 12- OCH_3) (TABLE VIII). Twenty carbon signals were observed in the ^{13}C NMR spectrum (TABLE IX). A comparison of the ^{13}C NMR data of **9** with those of icacinlactone B⁷⁸ and interpretation of the 2-dimensional NMR data (Figure 21) indicated that **9** was the 7-hydroxy derivative of icacinlactone B. The observation of the following NOESY correlations (Figure 21) revealed the presence of 5α -H, 6α -H, and 4α - CH_3 , as well as 7β -H and $3\beta,20$ -epoxy: H-5 (δ_{H} 2.54) correlated with H-1b (δ_{H} 1.94), H-6 (δ_{H} 4.93), and CH_3 -18 (δ_{H} 1.46); H-7 (δ_{H} 5.33) correlated with H-20a (δ_{H} 3.84); and H-1a (δ_{H} 2.75) correlated with H-20b (δ_{H} 3.73). The structure of **9**, 7α -hydroxyicacinlactone B, was defined as $3\beta,20:14,16$ -diepoxy- $3\alpha,7\alpha$ -dihydroxy-12-methoxy-17-*nor*-pimar-8(9),11,13(14),15-tetraen-19,6 β -olide.

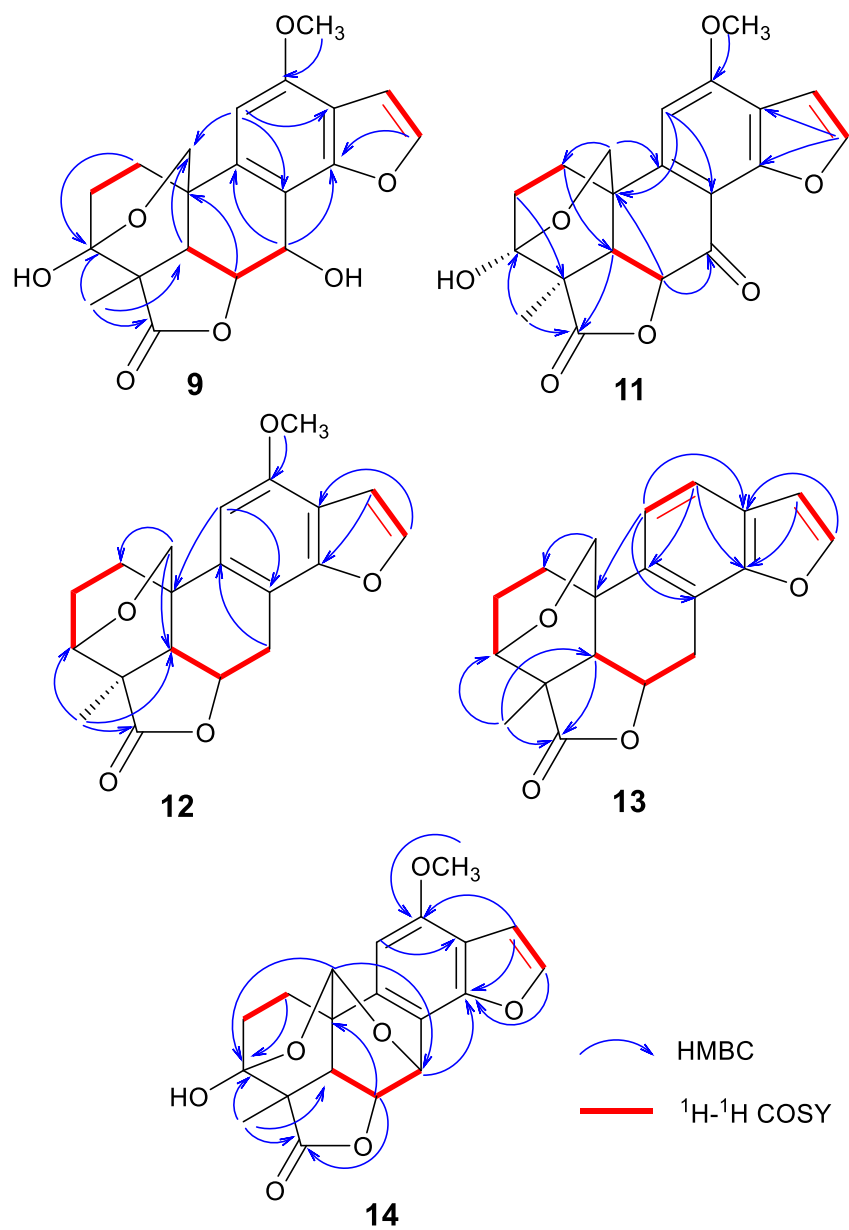


Figure 21. ^1H - ^1H COSY and selective HMBC for compounds 9 and 11-14

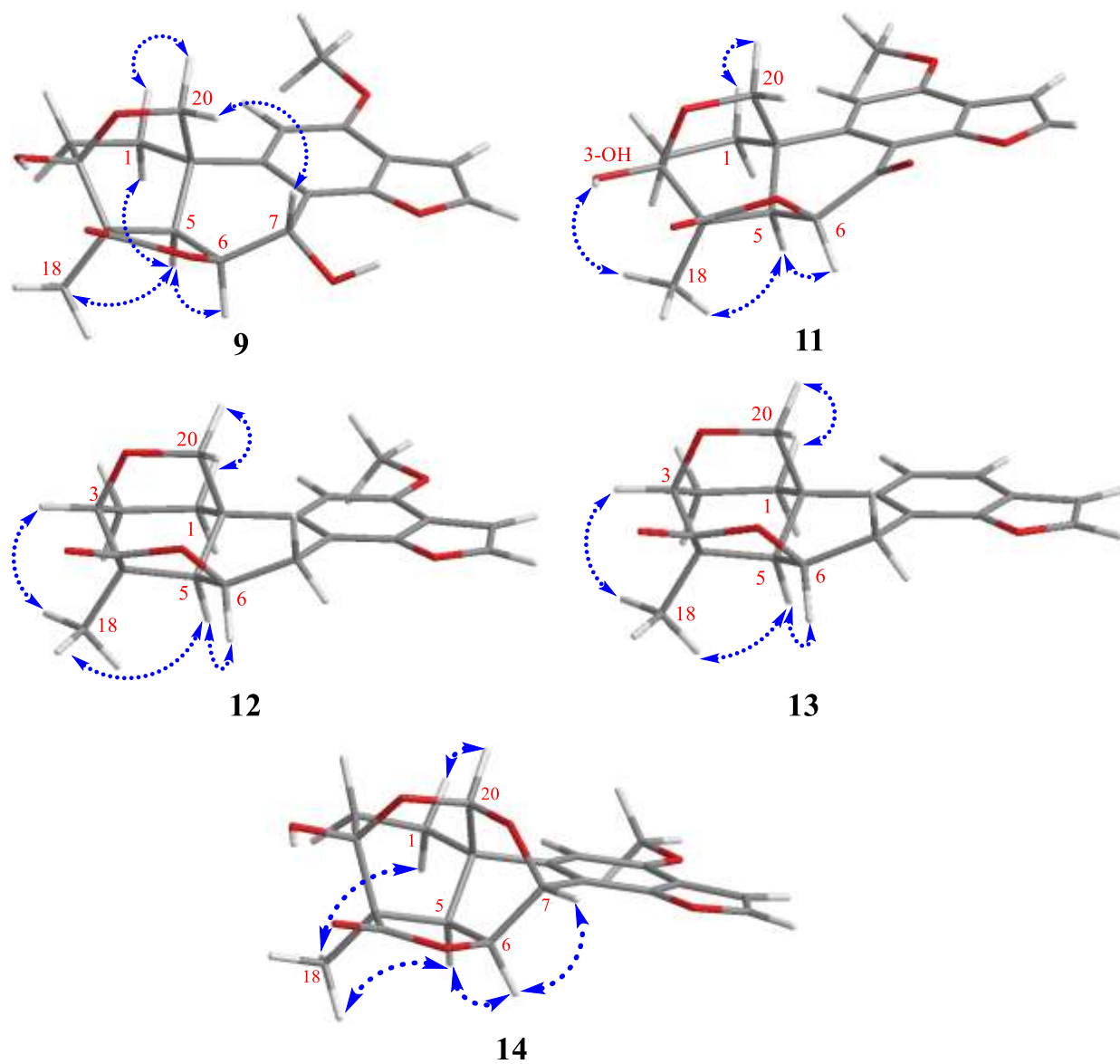


Figure 22. Key NOESY correlations for compounds 9 and 11-14

TABLE VIII. ^1H (400 MHz) NMR SPECTROSCOPIC DATA FOR COMPOUNDS 9 AND 11-14 (δ in ppm)

position	9^a δ_{H} (J in Hz)	11^b δ_{H} (J in Hz)	12^a δ_{H} (J in Hz)	13^a δ_{H} (J in Hz)	14^a δ_{H} (J in Hz)
1	2.75, ddd (4.6, 12.3, 12.3)	2.70, td (12.1, 5.1)	2.68, td (13.4, 2.2)	2.67, dd (13.0, 4.0)	2.24–2.32, m ^c
2	1.94, dddd (3.3, 3.7, 12.1, 12.5)	2.08, tt (12.0, 3.8)	1.74, m	1.76, dd (14.7, 12.0)	1.92, m
	2.29, ddd (4.6, 12.0, 14.0)	2.29, ddd (13.8, 11.7, 5.1)	2.15, m	2.15, m	2.38, m
	2.05, ddd (4.2, 11.9, 13.8)	2.21, ddd, (13.9, 11.7, 4.0)	2.06, qd (13.5, 5.0)	2.05, qd (13.2, 5.3)	
3			3.63, dt (11.9, 5.9)	3.63, dd (11.4, 5.3)	
4					
5	2.54, dd (2.0, 8.4)	2.85, dd (8.4, 2.3)	1.86, d (8.2)	1.88, d (2.1)	2.29, dd (2.3, 9.7) ^c
6	4.93, dd (4.1 8.4)	5.11, d (8.3)	4.59, m	4.61, m	4.67, dd (2.3, 9.7)
7	5.33, d (4.0)		3.25, dd (16.6, 1.4)	3.36, m	5.61, br d (2.2)
			3.06, dd (17.6, 4.4)	3.15, dd (18.1, 4.3)	
8					
9					
11	6.71, s	6.61, s	6.72, s	7.26, d (8.3)	6.70, s
12				7.45, d (8.3)	
15	6.85, d (2.2)	6.88, d (2.2)	6.82, d (2.2)	6.79, d (2.2)	6.91, d (2.2)
16	7.69, d (2.2)	7.69, d (2.2)	7.65, d (2.2)	7.74, d (2.2)	7.69, d (2.2)
18	1.46, s	1.53, s	1.46, s	1.47, s	1.42, s
20	3.84, dd (3.7, 9.8)	3.94, dd (10.3, 3.2)	4.57, dd (9.4, 2.4)	4.56, dd (10.9, 2.4)	4.99, d (2.2)
	3.73, dd (2.1, 9.7)	3.90, dd (10.2, 2.3)	4.47, d (11.0)	4.41, dd (10.9, 1.3)	
OCH ₃	3.94, s	4.05, s	3.92, s		3.98, s

^aData were measured in methanol-*d*₄. For CH₂, the deshielded signal was assigned as H_a, and the shielded signal as H_b. ^bData were measured in chloroform-*d*₄.

^cSignal was partially obscured.

TABLE IX. ^{13}C (100 MHz) NMR SPECTROSCOPIC DATA FOR COMPOUNDS 9 AND 11-14 (δ in ppm)

position	9^a δ_{C} , type	11^b δ_{C} , type	12^a δ_{C} , type	13^a δ_{C} , type	14^a δ_{C} , type
1	30.9, CH ₂	28.6, CH ₂	39.3, CH ₂	39.3, CH ₂	28.0, CH ₂
2	28.6, CH ₂	26.3, CH ₂	31.0, CH ₂	31.0, CH ₂	22.4, CH ₂
3	97.9, C	97.3, C	77.3, CH	77.3, CH	100.1, C
4	50.9, C	50.0, C	47.8, C	46.9, C	49.0, C
5	50.2, CH	49.1, CH	50.6, CH	50.4, CH	45.0, CH
6	85.7, CH	76.5, CH	63.1, CH	63.0, CH	78.0, CH
7	70.4, CH	186.1, C	32.6, C	32.9, C	68.1, CH
8	115.3, C	111.9, C	111.0, C	118.3, C	113.8, C
9	135.5, C	143.0, C	136.5, C	135.8, C	137.6, C
10	36.4, C	34.6, C	36.9, C	36.5, C	36.8, C
11	101.3, CH	100.1, CH	101.9, CH	121.4, CH	99.6, CH
12	154.5, C	158.9, C	153.3, C	120.0, CH	155.7, C
13	119.6, C	118.8, C	117.3, C	126.8, C	118.3, C
14	155.8, C	154.7, C	156.5, C	154.2, C	152.5, C
15	104.4, CH	103.8, CH	105.0, CH	107.6, CH	105.4, CH
16	145.4, CH	145.8, CH	145.2, CH	146.6, CH	145.7, CH
18	19.8, CH ₃	19.9, CH ₃	18.5, CH ₃	18.5, CH ₃	21.5, CH ₃
19	181.2, C	179.1, C	176.7, C	175.2, C	181.9, C
20	73.2, CH ₂	75.8, CH ₂	80.2, CH ₂	80.2, CH ₂	101.1, CH
OCH ₃	56.1, CH ₃	56.2, CH ₃	56.1, CH ₃		56.4, CH ₃

^aData were measured in methanol-*d*₄. ^bData were measured in chloroform-*d*₄.

2.3.4.2 7 β -Hydroxyicacinlactone B (10)

Compound **10** was isolated as a colorless amorphous powder. The ^1H spectrum displayed three olefinic protons at δ_{H} 7.69 (d, $J = 2.2$ Hz, H-16), 6.87 (d, $J = 2.2$ Hz, H-15) and 6.74 (s, H-11), a methyl group at δ_{H} 1.46 (s, CH_3 -18), and a methoxy group δ_{H} 3.96 (s, 12- OCH_3). A molecular formula of $\text{C}_{20}\text{H}_{20}\text{O}_7$ was inferred based upon the LC-MS analysis (m/z 373). Identification of the compound was accomplished primarily by comparing the ^1H spectrum with previously collected NMR data for 7 β -hydroxyicacinlactone B.⁷⁷ The two spectra are nearly identical upon comparison (Figure 108, Appendix A). Therefore, compound **10** was determined to be 7 β -hydroxyicacinlactone B.

2.3.4.3 7-Oxo-icacinlactone B (11)

7-Oxo-icacinlactone B (**11**): $[\alpha]_{\text{D}}^{20} = +3.0$ (c 0.1, MeOH); IR (film) ν_{max} 2905, 1751, 1678, 1597, 1299, 1267, 1142, 1099, 1059 cm^{-1} ; ^1H NMR (methanol- d_4 , 400 MHz), see TABLE VIII. ^{13}C NMR (methanol- d_4 , 100 MHz), see TABLE IX; (+)-HRESIMS m/z 363.1793 $[\text{M} + \text{H}]^+$ (calcd for $\text{C}_{20}\text{H}_{27}\text{O}_6^+$, 363.1802).

Compound **11** was obtained as a colorless amorphous crystal. A molecular formula of $\text{C}_{20}\text{H}_{18}\text{O}_7$ was proposed due to a protonated molecular ion at m/z 371.1108 $[\text{M} + \text{H}]^+$ (calculated for $\text{C}_{20}\text{H}_{19}\text{O}_7^+$, 371.1125), indicating 12 degrees of unsaturation. The ^1H NMR spectrum displayed three olefinic protons at δ_{H} 6.61 (s, H-11), 6.88 (d, $J = 2.2$ Hz, H-15), 7.69 (d, $J = 2.2$ Hz, H-16), a methyl signal at δ_{H} 1.53 (s, CH_3 -18), and a methoxy at δ_{H} 4.05 (s, 12- OCH_3). The ^{13}C NMR spectrum displayed 20 carbons signals corresponding to one methyl, one methoxy, three methylenes, three olefinic methines, two aliphatic methines, one dioxygenated secondary carbon, two oxygenated tertiary carbons, two carbonyls, and five quaternary carbons. A comparison of NMR data with icacinlactone B⁷⁸ suggested the compound was an oxo-derivative

at C-7 (TABLE VIII). This was supported by the significant deshielding of C-7 from δ_c 25.7 to 186.1 and its apparent shift from a methylene to a quaternary resonance with a chemical shift detective in the value range typical of carbonyls (TABLE IX). Three spin systems were identified from the ^1H - ^1H COSY spectrum: H-1a (δ_H 2.70)/H-2a (δ_H 2.29), H-5 (δ_H 2.85)/H-6 (δ_H 5.11), and H-15 (δ_H 6.88)/H-16 (δ_H 7.69) (Figure 21). Interpretation of the HMBC correlations confirm the structural similarity with icacinlactone B. The presence of 6,19- γ -lactone and 3 β ,20-epoxy bridge moieties was confirmed in addition to all other connectivity. The unassigned signal at δ_c 186.1 demonstrated correlation with H-6, which assisted to confirm the placement of the non-lactone carbonyl signal at C-7 (Figure 21). The relative configuration was proposed to be H-6 (δ_H 5.11)/H-5 (δ_H 2.85)/H-18 (δ_H 1.53)/3-OH (δ_H 4.17) in the α -position and the C3-C20 epoxy bridge in the β -position, the same relative configuration of icacinlactone B, based on the following NOESY results: CH₃-18 with H-5 and the C-3 hydroxy group, and H-9 with H-5 (Figure 22). The absolute configuration was determined to be 3*S*, 4*R*, 5*R*, 6*S*, and 10*R* based on crystal x-ray diffraction (Figure 23). The structure of the novel compound was defined as (3*S*,4*R*,5*R*,6*S*,10*R*)-3 β ,20:14,16-diepoxy-3 α -hydroxy-7-oxo-12-methoxy-17-nor-pimar-8(9),11,13(14),15-tetraen-19,6 β -olide and given the trivial name 7-oxo-icacinlactone B.

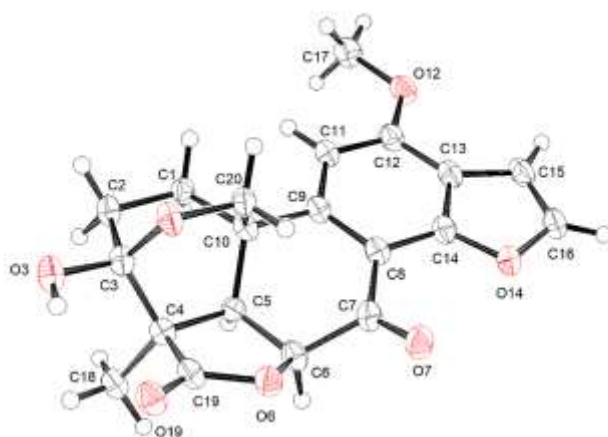


Figure 23. ORTEP representation of compound 11

2.3.4.4 3-Dehydroxyicacinlactone B (12)

3-Dehydroxyicacinlactone B (12): $[\alpha]_D^{20} = +4.2$ (*c* 0.1, MeOH); IR (film) ν_{\max} 3399, 2939, 1711, 1618, 1499, 1377, 1303, 1157, 1100, 1072, 1043 cm^{-1} ; ^1H NMR (methanol- d_4 , 400 MHz), see TABLE VIII; ^{13}C NMR (methanol- d_4 , 100 MHz), see TABLE IX; (+)-HRESIMS m/z 341.1385 $[\text{M} + \text{H}]^+$ (calcd for $\text{C}_{20}\text{H}_{21}\text{O}_5^+$, 341.1383).

Compound **12** was obtained as a white amorphous powder. HRESIMS detected a protonated molecular ion at m/z 341.1385 $[\text{M} + \text{H}]^+$ (calculated for $\text{C}_{20}\text{H}_{21}\text{O}_5^+$, 341.1383), suggesting a molecular formula of $\text{C}_{20}\text{H}_{20}\text{O}_5$, implying eleven degrees of unsaturation. The ^1H spectrum displayed resonances for three olefinic protons at δ_{H} 7.65 (d, $J = 2.2$ Hz, H-16), 6.82 (d, $J = 2.2$ Hz, H-15), and 6.72 (s), one methyl group at δ_{H} 1.46 (s, CH_3 -18), and one methoxy group at δ_{H} 3.92 (s, 12- OCH_3) (TABLE VIII). Nineteen resonances were identified in the ^{13}C spectra and a twentieth obscured resonance was determined with the assistance of the HSQC experiment (TABLE IX). The resonances include one methyl, one methoxy, four methylenes, three aliphatic methines, four olefinic methines, two oxygenated tertiary carbon, one carbonyl, and four quaternary carbons. Comparison with the ^1H and ^{13}C results of icacinlactone B⁷⁸ indicated that the compound was a dehydroxy-derivative indicated by the shielding of C-3 from δ_{C} 96.9 to 77.3. The C-6 signal also demonstrated a slight shift upfield from δ_{C} 75.0 to 63.1. This proposed structure was explored via analysis of ^1H - ^1H COSY, HSQC, and HMBC NMR data (Figure 21). The ^1H - ^1H COSY spectrum demonstrated three spin systems: H-1a (δ_{H} 2.68)/H-2 (δ_{H} 2.15)/H-3 (δ_{H} 3.63), H-5 (δ_{H} 1.86)/H-6 (δ_{H} 4.59)/ H-7a (δ_{H} 3.25), and H-15 (δ_{H} 7.65)/H-16 (δ_{H} 6.82). Interpretation of the spectrum from an HMBC experiment was used to confirm the flat structure of compound **12**. The proton signal for CH_3 -18 correlated with the C-19 (δ_{C} 176.7) lactone carbon, the methine carbon at C-5 (δ_{C} 50.6), and the oxygenated methine carbon at δ_{C} 77.3. This

carbon was assigned to C-3 which was further confirmed by the assignment of the 3,20-epoxy group based on correlations between H-20a (δ_H 4.57) with C-1 (δ_C 39.3) and C-5 (δ_C 50.6). The correlation of the carbon resonance at δ_C 153.3 with the methoxy proton signal was used to assign the methoxy group at C-12. In addition, correlations between C-8 (δ_C 111.0), C-10 (δ_C 36.9), C-12 (δ_C 153.3), and C-13 (δ_C 117.3) with H-11 (δ_H 6.72) was used to confirm the placement of the methoxy group. These connectivities were consistent with observed correlations of C-14 (δ_C 156.5) correlating with H-15 (δ_H 6.82) and C-13 (δ_C 117.3) correlating with H-16 (δ_H 7.65), which were used to assign the aromatic signals. A NOESY experiment resulted in the following correlations: H-18/H-3, H-18/H-6, H-5/H-3, and H-20b/H-1a (Figure 22). These results imply H-3, H-5, H-6, and CH₃-18 are in the α -orientation and the 3-20 epoxy bridge is β -oriented, which is consistent with icacinlactone B. Altogether, compound **12** was identified as 3 β ,20:14,16-diepoxy-7 α -hydroxy-12-methoxy-17-*nor*-pimar-8(9),11,13(14),15-tetraen-19,6 β -olide and given the trivial name 3-dehydroxyicacinlactone B.

2.3.4.5 3-Dehydroxyicacinlactone A (13)

3-Dehydroxyicacinlactone A (13): [α]_D²⁰ = +5.5 (*c* 0.1, MeOH); IR (film) ν_{\max} 1716, 1698 cm⁻¹; ¹H NMR (methanol-*d*₄, 400 MHz), see TABLE VIII; ¹³C NMR (methanol-*d*₄, 100 MHz), see TABLE IX; (+)-HRESIMS *m/z* 311.1289 [M + H]⁺ (calcd for C₁₉H₁₉O₄⁺, 311.1288).

Compound **13** was obtained as a white amorphous powder. HRESIMS detected a protonated molecular ion at *m/z* 311.1289 [M+H]⁺ (calculated for C₁₉H₁₉O₄⁺, 311.1288), suggesting a molecular formula of C₁₉H₁₈O₄. The ¹H spectrum displayed resonances for four olefinic protons at δ_H 7.26 (d, *J* = 8.3, H-11), 7.45 (d, *J* = 8.3, H-12), 6.79 (d, *J* = 2.2, H-15), and 7.74 (d, *J* = 2.2, H-16) and one methyl group δ_H 1.47 (s, CH₃-18) (TABLE VIII). Eighteen

resonances were identified in the ^{13}C spectra and a nineteenth obscured resonance was determined with the assistance of the HSQC experiment (TABLE IX). The resonances include one methyl, four methylenes, three aliphatic methines, four olefinic methines, one oxygenated tertiary carbon, one carbonyl, and four quaternary carbons. Comparison with the ^1H and ^{13}C results of icacinlactone A⁷⁸ suggested that the compound was a dihydroxy-derivative indicated by the shielding of C-3 from δ_{C} 98.2 to 77.3. The C-6 signal also had a significant shift upfield from δ_{C} 75.9 to 63.0. This proposed structure was confirmed via analysis of ^1H - ^1H COSY, HSQC, and HMBC NMR data (Figure 21). Four spin systems were identified from the ^1H - ^1H COSY spectrum: H-1 (δ_{H} 2.67)/H-2 (δ_{H} 2.15)/H-3 (δ_{H} 3.63), H-5 (δ_{H} 1.88)/H-6 (δ_{H} 4.61)/H-7 (δ_{H} 3.36), H-11 (δ_{H} 7.26)/H-12 (δ_{H} 7.45), and H-15 (δ_{H} 6.79)/H-16 (δ_{H} 7.74). The observed HMBC correlations between CH_3 -18 and C-3, C-19, and C-5 in addition to H-20 with C-1 and C-5 was used to assign the 3,20-epoxy bridge. Other HMBC correlations were consistent with icacinlactone A. The relative configuration was similarly determined to be consistent with icacinlactone A. A NOESY experiment determined H-3, H-5, H-6, and CH_3 -18 are α -oriented and the 3-20 epoxy bridge is β -oriented based on the following correlations: H-18/H-3, H-18/H-5, H-5/H-6, and H-20b/H-1a (Figure 22). Altogether, this compound was identified as 3 β ,20:14,16-diepoxy-17-norpimar-8(9),11,13(14),15-tetraen-19,6 β -olide and given the trivial name 3-dehydroxyicacinlactone A.

2.3.4.6 **Icacinlactone L (14)**

Icacinlactone L (14): Colorless amorphous powder; $[\alpha]_{\text{D}}^{20} = -13$ (c 0.1, MeOH); IR (film) ν_{max} 3382, 2910, 2848, 1739, 1602, 1355, 1238, 1179, 1117, 1029, 986 cm^{-1} ; UV $_{\text{max}}$: 218, 252, 260 nm; ^1H NMR (methanol- d_4 , 400 MHz), see TABLE VIII; ^{13}C NMR

(methanol- d_4 , 100 MHz), see TABLE IX; (+)-HRESIMS m/z 371.1138 $[M + H]^+$ (calcd for $C_{20}H_{19}O_7^+$, 371.1125).

Compound **14** was obtained as a colorless amorphous powder. Its HRESIMS showed a protonated molecular ion at m/z 371.1138 $[M + H]^+$ (calcd for $C_{20}H_{19}O_7^+$, 371.1125), suggesting a molecular formula of $C_{20}H_{18}O_7$ with 12 indices of hydrogen deficiency. The IR absorption at 1739 cm^{-1} indicated the presence of a γ -lactone moiety. The ^1H NMR spectrum displayed resonances for three olefinic protons at δ_H 6.70 (s, H-11), 6.91 (d, $J = 2.2\text{ Hz}$, H-15), and 7.69 (d, $J = 2.2\text{ Hz}$, H-16), and a methyl at δ_H 1.42 (s, CH_3 -18) (TABLE VIII). The ^{13}C NMR spectrum exhibited 20 carbon signals corresponding to a methyl, a methoxy, two methylenes, seven methines, a dioxygenated secondary carbon, two oxygenated tertiary carbons, a carbonyl carbon, and five quaternary carbons (TABLE IX). With the aid of an HSQC experiment, all proton signals were assignable to their attached carbons. The ^1H - ^1H COSY spectrum displayed three coupled spin systems, i.e. H-1 (δ_H 2.24–2.32, 1.92)/H-2 (δ_H 2.38), H-5 (δ_H 2.29)/H-6 (δ_H 4.67)/H-7 (δ_H 5.61), and H-15 (δ_H 6.91)/H-16 (δ_H 7.69), allowing the assignment of connectivity of these fragments (Figure 21). The presence of benzofuranyl and 6,19- γ -lactone moieties were proposed based on the interpretation of the HMBC data (Figure 21). The methoxy group was attached at C-12 (δ_C 155.7). The dioxygenated secondary carbon (δ_C 100.1) exhibited HMBC correlation to CH_3 -18 (δ_H 1.42, s) and was, therefore, assignable to C-3. C-10 (δ_C 36.8) showed HMBC correlations with H-2, H-11, and H-6. It is noteworthy that the proton at δ_H 4.99 (H-20) correlated to C-3 (δ_C 100.1), C-5 (δ_C 45.0), C-7 (δ_C 68.1), and C-10 (δ_C 36.8) in the HMBC spectrum, indicating the presence of an acetal moiety at C-20 (δ_C 101.1). The 2D structure was thus elucidated as shown (Figure 20). To determine the relative configuration, a NOESY experiment was performed. The observation of the following NOESY correlations indicated the

α -orientations of H-5, H-6, H-7, and CH₃-18, and β -orientations of the 3,20- and 7,20-epoxy groups: CH₃-18 correlated to H-5 and H-1a; H-6 correlated with H-5 and H-7; and H-20 correlated with H-1b (Figure 22). Consequently, the structure of icacinlactone L was defined as 3 β ,20:7 β ,20:14,16-triepoxy-3 α -hydroxy-12-methoxy-17-*nor*-pimar-8(9),11,13(14),15-tetraen-19,6 β -olide. It is the first example of a 17-*nor*-pimarane bearing a unique C-20 acetal group from *Icacina* plants.

2.3.4.7 **Icacinlactone D (15)**

Icacinlactone D was isolated as a white amorphous powder. A molecular formula of C₂₀H₂₀O₇ was suggested based upon the LC-MS result of the protonated molecular ion as m/z 373 [M+H]⁺. The ¹H NMR displayed resonances for three olefinic protons at δ_H 7.65 (d, J = 2.2 Hz, H-16), 6.85 (d, J = 2.2 Hz, H-15), and 6.65 (s, H-11), a methyl group at δ_H 1.37 (s, CH₃-18), and a methoxy group at δ_H 3.95 (s, 12-OCH₃). Shimadzu LabSolutions software was used to analyze HPLC-MS data of the unknown compound and compare with a library of previously isolated diterpenoids. Additionally, the ¹H spectra of the unknown compound and the previously isolated known compound were compared and found to be nearly identical (Figure 144, Appendix A). Based upon the collective results, the compound was determined to be icacinlactone D.

2.3.4.8 **Icacinlactone H (2 β -Hydroxy-icacinlactone B) (16)**

Icacinlactone H was isolated as a white amorphous powder. The ESIMS showed a protonated molecular ion at m/z 373 [M+H]⁺ suggesting a molecular formula of C₂₀H₂₀O₇. The ¹H NMR displayed resonances for three olefinic protons at δ_H 7.67 (d, J = 2.2 Hz, H-16), 6.85 (d, J = 2.2 Hz, H-15), and 6.68 (s, H-11), and a methyl signal at δ_H 1.44 (s, CH₃-18). Shimadzu LabSolutions software was used to analyze HPLC-MS data of the unknown compound and

compare with a library of previously isolated diterpenoids. The highest similarity score compound match was icacinlactone H with a score of 86/100 with the next highest score of 72/100. Additionally, the ^1H spectra of the unknown compound and the previously isolated known compound were compared and found to be nearly identical (Figure 147, Appendix A). Based upon the collective results, the compound was determined to be icacinlactone H.

2.3.5 Isolation and Structure Elucidation of 19-nor-pimarane diterpenoids

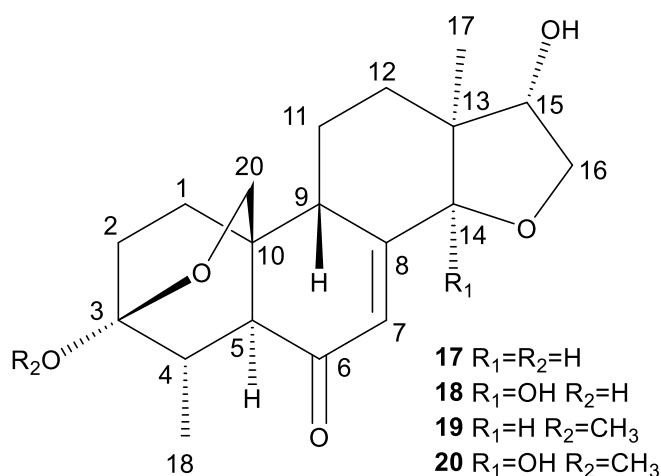


Figure 24. Isolated 19-nor-pimarane diterpenoids from *I. trichantha*

The EtOAc-soluble fraction of an acetone extract of the tubers of *I. trichantha* was subjected to repeated column chromatography over silica gel, MCI[®] gel, and reverse phase HPLC to afford four new compounds (**17** – **20**). Their planar structures were elucidated based on HRESIMS and NMR data, while the absolute configurations were determined by electronic circular dichroism analysis.

2.3.5.1 Icatrichanone (17)

Icatrichanone (17): colorless amorphous powder; $[\alpha]_{\text{D}}^{25} = -48$ (*c* 0.1, MeOH); UV_{max}: 199, 245 nm; IR ν_{max} 3361, 2921, 1670, 1632, 1465, 1378, 1088, 1047 cm⁻¹; ¹H NMR (methanol-*d*₄, 400 MHz), see TABLE X; ¹³C NMR (methanol-*d*₄, 100 MHz), see TABLE XI; (+)-HRESIMS *m/z* 335.1837 [M + H]⁺ (calcd for C₁₉H₂₇O₅⁺, 335.1853).

Compound **17** was obtained as a colorless amorphous powder. A molecular formula of C₁₉H₂₆O₅ (*m/z* 335.1840 [M+H]⁺; calculated for C₁₉H₂₇O₅⁺, 335.1859) was suggested based on the observed protonated molecular obtained with HRESIMS. The ¹³C NMR spectrum exhibited nineteen carbon signals. DEPT NMR experiments helped assign the carbons as two methyls, six methylenes, six methines, one carbonyl, one dioxygenated secondary carbon, and three quaternary carbons. The ¹H NMR displayed an isolated singlet olefinic proton at δ_{H} 5.97 (s, H-7) and two methyls at δ_{H} 0.99 (s, H-17) and 1.09 (d, *J* = 6.8 Hz, H-18) (TABLE X). All proton signals were assigned to their corresponding carbon by the HSQC experiment (TABLE XI).

TABLE X. ¹H (400 MHz) NMR SPECTROSCOPIC DATA OF COMPOUNDS 17-20 (δ in ppm)

position	17^a δ _H (J in Hz)	18^a δ _H (J in Hz)	19^a δ _H (J in Hz)	20^b δ _H (J in Hz)
1	1.84, m ^c	1.85, m ^c	1.83, m	1.83, m
	1.70, m	1.71, dd (11.7, 1.6)	1.72, dd (11.2, 2.2)	1.65, dd (9.4, 4.7)
2	2.03, tdd (15.7, 7.5, 4.8)	2.03, dt (12.5, 1.9)	2.00, m	2.07-2.12, m
	1.84, m ^c	1.83, m ^c	1.93, dd (10.7, 2.7)	1.91-1.98, m
4	2.67, m	2.69, m	2.80, qdd (7.2, 3.5, 2.3)	2.97, m
5	2.27, dd (4.0, 2.0)	2.26, dd (4.0, 2.1)	2.26, dd (3.8, 2.0)	2.10, m ^c
7	5.97, s	6.22, s	5.98, s	6.29, s
9	2.18, dd (12.6, 3.7)	2.13, dd (12.7, 3.7)	2.16, dd (12.2, 3.7)	2.10, m ^c
11	1.86, m ^b	1.86, m ^c	1.87, m	2.07-2.12, m
	1.63, m	1.66, dt (12.4, 3.6)	1.65, tdd (12.4, 9.5, 2.7)	1.91-1.98, m
12	1.48, m	1.53, dt (13.7, 3.3)	1.48, m	1.55-1.62, m
		1.41, ddd (13.6, 12.6, 4.3)	1.45, m	1.32, ddd (13.7, 13.1, 4.1)
14	4.02, s		4.02, s	
15	3.85, dd (10.8, 4.7)	3.84, dd (5.4, 1.5)	3.84, dd (4.8, 1.3)	3.89, dd (9.0, 5.8)
16	4.43, dd (10.1, 4.9)	4.47, dd (10.0, 5.4)	4.44, dd (10.0, 4.8)	4.50, dd (10.6, 5.3)
	3.73, dd (10.3, 1.1)	3.95, dd (10.0, 1.5)	3.73, dd (10.0, 1.3)	4.07, d (10.5)
17	0.99, s	1.05, s	0.99, s	1.06, s ^c
18	1.09, d (7.2)	1.11, d (7.2)	1.03, d (7.2)	1.05, br d (7.1) ^c
20	3.80, dd (9.0, 2.9)	3.77, dd (9.2, 2.9)	3.80, dd (9.1, 3.2)	3.86, dd (9.4, 3.5)
	3.63, dd (9.0, 2.0)	3.62, dd (9.0, 2.1)	3.62, dd (9.1, 2.1)	3.61, dd (9.3, 2.2)
OCH ₃			3.26, s	3.31, s
14-OH				3.10, s
15-OH				2.79, d (9.3)

^aData measured in methanol-*d*₄. ^bData measured in chloroform-*d*. ^cSignal partially obscured. For CH₂, the deshielded signal was assigned as H_a, and the shielded signal as H_b.

TABLE XI. ^{13}C (100 MHz) NMR SPECTROSCOPIC DATA OF COMPOUNDS 17-20 (δ in ppm)

position	17^a δ_C	18^a δ_C	19^a δ_C	20^b δ_C
1	30.3, CH ₂	30.5, CH ₂	30.1, CH ₂	29.7, CH ₂
2	27.9, CH ₂	27.9, CH ₂	25.4, CH ₂	25.6, CH ₂
3	98.7, C	98.7, C	101.9, C	100.2, C
4	37.4, CH	37.3, CH	34.5, CH	32.1, CH
5	53.7, CH	53.2, CH	53.5, CH	52.3, CH
6	200.5, C	201.0, C	200.4, C	198.3, C
7	124.8, CH	124.0, CH	124.9, CH	123.6, CH
8	163.2, C	162.9, C	163.2, C	159.1, C
9	39.4, CH	41.3, CH	39.3, CH	40.0, CH
10	36.7, C	37.0, C	36.7, C	35.9, C
11	26.5, CH ₂	26.4, CH ₂	26.5, CH ₂	25.6, CH ₂
12	32.9, CH ₂	34.9, CH ₂	32.9, CH ₂	33.7, CH ₂
13	52.5, C	55.1, C	52.5, C	54.1, C
14	87.3, CH	106.4, C	87.3, CH	106.0, C
15	79.8, CH	79.6, CH	79.8, CH	79.1, CH
16	76.8, CH ₂	76.1, CH ₂	76.8, CH ₂	76.0, CH ₂
17	15.2, CH ₃	13.7, CH ₃	15.2, CH ₃	13.2, CH ₃
18	18.8, CH ₃	18.8, CH ₃	18.4, CH ₃	18.5, CH ₃
20	72.2, CH ₂	72.2, CH ₂	72.1, CH ₂	71.4, CH ₂
OCH ₃			49.6, CH ₃	49.4, CH ₃

^aData measured in methanol-*d*₄. ^bData measured in chloroform-*d*.

Four coupled spin systems were identified by interpreting correlations in the ^1H - ^1H COSY experiment: H-1 (δ_{H} 1.84, 1.70) / H-2 (δ_{H} 2.03, 1.84), H-18 / H-4 (δ_{H} 2.67) / H-5 (δ_{H} 2.27), H-9 (δ_{H} 2.18) / H-11 (δ_{H} 1.86, 1.63) / H-12 (δ_{H} 1.48), and H-15 (δ_{H} 3.85) / H-16 (δ_{H} 4.43, 3.73). Interpretation of HMBC data led to the proposed flat structure of **1** (Figure 25). Establishment of the bicyclic A-ring was completed with experimental NMR data and comparison with previously reported results. The chemical shift of C-20 (δ_{C} 72.2) suggested an oxygenated methylene carbon. The associated protons (δ_{H} 3.80, 3.63) correlated with C-1 (δ_{C} 30.3), C-3 (δ_{C} 98.7), and C-5 (δ_{C} 53.7). These signals and the distinguished chemical shift of C-3 suggested a 3,20-ether bridge that is common in other pimaranes reported from this species. The correlation between H-18 and C-3 further evidenced this interpretation. Previously reported pimarane diterpenes from *Icacina* possess a γ -lactone moiety usually involving C-4, C-19, and C-6. The absence of a characteristic lactone carbon signal and the presence of a carbon signal in the ketone chemical shift range suggested the absence of the lactone group. The observed signals from H-5 (δ_{H} 2.27) to C-10 (δ_{C} 36.7) and C-6 (δ_{C} 200.5) helped establish the B-ring and assign the suspected ketone carbon.

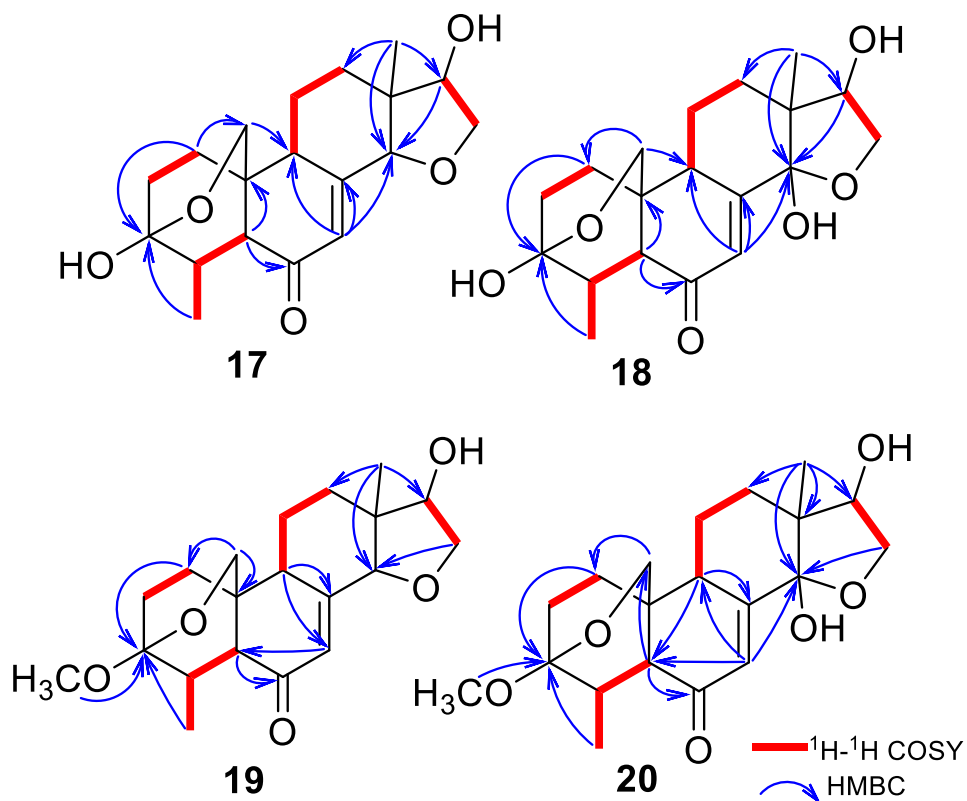


Figure 25. ^1H – ^1H COSY and selective HMBC for compounds **17**–**20**

Next, the observed correlations of the methyl protons of H-17 (δ_{H} 0.99) with C-13 (δ_{C} 52.5), C-14 (δ_{C} 87.3), and C-15 (δ_{C} 79.8) suggested the presence of a benzofuran group. A correlation to C-14 from H-15 (δ_{H} 3.85) and H-7 (δ_{H} 5.97) supported its association with the benzofuran and the location of the C-7 (δ_{C} 124.8), C-8 (δ_{C} 163.2) alkene group, respectively. The lone olefinic proton H-7 correlation with C-8 confirms the unsaturated bond. The other key correlation is with C-9 (δ_{C} 39.4), which along with H-20 (δ_{H} 3.80, 3.63), helped support the location of the alkene in the B-ring and established the C-ring. The correlation between H-17 and C-12 (δ_{C} 32.9) supported this as well to give the proposed structure for **17**. The relative configuration was determined by interpretation of NOESY results (Figure 26). Key correlations observed include H-9/H-20, H-4/H-18, H-7/H-14/H-17, and H-15/H-14. All previous pimaranes

reported from *I. trichantha* whose C-9 is a methine share the same β -orientation for its proton. Therefore, we assume the C-20/C-10 bond to also be in β -orientation while H-5 and H-18 are configured in α -orientation. The correlation between H-7 and H-14 provided strong evidence H-14 and thus H-17 were in the same α -orientation. H-15 demonstrating correlation with H-12 suggests an opposite orientation from H-17.

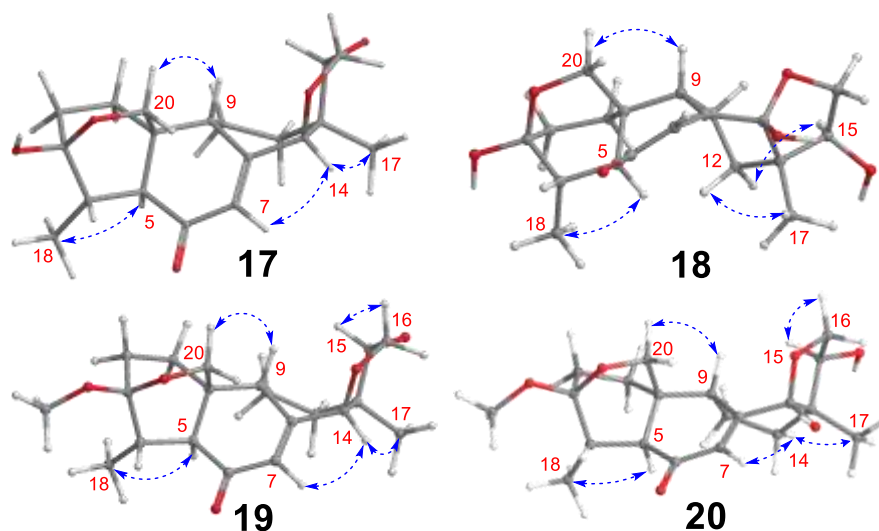


Figure 26. Key NOESY correlations for compounds 17-20

Absolute configuration of **17** was determined with electronic circular dichroism (ECD) calculations. Using the time-dependent density functional theory (TDDFT) method, the calculated ECD spectrum was generated along with its enantiomer based upon the determined relative configuration. The experimental ECD spectrum of **17** had similar Cotton effects as the calculated ECD for the proposed structure of **17** (Figure 27). Together, the determined structure of **17**, given the trivial name icatrichanone, is (3*S*,4*S*,5*S*,9*S*,10*S*,13*S*,14*S*,15*S*)-3,20:14 β ,16-diether-3,15 α -dihydroxy-6-oxo-19-nor-pimar-7-ene. This is the first reported 19-nor-pimarane from this species.

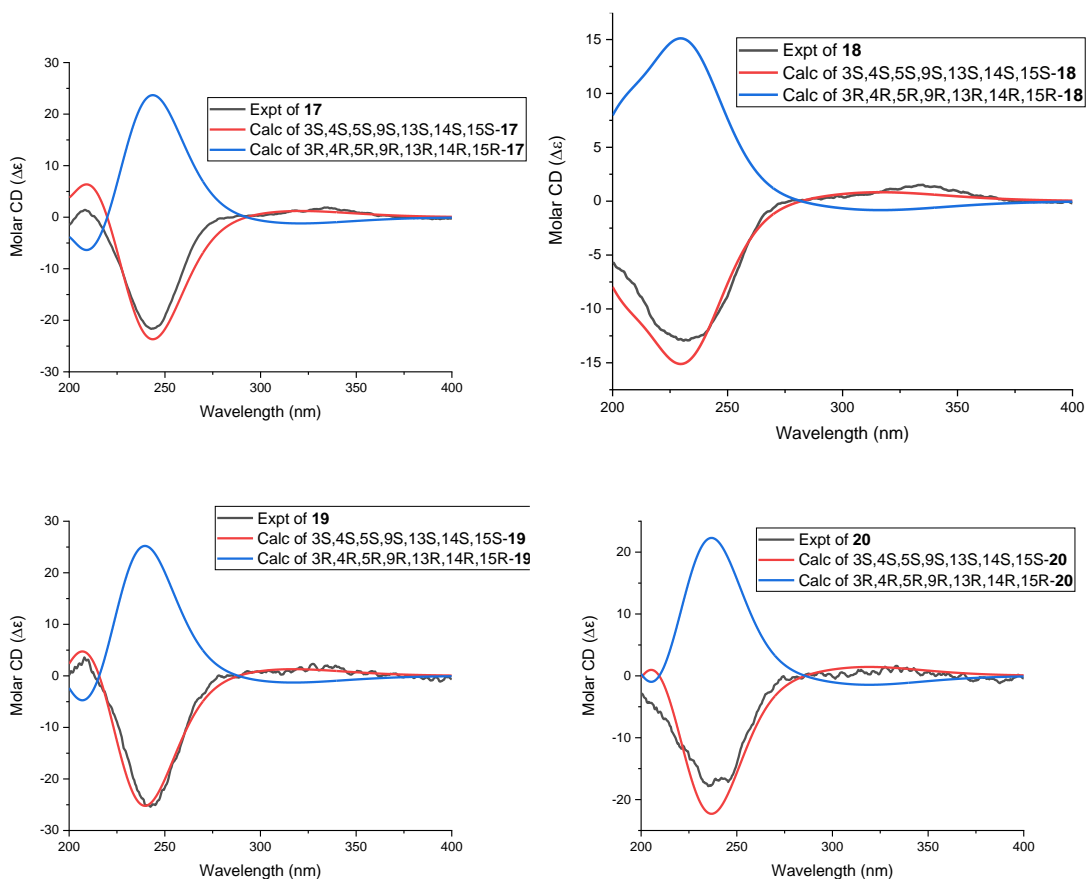


Figure 27. Experimental ECD spectra for 17-20, and the calculated ECD spectra for 17-20, and their enantiomers.

2.3.5.2 14-Hydroxyicatrichanone (18)

14-Hydroxyicatrichanone (18): Colorless amorphous powder; $[\alpha]_D^{25} = -165$ (c 0.33, MeOH); UV_{max}: 199, 242 nm; IR ν_{max} 3368, 2935, 1669, 1042; ; ^1H NMR (methanol- d_4 , 400 MHz), see TABLE X; ^{13}C NMR (methanol- d_4 , 100 MHz), see TABLE XI; (+)-HRESIMS m/z 351.1817 $[\text{M} + \text{H}]^+$ (calcd for $\text{C}_{19}\text{H}_{27}\text{O}_6$, 351.1802).

Compound **18** was isolated as a colorless amorphous powder. The HRESIMS result (m/z 351.1817 $[\text{M}+\text{H}]^+$; calculated for $\text{C}_{19}\text{H}_{27}\text{O}_6^+$, 351.1802) suggested a molecular formula of

$C_{19}H_{26}O_6$ with seven degrees of unsaturation. The ^{13}C NMR spectrum displayed twenty carbons corresponding to two methyls, a methoxy, six methylenes, five methines, a carbonyl, two dioxygenated secondary carbons, and three quaternary carbons. These assignments were confirmed with DEPT NMR (TABLE XI). All proton signals were assigned to their respective carbon including an isolated singlet olefinic proton at δ_H 6.22 (s, H-7) and two methyls at δ_H 1.05 (s, H-17) and 1.11 (d, $J = 7.2$ Hz, H-18) (TABLE X). The 1H - 1H COSY spectrum allowed the unambiguous assignment of coupled spin systems H-1 (δ_H 1.85, 1.71) / H-2 (δ_H 2.03, 1.83), H-18 (δ_H 1.11) / H-4 (δ_H 2.69) / H-5 (δ_H 2.26), H-9 (δ_H 2.13) / H-11 (δ_H 1.86, 1.66) / H-12 (δ_H 1.53, 1.41), and H-15 (δ_H 3.84) / H-16 (δ_H 4.47, 3.95). Upon comparison with the 1H - 1H COSY, HSQC, and HMBC NMR data of **17**, it became clear that compound **18** is a similar structure. The 3,20-ether moiety and ketone were clearly identified. The quaternary carbon at δ_C 106.4 had HMBC correlations with H-7 (δ_H 6.22), H-15 (δ_H 3.84), and H-17 (δ_H 1.05) which led to its assignment as C-14 (Figure 25). In comparison with **17**, C-14 was deshielded by 19.1 ppm. This led to speculation of a substitution with a hydroxyl group. The 2D structure of **18** was thus proposed as shown (Figure 24). NOESY was used to determine the relative configuration. The observed correlations of H-18 with H-5 and H-9 with H-20a (δ_H 3.77) indicated their assignments as α -orientation and β -orientation, respectively. In the benzofuran ring portion, H-15 correlated with H-12, indicating a β -orientation. H-17 only showed a strong correlation with H-12 as well, so the orientation was assumed to be similar to **17** (Figure 26). The ECD spectra for (3*S*,4*S*,5*S*,9*S*,10*S*,13*S*,14*S*,15*S*)-**18** and its enantiomer were calculated using the TDDFT method. The experimental ECD spectrum for **18** closely matched the calculated spectrum for (3*S*,4*S*,5*S*,9*S*,10*S*,13*S*,14*S*,15*S*) (Figure 27). Therefore, the structure of **18**, given the trivial name

14-hydroxy-icatrichanone, was determined to be (3*S*,4*S*,5*S*,9*S*,10*S*,13*S*,14*S*,15*S*)-3,20:14 β ,16-diether-3,14 α ,15 α -trihydroxy-6-oxo-19-nor-pimar-7-ene.

2.3.5.3 **3-Methoxyicatrichanone (19)**

3-O-Methylicatrichanone (19): Colorless amorphous powder; $[\alpha]_D^{25} = -63$ (*c* 0.03, MeOH); UV_{max}: 200, 242 nm; IR ν_{max} 3342, 2943, 1631, 1026; ; ^1H NMR (methanol-*d*₄, 400 MHz), see TABLE X; ^{13}C NMR (methanol-*d*₄, 100 MHz), see TABLE XI; (+)-HRESIMS m/z 349.2014 $[\text{M} + \text{H}]^+$ (calcd for C₂₀H₂₉O₅, 349.2010).

Compound **19** was isolated as a white amorphous powder. A molecular formula of C₂₀H₂₈O₅ with seven degrees of unsaturation was suggested by HRESIMS (m/z 349.2014 $[\text{M} + \text{H}]^+$; calculated for C₂₀H₂₉O₅⁺, 349.2010). The ^{13}C NMR spectrum displayed twenty carbons corresponding to two methyls, a methoxy, six methylenes, six methines, a carbonyl, a dioxygenated secondary carbon, and three quaternary carbons. The ^1H NMR spectrum displayed an isolated olefinic proton at δ_{H} 5.98 (s, H-7), a methoxy at δ_{H} 3.26 (s, 3-OCH₃), and two methyls at δ_{H} 0.99 (s, H-17) and 1.03 (d, $J = 7.2$ Hz, H-18) (TABLE X). HSQC was used to designate proton signals to their respective carbon. Initial impression of the HSQC, COSY, and HMBC spectra for compound **19** suggested a similarity with **17** and **18** (Figure 25). The ^1H - ^1H COSY spectrum displayed four coupled spin systems: H-1 (δ_{H} 1.83, 1.72) / H-2 (δ_{H} 2.00, 1.93), H-18 (δ_{H} 1.03) / H-4 (δ_{H} 2.80) / H-5 (δ_{H} 2.26), H-9 (δ_{H} 2.16) / H-11 (δ_{H} 1.87, 1.65) / H-12 (δ_{H} 1.48, 1.45), and H-15 (δ_{H} 3.84) / H-16 (δ_{H} 4.44, 3.73). Long range coupling was also observed between H-20 and H-5. HMBC experiment was used to determine the planar structure. The downfield carbon C-3 (δ_{C} 101.9) correlated with H-2, H-18, and H-20 (δ_{H} 3.80, 3.62). Combined with the observed correlation signals between H-20 and C-1 (δ_{C} 30.1), C-5 (δ_{C} 53.5), and C-10 (δ_{C} 36.7), and the COSY observed H-18/H-4/H-5 spin system, a 3,20-ether bridge was proposed. Finally,

the correlation of the methoxy proton signal (δ_{H} 3.26) with C-3 strongly suggested the substitution of 3-hydroxyl with a methoxy group. The observed correlation between H-5 and the ketone signal (δ_{C} 200.4) was essential to establish the position of the carbonyl at C-6. Taken with correlations between H-7 (δ_{H} 5.98) with C-5 and H-9 with C-7 (δ_{C} 124.9), the alkene group was assigned in the β to the carbonyl. Observed correlations of methyl H-17 (δ_{H} 0.99) with C-12 (δ_{C} 32.9), C-13 (δ_{C} 52.5), C-14 (δ_{C} 87.3), and C-15 (δ_{C} 79.8) helped assign its location bonded to the quaternary C-13. The benzofuran group was obvious upon comparison with NMR results for compound **1**. Relative configuration was determined with the NOESY experiment (Figure 26). The spectrum showed observed correlations for H-5 with H-18 and H-9 with H-20. H-5 and H-18 were assigned in α -orientation while H-9 and H-20 as β -orientation, the same configurations as compounds **17** and **18**. Both H-7 and methyl group H-17 correlated with H-14, suggesting both are in α -orientation. Finally, H-15 correlated with the equatorial H-16 proton, so both were assigned in β -orientation. Using the TDDFT method, the ECD spectra for **19** and its enantiomer were calculated and compared with the experimental ECD (Figure 27). The observed Cotton effects were closer to (3*S*,4*S*,5*S*,9*S*,10*S*,13*S*,14*S*,15*S*)-**19**. Therefore, compound **19** was determined to be (3*S*,4*S*,5*S*,9*S*,10*S*,13*S*,14*S*,15*S*)-3,20:14,16-diether-15 α -hydroxy-3 β -methoxy-6-oxo-19-nor-pimar-7-ene and given the trivial name 3-methoxy-icatrchanone.

2.3.5.4 3-Methoxy-14-hydroxyicatrchanone (20)

3-O-Methyl-14-hydroxyicatrchanone (20): Colorless amorphous powder; $[\alpha]_{\text{D}}^{25} = -34$ (*c* 0.1, MeOH); UV_{max}: 203, 240 nm; IR ν_{max} 3424, 2933, 1673, 1044; ; ^1H NMR (chloroform-*d*, 400 MHz), see TABLE X; ^{13}C NMR (chloroform-*d*, 100 MHz), see TABLE XI; (+)-HRESIMS m/z 365.1982 $[\text{M} + \text{H}]^+$ (calcd for $\text{C}_{20}\text{H}_{29}\text{O}_6$, 365.1959).

Compound **20** was isolated as a colorless amorphous powder. A molecular formula of $C_{20}H_{28}O_6$ with seven degrees of unsaturation was suggested by HRESIMS (m/z 365.1982 $[M+H]^+$; calculated for $C_{20}H_{29}O_6^+$, 365.1958). The ^{13}C NMR spectrum displayed twenty carbons corresponding to two methyls, a methoxy, six methylenes, six methines, a carbonyl, a dioxygenated secondary carbon, and three quaternary carbons. The 1H NMR spectrum displayed an isolated olefinic proton at δ_H 6.29 (s, H-7), a methoxy at δ_H 3.31 (s, 3-OCH₃), and two methyls at δ_H 1.06 (s, CH₃-17) and 1.05 (d, J = 7.1 Hz, CH₃-18) (TABLE X). The 1H - 1H COSY spectrum displayed four coupled spin systems H-1 (δ_H) / H-2 (δ_H), H-18 (δ_H 1.05) / H-4 (δ_H 2.94) / H-5 (δ_H 2.08), H-9 (δ_H 2.17) / H-11 (δ_H 1.57, 1.86) / H-12 (δ_H 1.48), and H-15 (δ_H 3.93) / H-16 (δ_H 3.80, 4.40). Comparison of ^{13}C NMR results, along with assessment of 1H - 1H COSY, HSQC, and HMBC data suggested **20** is the 3-methoxy, 14-hydroxy derivative of **17** (Figure 24).

Relative configuration was determined with NOESY experiment. Observed correlations included H-9 with H-20a (δ_H 3.86), H-5 with H-2, H-15 with equatorial H-16a, consistent with the orientations determined in compounds **17-19**. NMR experiments for **20** were obtained in chloroform-*d* solvent, which allowed visualization of correlations between 14-OH (δ_H 3.10) with H-7 and 17-CH₃. Therefore, the proposed orientations are as follows: H β -9, 3 β -20-ether, 15 β -H and 5 α -H, 17 α -CH₃, 18 α -CH₃, and 14 α -OH (Figure 26). Finally, the absolute configuration for **20** was determined to be 3*S*,4*S*,5*S*,9*S*,10*S*,13*S*,14*S*,15*S* by ECD. The experimental ECD spectrum for **20** had more similar Cotton effects with the calculated ECD spectra of (3*S*,4*S*,5*S*,9*S*,10*S*,13*S*,14*S*,15*S*)-**20** than its enantiomer, which were calculated using the TDDFT method (Figure 27). Compound **20** was thus determined to be (3*S*,4*S*,5*S*,9*S*,10*S*,13*S*,14*S*,15*S*)-3,20:14 β ,16-diether-14 α ,15 α -dihydroxy-3 β -methoxy-6-oxo-19-nor-pimar-7-ene and given the trivial name 3-methoxy-14-hydroxy-icatrichanone.

2.3.5.5 Biogenesis Discussion

Several *nor*-pimaranes have been reported from *I. trichantha*, but the only compound with a similar 19-*nor*-structure is icacintrichanone (**22**), which is actually a 17,19-di-*nor*-pimarane.⁸⁹ A review of the literature shows several 19-*nor*-diterpenoids derived from plant species in the Erythroxylaceae,¹⁴⁴ Annonaceae,¹⁴⁵ Meliaceae,¹⁴⁶ Euphorbiaceae,¹⁴⁷ and Araliaceae¹⁴⁸ families. One group that reported¹⁴⁹ such a compound (19-*nor*-kauran-4 α -ol-17-oic acid), coincidentally also from a West African species *Annona senegalensis* known to produce kaurene diterpenoids,^{150,151} hypothesized the *nor*-diterpenoid may be an artifact due to oxidation.¹⁵⁰ Isolated kaurenes possessed aldehyde and carboxylic acid groups at the C-4 position, which the authors suspected oxidized spontaneously to a hydroxy group, resulting in the *nor*-diterpenoid. However, there were no reports of structural analogues with oxidation at C-6 as observed with compounds **17** – **20**. Though this natural product was similarly a 19-*nor*-diterpenoid, we suspect their respective biogenesis differed. However, compounds **19** and **20** are suspected to be artifacts resultant of the isolation process using methanol solvent. Previous reports of isolation of compounds with hemiketal groups determined isolation schemes can result in artifacts with converted hemiacetyl groups.¹⁵²

At initial examination, the structural similarity between compound **1** and chemotaxonically prominent humirianthol suggests a possible modification via decarboxylation of the lactone moiety. A search of the literature did not produce examples of such a transformation except for one recent report. A closely related 19-*nor*-diterpenoid, *nor*-annonalide, was reported following bioconversion of annonalide by growing cells of *Fusarium oxysporum* f. sp. *tracheiphilum* (UFCM 0089) cells.¹⁵³ The proposed pathway has been applied to compound **17** (Figure 28). The *nor*-annonalide structure is nearly identical to icatrighanone

just as annonalide is similar to humirianthol (compound **V**) with the only major difference being the loss of the tetrahydrofuran D-ring due to lack of cyclization of a hydroxyacetal. The proposed pathway identified the formation of a C-4 carboxylic acid intermediate (compound **V**) via hydrolysis as important to the bioconversion process. This intermediate is similar to the *syn*-pimaradien-19-oic acid product (compound **II**) of CYP99A3 catalyzed reactions of the momilactones,^{154,155} lactone diterpenoids structurally similar to those from *I. trichantha*. Based on theoretical modeling, the intermediate could plausibly interact with the catalytic site of pyruvate decarboxylase to produce the final product. We hypothesize a similar biogenetic pathway may have resulted in compounds **17** – **20**.

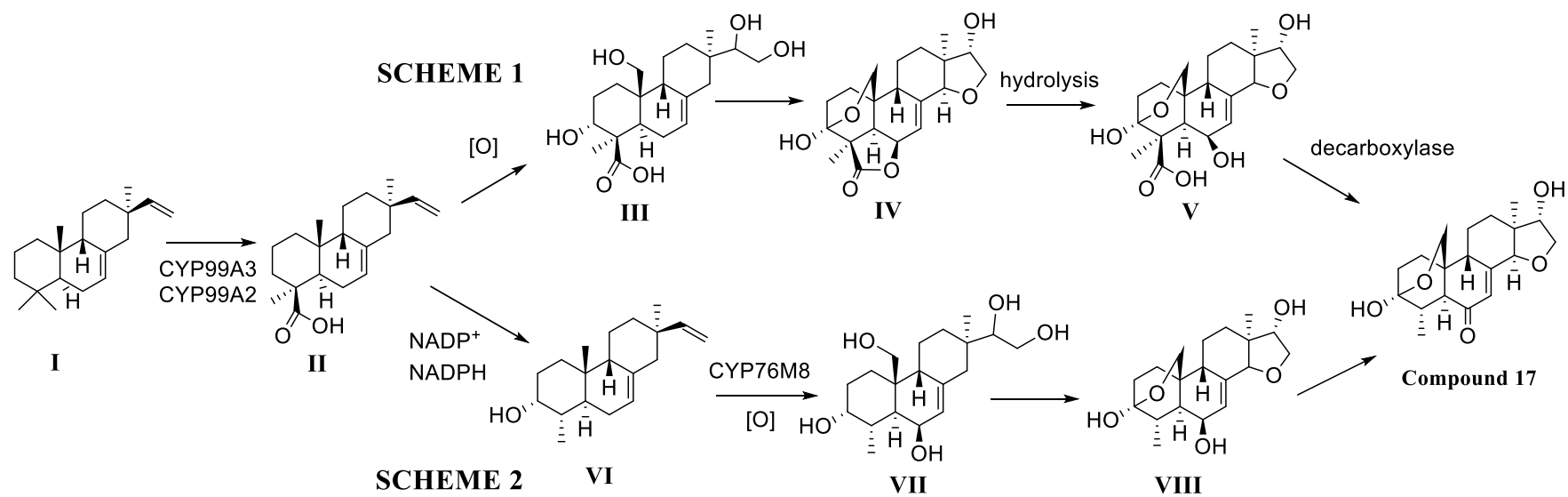


Figure 28. Proposed biogenesis for compound 17 via Scheme 1 and Scheme 2

An alternative biogenetic pathway was suggested based upon two observations from the literature. First, higher plants possess step-wise mechanisms for the demethylation of C-4 dimethyl-sterols in the biosynthesis of phytosterols. There is well-established evidence these processes involve the demethylation of C-4 intermediates,^{156,157} decarboxylation of C-4^{158–160} or other alternative mechanisms that result in a product with only one methyl group removed. Second, another closely related 19-*nor*-diterpenoid, momilactone E, was previously isolated from *Oryza sativa*.¹⁶¹ No indication of the possibility of momilactone E being an artifact has been published to our knowledge. We propose a possible biogenesis for compounds **17** – **20** combining these two concepts (Figure 28) where the C-4 decarboxylation occurs earlier in the biogenetic pathway than Scheme 1. *O. sativa* is well-known to produce momilactones, and a biogenetic pathway has been proposed^{154,155} that involves the mevalonate pathway to produce a (9 β H)-pimara-7,15-diene precursor (compound **I**). Cytochrome P450s, including CYP99A2 and CYP99A3,¹⁵⁴ are also involved to produce syn-pimara-7,15-dien-19-oic acid (compound **II**) from which further lactone derivatives can be formed, such as humirianthol. Alternatively, these enzymes may not be involved and there is only C-4 demethylation of the precursor. A study of *O. sativa* biosynthetic gene clusters also identified hydroxylase activity due to CYP76M6 and CYP76M8, which can result in β -hydroxylation of C-6.¹⁶² Therefore, oxidation of a 4 α -methyl intermediate (compound **VI**) that is also hydroxylated by CYP76M6/CYP76M8 or a similar enzyme, may results in a 19-*nor*-diterpenoid with oxidation at C-6 specifically (compound **VII/VIII**). Along this line of thought, the alternative biogenetic pathway in Scheme 2 is proposed. This scheme may also explain the unique structure of momilactone E since no biogenesis has been proposed to our knowledge. However, the biosynthetic origin for icatrichanone and related compounds is currently unclear and requires further analysis.

2.3.6 Isolation and Structure Elucidation of Di-*nor*-pimaranes

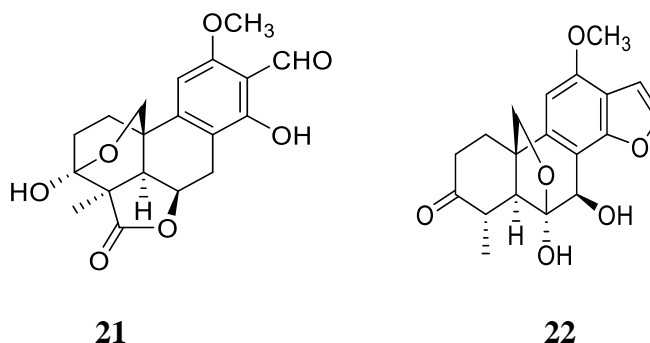


Figure 29. Isolated di-*nor*-pimaranes from *I. trichantha*

2.3.6.1 Icacinlactone K (21)

Icacinlactone K (21): needle-like crystal; mp 188–189 °C; $[\alpha]_D^{20} = +39$ (*c* 0.1, MeOH); IR (film) ν_{\max} 3500, 2916, 2849, 1730, 1630, 1440, 1418, 1352, 1234, 1180, 1128, 1113, 1044, 960 cm^{-1} ; UV_{\max} : 211, 284 nm; ^1H NMR (methanol- d_4 , 400 MHz) and ^{13}C NMR (methanol- d_4 , 100 MHz), see TABLE XII; (+)-HRESIMS m/z 361.1292 $[\text{M} + \text{H}]^+$ (calcd for $\text{C}_{19}\text{H}_{21}\text{O}_7^+$, 361.1282).

Compound **21** was obtained as a needle-like crystal. A molecular formula of $\text{C}_{19}\text{H}_{20}\text{O}_7$ with 10 indices of hydrogen deficiency was suggested by HRESIMS (m/z 361.1292 $[\text{M} + \text{H}]^+$; calcd for $\text{C}_{19}\text{H}_{21}\text{O}_7^+$, 361.1282) with the aid of ^{13}C NMR spectroscopic data. IR absorptions at 1730 and 1630 cm^{-1} indicated the presence of γ -lactone and conjugated formyl moieties, respectively. In the ^1H NMR spectrum, signals for formyl at δ_{H} 10.31 (s, H-15), methyl at δ_{H} 1.45 (s, CH_3 -18), methoxy at δ_{H} 3.95 (s, 12- OCH_3), and an isolated aromatic proton at δ_{H} 6.54 (s, H-11) were observed (TABLE XII). Nineteen carbons were displayed in the ^{13}C NMR spectrum (TABLE XII). A comparison of the ^{13}C NMR data of **21** with those of icacinlactone A⁷⁸ revealed similarities except for those of the benzofuranyl moiety of the latter. Using ^1H – ^1H COSY, HSQC, and HMBC

analyses (Figure 30), connectivities across the C-1–C-10 bicyclic ring, as well as the presence of 3,20-epoxy and 19,6-lactone moieties, became obvious. The observation of HMBC correlations from H-7 (δ_{H} 4.00, dd, $J = 9.7, 17.3$ Hz) to C-5 (δ_{C} 51.3), C-6 (δ_{C} 75.7), C-8 (δ_{C} 114.4), C-9 (δ_{C} 150.5), as well as an oxygenated tertiary carbon at δ_{C} 161.5, led to the assignment of the latter signal to C-14. The olefinic carbon at δ_{C} 99.3 was assignable to C-11 since its proton (δ_{H} 6.54, H-11) displayed HMBC correlations with both C-8 and C-10 (δ_{C} 37.7). Subsequently, the assignments of C-12 (δ_{C} 162.8), C-13 (δ_{C} 110.8), and C-15 (δ_{C} 195.4) were possible on the basis of the following HMBC correlations: H-11 with C-12 and C-13; H-15 (δ_{H} 10.31, s) with C-13 and C-14. The 2D structure of **21** was thus proposed as shown. The relative configuration of **21** was established on the basis of NOESY results (Figure 31). Finally, the absolute configuration was determined as (3*S*, 4*R*, 5*R*, 6*R*, 10*R*) by single-crystal X-ray diffraction (Figure 32). Furthermore, calculations of the ECD spectra of **21** and its enantiomer were performed using the TDDFT method. The calculated ECD spectrum for **21** matched its experimental data, showing similar Cotton effects (Figure 33). Collectively, these permitted definition of the structure of compound **21**, icacinlactone K, as (3*S*,4*R*,5*R*,6*R*,10*R*)-3 β ,20-epoxy-13-formyl-3 α ,14-dihydroxy-12-methoxy-16,17-*dinor*-pimar-8(9),11,13(14)-trien-19,6 β -olide. It is the first report of a 16,17-*dinor*-pimarane from *Icacina* plants. Theoretically, compound **21** could have been derived from the loss of either C15/C-16 or C16/C-17. The latter case (i.e., 16,17-*di-nor*-pimarane structure) is preferred because several other compounds obtained from the same plant belong to 17-*nor*-pimaranes.

TABLE XII. ^1H (400 MHz) AND ^{13}C (100 MHz) NMR OF COMPOUND 21 AND 22 (δ in ppm)

position	21^a		22^a	
	δ_{C}	δ_{H} (J in Hz)	δ_{C}	δ_{H} (J in Hz)
1	30.2, CH ₂	2.71, ddd (4.4, 12.6, 12.6) 1.92, dddd/tt-like (3.7, 4.5, 11.9, 12.6)	29.7, CH ₂	2.72–2.79, m ^b 2.33, ddd (4.9, 13.7, 13.7)
2	28.3, CH ₂	2.29, ddd (4.4, 11.9, 16.6) 2.07, ddd (4.5, 12.6, 16.6)	37.8, CH ₂	2.80–2.90, m ^b 2.46, ddd (2.1, 4.9, 13.7)
3	98.2, C		215.1, C	
4	50.7, C		41.7, CH	2.79–2.85, m
5	51.3, CH	2.36, dd (2.0, 8.0)	54.0, CH	2.27, d (10.9)
6	75.7, CH	5.10, ddd (5.8, 8.0, 9.7)	109.9, C	
7	25.0, CH ₂	4.00, dd (9.7, 17.3) 2.58, dd (5.8, 17.3)	72.7, CH	4.85
8	114.4, C		115.0, C	
9	150.5, C		143.9, C	
10	37.7, C		49.9, C	
11	99.3, CH	6.54, s	99.2, CH	6.63, s
12	162.8, C		154.7, C	
13	110.8, C		118.0, C	
14	161.5, C		157.0, C	
15	195.4, CH	10.31, s	104.8, CH	6.84, d (2.2)
16			145.3, CH	7.67, d (2.2)
18	19.9, CH ₃	1.45, s	14.6, CH ₃	1.26, d (6.3)
19	181.4, C			
20	71.5, CH ₂	4.12, dd (3.7, 9.5) 3.80, dd (2.0, 9.5)	74.2, CH ₂	4.66, d (7.6) 3.35 ^b
OCH ₃	56.5, CH ₃	3.95, s	56.1, CH ₃	3.93, s

^aData were measured in methanol-*d*₄. For CH₂, the deshielded signal was assigned as H_a, and the shielded signal as H_b. ^bSignal was partially obscured.

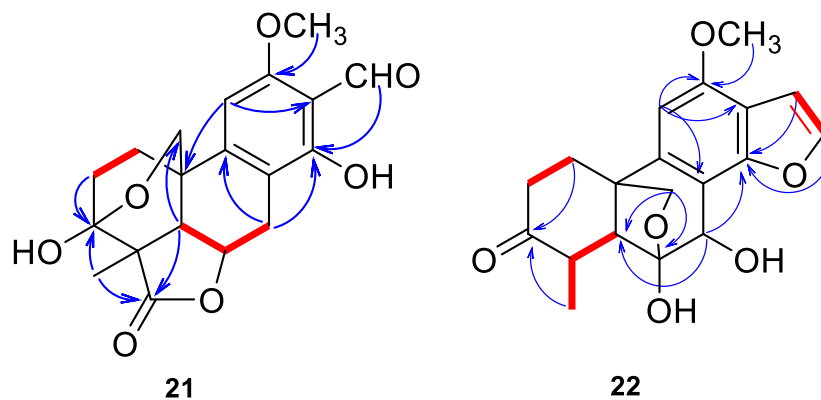


Figure 30. ^1H - ^1H COSY and select HMBC correlations for compounds 21 and 22

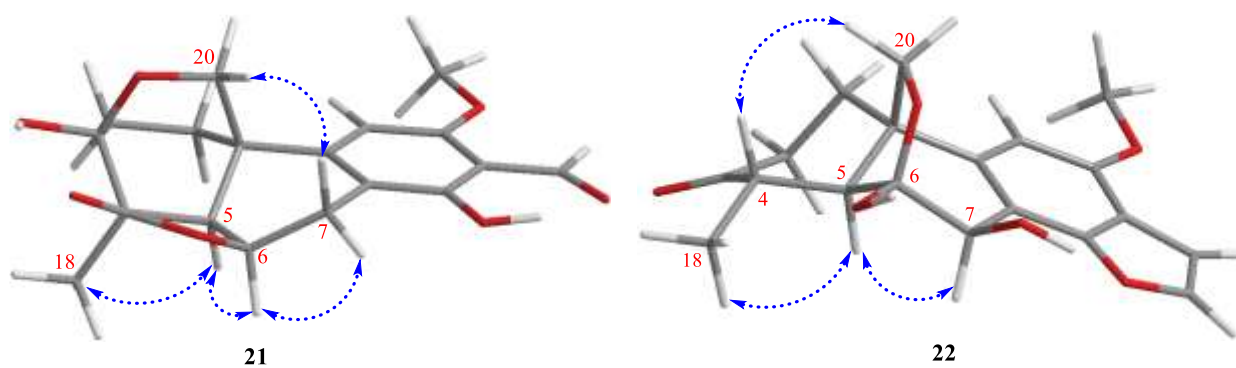


Figure 31. Key NOESY correlations for compounds 21 and 22

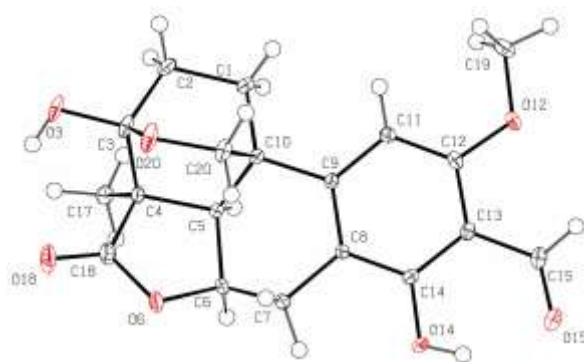


Figure 32. ORTEP representation of compound 21

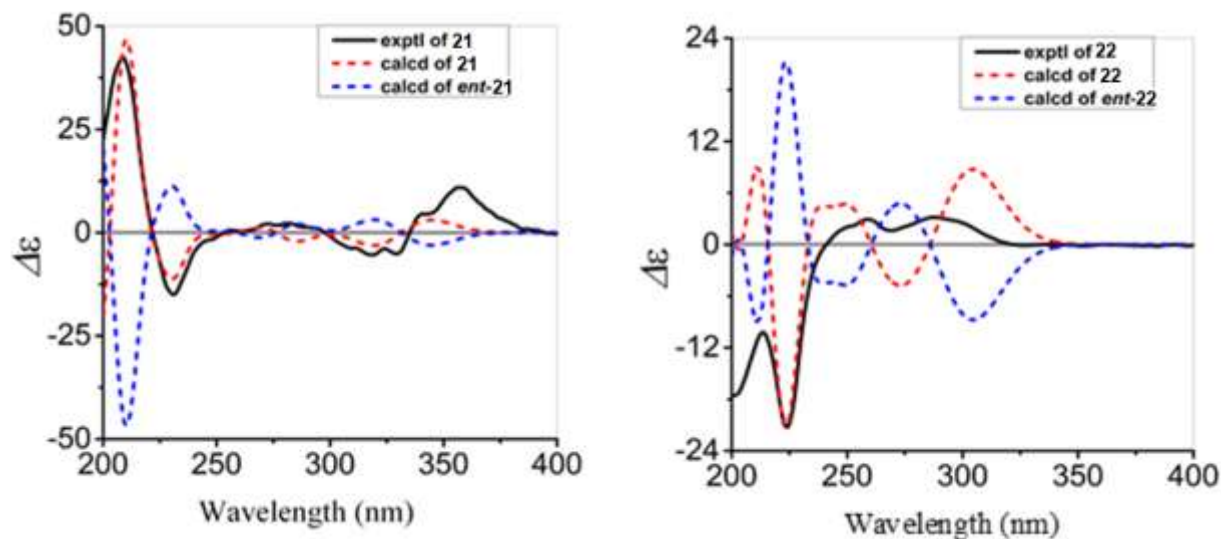


Figure 33. Experimental ECD spectra for **21** and **22**, and the calculated ECD spectra for **21** and **22**, and their enantiomers.

2.3.6.2 Icacintrichanone (**22**)

Icacintrichanone (**22**): Colorless amorphous powder; $[\alpha]_{\text{D}}^{20} = -36$ (c 0.1, MeOH); IR (film) ν_{max} 3394, 2916, 2849, 1739, 1708, 1497, 1463, 1371, 1304, 1239, 1206, 1165, 1118, 1032, 988 cm^{-1} ; UV $_{\text{max}}$: 217, 250, 260 nm; ^1H NMR (methanol- d_4 , 400 MHz) and ^{13}C NMR (methanol- d_4 , 100 MHz), see TABLE XII; (+)-HRESIMS m/z 327.1246 $[\text{M} + \text{H} - \text{H}_2\text{O}]^+$ (calcd for $\text{C}_{19}\text{H}_{19}\text{O}_5$, 327.1227).

Compound **22** was obtained as a colorless amorphous powder. HRESIMS suggested a molecular formula of $\text{C}_{19}\text{H}_{20}\text{O}_6$ with 10 indices of hydrogen deficiency (m/z 327.1246 $[\text{M} + \text{H} - \text{H}_2\text{O}]^+$; calcd for $\text{C}_{19}\text{H}_{19}\text{O}_5^+$, 327.1227). The presence of a dialkylketo group was indicated by the IR absorption at 1739 cm^{-1} . The ^1H NMR spectrum displayed three olefinic protons at δ_{H} 7.67 (d, $J = 2.2$ Hz, H-16), 6.84 (d, $J = 2.2$ Hz, H-15), and 6.63 (s, H-11), and a methyl at δ_{H} 1.26 (d, $J = 6.3$ Hz, CH_3 -18) (TABLE XII). The ^{13}C NMR spectrum exhibited 19 carbon signals corresponding to a methyl, a methoxy, three methylenes, six methines, a dioxygenated secondary carbon, two oxygenated tertiary carbons, a carbonyl carbon, and four quaternary carbons

(TABLE XII). Three coupled spin systems were revealed by the following ^1H - ^1H COSY correlations: H-1a (δ_{H} 2.72–2.79)/H-2b (δ_{H} 2.46), CH₃-18/H-4 (δ_{H} 2.79–2.85)/H-5 (δ_{H} 2.27), and H-15/H-16, allowing the establishment of fragments corresponding to C-1/C-2, C-18/C-4/C-5, and C-15/C-16 (Figure 30). In the HMBC spectrum, both H-1a and CH₃-18 correlated to the carbonyl carbon at δ_{C} 215.1, leading to the connectivity between C-2 and C-4 via C-3 (δ_{C} 215.1). A benzofuran moiety was proposed based on the HMBC correlations as shown in Figure 30. A methoxy group was attached to C-12 (δ_{C} 154.7). The proton at δ_{H} 4.85 showing HMBC correlations with C-5 (δ_{C} 54.0), C-9 (δ_{C} 143.9), and C-14 (δ_{C} 157.0) was assigned to H-7. On the other hand, observation of HMBC correlations from H-20b (δ_{H} 3.35) to C-5, C-6 (δ_{C} 109.9), C-9, and C-10 (δ_{C} 49.9) revealed the presence of 6,20-epoxy and C-6 hemiketal functional groups. The 2D structure of **22** was thus elucidated as shown. In the NOESY spectrum, H-5 correlated with both H-7 (δ_{H} 4.85) and CH₃-18, while H-4 correlated with H-20a (δ_{H} 4.66), indicating the α -orientations of H-5, H-7, and CH₃-18, as well as the β -orientations of H-4 and the 6,20-epoxy group (Figure 31). To determine the absolute configuration of **22**, the ECD spectra for (4*S*, 5*S*, 6*S*, 7*R*, 10*R*)-**22** and its enantiomer were calculated using the TDDFT method (Figure 33). The experimental ECD spectrum of **22** revealed the absolute configuration of **22** as (4*S*, 5*S*, 6*S*, 7*R*, 10*R*). Consequently, the structure of **22**, icacintrichanone, was defined as (4*S*,5*S*,6*S*,7*R*,10*R*)-6 β ,20:14,16-diepoxy-6 α ,7 β -dihydroxy-12-methoxy-3-oxo-17,19-dinor-pimar-8(9),11,13(14),15-tetraene. It is the first example of a 17,19-dinor-pimarane from *Icacina* plants. Another similar but simpler compound, 17,19-dinor-pimar-8(9),11,13(14)-triene, was detected in the sediments of a deltaic environment.¹⁶³

This is the first report of the isolation of a 16,17-dinor-pimarane (**21**) and a 17,19-dinor-pimarane (**22**) from *Icacina* plants. Theoretically, compound **21** could have been

derived from the loss of either C15/C-16 or C16/C-17. The latter case (i.e. 16,17-dinor-pimarane structure) is preferred because several other compounds obtained from the same plant belong to 17-*nor*-pimaranes.

2.3.7 Other compounds

2.3.7.1 Pinoresinol (23)

(+)-*Pinoresinol* (**23**): White amorphous powder; $[\alpha]_D^{20} = +26$ (*c* 0.3, MeOH); IR (film) ν_{\max} 1526, 1273, 1036 cm^{-1} ; ^1H NMR (methanol-*d*₄, 400 MHz) δ 6.97 (2H, d, *J* = 1.9 Hz, H-2'/H-2"), 6.83 (2H, dd, *J* = 8.1, 1.9 Hz, H-6'/H-6"), 6.79 (2H, d, *J* = 8.1 Hz, H-5'/H-5"), 4.73 (2H, d, *J* = 4.2 Hz, H-2/H-6), 4.26 (2H, dd, *J* = 9.1, 6.8 Hz, H-4a/H-8a), 3.88 (6H, s, OCH₃), 3.85 (2H, dd, *J* = 9.1, 3.5 Hz, H-4b/H-8b), 3.17 (2H, m, H-1/H-5); ^{13}C NMR (methanol-*d*₄, 100 MHz) δ 149.2 (C-3', C-3"), 147.5 (C-4', C-4"), 133.7 (C-1', C-1"), 120.1 (C-6', C-6"), 116.1 (C-5', C-5"), 111.0 (C-2', C-2"), 87.5 (C-2, C-6), 72.6 (C-4, C-8), 56.4 (OCH₃, OCH₃), 55.4 (C-1, C-5); (+)-HRESIMS *m/z* 341.1364 [*M* + *H* - H₂O]⁺ (calcd for C₂₀H₂₁O₅, 341.1383).

Compound **23** was obtained as a white amorphous powder. HRESIMS suggested a molecular formula of C₂₀H₂₂O₆ (*m/z* 341.1364 [*M*+*H*-H₂O]⁺; calculated for C₂₀H₂₁O₅, 341.1383). The ^1H NMR spectrum displayed three olefinic protons at δ_{H} 6.97 (d, *J* = 1.9, H-2' and H-2"), 6.83 (dd, *J* = 8.1, 1.9, H-6' and H-6"), and 6.79 (d, *J* = 8.1, H-5' and H-5"). The ^{13}C NMR spectrum presented ten carbon signals corresponding to a methoxy, a methylene, two aliphatic methines, three olefinic methines, two oxygenated aromatic carbons, and one quaternary carbon. The disagreement between the mass spectrometry-suggested molecular formula and the observed signals in the ^{13}C NMR spectrum was obvious; therefore, a structure with symmetry was proposed to account for the discrepancy. Analysis and interpretation of 2-D NMR data

(Appendix A) was carried out to determine the structure. First, the ^{13}C resonances at δ_{C} 149.2 (C-3'), 147.5 (C-4'), 133.7 (C-1'), 120.1 (C-6'), 116.1 (C-5'), and 111.0 (C-2') suggested the presence of a substituted aromatic ring. After assignment of proton signals with their respective carbons with an HSQC experiment, interpretation of the measured J -coupling in the ^1H spectrum was used to assign the three aromatic carbons. Interpretation of the olefinic proton at δ_{H} 6.83 was most important due to the observed doublet of doublet splitting with measured J -values of 8.1 and 1.9 Hz, suggesting the remaining two protons are oriented *ortho* and *meta* to the selected proton, respectively. The ^1H - ^1H COSY spectrum displayed correlations, but these were eventually determined to be mostly due to the aromatic proton coupling. The only verified spin system present was H-1 (δ_{H} 3.17)/ H-2 (δ_{H} 4.73) and H-5 (δ_{H} 3.17)/H-6 (δ_{H} 4.73). An HMBC experiment was vital to complete the structure elucidation. The methoxy proton signal at δ_{H} 3.88 (3'-OCH₃) and a olefinic proton at δ_{H} 6.79 (H-5' and H-5'') correlated with δ_{C} 149.2 (C-3') suggesting C-3'/C-3'' is positioned *meta* to C-5'/C-5'' and substituted with a methoxy group. Both olefinic protons at δ_{H} 6.97 (H-2' and H-2'') and 6.83 (H-6' and H-6'') correlated with δ_{C} 147.5 (C-4'), implying their *meta* positions to each other. The deshielded chemical shift of C-4'/C-4'' implied a hydroxy substitution. Finally, the correlation between H-5'/H-5'' and δ_{C} 133.7 (C-1') suggested C-1'/C-1'' connects with the rest of the structure. This was confirmed by the correlation between H-6'/H-6'' and C-2/C-6 (δ_{C} 87.5). Finally, the correlation between δ_{H} 4.26 and δ_{C} 55.4 (C-1/C-5) and C-2/C-6 established the tetrahydrofuran ring with a line symmetry across the C-1/C-5 bond. A NOESY experiment displayed correlations between H-1/H-5 and the deshielded proton H-4a in addition to H-2/H-6 with the shielded H-4b. This suggests the relative configuration of H-1/H-5 is opposite to H-2/H-6. A search of the literature and comparison of results suggested (+)-pinoresinol as a match based on the interpretation of spectroscopic data and

comparison of optical rotation.¹⁶⁴ This is the first reported isolation of a lignan from the genus *Icacina*. Though (+)-pinoresinol is well-known lignan found throughout nature,¹⁶⁵ its reported biological activity includes antibacterial,¹⁶⁶ chemoprevention,¹⁶⁷ and cytotoxicity.¹⁶⁸

2.3.7.2 16-Methylethylidene-humirianthenolide C (24)

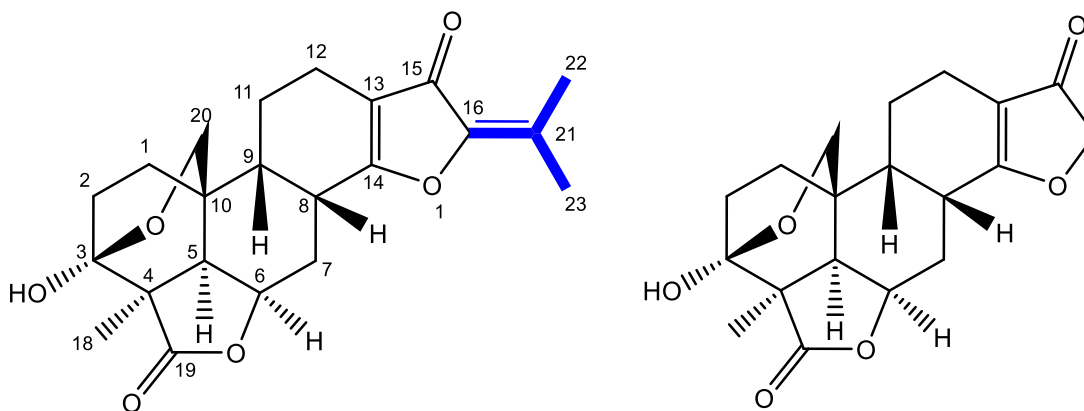


Figure 34. Artifact of humirianthenolide C structural analogue (modification highlighted in blue)

Compound **24** was obtained as a white amorphous powder. A molecular formula of $C_{22}H_{26}O_6$ with ten degrees of unsaturation was suggested by HRESIMS (m/z 387.1836 $[M+H]^+$; calculated for $C_{22}H_{27}O_6^+$, 387.1802). The ^{13}C NMR spectrum displayed twenty-two carbons corresponding to three methyls, six methylenes, four methines, two carbonyls, a dioxygenated secondary carbon, two oxygenated tertiary carbons, and four quaternary carbons. The 1H NMR spectrum displayed three methyl signals at δ_H 2.27 (s, CH_3 -22), 2.04 (s, CH_3 -23), and 1.36 (s, CH_3 -18). All proton signals were correlated with their connected carbons via an HSQC experiment (Table XIII). Two coupled spin systems were determined from a 1H - 1H COSY experiment: H-1 (δ_H 1.95)/ H-2 (δ_H 1.84) and H-5 (δ_H 2.28)/ H-6 (δ_H 4.77)/ H-7 (δ_H 2.54)/ H-8 (δ_H 2.87)/ H-9 (δ_H 1.66)/ H-11 (δ_H 2.11)/ H-12 (δ_H 2.37). Compound **24** was suspected to be a

structural analogue of humirianthenolide C (Figure 34) upon interpretation of an HMBC experiment (Figure 35).¹⁶⁹

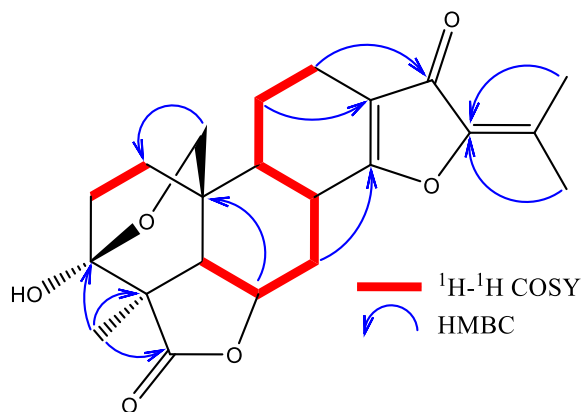


Figure 35. Key COSY and HMBC correlations for compound 24

Comparison of the ^1H and ^{13}C NMR data with unpublished data previously obtained from the C.T. Che research group confirms this similarity. The ^1H spectra were similar except for noticeable differences in the aliphatic chemical shift region (Figure 207, Appendix A). The measured J -coupling values gathered from the ^1H NMR data, when available, were the same as previously reported values for the corresponding assigned protons.⁷⁶ The ^{13}C chemical shifts for atoms in the A- and B- rings were nearly identical, but the δ_{C} values in the furanone ring (i.e. C-13, C-14, C-15, and C-16) were noticeably different (Table XIII). Methyl groups CH_3 -22 and CH_3 -23 demonstrated HMBC correlations with alkene carbon signals at δ_{C} 146.3 (C-16) and 134.5 (C-21), providing further evidence for the addition of a methylethyldiene group to the furanone ring. The relative configuration from a NOESY experiment was also in agreement. Such a structure is highly unusual for a diterpenoid based upon previously proposed biosynthetic pathways and the nature of the structural difference. Therefore, it was hypothesized that

compound **24** is an artifact resultant from the use of aqueous acetone as an extraction solvent and occasional chromatographic solvent as well.

The methylethylidene furanone moiety in proposed structure of **24** bears resemblance to several natural products, including an aromatic from roasted coffee¹⁷⁰ and cytotoxic diterpenoids isolated from plants.^{171,172} However, the compound was determined to be an artifact due to 1) the close resemblance of the proposed structure with a previously reported compound from the species; and 2) established organic synthesis mechanisms of α,β -unsaturated ketone via aldol condensation. Alternative mechanisms were explored involving Maillard reaction¹⁷³ and cyclization reactions.¹⁷⁴ Ultimately, literature reports of the complete synthesis of pseudodefectusin supports the hypothesis. Both synthesis schemes report the conversion of the furanone ring via condensation with acetone.^{175,176} Adopting these findings led to a proposed biogenesis involving methoxy (methanol)-catalyzed ketol-condensation with acetone (Figure 36). It should be noted the reported synthesis involved the use of metallic or acid catalysts along with temperature change, whereas compound **24** could only have been generated at room temperature during the extraction and/or separation steps. While the mechanism of its formation remains unclear, the possibility of enzymatic reactions cannot be excluded. It is also noteworthy that aldol condensation may occur at room temperature under slightly basic conditions without catalyst.^{177,178}

TABLE XIII. ^1H (900 MHz) AND ^{13}C (226 MHz) NMR OF COMPOUND 24 (δ in ppm)

position	24^a	δ_{H} (J in Hz)	Humirianthenolide C^c
	δ_{C}		δ_{C}
1	31.3, CH ₂	1.95, dt (12.3, 3.4) 1.63, dt (12.1, 6.2)	31.3, CH ₂
2	18.0, CH ₂	1.84, td (12.9, 2.9) 1.50, tdd (13.4, 11.5, 5.8)	17.9, CH ₂
3	97.8, C		97.8, C
4	53.2, C		53.2, CH
5	45.8, CH	2.28, m ^b	45.8, CH
6	75.9, CH	4.77, t (5.3)	75.7, CH
7	27.6, CH ₂	2.54, ddd (16.3, 5.6, 1.5) 1.91, ddd (16.3, 13.0, 5.5)	27.3, CH ₂
8	29.7, CH	2.87, dt (12.1, 4.5)	30.9, C
9	38.6, CH	1.66, ddd (12.1, 4.5, 2.6)	38.5, C
10	33.1, C		33.1, C
11	29.4, CH ₂	2.11, ddt (11.7, 4.1, 2.5) 1.84, m ^b	29.4, CH ₂
12	19.1, CH ₂	2.37, ddd (16.3, 5.8, 1.5) 2.09, dd (11.6, 6.0)	18.8, CH ₂
13	115.5, C		112.8, C
14	181.6, C		194.5, C
15	187.5, C		204.1, CH
16	146.3, C		76.7, C
18	17.5, CH ₃	1.36, s	17.4, CH ₃
19	181.1, C		180.9, C
20	74.3, CH ₂	4.36, dd (9.4, 3.5) 3.63, dd (9.5, 1.8)	74.2, CH ₂
21	134.5, C		
22	19.9, CH ₃	2.04, s	
23	17.2, CH ₃	2.27, s	

^aData were measured in methanol-*d*₄. For CH₂, the deshielded signal was assigned as H_a, and the shielded signal as H_b. ^bSignal was partially obscured. ^cUnpublished data measured in methanol-*d*₄ for reference.

2.4 Conclusion

Icacina plants are rich in a variety of diterpenoids including (9 β -H)-pimaranes, 17-*nor*-(9 β -H)-pimaranes, and 17-*nor*-pimaranes.^{63,72,76,78} A (9 β -H)-pimarane pathway has been proposed for their biosynthesis.⁷⁹ In summary, fifteen new *Icacina* diterpenoids were isolated from the tuber of *I. trichantha*, at least one of which is suspected to be a purification artifact. Among these is the first report of the isolation of 19-*nor*-pimaranes (**17-20**), a 16,17-di-*nor*-pimarane (**21**), and a 17,19-di-*nor*-pimarane (**22**), from *Icacina* plants. The first report of a lignan (**23**) from genus *Icacina* was also achieved. The unusual 19-*nor*-pimarane subclass are characterized by the lack of a γ -lactone ring between C-4 and C-6 in comparison with all other reported pimaranes from *Icacina*. These findings highlight the chemotaxonomic importance of the *Icacina* genus and their capacity to produce a variety of unique diterpenoids. They represent an expansion of the structural diversity from an already unique field of 9 β H-pimaranes discovered from this genus. The biological activity of the novel compounds will be discussed further in the following chapter.

3. BIOLOGICAL ACTIVITY OF SELECT PIMARANES

This chapter is reproduced (adapted) in part with permissions from Zhao, M.; Guo, B.; Onakpa, M. M.; Wong, T.; Wakasa, K.; Che, C. T.; Warpeha, K. Activity of Icacinol from *Icacina Trichantha* on Seedling Growth of *Oryza Sativa* and *Arabidopsis Thaliana*. *J. Nat. Prod.* **2017**, *80* (12), 3314–3318, DOI: 10.1021/acs.jnatprod.7b00668. Copyright 2017 American Chemical Society; and Guo, B.; Onakpa, M. M.; Huang, X.-J.; Santarsiero, B. D.; Chen, W.-L.; Zhao, M.; Zhang, X.-Q.; Swanson, S. M.; Burdette, J. E.; Che, C.-T. Di -nor - and 17- nor -Pimaranes from *Icacina Trichantha*. *J. Nat. Prod.* **2016**, *79* (7), 1815–1821, DOI: 10.1021/acs.jnatprod.6b00289. Copyright 2016 American Chemical Society.

3.1 Introduction

There is a global need for increased food production in future decades due to continued population growth.¹⁷⁹ However, annual crop yields have been slowly decreasing and will need to be improved to meet these demands. Adding to this pressure is the looming threat of climate change and its agricultural effects. Rising global temperatures and increased atmospheric greenhouse gas levels will lower crop yields by simultaneously inhibiting crop output and increasing plant loss due to pests.^{180,181} Though estimated losses varies for different crops, weeds account for 34% of potential crop loss on average compared with 18% and 16% caused by animals and pathogens, respectively.^{182,183} Weeds such as *Erigeron canadensis*, *Commelina cumminus*, and *Arabidopsis thaliana* compete for nutrients, water, and light, negatively impacting the growth and production of planted crops. Weed control is a necessary aspect of agriculture but historically labor-intensive and costly. Fortunately, herbicides emerged as an extremely effective and economical solution. Since their commercial deployment in the 1940's, herbicides are the most common method for weed control.¹⁸⁴ Unfortunately, their extensive use also served as an evolutionary selective pressure that has led to growing herbicide resistance in weeds, similar to the phenomena of antibiotic resistance development. Therefore, new herbicide targets and mechanisms of action are needed.¹⁸⁵ The need for weed management affects crops worldwide, including rice cultivars (*Oryza sativa*) an important staple crop for populations across the globe.^{186,187} The additional negative side effects of synthetic herbicides makes the concept of naturally-derived agents attractive as being safer and more sustainable.^{188,189}

Natural products have been important for agriculture as a chemical basis to develop herbicides, pesticides, and fungicides to protect crops.^{190,191} A natural product-based approach to develop new herbicides is advantageous due to the chemical diversity of natural products that

could potentially lead to new modes of action and targets, and are likely more practical in the current environment of increased government regulation of harmful substances and societal demands and expectations of food that is consumed.^{192,193} Allelopathy is a biological process where an organism produces and releases a chemical entity into its surrounding environment as a defense mechanism by manipulating the development of competitors or other harmful organisms. These allelochemicals can inhibit other plants, fungi, or microorganisms through a variety of mechanisms and can be exploited for agricultural purposes.¹⁹⁴

The pimaranes from *I. trichantha* were examined for herbicidal activity because of the structural similarity to the previously reported momilactones from rice plants. This class of diterpenoids were studied and found to be very important for the rice plant's allelopathy, especially momilactone B. Research suggests these phytochemicals are secreted from the roots throughout the plant's lifecycle and can be absorbed by other plant species.^{195,196} However, there is limited information on the phytotoxic mechanism of action. One study suggests momilactone B inhibits seedling growth by disrupting several proteins involved in the metabolic process for cell structure production and seedling growth, including subtilisin-like serine protease and cruciferin 2, in *Arabidopsis thaliana*.¹⁹⁷

Cancer remains the second leading cause of death in the US and is a serious health issue worldwide. Advances in cancer diagnosis and treatment has led to better survival rates, but continued drug development is needed. Prostate cancer (PC) is a particular area of concern as it is in the top three cause of death due to cancer for men in the US.¹⁹⁸ One of the treatment strategies for PC is disrupting androgen hormone production, known as androgen-deprivation therapy, or targeting the androgen receptor itself.¹⁹⁹ Carnosol, a phytochemical diterpenoid found in several plants, has been shown to target androgen receptor and disrupt its activity.²⁰⁰ Natural

products have played an important role as the source for many cancer treatments in the clinic,^{201–203} but current chemotherapy comes with harmful side effects.²⁰⁴ An alternative approach has been to develop therapeutic agents to prevent, inhibit, or reverse the onset of cancer before it progresses, known as chemoprevention.²⁰⁵ As with chemotherapeutic drugs, natural products are often looked to for chemopreventive agents due to generally lower toxicity and side effect compared to synthetic drugs.^{206,207} Dietary plants are often examined for their role in cancer prevention due to the presence of a complex mixture of chemical agents possibly targeting multiple pathways in cancerous cells.^{208–210} Reports of *Icacina trichantha* consumption by the indigenous population to treat a variety of ailments, including “soft tumors”⁶², and published articles of the anti-inflammatory¹¹⁰ and anti-oxidant⁹² activity of extracts *in vivo* prompted further examination of its anticancer potential.

3.2 Anti-germination Materials and Methods

3.2.1 General Experimental Procedures.

Chemicals for plant experiments and sterile plastics (square Petri dishes, Phytatrays, and Phytatray II), unless otherwise noted, were obtained from Sigma-Aldrich (St. Louis, MO, USA). Seeds were sterilized in bleach solution (49% sodium hypochlorite [6.05%], 49% sterile water, 2% 0.1% Triton X-100) with vigorous shaking for 5 min, then four washes with sterile water. All materials in contact with seeds or plants were sterilized by autoclaving or purchased sterile (gamma irradiated) or sterile (0.22 μm) filtered molecular biology grade water). In order to test specific chemical concentrations per area, 0.5 \times MS minimal medium trays were made (50 mL Phytatray, 50 mL vertical tray) for

seed germination and plant growth.²¹¹ Rice when transplanted went into an autoclaved soil/sand mix.

Human melanoma cancer cells MDA-MB-435, human breast cancer cells MDA-MB-231, human ovarian cancer cells OVCAR3, human colorectal cancer cells HCT116, human prostate cancer cells 22Rv1, and PC3 were purchased from the American Type Culture Collection (Manassas, VA).

3.2.2 Plant Material.

Tubers of *Ipomoea trichantha* Oliv. were collected in June 2011 from the Orba village in Nsukka of the Enugu State, Nigeria, and authenticated by Prof. B.O. Olorede of the Botany Department, University of Abuja, Nigeria, and Mr. A. Ozioko, botanist at the BDCP Laboratories, Nsukka, Nigeria. A voucher specimen (UNN/FVM 456) was deposited in the pharmacology laboratory at the University of Nigeria, Nsukka, Nigeria.

3.2.3 Extraction and Isolation.

The powdered tubers of *I. trichantha* (1.5 kg) were extracted with 80% aqueous MeOH by percolation to yield 166 g of dry crude extract, which was partitioned into petroleum ether-soluble (S1, 11 g), EtOAc-soluble (S2, 17 g), BuOH-soluble (S3, 15 g), and H₂O-soluble (S4, 128 g) fractions. The EtOAc-soluble fraction (S2) was further fractionated. A precipitate from subfractions 47–53 was purified by further chromatography using a mixture of DCM and MeOH to yield icacinol (1), a crop of 50 mg of crystals of which was finally obtained. This compound exhibited physical and spectroscopic parameters consistent with literature data;⁷⁶

3.2.4 Plant Growth Response Screening Materials.

Stock solutions were made of all final extract fractions at 10 µg/mL, with icacinol (1) resuspended to a 265 µM solution in sterile DMSO, then were diluted for use in 0.5× MS²¹² for experiments described herein. *Arabidopsis thaliana* Columbia WT seed was originally obtained from ABRC/ TAIR.²¹³ Bulk seed stocks were grown as previously reported.³⁰ Seeds of *Oryza sativa* (rice) Nipponbare (obtained from K. Warpeha) were sterilized and sown in the same manner as *Arabidopsis* seed, as described,²¹¹ but incubated at 28 °C for germination.

3.2.5 Assays for Growth Responses.

Seeds were surface sterilized in bleach solution, then rinsed in sterile water and plated on 0.5× MS (pH 5.8) in Phytatrays (Sigma) with no sucrose and no added vitamins as described,²¹¹ but instead of a cold treatment, were given a 48 h darkness treatment at 20°C. At the time of planting, a plant extract of S2 or 1 or DMSO (empty vehicle control) was diluted in 0.5× MS, then was added to 0.8% low melt agarose (0.5× MS; top agarose) when the autoclaved media fell below 50 °C, mixed well, then poured and allowed to solidify with sterilized and washed seeds in the top agarose in a thin layer. Dilutions of chemicals derived from the plant were initially made at 1:20 to 1:5000 (depending on the experiment) from extract stock in DMSO (described above), diluted with 0.5× MS right before plating. After sowing seeds on plates, the plates were placed into black boxes and moved to a 20 °C complete darkness room for 48 h, then subsequently moved to white light at 120 µmol m⁻² s⁻¹, at 20 °C for *Arabidopsis* and 28°C for rice.

3.2.6 Vertical Growth Assays of *Arabidopsis*.

On sterile square Petri plates seeds were lined up in a row, 2.5 cm from the designated top edge and 2.0 cm between each row. A 10 μ L aliquot of seed in top agarose was spotted onto a 0.5 \times MS Phytatray base plate of different dilutions of S2 or 1. Plated, sterilized seed plates were turned vertically, secured into light-tight black Plexiglas boxes, sealed with aluminum foil, and then were cold placed in a dark room at 20 °C for 48 h. After 48 h the plates were moved to one of several locations: to a 24 h 20 °C dark environmental room (continuous darkness, i.e., Dc) or a white light environmental room where lights were on for 24 h continuously (Wc) or the lighting regime was 16:8 (16 h light, 8 h darkness),²¹⁴ for varying numbers of days, ranging from 0 to 60 days, depending on the experiment. Light sources, including dim green light for handling darkgrown seedlings, have been described.^{214,215} The fluence rate received by the vertical plates and Phytatrays determined by a LiCor meter was 120 μ mol m⁻² s⁻¹.

3.2.7 Germination and Phenotyping.

Successful germination was determined under a dissecting scope by viewing rice and *Arabidopsis* seeds every 12 h post-sowing, scoring complete emergence of the radical as previously described.²¹⁵ Phenotypic responses on untreated (control) and experimental extract plates were determined by comparison of chemically treated seeds to untreated plants (DMSO vehicle control) and counted on a Zeiss Stereo Discovery V.8 microscope at 1 \times using Axiovision (Zeiss). Plates were photographed at different times after stratification using a Nikon Coolpix on a light box or black background. At least three sets of 30 seeds were scored for each germination assay on Phytatrays at 24, 48, and 72 h poststratification.

3.2.8 Vegetative Assessment.

Rice and *Arabidopsis* seeds were sown on Phytatray II to assess how they would grow over 7–60 days, depending on the experiments. At 4 weeks, rice seedlings were transferred to a soil/sand mix submerged in water in white catering 1 gallon buckets, where they were moved to a greenhouse of similar fluence levels and where the daytime temperature was above 25 °C, in order to grow long-term, including for seed sets (rice grains per panicle). Sets of plants were washed and dried to determine root and shoot dried weight at 6 weeks. Images and samples (100 seedlings \times 3 replicates) for chlorophyll extraction²¹⁶ and anthocyanin extraction²¹⁷ were taken at 2 weeks. Seedlings were imaged on a dissecting scope at various times to capture phenotypes as indicated in the figures.

3.2.9 Statistical Analysis.

Phenotypes and plant responses were quantitated, and the values entered into GraphPad/Prism V.5 for Mac, similar to the manner described previously.²¹¹ Equal variances were not assumed in plant materials (seeds and seedlings), and differences of means compared (typically to the DMSO control data) were assessed by unpaired t test (two-tailed) with Welch's correction.

3.3 Anti-germination Results and Discussion

Fractions from solvent partitioning of *I. trichantha* tuber and isolated icacinol (**1**) compound were analyzed for effect on seedling growth of rice (*Oryza sativa*) and *Arabidopsis* weeds. Fractions S1 (petroleum ether-soluble), S2 (EtOAc-soluble fraction), S3 (BuOH-soluble), S4 (H₂O-soluble), and **1** were mixed in top agarose with seeds at concentrations indicated in

Figure 37. Seed germination was scored 72 h postplating. Only the EtOAc-soluble fraction demonstrated growth inhibition. At a concentration of 10 ng/mL, rice seed germination showed no change from the DMSO control after 72 hours. However, *Arabidopsis* germination was inhibited by 88%, suggesting a selective anti-germination activity. Icacinol was also analyzed and demonstrated a more pronounced selective inhibition of weed growth. Weed germination was 36% at 56 μ M concentration while rice seeds germinated at nearly 100%.

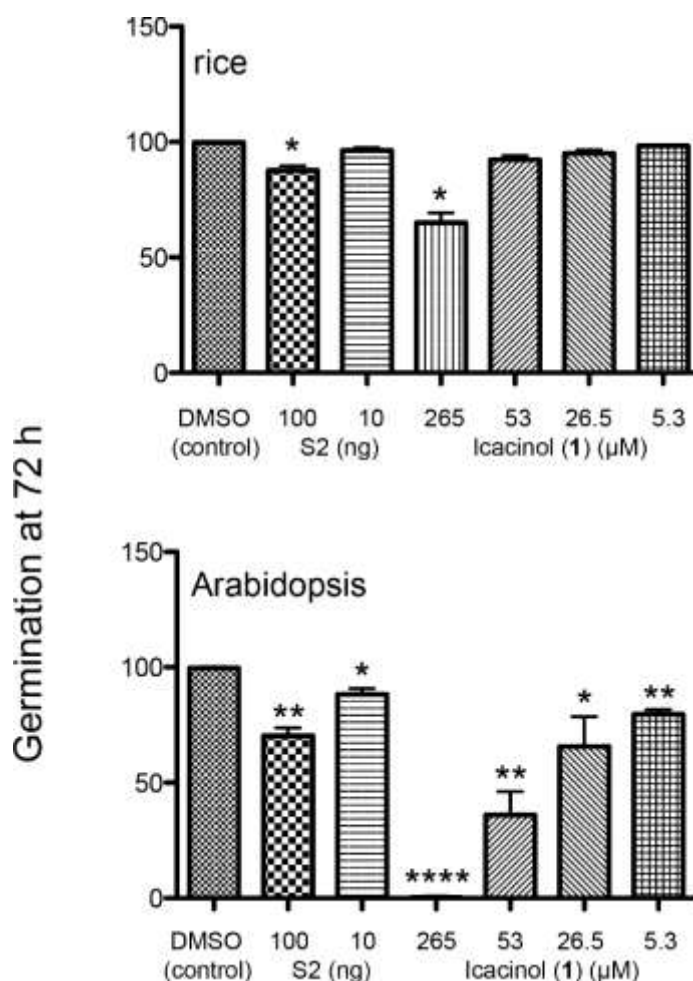


Figure 37. *Ipacina trichantha* fractions and icacinol (1) effects on seed germination.

The observed inhibitory activity was then tested on seedlings of rice and weed. The growth of young seedlings was observed over the course of two weeks with treatment of either fraction

S2 or compound **1**. At end of the treatment period, rice seedlings were observed to have been delayed in growth and development compared with the negative control (Figure 38). However, no rice seedlings were lost due to treatment and ultimately developed as normal. A similar observation was made for *Arabidopsis* seedlings.

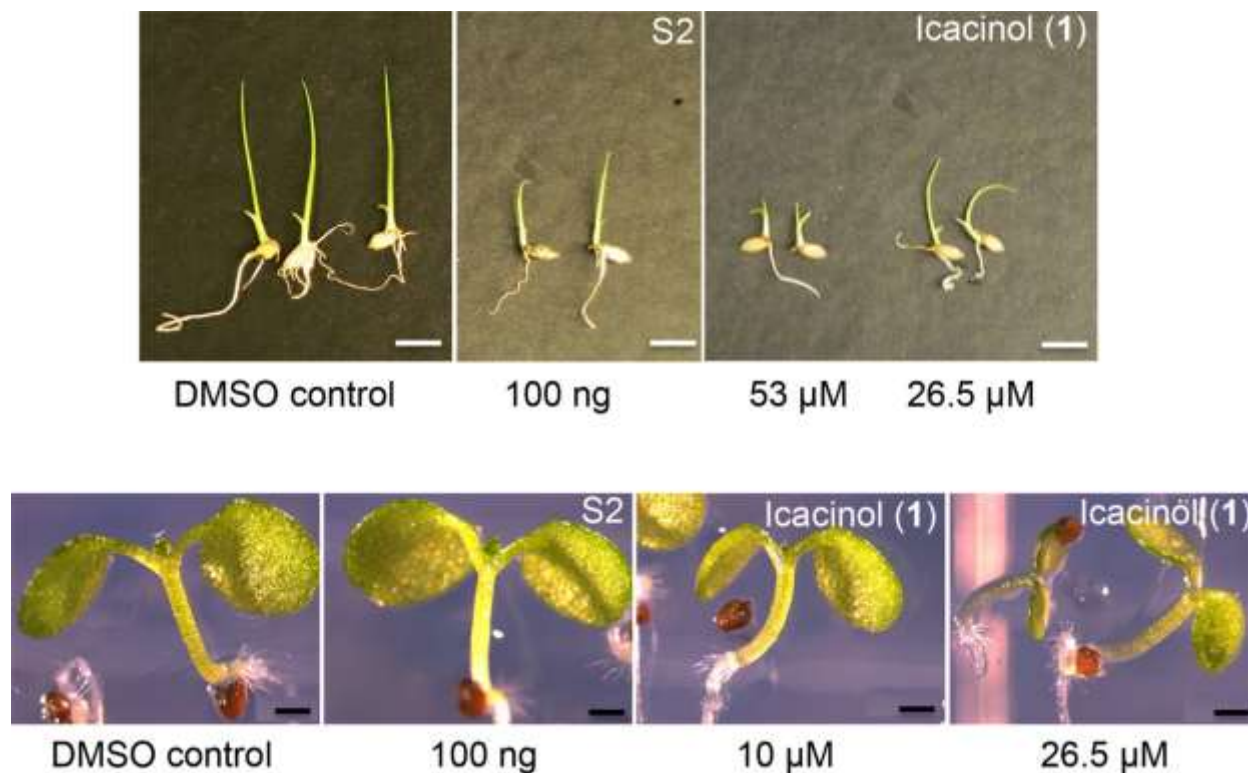


Figure 38. *I. trichantha* EtOAc-extract and icacinol (1) impact on vegetative growth. Images are representative. Top panel rice (size bar 2 cm), lower panel Arabidopsis (size bar 250 μm).

A longer six-week study was also carried out to measure the biomass change in seedlings treated with plant extract and compound **1** after sowing. For rice seeds, the average biomass difference from the 56 μ M icacinol treatment group was 90.4%, which was statistically significant but comparable to the negative control mean of 99.6%. The number of rice grains produced was also comparable to the control. There was a much stronger response in *Arabidopsis* seeds treated with the same concentration, with mean biomass reduced to 64.4% compared with 99.8% for the negative control group, and seeds did not reach their reproductive stage (Figure 39).

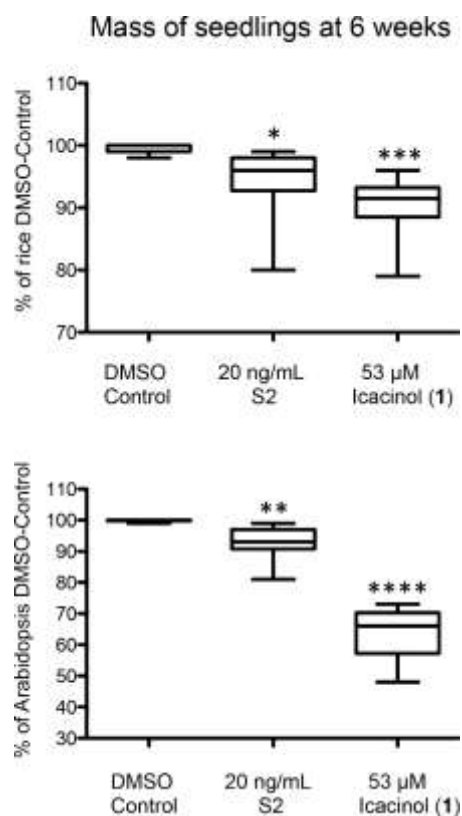


Figure 39. *Icacina trichantha* extract and icacinol (1) impacts on longer term vegetative growth. * $P < 0.05$; ** $P < 0.01$; *** $P < 0.001$; **** $P < 0.0001$.

EtOAc-extract of *I. trichantha* tuber was found to be the most active on plant germination responses among the tested fractions. Pure icacinol (1) isolated from that fraction was found to be even more active. Importantly, there was a clear difference in seed germination between *Arabidopsis* (a eudicot) and rice (a monocot), where *Arabidopsis* germination was severely impaired under experimental treatment conditions. The chief difference of monocots and eudicots in germination is related to the fact that the monocot seed leaf is thin and the endosperm to feed the seed leaf is outside of the leaf itself, whereas the eudicots such as *Arabidopsis* have two seed leaves with an endosperm to feed the embryonic plant. In addition, *Arabidopsis* is a very fast-growing weed-like plant, with photosynthesizing cotyledons. It is possible that the metabolic interactions in the cotyledons of *Arabidopsis* are disrupted in the process of germination and the concomitant greening process, as *Arabidopsis* cotyledons develop and photosynthesize within 2–3 days in summer (i.e., 16:8 light/dark cycle) conditions.¹³²

3.4 Cytotoxicity Materials and Methods

3.4.1 General Experimental Procedures.

Human melanoma cancer cells MDA-MB-435, human breast cancer cells MDA-MB-231, human ovarian cancer cells OVCAR3, human colorectal cancer cells HCT116, human prostate cancer cells 22Rv1, and PC3 were purchased from the American Type Culture Collection (Manassas, VA).

3.4.2 Plant Material.

Tubers of *Icacina trichantha* Oliv. were collected in June 2011 from the Orba village in Nsukka of the Enugu State, Nigeria, and authenticated by Prof. B.O. Olorede of the Botany Department, University of Abuja, Nigeria, and Mr. A. Ozioko, botanist at the

BDCP Laboratories, Nsukka, Nigeria. A voucher specimen (UNN/FVM 456) was deposited in the pharmacology laboratory at the University of Nigeria, Nsukka, Nigeria.

3.4.3 Extraction and Isolation.

See Chapter 2, Section 2.2.3, page 51.

3.4.4 Cytotoxicity Assays.

The MDA-MB-435, MDA-MB-231, and OVCAR3 cell lines were propagated at 37°C in 5% CO₂ in RPMI-1640 medium, supplemented with 10% FBS, penicillin (100 units/mL), and streptomycin (100 µg/mL). Cells in log phase growth were harvested by trypsinization followed by two washings to remove all traces of enzyme. A total of 5,000 cells were seeded per well of a 96-well clear, flat-bottom plate (Microtest 96®, Falcon) and incubated overnight (37°C in 5% CO₂). Samples dissolved in DMSO were then diluted and added to the appropriate wells (concentrations: 20, 4, 0.8, 0.16, and 0.032 µM; total volume: 100 µL; DMSO: 0.5%). The cells were incubated in the presence of test substance for 72 h at 37°C and evaluated for viability with a commercial absorbance assay (CellTiter 96® AQueous One Solution Cell Proliferation Assay, Promega Corp, Madison, WI) that measured viable cells. IC₅₀ values are expressed in µM relative to the solvent (DMSO) control. Taxol was used for positive control.

HCT-116 cells were cultured in McCoy's 5A with L-glutamine supplemented with 10% FBS and 1% penicillin/streptomycin. PC-3 cells were cultured in F-12K medium supplemented with 10% FBS and 1% penicillin/streptomycin. 22Rv1 cells were cultured in RPMI-1640 medium supplemented with 10% FBS and 1% penicillin/streptomycin. Cells in log phase growth were harvested by trypsinization followed by two washings to remove all traces of enzyme. A total of 10,000 cells were seeded per well of a 96-well clear, flat-bottom plate

(Microtest 96[®], Falcon) and incubated overnight (37°C in 5% CO₂). Following incubation, media was replaced with media containing the test compounds in serial dilution ranging from 100 μ M to 5 μ M in triplicate for 48-72 hrs. DMSO was used to solubilize compounds with the final DMSO concentration in the media 0.1%. Vehicle controls were employed in all experiments. Cell viability following treatment was determined by 3-(4, 5-dimethylthiazol-2-yl)-2, 5-diphenyltetrazolium bromide (MTT) assay as previously described.²¹⁸ After incubating the cells with test compounds, test media was replaced with media containing MTT reagent (Sigma-Aldrich) at a final concentration of 0.5 mg/mL. The cells were incubated for a period of 1 h and the media was discarded, and the formazan crystals were solubilized in DMSO on a plate shaker protected from light at all times. The reading was taken at a wavelength of 570 nm and the viability was calculated with respect to control (0.01% DMSO). IC₅₀ was calculated with GraphPad Prism 5.0. using Non-linear regression analysis.

3.5 Cytotoxicity Results and Discussion

Based upon reported ethnomedicinal reports of *I. trichantha* tuber use in West African traditional to treat “soft tumors,”⁶² cytotoxicity assays were conducted to assist with bioassay-guided fractionation and to determine the anticancer potential of isolated phytochemicals. Compounds **5**, **6**, **7**, **9**, **14**, and **17-22** were evaluated for cytotoxic activity against MDA-MB-435 (human melanoma cancer), MDA-MB-231 (human breast cancer), and OVCAR3 (human ovarian cancer) cell lines. Compound **13** was screened against the MDA-MB-435 cell line. Compounds **11-12** were evaluated against the HT-29 (human colorectal cancer) cell line. Compound **7** was the most active, with IC₅₀ values of 1.48–3.23 μ M; compound **6** showed IC₅₀ values of 2.91–7.60 μ M. Compounds **9**, **14**, **21**, and

22 did not show significant cytotoxicity at concentrations up to 20 μ M (TABLE XIV).

Collectively, the reported cytotoxicity data of (9 β -H)-pimarane and derivatives^{76–78} showed that compounds possessing a 9 β -hydrogen are cytotoxic while those with an aromatic C-ring are inactive.

Compounds **17** – **20** were assessed for cytotoxicity (TABLE XIV) against the MDA-MB-435 human melanoma cell line but did not show measurable inhibitory activity. Compounds **18** and **19** were also screened against the MDA-MB-231 and OVCAR3 cell lines but were found to be inactive as well. This is in sharp contrast to the significantly stronger activity against the same cell lines by humirianthol (**2**) and icacinol (**1**), which possess an γ -lactone ring between C-4 and C-6.⁷⁶ This suggests that the lactone moiety is essential to activity, though a possible mechanism of action cannot be proposed at this time.

It is thus proposed that the presence of a 9 β -hydrogen or an alicyclic C-ring in addition to the γ -lactone moiety in these structures is essential for their cytotoxicity, though more detailed supportive evidence is still required.

TABLE XIV. CYTOTOXIC ACTIVITY OF ISOLATED NOVEL COMPOUNDS

compound	IC ₅₀ (μ M)			
	MDA-MB-435	MDA-MB-231	OVCAR3	HT-29
5	>20	>20	>20	NT ^a
6	2.91	7.60	7.53	NT
7	1.48	2.85	3.23	NT
9	> 20	> 20	> 20	NT
11	NT	NT	NT	> 20
12	NT	NT	NT	> 20
13	> 20	NT	NT	NT
14	> 20	> 20	> 20	NT
17	> 20	> 20	> 20	NT
18	> 20	> 20	> 20	NT
19	> 20	> 20	> 20	NT
20	> 20	> 20	> 20	NT
21	> 20	> 20	> 20	NT
22	> 20	> 20	> 20	NT
1^b	1.25 ^c	7.30 ^c	7.55 ^c	4.23
2^b	1.65 ^c	3.73 ^c	4.12 ^c	4.94
Taxol	0.1 nM	171.4 nM	1.45 nM	13.0 nm

^a Not tested. ^b Included for reference^{76,78}

Select isolated compounds were chosen for further cytotoxicity testing in human colorectal and prostate cancer cell lines. Icacinol (**1**) and humirianthol (**2**) were chosen based upon their previously reported anticancer activity. Icacinlactone E (**8**) was also tested for comparison due to its inactivity and structural diversity. The compounds were screened against HCT-116 colorectal cancer cells and prostate cancer cells PC-3 and 22Rv1 (TABLE XV). Due to the clinical importance of hormonal therapy targeting AR for treatment of prostate cancer, both AR-positive (22Rv1) and AR-negative (PC-3) cell lines were used.^{199,200,219} Compound **2** demonstrated a much stronger cytotoxic response in the three cancer cell lines compared with previous experiments with human ovarian, breast, and melanoma cancers. In both prostate cells, its IC₅₀ was measured in the nanomolar level, suggesting promising therapeutic potential. On the other hand, the cytotoxic activity range of compound **1** (1.63 – 6.43 μ M) was comparable with previous results. Surprisingly, compound **8** showed similar activity levels as compound **1**, which is a sharp contrast to previous measured activity. Overall, all three compounds showed moderate to significant cytotoxic activity against the three cell lines, with AR-positive 22Rv1 cells the most sensitive.

TABLE XV. CYTOTOXIC ACTIVITY OF ICACINOL (1), HUMIRIANTHOL (2), AND ICACINLACTONE E (8)

compound	IC ₅₀ (μ M) ^a		
	PC-3	22Rv1	HCT-116
1	6.43	1.63	3.13
2	60.1 (nM)	4.29 (nM)	0.410
8	1.04	3.21	4.55

^aMeasured against negative DMSO-vehicle control.

These findings were also compared with literature reported resorts of other diterpenoids screened against the same cell lines (Figure 40). Melanocane A and B isolated from the roots of *Aralia melanocarpa* showed relative IC_{50} values of 6.92 and 4.33 μM , respectively against PC-3 cells.²²⁰ Aerial parts of *Orthosiphon stamineus* yielded orthosiphol E and was similarly tested against PC-3 with reported relative IC_{50} values of 28.7 μM .²²¹ Sphaeropsidin A, a pimarane with a lactone moiety, was isolated *in vitro* from a phytotoxic fungus, *Sphaeropsis sapinea f. sp. Cupressi*, and was later screened against PC-3, with a reported relative IC_{50} values of 2.5 μM .²²² Interestingly, sphaeropsidin A performed similarly to compound 1, 2, and 8 against PC-3 cells, suggesting a possible structure-activity relationship from the presence of a lactone group.

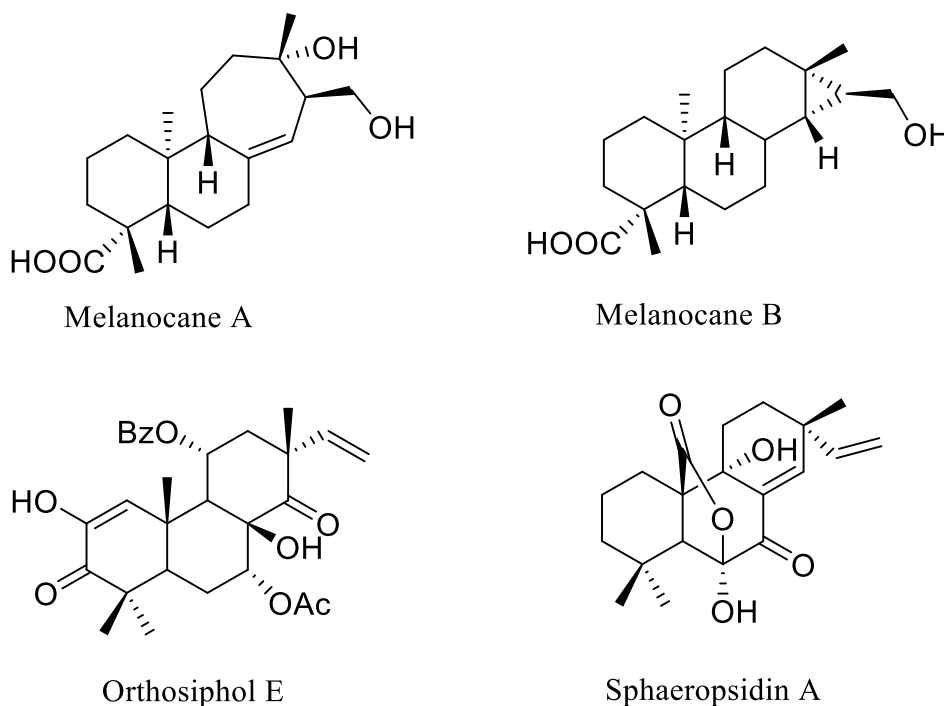


Figure 40. Related pimarane diterpenoids screened against PC-3 cancer cells

3.6 Conclusion

The discovery of the potential herbicidal activity of icacinol (**1**) now adds to our knowledge of the (9 β H)-pimarane diterpenes. These versatile molecules seem to be the natural choice for plant defense during evolution, and they can serve as prototypes for other lead compounds in the search for selective herbicides, antifungal agents, and related agricultural substances. Further studies on natural sources to enrich structural diversity of momilactone-like molecules and discovery of more promising lead compounds and adjuvants for treatment are desirable goals for weed management.

In summary, fourteen new *Icacina* diterpenoids were isolated from the tuber of *I. trichantha*, all belonging to the pimarane subclass. In comparison with the cytotoxic activity of other pimarane-type compounds found in *Icacina*, the presence of a 9 β -hydrogen or an alicyclic C-ring in addition to the γ -lactone moiety in these structures seems to be essential for their cytotoxicity. These results provide insight into their structure-activity relationship in human cancer cells and could be helpful in any medicinal chemistry structural modifications to improve their activity. A mechanism of action or target-binding information cannot be proposed at this time but warrants further study.

4. CONCLUSIONS AND PERSPECTIVES

Natural product research continues to find new and interesting chemistry in the hope of discovering unique biological targets or mechanisms of action.¹¹ Over the past century, natural products have directly and indirectly inspired a majority of developed drugs.¹⁵ Screening of medicinal plants reportedly used by traditional medicine systems is a rational approach to drug discovery.²⁴ This tactic can increase the likelihood of isolating an active compound or compounds that have similar biological activity as the reported medicinal application.²³ Plants have been a fertile source of important drugs such as taxanes¹²¹ and podophyllotoxins.²²³ Plants are also prolific producers of terpenes, the largest chemical class of natural products, that have also demonstrated a variety of biological activities.²²⁴ The pimarane-class diterpenoids reported from *Icacina trichantha* have demonstrated moderate cytotoxic and anti-germination activity but are still poorly understood overall.

Icacina trichantha (Oliv. Icacinaceae) is an ethnomedicinal plant endemic to West Africa and is primarily utilized for the local traditional medicine system. Extracts of the tuber are reportedly orally administered to treat malaria, hepatitis, and tumors, though its clinical effectiveness is unknown. It is commonly found among rural vegetative areas, and the local populace frequently uses tinctures as an emetic to treat poisonings.^{62,108} There are also reports of the tuber being consumed during periods of famine.¹⁰⁷ Plant extract was used for initial biological experiments *in vivo* that confirmed the emetic activity⁷⁵ and also demonstrated moderate anti-inflammatory,¹¹⁰ anti-hepatotoxic,⁹⁹ and anti-oxidant activity.⁹² Beginning in 2014, the first phytochemical analysis of this species began with a collaboration between the University of Illinois at Chicago, the University of Nigeria, and the University of Abuja. The first publication by collaborator Dr. Monday M. Onakpa reported diterpenoids belonging to the

rare pimarane chemical class.²²⁵ Publications from continued research established that *I. trichantha* is chemotaxonomically defined by these unusual natural products.^{77–79}

The study of *I. trichantha* was continued with new plant material provided by collaborators from Nigeria with two primary goals: 1) isolate and purify novel bioactive compounds to expand the chemotaxonomic profile of the species and 2) collect more materials of previously reported active pimaranes to continue biological assessment these compounds. A bioassay-guided fractionation approach was used to apply orthogonal chromatographic methods to separate and purify target compounds. Isolated metabolites were spectroscopically analyzed, primarily relying on NMR and MS, to elucidate their structures. This resulted in fourteen novel compounds belonging to the rare pimarane diterpene class²²⁶ in addition to eight previously reported, one artifact, and a well-known lignan that was the first reported from this genus. Included in these newly reported phytochemicals are the first reported 16,17-di-*nor*-pimarane (**21**, icacinlactone K), 17,19-di-*nor*-pimarane (**22**, icacintrichanone), and 19-*nor*-pimaranes (**17** – **20**, icatrichanone, 14-hydroxyicatrichanone, 3-methoxyicatrichanone, and 3-methoxy-14-hydroxyicatrichanone) from the *Icacina* genus. These findings expanded our understanding of the chemical diversity within this medicinal plant and added to the chemical diversity of terpene natural products.

Though there are reports of 19-*nor*-pimaranes isolated from natural sources,^{145,146,161,220} they are an unusual subclass of natural products. The pimaranes from *I. trichantha* are particularly interesting due to the single methyl group at the C-4 position. Terpene synthesis typically results in a dimethyl group at that structural position due to the arrangement of the isoprenyl building blocks.^{120,159} The proposed biogenesis for the pimarane lactones that have come to represent this species¹⁵⁵ were not immediately applicable to the 19-*nor*-pimaranes.

Therefore, a search of the literature was conducted for other examples in natural products or possible mechanisms. Ultimately, the biogenetic picture is still unclear with one possibility of a post-genesis modification¹⁵³ or a pathway involving sterol synthesis-like mechanisms.²²⁷

Overall, the phytochemical work presented here and in previous reports^{77–79,225} establishes pimarane diterpenoids as a chemotaxonomic marker for *Icacina trichantha* and the *Icacina* genus in general. The identified compounds include 9 β H-pimaranes, *nor*-pimaranes, and di-*nor*-pimaranes and are also characterized by a γ -lactone moiety in most cases, making this species a natural source for a rare class of compounds.

Processing the large amount of plant material required workflows to dereplicate previously reported compounds so as to focus on novel compounds and the development of efficient purification methods to procure large samples of the bioactive compounds of interest, particularly humirianthol (compound **2**) and icacinol (compound **1**). A dereplication process was developed that relied upon a Shimadzu single quadrupole MS detector and data processing software. A library was gradually built that uses parameters from ESI-MS and HPLC-UV to characterize each compound. Initial identification relied upon comparison of the specific ¹H spectrum for each compound¹³⁸ that was obtained and compared with a repository of all previously isolated compounds from *I. trichantha*. This process yielded a growing stockpile of these unique pimaranes, including compounds **1** and **2**.

Weeds are the prevalent pest that hinders crop production in agricultural.^{180,228} Herbicides are heavily relied upon to efficiently remove these pests and maintain food output. However, their continued use has led to prevalence of herbicide-resistant weeds, requiring new treatments to be developed.^{184,192} Extract of *I. trichantha* and compound **1** were examined for anti-germination activity against *Arabidopsis* weed.¹³² *Oryza sativa* rice seedlings were also treated to

determine selective protection. Results determined that compound **1** discriminately inhibited Arabidopsis seed germination and growth. Comparatively, rice seed germination and germination were only minorly affected by treatment. This selective activity suggests further interrogation of herbicidal activity and selectivity is warranted.

All isolated compounds were screened against human cancer cell lines. *2β*-Hydroxyhumirianthenolide C (compound **7**) was the most active, with IC₅₀ values of 1.48, 2.85, and 3.23 μM against MDA-MB-435, MDA-MB-231, and OVCAR3, respectively. *7α*-Hydroxicacenone (compound **6**) showed IC₅₀ values of 2.91, 7.60, and 7.53 μM against the same three cell lines. All other compounds were determined to be inactive. Compounds **1** and **2** demonstrated moderate cytotoxicity in previous reports²²⁵ and are the most abundant metabolites in *I. trichantha* extract. Both compounds were screened against PC-3, 22Rv1, and HCT-116 cancer cells. Compound **1** displayed similar cytotoxic levels as other cell lines. However, compound **2** reported IC₅₀ values of 4.29 nM and 60.1 nM against 22Rv1 and PC-3, respectively. These results indicate promising cytotoxic activity against both prostate carcinoma lines, in particular the AR-positive 22Rv1 cells.

Based upon the interesting biological activity, further exploration of structure-activity relationships should be considered. Medicinal chemistry is routinely applied to natural products to improve desirable traits for drug development.²²⁹ The structural diversity of the pimaranes from *I. trichantha* and their corresponding cytotoxic activity has already provided some insight into potential pharmacophores. Observed activities indicate that the γ -lactone moiety and the 9 β H-pimarane configuration are important.

Due to the unique pimarane diterpene chemical structures characteristic of the *Icacina* genus, further research focus should shift away from chemical analysis and towards assessing

biological targets and mechanisms of action. Regarding the anticancer activity observed in prostate cancer cells, a simple test should determine binding of AR receptor. Development of alternatives to hormonal therapy would be beneficial to clinical treatment of aggressive prostate cancers.²⁰⁰ Proteomics is a powerful biochemical tool that could provide insight into possible pathways and mechanism of action of the observed cytotoxicity.²³⁰ Treatment of normal human prostate cells, such as RWPE-1, would be needed to determine specificity and as a comparison to treated cancer cells to determine changes in protein expression. Finally, preliminary screening of other biological activity in line with reported ethnomedicinal use, such as Sickle cell disorder,⁶⁴ should be further explored.

African traditional medicine is a very deep and fascinating topic that was only discussed superficially in this dissertation. But I believe the spiritual aspect of African TM is important to consider in the context of *Icacina*. Spiritual healing is an important aspect of the African TM philosophy where sickness can be caused by an imbalance from bad or evil spirits. Purging a patient can help restore their spiritual balance, which I believe is one of the primary reasons *Icacina trichantha* seemingly has such widespread utilization in the local traditional medicine system. Its primary physiological action is acute emesis, so much so that its common name among different ethnicities refers to this property. Such an herb would naturally play a large role for a traditional healer to treat many different diseases, though mainly in the spiritual sense. It is possible that there is TM knowledge that *I. trichantha* has a specific desirable physiological action besides emesis that was developed over repeated observations of treated patients. However, this type of information has not been found and a precise explanation of the medicinal action of *I. trichantha* in TM is unclear from the literature. Such privileged information may be difficult to determine due to the lack of a strong written record of African TM. More detailed

analysis and explanation from traditional practitioners familiar with the plant would be illuminating. In addition, the preservation of traditional medicinal knowledge is important in the larger sense of maintaining the local cultural history and anthropological research.

The traditional medicine role of *Icacina trichantha* is unclear at this point. I would argue it is also somewhat dubious. There have been several medicinal plants touted for their vast beneficial properties. Herbs such as turmeric and ginseng are widely used in traditional medicine and thus were closely studied. However, the results have been underwhelming and have not yielded the expected motherlode of highly active compounds.^{231,232} It is safe to assume *I. trichantha* would follow a similar path if a chemical analysis were to continue. There is little need to continue a phytochemical study of this plant since there is strong evidence this genus primarily produces pimarane diterpenoids. Minor constituents of new types of pimaranes could be discovered to expand the known natural chemical space. However, research has indicated the 9 β H-pimarane subclass are almost exclusively active for cytotoxicity and anti-germination. These compounds should be screened for other activities. Bioassays based on other reported traditional uses, such as Sick cell, should be considered but I believe screening should be established primarily upon their unique chemistry. These compounds are unique and difficult to synthesize. *Icacina trichantha* serves as a readily available producer of these compounds and can continue in that role while the focus shifts to biological screenings and medicinal chemistry of the pimaranes.

The historic and global impact of the field of pharmacognosy cannot be understated. Natural products are an incredibly important resource for humanity. Their inherent chemical diversity extends beyond the current synthetic chemical space, a product of the evolution and natural selection of every living organism that uses specialized metabolites for survival.^{14,207}

Research of this field has greatly benefited our world with new and effective chemical tools in the fields of medicine^{22,233} and agriculture.^{189,191} The study of natural products and traditional medicine provide a global benefit in addition to a deeper understanding of our environment and the people living in it. Nature is an extremely talented chemist able to produce compounds beyond humanity's current capacity. However, a vast majority of that potential remains undiscovered. I humbly present this work to add to the collective knowledge of our world and hope that it may be beneficial to future natural product research.

REFERENCES

- (1) Pharmacy. *Encyclopædia Britannica*; 2019.
- (2) Alamgir, A. N. M.; Rainsford, K. D. *Progress in Drug Research Series Editor: Therapeutic Use of Medicinal Plants and Their Extracts: Volume 1 Pharmacognosy*; 2017; Vol. 1.
- (3) Solecki, R. S. Shanidar IV, a Neanderthal Flower Burial in Northern Iraq. *Science* (80-.). **1975**, 190 (4217), 880–881.
- (4) Huang, K. C. 1917-. *The Pharmacology of Chinese Herbs*, 2nd ed.; Williams, W. M., Ed.; CRC Press: Boca Raton, 1999.
- (5) Tirtha, S. S.; Uniyal, R. C.; S, andhu.; Chandhok, J. K. *Ayurveda Encyclopedia : Natural Secrets to Healing, Prevention, & Longevity*; Sat Yuga Press: Bayville, UNITED STATES, 2007.
- (6) Saad, B.; Said, O. *Greco-Arab and Islamic Herbal Medicine : Traditional System, Ethics, Safety, Efficacy, and Regulatory Issues*; John Wiley & Sons, Incorporated: Hoboken, UNITED STATES, 2011.
- (7) Kapoor, L. D. *Handbook of Ayurvedic Medicinal Plants*; Routledge, 2017, DOI: 10.1201/9780203719473.
- (8) Cragg, G. M.; Newman, D. J. Natural Products: A Continuing Source of Novel Drug Leads. *Biochim. Biophys. Acta - Gen. Subj.* **2013**, 1830 (6), 3670–3695, DOI: 10.1016/j.bbagen.2013.02.008.
- (9) World Health Organization. *Traditional Medicine: Growing Needs and Potential. Geneva: World Health Organization; 2002; 2002.*
- (10) World Health Organization. *WHO Guidelines on Developing Consumer Information on Proper Use of Traditional, Complementary and Alternative Medicine*; Geneva: World Health Organization, 2004.
- (11) Filho, V. C. *Natural Products as Source of Molecules with Therapeutic Potential*; 2018, DOI: 10.1007/978-3-030-00545-0.
- (12) World Health Organization. *WHO Global Report on Traditional and Complementary Medicine 2019*; 2019.
- (13) Smith, T.; Gillespie, M.; Eckl, V.; Knepper, J.; Morton-Reynolds, C. Herbal Supplement Sales in US Increase by 9.4% in 2018. *HerbalGram* **2019**, 123, 62–73.
- (14) Newman, D. J.; Cragg, G. M.; Snader, K. M. The Influence of Natural Products upon Drug Discovery. *Nat. Prod. Rep.* **2000**, 17 (3), 215–234, DOI: 10.1039/a902202c.
- (15) Newman, D. J.; Cragg, G. M. Natural Products as Sources of New Drugs from 1981 to 2014. *J. Nat. Prod.* **2016**, 79 (3), 629–661, DOI: 10.1021/acs.jnatprod.5b01055.
- (16) Shen, B. A New Golden Age of Natural Products Drug Discovery. *Cell* **2015**, 163 (6), 1297–1300, DOI: 10.1016/J.CELL.2015.11.031.
- (17) Wu, K.; Wu, C.; Dou, J.; Ghantous, H.; Lee, S.; Yu, L. A Update of Botanical Drug Development in the United States: Status of Applications. *Planta Med.* **2015**, 81 (11), 8847620, DOI: 10.1055/s-0035-1556235.
- (18) Mikulic, M. Number of Botanical Investigational New Drug Applications Submitted to the FDA from 2002 to 2016. Statista 2018.
- (19) Chen, S. T.; Dou, J.; Temple, R.; Agarwal, R.; Wu, K.-M.; Walker, S. New Therapies

- from Old Medicines. *Nat. Biotechnol.* **2008**, 26 (10), 1077–1083, DOI: 10.1038/nbt1008-1077.
- (20) Ahn, K. The Worldwide Trend of Using Botanical Drugs and Strategies for Developing Global Drugs. *BMB Rep.* **2017**, 50 (3), 111–116, DOI: 10.5483/bmbrep.2017.50.3.221.
 - (21) Brinckmann, J. A. Reproducible Efficacy and Safety Depend on Reproducible Quality: Matching the Various Quality Standards That Have Been Established for Botanical Ingredients with Their Intended Uses in Cosmetics, Dietary Supplements, Foods, and Medicines. *HerbalGram* **2011**, 91, 40–55.
 - (22) Schmidt, B.; Ribnicky, D. M.; Poulev, A.; Logendra, S.; Cefalu, W. T.; Raskin, I. A Natural History of Botanical Therapeutics. *Metabolism.* **2008**, 57 (SUPPL. 1), S3, DOI: 10.1016/j.metabol.2008.03.001.
 - (23) Fabricant, D. S.; Farnsworth, N. R. The Value of Plants Used in Traditional Medicine for Drug Discovery. *Environ. Health Perspect.* **2001**, 109, 69, DOI: 10.2307/3434847.
 - (24) Farnsworth, N. R.; Akerele, O.; Bingel, A. S.; Soejarto, D. D.; Guo, Z. Medicinal Plants in Therapy. *Bull. World Health Organ.* **1985**, 63 (6), 965–981, DOI: 10.1016/0378-8741(87)90016-x.
 - (25) Wang, J.; Zhang, C. J.; Chia, W. N.; Loh, C. C. Y.; Li, Z.; Lee, Y. M.; He, Y.; Yuan, L. X.; Lim, T. K.; Liu, M.; et al. Haem-Activated Promiscuous Targeting of Artemisinin in Plasmodium Falciparum. *Nat. Commun.* **2015**, 6, DOI: 10.1038/ncomms10111.
 - (26) Abdullahi, A. A. Trends and Challenges of Traditional Medicine in Africa. *African J. Tradit. Complement. Altern. Med.* **2011**, 8 (5 SUPPL.), 115–123, DOI: 10.4314/ajtcam.v8i5S.5.
 - (27) Innocent, E. Trends and Challenges toward Integration of Traditional Medicine in Formal Health-Care System: Historical Perspectives and Appraisal of Education Curricula in Sub-Sahara Africa. *J. Intercult. Ethnopharmacol.* **2016**, 5 (3), DOI: 10.5455/jice.20160421125217.
 - (28) Gqaleni, N.; Moodley, I.; Kruger, H.; Ntuli, A.; McLeod, H. Traditional and Complementary Medicine Policy. *South African Heal. Rev.* **2007**, 175–188.
 - (29) Iwu, M. M. *Handbook of African Medicinal Plants*; CRC Press: Boca Raton, 1993.
 - (30) Ozioma, E.-O. J. Herbal Medicines in African Traditional Medicine; Builders, O. A. N. C. E.-P. F., Ed.; IntechOpen: Rijeka, 2019; p Ch. 10, DOI: 10.5772/intechopen.80348.
 - (31) Raphael, E. C. Traditional Medicine in Nigeria: Current Status and the Future. *Research Journal of Pharmacology.* 2011, pp 90–94, DOI: 10.3923/rjpharm.2011.90.94.
 - (32) Abd El-Ghani, M. M. AGRICULTURE AND BIOLOGY JOURNAL OF NORTH AMERICA Traditional Medicinal Plants of Nigeria: An Overview. **2016**, No. October, 220–247, DOI: 10.5251/abjna.2016.7.5.220.247.
 - (33) Mahomoodally, M. F. Evidence - Based Complementary and Alternative Medicine Traditional Medicines in Africa : An Appraisal of Ten Potent African Medicinal Plants. *Evidence-based Complement. Altern. Med.* **2013**, 2013, 1–10.
 - (34) Aslam, J.; Khan, S. H.; Siddiqui, Z. H.; Fatima, Z.; Maqsood, M.; Bhat, M. A.; Nasim, S. A.; Ilah, A.; Ahmad, I. Z.; Khan, S. A. Catharanthus Roseus (L.) G. Don. An Important Drug: It's Applications and Production. *Int. J. Compr. Pharm.* **2010**, 4 (12), 1–16.
 - (35) David, B.; Wolfender, J. L.; Dias, D. A. The Pharmaceutical Industry and Natural Products: Historical Status and New Trends. *Phytochem. Rev.* **2015**, 14 (2), 299–315, DOI: 10.1007/s11101-014-9367-z.
 - (36) Linder, H. P. The Evolution of African Plant Diversity . *Frontiers in Ecology and*

- Evolution* . 2014, p 38.
- (37) Van Wyk, B.-E. A Review of Commercially Important African Medicinal Plants. *J. Ethnopharmacol.* **2015**, 176, 118–134, DOI: <https://doi.org/10.1016/j.jep.2015.10.031>.
 - (38) Hostettmann, K.; Marston, A.; Wolfender, K. N. and J.-L. The Potential of African Plants as a Source of Drugs. *Current Organic Chemistry*. 2000, pp 973–1010, DOI: <http://dx.doi.org/10.2174/1385272003375923>.
 - (39) Ntie-Kang, F.; Zofou, D.; Babiaka, S. B.; Meudom, R.; Scharfe, M.; Lifongo, L. L.; Mbah, J. A.; Mbaze, L. M.; Sippl, W.; Efange, S. M. N. AfroDb: A Select Highly Potent and Diverse Natural Product Library from African Medicinal Plants. *PLoS One* **2013**, 8 (10), e78085, DOI: 10.1371/journal.pone.0078085.
 - (40) Iwu, M. M. *Handbook of African Medicinal Plants, Second Edition*; Taylor & Francis, 2014.
 - (41) Neuwinger, H. D. *African Traditional Medicine: A Dictionary of Plant Use and Applications. With Supplement: Search System for Diseases.*; Medpharm: Stuttgart, 2000.
 - (42) Bosch, C. H.; Siemonsma, J. S.; Lemmens, R. H. M. J.; Oyen, L. P. A. *Plant Resources of Tropical Africa. Basic List of Species and Commodity Grouping.*; Programme PROTA: Wageningen, 2002.
 - (43) Joppa, L. N.; Pfaff, A. Global Protected Area Impacts. *Proc. R. Soc. B Biol. Sci.* **2011**, 278 (1712), 1633–1638, DOI: 10.1098/rspb.2010.1713.
 - (44) Green, J. M. H.; Larrosa, C.; Burgess, N. D.; Balmford, A.; Johnston, A.; Mbilinyi, B. P.; Platts, P. J.; Coad, L. Deforestation in an African Biodiversity Hotspot: Extent, Variation and the Effectiveness of Protected Areas. *Biol. Conserv.* **2013**, 164, 62–72, DOI: <https://doi.org/10.1016/j.biocon.2013.04.016>.
 - (45) Simoben, C. V; Ntie-Kang, F.; Lifongo, L. L.; Babiaka, S. B.; Sippl, W.; Mbaze, L. M. The Uniqueness and Therapeutic Value of Natural Products from West African Medicinal Plants, Part III: Least Abundant Compound Classes. *RSC Adv.* **2014**, 4 (75), 40095–40110, DOI: 10.1039/C4RA05376A.
 - (46) Ntie-Kang, F.; Lifongo, L. L.; Simoben, C. V; Babiaka, S. B.; Sippl, W.; Mbaze, L. M. The Uniqueness and Therapeutic Value of Natural Products from West African Medicinal Plants. Part I: Uniqueness and Chemotaxonomy. *RSC Adv.* **2014**, 4 (54), 28728–28755, DOI: 10.1039/C4RA03038A.
 - (47) Ntie-Kang, F.; Lifongo, L. L.; Simoben, C. V; Babiaka, S. B.; Sippl, W.; Mbaze, L. M. The Uniqueness and Therapeutic Value of Natural Products from West African Medicinal Plants, Part II: Terpenoids, Geographical Distribution and Drug Discovery. *RSC Adv.* **2014**, 4 (67), 35348–35370, DOI: 10.1039/C4RA04543B.
 - (48) Burkill, H. M. *The Useful Plants of West Tropical Africa. Volume 2: Families E-I.*; Royal Botanic Gardens: Kew, 1994.
 - (49) The Plant List Version 1.1 <http://www.theplantlist.org/> (accessed Mar 12, 2019).
 - (50) Paris., S. d'Histoire N. de. *Mémoires de La Société d'Histoire Naturelle de Paris.*; 1823.
 - (51) Raynal, J. Changement Du Nom de l'espece-Type d'Icacina Juss. *Adansonia* **1975**, 15, 193–194.
 - (52) Garden., M. B. Tropicos.org. <http://www.tropicos.org/Name/50085145> (accessed Nov 30, 2019).
 - (53) Kaplan, M. A. C.; Ribeiro, J.; Gottlieb, O. R. Chemogeographical Evolution of Terpenoids in Icacinaceae. *Phytochemistry* **1991**, 30 (8), 2671–2676, DOI: 10.1016/0031-9422(91)85121-F.

- (54) Group, T. A. P. An Ordinal Classification for the Families of Flowering Plants. *Ann. Missouri Bot. Gard.* **1998**, 85 (4), 531–553, DOI: 10.2307/2992015.
- (55) Kårehed, J. Multiple Origin of the Tropical Forest Tree Family Icacinaceae. *Am. J. Bot.* **2001**, 88 (12), 2259–2274, DOI: 10.2307/3558388.
- (56) Chase, M. W.; Christenhusz, M. J. M.; Fay, M. F.; Byng, J. W.; Judd, W. S.; Soltis, D. E.; Mabberley, D. J.; Sennikov, A. N.; Soltis, P. S.; Stevens, P. F.; et al. An Update of the Angiosperm Phylogeny Group Classification for the Orders and Families of Flowering Plants: APG II. *Bot. J. Linn. Soc.* **2016**, 181 (1), 1–20, DOI: 10.1111/boj.12385.
- (57) Oliver, D. *Flora of Tropical Africa /by Daniel Oliver ... Assisted by Other Botanists.*; L. Reeve and co.; London :, 1868; Vol. v.1 (1868), DOI: 10.5962/bhl.title.42.
- (58) Reveal, J. L.; Reveal, J. L. New Ordinal Names for Extant Vascular Plants. *Phytologia*. **1993**, 74, 173–177.
- (59) Gardens, R. B. *Icacina trichantha* - Royal Botanic Gardens
<http://specimens.kew.org/herbarium/K000226065> (accessed Sep 12, 2019).
- (60) M. Ubom, R. Ethnobotany and Biodiversity Conservation in the Niger Delta, Nigeria. *Int. J. Bot.* **2010**, 6 (3), 310–322, DOI: 10.3923/ijb.2010.310.322.
- (61) Conservatoire et Jardin botaniques de la Ville de Genève and South African National Biodiversity Institute, P. African Plant Database (version 3.4.0) <http://www.ville-ge.ch/musinfo/bd/cjb/africa/> (accessed Jan 12, 2019).
- (62) Burkill, H. M. The Useful Plants of West Tropical Africa. *R. Bot. Gard. Kew, UK* **1985**, 2nd editio, 4–8, DOI: 10.1097/NAQ.0b013e318258ba14.
- (63) On'Okoko, P.; Vanhaelen, M.; Vanhaelen-Fastré, R.; Declercq, J. P.; Van Meerssche, M. Icacenone, a Furanoditerpene with a Pimarane Skeleton from *Icacina Mannii*. *Phytochemistry* **1985**, 24 (10), 2452–2453, DOI: 10.1016/S0031-9422(00)83067-8.
- (64) Amujoyegbe, O. O.; Idu, M.; Agbedahunsi, J. M.; Erhabor, J. O. Ethnomedicinal Survey of Medicinal Plants Used in the Management of Sickle Cell Disorder in Southern Nigeria. *J. Ethnopharmacol.* **2016**, 185, 347–360, DOI: <https://doi.org/10.1016/j.jep.2016.03.042>.
- (65) Madge, C. Therapeutic Landscapes of the Jola, The Gambia, West Africa. *Health Place* **1998**, 4 (4), 293–311, DOI: 10.1016/S1353-8292(98)00033-1.
- (66) Gill, L. S. *Ethnomedical Uses of Plants in Nigeria*; Uniben Press, 1992.
- (67) Bouquet, A. Féticheurs et Médecines Traditionnelles Du Congo (Brazzaville). *ORSTOM* **1969**, 36.
- (68) le Grand, A.; Wondergem, P. . Les Phytothérapies Anti-Infectieuses de La Forêtsavane, Senegal (Afrique Occidentale) I. Un Inventaire. *J. Ethnopharmacol.* **1987**, 21 (2), 109–125, DOI: 10.1016/0378-8741(87)90122-X.
- (69) Okieimen, E. F.; Owolabi, O. J.; Iyekowa, O.; Jonathan, E. M. Uterine Contractile Activity of Extract of *Icacina Trichantha* on Albino Non-Pregnant Rat Uterus. *Trop. J. Nat. Prod. Res.* **2018**, 2 (3), 118–121, DOI: 10.26538/tjnpr/v2i3.3.
- (70) Borokini, Israel Clement M, D. N. . and E. D. . Ethnobiological Survey of Traditional Medicine Practice for Circulatory and Nervous System Related Diseases in Oyo State , Nigeria. *Topclass J. Herb. Med.* **2013**, 2 (6), 111–120.
- (71) Kerharo, J.; Adam, J. G. Les Plantes Médicinales, Toxiques et Magiques Des Niominka et Des Socé Des Iles Du Saloum (Sénégal). *Acta Trop Suppl* **1964**, 8, 279–334.
- (72) On'okoko, P.; Vanhaelen, M.; Vanhaelen-Fastré, R.; Declercq, J. P.; Van Meerssche, M. The Constitution of Icacinol, a New Diterpene with a Pimarane Skeleton from *Icacina Claessensis*. *Tetrahedron* **1985**, 41 (4), 745–748, DOI: 10.1016/S0040-4020(01)96452-X.

- (73) Ajibesin, K. K.; Ekpo, B. A.; Bala, D. N.; Essien, E. E.; Adesanya, S. A. Ethnobotanical Survey of Akwa Ibom State of Nigeria. *J. Ethnopharmacol.* **2008**, *115* (3), 387–408, DOI: 10.1016/j.jep.2007.10.021.
- (74) Bassey and Effiong. Preliminary Investigation of Herbs Used in Paediatric Care among the People of Akwa Ibom State, Nigeria. *J. Nat. Prod. Plant Resour.* **2011**, *1* (3), 33–42.
- (75) Asuzu, I. U.; Ugwueze, E. E. Screening of Icacin Trichantha Extracts for Pharmacological Activity. *J. Ethnopharmacol.* **1990**, *28* (2), 151–156, DOI: 10.1016/0378-8741(90)90024-N.
- (76) Onakpa, M. M.; Zhao, M.; Gödecke, T.; Chen, W. L.; Che, C. T.; Santarsiero, B. D.; Swanson, S. M.; Asuzu, I. U. Cytotoxic (9 β H)-Pimarane and (9 β H)-17-Norpimarane Diterpenes from the Tuber of Icacin Trichantha. *Chem. Biodivers.* **2014**, *11* (12), 1914–1922, DOI: 10.1002/cbdv.201400151.
- (77) Zhao, M.; Onakpa, M. M.; Santarsiero, B. D.; Chen, W.-L.; Szymulanska-Ramamurthy, K. M.; Swanson, S. M.; Burdette, J. E.; Che, C.-T. (9 β H)-Pimaranes and Derivatives from the Tuber of Icacin Trichantha. *J. Nat. Prod.* **2015**, *78* (11), 2731–2737, DOI: 10.1021/acs.jnatprod.5b00688.
- (78) Zhao, M.; Onakpa, M. M.; Chen, W.-L.; Santarsiero, B. D.; Swanson, S. M.; Burdette, J. E.; Asuzu, I. U.; Che, C.-T. 17-Norpimaranes and (9 β H)-17-Norpimaranes from the Tuber of Icacin Trichantha. *J. Nat. Prod.* **2015**, *78* (4), 789–796, DOI: 10.1021/np5010328.
- (79) Zhao, M.; Onakpa, M. M.; Santarsiero, B. D.; Huang, X. J.; Zhang, X. Q.; Chen, J.; Cheng, J. J.; Longnecker, R.; Che, C. T. Icacinlactone H and Icacintrichantholide from the Tuber of Icacin Trichantha. *Org. Lett.* **2015**, *17* (15), 3834–3837, DOI: 10.1021/acs.orglett.5b01806.
- (80) On'okoko, P.; Hans, M.; Colau, B.; Hootelé, C.; Declercq, J. P.; Germain, G.; van Meeressche, M. L'icacine, Nouvel Alcaloïde Diterpenique De Icacin Gussfeldtii. *Bull. des Sociétés Chim. Belges* **1977**, *86* (9), 655–661, DOI: 10.1002/bscb.19770860902.
- (81) On'okoko, P.; Vanhaelen, M. Two New Diterpene-Based Alkaloids from Icacin Guesfeldtii. *Phytochemistry* **1980**, *19* (2), 303–305, DOI: 10.1016/S0031-9422(00)81979-2.
- (82) Vanhaelen, M.; Planchon, C.; Vanhaelen-Fastré, R.; On'Okoko, P. Terpenic Constituents from Icacin Senegalensis. *J. Nat. Prod.* **1987**, *50* (2), 312, DOI: 10.1021/np50050a048.
- (83) Soicke, H.; Görler, K.; Waring, H. Terpenic Constituents from Icacin Senegalensis. *Planta Med.* **1991**, *57* (01), 86–87, DOI: 10.1055/s-2006-960030.
- (84) Manga, A.; Gassama, A.; Sy, G. Y.; Bassene, E.; Lavaud, C. Structural Determination of New Flavones C-Glycosides and Trans (S, E)-(-) Clovamide Isolated Icacin Senegalensis Juss Leaves (Icacinaceae). *J. Soc. Ouest-Afr. Chim* **2013**, *35*, 15–27.
- (85) Sun, M. Identification of Diterpenoids From Icacin Oliviformis, University of Illinois at Chicago, 2019.
- (86) Zhou, J.; Wu, Z.; Guo, B.; Sun, M.; Onakpa, M. M.; Yao, G.; Zhao, M.; Che, C. Modified Diterpenoids from the Tuber of Icacin Oliviformis as Protein Tyrosine Phosphatase 1B Inhibitors. *Org. Chem. Front.* **2020**, DOI: 10.1039/C9QO01320B.
- (87) Otun, K. O.; Onikosi, D. B.; Ajiboye, A. T.; Jimoh, A. A. Chemical Composition, Antioxidant and Antimicrobial Potentials of Icacin Trichantha Oliv. Leaf Extracts. *Res. J. Phytochem.* **2015**, *9* (4), 161–174, DOI: 10.3923/rjphyto.2015.161.174.
- (88) Aderonke, S. T.; Ayorinde Babatunde, J.; Temitope Adesola, O.; Uchennaya Okereke, O.; Innocent, C.; Oluwaseun Elisha, M.; Lanre Abolaji, O.; Olubunmi Abiola, M. Evaluation

- of Retinoblastoma (Rb) and Protein-53 (P53) Gene Expression Levels in Breast Cancer Cell Lines (MCF- 7) Induced with Some Selected Cytotoxic Plants. *J. Pharmacogn. Phyther.* **2013**, 5 (7), 120–126, DOI: 10.5897/JPP2013.0270.
- (89) Guo, B.; Onakpa, M. M.; Huang, X.-J.; Santarsiero, B. D.; Chen, W.-L.; Zhao, M.; Zhang, X.-Q.; Swanson, S. M.; Burdette, J. E.; Che, C.-T. Di -nor - and 17- nor -Pimaranes from *Icacina Trichantha*. *J. Nat. Prod.* **2016**, 79 (7), 1815–1821, DOI: 10.1021/acs.jnatprod.6b00289.
- (90) Timothy, O.; Idu, M.; Olorunfemi, D. I.; Ovuakporie-Uvo, O. Cytotoxic and Genotoxic Properties of Leaf Extract of *Icacina Trichantha* Oliv. *South African J. Bot.* **2014**, 91, 71–74, DOI: 10.1016/j.sajb.2013.11.008.
- (91) . M. O. S.; . O. A. O.; . O. B. F.; . S. I. I.-A. Free Radical Scavenging Activity of Some Nigerian Medicinal Plant Extracts. *Pakistan J. Biol. Sci.* **2006**, 9 (8), 1438–1441, DOI: 10.3923/pjbs.2006.1438.1441.
- (92) Onakpa, M. M.; Ode, J. O.; Ajagbonna, O. P. and Asuzu, I. U. In Vivo and in Vitro Antioxidant Effects of *Icacina Trichantha* Tuber Extract. *Niger. Vet. J.* **2016**, 37 (3), 148–154–154.
- (93) Alawode, T. T.; Lajide, L.; Owolabi, B. J.; Olaleye, M. T. Investigation into the Antioxidant and In Vitro Anti-Inflammatory Use of the Leaves and Tuber Extracts of *Icacina Trichantha*. *J. Chem Soc. Niger.* **2018**, 43 (4), 699–706.
- (94) Timothy, O.; Idu, M. Preliminary Phytochemistry and in Vitro Antimicrobial Properties of Aqueous and Methanol Extracts of *Icacina Trichantha* Oliv. Leaf. *Int. J. Med. Aromat. Plants* **2011**, 1 (3), 184–188.
- (95) Shagal, M. H. Antimicrobial and Phytochemical Screening of *Icacina Trichantha*. *Am. J. Biomed. Life Sci.* **2013**, 1 (2), 37, DOI: 10.11648/j.ajbls.20130102.11.
- (96) le Grand, A.; Wondergem, P. A.; Verpoorte, R.; Pousset, J. L. Anti-Infectious Phytotherapies of the Tree-Savannah of Senegal (West-Africa) II. Antimicrobial Activity of 33 Species. *J. Ethnopharmacol.* **1988**, 22 (1), 25–31, DOI: 10.1016/0378-8741(88)90227-9.
- (97) David-Oku, E.; Bassey, S. C.; Obiajunwa-Otteh, J. I.; Ekpenyong, E. U. Comparative Phytochemical and Antimicrobial Activities of Polar Solvents Tuber Extracts of *Icacina Senegalensis* A. Juss (Icacinaceae). *Med. Res. Arch.* **2017**, 5 (11), 1–9, DOI: 10.18103/mra.v5i11.1501.
- (98) Sarr, S. O.; Perrotey, S.; Fall, I.; Ennahar, S.; Zhao, M.; Diop, Y. M.; Candolfi, E.; Marchioni, E. *Icacina Senegalensis* (Icacinaceae), Traditionally Used for the Treatment of Malaria, Inhibits in Vitro Plasmodium Falciparum Growth without Host Cell Toxicity. *Malar. J.* **2011**, 10, 1–10, DOI: 10.1186/1475-2875-10-85.
- (99) Asuzu, I. U.; Abubaker, I. I. The Emetic, Antihepatotoxic, and Antinephrotoxic Effects of an Extract from *Icacina Trichantha*. *J. Herbs, Spices Med. Plants* **1996**, 3 (4), 9–20, DOI: 10.1300/J044v03n04_03.
- (100) Okunji, C. O.; Iwu, M. M. Control of Schistosomiasis Using Nigerian Medicinal Plants as Molluscicides. *Int. J. Crude Drug Res.* **1988**, 26 (4), 246–252, DOI: 10.3109/13880208809053927.
- (101) Edori, O. S.; Ekpote, O. A. Phytochemical Screening of Aqueous Extract of *Icacina Trichantha* Roots and Its Effect on Mortality of Wood Termite. *World J. Pharm. Res.* **2015**, 4 (10), 213–224.
- (102) Ezeigbo, I. I. Antidiabetic Potential of Methanolic Leaf Extracts of *Icacina Trichantha* in

- Alloxan-Induced Diabetic Mice. *Int. J. Diabetes Dev. Ctries.* **2010**, 30 (3), 150–152, DOI: 10.4103/0973-3930.66511.
- (103) Monday, O. M.; Uzoma, A. I. Histological Changes and Antidiabetic Activities of Icacina Trichantha Tuber Extract in Beta-Cells of Alloxan Induced Diabetic Rats. *Asian Pac. J. Trop. Biomed.* **2013**, 3 (8), 628–633, DOI: 10.1016/S2221-1691(13)60127-6.
- (104) Akuodor, G.; Udia, P.; Bassey, A.; Chilaka, K.; Okezie, O. Antihyperglycemic and Antihyperlipidemic Properties of Aqueous Root Extract of Icacina Senegalensis in Alloxan Induced Diabetic Rats. *J. Acute Dis.* **2014**, 3 (2), 99–103, DOI: 10.1016/s2221-6189(14)60025-1.
- (105) Akinwumi, K. A.; Odunola, O. A.; Olashore, H. O. The Toxicity of Methanolic Extract of Icacina Trichantha Leaves in Wistar Rats. *J. Food, Agric. Environ.* **2011**, 9 (2), 145–147.
- (106) Timothy, O.; Igbe, I.; Idu, M.; Eze, G. I.; Edosuyi, O. Acute and Sub-Chronic Toxicity Studies of Aqueous Extract of Icacina Trichantha Oliv . Leaves in Rodents. *Nig. J. Nat. Prod. Med.* **2018**, 22, 103–114, DOI: 10.4314/njnp.v22i1.3.
- (107) U., A. I.; I., A. I. The Effects of Icacina Trichantha Tuber Extract on the Nervous System. *Phyther. Res.* **1995**, 9 (1), 21–25, DOI: 10.1002/ptr.2650090106.
- (108) Asuzu, I. U.; Egwu, O. K. Search for the Centrally Active Component of Icacina Trichantha Tuber. *Phytomedicine* **1998**, 5 (1), 35–39, DOI: 10.1016/S0944-7113(98)80057-3.
- (109) David-Oku, E.; Akuodor, G. C.; Edet, E. E.; Ogbuji, G. K.; Obiajunwa-Otteh, J. I.; Aja, D. O. J. Antinociceptive, Anti-Inflammatory and Antipyretic Effects of Ethanolic Root Bark Extract of Icacina Senegalensis in Rodents. *J. Appl. Pharm. Sci.* **2016**, 6 (2), 104–108, DOI: 10.7324/JAPS.2016.60215.
- (110) Asuzu, I. U.; Sosa, S.; Loggia, R. Della. The Antiinflammatory Activity of Icacina Trichantha Tuber. *Phytomedicine* **1999**, 6 (4), 267–272, DOI: 10.1016/S0944-7113(99)80019-1.
- (111) David-Oku, E.; Obiajunwa-Otteh, J. I. A Combination of the Leaves and Tuber of Icacina Senegalensis A. Juss (Icacinaceae) Improves the Antimalarial Activity of the Plant in Mice. *J. Coast. Life Med.* **2015**, 3 (10), 821–825, DOI: 10.12980/jclm.3.2015j5-93.
- (112) Onyeonagu, C. C.; Asiegbu, J. E. Frequency of Collection, Distance from Source of Collection, Seasonality and Preference Rating of Identified Forage Species in Nsukka Rural Communities of Enugu State, Nigeria. *J. Trop. Agric. Food, Environ. Ext.* **2006**, 5 (2), 33–39.
- (113) Agbo, I. .; Odo, G. . The Effect of Hypochlorite Oxidation and Acetylation on Some of the Physicochemical Properties of Icacina Trichantha Starch. *Bio-Research* **2010**, 8 (1), 593–597, DOI: 10.4314/br.v8i1.62539.
- (114) Golly, M. K.; Amadotor, B. Nutritional Composition of the Seed of Icacina Senegalensis/Oliviformis (False Yam). *Pakistan Journal of Nutrition.* 2013, pp 80–84, DOI: 10.3923/pjn.2013.80.84.
- (115) Umoh, E. O.; Iwe, M. O. Effects of Processing on the Nutrient Composition of False Yam (Icacina Trichantha) Flour. *Niger. Food J.* **2014**, 32 (2), 1–7, DOI: 10.1016/s0189-7241(15)30111-9.
- (116) Sunday, E. A.; Israel, A. U.; Odey, T. Proximate Analysis and Mineral Element Composition of False Yam (Icacina Trichantha) Tuber and Oyster Mushroom (Pleurotus Ostreatus). *Int. J. Chem. Sci.* **2016**, 1 (1), 31–39.
- (117) Roessler, R.; Amprako, L.; Sayibu, A. R.; Mohammed, A.; Menezes, R. C.; Hölscher, D.;

- Alenyorege, B.; Dei, H. K.; Steiner, C. Effects of False Yam Tuber Meals and Charcoal on Broiler Chicken Production and Blood Parameters. *South African J. Anim. Sci.* **2017**, *47* (6), 842–853, DOI: 10.4314/sajas.v47i6.12.
- (118) Okosun, S. E.; Eguaoje, A. S.; Ehebha, E. T. E. Hematology and Blood Serum Chemistry of Albino Rat Fed Variouslly Processed False Yam (*Icacina Trichantha*) Root Tuber at Varying Replacement Levels for Maize. *Asian J. Res. Anim. Vet. Sci.* **2018**, *1* (3), 1–8, DOI: 10.9734/AJRAVS/2018/41041.
- (119) S. E., O.; S., E. A.; D. O., O. The Performance Characteristics and Economic Evaluation of Weaner Rabbits Fed Varying Levels of Sundried False Yam (*Icacina Tricantha*) Meal. *Int. J. Appl. Sci.* **2019**, *2* (1), p1, DOI: 10.30560/ijas.v2n1p1.
- (120) Ruzicka, L. The Isoprene Rule and the Biogenesis of Terpenic Compounds. *Experientia* **1953**, *9* (10), 357–367, DOI: 10.1007/BF02167631.
- (121) Rowinsky Eric K., M. D. THE DEVELOPMENT AND CLINICAL UTILITY OF THE TAXANE CLASS OF ANTIMICROTUBULE CHEMOTHERAPY AGENTS. *Annu. Rev. Med.* **1997**, *48* (1), 353–374, DOI: 10.1146/annurev.med.48.1.353.
- (122) Kerr, P. G. Plants and Tuberculosis. In *Fighting Multidrug Resistance with Herbal Extracts, Essential Oils and Their Components*; Elsevier, 2013; pp 45–64, DOI: 10.1016/B978-0-12-398539-2.00005-7.
- (123) Liu, H.; Zhang, L.; Chen, Y.; Li, S.; Tan, G.; Sun, Z.; Pan, Q.; Ye, W.; Li, H.; Zhang, W. Cytotoxic Pimarane-Type Diterpenes from the Marine Sediment-Derived Fungus *Eutypella* Sp. FS46. *Nat. Prod. Res.* **2017**, *31* (4), 404–410, DOI: 10.1080/14786419.2016.1169418.
- (124) Qin-Feng, Z.; Yan-Yan, Q.; Zhi-Jun, Z.; Min, F.; Ran, B.; Jia, S.; Xing-De, W.; Li-Dong, S.; Qin-Shi, Z. Vibsan-Type Diterpenoids from *Viburnum Odoratissimum* and Their Cytotoxic and HSP90 Inhibitory Activities. *Chem. Biodivers.* **2018**, *0* (0), 1800049, DOI: 10.1002/cbdv.201800049.
- (125) Xiaoli, W.; Kunlai, S.; Bin, W. Bioactive Pimarane Diterpenes from the Arctic Fungus *Eutypella* Sp. D-1. *Chem. Biodivers.* **2017**, *15* (2), e1700501, DOI: 10.1002/cbdv.201700501.
- (126) Ni, L.; Zhong, X.-H.; Chen, X.-J.; Zhang, B.-J.; Bao, M.-F.; Cai, X.-H. Bioactive Norditerpenoids from *Cephalotaxus Fortunei* Var. *Alpina* and *C. Lanceolata*. *Phytochemistry* **2018**, *151*, 50–60, DOI: 10.1016/j.phytochem.2018.04.007.
- (127) Rozimamat, R.; Hu, R.; Aisa, H. A. New Isopimarane Diterpenes and Nortriterpene with Cytotoxic Activity from *Ephorbia Alata* Boiss. *Fitoterapia* **2018**, *127*, 328–333, DOI: 10.1016/j.fitote.2018.02.026.
- (128) Oliver, D. *Flora of Tropical Africa /by Daniel Oliver ... Assisted by Other Botanists.*; L. Reeve and co.; London :, 1868, DOI: 10.5962/bhl.title.42.
- (129) Gbolade, A. Ethnobotanical Study of Plants Used in Treating Hypertension in Edo State of Nigeria. *J. Ethnopharmacol.* **2012**, *144* (1), 1–10, DOI: 10.1016/j.jep.2012.07.018.
- (130) Park, H.; Yoda, N.; Fukaya, H.; Aoyagi, Y.; Takeya, K. Rakanmakilactones A–F, New Cytotoxic Sulfur-Containing Norditerpene Dilactones from Leaves of *Podocarpus Macrophyllus* Var. *Maki*. *Tetrahedron* **2004**, *60* (1), 171–177, DOI: 10.1016/j.tet.2003.10.083.
- (131) Adou, E.; Williams, R. B.; Schilling, J. K.; Malone, S.; Meyer, J.; Wisse, J. H.; Frederik, D.; Koese, D.; Werkhoven, M. C. M.; Snipes, C. E.; et al. Cytotoxic Diterpenoids from Two Lianas from the Suriname Rainforest. *Bioorganic Med. Chem.* **2005**, *13* (21), 6009–

- 6014, DOI: 10.1016/j.bmc.2005.07.026.
- (132) Zhao, M.; Guo, B.; Onakpa, M. M.; Wong, T.; Wakasa, K.; Che, C. T.; Warpeha, K. Activity of Icacinol from *Icacina Trichantha* on Seedling Growth of *Oryza Sativa* and *Arabidopsis Thaliana*. *J. Nat. Prod.* **2017**, *80* (12), 3314–3318, DOI: 10.1021/acs.jnatprod.7b00668.
 - (133) Kabsch, W. XDS. *Acta Crystallogr. Sect. D Biol. Crystallogr.* **2010**, *66* (2), 125–132, DOI: 10.1107/S0907444909047337.
 - (134) Sheldrick, G. M. Crystal Structure Refinement with SHELXL. *Acta Crystallogr. Sect. C Struct. Chem.* **2015**, *71* (1), 3–8, DOI: 10.1107/S2053229614024218.
 - (135) Gaussian 09, Revision A.02, M. J. Frisch, G. W. Trucks, H. B. Schlegel, G. E. Scuseria, M. A. Robb, J. R. Cheeseman, G. Scalmani, V. Barone, G. A. Petersson, H. Nakatsuji, X. Li, M. Caricato, A. Marenich, J. Bloino, B. G. Janesko, R. Gomperts, B. Mennucci, 2016. No Title.
 - (136) Bruhn, T.; Schaumlöffel, A.; Hemberger, Y.; Pescitelli, G. SpecDis Version 1.70, Berlin, Germany. 2017.
 - (137) Bruhn, T.; Schaumlöffel, A.; Hemberger, Y.; Bringmann, G. SpecDis: Quantifying the Comparison of Calculated and Experimental Electronic Circular Dichroism Spectra. *Chirality* **2013**, *25* (4), 243–249, DOI: 10.1002/chir.22138.
 - (138) Pauli, G. F.; Chen, S.-N.; Lankin, D. C.; Bisson, J.; Case, R. J.; Chadwick, L. R.; Gödecke, T.; Inui, T.; Kronic, A.; Jaki, B. U.; et al. Essential Parameters for Structural Analysis and Dereplication by ¹H NMR Spectroscopy. *J. Nat. Prod.* **2014**, *77* (6), 1473–1487, DOI: 10.1021/np5002384.
 - (139) Yang, J. Y.; Sanchez, L. M.; Rath, C. M.; Liu, X.; Boudreau, P. D.; Bruns, N.; Glukhov, E.; Wodtke, A.; De Felicio, R.; Fenner, A.; et al. Molecular Networking as a Dereplication Strategy. *J. Nat. Prod.* **2013**, *76* (9), 1686–1699, DOI: 10.1021/np400413s.
 - (140) Dieckmann, R.; Graeber, I.; Kaesler, I.; Szewzyk, U.; von Döhren, H. Rapid Screening and Dereplication of Bacterial Isolates from Marine Sponges of the Sula Ridge by Intact-Cell-MALDI-TOF Mass Spectrometry (ICM-MS). *Appl. Microbiol. Biotechnol.* **2005**, *67* (4), 539–548, DOI: 10.1007/s00253-004-1812-2.
 - (141) Funari, C. S.; Eugster, P. J.; Martel, S.; Carrupt, P.-A.; Wolfender, J.-L.; Silva, D. H. S. High Resolution Ultra High Pressure Liquid Chromatography–Time-of-Flight Mass Spectrometry Dereplication Strategy for the Metabolite Profiling of Brazilian *Lippia* Species. *J. Chromatogr. A* **2012**, *1259*, 167–178, DOI: <https://doi.org/10.1016/j.chroma.2012.03.069>.
 - (142) van Elswijk, D. A.; Schobel, U. P.; Lansky, E. P.; Irth, H.; van der Greef, J. Rapid Dereplication of Estrogenic Compounds in Pomegranate (*Punica Granatum*) Using on-Line Biochemical Detection Coupled to Mass Spectrometry. *Phytochemistry* **2004**, *65* (2), 233–241, DOI: <https://doi.org/10.1016/j.phytochem.2003.07.001>.
 - (143) Graebner, I. B.; Mostardeiro, M. A.; Ethur, E. M.; Burrow, R. A.; Dessoy, E. C. S.; Morel, A. F. Diterpenoids from *Humirianthera Ampli*. *Phytochemistry* **2000**, *53* (8), 955–959, DOI: 10.1016/S0031-9422(99)00585-3.
 - (144) Martin, A.; Murray, R. D. H. Constituents of *Erythroxylon Monogynum* Roxb. Part IV. Two Norditerpenoid Tertiary Alcohols and Three Diterpenoid Epoxides. *J. Chem. Soc. C Org.* **1968**, 2529, DOI: 10.1039/j39680002529.
 - (145) Wu, Y. C.; Hung, Y. C.; Chang, F. R.; Cosentino, M.; Wang, H. K.; Lee, K. H. Identification of Ent-16 β ,17-Dihydroxykauran-19-Oic Acid as an Anti- HIV Principle and

- Isolation of the New Diterpenoids Annosquamosins A and B from *Annona Squamosa*. *J. Nat. Prod.* **1996**, 59 (6), 635–637, DOI: 10.1021/np960416j.
- (146) Luo, X. D.; Wu, S. H.; Ma, Y. B.; Wu, D. G. Ent-Pimarane Derivatives from *Dysoxylum Hainanense*. *Phytochemistry* **2001**, 57 (1), 131–134, DOI: 10.1016/S0031-9422(00)00482-9.
- (147) Grace, M. H.; Jin, Y.; Wilson, G. R.; Coates, R. M. Structures, Biogenetic Relationships, and Cytotoxicity of Pimarane-Derived Diterpenes from *Petalostigma Pubescens*. *Phytochemistry* **2006**, 67 (16), 1708–1715, DOI: 10.1016/j.phytochem.2005.09.026.
- (148) Jung, H. J.; Jung, H. A.; Kang, S. S.; Lee, J. H.; Cho, Y. S.; Moon, K. H.; Choi, J. S. Inhibitory Activity of *Aralia Continentalis* Roots on Protein Tyrosine Phosphatase 1B and Rat Lens Aldose Reductase. *Arch. Pharm. Res.* **2012**, 35 (10), 1771–1777, DOI: 10.1007/s12272-012-1009-7.
- (149) Adesogan, E. K.; Durodola, J. I. Antitumour and Antibiotic Principles of *Annona Senegalensis*. *Phytochemistry* **1976**, 15 (8), 1311–1312, DOI: 10.1016/0031-9422(76)85100-X.
- (150) Eshiet, I. T. U.; Akisanya, A.; Taylor, D. A. H. Diterpenes from *Annona Senegalensis*. *Phytochemistry* **1971**, 10 (12), 3294–3295, DOI: 10.1016/S0031-9422(00)97396-5.
- (151) Fatope, M. O.; Audu, O. T.; Takeda, Y.; Zeng, L.; Shi, G.; Shimada, H.; McLaughlin, J. L. Bioactive Ent-Kaurene Diterpenoids from *Annona Senegalensis*. *J. Nat. Prod.* **1996**, 59 (3), 301–303, DOI: 10.1021/np9601566.
- (152) Britton, R.; Roberge, M.; Berisch, H.; Andersen, R. J. Antimitotic Diterpenoids from *Erythropodium Caribaeorum*: Isolation Artifacts and Putative Biosynthetic Intermediates. *Tetrahedron Lett.* **2001**, 42 (16), 2953–2956, DOI: 10.1016/S0040-4039(01)00347-1.
- (153) Gomes, A. O. C. V.; Brito, M. V.; Marques, R. A.; Lima, L. B.; Cavalcante, I. M.; Vieira, T. D. N.; Nunes, F. M.; Lima, M. A. S.; Uchôa, D. E.; Lima, C. S.; et al. Multi-Step Bioconversion of Annonalide by *Fusarium Oxysporum* f. Sp. *Tracheiphilum* and Theoretical Investigation of the Decarboxylase Pathway. *J. Mol. Struct.* **2020**, 1204, DOI: 10.1016/j.molstruc.2019.127514.
- (154) Wang, Q.; Hillwig, M. L.; Peters, R. J. CYP99A3: Functional Identification of a Diterpene Oxidase from the Momilactone Biosynthetic Gene Cluster in Rice. *Plant J.* **2011**, 65 (1), 87–95, DOI: 10.1111/j.1365-313X.2010.04408.x.
- (155) Zhao, M.; Cheng, J.; Guo, B.; Duan, J.; Che, C.-T. Momilactone and Related Diterpenoids as Potential Agricultural Chemicals. *J. Agric. Food Chem.* **2018**, 66 (30), 7859–7872, DOI: 10.1021/acs.jafc.8b02602.
- (156) Sonawane, P. D.; Pollier, J.; Panda, S.; Szymanski, J.; Massalha, H.; Yona, M.; Unger, T.; Malitsky, S.; Arendt, P.; Pauwels, L.; et al. Plant Cholesterol Biosynthetic Pathway Overlaps with Phytosterol Metabolism. *Nat. Plants* **2016**, 3 (December), DOI: 10.1038/nplants.2016.205.
- (157) Darnet, S.; Rahier, A. Plant Sterol Biosynthesis: Identification of Two Distinct Families of Sterol 4 α -Methyl Oxidases. *Biochem. J.* **2004**, 378 (3), 889–898, DOI: 10.1042/BJ20031572.
- (158) Pascal, S.; Taton, M.; Rahier, A. Plant Sterol Biosynthesis: Identification of a NADPH Dependent Sterone Reductase Involved in Sterol-4 Demethylation. *Arch. Biochem. Biophys.* **1994**, 312 (1), 260–271, DOI: 10.1006/abbi.1994.1308.
- (159) Bouvier, F.; Rahier, A.; Camara, B. Biogenesis, Molecular Regulation and Function of Plant Isoprenoids. *Prog. Lipid Res.* **2005**, 44 (6), 357–429, DOI:

- 10.1016/j.plipres.2005.09.003.
- (160) Rahier, A.; Darnet, S.; Bouvier, F.; Camara, B.; Bard, M. Molecular and Enzymatic Characterizations of Novel Bifunctional 3β -Hydroxysteroid Dehydrogenases/C-4 Decarboxylases from *Arabidopsis Thaliana*. *J. Biol. Chem.* **2006**, *281* (37), 27264–27277, DOI: 10.1074/jbc.M604431200.
 - (161) Cho, J. G.; Cha, B. J.; Minlee, S.; Shrestha, S.; Jeong, R. H.; Sunglee, D.; Kim, Y. C.; Lee, D. G.; Kang, H. C.; Kim, J.; et al. Diterpenes from the Roots of *Oryza Sativa* L. and Their Inhibition Activity on NO Production in LPS-Stimulated RAW264.7 Macrophages. *Chem. Biodivers.* **2015**, *12* (9), 1356–1364, DOI: 10.1002/cbdv.201400239.
 - (162) Wang, Q.; Hillwig, M. L.; Okada, K.; Yamazaki, K.; Wu, Y.; Swaminathan, S.; Yamane, H.; Peters, R. J. Characterization of CYP76M5-8 Indicates Metabolic Plasticity within a Plant Biosynthetic Gene Cluster. *J. Biol. Chem.* **2012**, *287* (9), 6159–6168, DOI: 10.1074/jbc.M111.305599.
 - (163) Albaigés, J.; Grimalt, J.; Bayona, J. M.; Risebrough, R.; de Lappe, B.; Walker, W. Dissolved, Particulate and Sedimentary Hydrocarbons in a Deltaic Environment. *Org. Geochem.* **1984**, *6*, 237–248, DOI: [https://doi.org/10.1016/0146-6380\(84\)90045-7](https://doi.org/10.1016/0146-6380(84)90045-7).
 - (164) Moon, S. S.; Rahman, A. A.; Kim, J. Y.; Kee, S. H. Hanultarin, a Cytotoxic Lignan as an Inhibitor of Actin Cytoskeleton Polymerization from the Seeds of *Trichosanthes Kirilowii*. *Bioorganic Med. Chem.* **2008**, *16* (15), 7264–7269, DOI: 10.1016/j.bmc.2008.06.032.
 - (165) Schroeder, F. C.; del Campo, M. L.; Grant, J. B.; Weibel, D. B.; Smedley, S. R.; Bolton, K. L.; Meinwald, J.; Eisner, T. Pinoresinol: A Lignol of Plant Origin Serving for Defense in a Caterpillar. *Proc. Natl. Acad. Sci.* **2006**, *103* (42), 15497–15501, DOI: 10.1073/pnas.0605921103.
 - (166) Zhou, H.; Ren, J.; Li, Z. Antibacterial Activity and Mechanism of Pinoresinol from *Cinnamomum Camphora* Leaves against Food-Related Bacteria. *Food Control* **2017**, *79*, 192–199, DOI: <https://doi.org/10.1016/j.foodcont.2017.03.041>.
 - (167) Fini, L.; Hotchkiss, E.; Fogliano, V.; Graziani, G.; Romano, M.; De Vol, E. B.; Qin, H.; Selgrad, M.; Boland, C. R.; Ricciardiello, L. Chemopreventive Properties of Pinoresinol-Rich Olive Oil Involve a Selective Activation of the ATM–P53 Cascade in Colon Cancer Cell Lines. *Carcinogenesis* **2007**, *29* (1), 139–146, DOI: 10.1093/carcin/bgm255.
 - (168) López-Biedma, A.; Sánchez-Quesada, C.; Beltrán, G.; Delgado-Rodríguez, M.; Gaforio, J. J. Phytoestrogen (+)-Pinoresinol Exerts Antitumor Activity in Breast Cancer Cells with Different Oestrogen Receptor Statuses. *BMC Complement. Altern. Med.* **2016**, *16* (1), 350, DOI: 10.1186/s12906-016-1233-7.
 - (169) Das G.B. Zoghbi, M.; F. Roque, N.; Gottlieb, H. E. Humirianthenolides, New Degraded Diterpenoids from *Humirianthera Rupestris*. *Phytochemistry* **1981**, *20* (7), 1669–1673, DOI: 10.1016/S0031-9422(00)98552-2.
 - (170) Gianturco, M. A.; Friedel, P.; Giammarino, A. S. The Volatile Constituents of Coffee—III. *Tetrahedron* **1964**, *20* (7), 1763–1772, DOI: 10.1016/S0040-4020(01)99177-X.
 - (171) Wang, T.; Tang, F.; Zhang, Y.-H.; Chen, Z. A Natural Diterpenoid Kamebacetal A with Anti-Tumor Activity: Theoretical and Experimental Study. *J. Mol. Struct.* **2010**, *975* (1), 317–322, DOI: <https://doi.org/10.1016/j.molstruc.2010.04.044>.
 - (172) Takeda, Y.; Matsumoto, T.; Otsuka, H. Longirabdolide C, a New Diterpenoid from *Rabdosia Longituba*. *J. Nat. Prod.* **1994**, *57* (5), 650–653, DOI: 10.1021/np50107a015.
 - (173) Pischetsrieder, M.; Severin, T. Maillard Reaction of Maltose - Isolation of 4-(Glucopyranosyloxy)-5-(Hydroxymethyl)-2-Methyl-3(2H)-Furanone. *J. Agric. Food*

- Chem.* **1994**, 42 (4), 890–892, DOI: 10.1021/jf00040a010.
- (174) Corey, E. J.; Ensley, H. E.; Suggs, J. W. Convenient Synthesis of (S)-(-)-Pulegone from (-)-Citronellol. *J. Org. Chem.* **1976**, 41 (2), 380–381, DOI: 10.1021/jo00864a047.
- (175) Saito, F.; Kuramochi, K.; Nakazaki, A.; Mizushima, Y.; Sugawara, F.; Kobayashi, S. Synthesis and Absolute Configuration of (+)-Pseudodefectusin: Structural Revision of Aspergione B. *European J. Org. Chem.* **2006**, No. 21, 4796–4799, DOI: 10.1002/ejoc.200600702.
- (176) Kuramochi, K.; Saito, F.; Nakazaki, A.; Takeuchi, T.; Tsubaki, K.; Sugawara, F.; Kobayashi, S. Synthesis of Pseudodefectusin and Ustusorane C: Structural Revision of Aspergione A and B. *Biosci. Biotechnol. Biochem.* **2010**, 74 (8), 1635–1640, DOI: 10.1271/bbb.100241.
- (177) Raston, C. L.; Scott, J. L. Chemoselective, Solvent-Free Aldol Condensation Reaction. *Green Chem.* **2000**, 2 (2), 49–52, DOI: 10.1039/A907688C.
- (178) Crouch, R. D.; Richardson, A.; Howard, J. L.; Harker, R. L.; Barker, K. H. The Aldol Addition and Condensation: The Effect of Conditions on Reaction Pathway. *J. Chem. Educ.* **2007**, 84 (3), 475, DOI: 10.1021/ed084p475.
- (179) Pradhan, P.; Fischer, G.; van Velthuizen, H.; Reusser, D. E.; Kropp, J. P. Closing Yield Gaps: How Sustainable Can We Be? *PLoS One* **2015**, 10 (6), e0129487.
- (180) Korres, N. E.; Norsworthy, J. K.; Tehranchian, P.; Gitsopoulos, T. K.; Loka, D. A.; Oosterhuis, D. M.; Gealy, D. R.; Moss, S. R.; Burgos, N. R.; Miller, M. R.; et al. Cultivars to Face Climate Change Effects on Crops and Weeds: A Review. *Agron. Sustain. Dev.* **2016**, 36 (1), 12, DOI: 10.1007/s13593-016-0350-5.
- (181) Deutsch, C. A.; Tewksbury, J. J.; Tigchelaar, M.; Battisti, D. S.; Merrill, S. C.; Huey, R. B.; Naylor, R. L. Increase in Crop Losses to Insect Pests in a Warming Climate. *Science* (80-.). **2018**, 361 (6405), 916 LP – 919, DOI: 10.1126/science.aat3466.
- (182) Oerke, E.-C.; Dehne, H.-W. Safeguarding Production—Losses in Major Crops and the Role of Crop Protection. *Crop Prot.* **2004**, 23 (4), 275–285, DOI: <https://doi.org/10.1016/j.cropro.2003.10.001>.
- (183) OERKE, E.-C. Crop Losses to Pests. *J. Agric. Sci.* **2006**, 144 (1), 31–43, DOI: 10.1017/S0021859605005708.
- (184) Owen, M. D.; Zelaya, I. A. Herbicide-Resistant Crops and Weed Resistance to Herbicides. *Pest Manag. Sci.* **2005**, 61 (3), 301–311, DOI: 10.1002/ps.1015.
- (185) Délye, C.; Jasieniuk, M.; Le Corre, V. Deciphering the Evolution of Herbicide Resistance in Weeds. *Trends Genet.* **2013**, 29 (11), 649–658, DOI: <https://doi.org/10.1016/j.tig.2013.06.001>.
- (186) Tshewang, S.; Sindel, B. M.; Ghimiray, M.; Chauhan, B. S. Weed Management Challenges in Rice (*Oryza Sativa* L.) for Food Security in Bhutan: A Review. *Crop Prot.* **2016**, 90, 117–124, DOI: <https://doi.org/10.1016/j.cropro.2016.08.031>.
- (187) Linares, O. F. African Rice (*Oryza Glaberrima*): History and Future Potential. *Proc. Natl. Acad. Sci.* **2002**, 99 (25), 16360–16365, DOI: 10.1073/pnas.252604599.
- (188) Li, H.-Y.; Wei, W.-J.; Ma, K.-L.; Zhang, J.-Y.; Li, Y.; Gao, K. Phytotoxic Neo-Clerodane Diterpenoids from the Aerial Parts of *Scutellaria Barbata*. *Phytochemistry* **2020**, 171, 112230, DOI: <https://doi.org/10.1016/j.phytochem.2019.112230>.
- (189) Harding, D. P.; Raizada, M. N. Controlling Weeds with Fungi, Bacteria and Viruses: A Review. *Frontiers in Plant Science*. 2015, p 659.
- (190) Hüter, O. F. Use of Natural Products in the Crop Protection Industry. *Phytochem. Rev.*

- 2011**, 10 (2), 185–194, DOI: 10.1007/s11101-010-9168-y.
- (191) Dayan, F. E.; Cantrell, C. L.; Duke, S. O. Natural Products in Crop Protection. *Bioorg. Med. Chem.* **2009**, 17 (12), 4022–4034, DOI: 10.1016/J.BMC.2009.01.046.
- (192) E, D. F.; K, O. D.; O, D. S. Rationale for a Natural Products Approach to Herbicide Discovery. *Pest Manag. Sci.* **2012**, 68 (4), 519–528, DOI: 10.1002/ps.2332.
- (193) O, D. S. Why Have No New Herbicide Modes of Action Appeared in Recent Years? *Pest Manag. Sci.* **2011**, 68 (4), 505–512, DOI: 10.1002/ps.2333.
- (194) Inderjit; Wardle, D. A.; Karban, R.; Callaway, R. M. The Ecosystem and Evolutionary Contexts of Allelopathy. *Trends Ecol. Evol.* **2011**, 26 (12), 655–662, DOI: <https://doi.org/10.1016/j.tree.2011.08.003>.
- (195) Kato-Noguchi, H.; Peters, R. J. The Role of Momilactones in Rice Allelopathy. *J. Chem. Ecol.* **2013**, 39 (2), 175–185, DOI: 10.1007/s10886-013-0236-9.
- (196) Kato-Noguchi, H.; Ota, K.; Kujime, H. Absorption of Momilactone A and B by *Arabidopsis Thaliana* L. and the Growth Inhibitory Effects. *J. Plant Physiol.* **2012**, 169 (15), 1471–1476, DOI: <https://doi.org/10.1016/j.jplph.2012.05.022>.
- (197) Kato-Noguchi, H.; Kitajima, S. Momilactone Sensitive Proteins in *Arabidopsis Thaliana*. *Nat. Prod. Commun.* **2015**, 10 (5), 1934578X1501000508, DOI: 10.1177/1934578X1501000508.
- (198) Siegel, R. L.; Miller, K. D.; Jemal, A. Cancer Statistics, 2016. *CA. Cancer J. Clin.* **2016**, 66 (1), 7–30, DOI: 10.3322/caac.21332.
- (199) Wang, G.; Zhao, D.; Spring, D. J.; DePinho, R. A. Genetics and Biology of Prostate Cancer. *Genes Dev.* **2018**, 32 (17–18), 1105–1140, DOI: 10.1101/gad.315739.118.
- (200) Johnson, J. J.; Syed, D. N.; Suh, Y.; Heren, C. R.; Saleem, M.; Siddiqui, I. A.; Mukhtar, H. Disruption of Androgen and Estrogen Receptor Activity in Prostate Cancer by a Novel Dietary Diterpene Carnosol: Implications for Chemoprevention. *Cancer Prev. Res.* **2010**, 3 (9), 1112 LP – 1123, DOI: 10.1158/1940-6207.CAPR-10-0168.
- (201) KINGHORN, A. D.; DE BLANCO, E. J. C.; LUCAS, D. M.; RAKOTONDRAIBE, H. L.; ORJALA, J.; SOEJARTO, D. D.; OBERLIES, N. H.; PEARCE, C. J.; WANI, M. C.; STOCKWELL, B. R.; et al. Discovery of Anticancer Agents of Diverse Natural Origin. *Anticancer Res.* **2016**, 36 (11), 5623–5637.
- (202) Subapriya, R.; Rajesh, A. Natural Products and Colon Cancer: Current Status and Future Prospects. *Drug Dev. Res.* **2008**, 69 (7), 460–471, DOI: 10.1002/ddr.20276.
- (203) Gordaliza, M. Natural Products as Leads to Anticancer Drugs. *Clin. Transl. Oncol.* **2007**, 9 (12), 767–776, DOI: 10.1007/s12094-007-0138-9.
- (204) Cella, D.; Peterman, A.; Hudgens, S.; Webster, K.; Socinski, M. A. Measuring the Side Effects of Taxane Therapy in Oncology. *Cancer* **2003**, 98 (4), 822–831, DOI: 10.1002/cncr.11578.
- (205) Benetou, V.; Lagiou, A.; Lagiou, P. Chemoprevention of Cancer: Current Evidence and Future Prospects. *F1000Research* **2015**, 4 (916), 916, DOI: 10.12688/f1000research.6684.1.
- (206) Ko, E.-Y.; Moon, A. Natural Products for Chemoprevention of Breast Cancer. *J. Cancer Prev.* **2015**, 20 (4), 223–231, DOI: 10.15430/JCP.2015.20.4.223.
- (207) Cragg, G. M.; Pezzuto, J. M. Natural Products as a Vital Source for the Discovery of Cancer Chemotherapeutic and Chemopreventive Agents. *Med. Princ. Pract.* **2016**, 25(suppl 2 (Suppl. 2), 41–59, DOI: 10.1159/000443404.
- (208) Singletary, K. Diet, Natural Products and Cancer Chemoprevention. *J. Nutr.* **2000**, 130

- (2), 465S-466S, DOI: 10.1093/jn/130.2.465S.
- (209) Khan, N.; Afaq, F.; Mukhtar, H. Apoptosis by Dietary Factors: The Suicide Solution for Delaying Cancer Growth. *Carcinogenesis* **2007**, *28* (2), 233–239, DOI: 10.1093/carcin/bgl243.
- (210) Johnson, J. J. Carnosol: A Promising Anti-Cancer and Anti-Inflammatory Agent. *Cancer Lett.* **2011**, *305* (1), 1–7, DOI: <https://doi.org/10.1016/j.canlet.2011.02.005>.
- (211) Para, A.; Muhammad, D.; Orozco-Nunnally, D. A.; Memishi, R.; Alvarez, S.; Naldrett, M. J.; Warpeha, K. M. The Dehydratase ADT3 Affects ROS Homeostasis and Cotyledon Development. *Plant Physiol.* **2016**, *172* (2), 1045 LP – 1060, DOI: 10.1104/pp.16.00464.
- (212) Hasegawa, M.; Mitsuhashi, I.; Seo, S.; Imai, T.; Koga, J.; Okada, K.; Yamane, H.; Ohashi, Y. Phytoalexin Accumulation in the Interaction Between Rice and the Blast Fungus. *Mol. Plant-Microbe Interact.* **2010**, *23* (8), 1000–1011, DOI: 10.1094/MPMI-23-8-1000.
- (213) Alonso, J. M. Genome-Wide Insertional Mutagenesis of *Arabidopsis Thaliana*. *Science* (80-.). **2003**, *301* (5633), 653–657, DOI: 10.1126/science.1086391.
- (214) WARPEHA, K. M.; GIBBONS, J.; CAROL, A.; SLUSSER, J.; TREE, R.; DURHAM, W.; KAUFMAN, L. S. Adequate Phenylalanine Synthesis Mediated by G Protein Is Critical for Protection from UV Radiation Damage in Young Etiolated *Arabidopsis Thaliana* Seedlings. *Plant. Cell Environ.* **2008**, *31* (12), 1756–1770, DOI: 10.1111/j.1365-3040.2008.01878.x.
- (215) Orozco-Nunnally, D. A.; Muhammad, D.; Mezzich, R.; Lee, B.-S.; Jayathilaka, L.; Kaufman, L. S.; Warpeha, K. M. Pirin1 (PRN1) Is a Multifunctional Protein That Regulates Quercetin, and Impacts Specific Light and UV Responses in the Seed-to-Seedling Transition of *Arabidopsis Thaliana*. *PLoS One* **2014**, *9* (4), e93371–e93371, DOI: 10.1371/journal.pone.0093371.
- (216) Pružinská, A.; Tanner, G.; Aubry, S.; Anders, I.; Moser, S.; Müller, T.; Ongania, K.-H.; Kräutler, B.; Youn, J.-Y.; Liljegren, S. J.; et al. Chlorophyll Breakdown in Senescent *Arabidopsis* Leaves. Characterization of Chlorophyll Catabolites and of Chlorophyll Catabolic Enzymes Involved in the Degreening Reaction. *Plant Physiol.* **2005**, *139* (1), 52 LP – 63, DOI: 10.1104/pp.105.065870.
- (217) Montgomery, B. L.; Yeh, K.-C.; Crepeau, M. W.; Lagarias, J. C. Modification of Distinct Aspects of Photomorphogenesis via Targeted Expression of Mammalian Biliverdin Reductase in Transgenic *Arabidopsis* Plants. *Plant Physiol.* **1999**, *121* (2), 629 LP – 640, DOI: 10.1104/pp.121.2.629.
- (218) Johnson, J. J.; Petiwala, S. M.; Syed, D. N.; Rasmussen, J. T.; Adhami, V. M.; Siddiqui, I. A.; Kohl, A. M.; Mukhtar, H. α -Mangostin, a Xanthone from Mangosteen Fruit, Promotes Cell Cycle Arrest in Prostate Cancer and Decreases Xenograft Tumor Growth. *Carcinogenesis* **2011**, *33* (2), 413–419, DOI: 10.1093/carcin/bgr291.
- (219) Tai, S.; Sun, Y.; Squires, J. M.; Zhang, H.; Oh, W. K.; Liang, C.-Z.; Huang, J. PC3 Is a Cell Line Characteristic of Prostatic Small Cell Carcinoma. *Prostate* **2011**, *71* (15), 1668–1679, DOI: 10.1002/pros.21383.
- (220) Jiang, Z.-Y.; Yang, C.-T.; Hou, S.-Q.; Tian, K.; Wang, W.; Hu, Q.-F.; Huang, X.-Z. Cytotoxic Diterpenoids from the Roots of *Aralia Melanocarpa*. *Planta Med.* **2016**, *82* (08), 742–746, DOI: 10.1055/s-0042-104349.
- (221) Takeda, Y.; Matsumoto, T.; Terao, H.; Shingu, T.; Futatsuishi, Y.; Nohara, T.; Kajimoto, T. Orthosiphon D and E, Minor Diterpenes from *Orthosiphon Stamineus*. *Phytochemistry* **1993**, *33* (2), 411–415, DOI: [https://doi.org/10.1016/0031-9422\(93\)85530-5](https://doi.org/10.1016/0031-9422(93)85530-5).

- (222) Wang, X.-N.; Bashyal, B. P.; Wijeratne, E. M. K.; U'Ren, J. M.; Liu, M. X.; Gunatilaka, M. K.; Arnold, A. E.; Gunatilaka, A. A. L. Smardaesidins A–G, Isopimarane and 20-nor-Isopimarane Diterpenoids from Smardaea Sp., a Fungal Endophyte of the Moss *Ceratodon Purpureus*. *J. Nat. Prod.* **2011**, 74 (10), 2052–2061, DOI: 10.1021/np2000864.
- (223) Canel, C.; Moraes, R. M.; Dayan, F. E.; Ferreira, D. Podophyllotoxin. *Phytochemistry* **2000**, 54 (2), 115–120, DOI: [https://doi.org/10.1016/S0031-9422\(00\)00094-7](https://doi.org/10.1016/S0031-9422(00)00094-7).
- (224) Gershenzon, J.; Dudareva, N. The Function of Terpene Natural Products in the Natural World. *Nat. Chem. Biol.* **2007**, 3 (7), 408–414, DOI: 10.1038/nchembio.2007.5.
- (225) Onakpa, M.; Zhao, M.; Gödecke, T.; Chen, W.; Swanson, S.; Uzoma, A.; Che, C. Bioactive Pimarane Diterpenes from *Icacina Trichantha*. *Planta Med.* **2014**, 80 (10), 1382530, DOI: 10.1055/s-0034-1382530.
- (226) Guo, B.; Onakpa, M. M.; Huang, X. J.; Santarsiero, B. D.; Chen, W. L.; Zhao, M.; Zhang, X. Q.; Swanson, S. M.; Burdette, J. E.; Che, C. T. Di-nor- and 17-nor-Pimaranes from *Icacina Trichantha*. *J. Nat. Prod.* **2016**, 79 (7), 1815–1821, DOI: 10.1021/acs.jnatprod.6b00289.
- (227) Rondet, S.; Taton, M.; Rahier, A. Identification, Characterization, and Partial Purification of 4 α - Carboxysterol-C3-Dehydrogenase/C4-Decarboxylase from *Zea Mays*. *Arch. Biochem. Biophys.* **1999**, 366 (2), 249–260, DOI: 10.1006/abbi.1999.1218.
- (228) Gianessi, L. P.; Reigner, N. P. The Value of Herbicides in U.S. Crop Production. *Weed Technol.* **2007**, 21 (2), 559–566, DOI: 10.1614/WT-06-130.1.
- (229) Lee, K.-H. Discovery and Development of Natural Product-Derived Chemotherapeutic Agents Based on a Medicinal Chemistry Approach. *J. Nat. Prod.* **2010**, 73 (3), 500–516, DOI: 10.1021/np900821e.
- (230) Faiella, L.; Piaz, F. D.; Bisio, A.; Tosco, A.; De Tommasi, N. A Chemical Proteomics Approach Reveals Hsp27 as a Target for Proapoptotic Clerodane Diterpenes. *Mol. Biosyst.* **2012**, 8 (10), 2637–2644, DOI: 10.1039/C2MB25171J.
- (231) Attele, A. S.; Wu, J. A.; Yuan, C. S. Ginseng Pharmacology: Multiple Constituents and Multiple Actions. *Biochem. Pharmacol.* **1999**, 58 (11), 1685–1693, DOI: 10.1016/S0006-2952(99)00212-9.
- (232) Sharma, R. A.; Gescher, A. J.; Steward, W. P. Curcumin: The Story so Far. *Eur. J. Cancer* **2005**, 41 (13), 1955–1968, DOI: 10.1016/j.ejca.2005.05.009.
- (233) Balunas, M. J.; Kinghorn, A. D. Drug Discovery from Medicinal Plants. *Life Sci.* **2005**, 78 (5), 431–441, DOI: 10.1016/J.LFS.2005.09.012.

APPENDICES

APPENDIX A. Spectroscopic Data and Figures

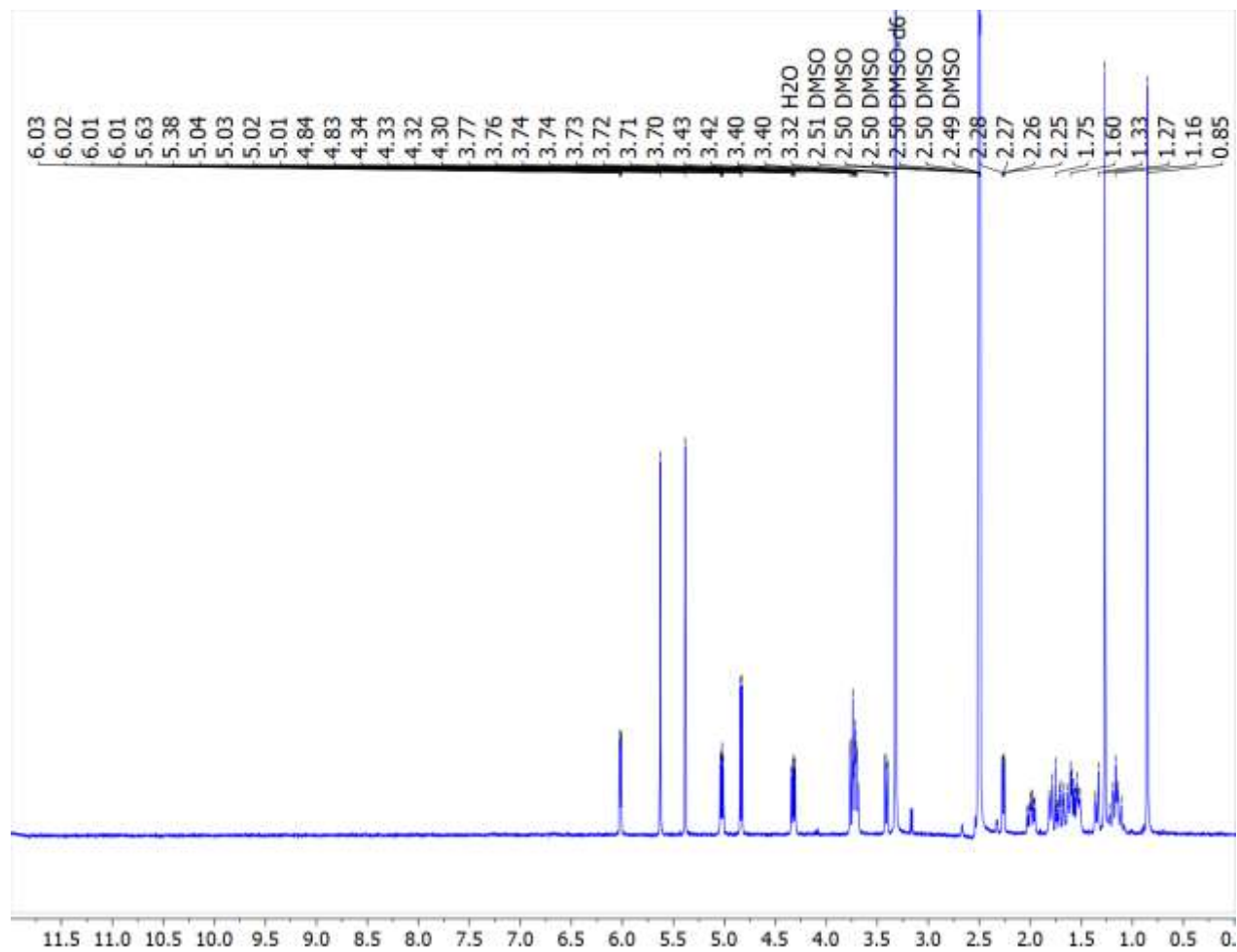


Figure 41. ^1H spectrum (400 MHz, $\text{DMSO-}d_6$) of icacinol

APPENDIX A (continued)

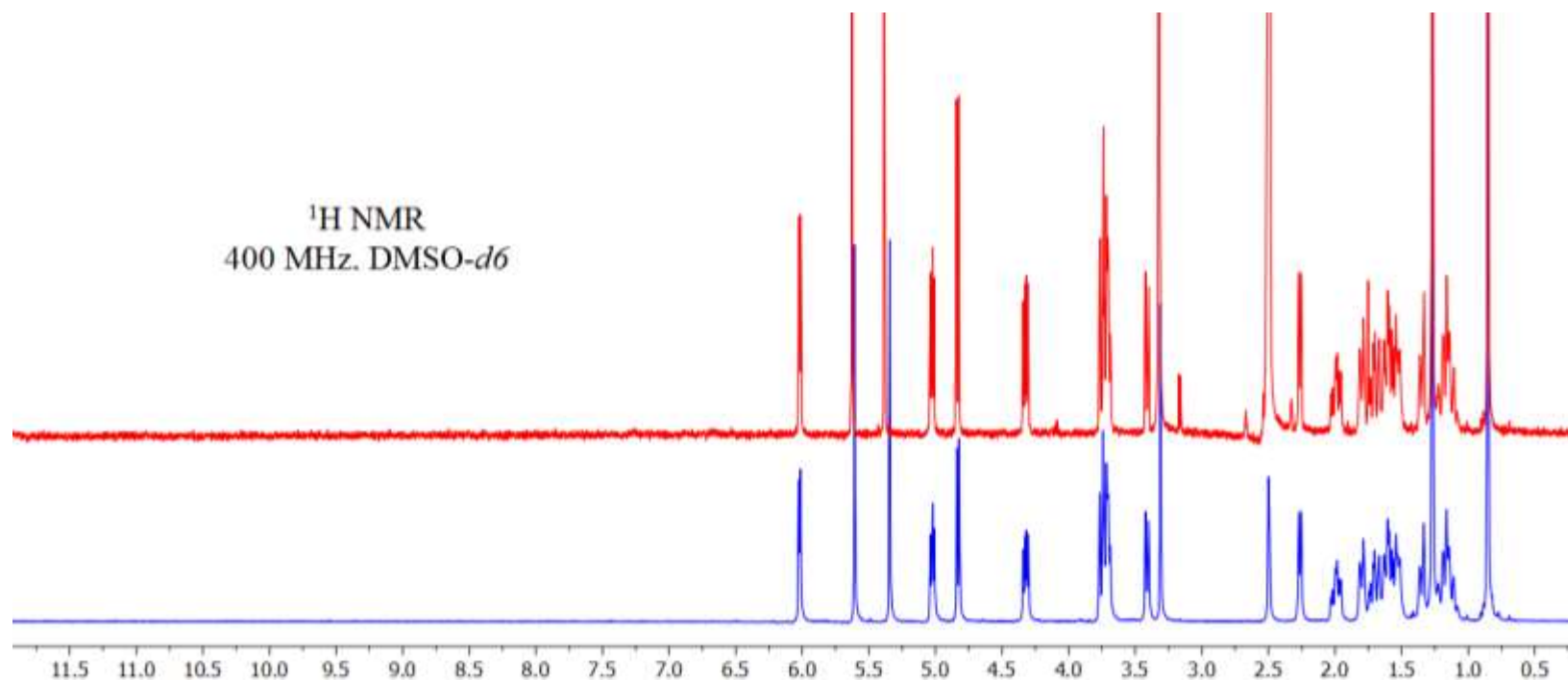


Figure 42. ^1H NMR (400 MHz, DMSO-*d*₆) spectra of compound 1 (red) and icacinol standard (blue)

APPENDIX A (continued)

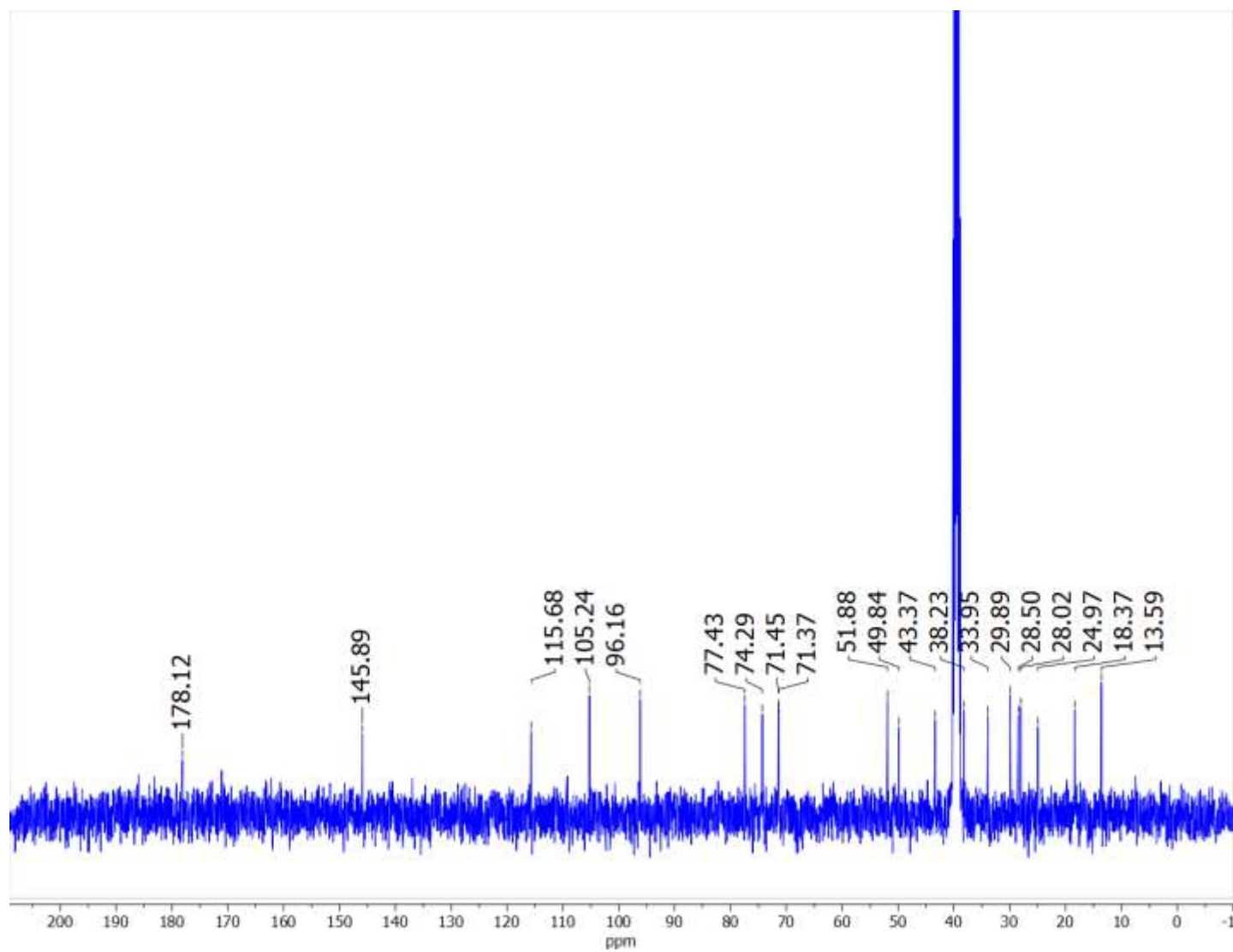


Figure 43. ^{13}C spectrum (100 MHz, $\text{DMSO-}d_6$) of icacinol

APPENDIX A (continued)

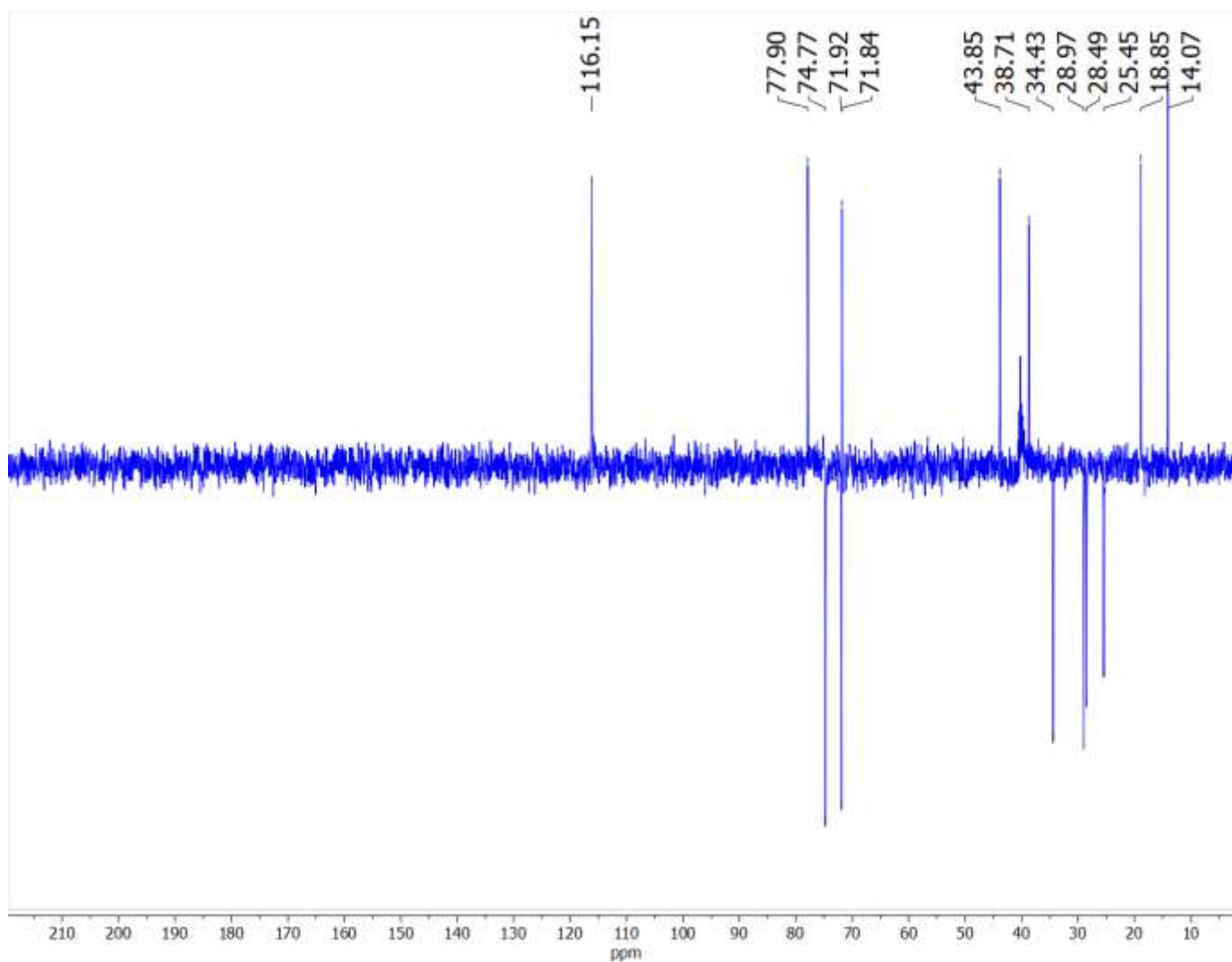


Figure 44. DEPT-135 spectrum (100 MHz, DMSO-*d*₆) of icacinol

APPENDIX A (continued)



Figure 45. LC-MS library similarity search for icacinol

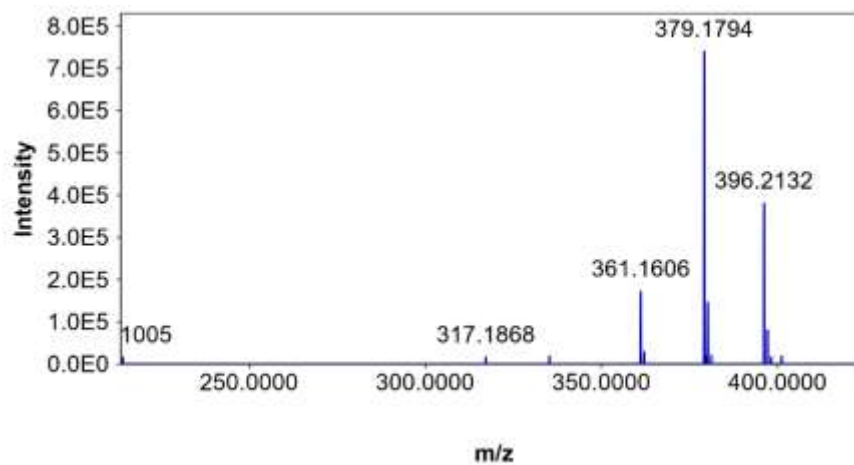


Figure 46. HRESIMS (positive mode) for icacinol

APPENDIX A (continued)

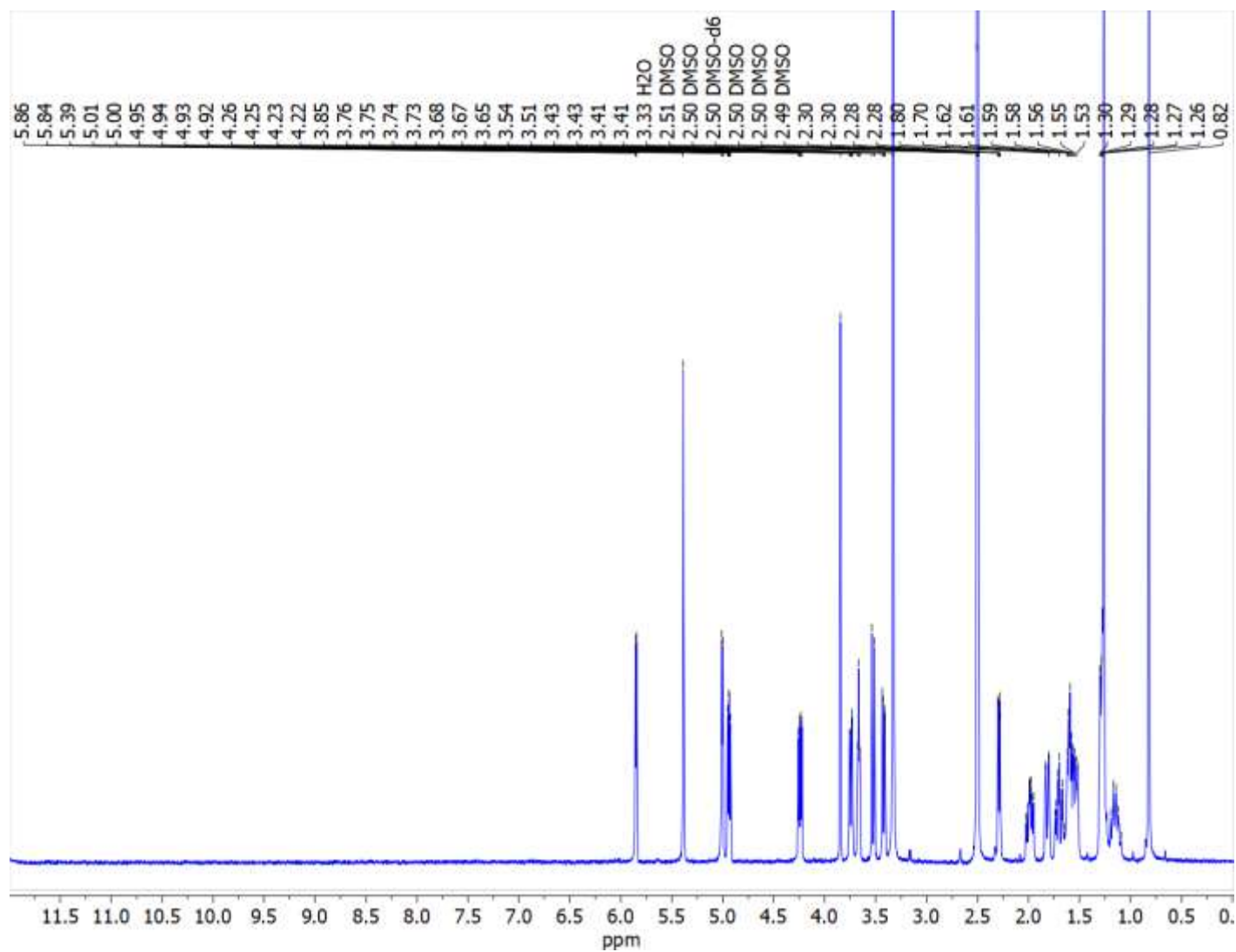


Figure 47. ¹H spectrum (400 MHz, DMSO-*d*₆) of humirianthol

APPENDIX A (continued)

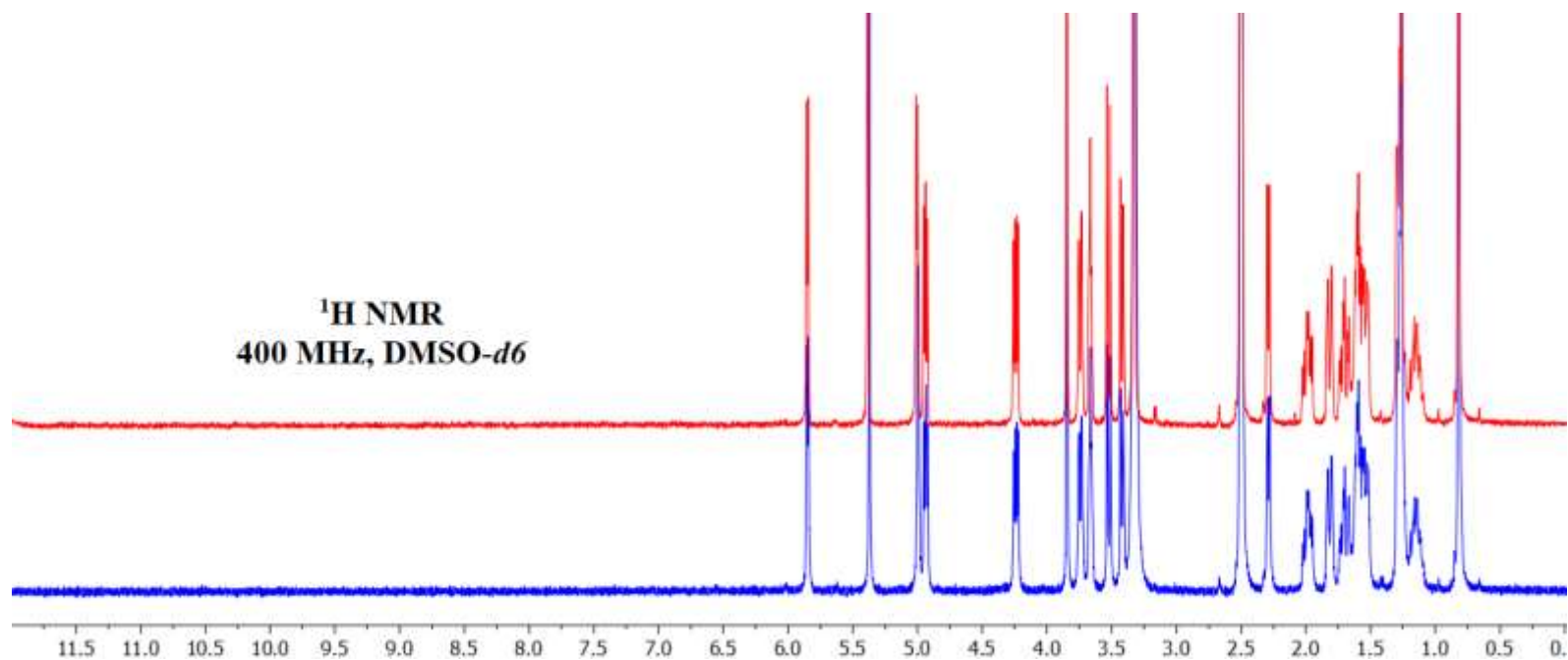


Figure 48. ¹H NMR (400 MHz, DMSO-*d*₆) spectra of isolated compound (red) and humirianthol standard (blue)

APPENDIX A (continued)

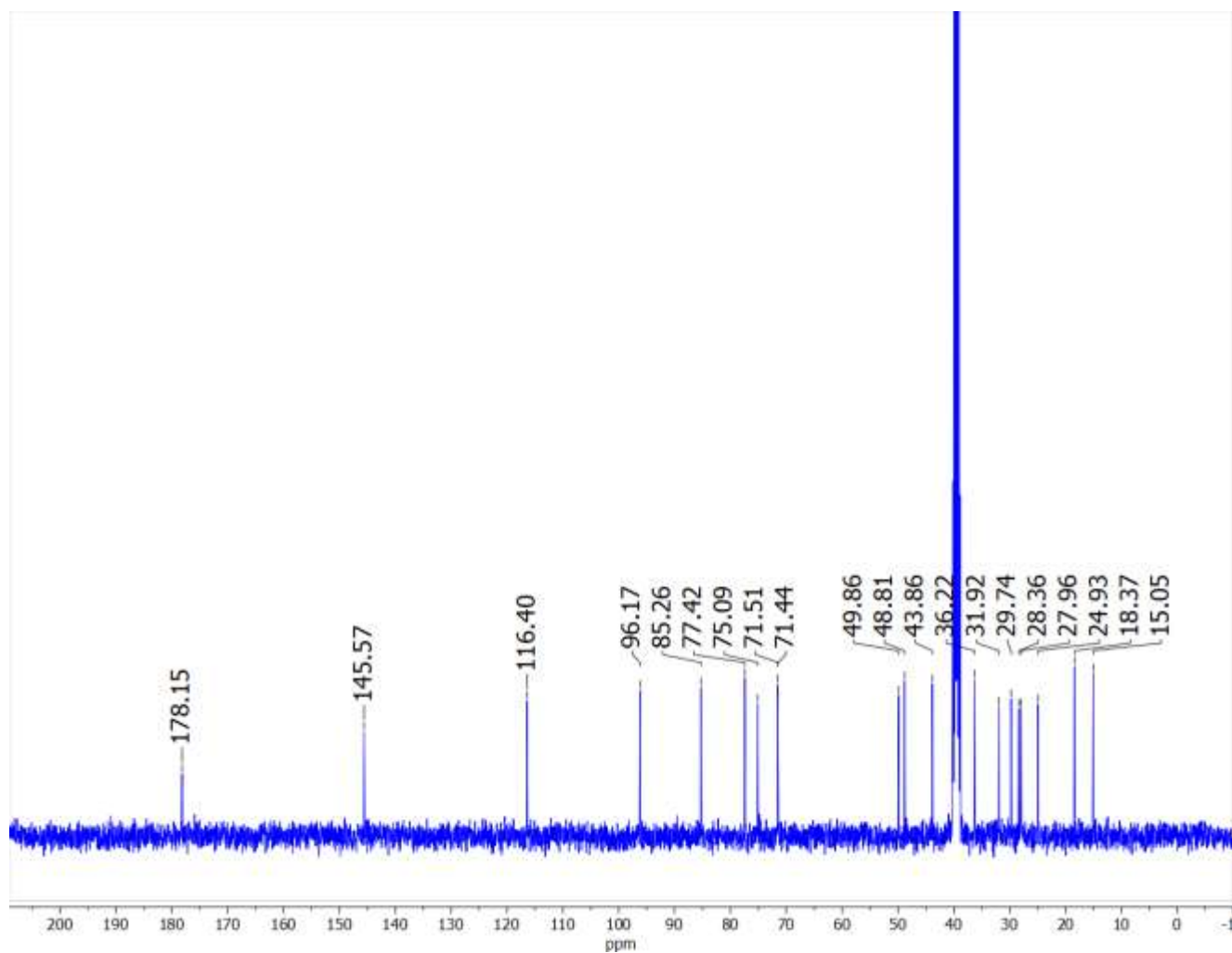
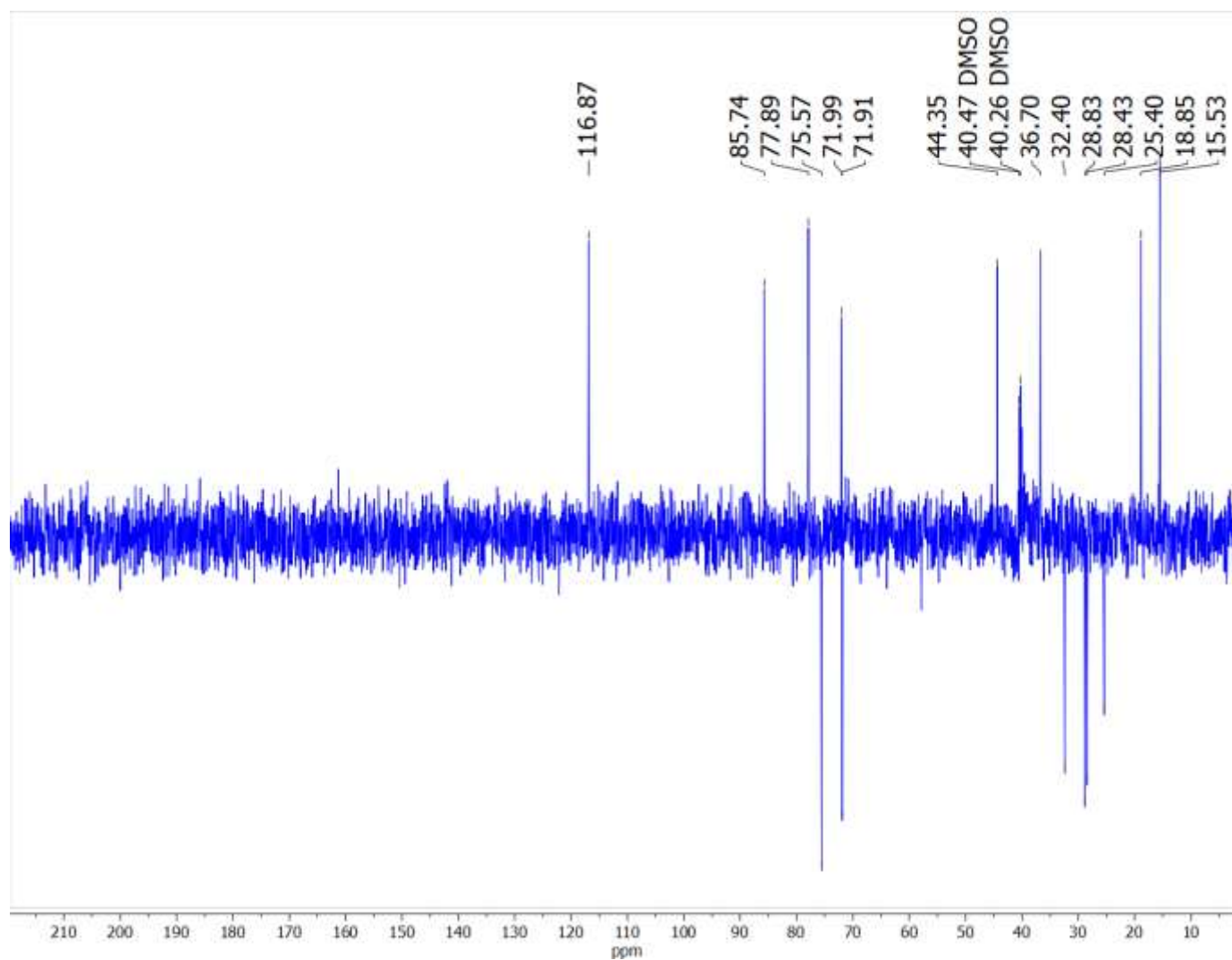


Figure 49. ^{13}C spectrum (100 MHz, $\text{DMSO-}d_6$) of humirianthol

APPENDIX A (continued)

**Figure 50. DEPT-135 spectrum (100 MHz, DMSO-*d*₆) of humirianthol**

APPENDIX A (continued)

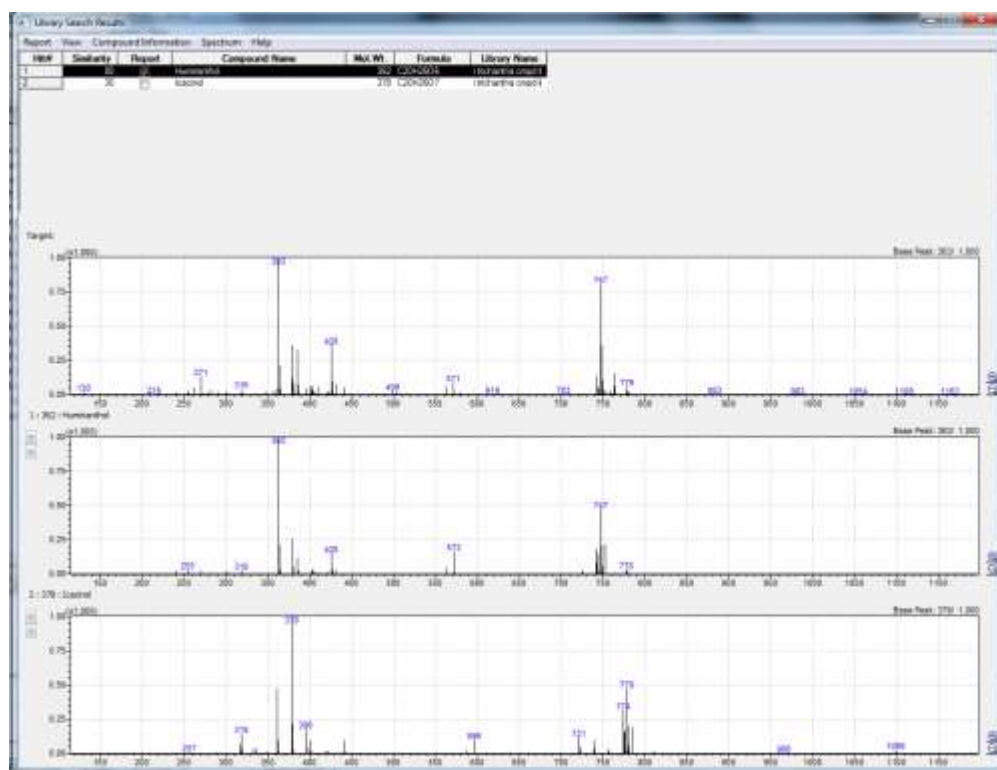


Figure 51. LC-MS library similarity search for humirianthol

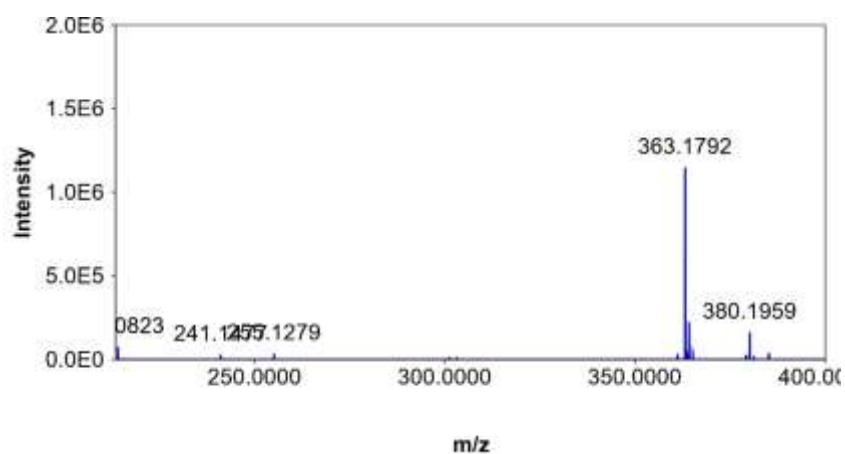


Figure 52. HRESIMS (positive mode) for humirianthol

APPENDIX A (continued)

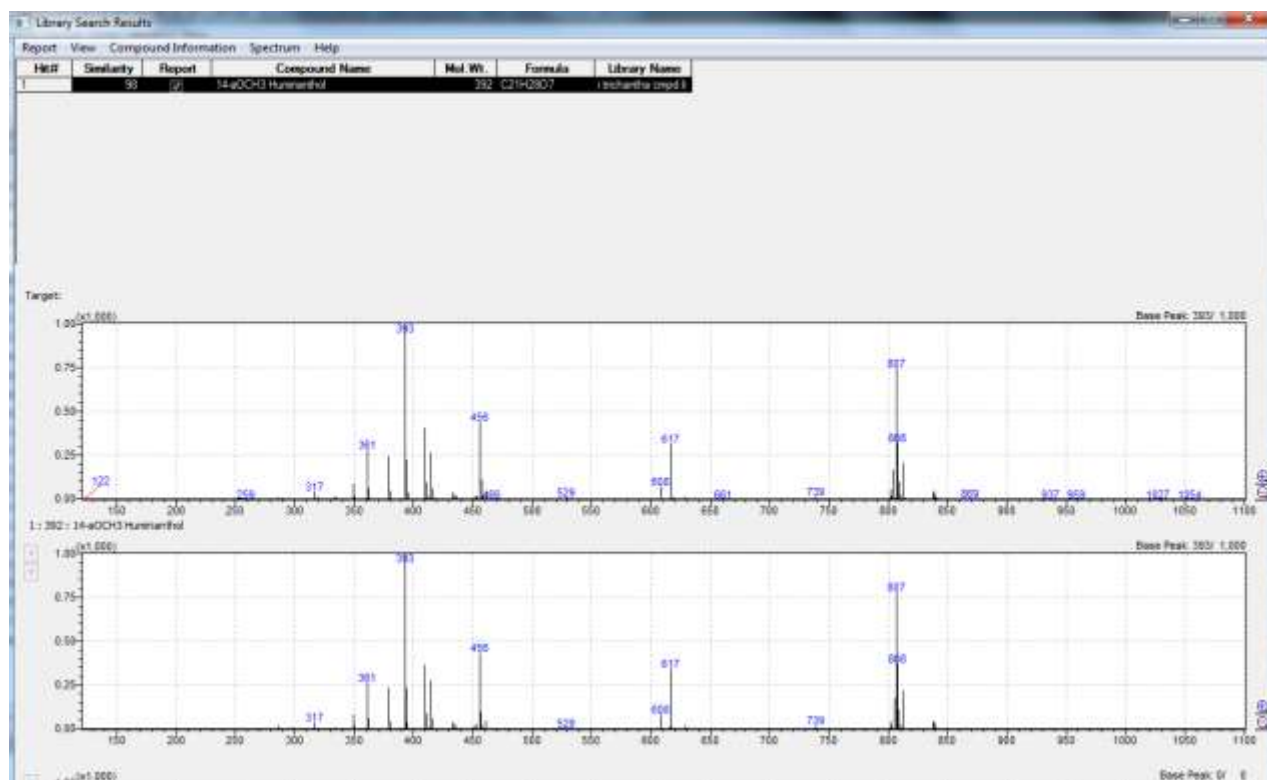


Figure 53. LC-MS library similarity search for 14- α OCH₃-humirianthol

APPENDIX A (continued)

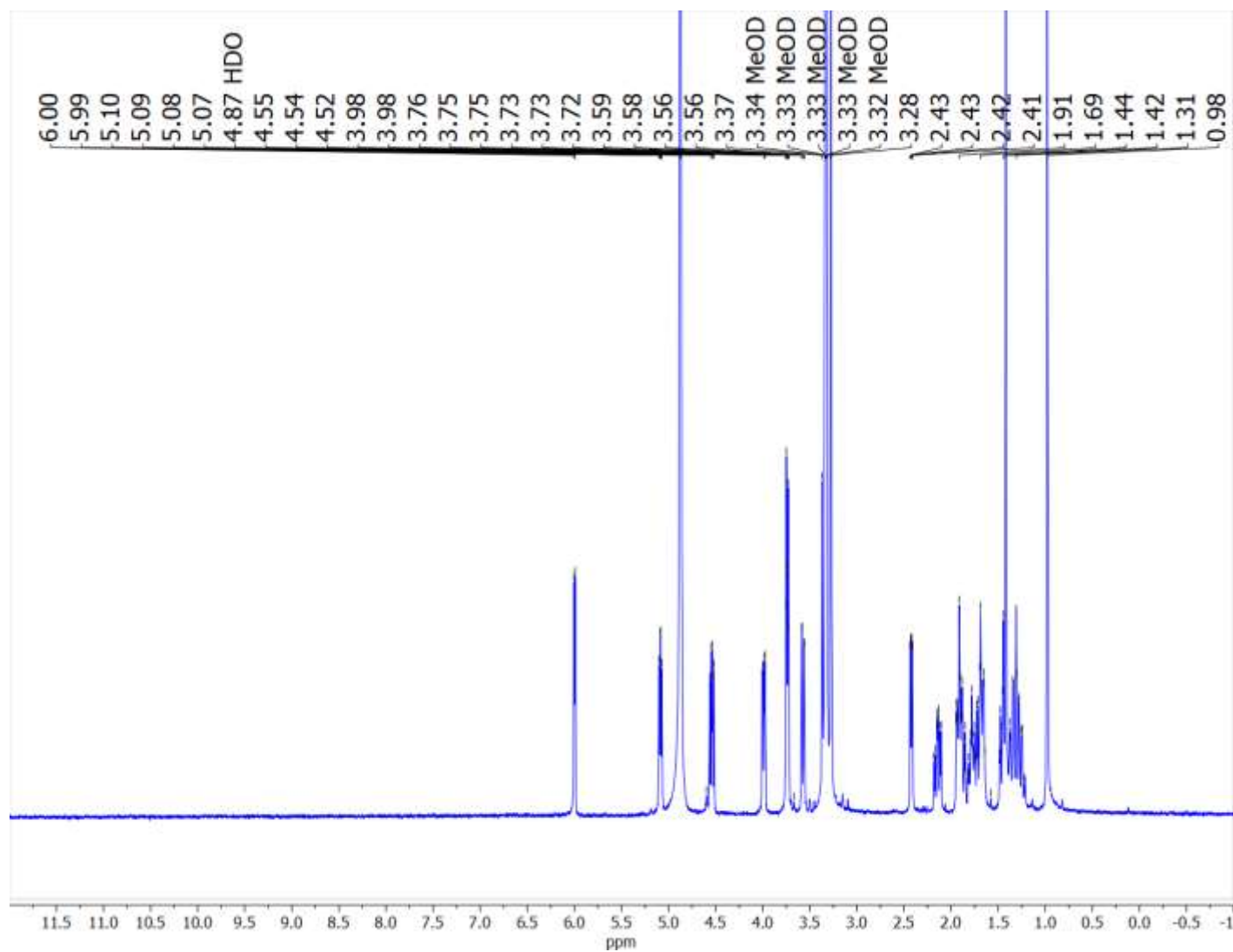


Figure 54. ¹H spectrum (400 MHz, CD₃OD) of 14- α -methoxy-humirianthol

APPENDIX A (continued)

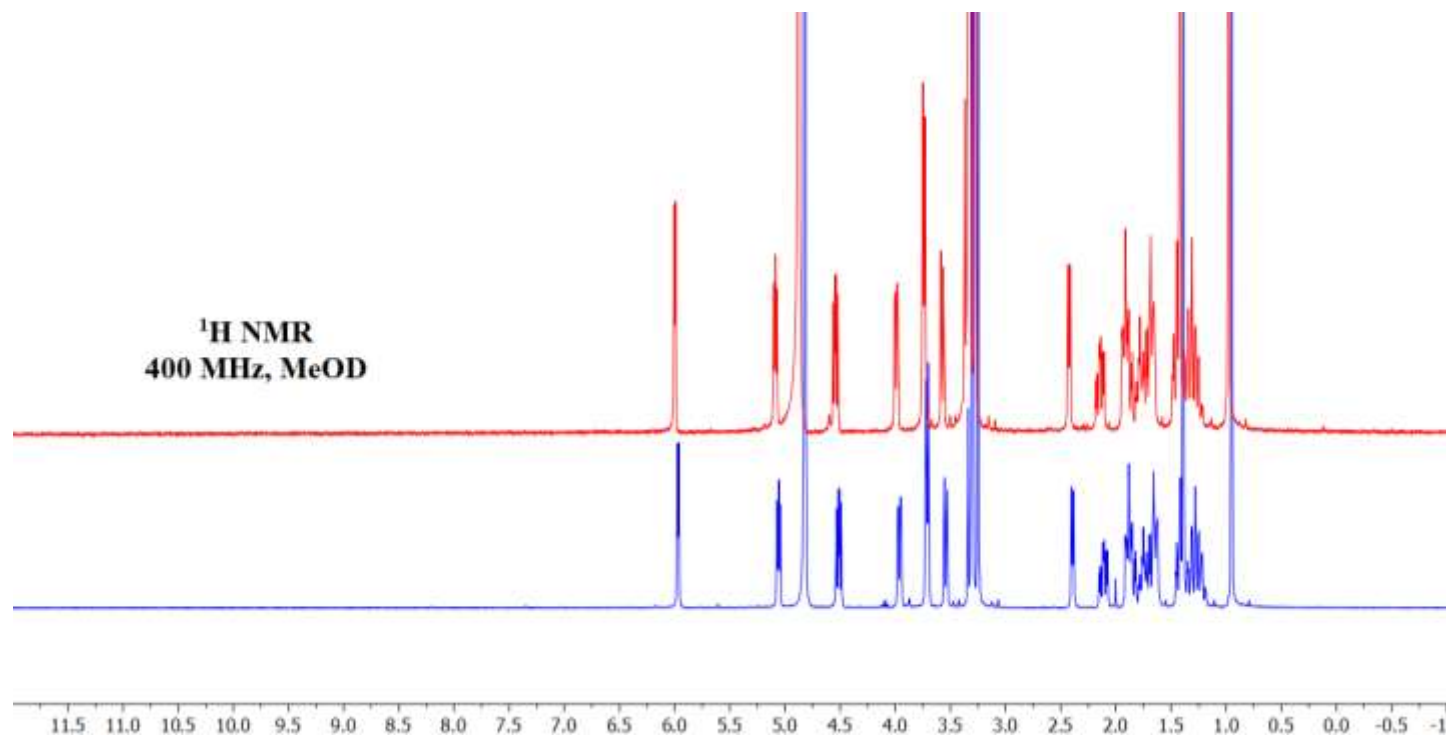


Figure 55. ¹H NMR (400 MHz, CD₃OD) spectra of isolated compound (red) and 14- α -methoxy-humirianthol standard (blue)

APPENDIX A (continued)

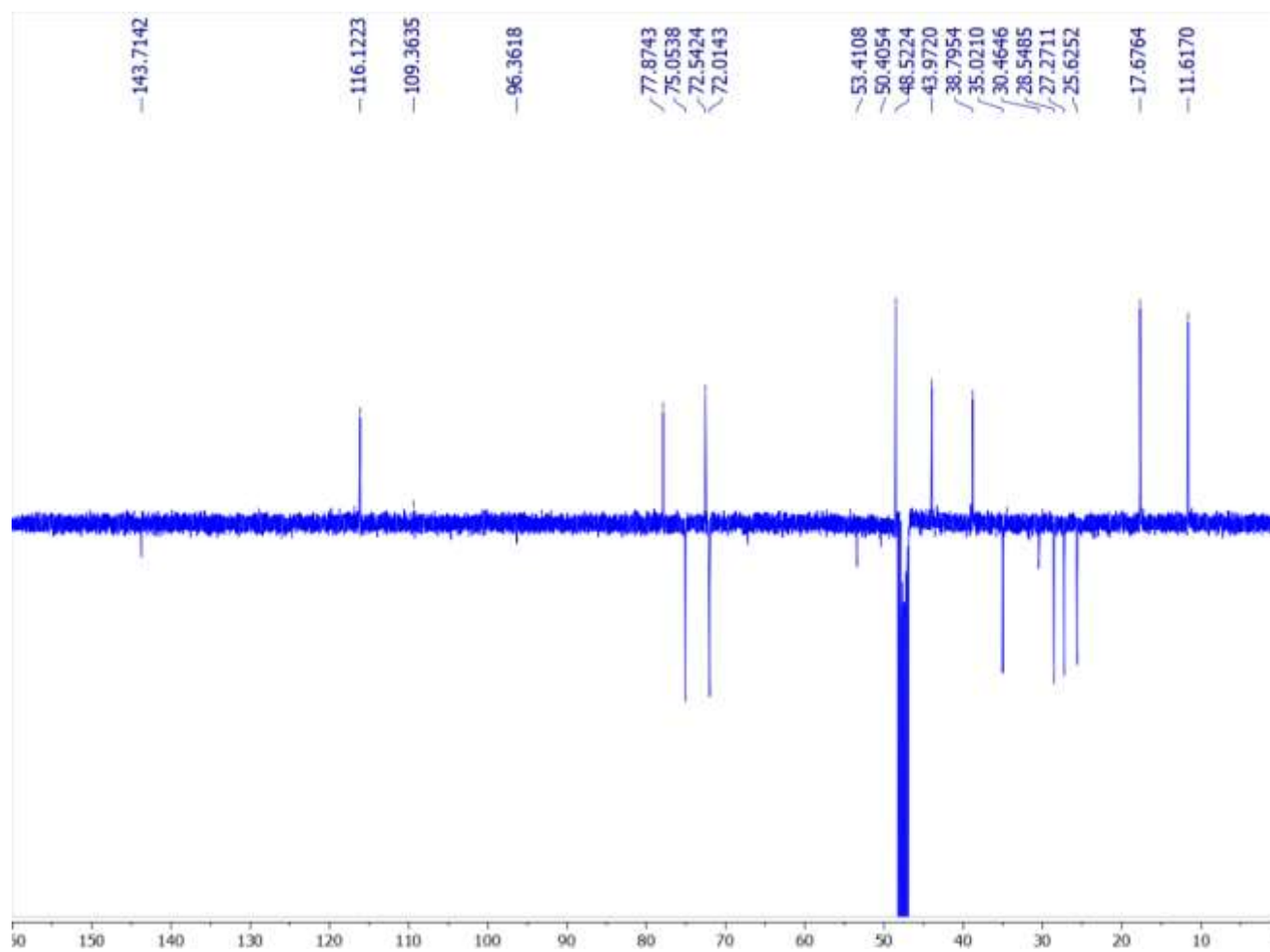


Figure 56. DEPTQ spectrum (100 MHz, CD₃OD) of 14- α -methoxy-humirianthol

APPENDIX A (continued)

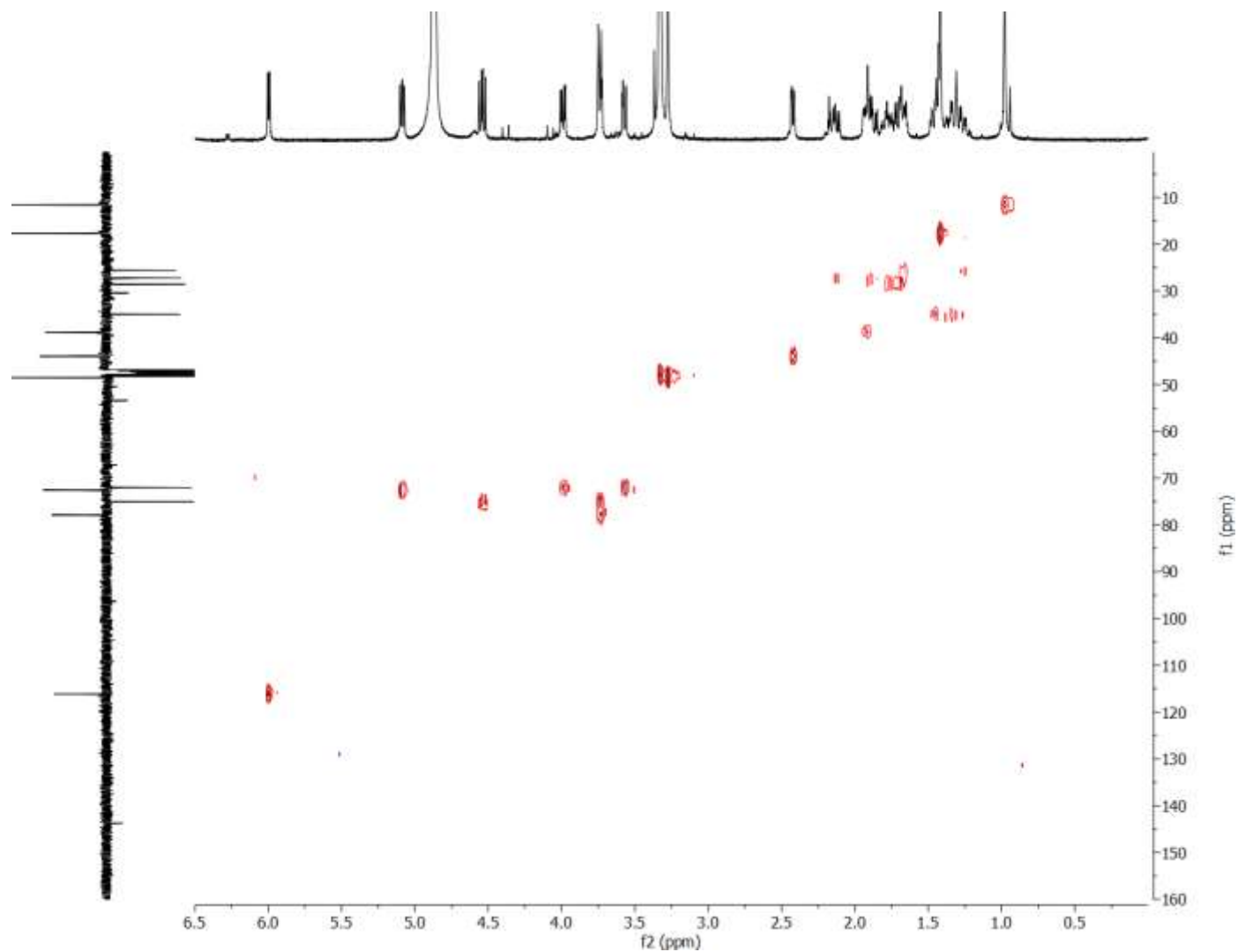


Figure 57. HSQC spectrum (400 MHz, CD₃OD) of 14- α - methoxy-humirianthol

APPENDIX A (continued)

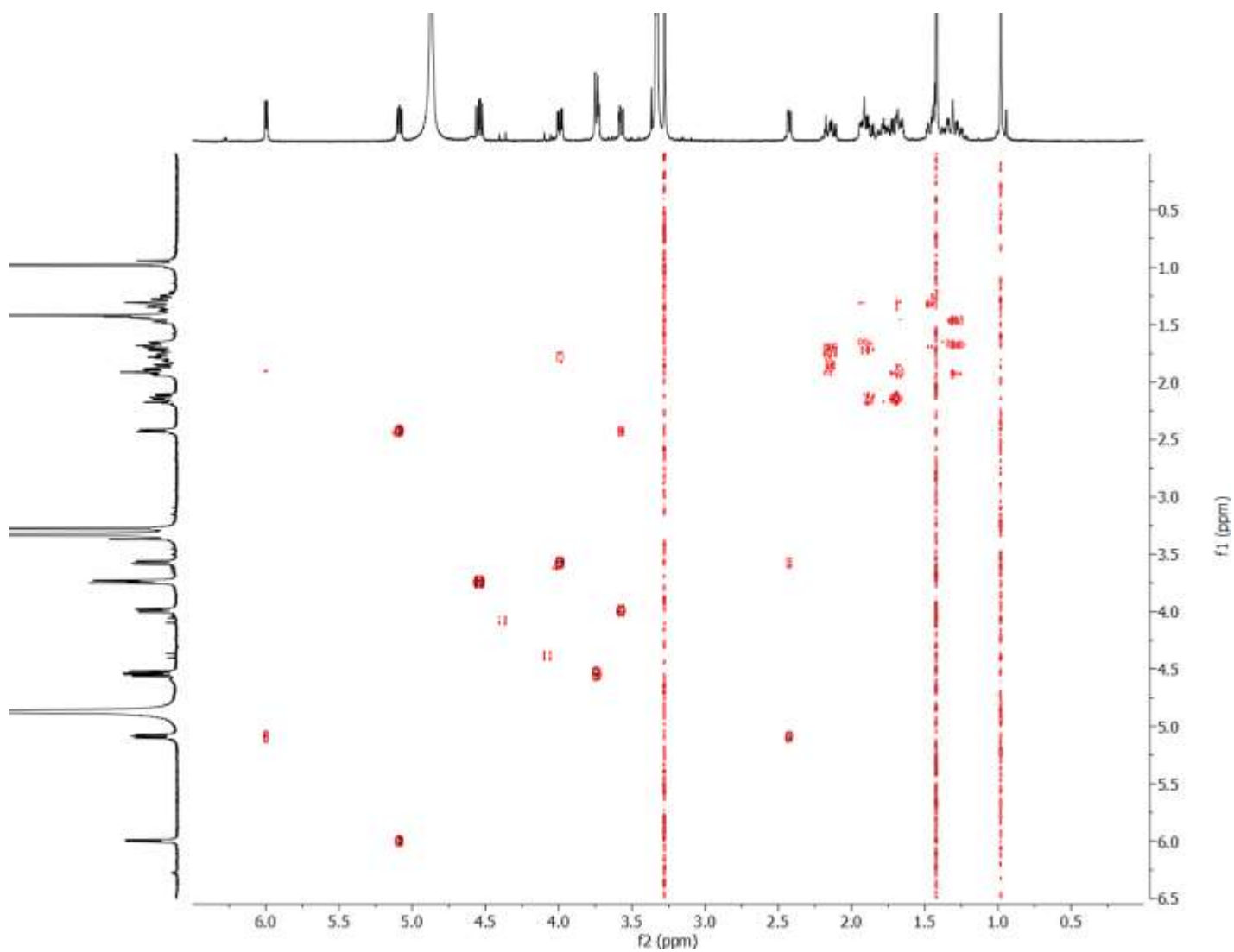


Figure 58. COSY spectrum (400 MHz, CD₃OD) of 14- α -methoxy-humirianthol

APPENDIX A (continued)

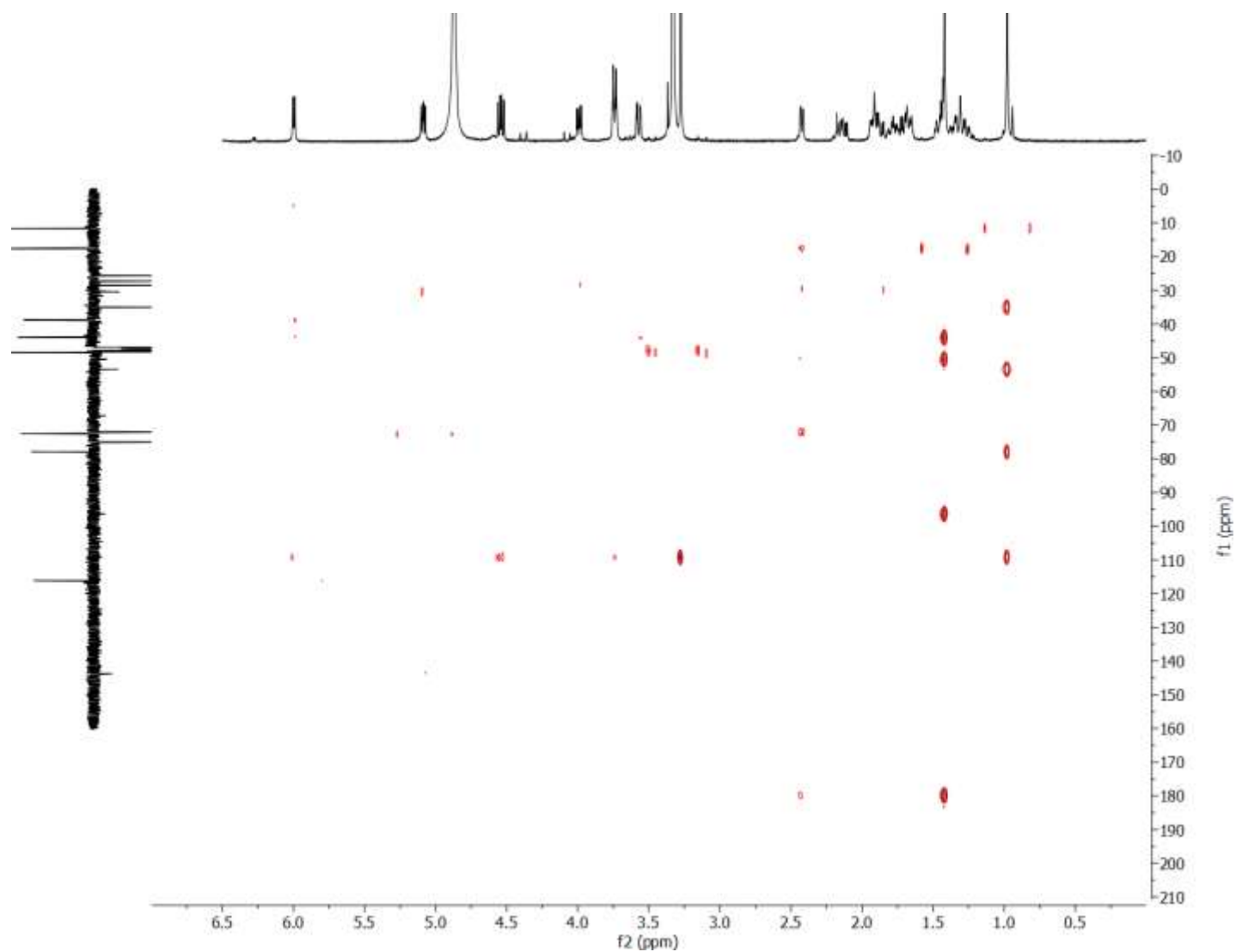


Figure 59. HMBC spectrum (400 MHz, CD₃OD) of 14- α -methoxy-humirianthol

APPENDIX A (continued)

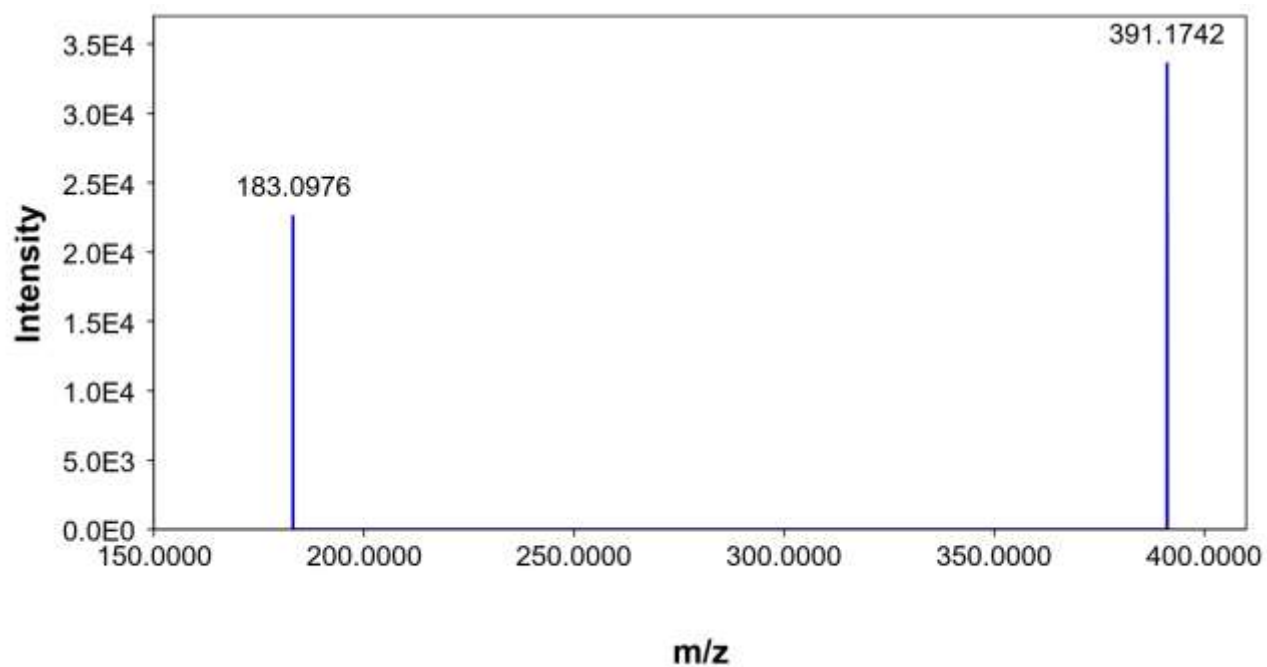


Figure 60. HRESIMS (negative mode) for icacinlactone I

APPENDIX A (continued)

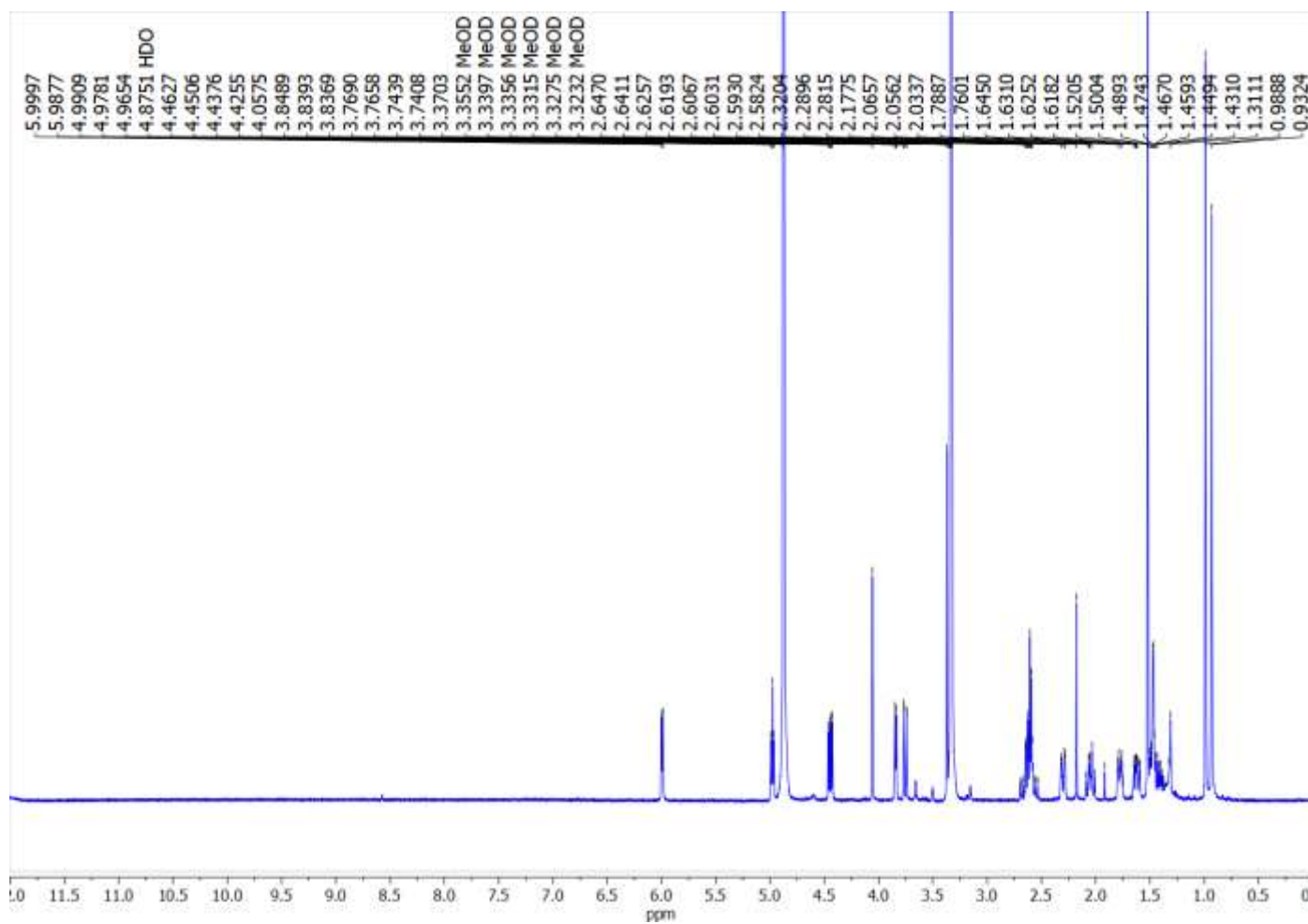


Figure 61. ^1H spectrum (400 MHz, CD_3OD) of icacinlactone I

APPENDIX A (continued)

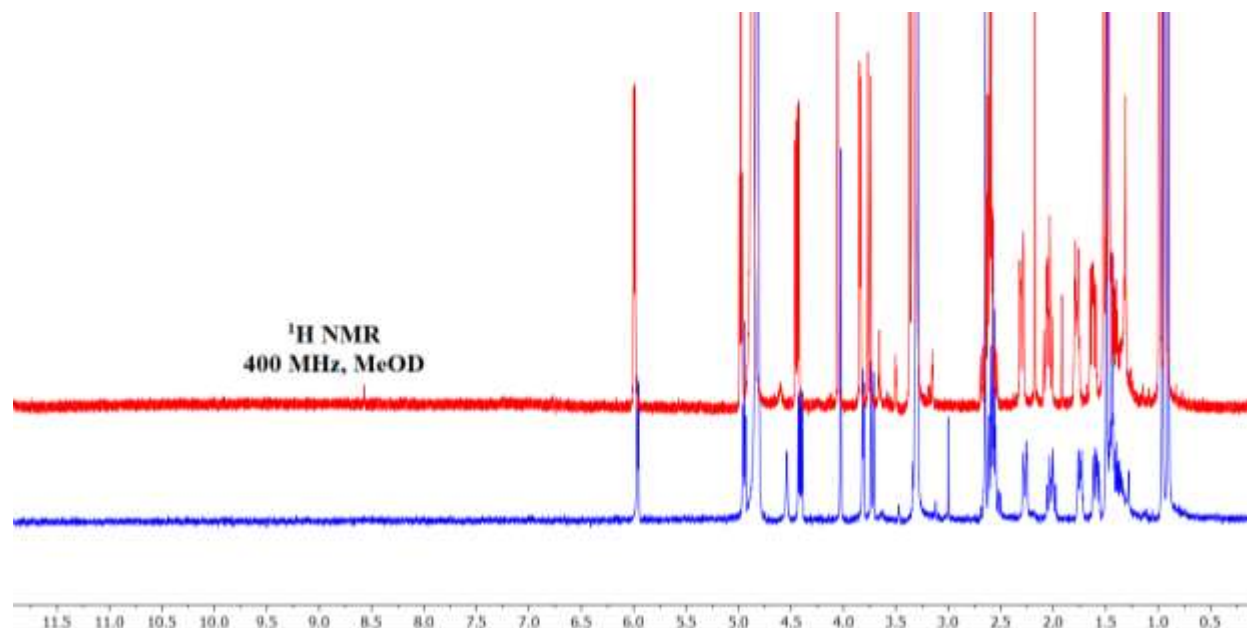


Figure 62. ^1H NMR (400 MHz, CD_3OD) spectra of isolated compound (red) and icacinlactone I standard (blue)

APPENDIX A (continued)

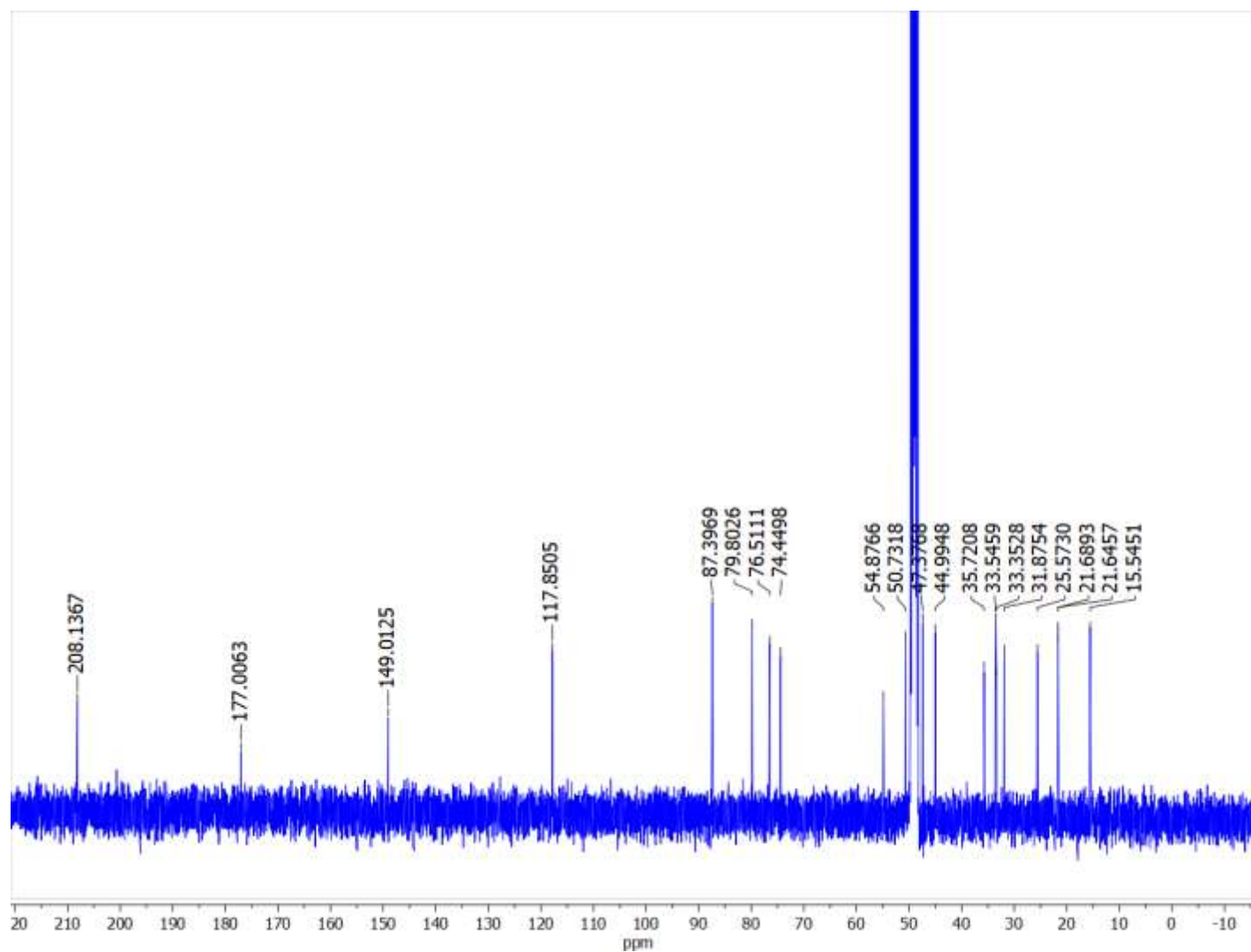


Figure 63. ¹³C spectrum (100 MHz, CD₃OD) of icacinlactone I

APPENDIX A (continued)

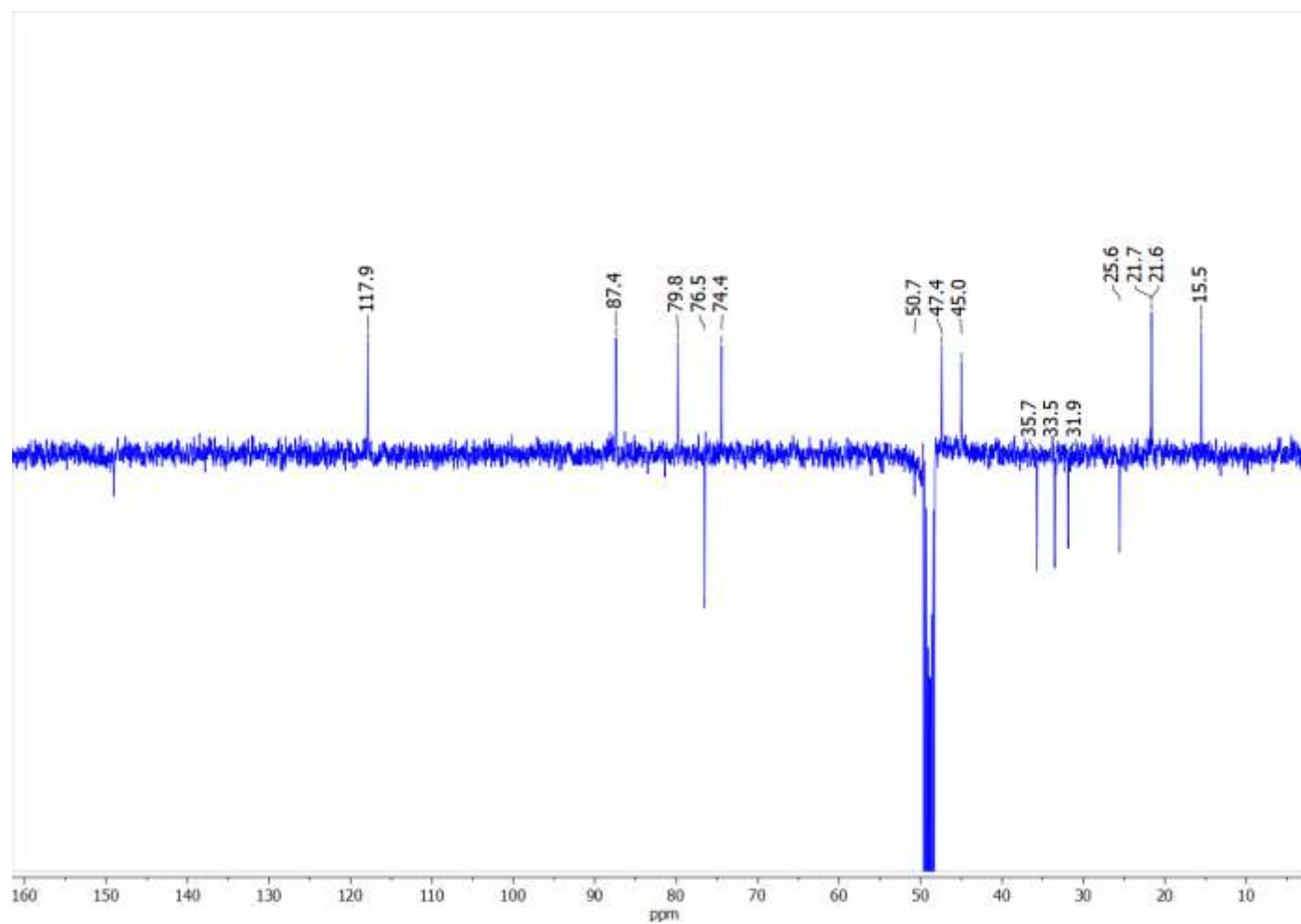


Figure 64. DEPT-135 spectrum (100 MHz, CD₃OD) of icacinlactone I

APPENDIX A (continued)

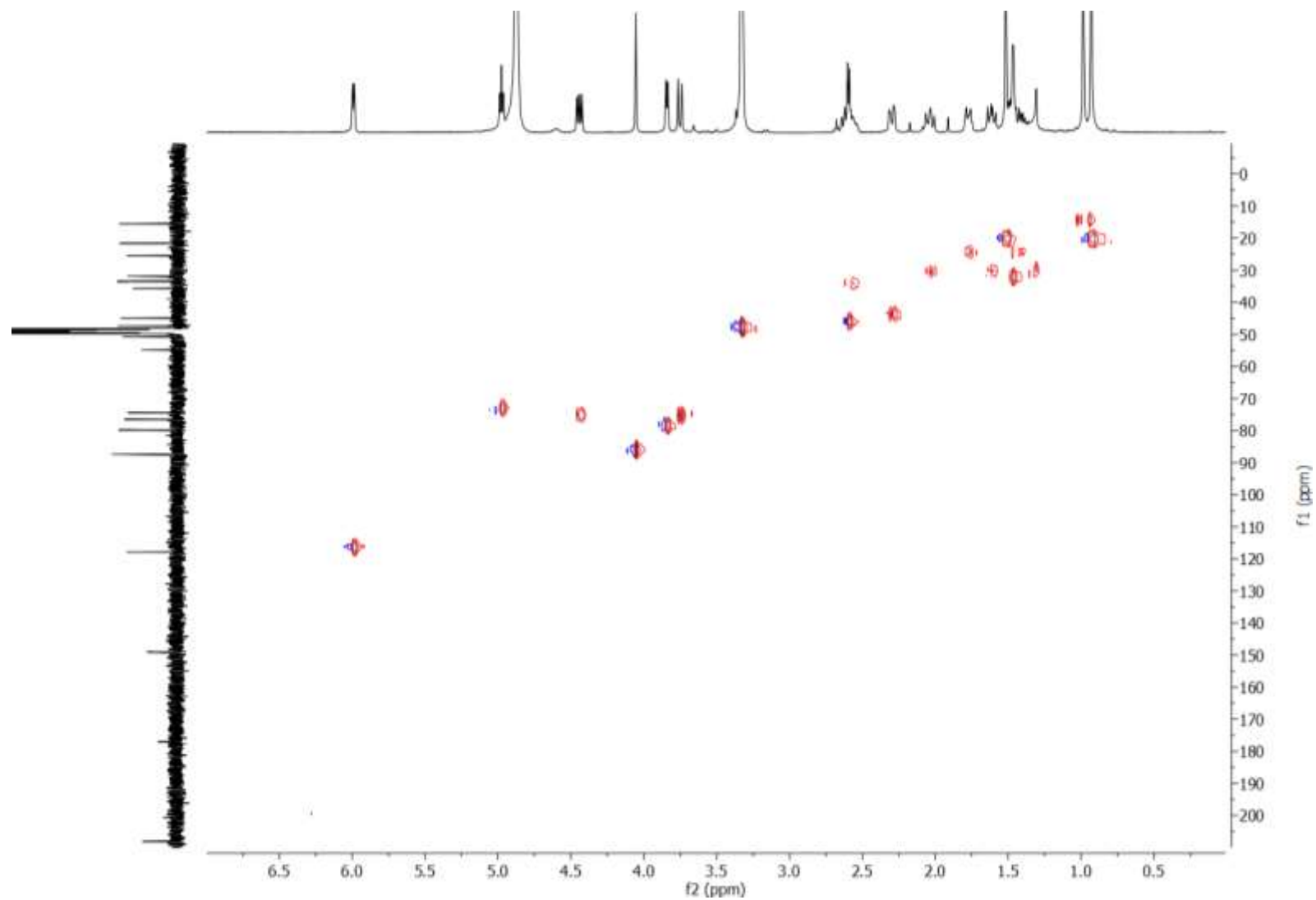


Figure 65. HSQC spectrum (400 MHz, CD_3OD) of icacinlactone I

APPENDIX A (continued)

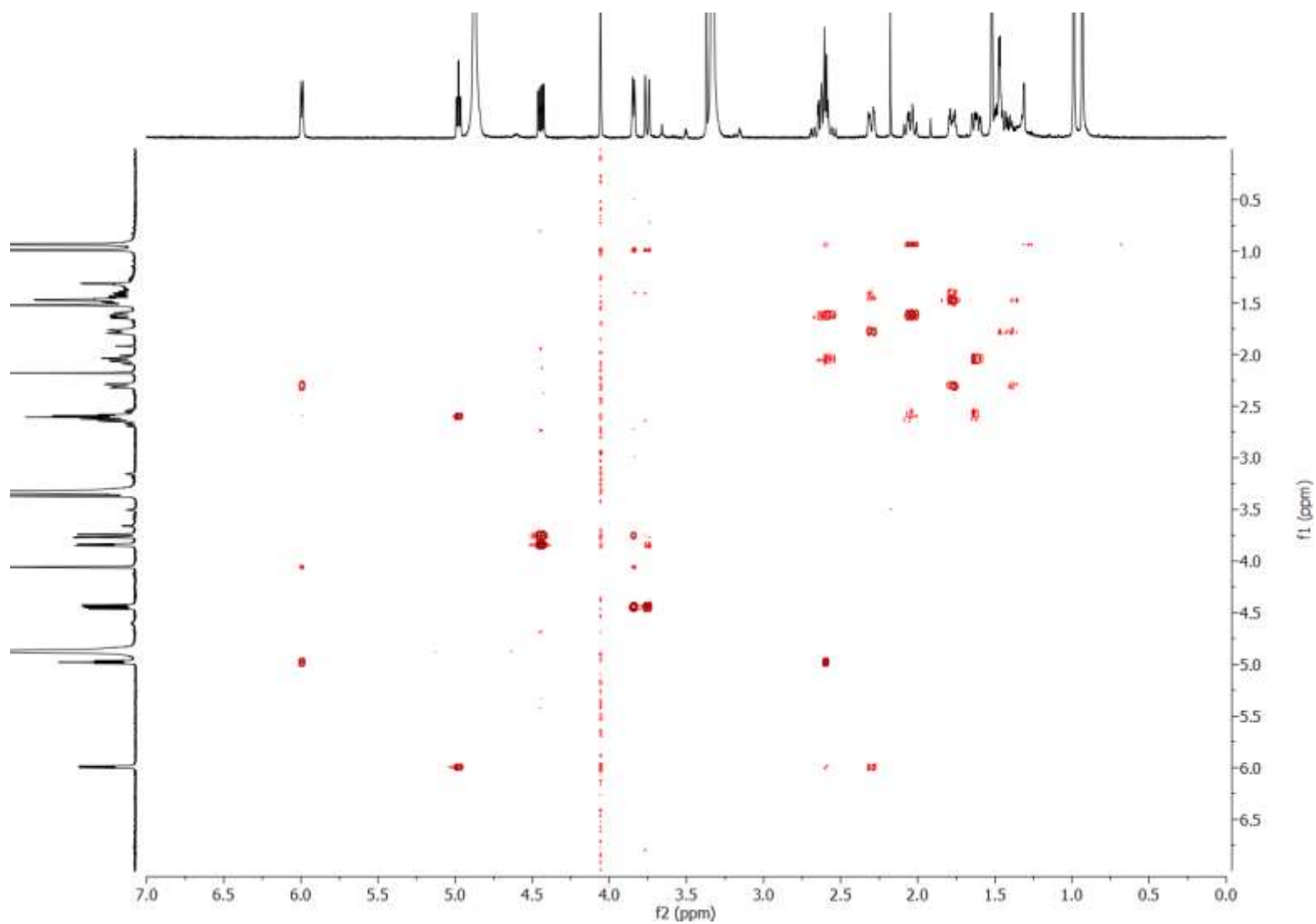


Figure 66. COSY spectrum (400 MHz, CD₃OD) of icacinlactone I

APPENDIX A (continued)

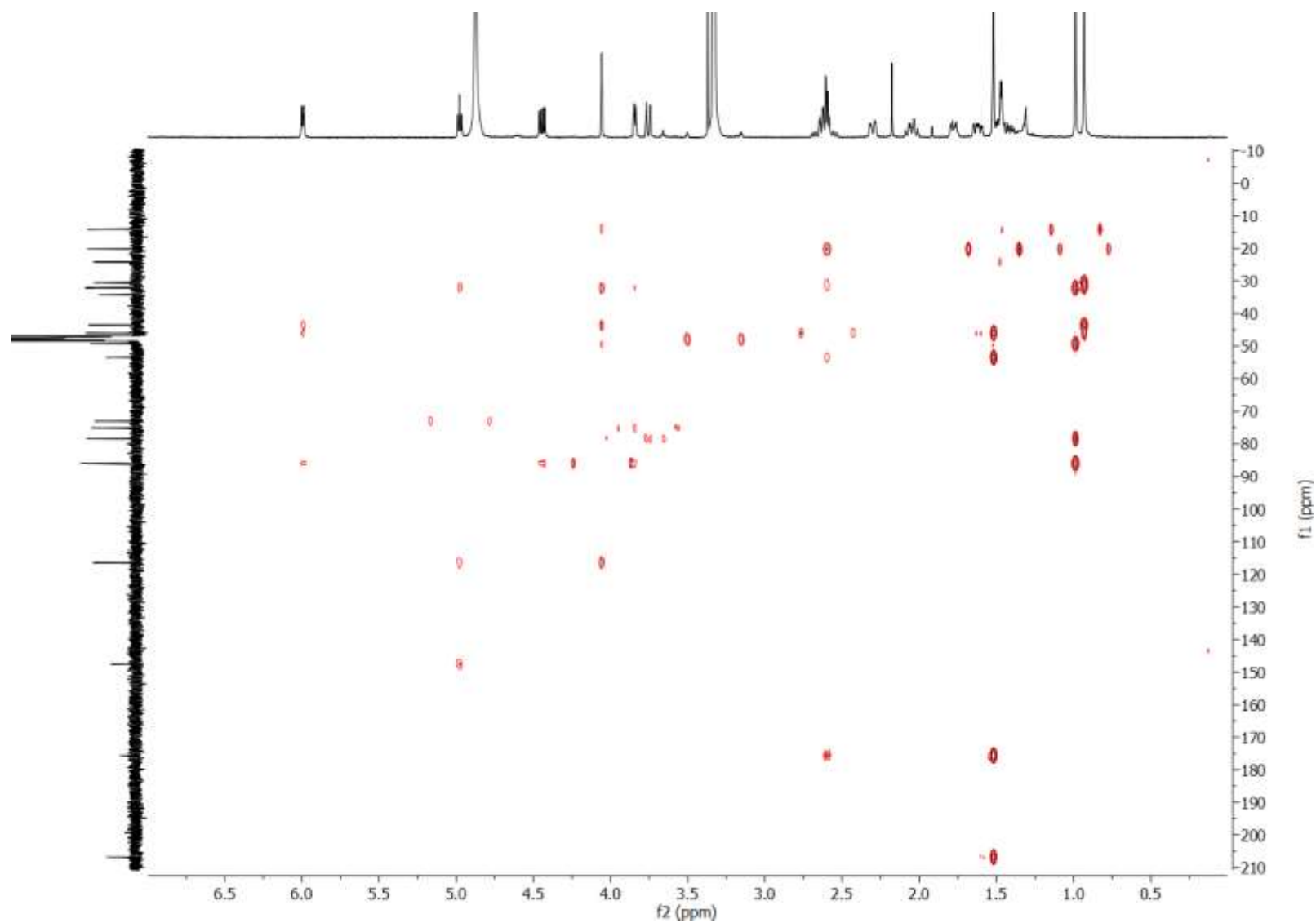


Figure 67. HMBC spectrum (400 MHz, CD₃OD) of icacinlactone I

APPENDIX A (continued)

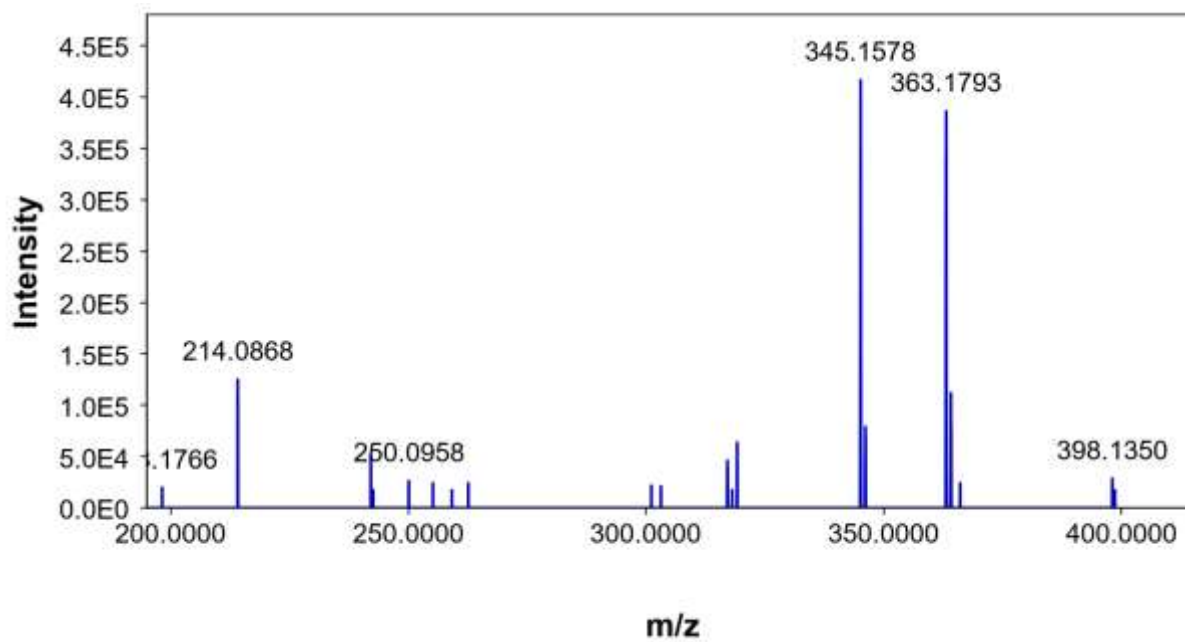


Figure 68. HRESIMS (positive mode) for 14-hydroxy-icacinlactone I

APPENDIX A (continued)

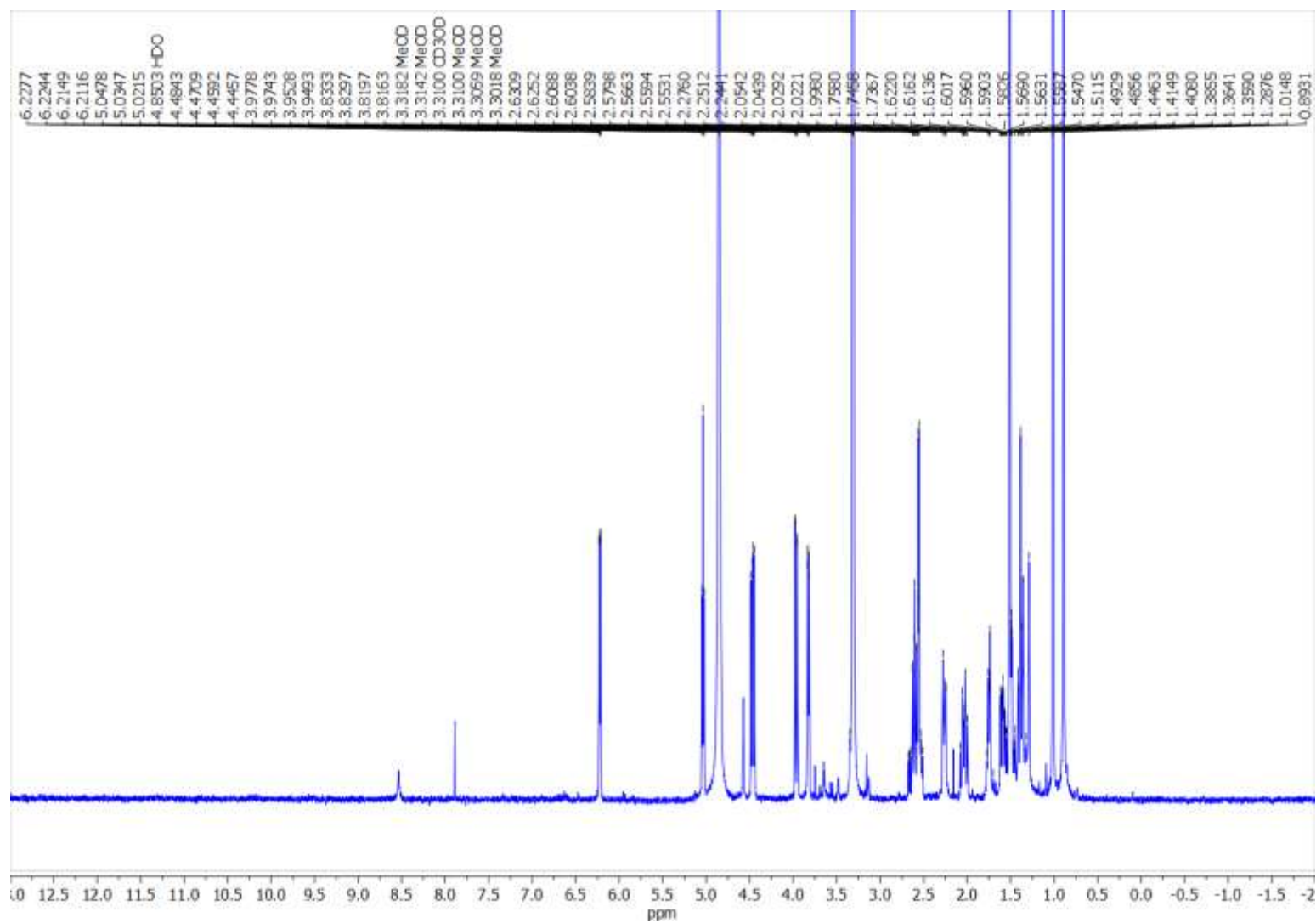


Figure 69. ^1H spectrum (400 MHz, CD_3OD) of 14-hydroxy-icacinlactone I

APPENDIX A (continued)

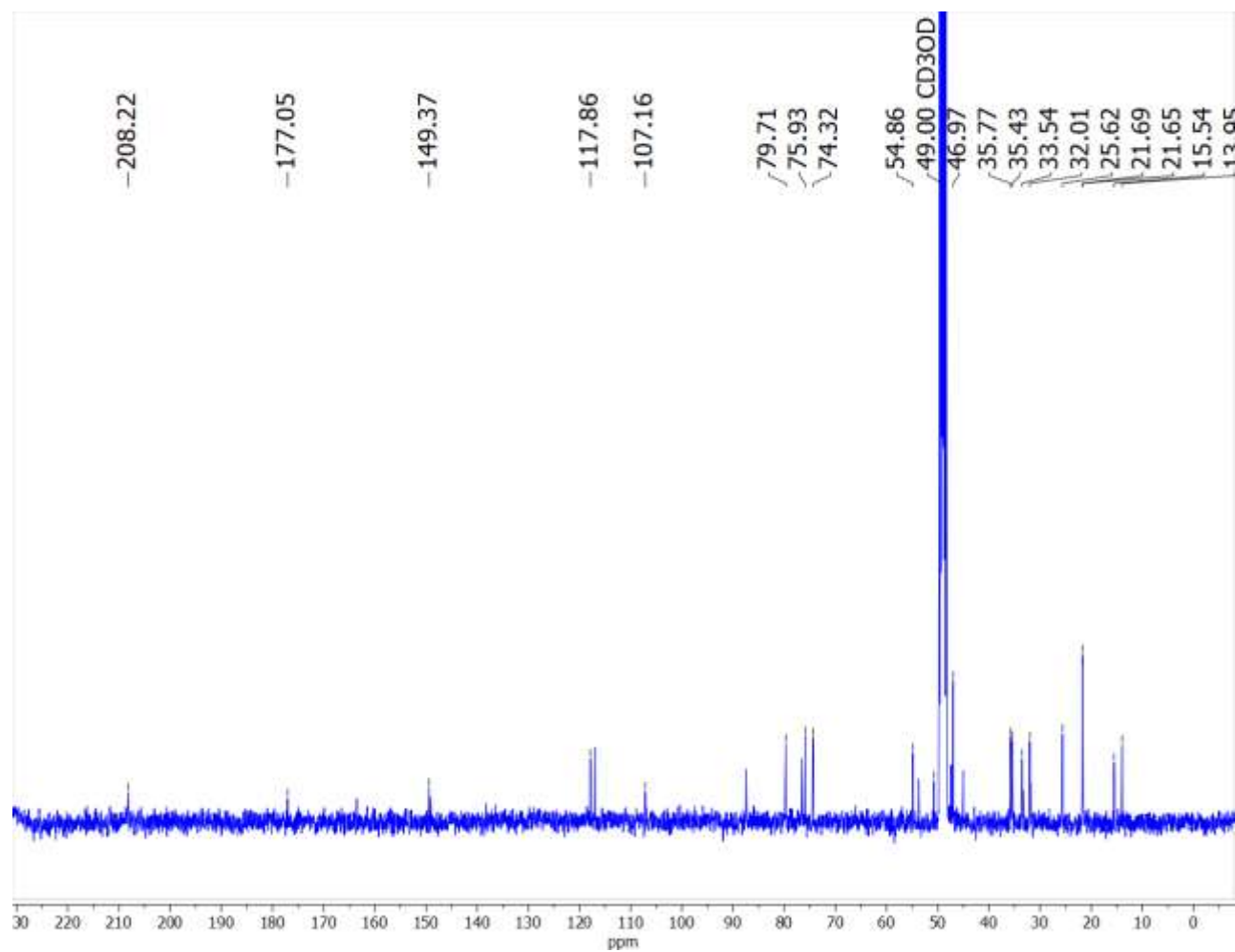


Figure 70. ^{13}C spectrum (100 MHz, CD_3OD) of 14-hydroxy-icacinlactone I

APPENDIX A (continued)

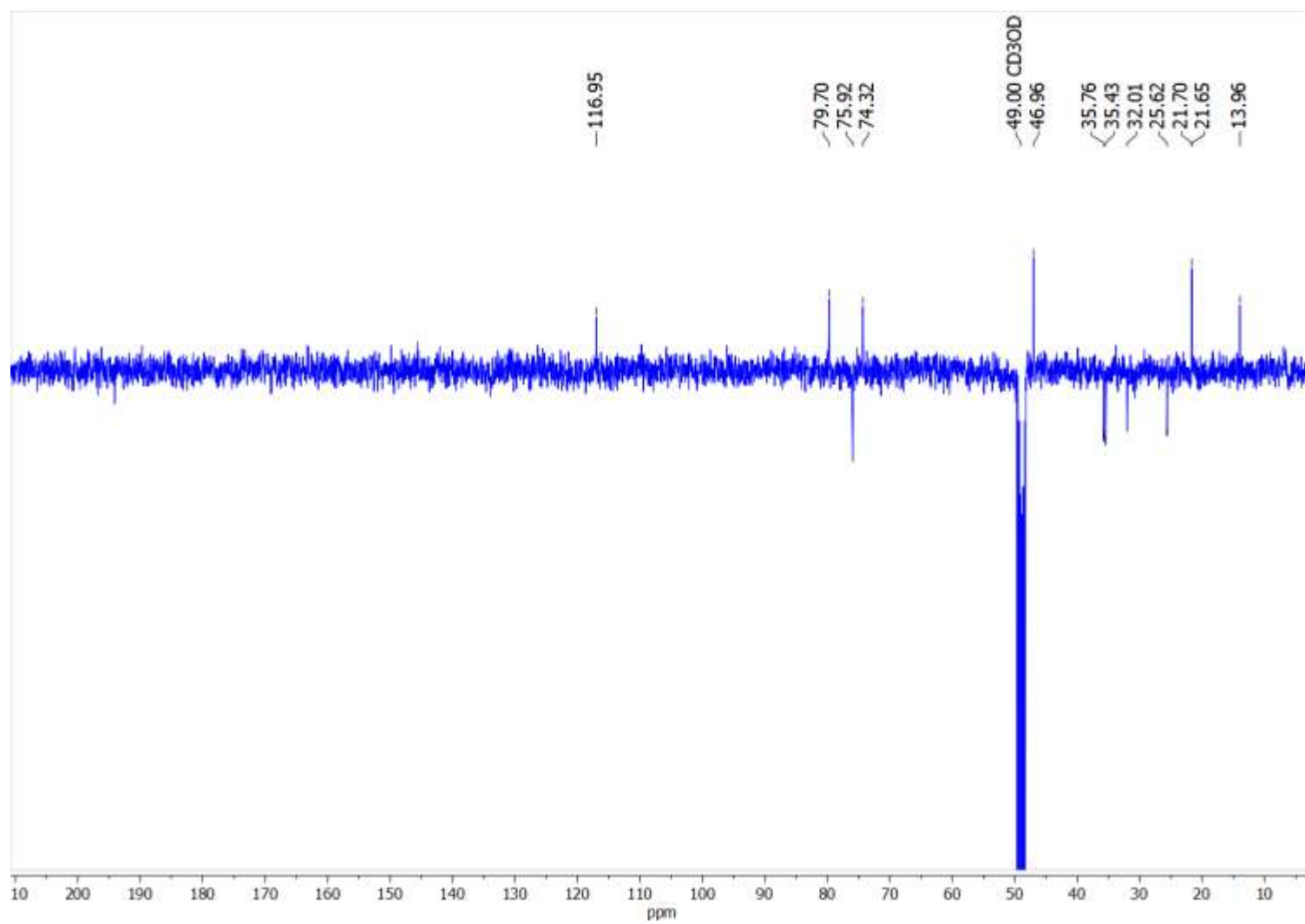


Figure 71. DEPT-135 spectrum (100 MHz, CD₃OD) of 14-hydroxy-icacinlactone I

APPENDIX A (continued)

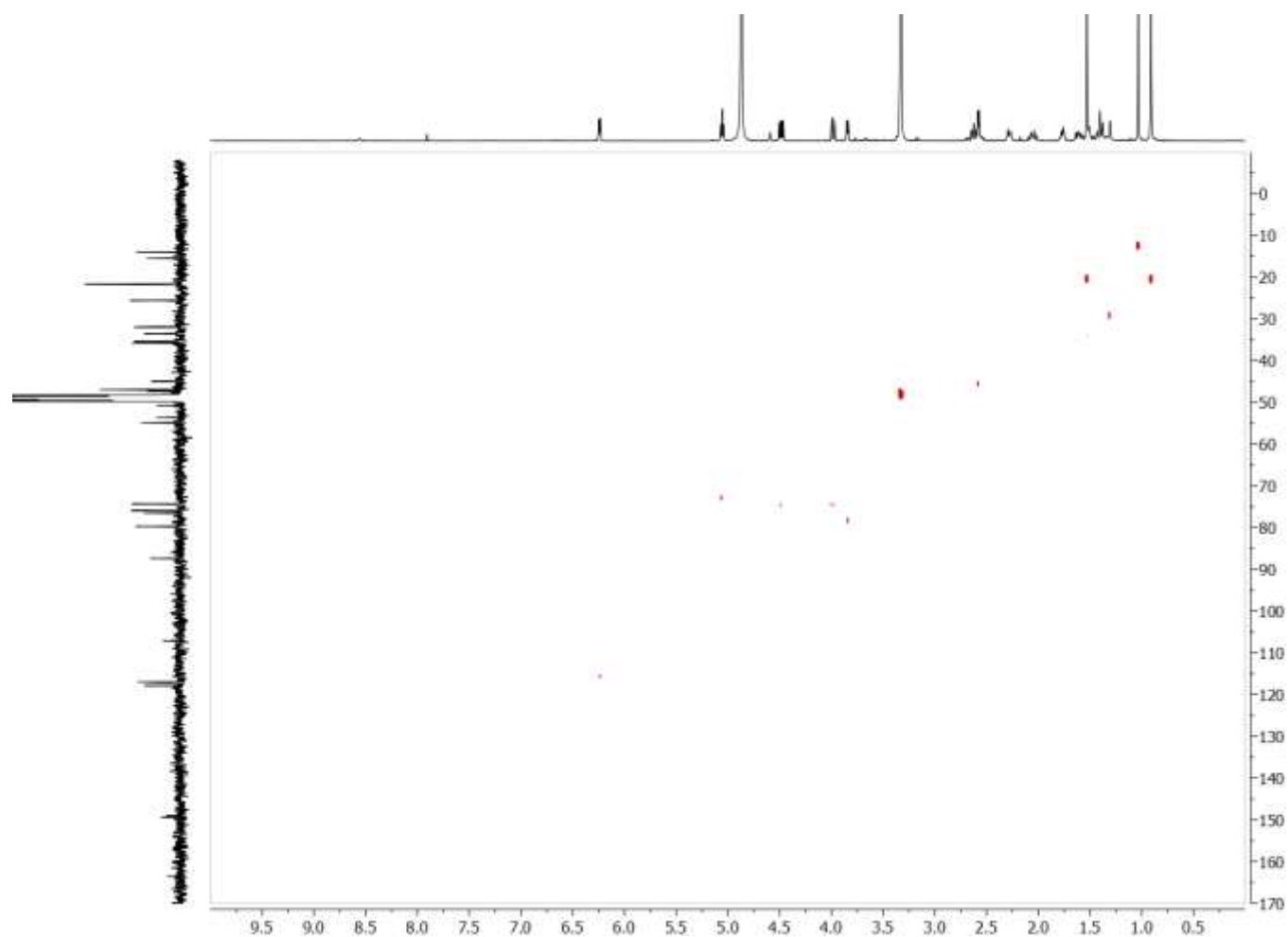


Figure 72. HSQC spectrum (400 MHz, CD₃OD) of 14-hydroxy-icacinlactone I

APPENDIX A (continued)

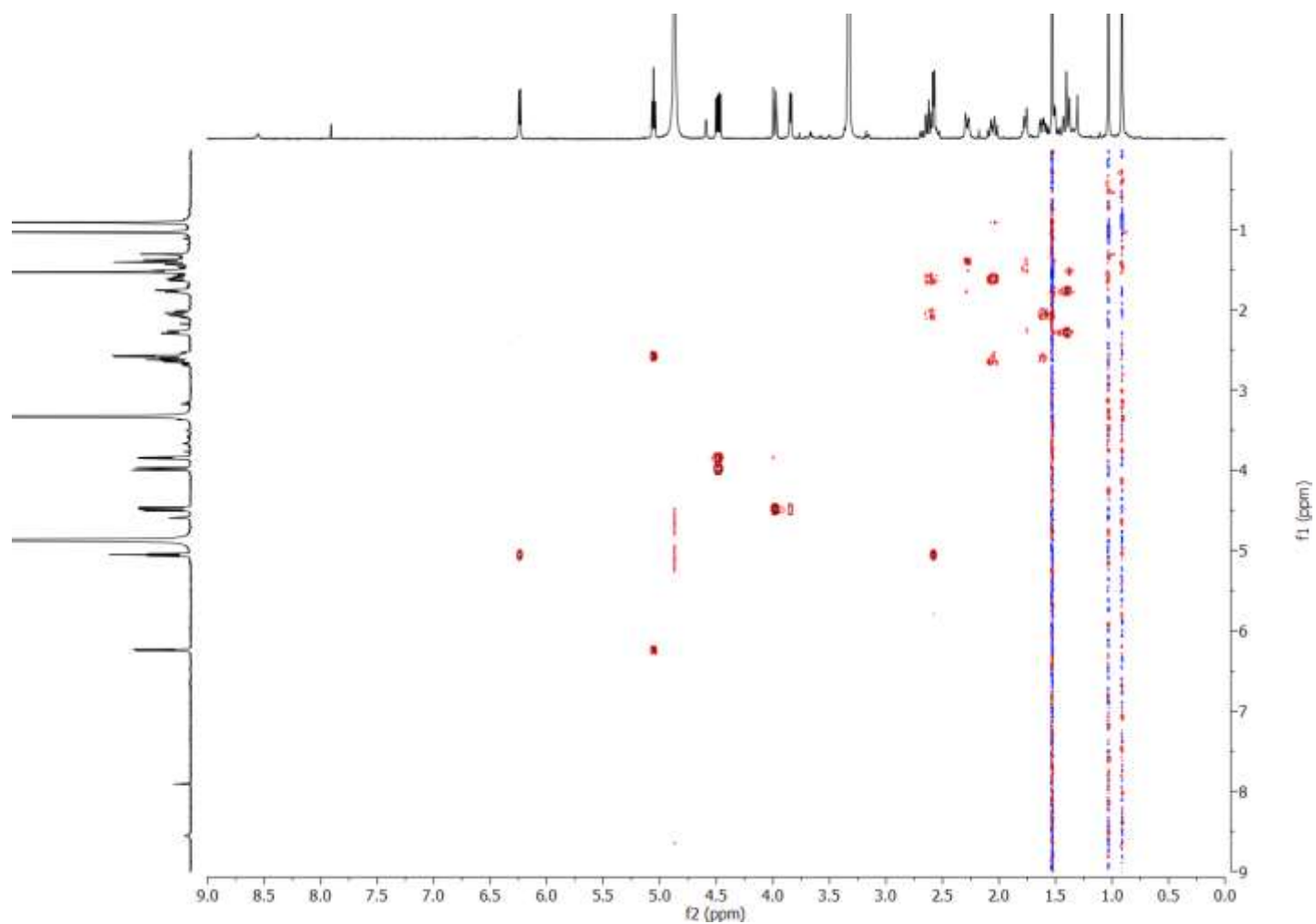


Figure 73. COSY spectrum (400 MHz, CD₃OD) of 14-hydroxy-icacinlactone I

APPENDIX A (continued)

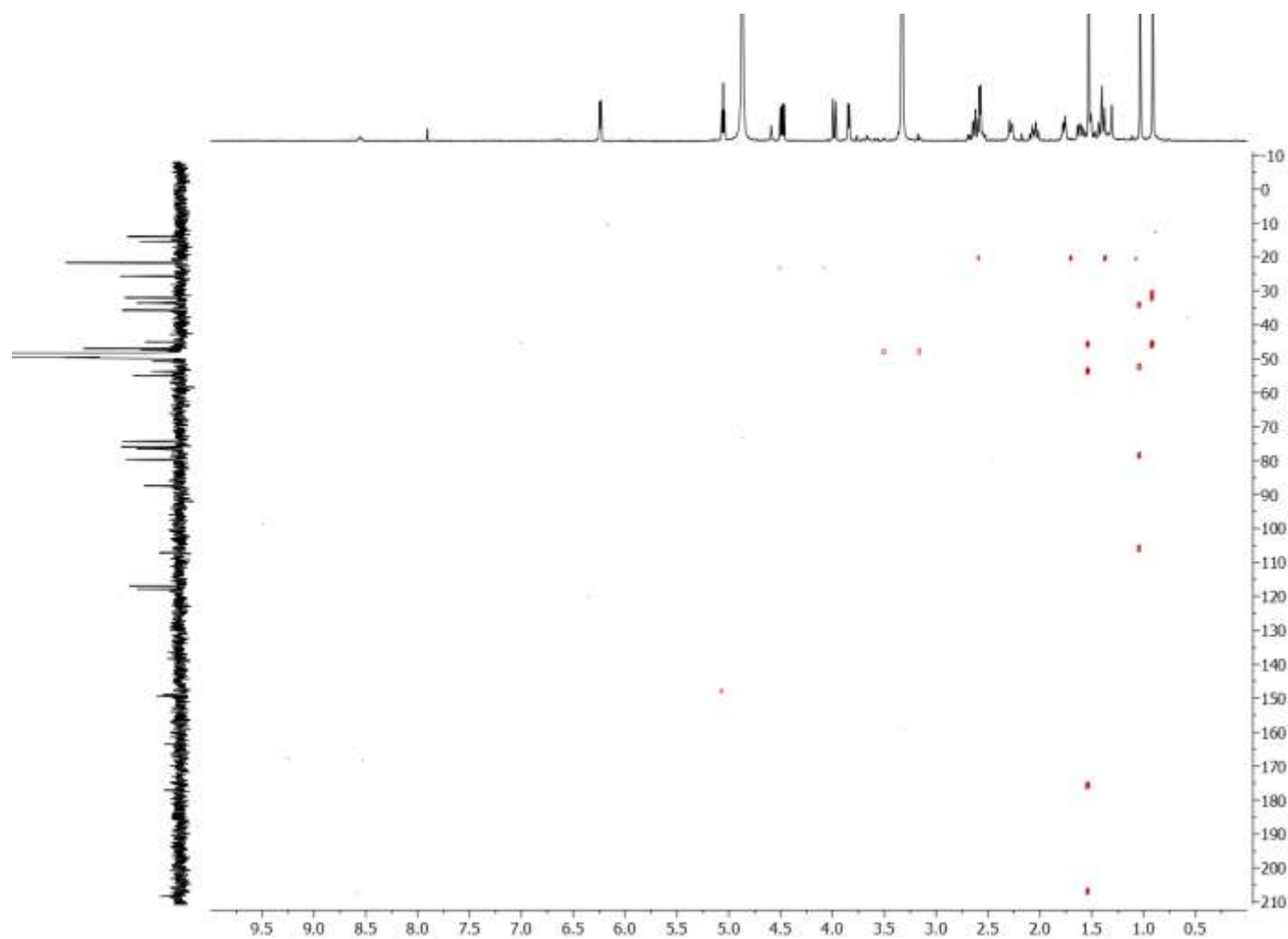


Figure 74. HMBC spectrum (400 MHz, CD_3OD) of 14-hydroxy-icacinlactone I

APPENDIX A (continued)

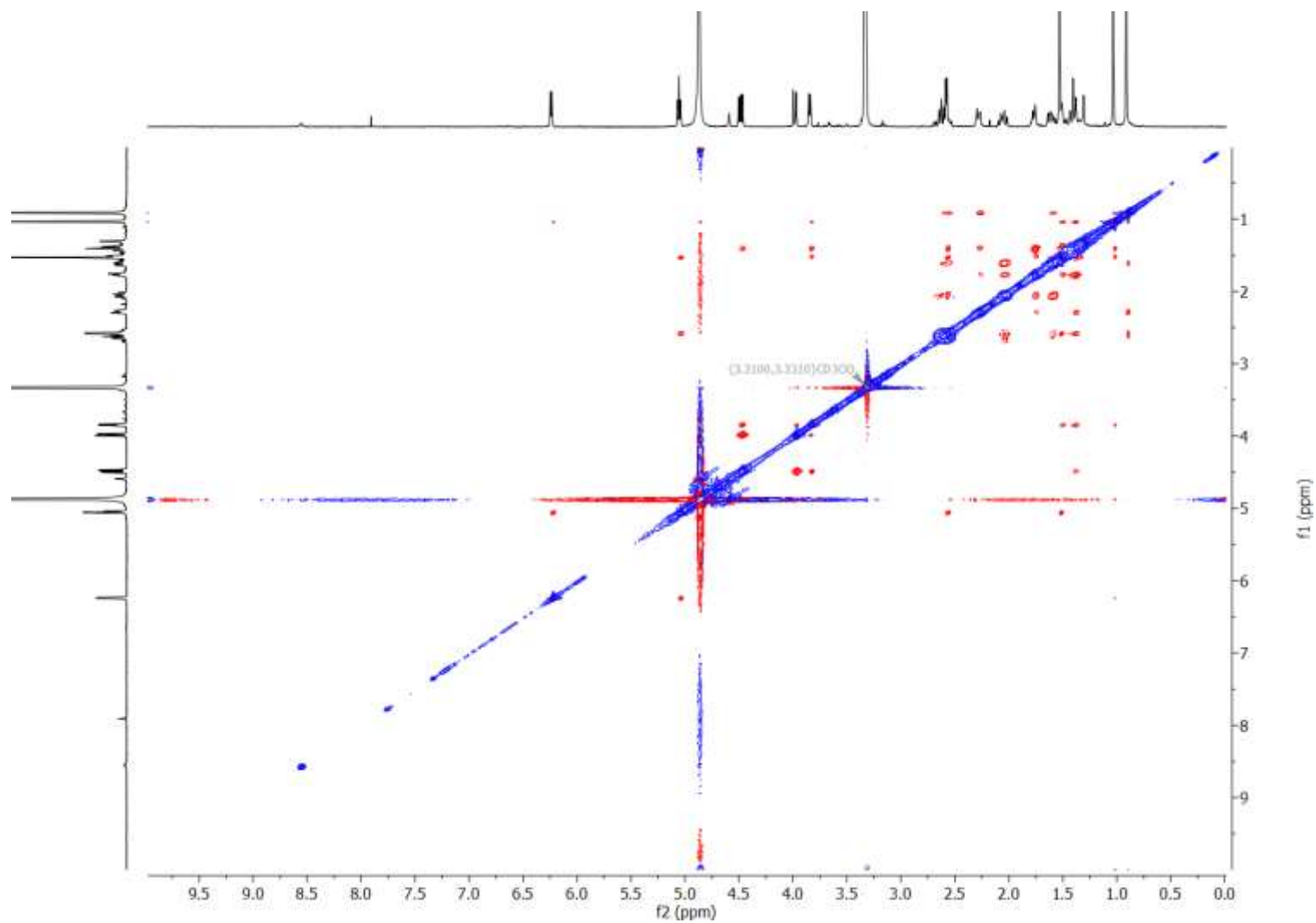


Figure 75. NOESY spectrum (400 MHz, CD₃OD) of 14-hydroxy-icacinlactone I

APPENDIX A (continued)

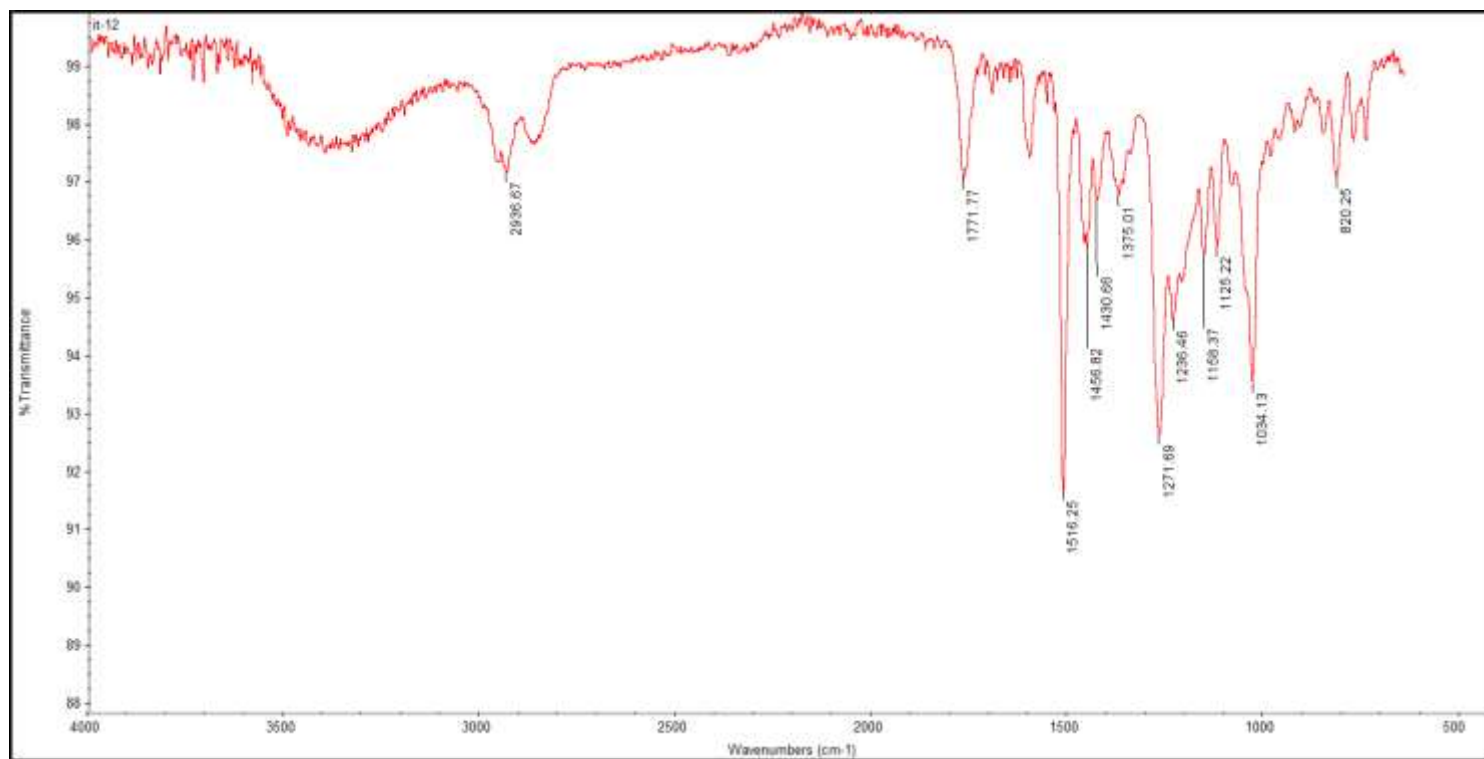
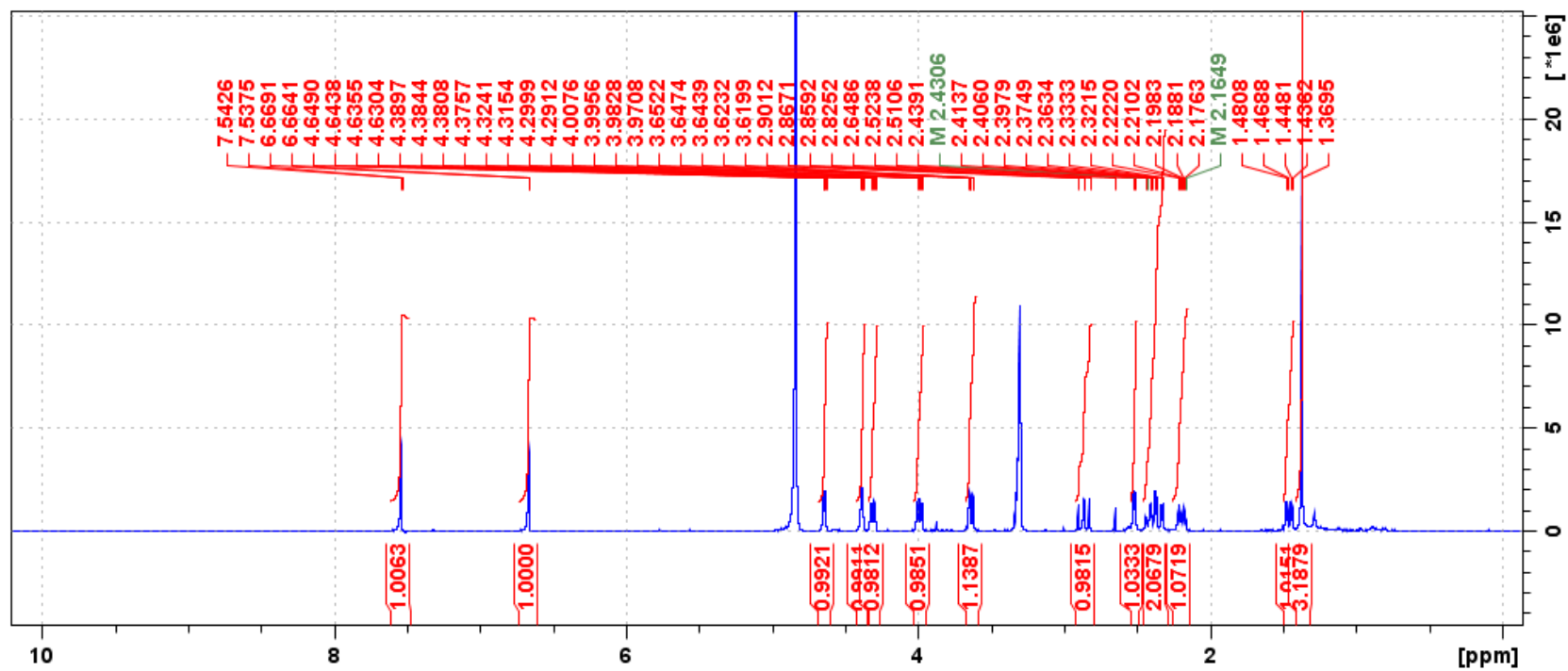


Figure 76. IR spectrum of 14-hydroxy-icacinlactone I

APPENDIX A (continued)

Figure 77. ^1H spectrum (400 MHz, CD_3OD) of 7 α -hydroxyicacenone

APPENDIX A (continued)

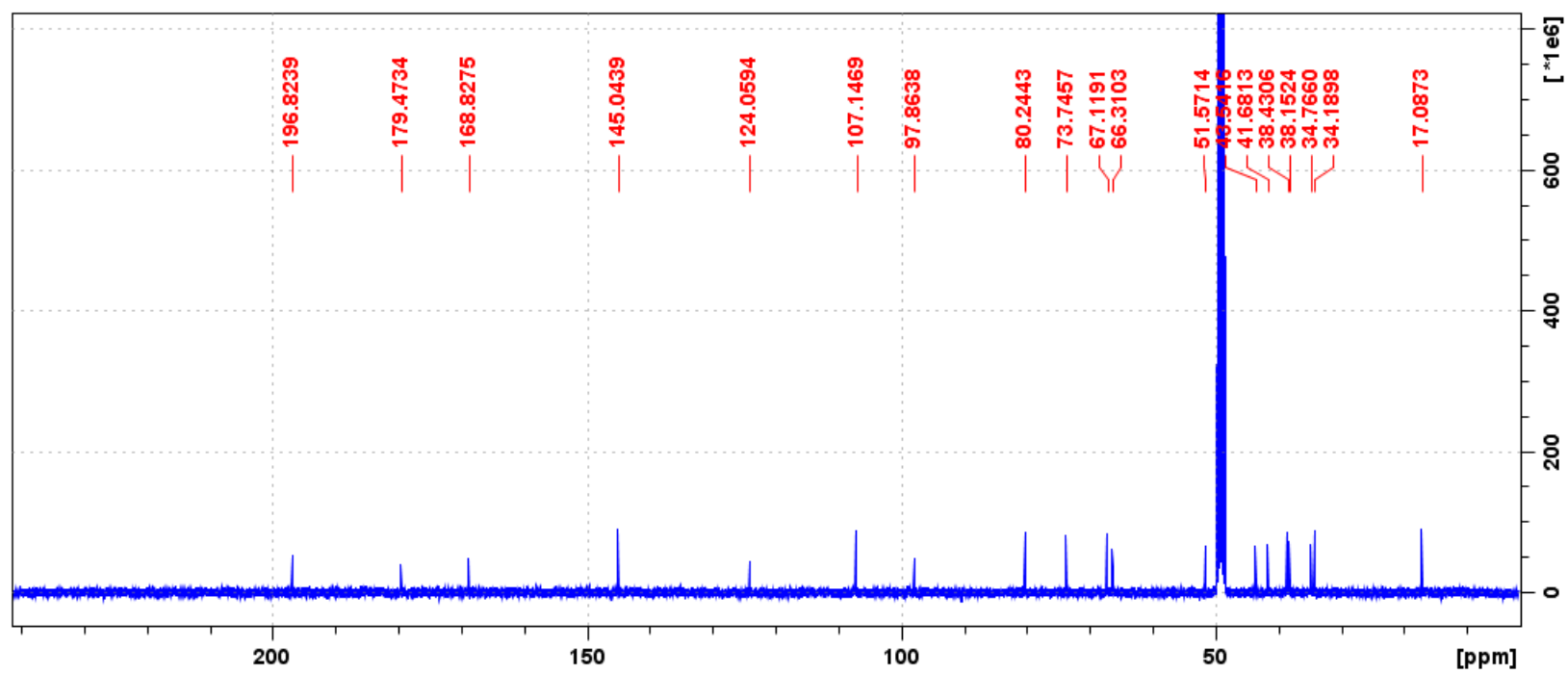


Figure 78. ^{13}C spectrum (100 MHz, CD_3OD) of 7 α -hydroxyicacenone

APPENDIX A (continued)

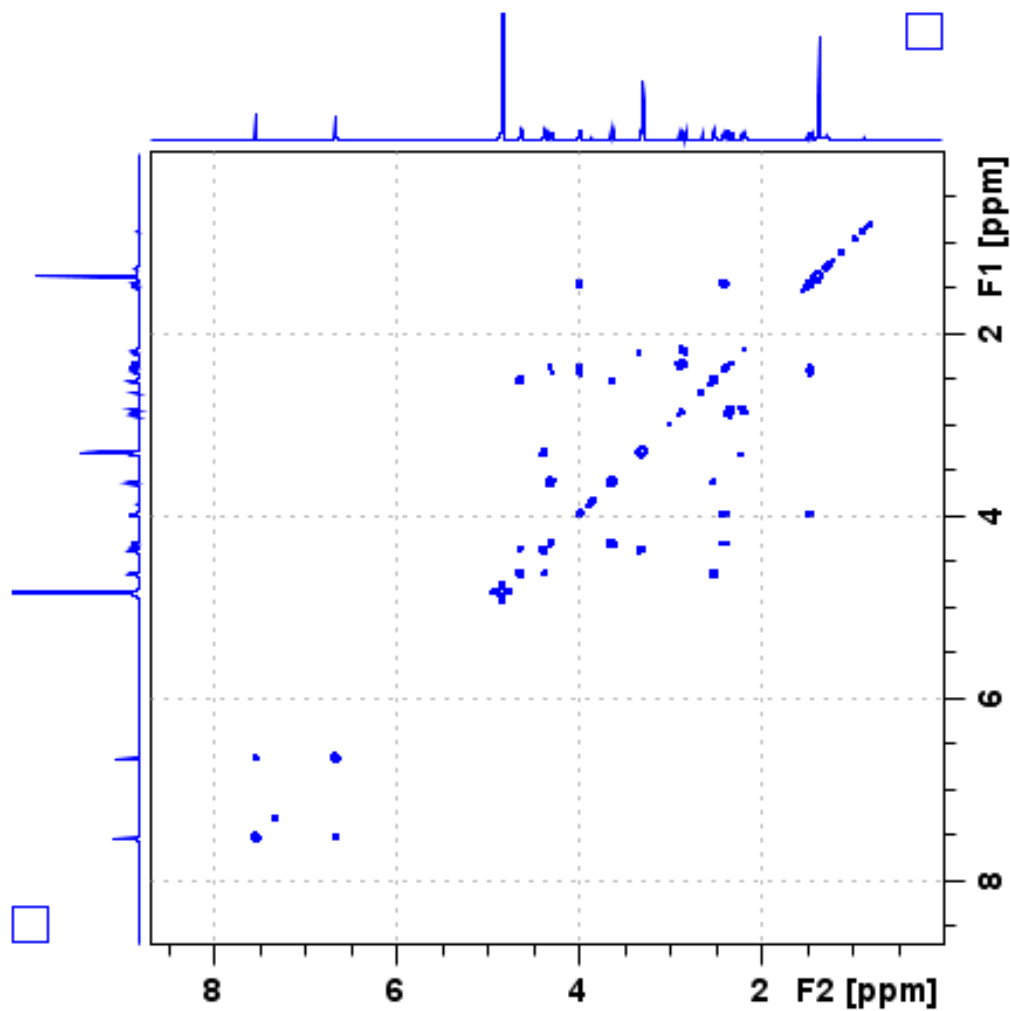


Figure 79. ^1H - ^1H COSY (400 MHz, CD_3OD) of 7 α -hydroxyicacenone

APPENDIX A (continued)

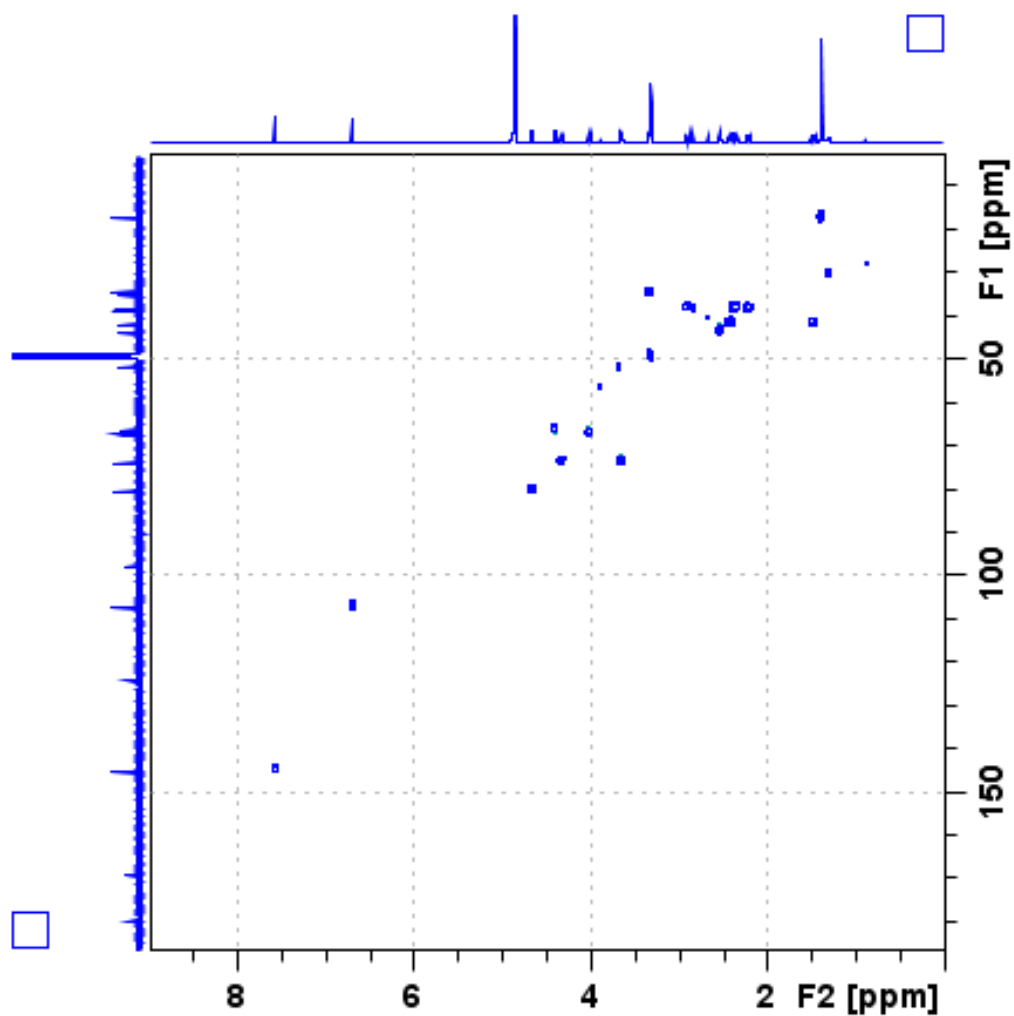


Figure 80. HSQC (400 MHz, CD₃OD) of 7 α -hydroxyicacenone

APPENDIX A (continued)

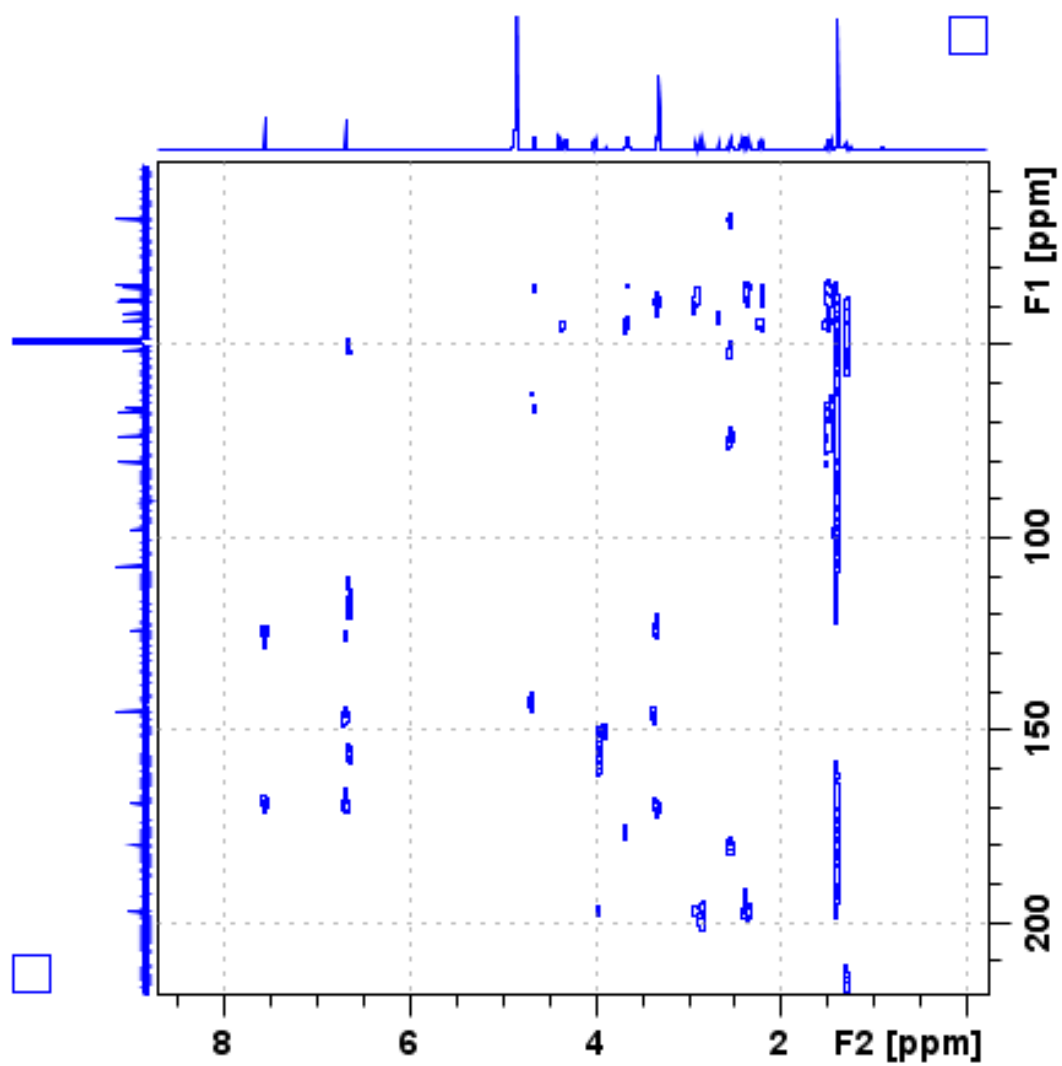


Figure 81. HMBC (400 MHz, CD₃OD) of 7 α -hydroxyicacenone

APPENDIX A (continued)

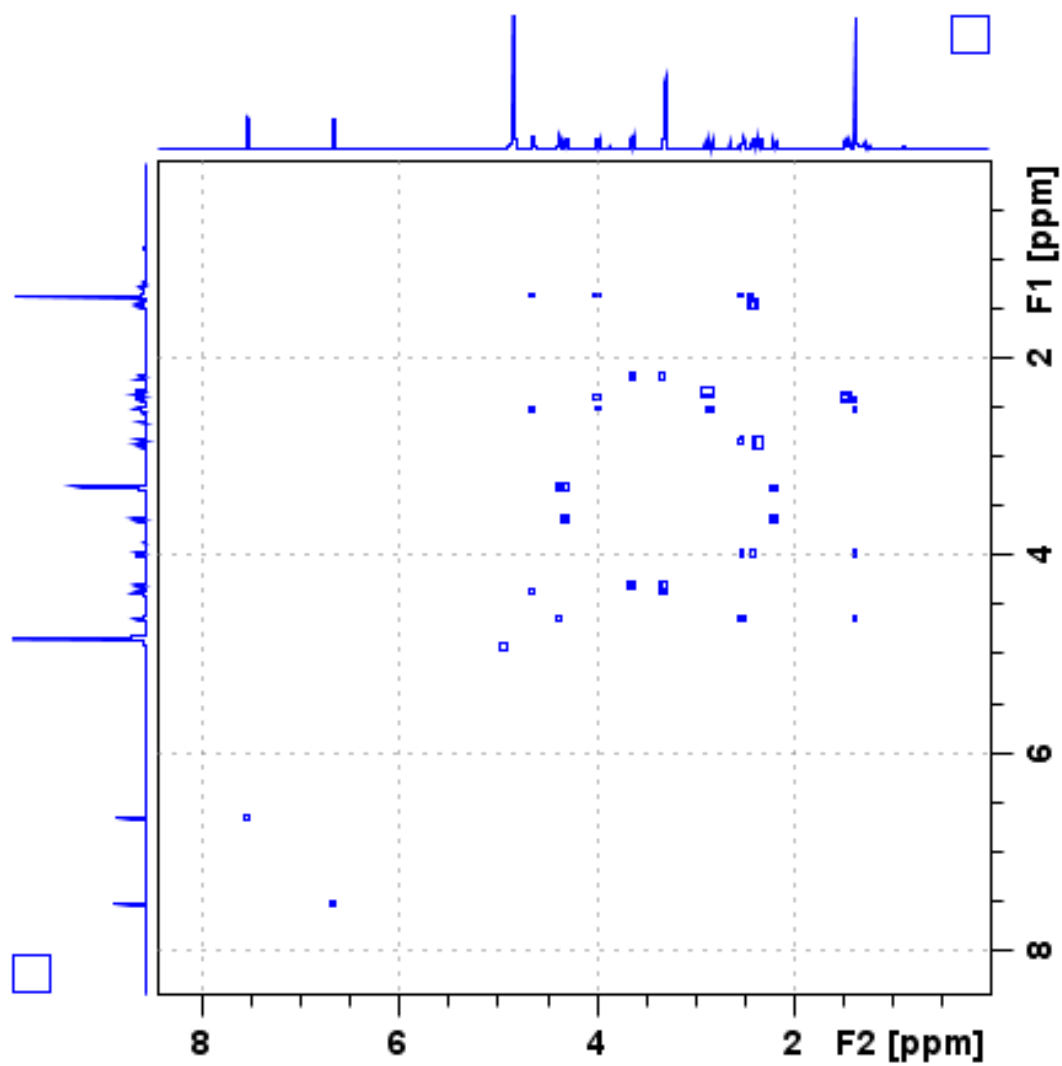
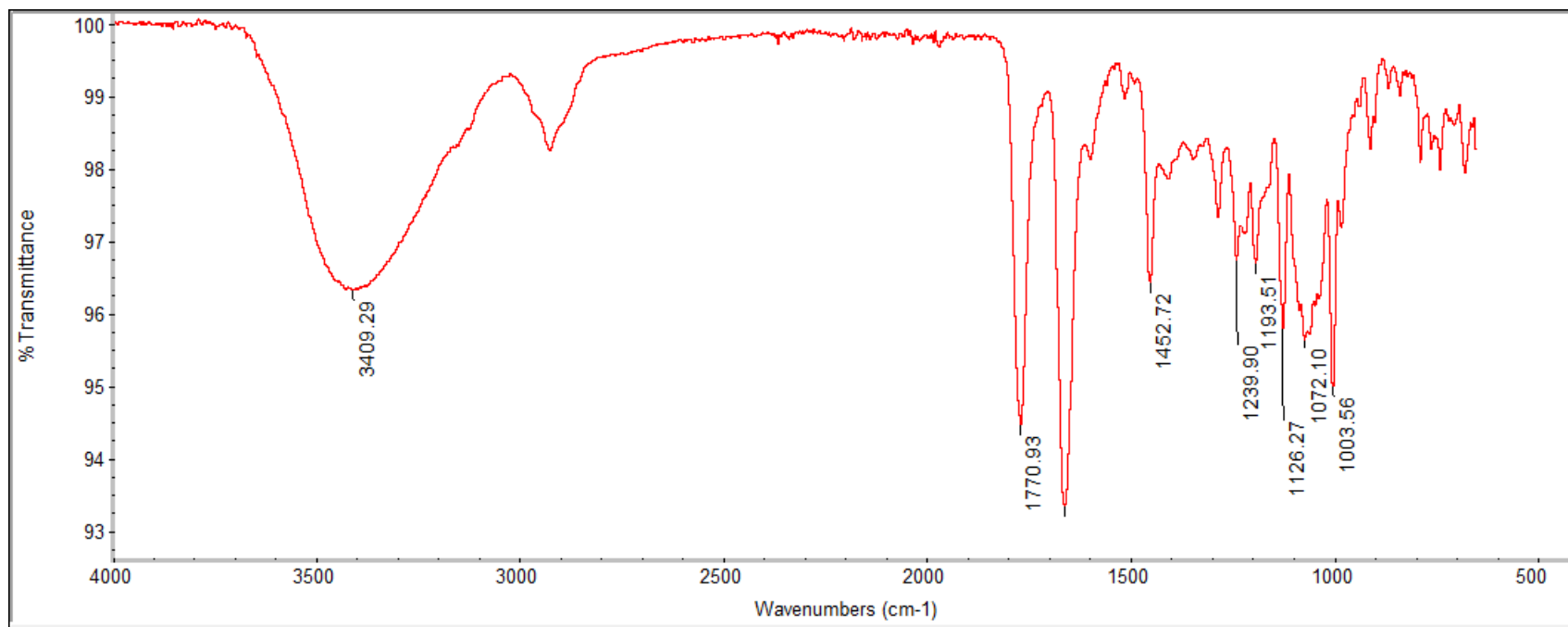
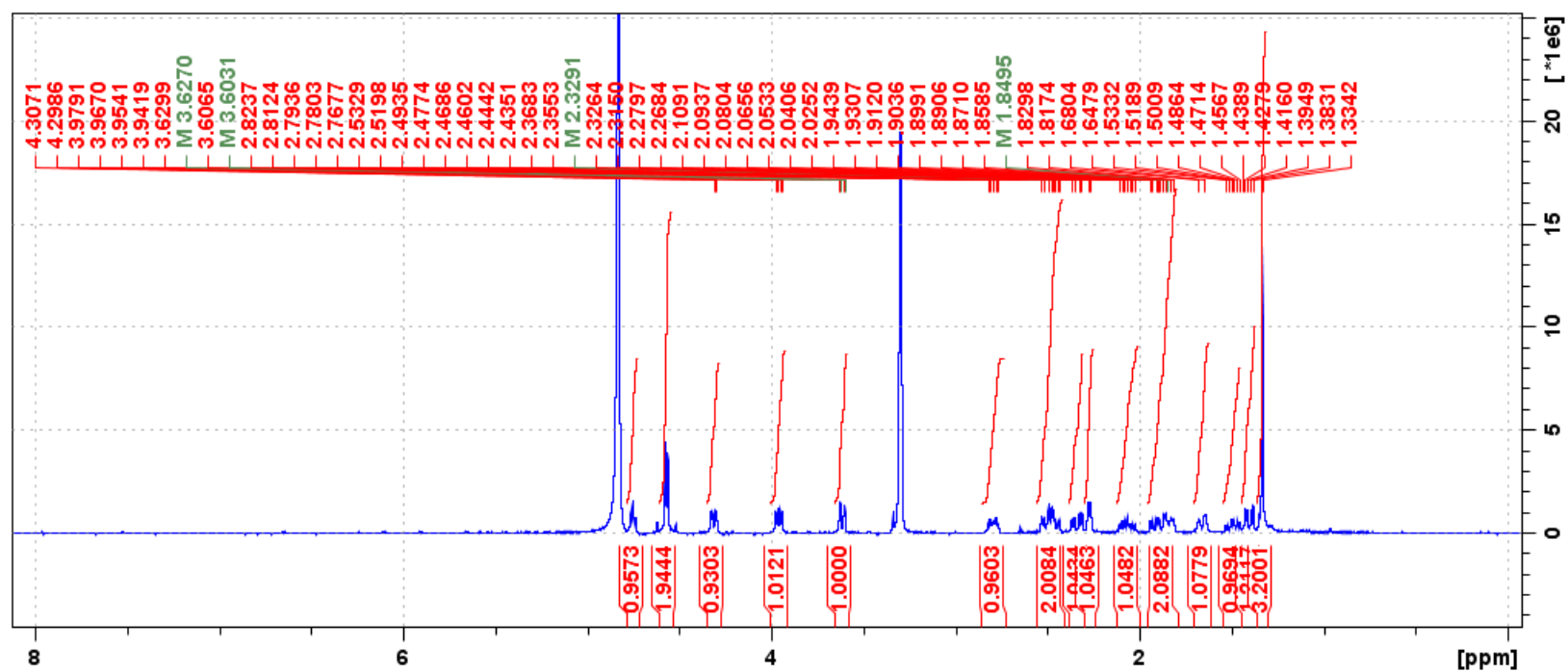


Figure 82. NOESY (400 MHz, CD_3OD) of 7 α -hydroxyicacenone

APPENDIX A (continued)

**Figure 83. IR Spectrum of 7α-hydroxyicacenone**

APPENDIX A (continued)

Figure 84. ¹H spectrum (400 MHz, CD₃OD) of 2β-hydroxyhumirianthenolide C

APPENDIX A (continued)

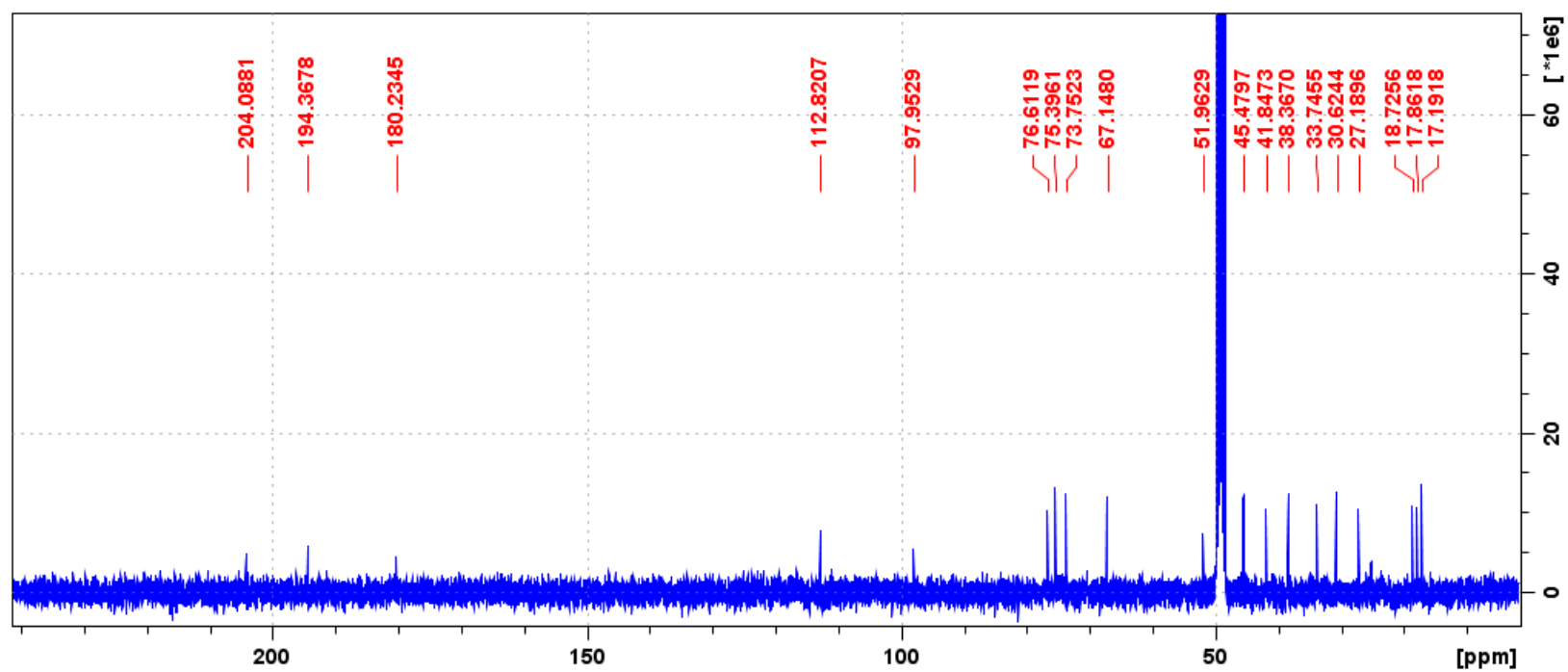


Figure 85. ¹³C spectrum (100 MHz, CD₃OD) of 2β-hydroxyhumirianthenolide C

APPENDIX A (continued)

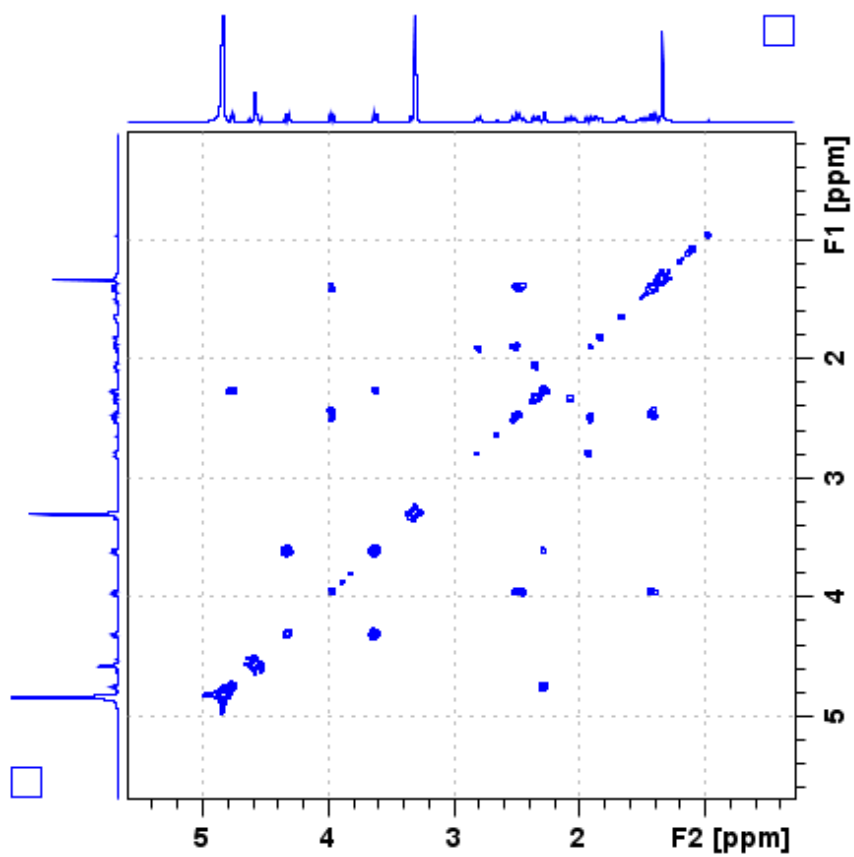


Figure 86. ^1H - ^1H COSY spectrum (400 MHz, CD_3OD) of 2 β -hydroxyhumirianthenolide C

APPENDIX A (continued)

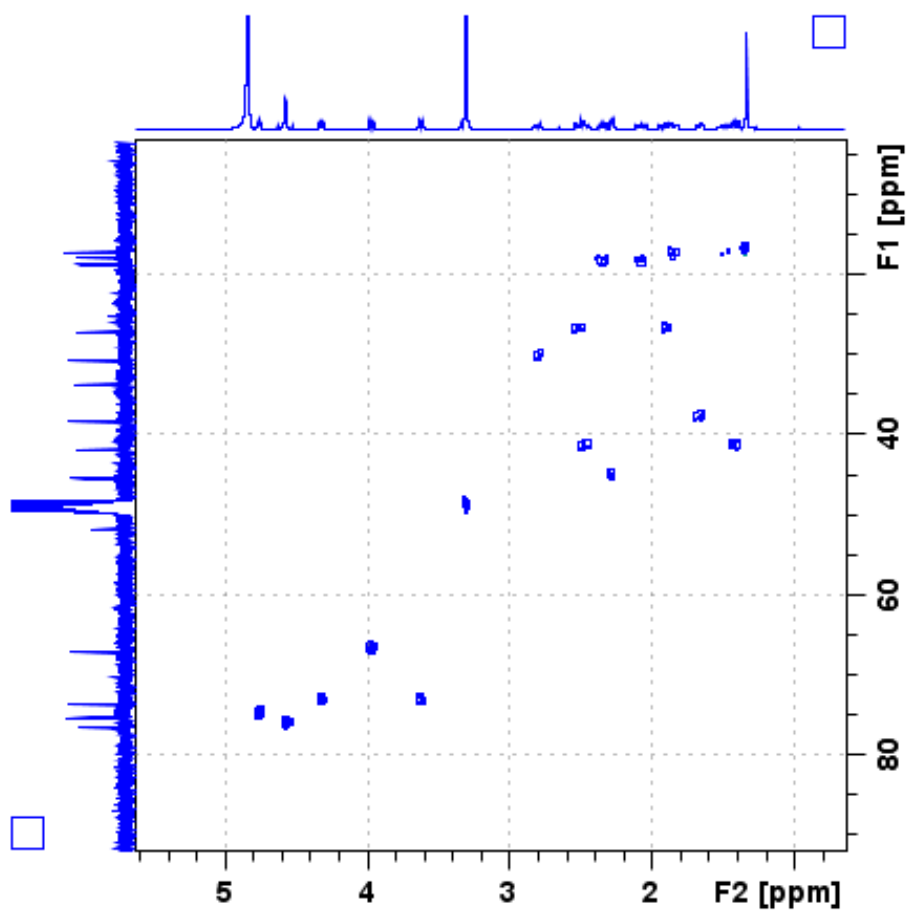


Figure 87. HSQC spectrum (400 MHz, CD₃OD) of 2β-hydroxyhumirianthenolide C

APPENDIX A (continued)

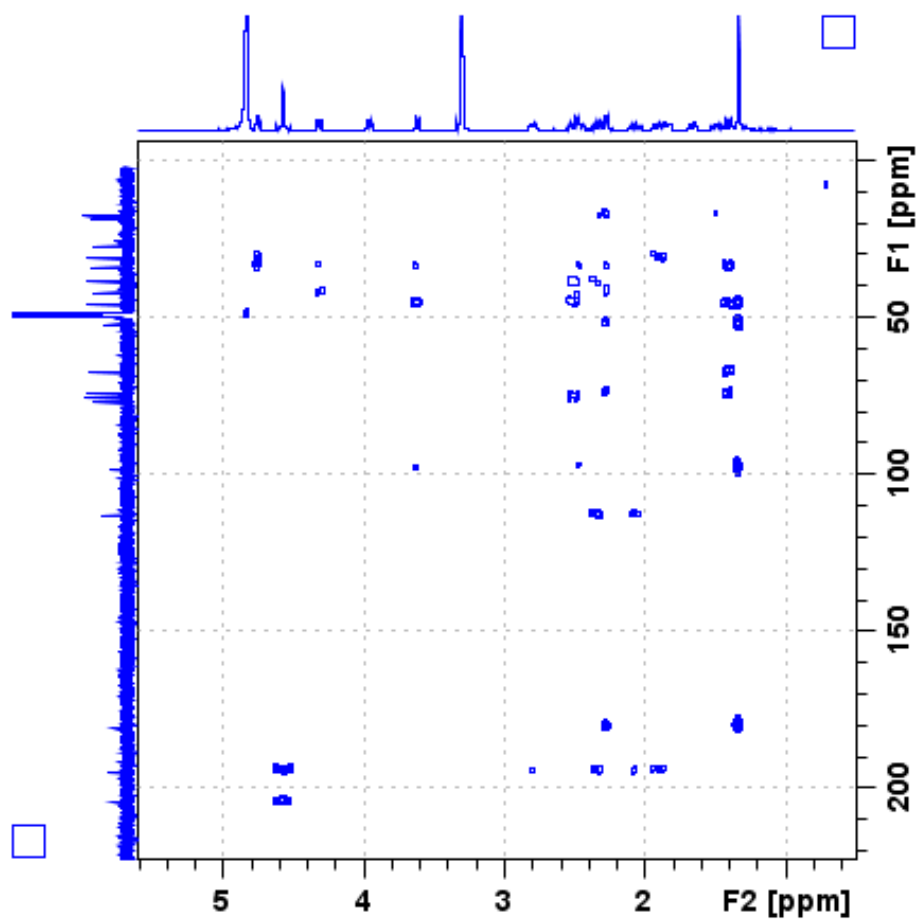


Figure 88. HMBC spectrum (400 MHz, CD_3OD) of 2 β -hydroxyhumirianthenolide C

APPENDIX A (continued)

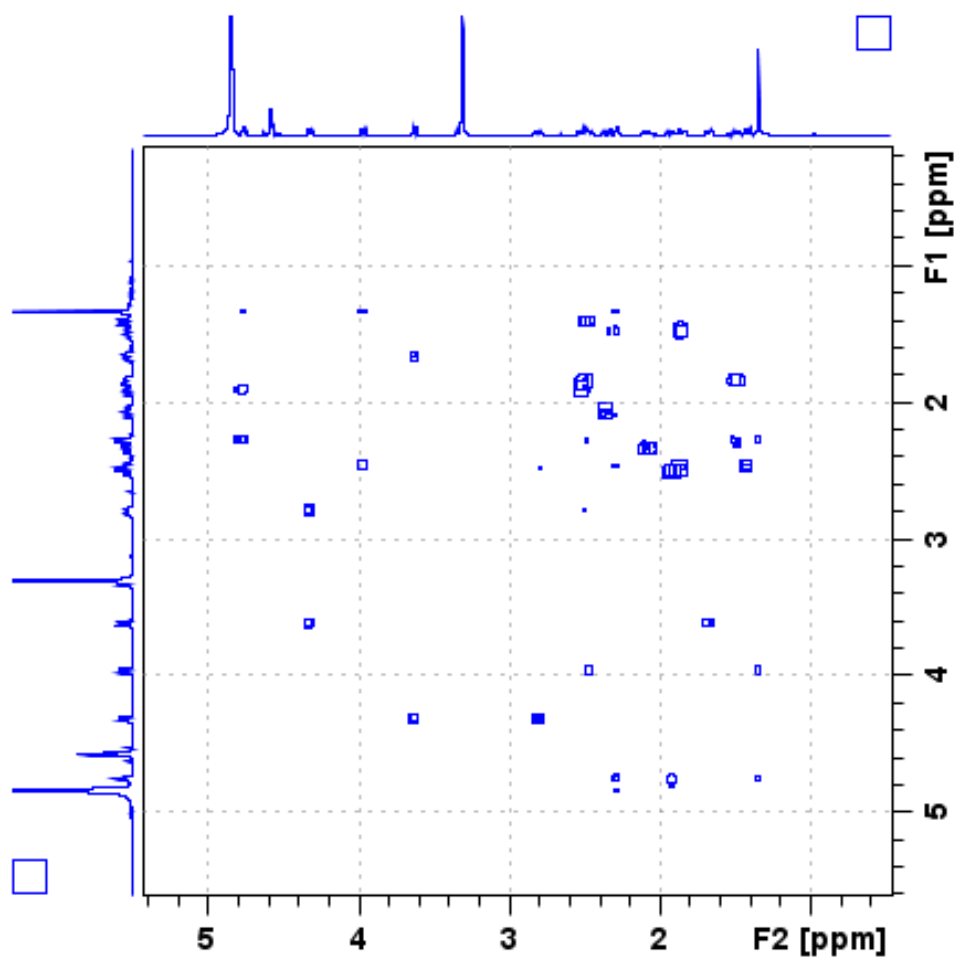


Figure 89. NOESY spectrum (400 MHz, CD₃OD) of 2β-hydroxyhumirianthenolide C

APPENDIX A (continued)

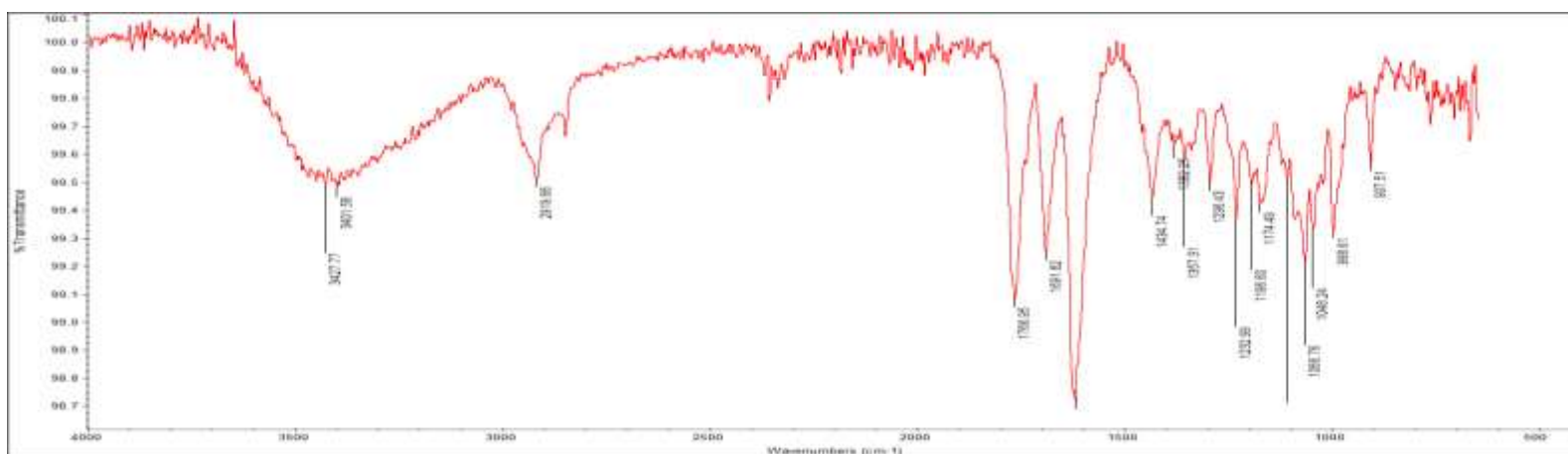


Figure 90. IR spectrum of 2β-hydroxyhumirianthenolide C

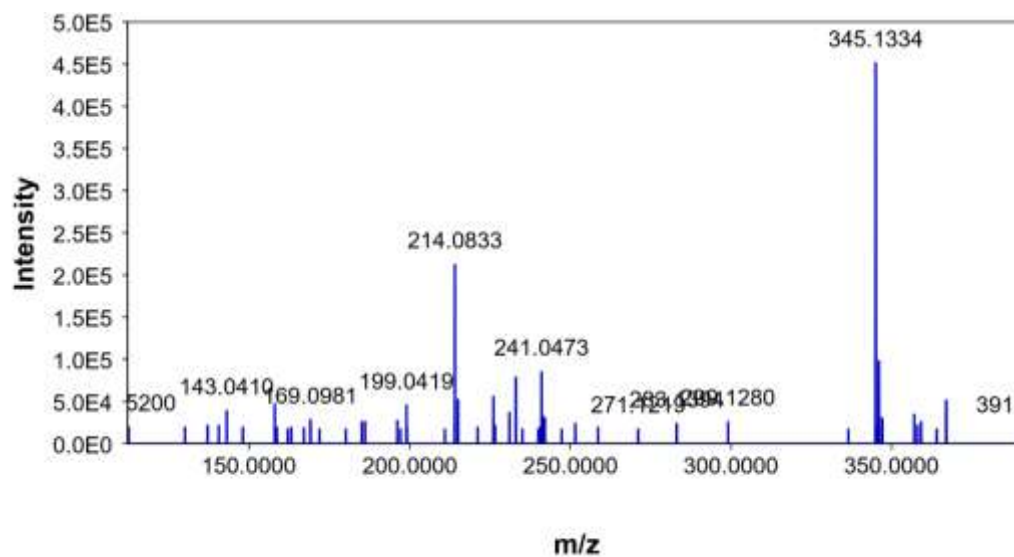


Figure 91. HRESIMS (positive mode) for icacinlactone E

APPENDIX A (continued)

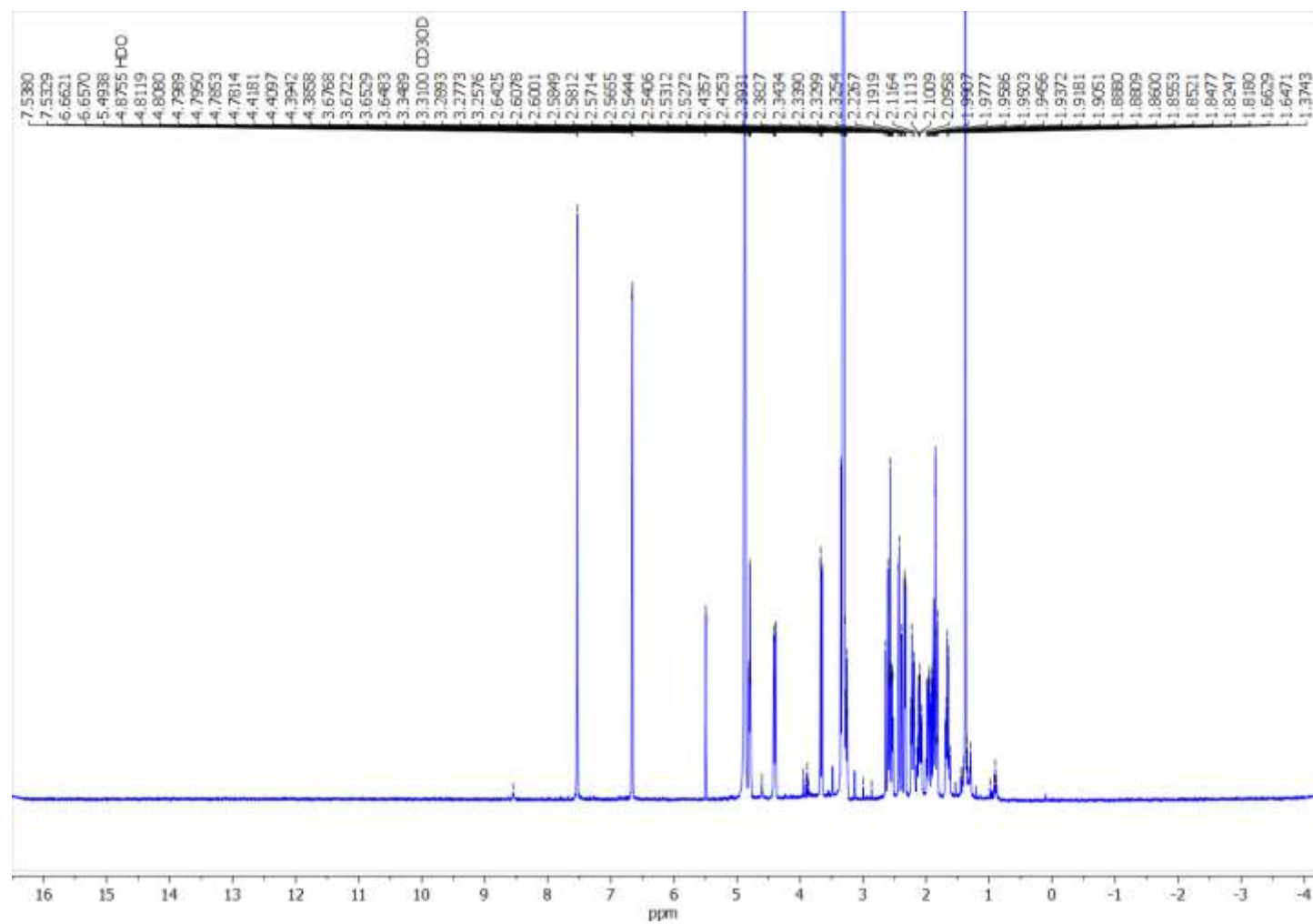


Figure 92. ¹H spectrum (400 MHz, CD₃OD) of icacinlactone E

APPENDIX A (continued)

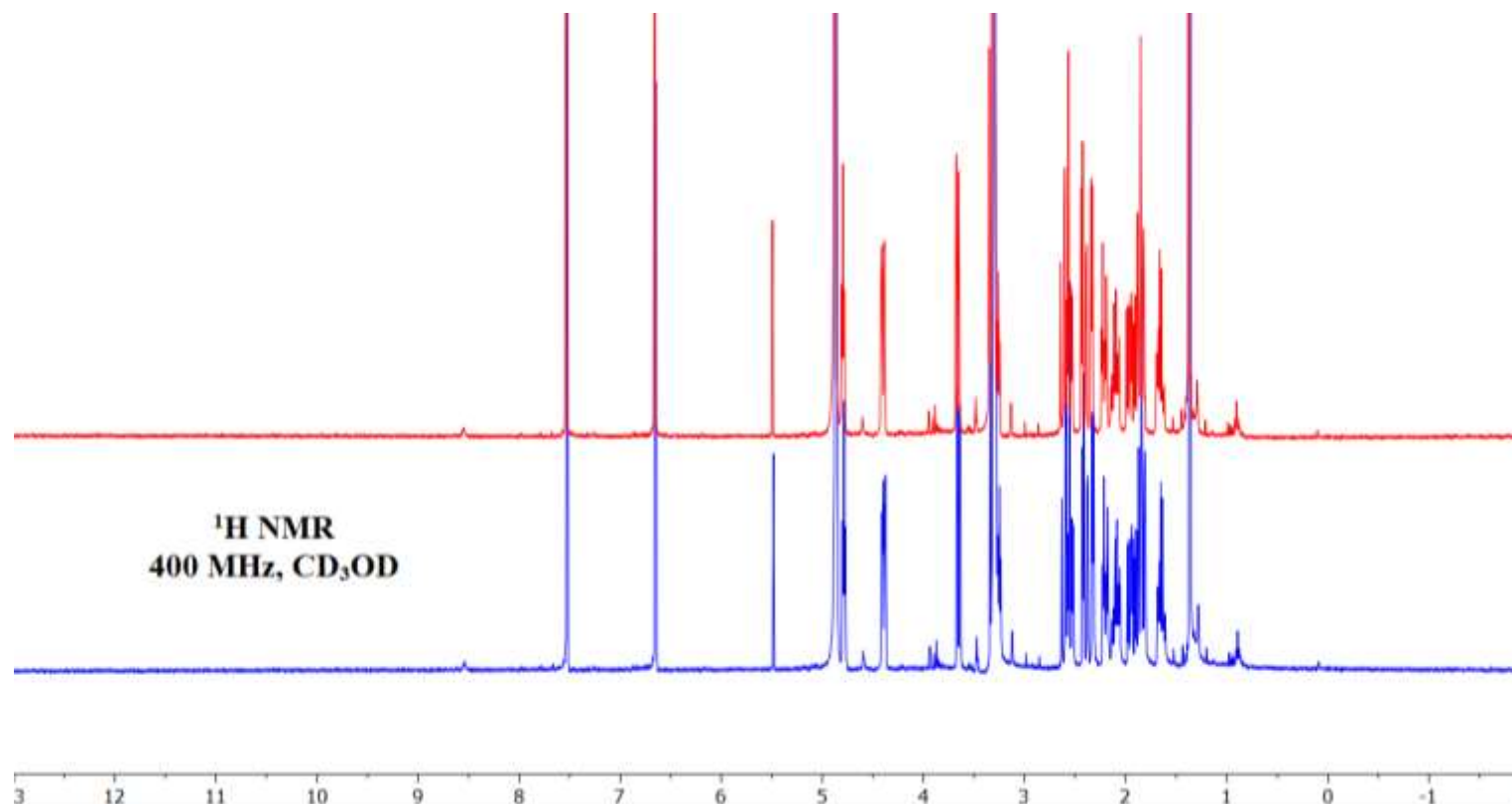


Figure 93. ^1H NMR (400 MHz, CD_3OD) spectra of compound 8 (red) and icacinlactone E standard (blue)

APPENDIX A (continued)

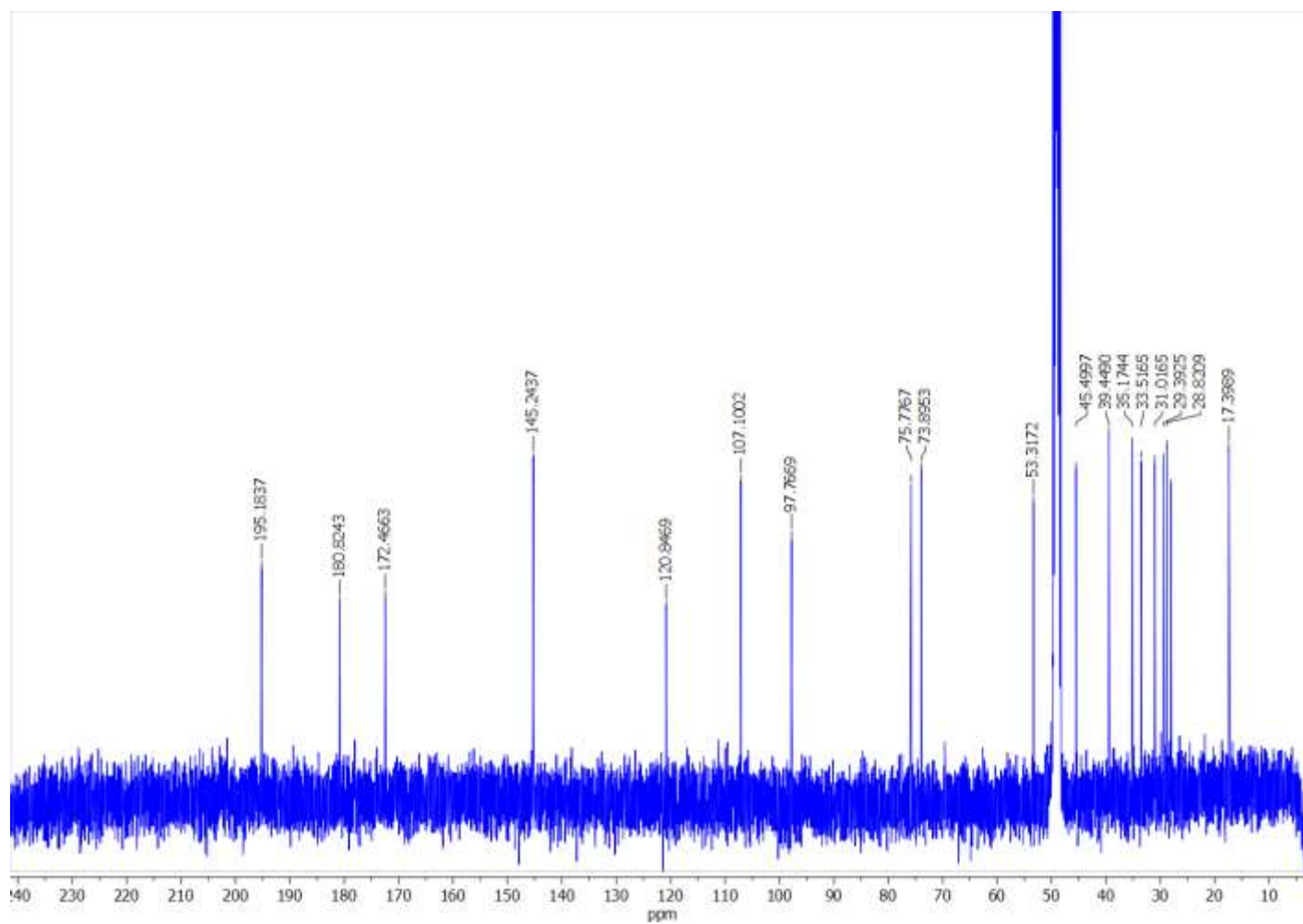


Figure 94. ¹³C spectrum (100 MHz, CD₃OD) of icacinlactone E

APPENDIX A (continued)

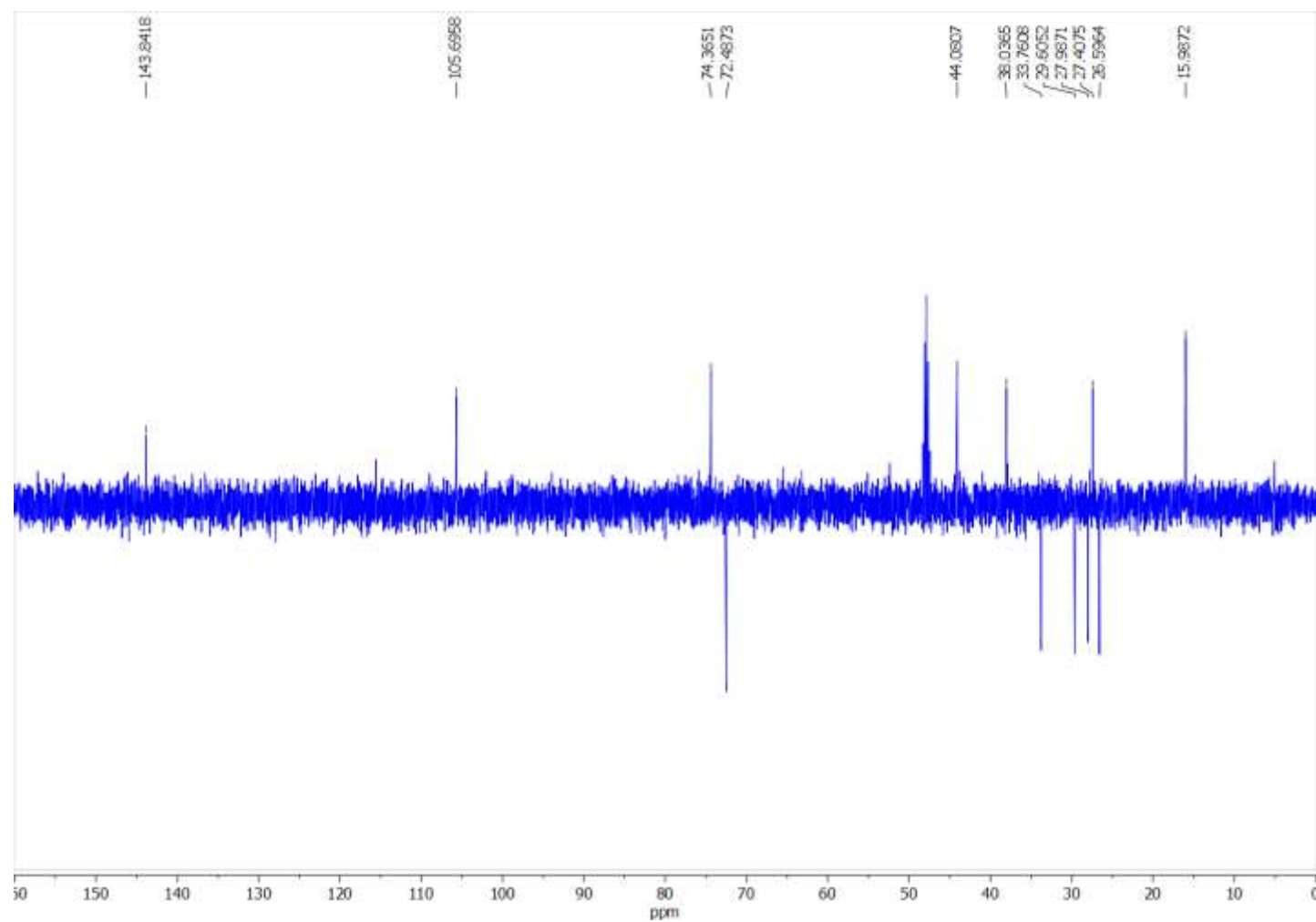


Figure 95. DEPT-135 spectrum (100 MHz, CD₃OD) of icacinlactone E

APPENDIX A (continued)

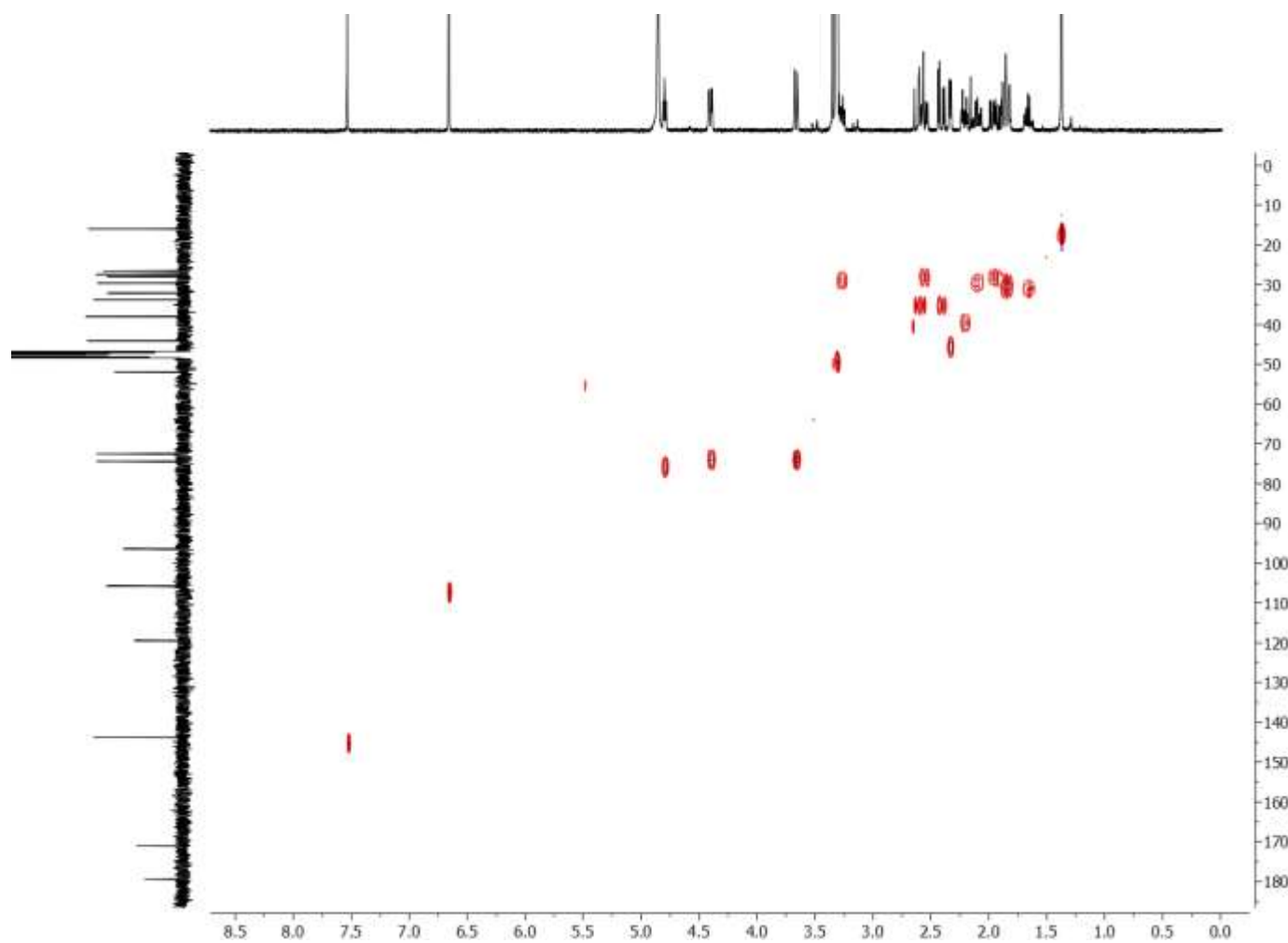


Figure 96. HSQC spectrum (400 MHz, CD_3OD) of icacinlactone E

APPENDIX A (continued)

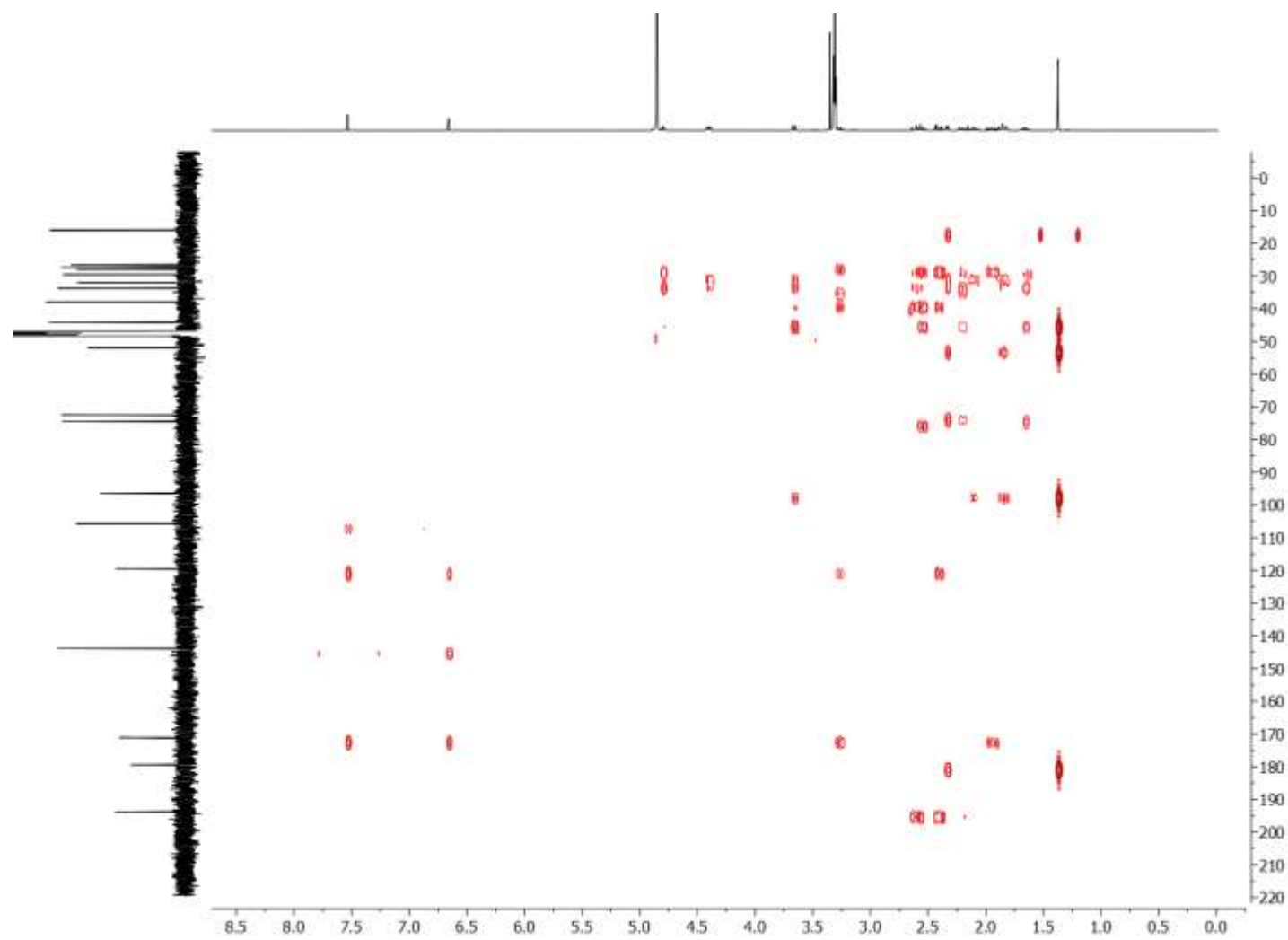


Figure 97. HMBC spectrum (400 MHz, CD_3OD) of icacinlactone E

APPENDIX A (continued)

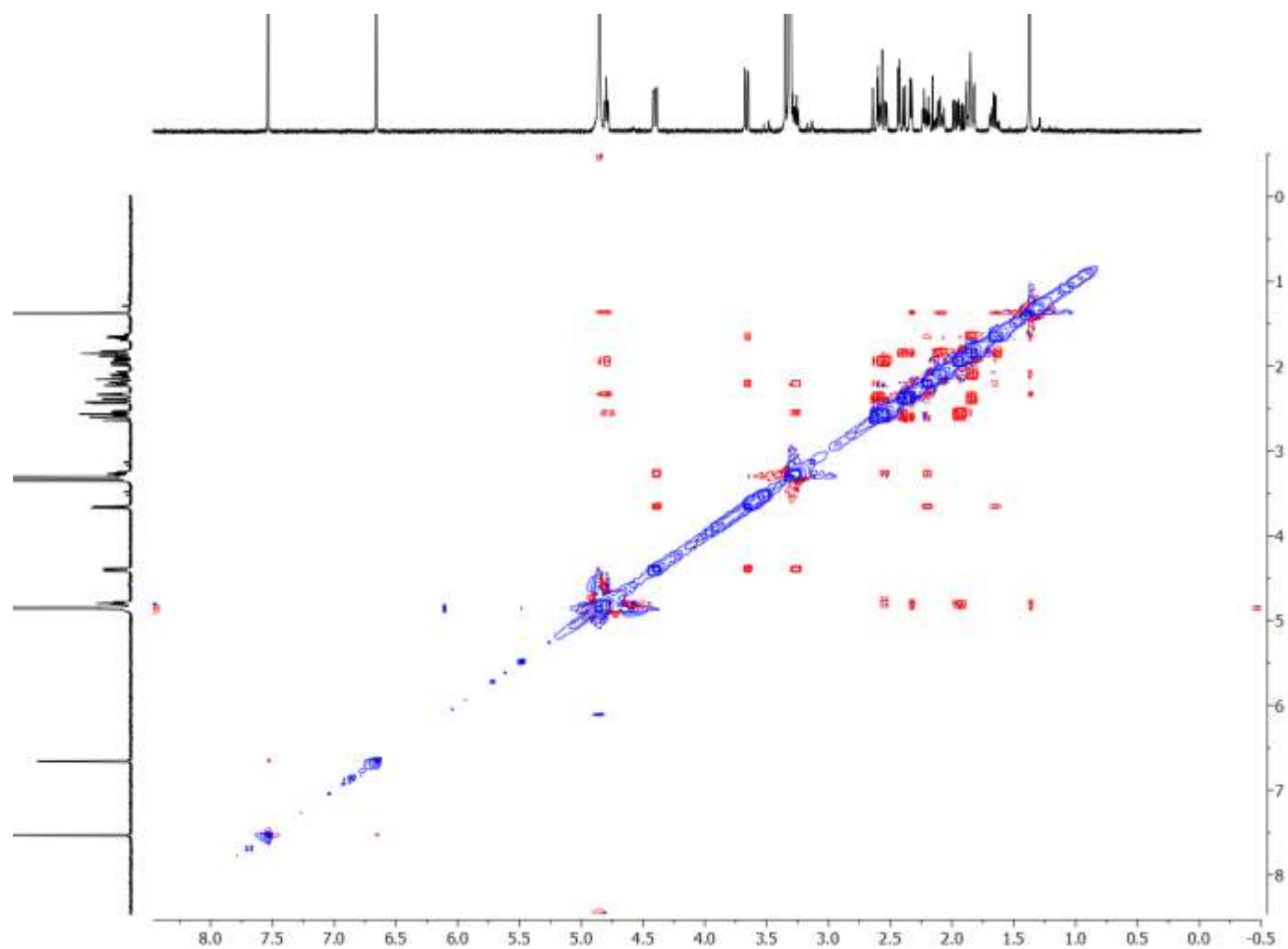


Figure 98. NOESY spectrum (400 MHz, CD₃OD) of icacinlactone E

APPENDIX A (continued)

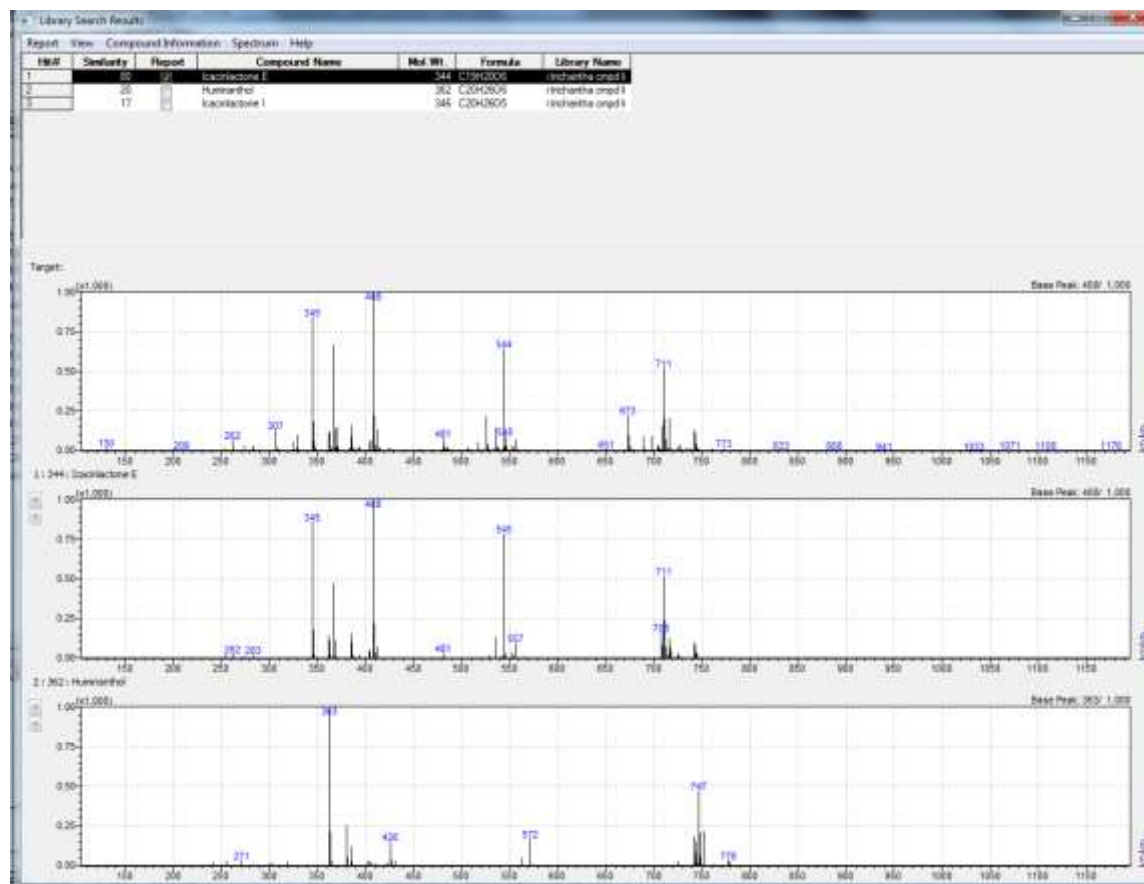
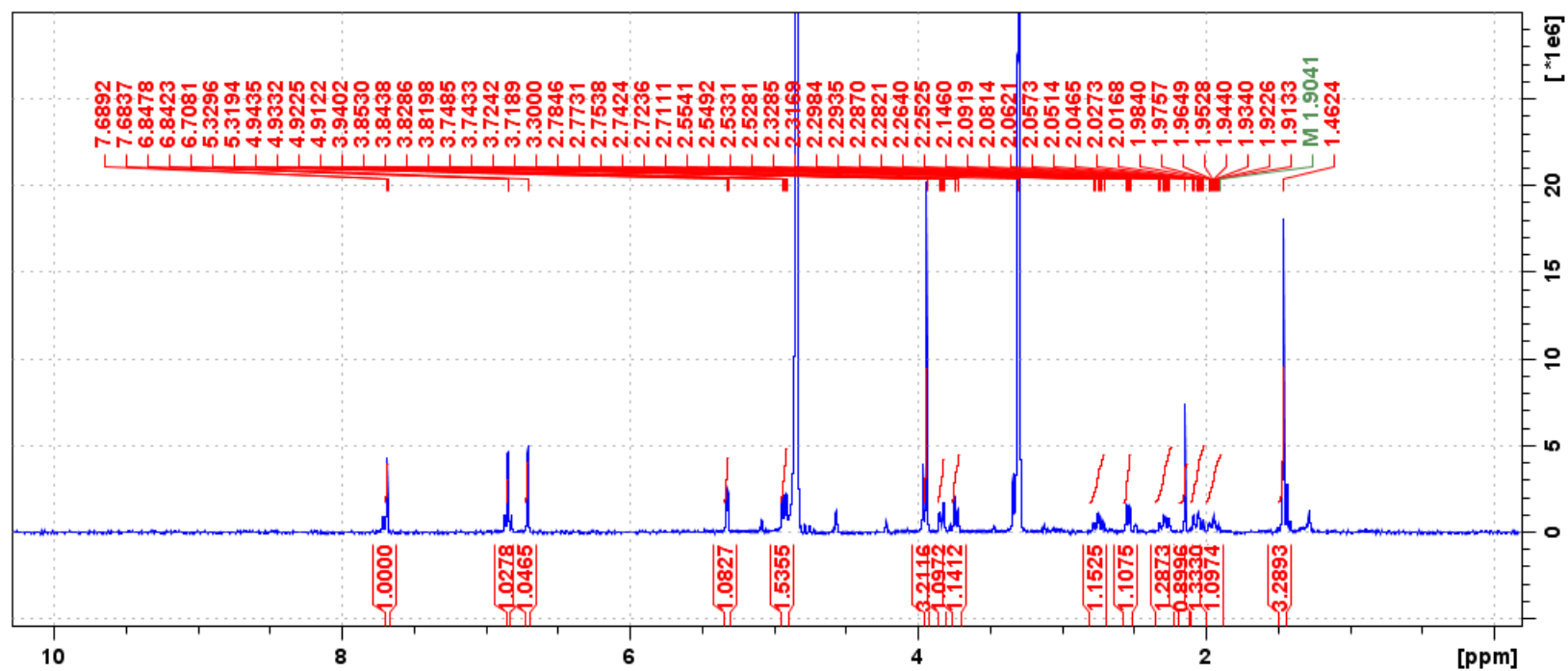


Figure 99. LC-MS library similarity search for icacinlactone E

APPENDIX A (continued)

Figure 100. ^1H spectrum (400 MHz, CD_3OD) of 7 α -hydroxyicacinlactone B

APPENDIX A (continued)

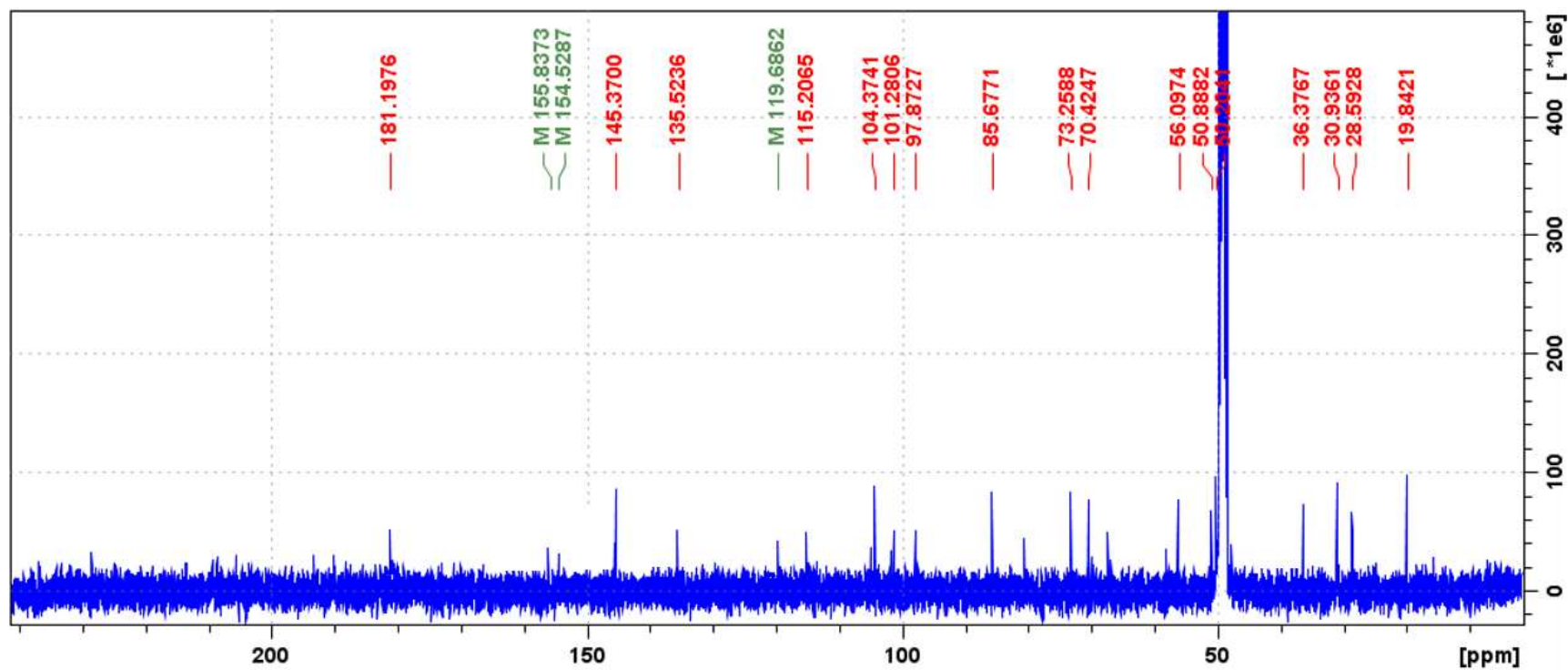


Figure 101. ¹³C spectrum (100 MHz, CD₃OD) of 7 α -hydroxyicacinlactone B

APPENDIX A (continued)

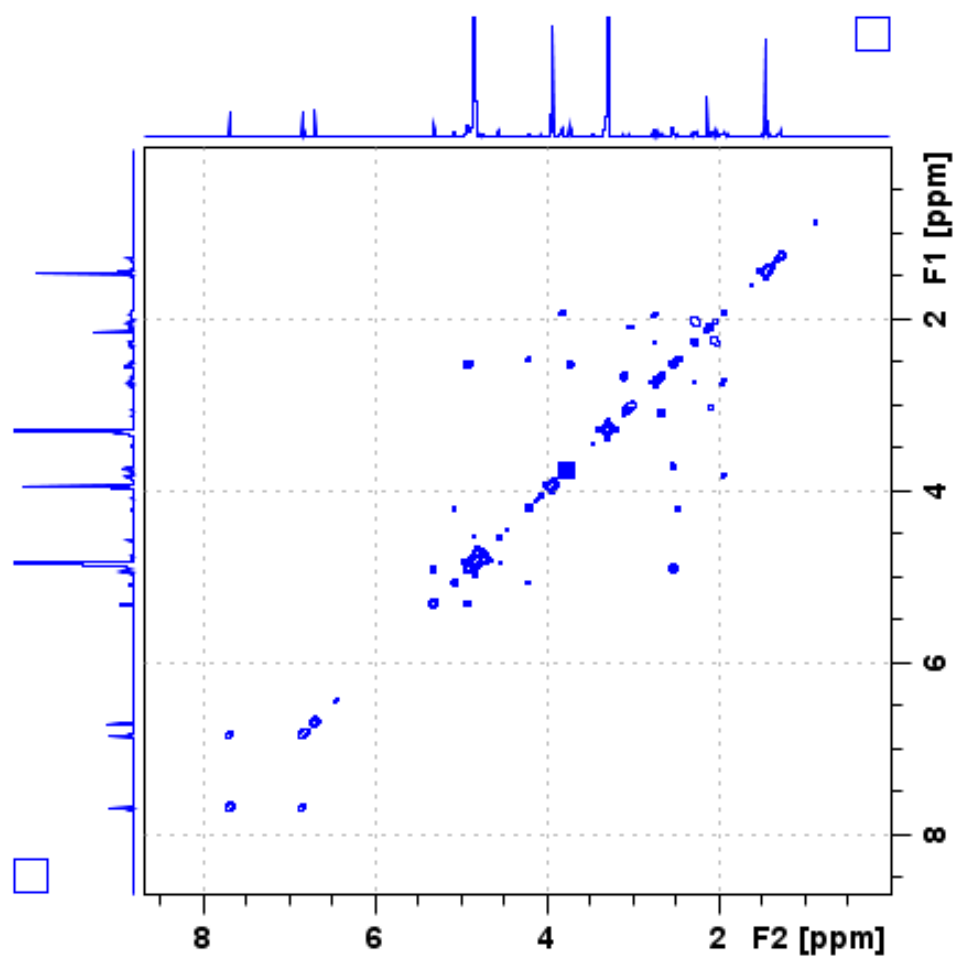


Figure 102. ^1H - ^1H COSY spectrum (400 MHz, CD_3OD) of 7α -hydroxyicacinlactone B

APPENDIX A (continued)

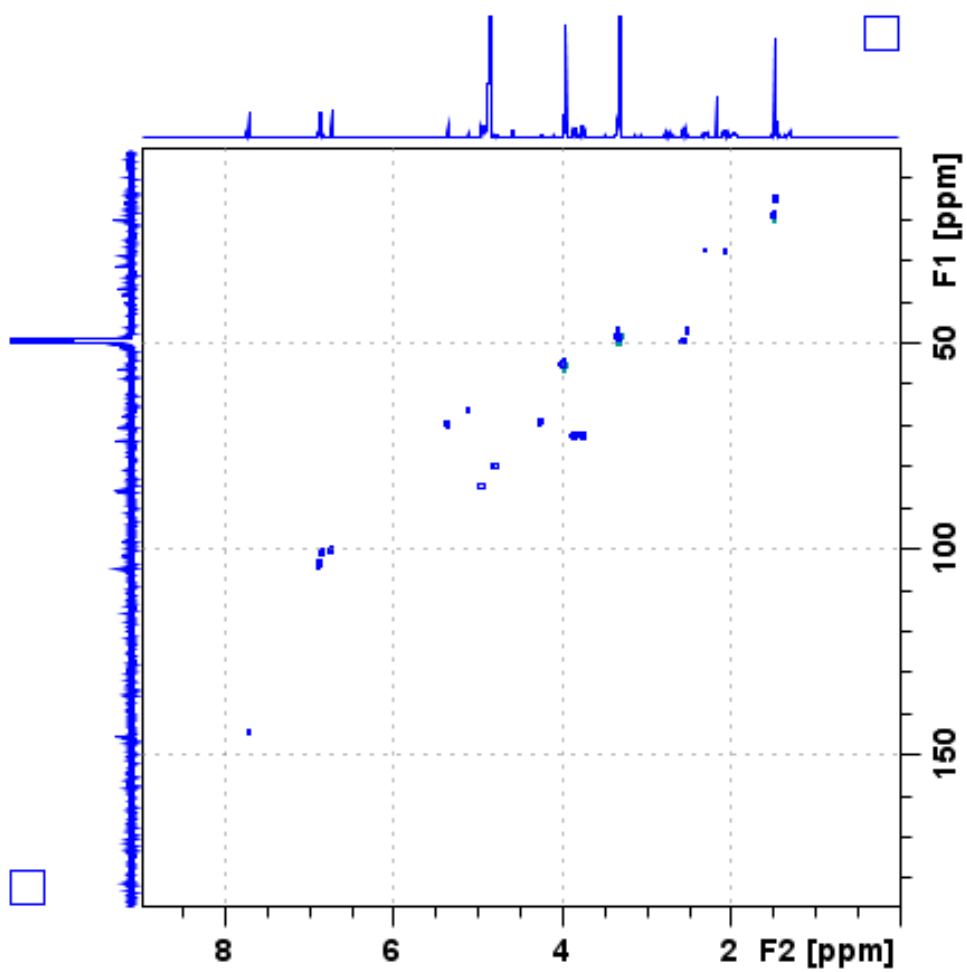


Figure 103. HSQC spectrum (400 MHz, CD₃OD) of 7 α -hydroxyicacinlactone B

APPENDIX A (continued)

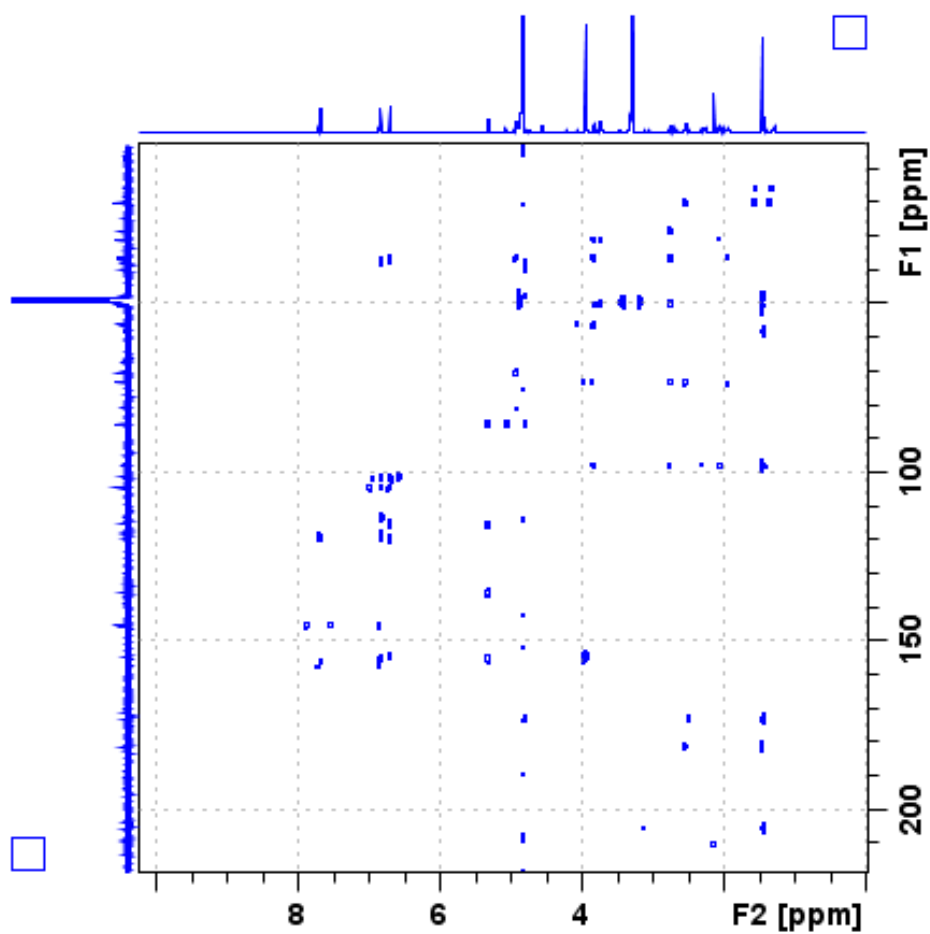


Figure 104. HMBC spectrum (400 MHz, CD₃OD) of 7 α -hydroxyicacinlactone B

APPENDIX A (continued)

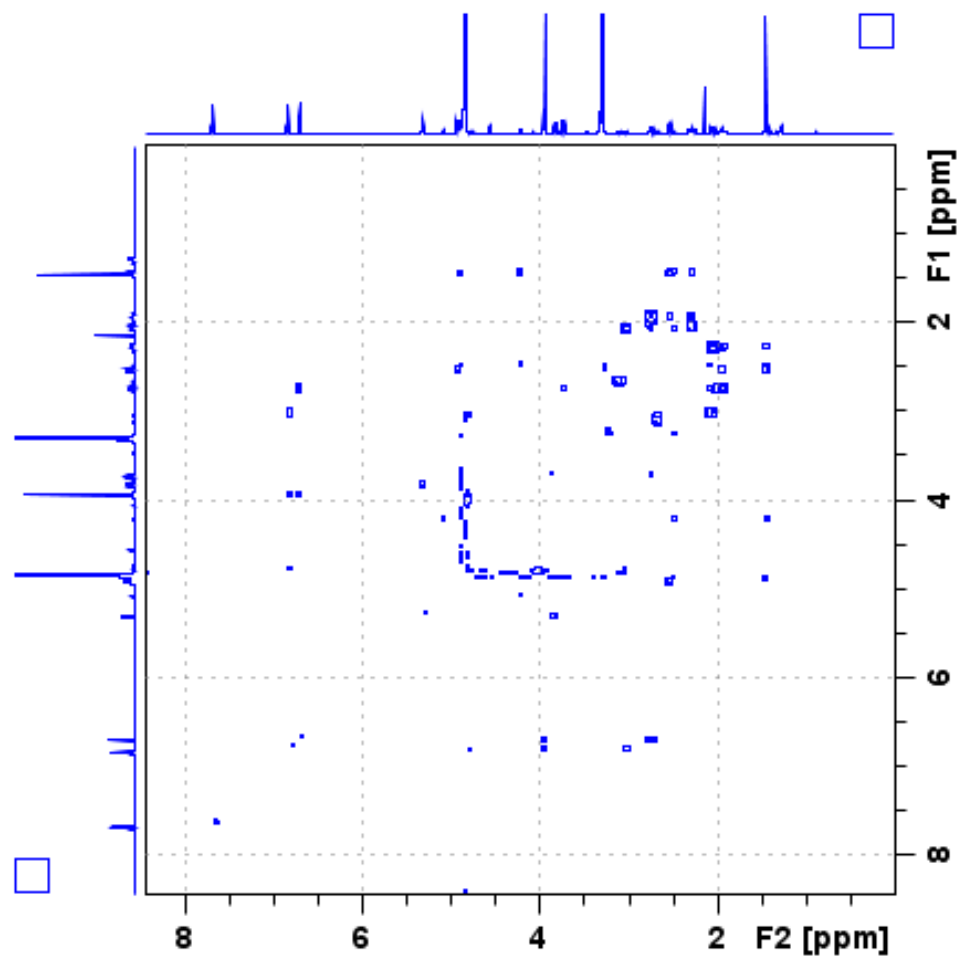
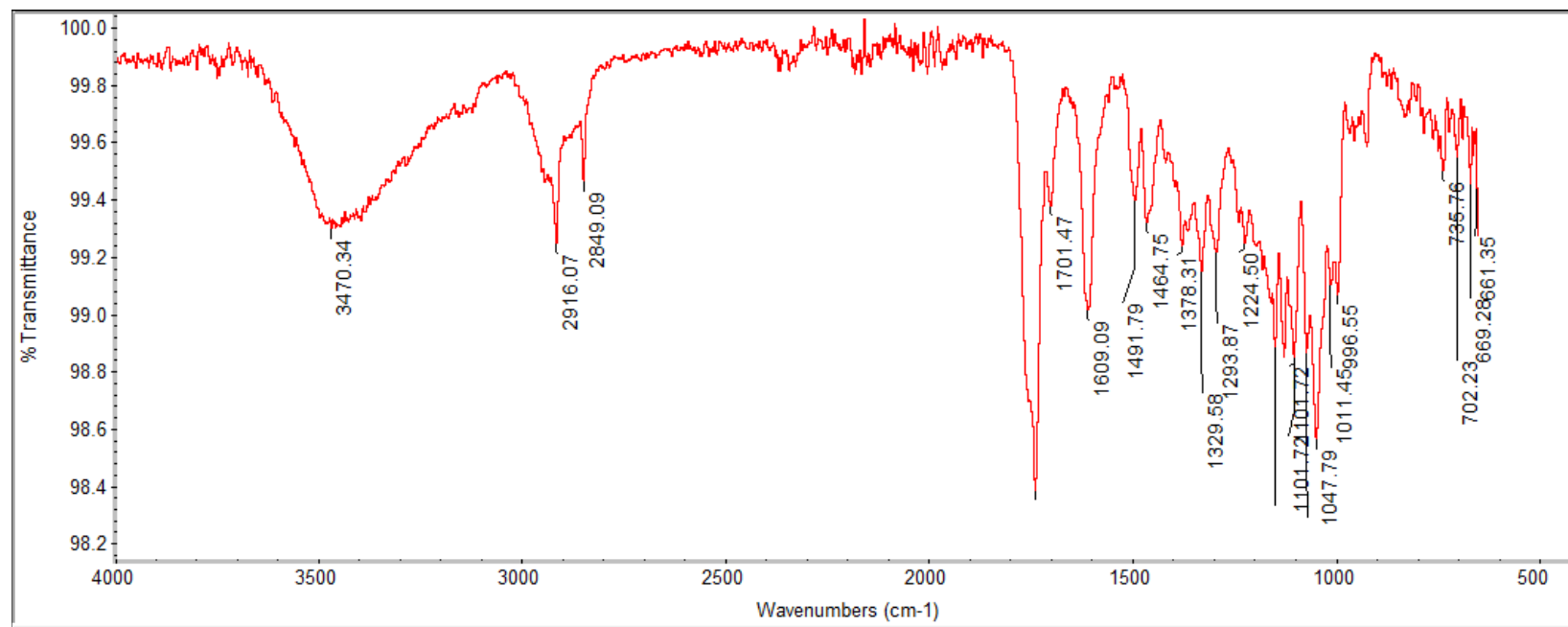


Figure 105. NOESY spectrum (400 MHz, CD₃OD) of 7 α -hydroxyicacinlactone B

APPENDIX A (continued)

**Figure 106. IR spectrum of 7 α -hydroxyicacinlactone B**

APPENDIX A (continued)

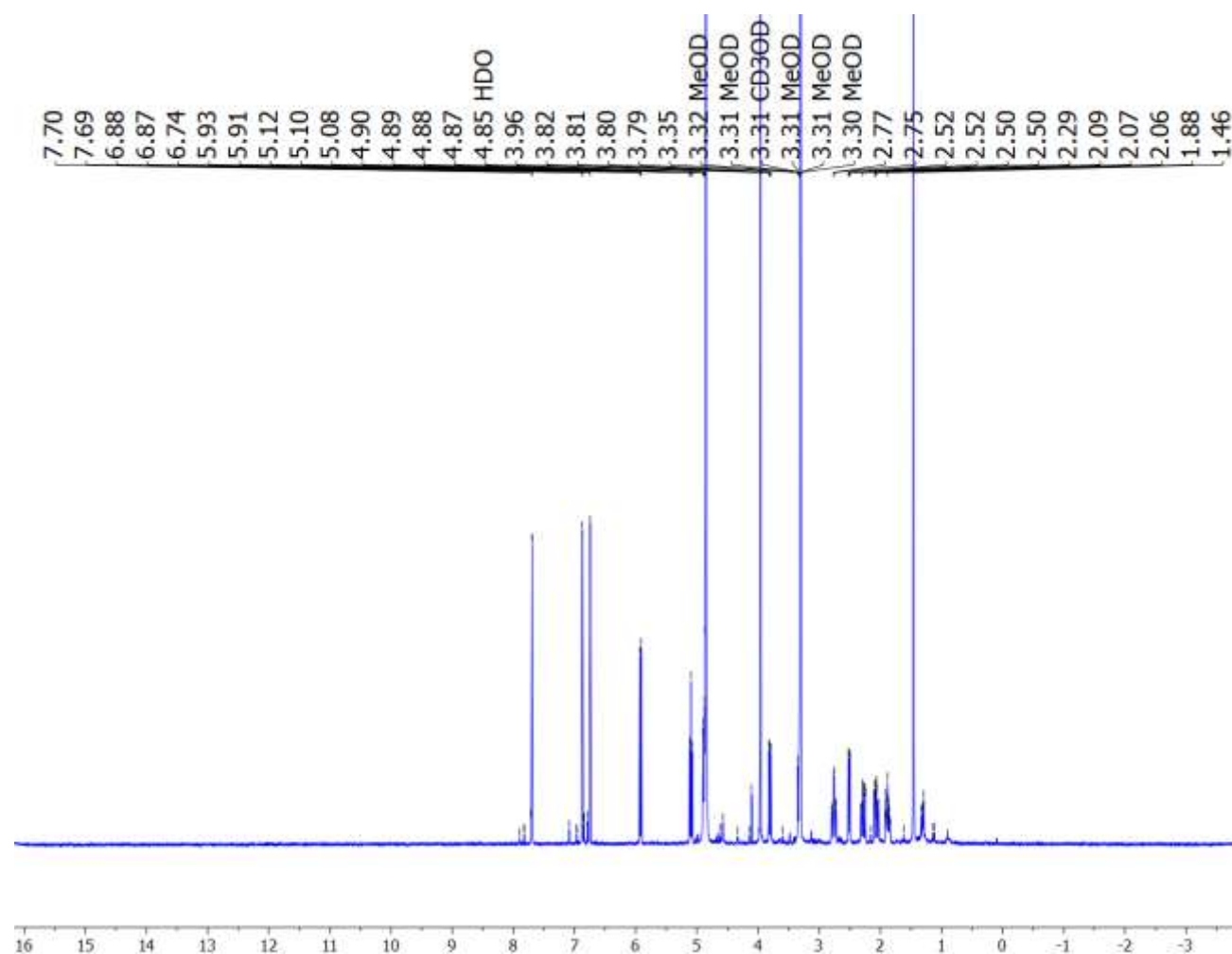


Figure 107. ¹H NMR (400 MHz, CD₃OD) spectrum of 7β-hydroxyacacilactone B

APPENDIX A (continued)

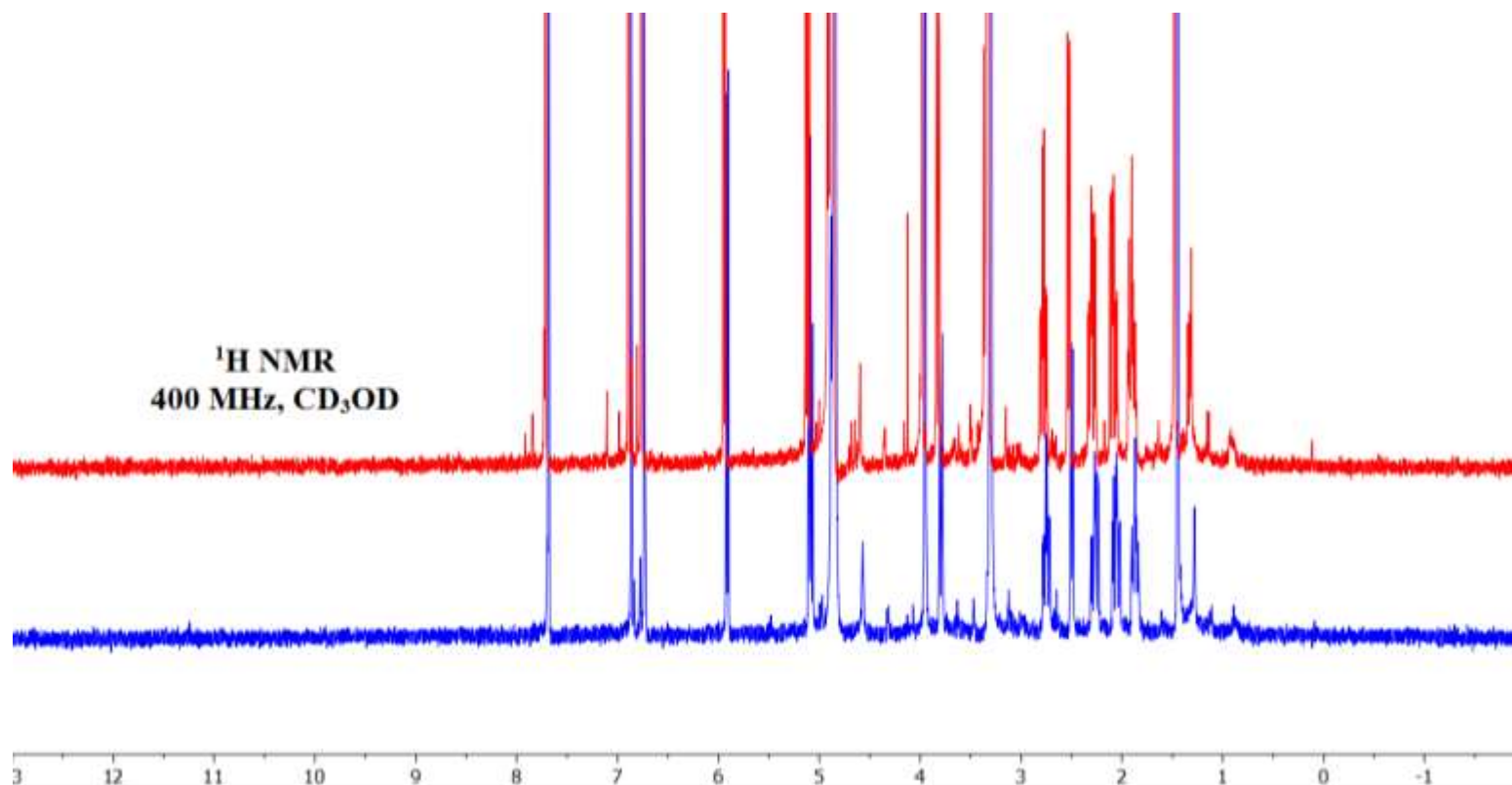


Figure 108. ¹H NMR (400 MHz, CD₃OD) spectra of compound 10 (red) and 7 β -hydroxyicacinlactone B standard (blue)

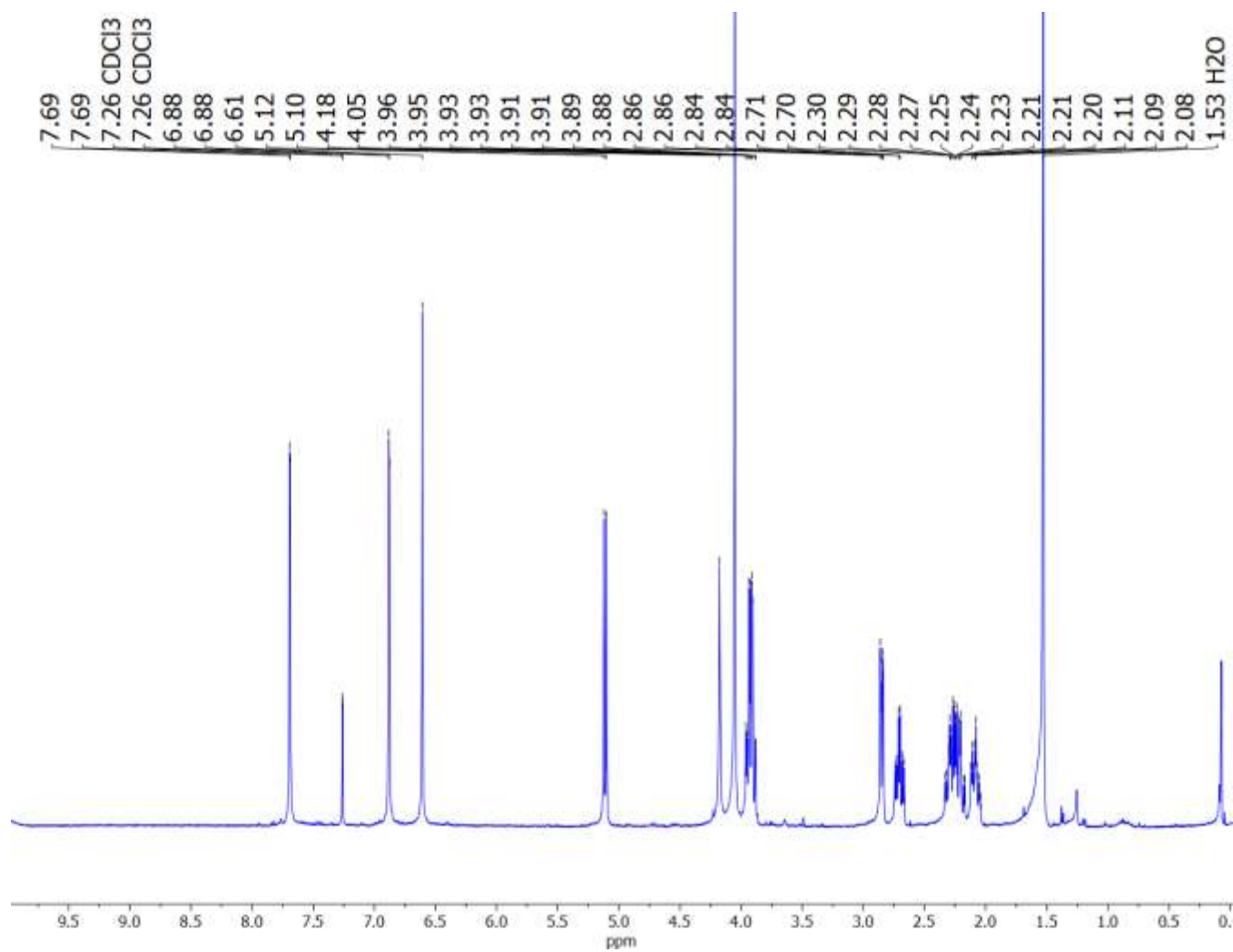


Figure 109. ^1H NMR (400 MHz, CDCl_3 -*d*) spectrum of 7-oxo-icacinlactone B

APPENDIX A (continued)

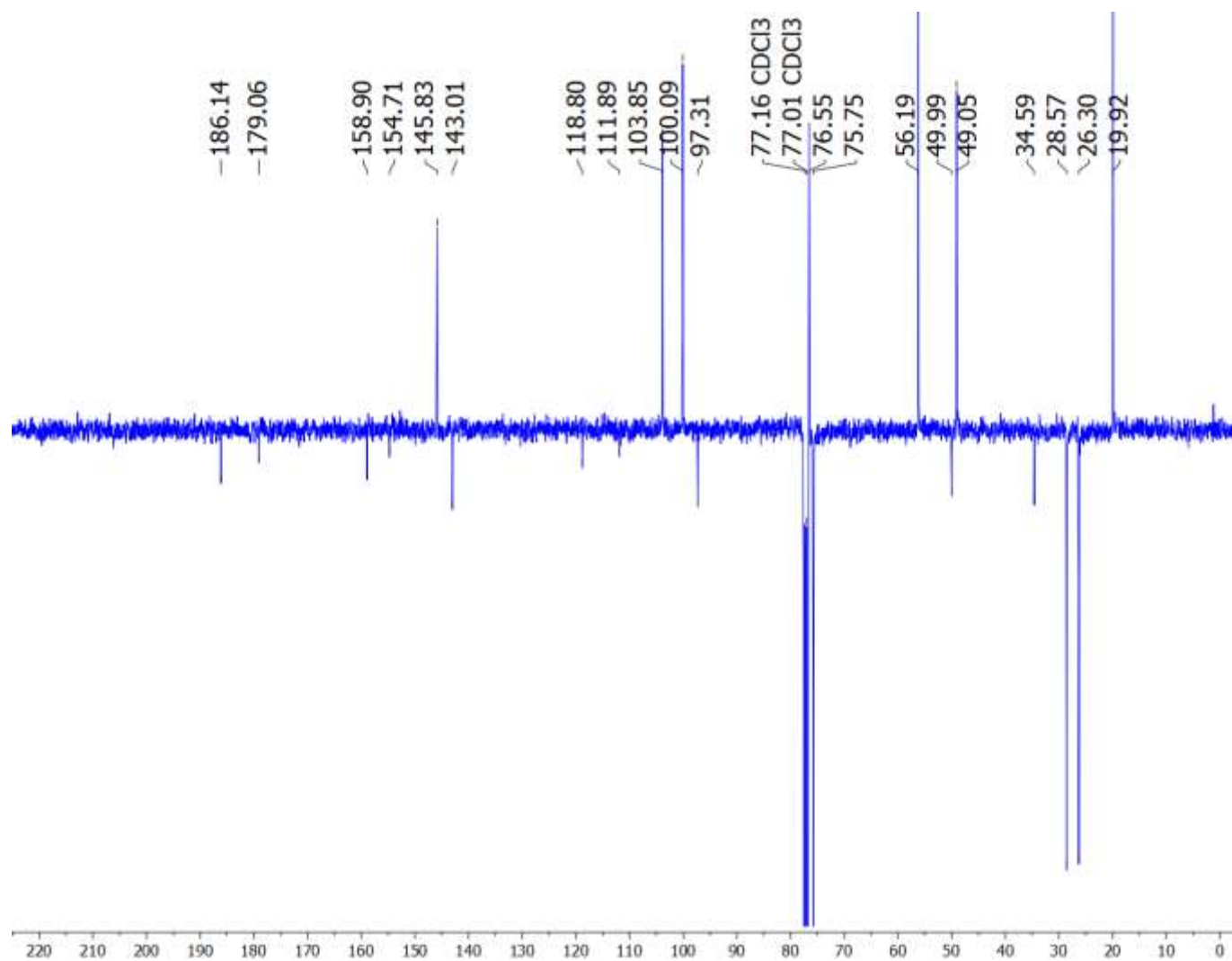


Figure 110. ^{13}C (100 MHz, $\text{CDCl}_3\text{-}d$) spectrum of 7-oxo-icacinlactone B

APPENDIX A (continued)

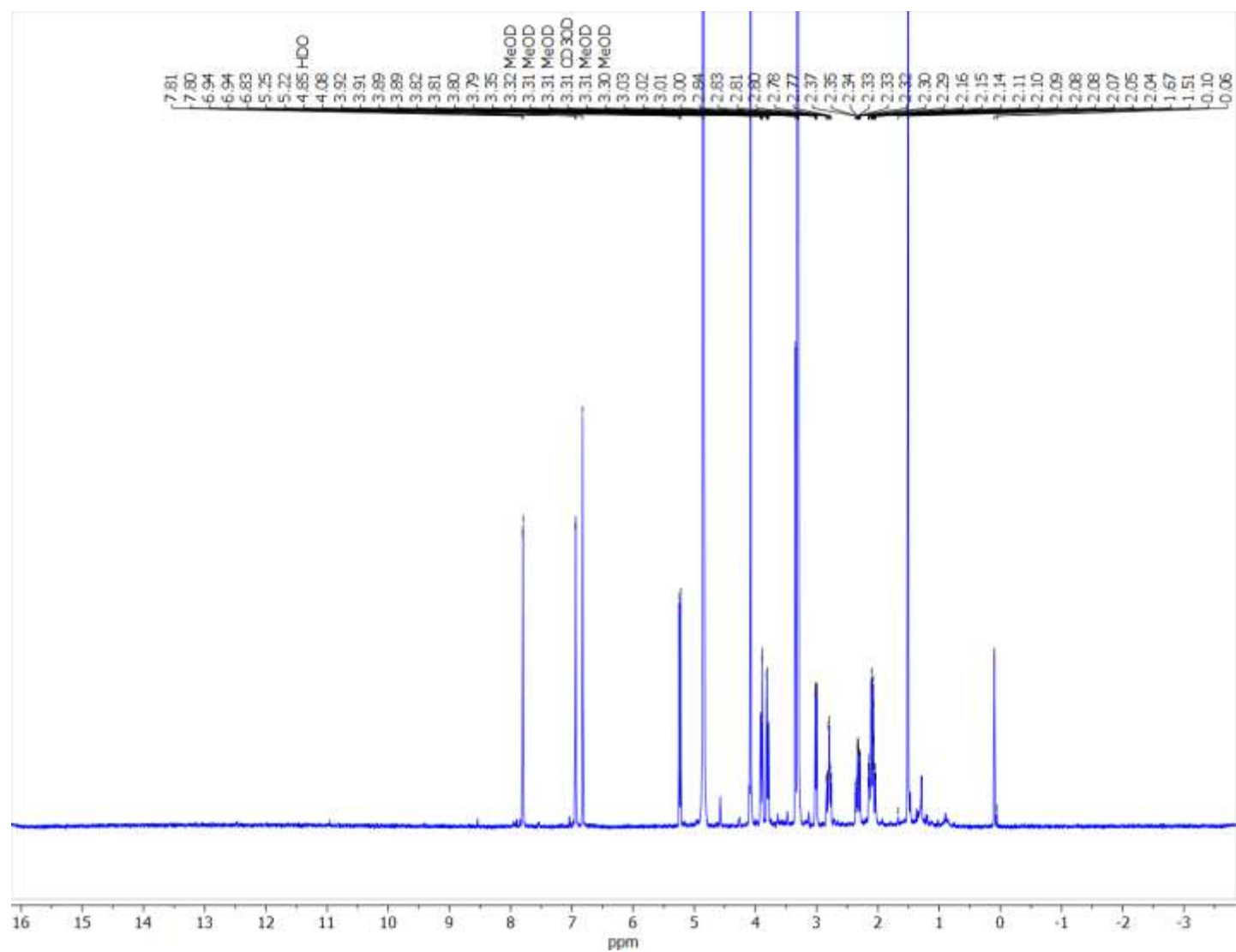


Figure 111. ¹H (400 MHz, CD₃OD) spectrum of 7-oxo-icacinlactone B

APPENDIX A (continued)

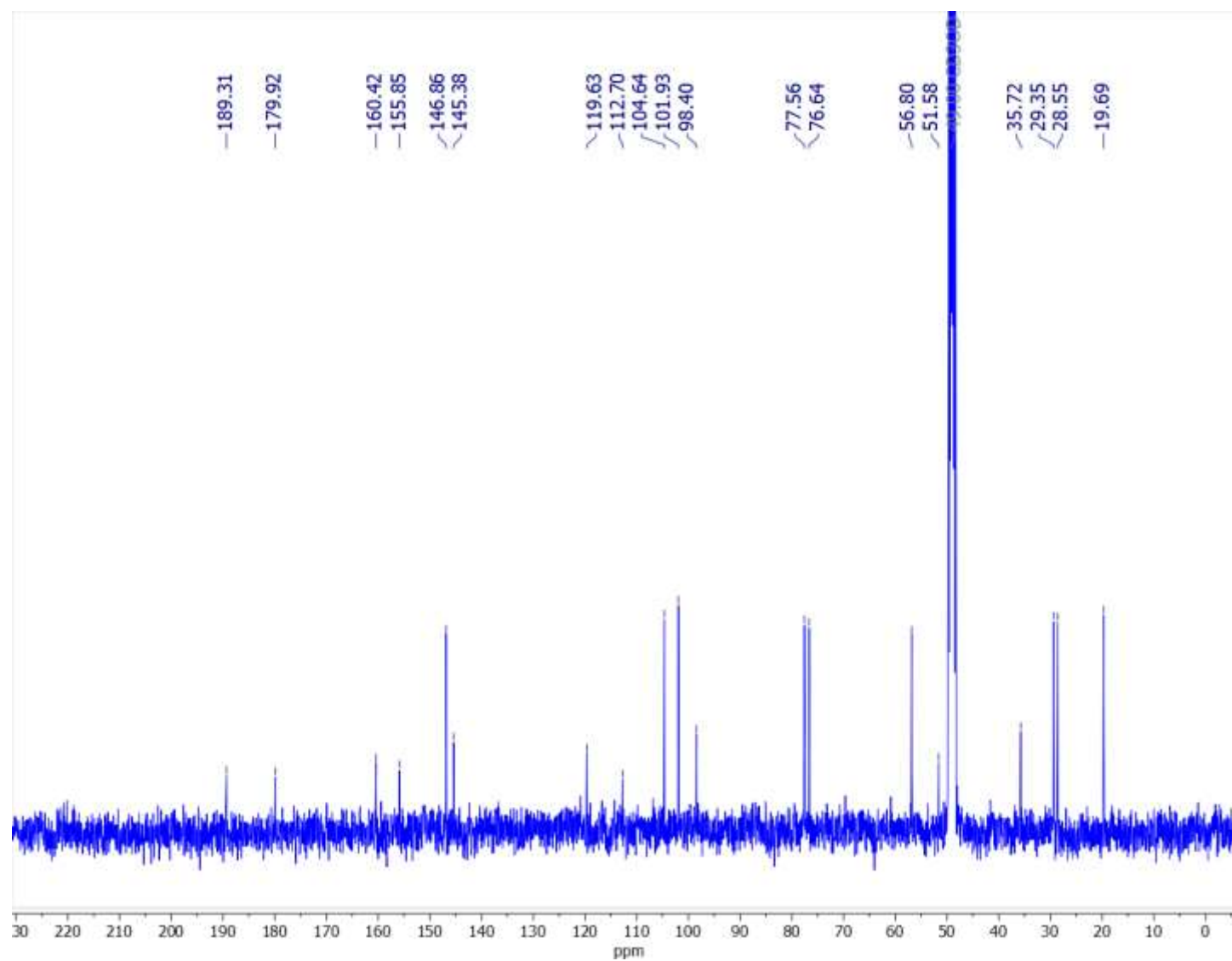


Figure 112. ¹³C (100 MHz, CD₃OD) spectrum of 7-oxo-icacinlactone B

APPENDIX A (continued)

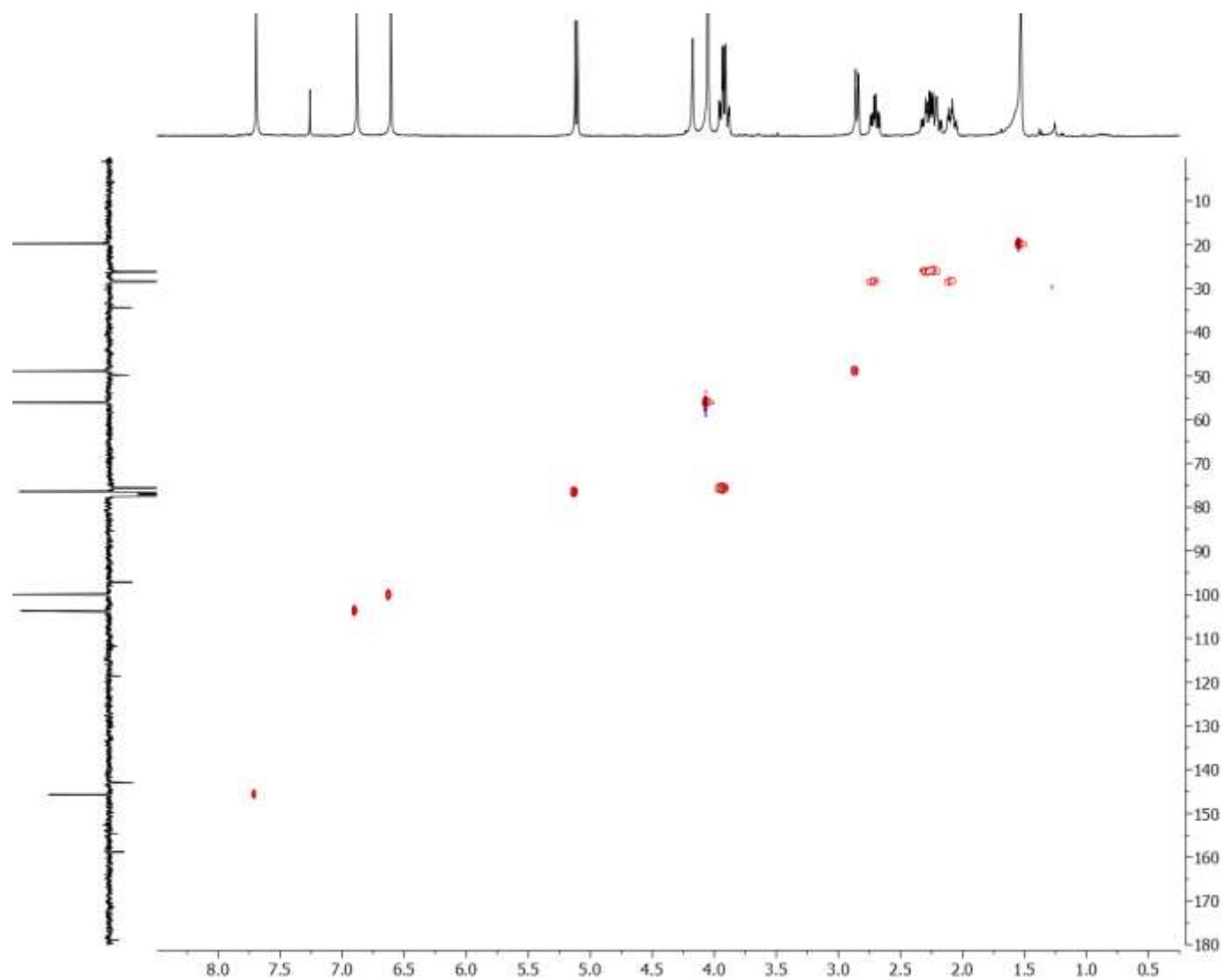


Figure 113. HSQC (400 MHz, CDCl_3-d) spectrum of 7-oxo-icacinlactone B

APPENDIX A (continued)

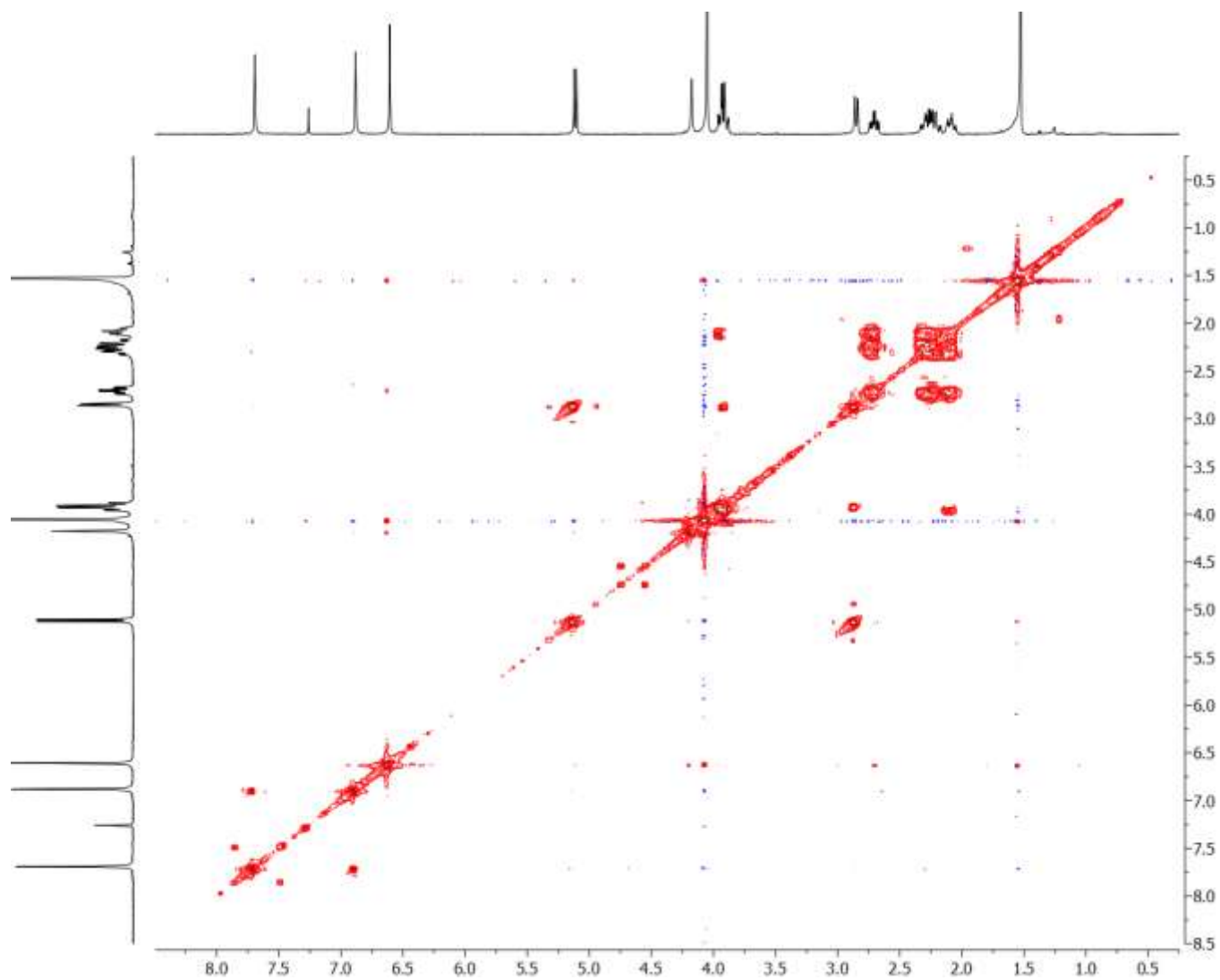


Figure 114. ^1H - ^1H COSY (400 MHz, $\text{CDCl}_3\text{-}d$) spectrum of 7-oxo-icacinlactone B

APPENDIX A (continued)

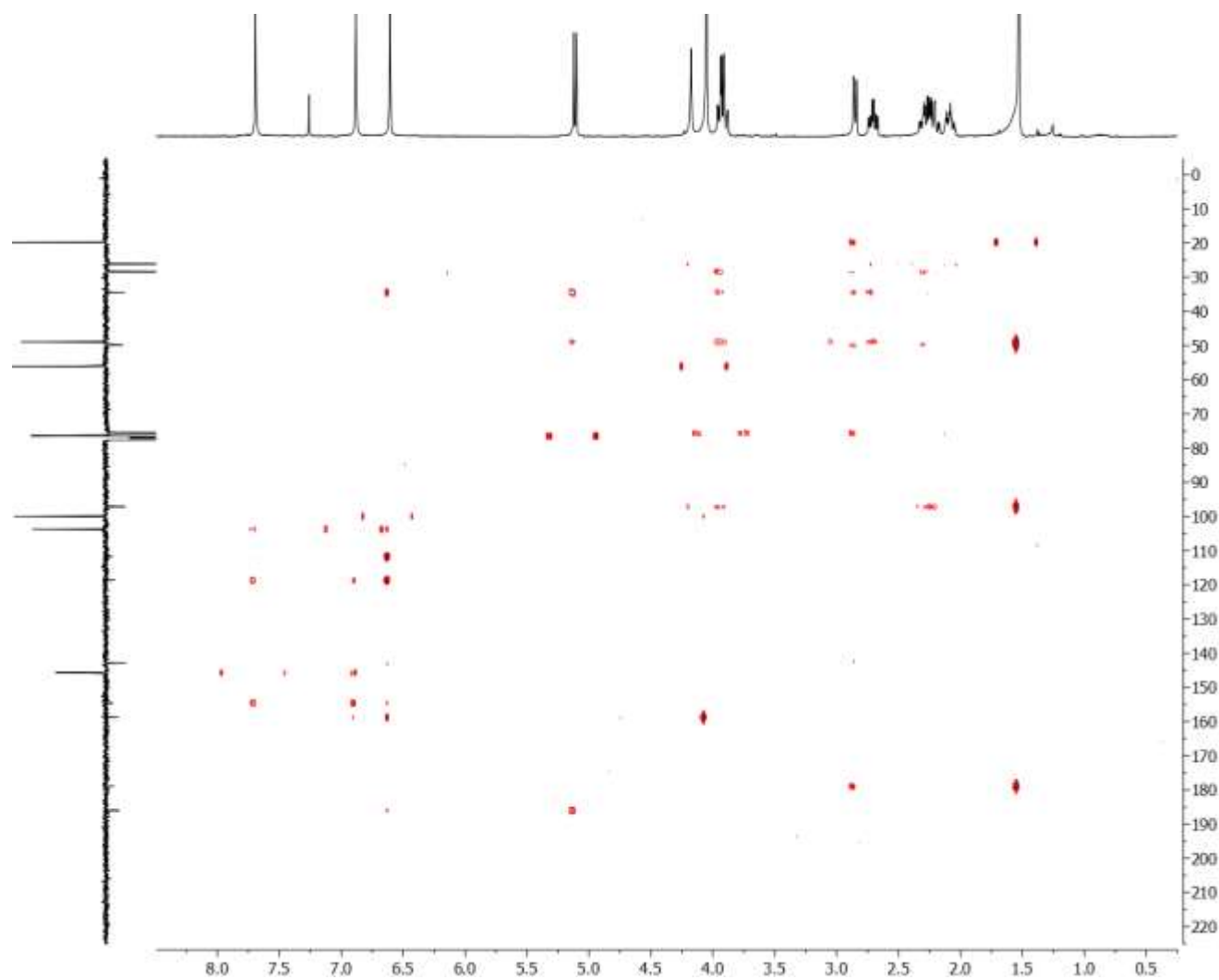


Figure 115. HMBC (400 MHz, CDCl_3-d) spectrum of 7-oxo-icacinlactone B

APPENDIX A (continued)

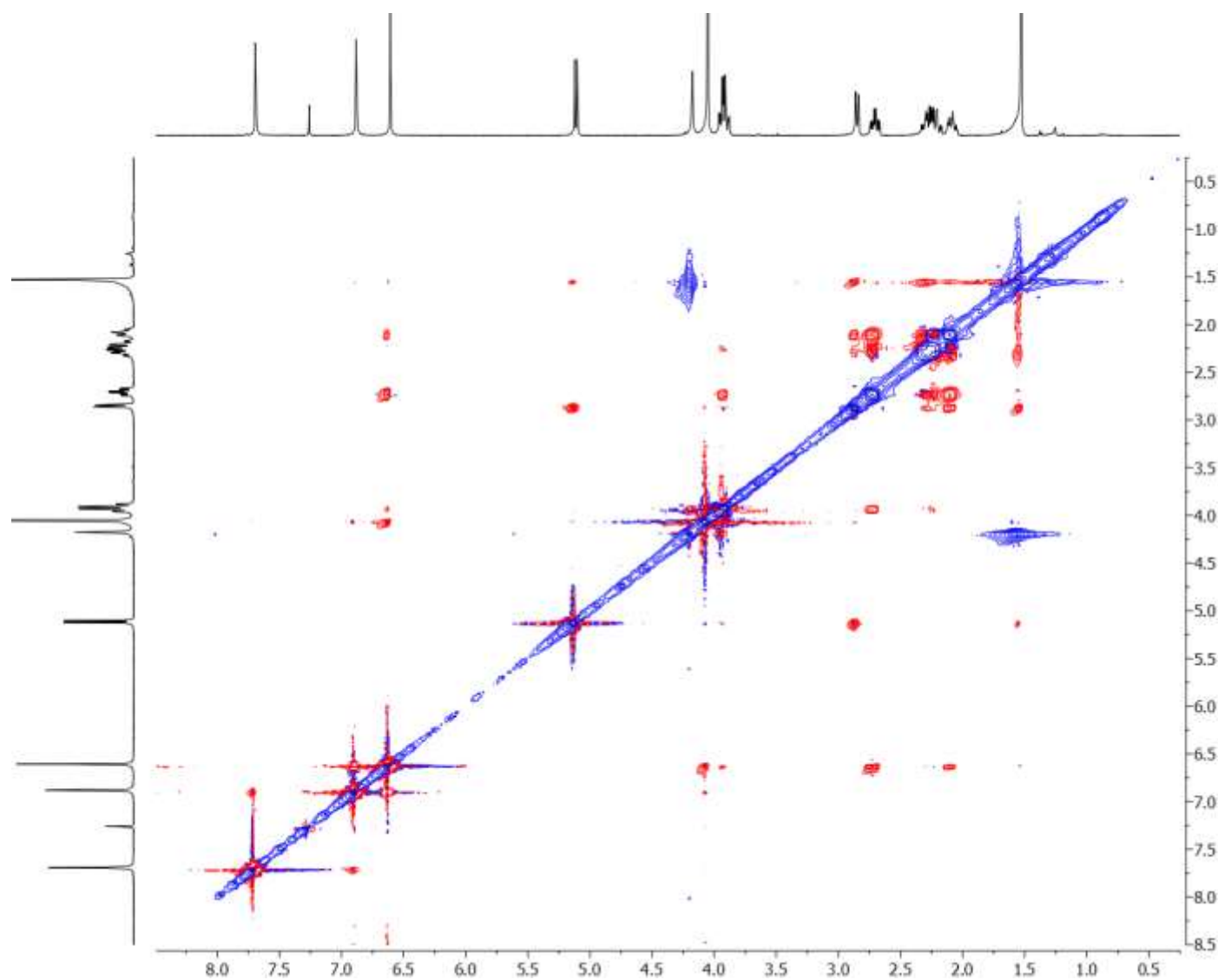
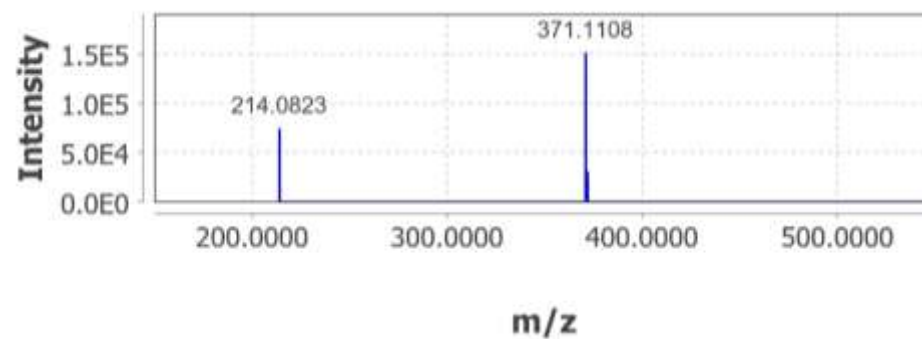
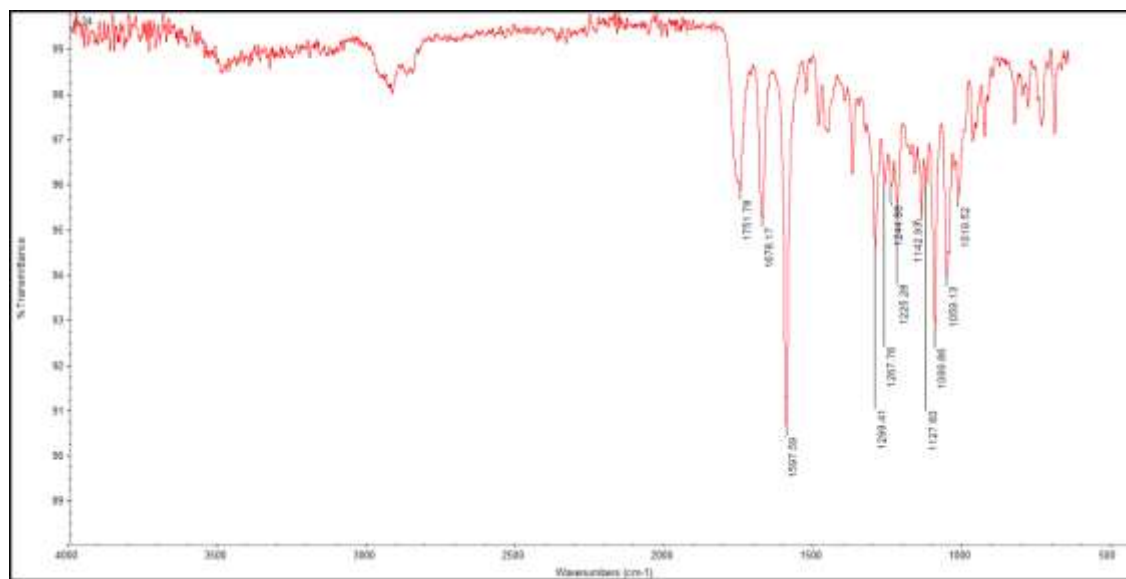


Figure 116. NOESY (400 MHz, CDCl₃-d) spectrum of 7-oxo-icacinlactone B

APPENDIX A (continued)

**Figure 117. HRESIMS (+) spectrum of 7-oxo-icacinlactone B****Figure 118. IR spectrum of 7-oxo-icacinlactone B**

APPENDIX A (continued)

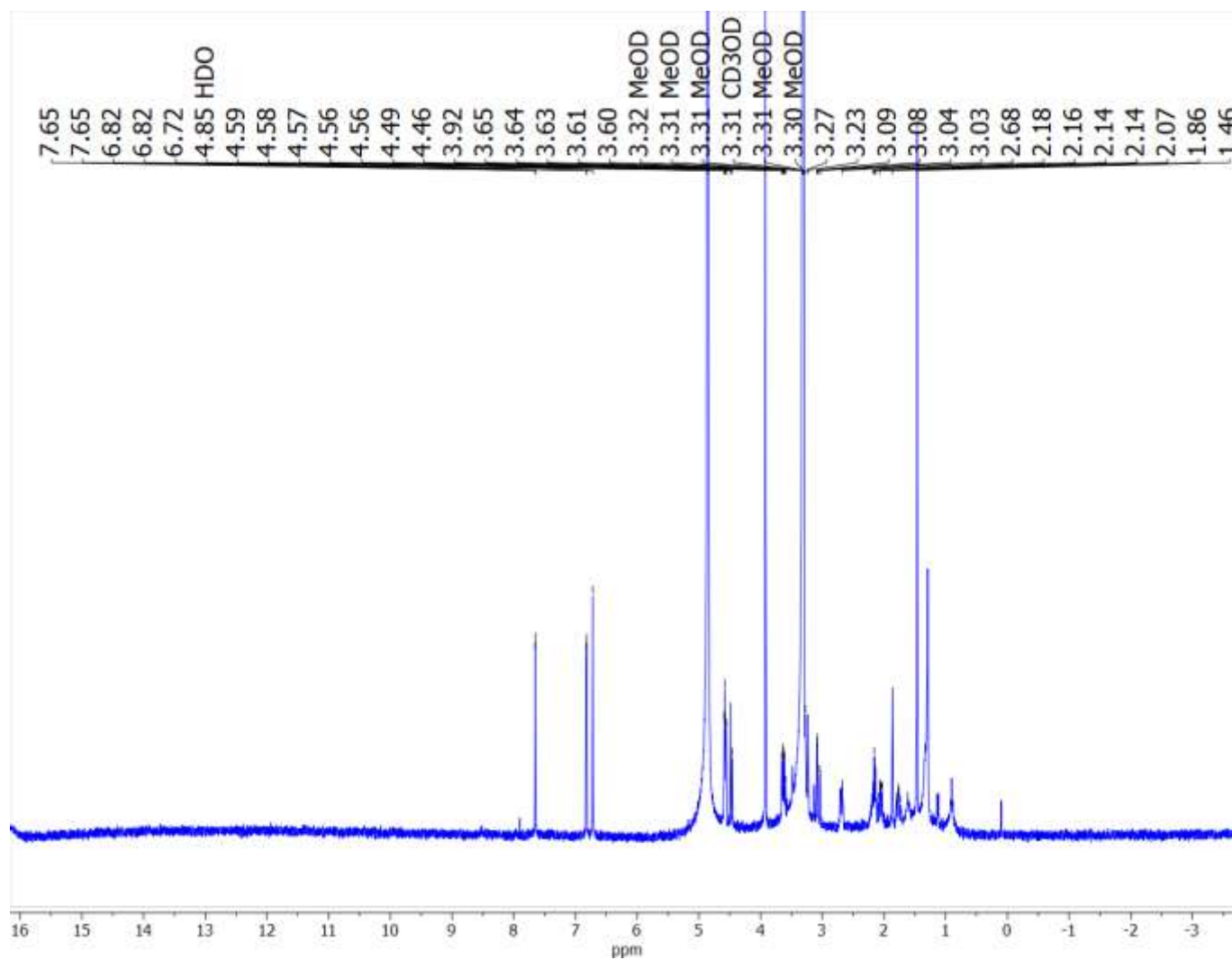


Figure 119. ¹H (400 MHz, CD₃OD) spectrum of 3-dehydroxy-icacinlactone B

APPENDIX A (continued)

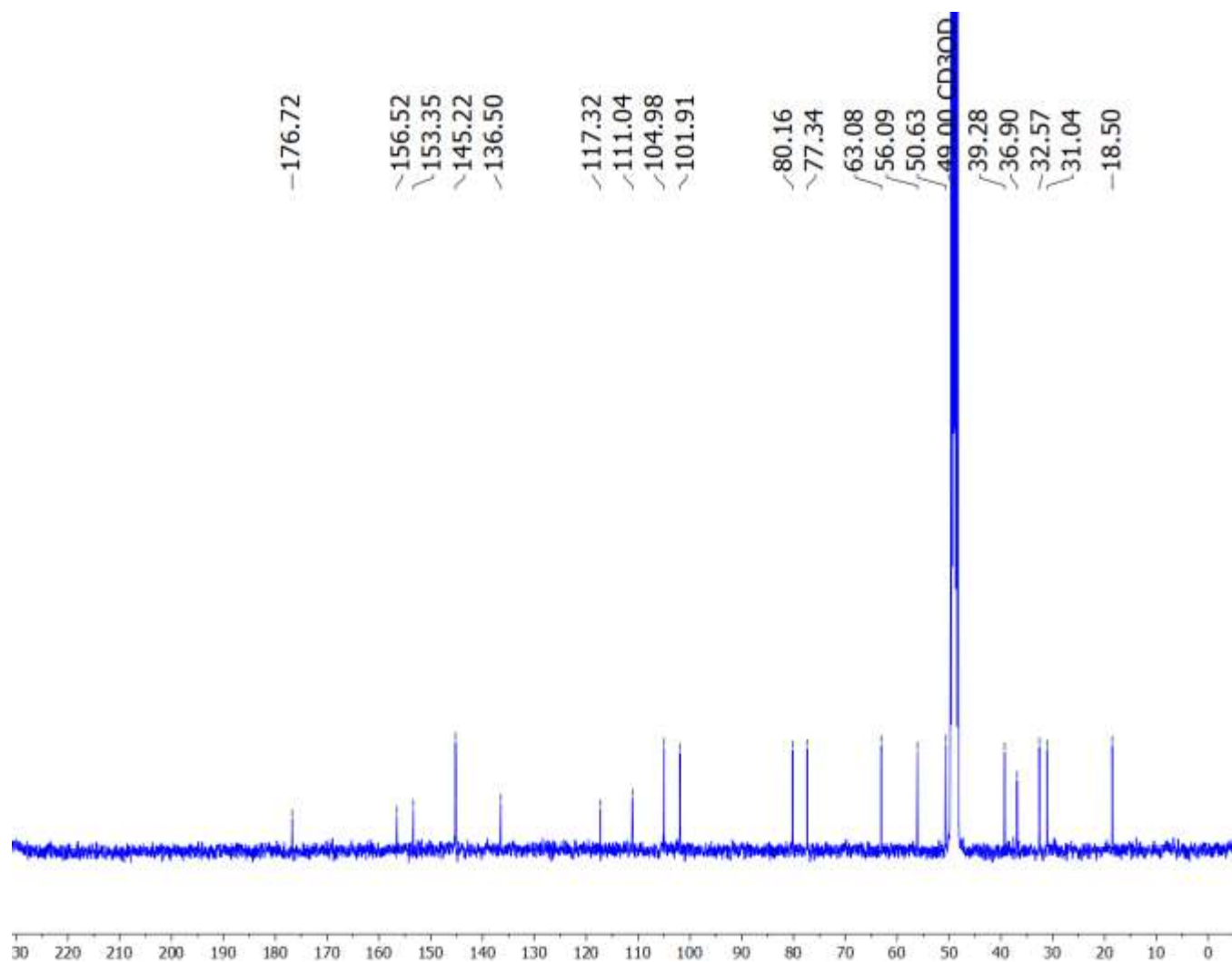


Figure 120. ¹³C (100 MHz, CD₃OD) spectrum of 3-dehydroxy-icacinlactone B

APPENDIX A (continued)

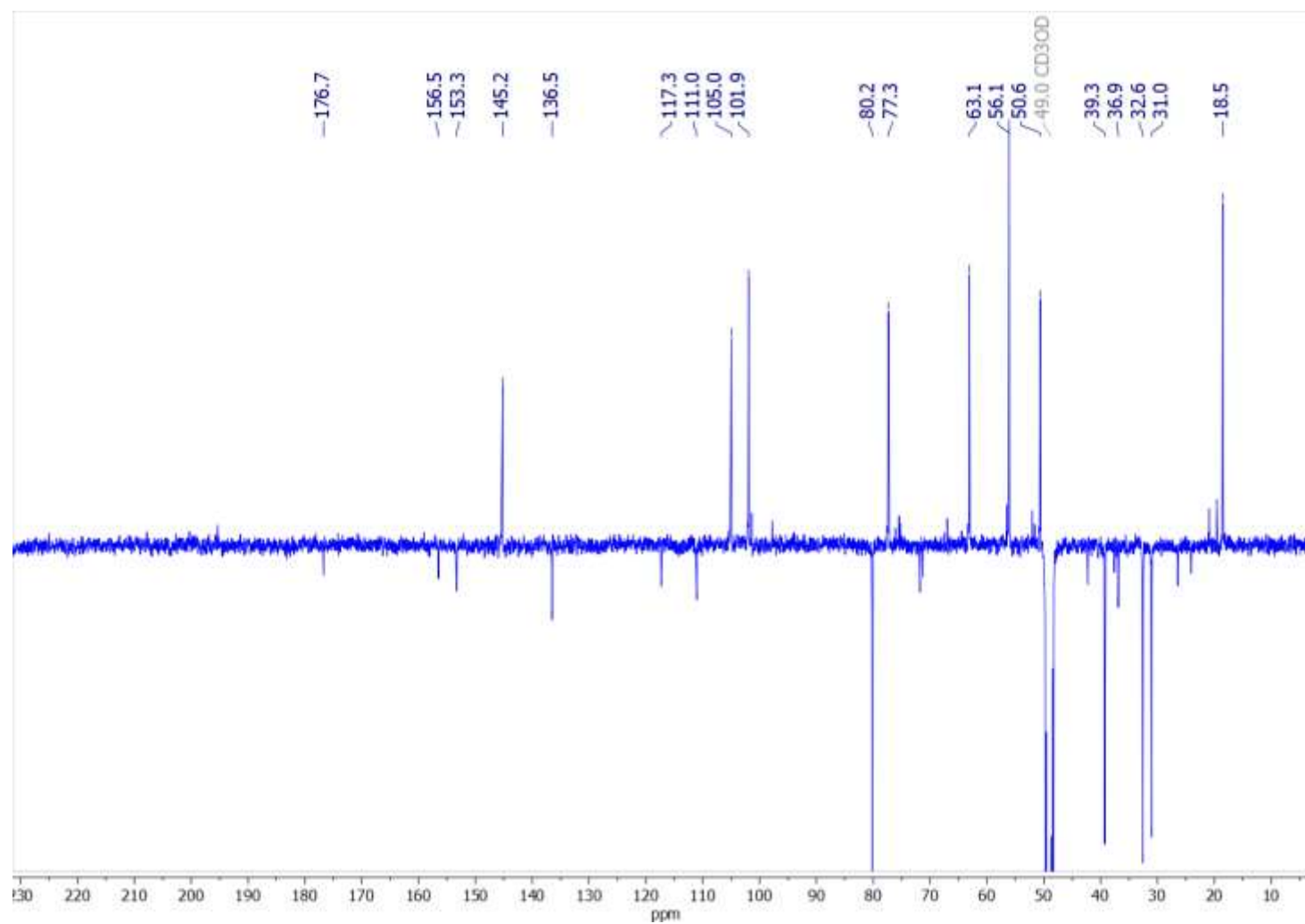


Figure 121. DEPTQ (100 MHz, CD₃OD) spectrum of 3-dehydroxy-icacinlactone B

APPENDIX A (continued)

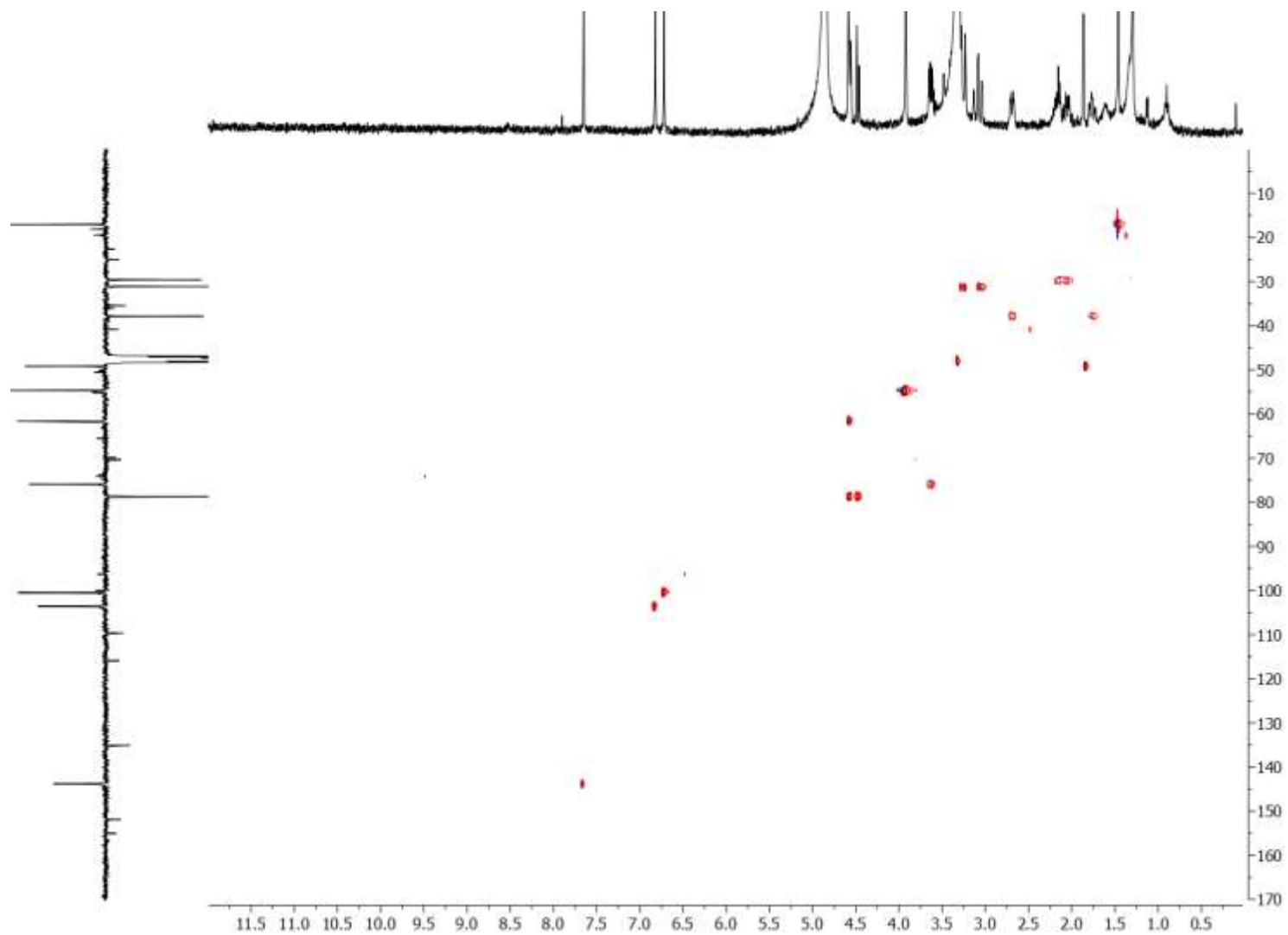


Figure 122. HSQC (400 MHz, CD_3OD) spectrum of 3-dehydroxy-icacinlactone B

APPENDIX A (continued)

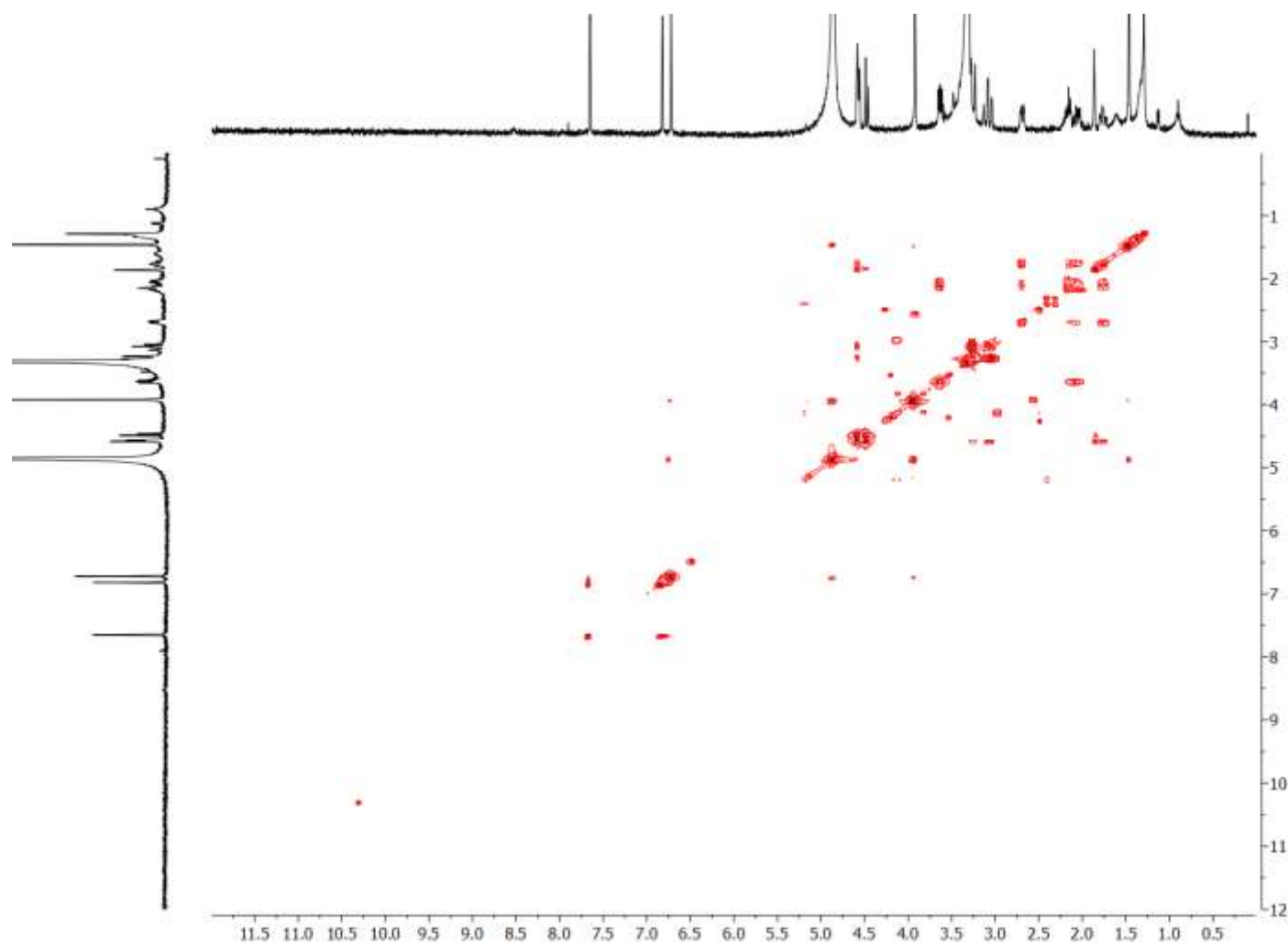


Figure 123. ^1H - ^1H (400 MHz, CD_3OD) spectrum of 3-dehydroxy-icacinlactone B

APPENDIX A (continued)

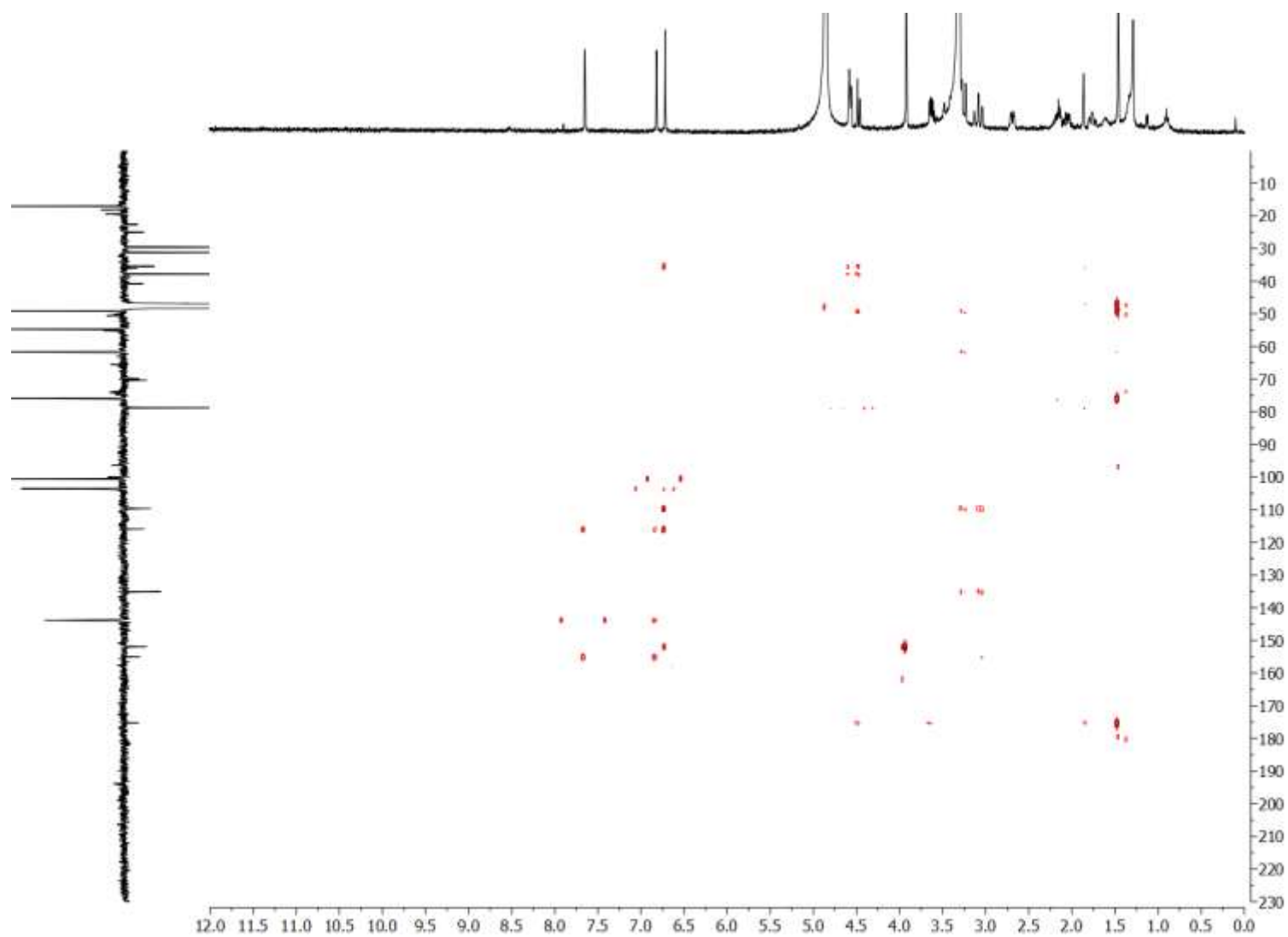


Figure 124. HMBC (400 MHz, CD_3OD) spectrum of 3-dehydroxy-icacinlactone B

APPENDIX A (continued)

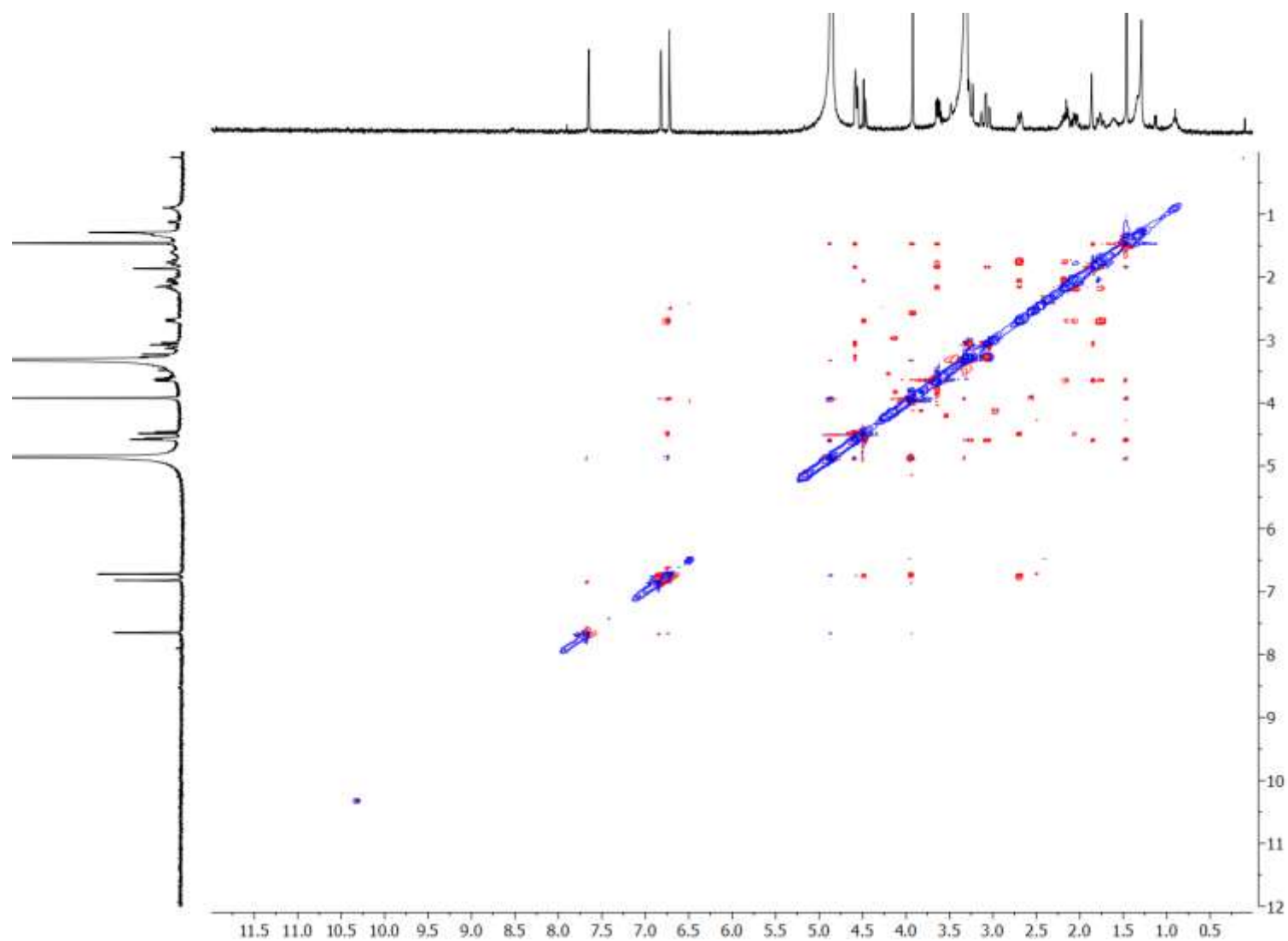


Figure 125. NOESY (400 MHz, CD₃OD) spectrum of 3-dehydroxy-icacinlactone B

APPENDIX A (continued)

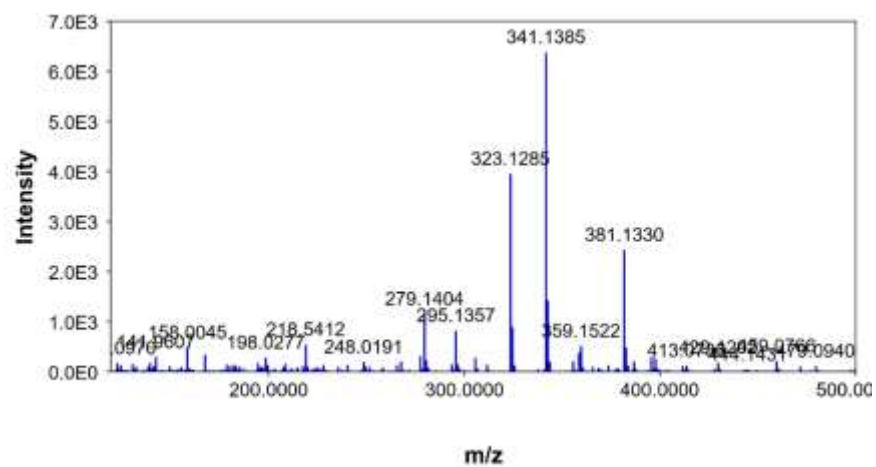


Figure 126. HRESIMS (+) spectrum of 3-dehydroxy-icacinlactone B

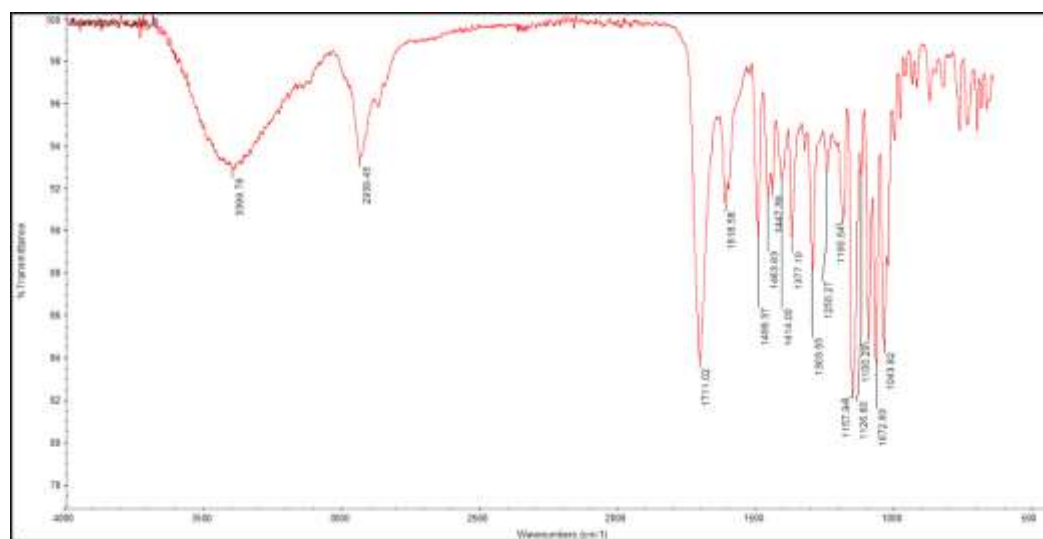


Figure 127. IR spectrum of 3-dehydroxy-icacinlactone B

APPENDIX A (continued)

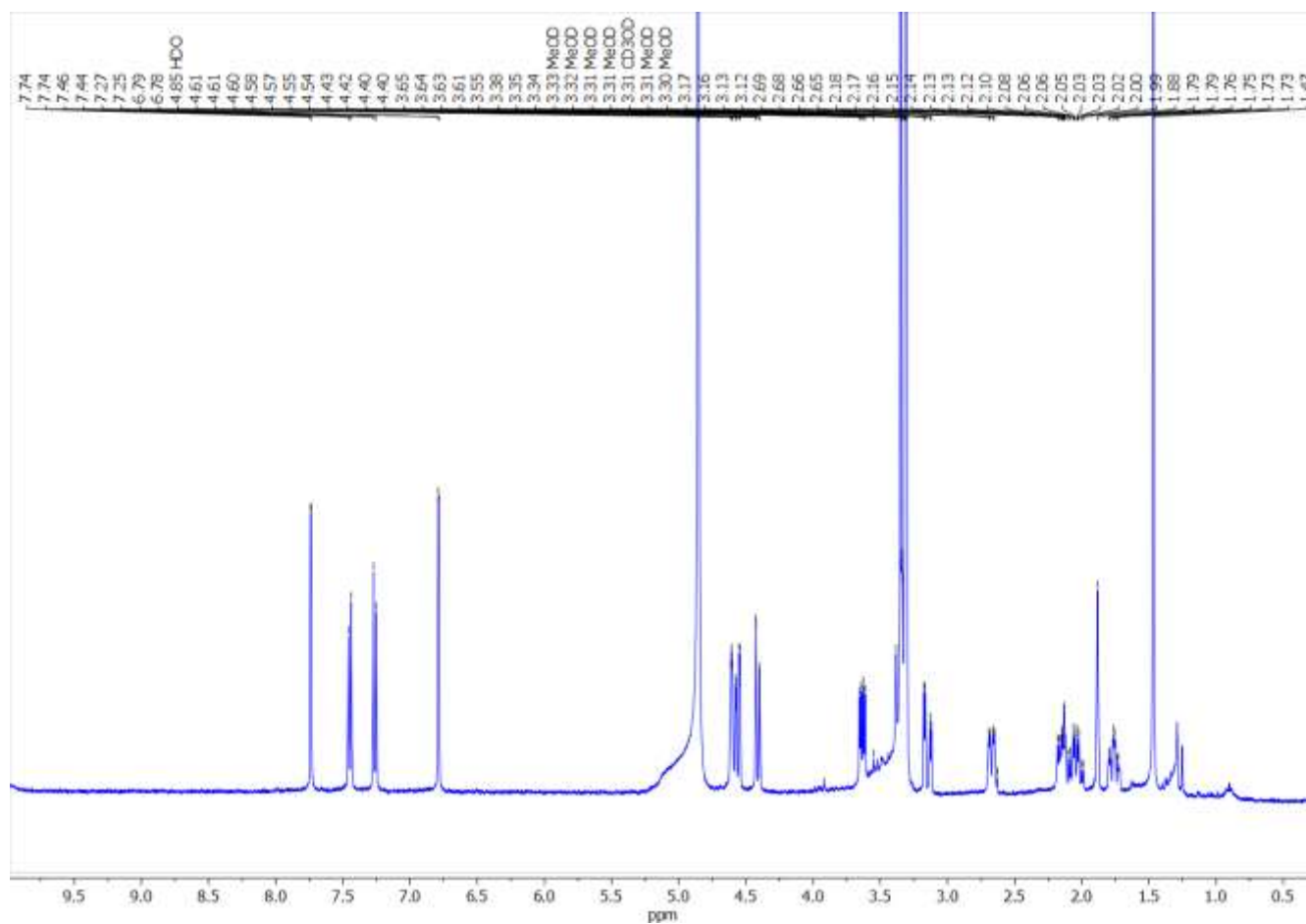


Figure 128. ^1H (400 MHz, CD_3OD) spectrum of 3-dehydroxy-icacinlactone A

APPENDIX A (continued)

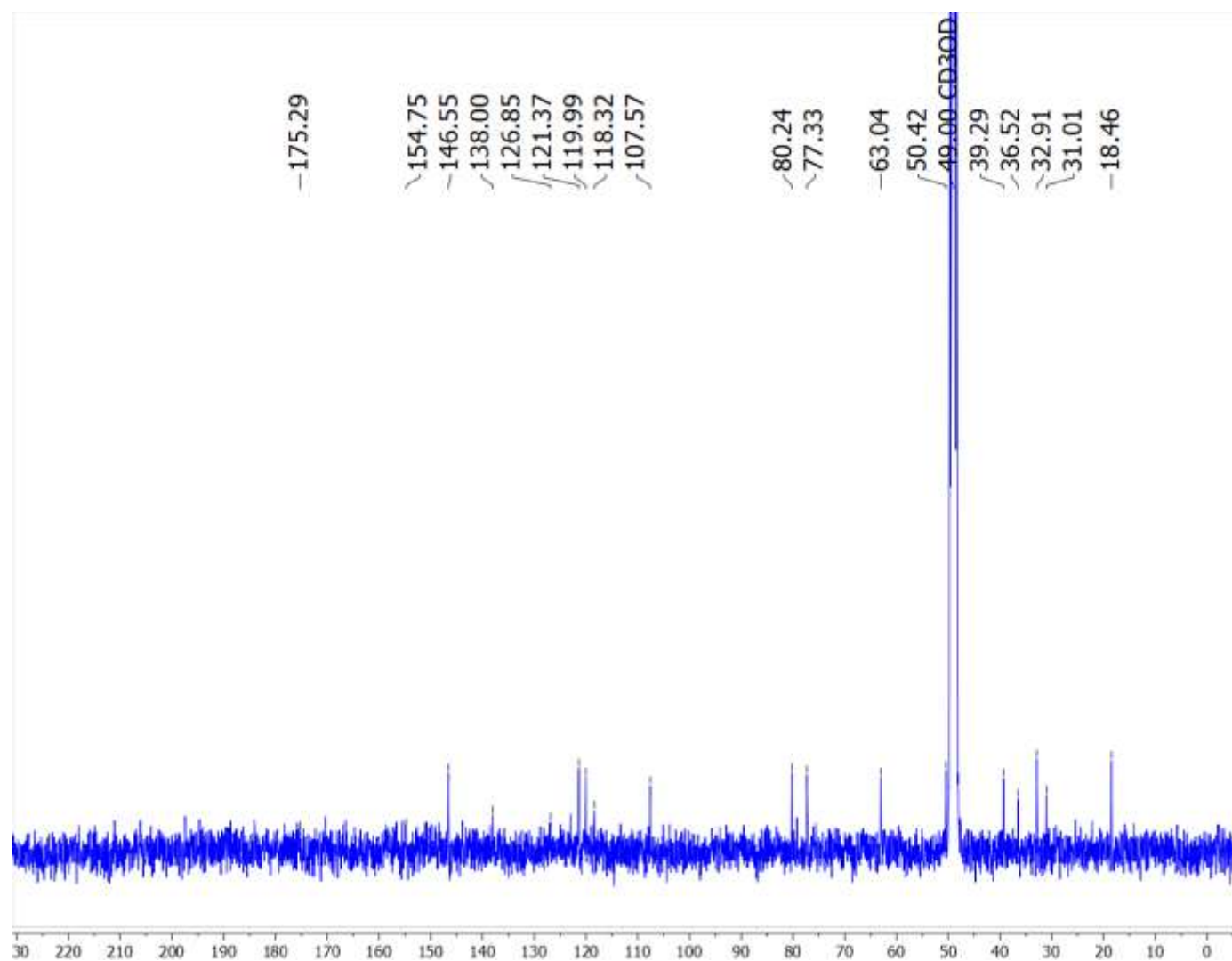


Figure 129. ^{13}C (100 MHz, CD_3OD) spectrum of 3-dehydroxy-icacinlactone A

APPENDIX A (continued)

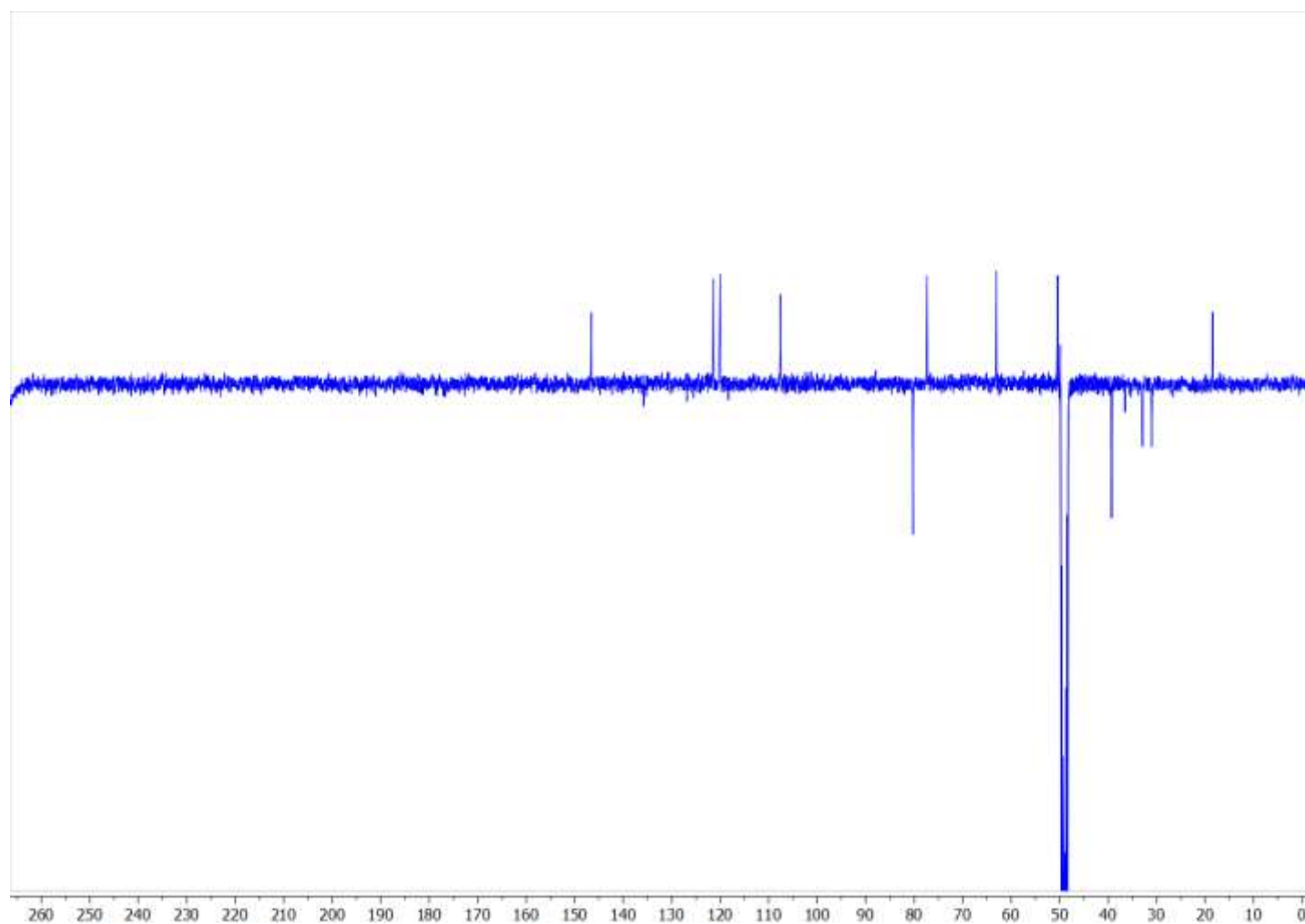


Figure 130. DEPTQ (100 MHz, CD₃OD) spectrum of 3-dehydroxy-icacinlactone A

APPENDIX A (continued)

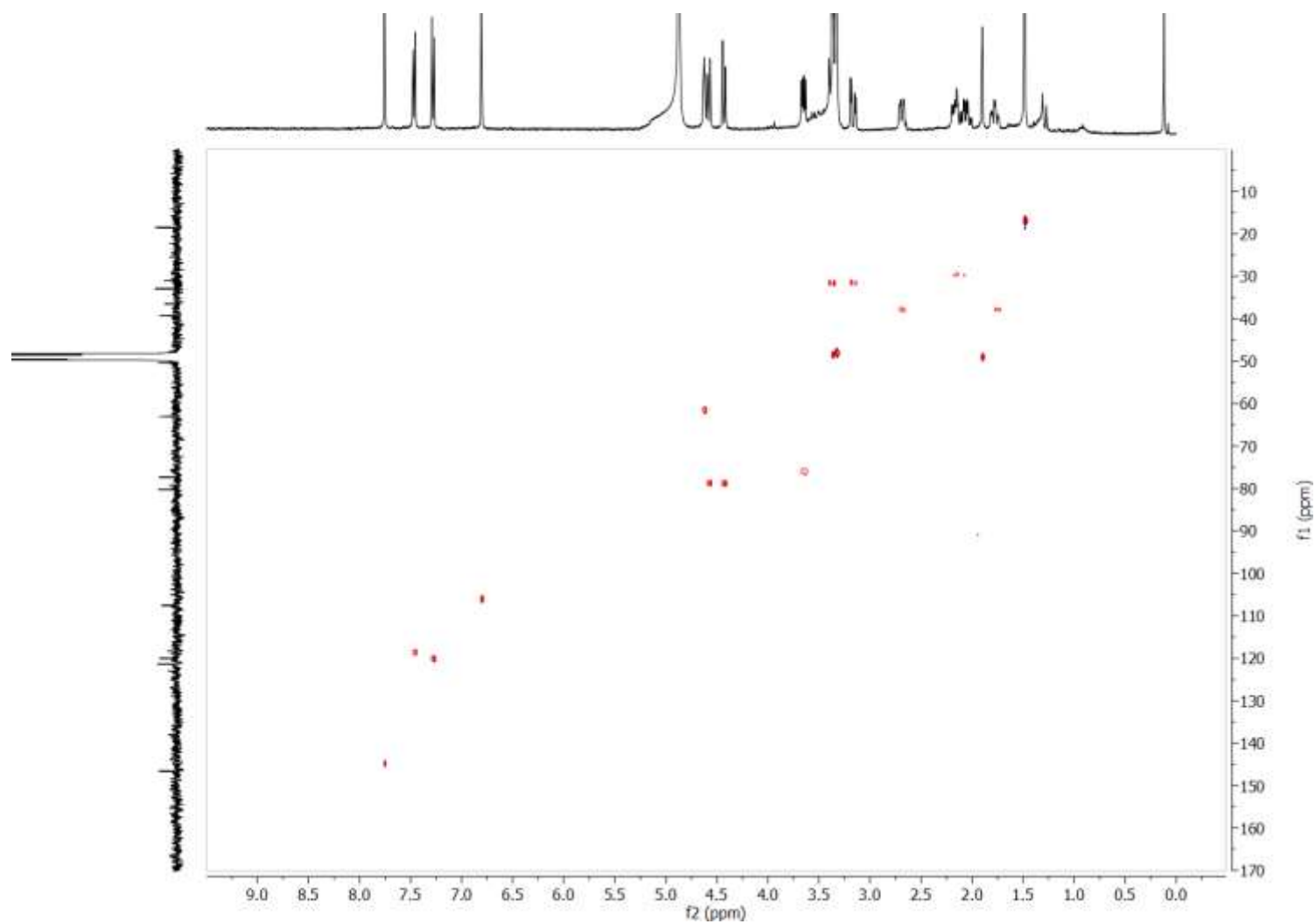


Figure 131. HSQC (400 MHz, CD_3OD) spectrum of 3-dehydroxy-icacinlactone A

APPENDIX A (continued)

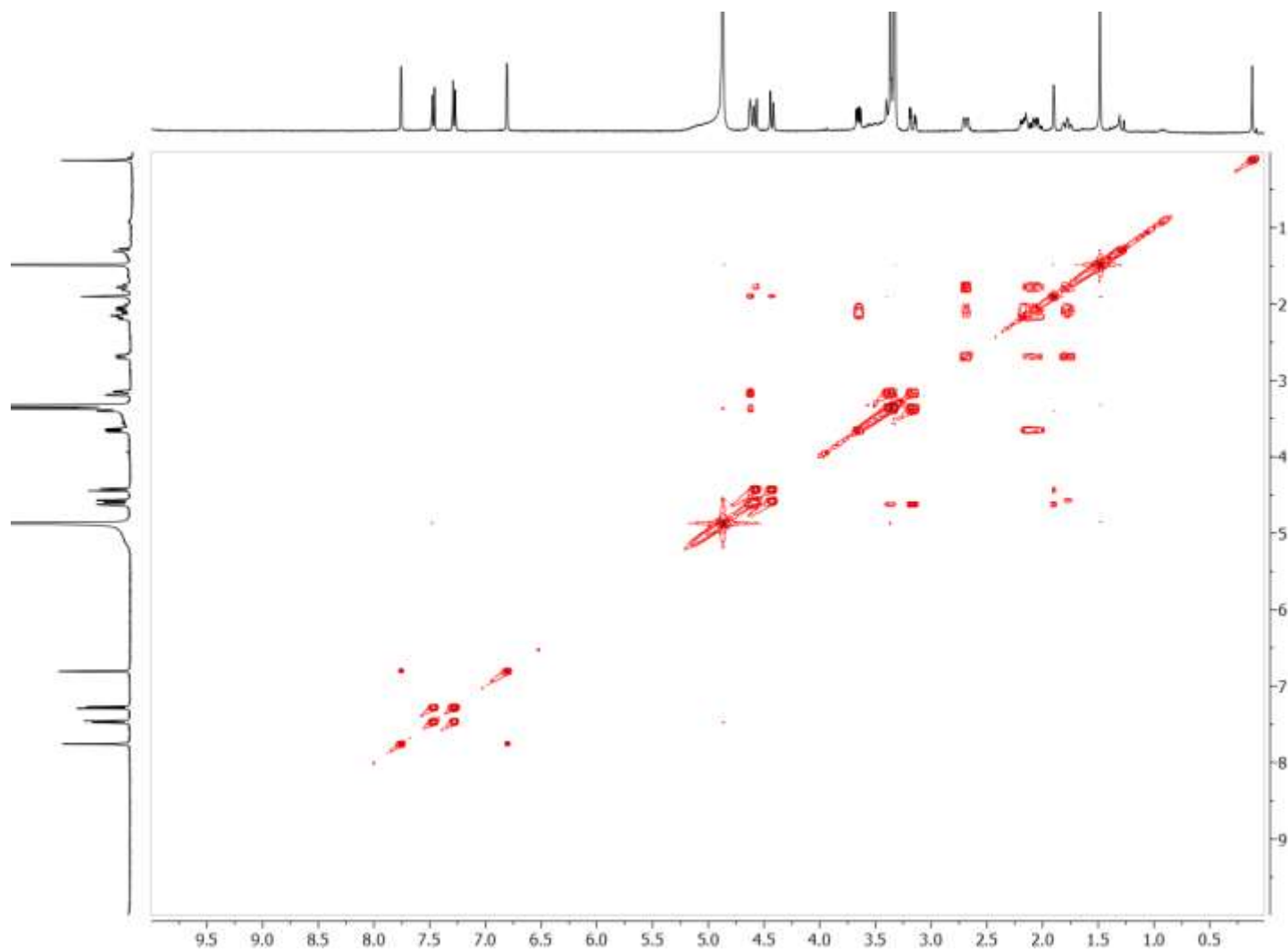


Figure 132. ^1H - ^1H COSY (400 MHz, CD_3OD) spectrum of 3-dehydroxy-icacinlactone A

APPENDIX A (continued)

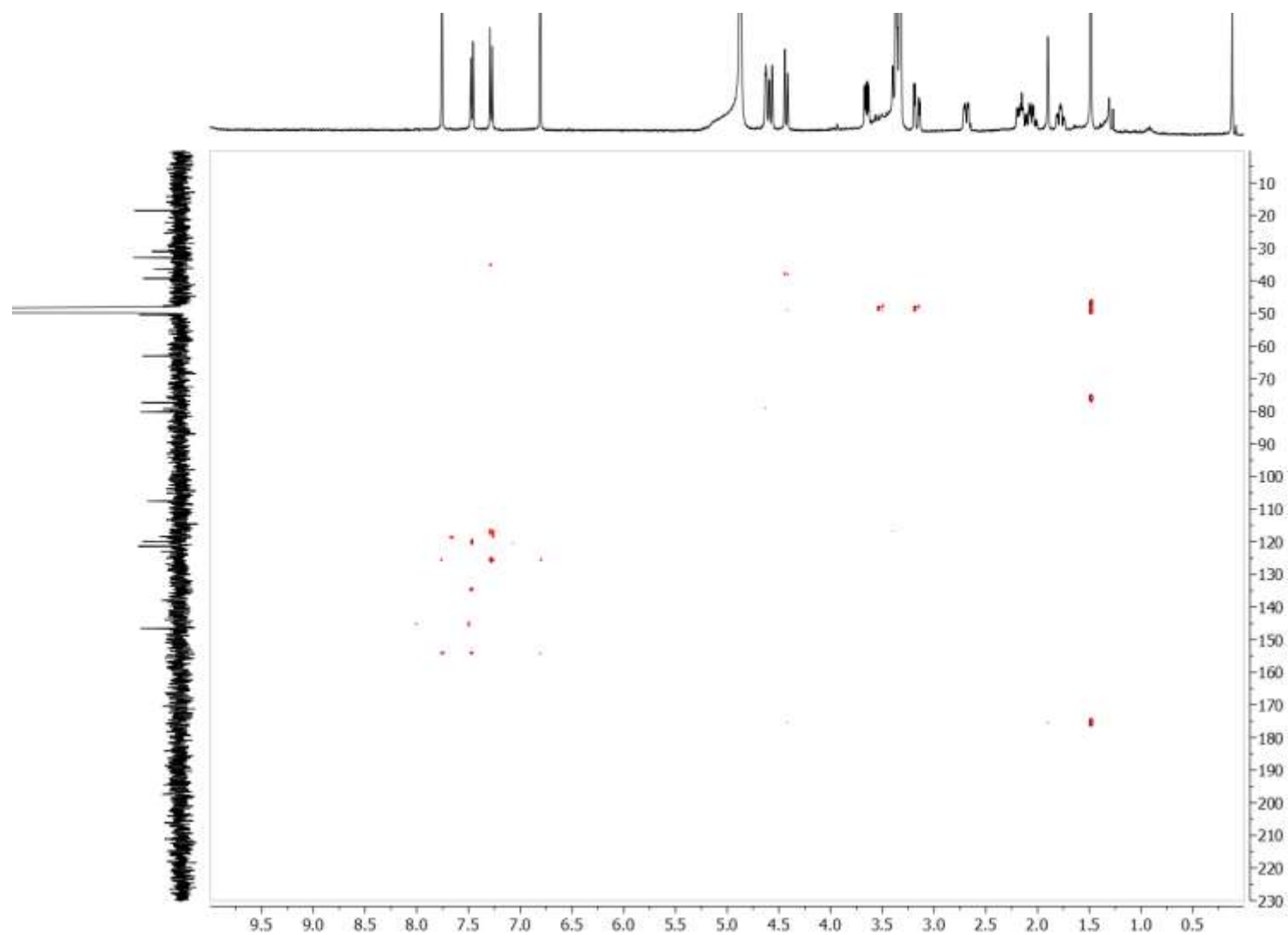


Figure 133. HMBC (400 MHz, CD₃OD) spectrum of 3-dehydroxy-icacinlactone A

APPENDIX A (continued)

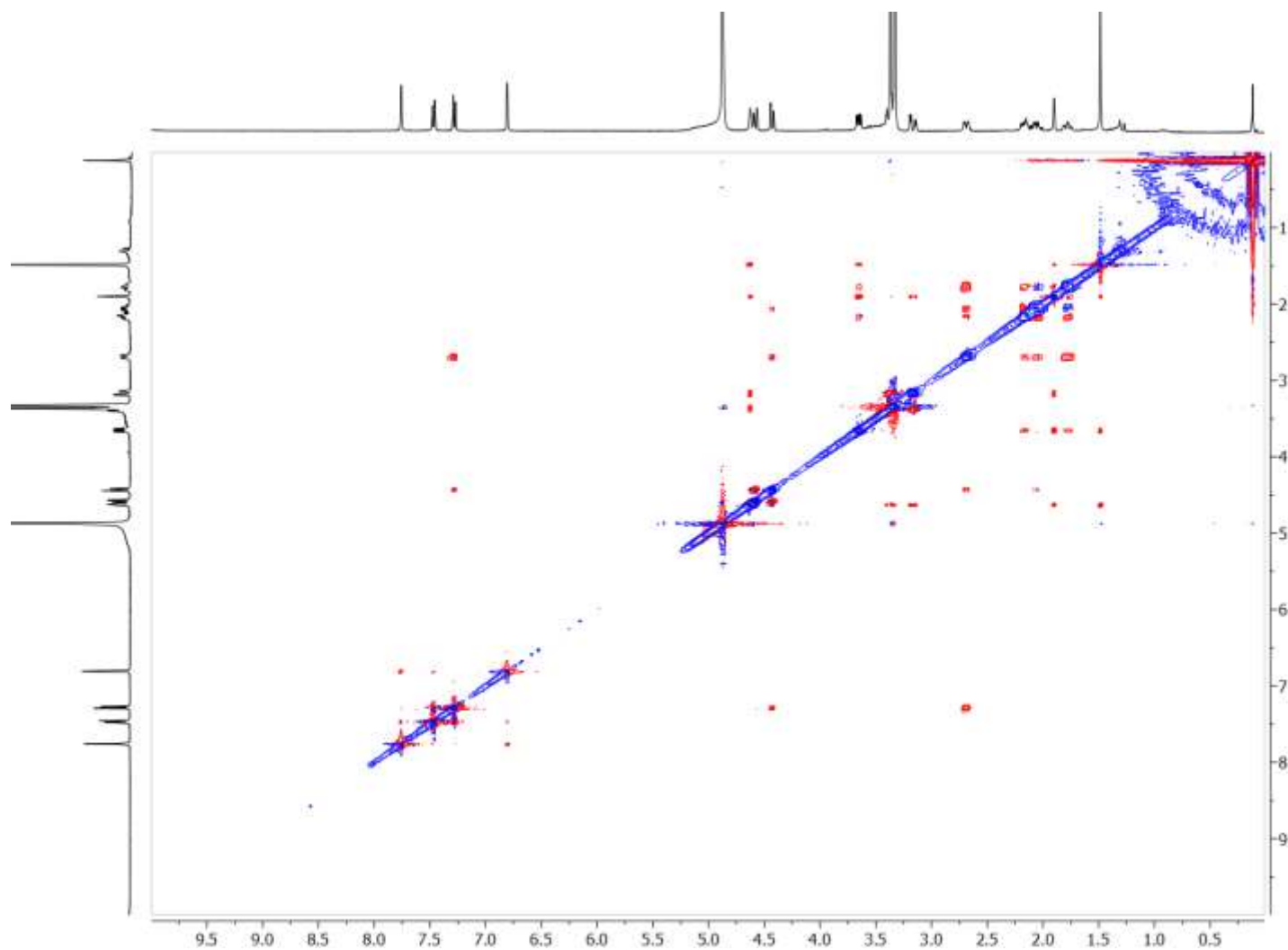


Figure 134. NOESY (400 MHz, CD₃OD) spectrum of 3-dehydroxy-icacinlactone A

APPENDIX A (continued)

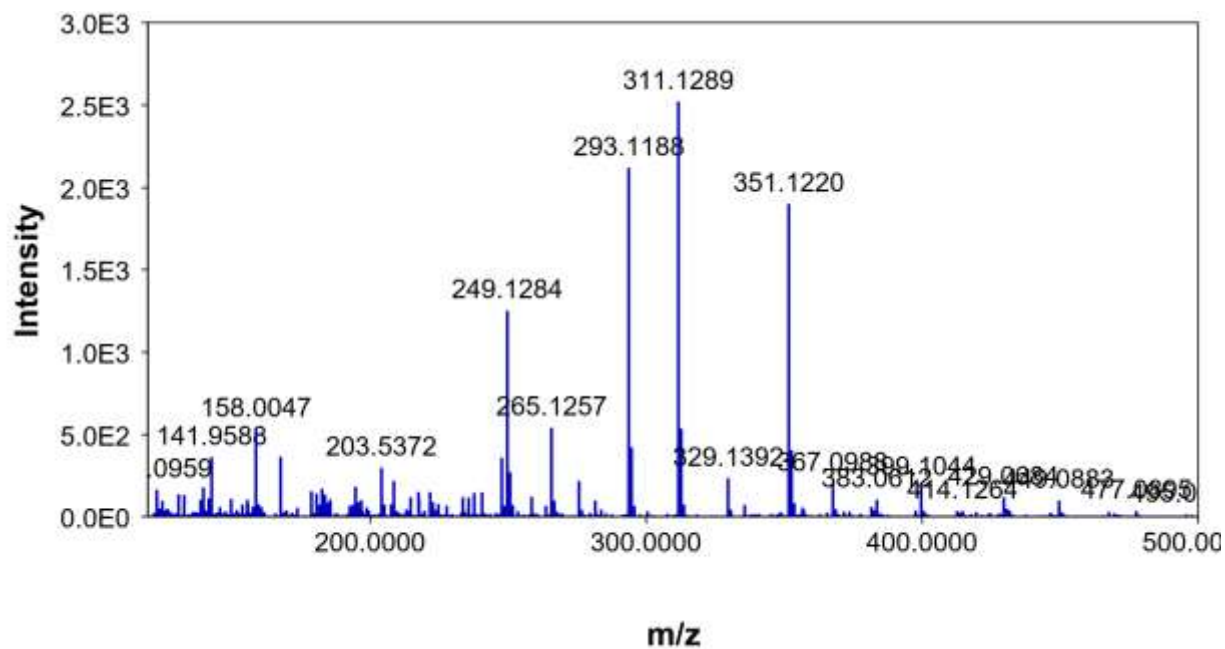
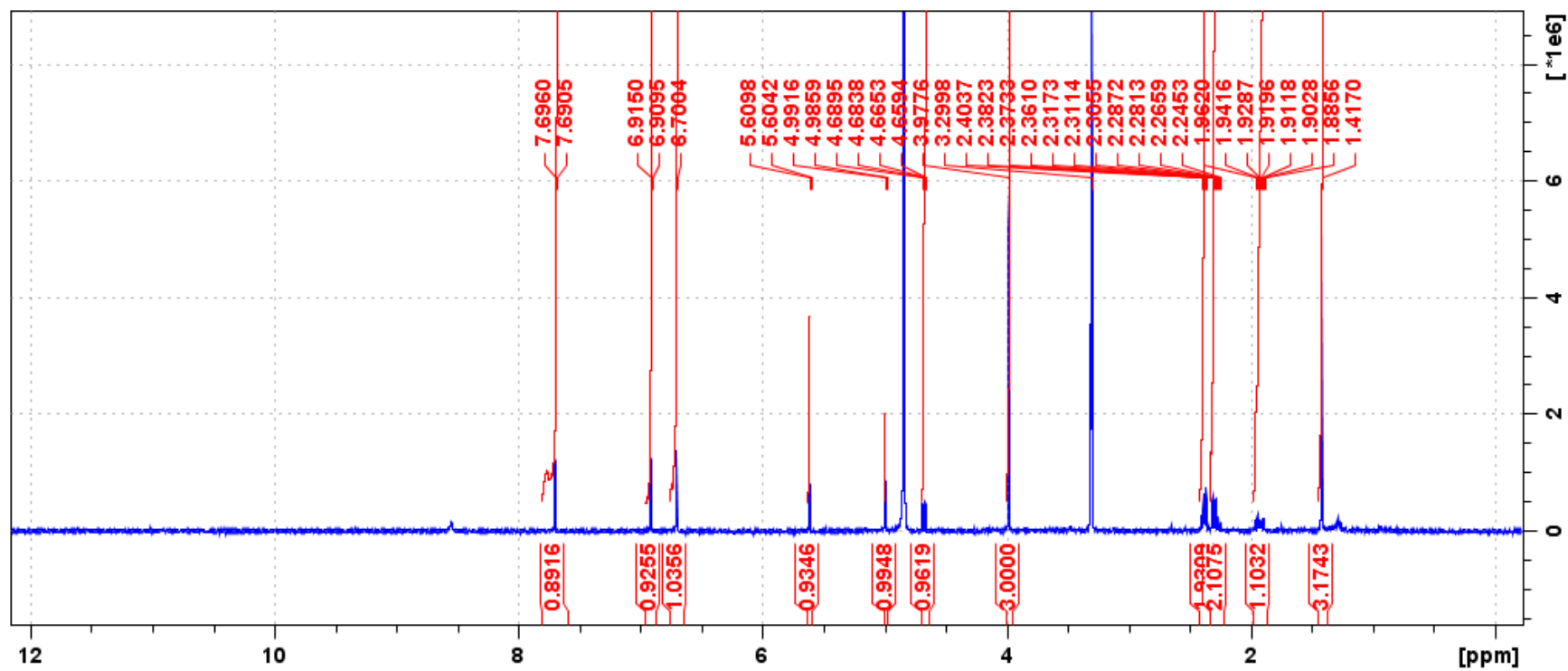
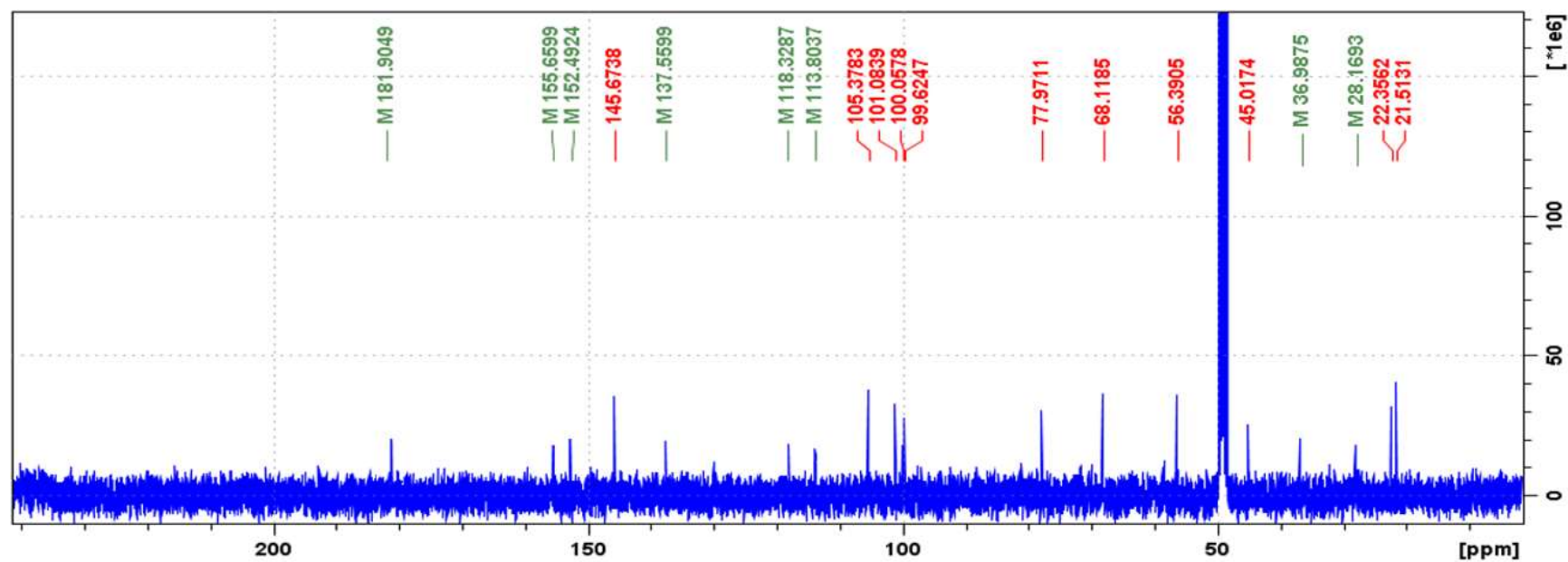


Figure 135. HRESIMS (+) spectrum of 3-dehydroxy-icacinlactone A

APPENDIX A (continued)

Figure 136. ^1H (400 MHz, CD_3OD) spectrum of icacinlactone L

APPENDIX A (continued)

Figure 137. ^{13}C (100 MHz, CD_3OD) spectrum of icacinlactone L

APPENDIX A (continued)

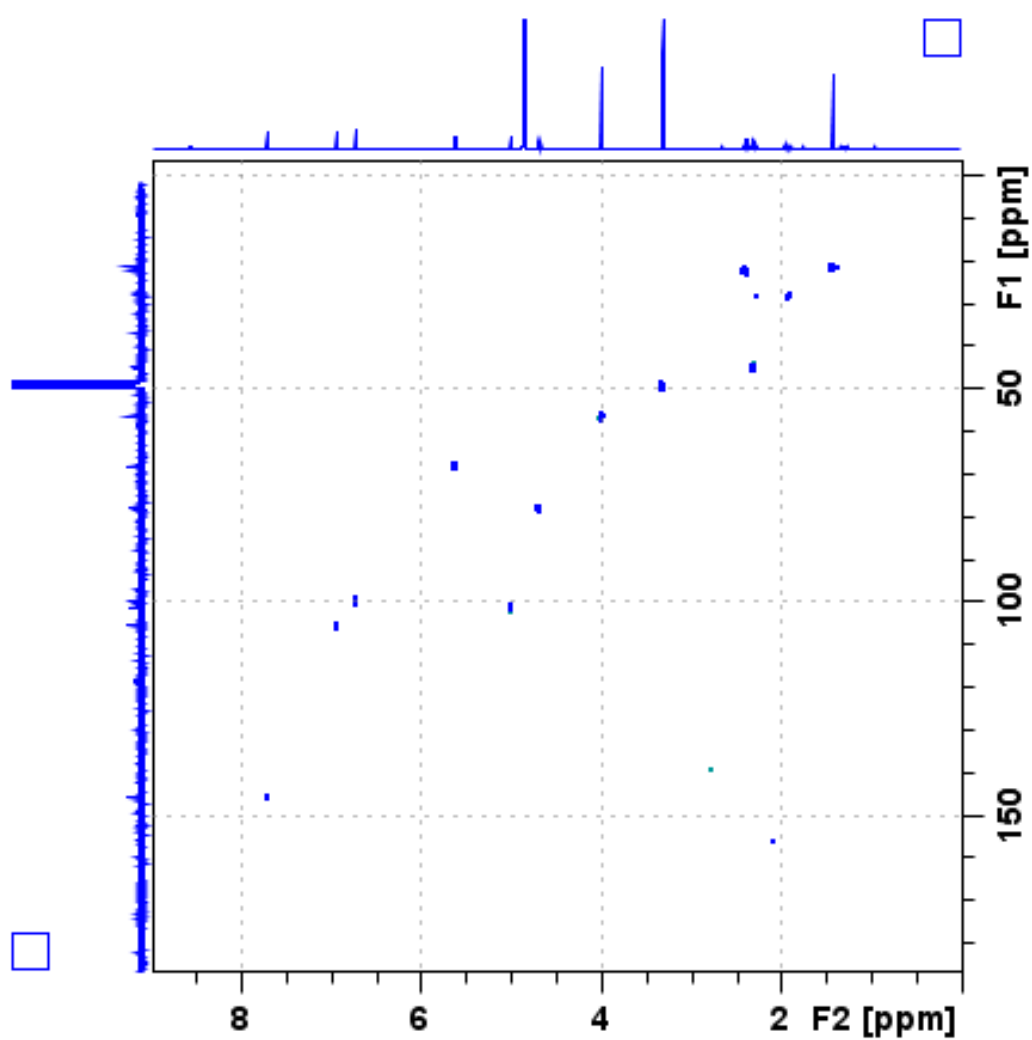


Figure 138. HSQC (400 MHz, CD₃OD) spectrum of icacinlactone L

APPENDIX A (continued)

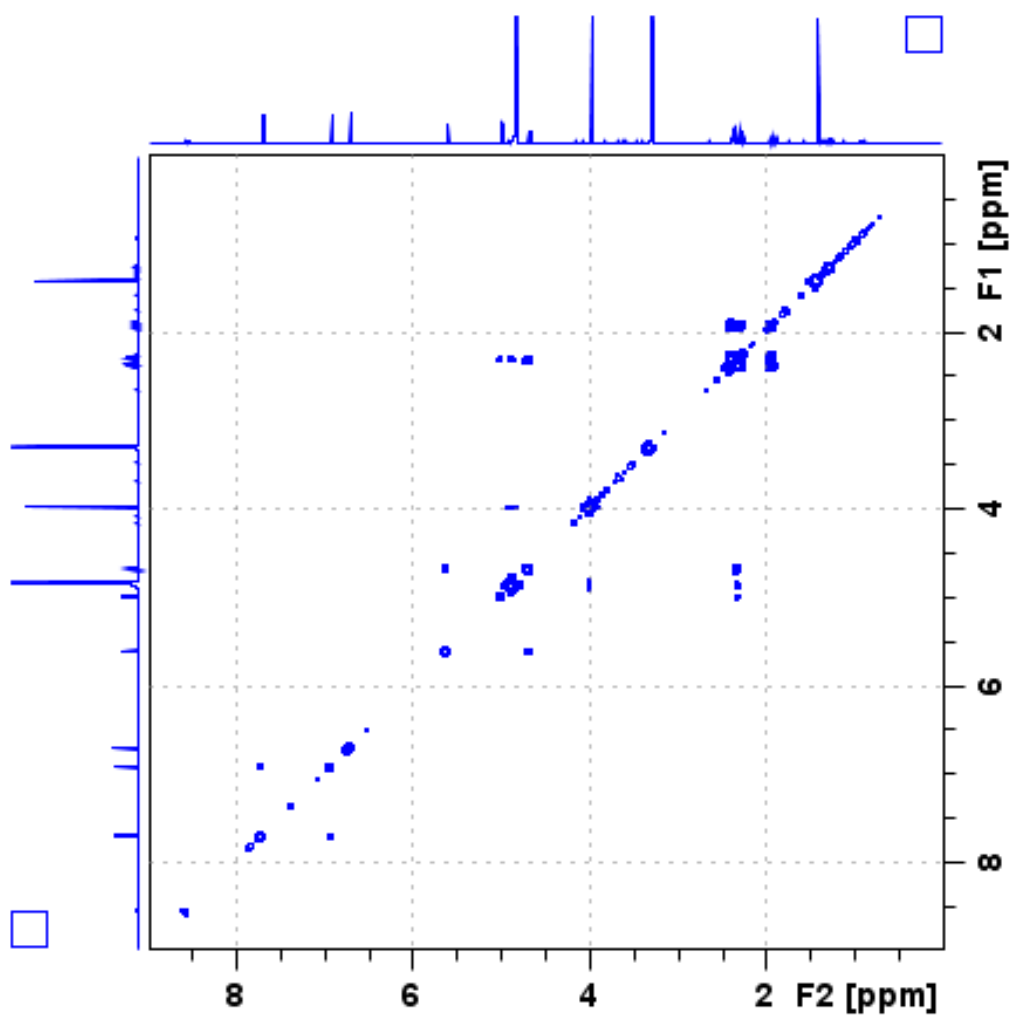


Figure 139. ^1H - ^1H COSY (400 MHz, CD_3OD) spectrum of icacinlactone L

APPENDIX A (continued)

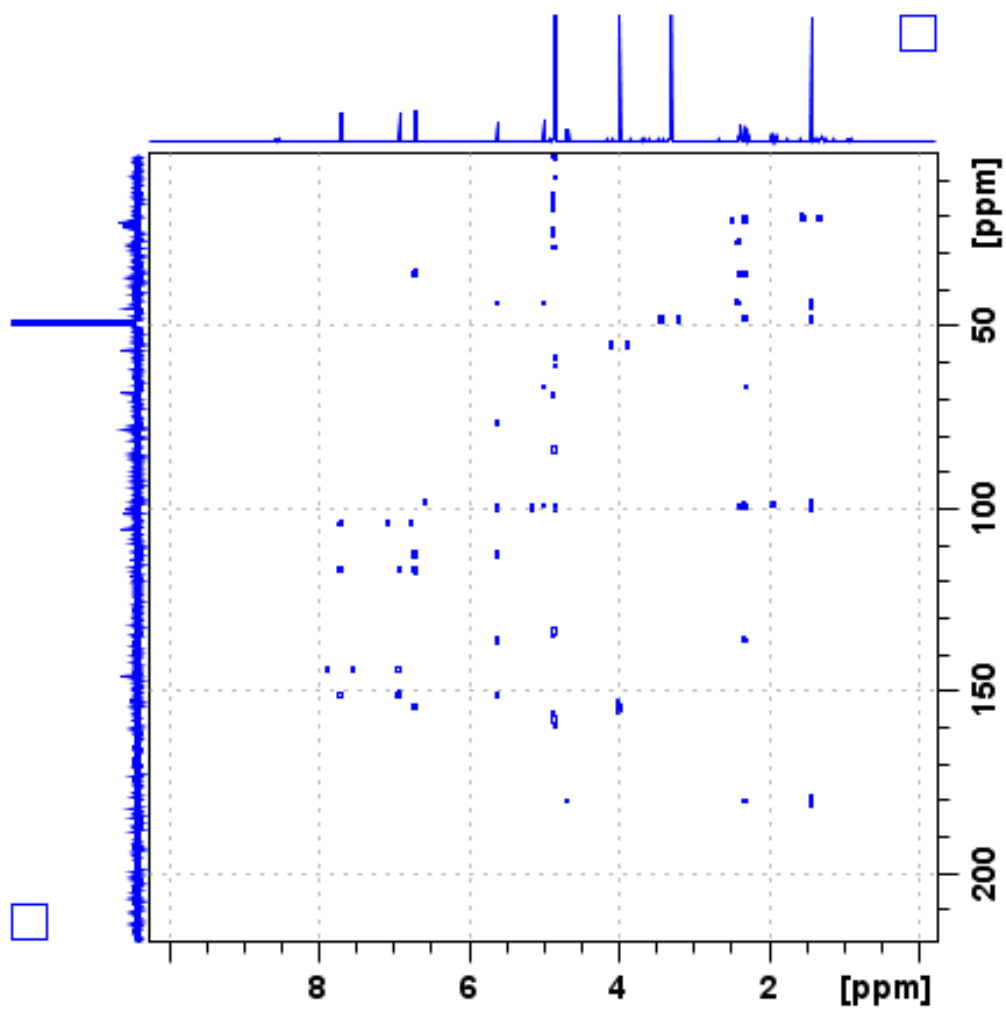


Figure 140. HMBC (400 MHz, CD₃OD) spectrum of icacinlactone L

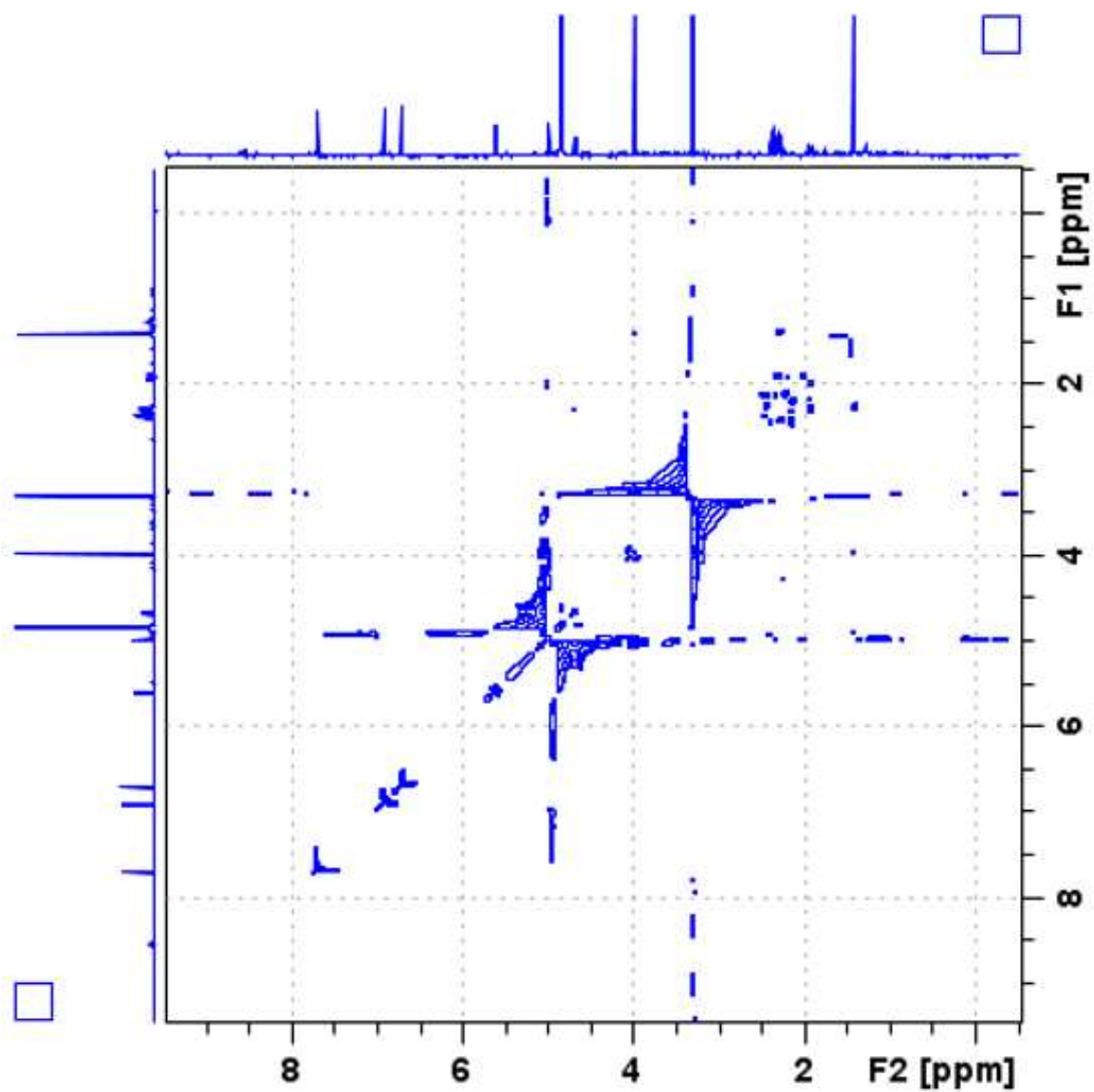
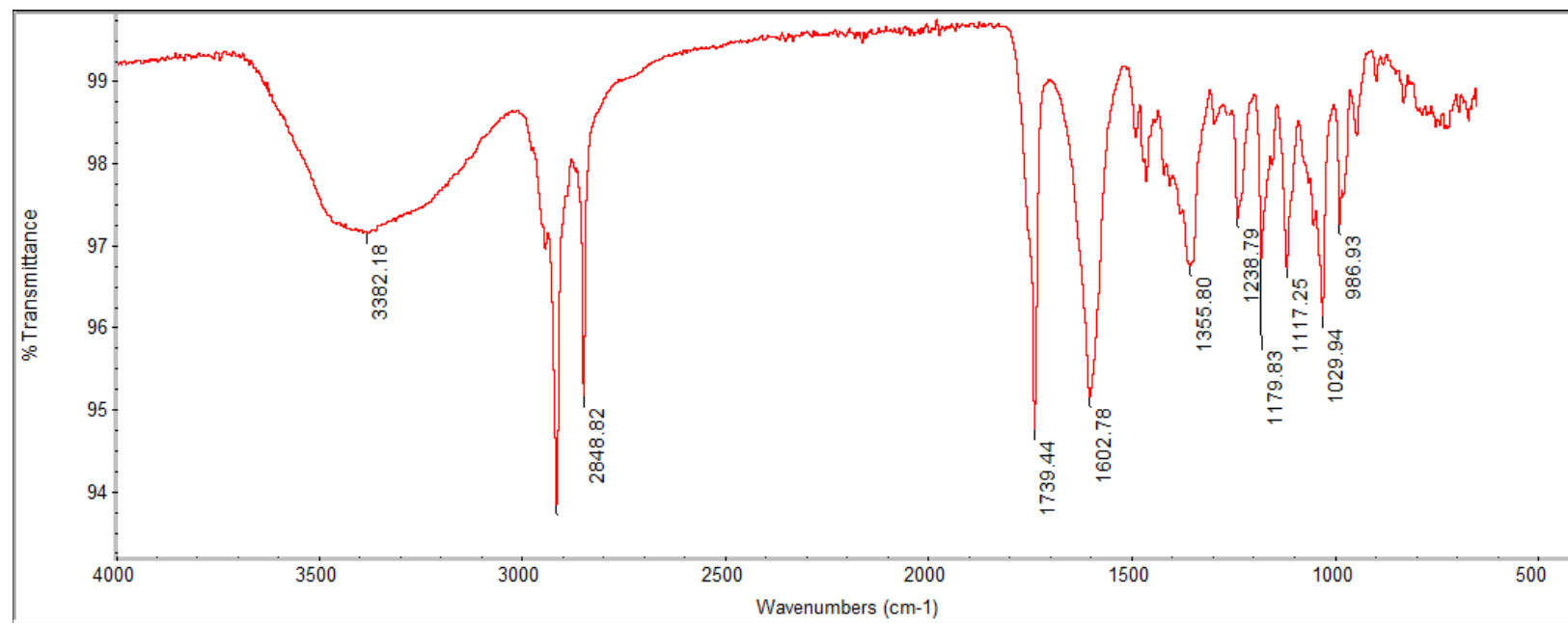


Figure 141. NOESY (400 MHz, CD₃OD) spectrum of icacinlactone L

APPENDIX A (continued)

**Figure 142. IR spectrum of icacinlactone L**

APPENDIX A (continued)

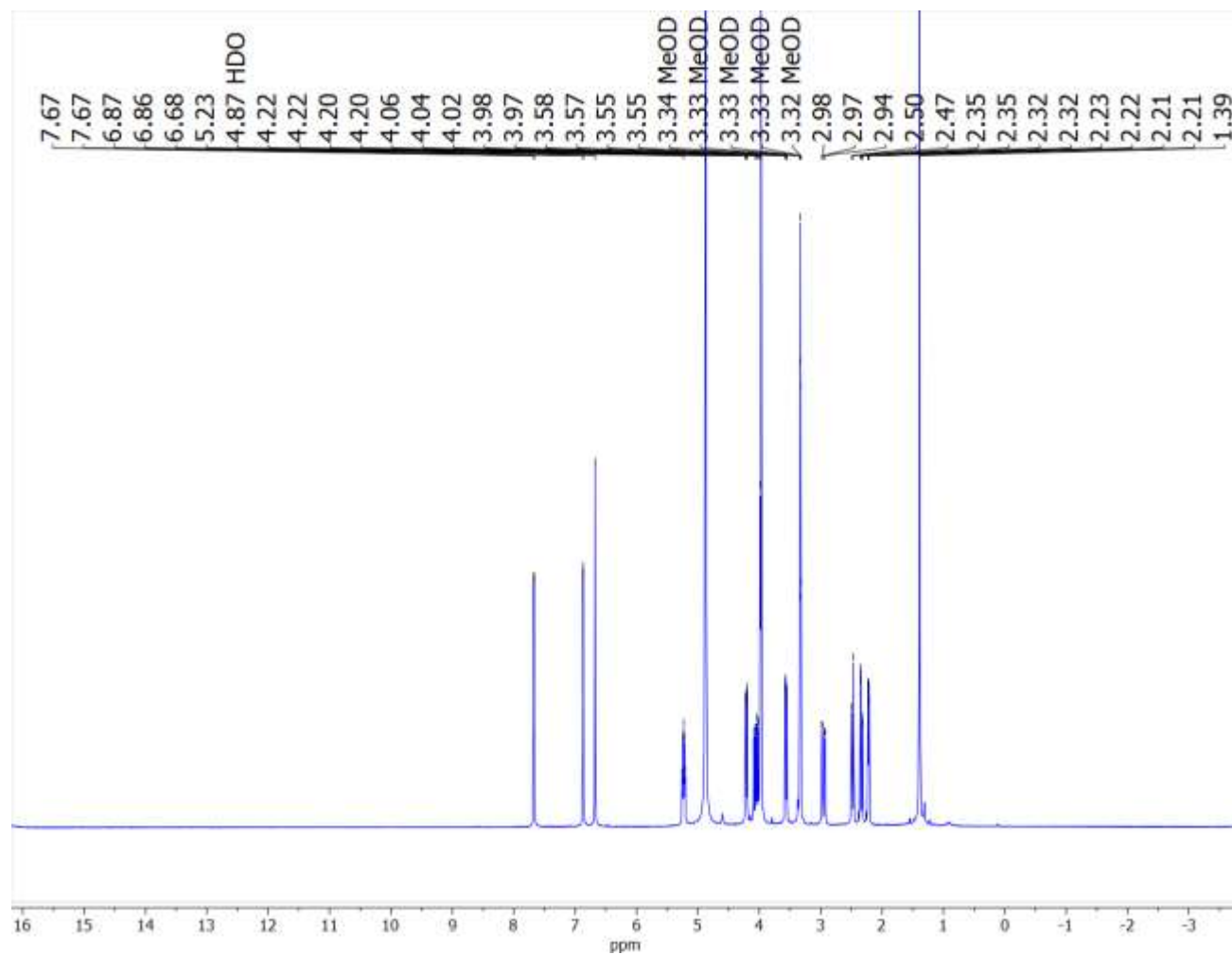


Figure 143. ¹H NMR (400 MHz, CD₃OD) spectrum of icacinlactone D

APPENDIX A (continued)

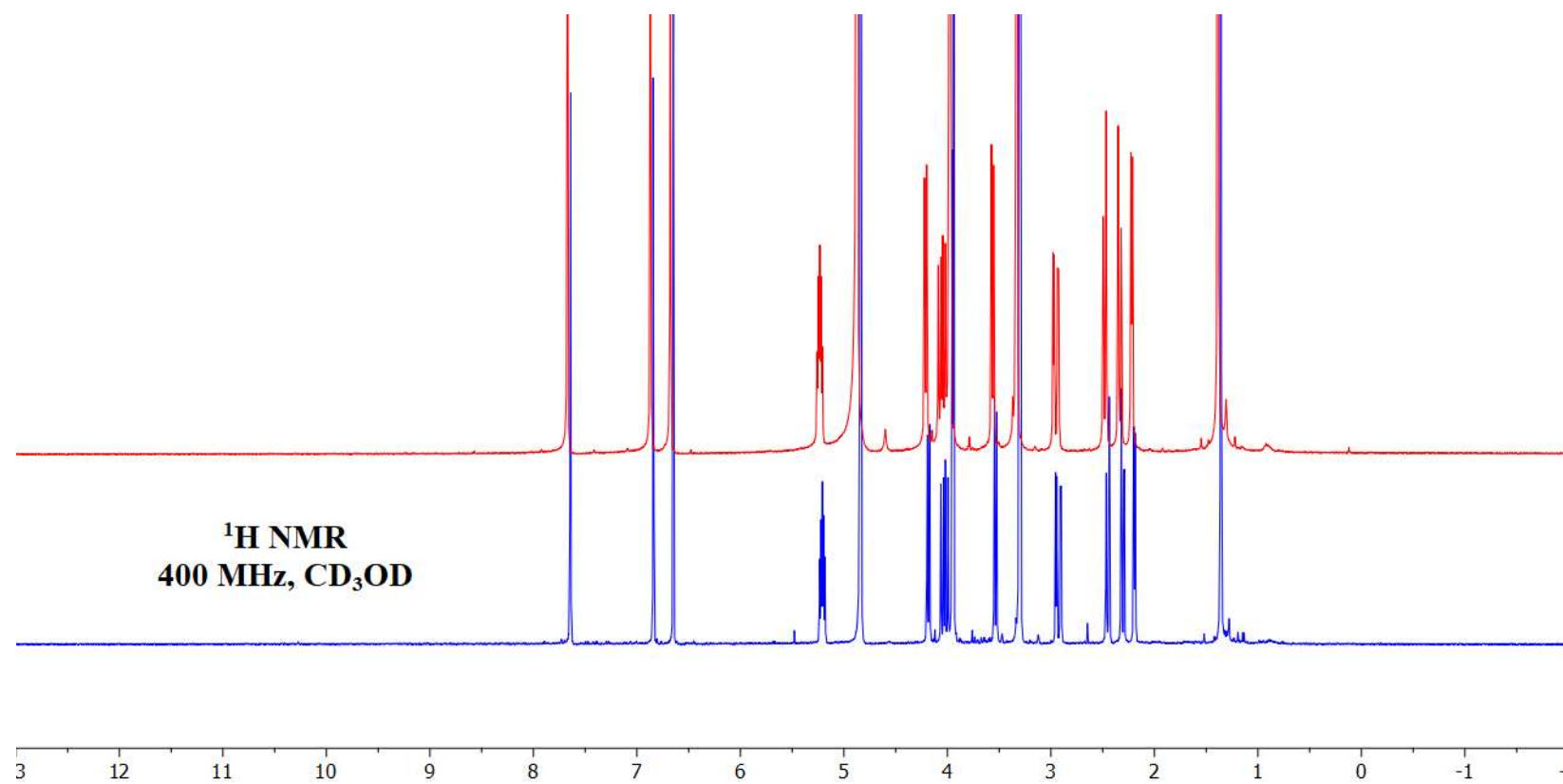
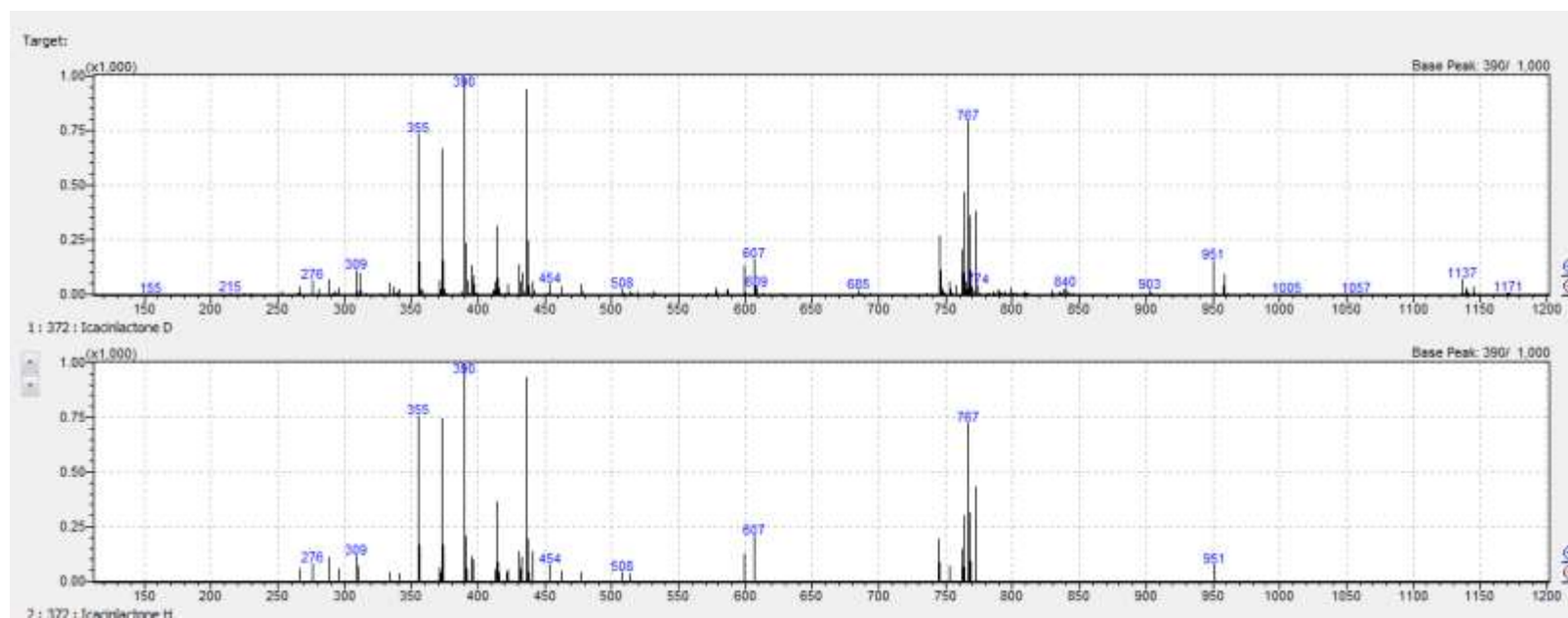


Figure 144. ¹H NMR (400 MHz, CD₃OD) spectra of compound 15 (red) and icacinlactone D standard (blue)

APPENDIX A (continued)

**Figure 145. LC-MS library similarity search for icacinlactone D**

APPENDIX A (continued)

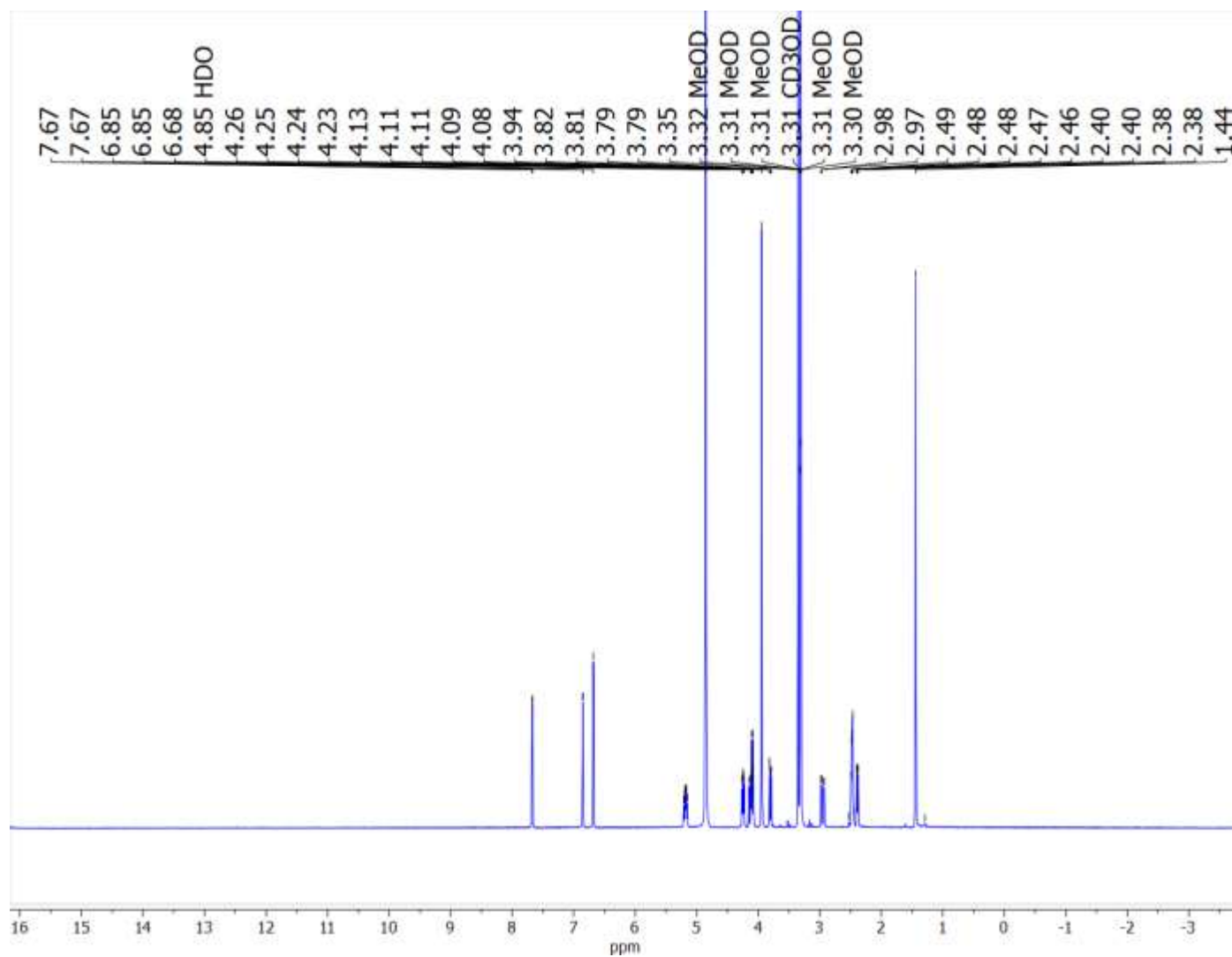


Figure 146. ^1H NMR (400 MHz, CD_3OD) spectrum of icacinlactone H

APPENDIX A (continued)

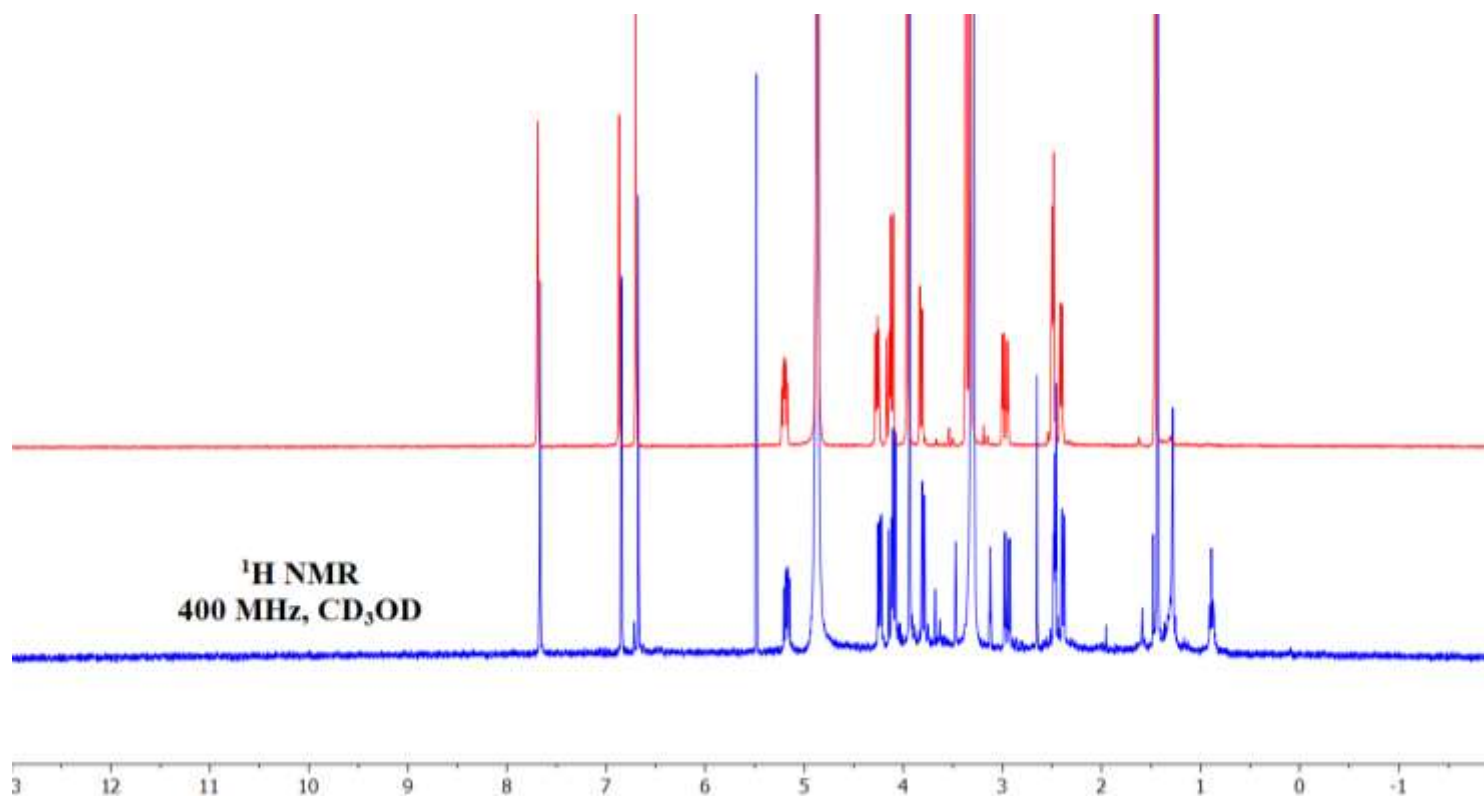


Figure 147. ^1H NMR (400 MHz) spectra of compound 15 (red) and icacinlactone H standard (blue)

APPENDIX A (continued)

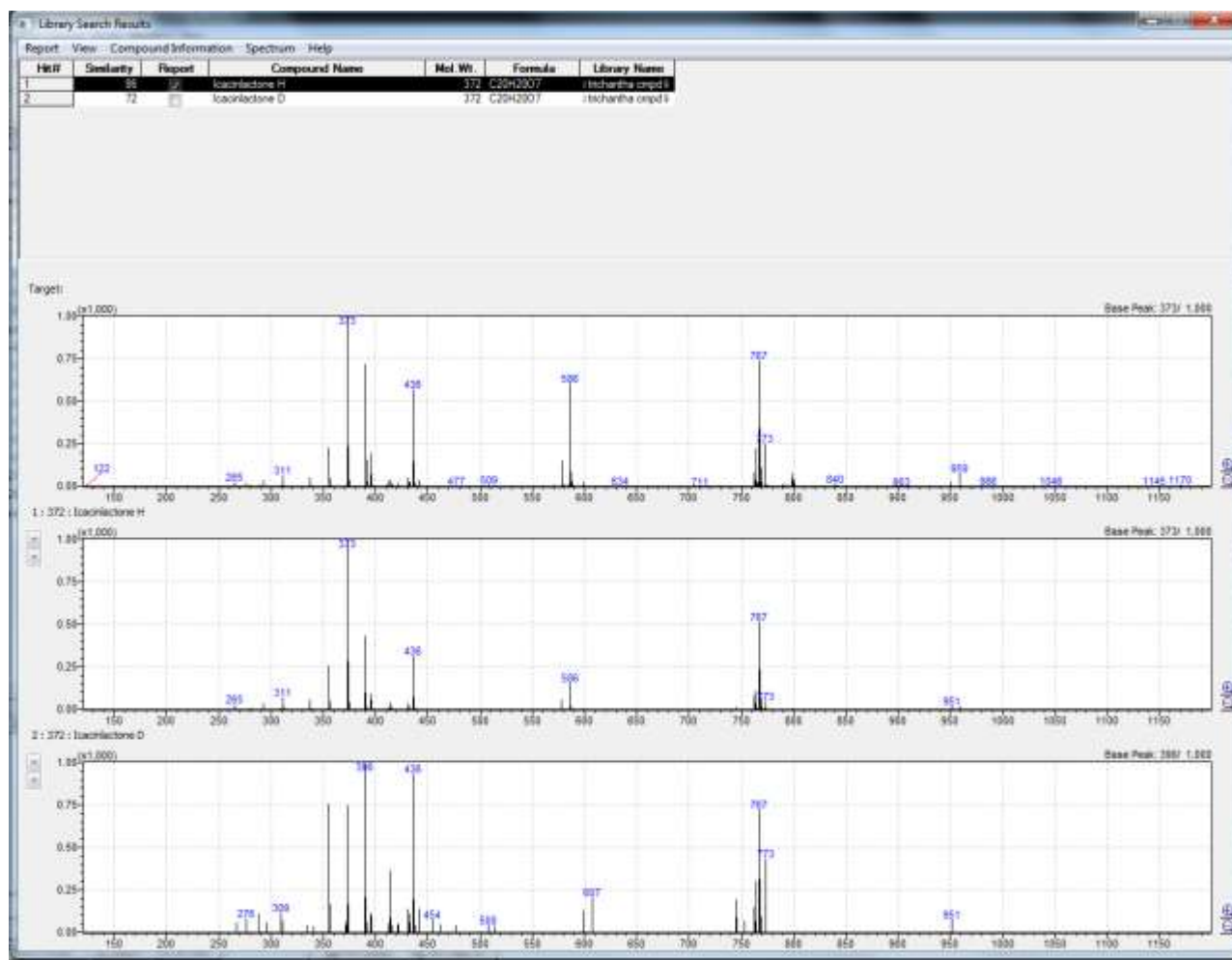
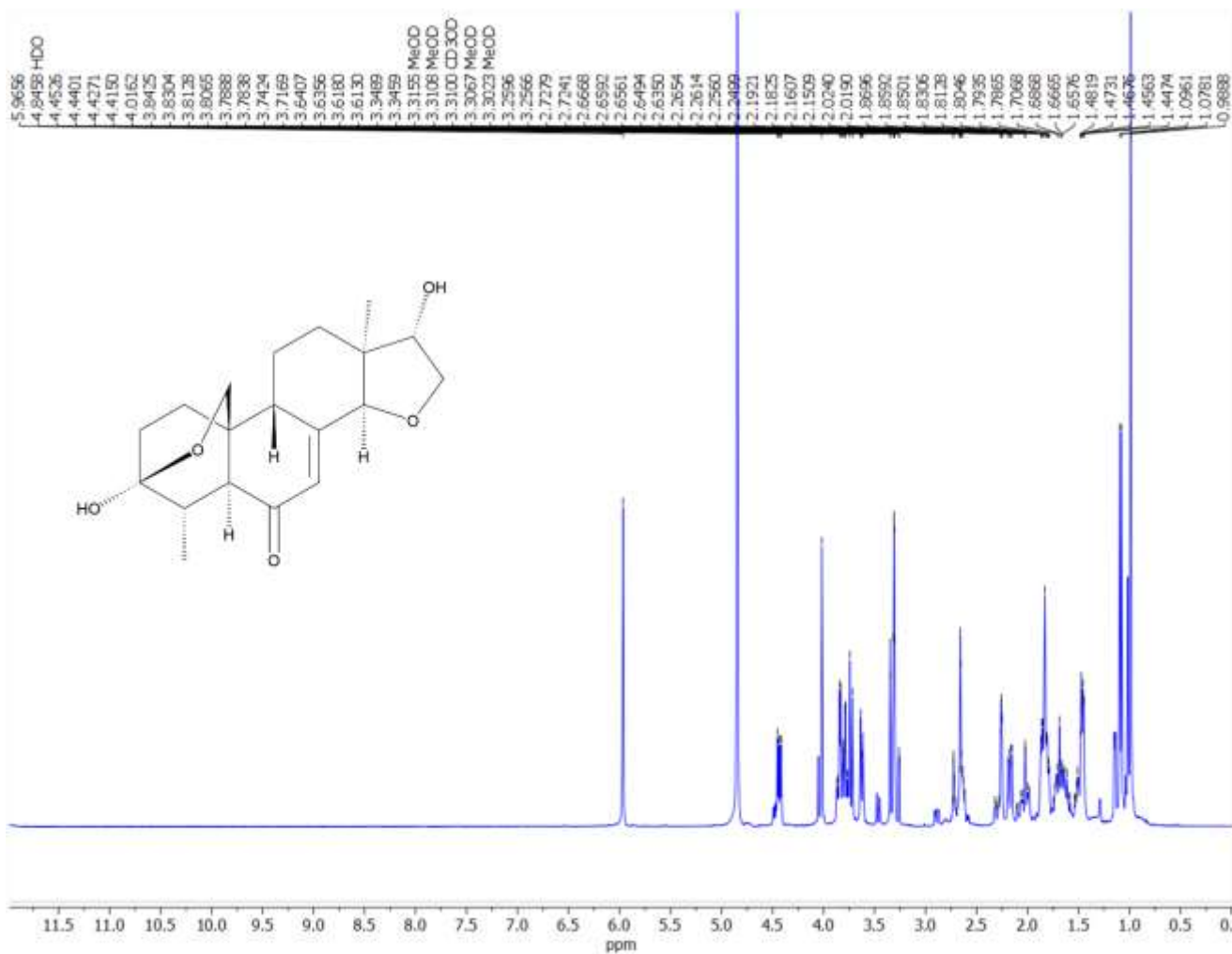


Figure 148. LC-MS library similarity search for icacinlactone H

APPENDIX A (continued)

Figure 149. ^1H NMR (400 MHz, CD_3OD) spectrum of icatrichanone

APPENDIX A (continued)

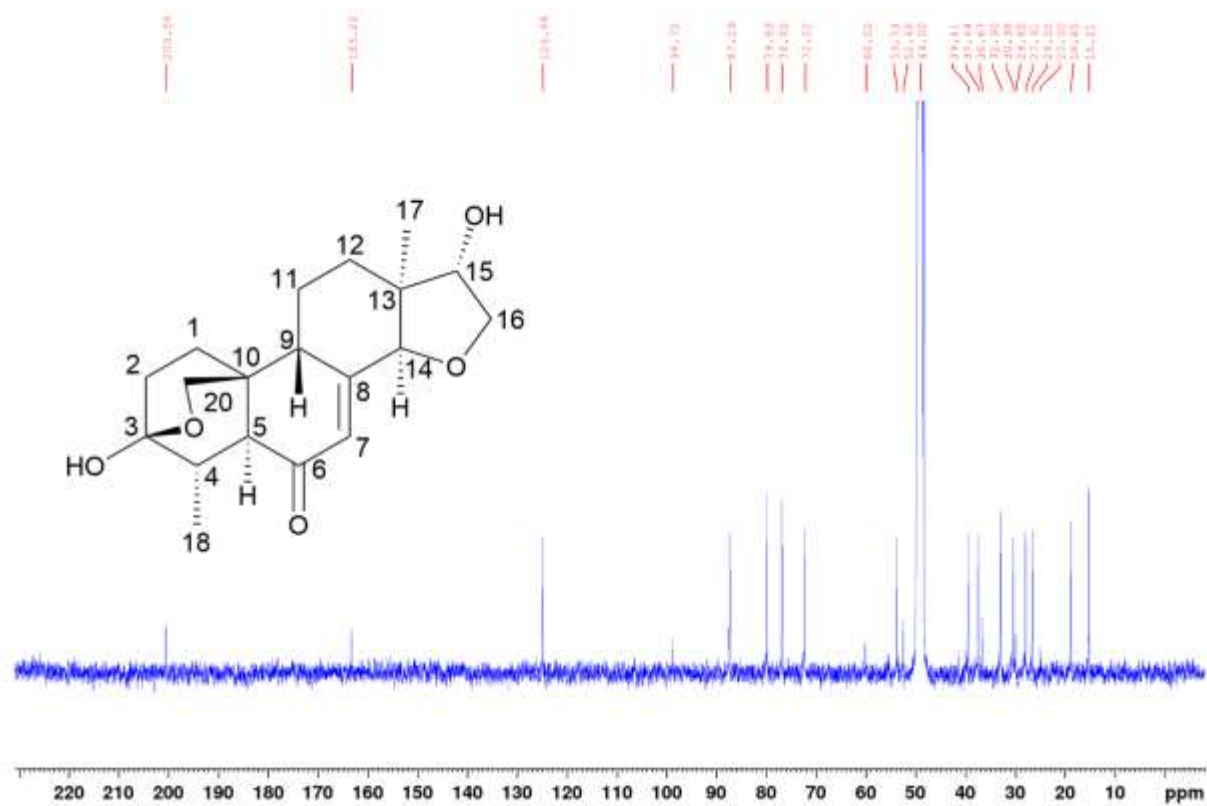


Figure 150. ^{13}C NMR (100 MHz, CD_3OD) spectrum of icatrichanone

APPENDIX A (continued)

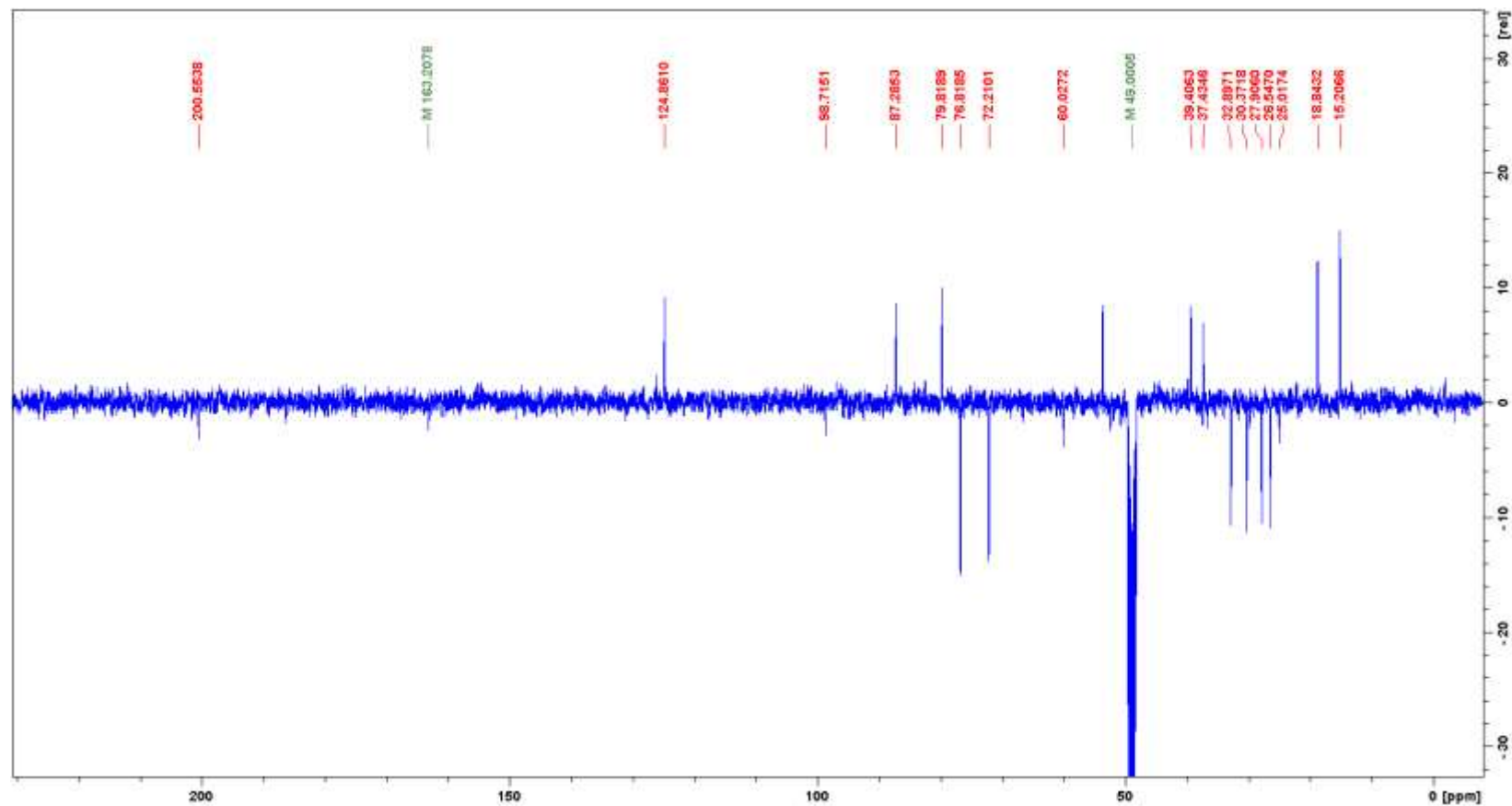


Figure 151. DEPTQ (100 MHz, CD₃OD) spectrum of icatrichanone

APPENDIX A (continued)

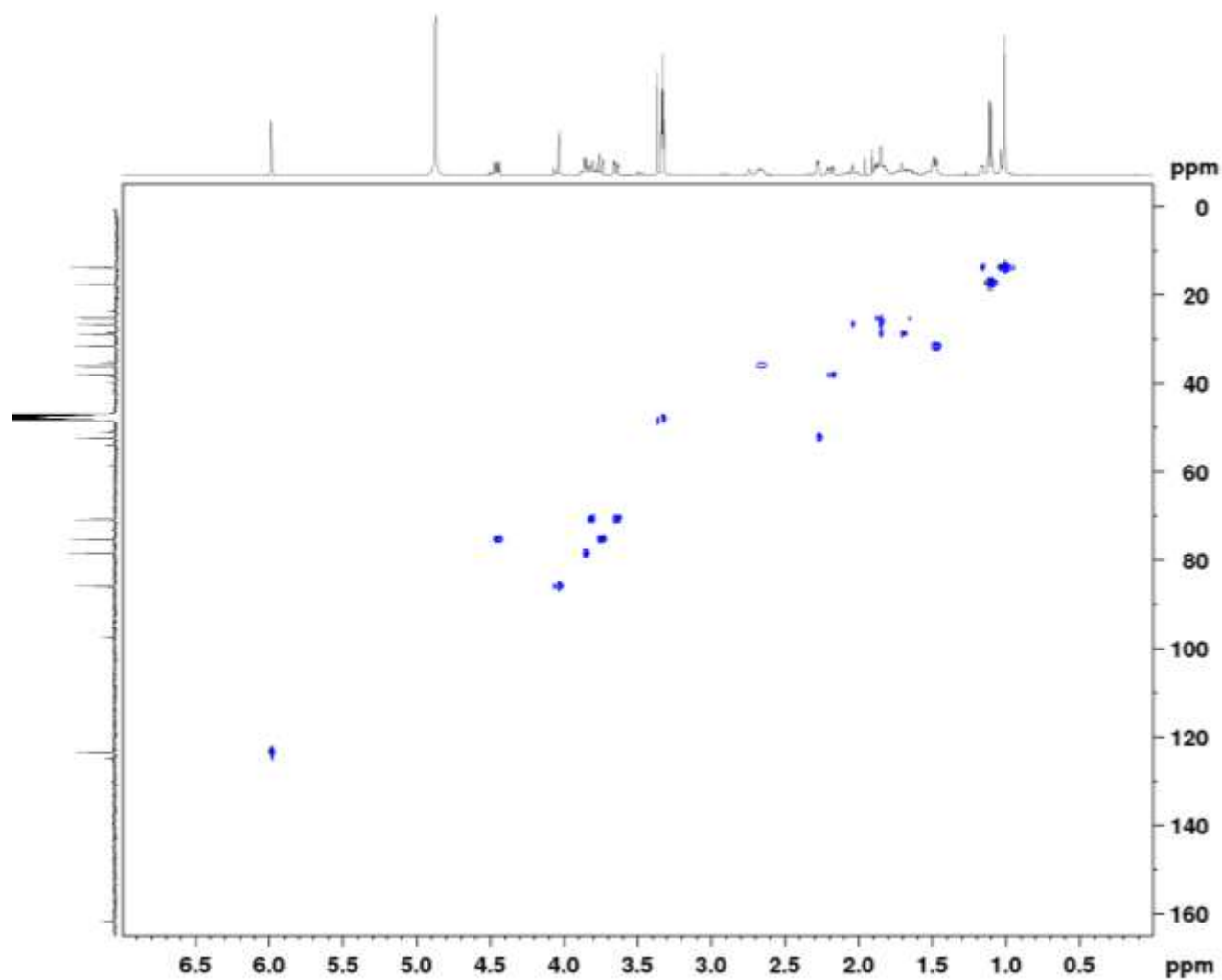


Figure 152. HSQC NMR (400 MHz, CD_3OD) spectrum of icatrichanone

APPENDIX A (continued)

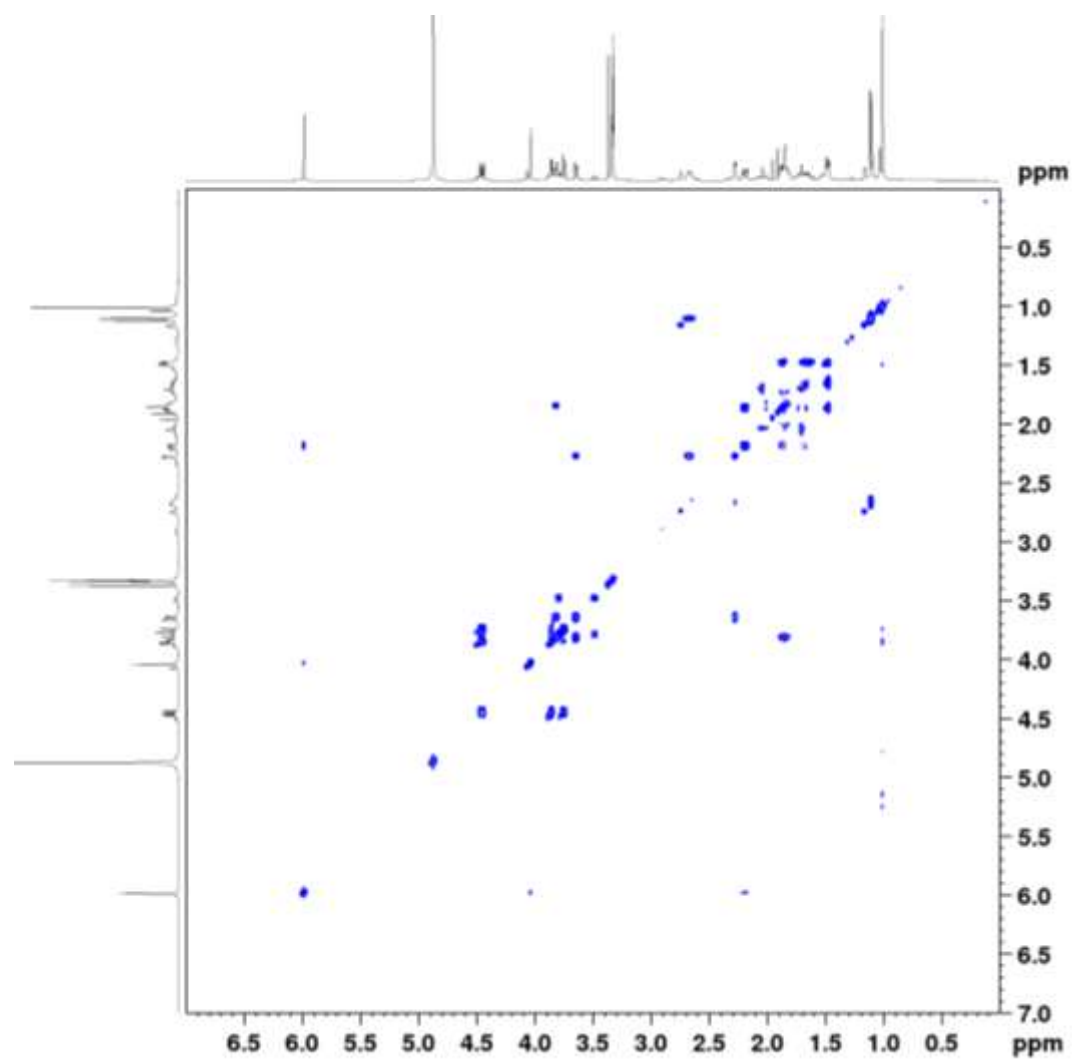


Figure 153. ^1H - ^1H COSY NMR (400 MHz, CD_3OD) spectrum of icatrichanone

APPENDIX A (continued)

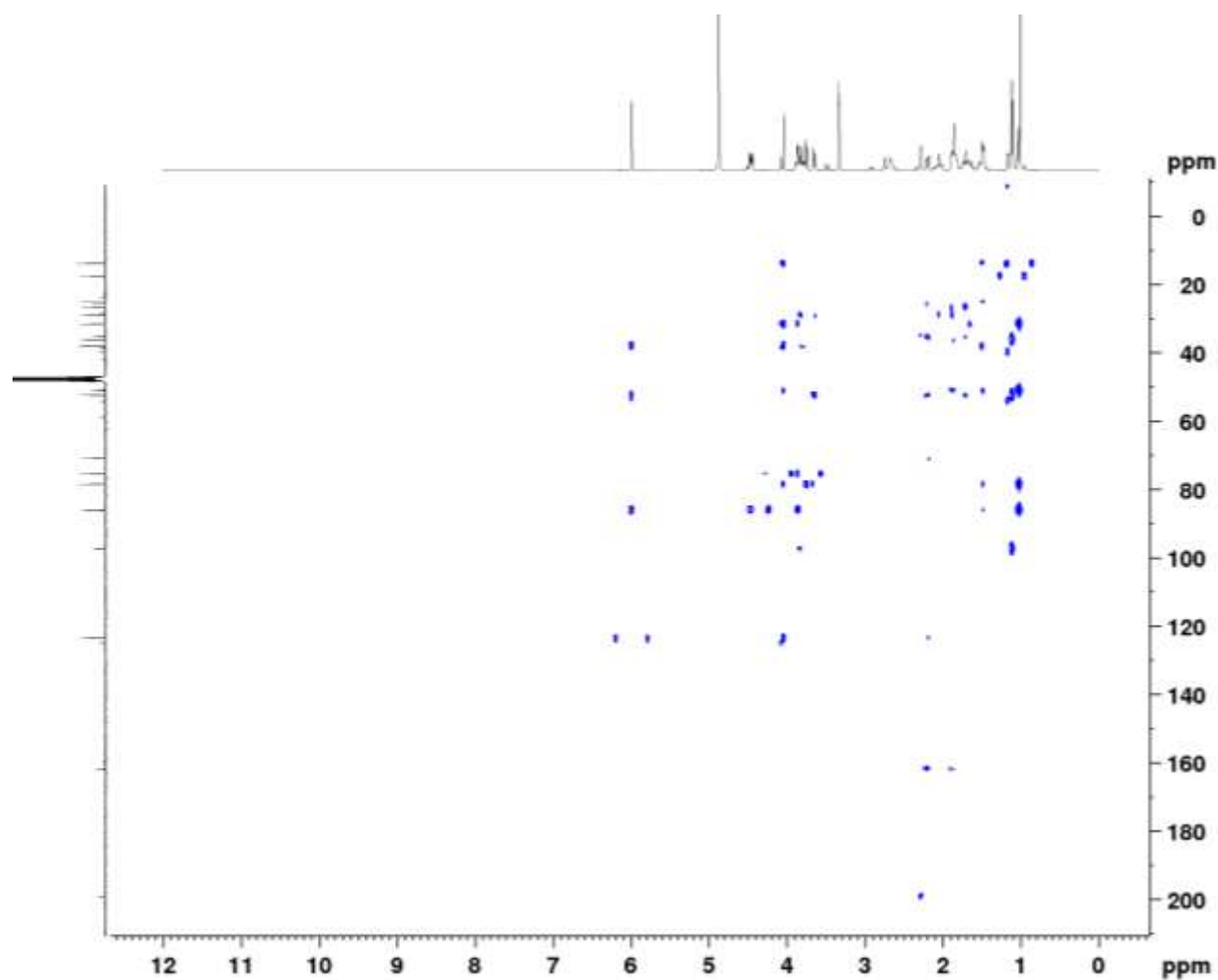


Figure 154. HMBC NMR (400 MHz, CD_3OD) spectrum of icatrichanone

APPENDIX A (continued)

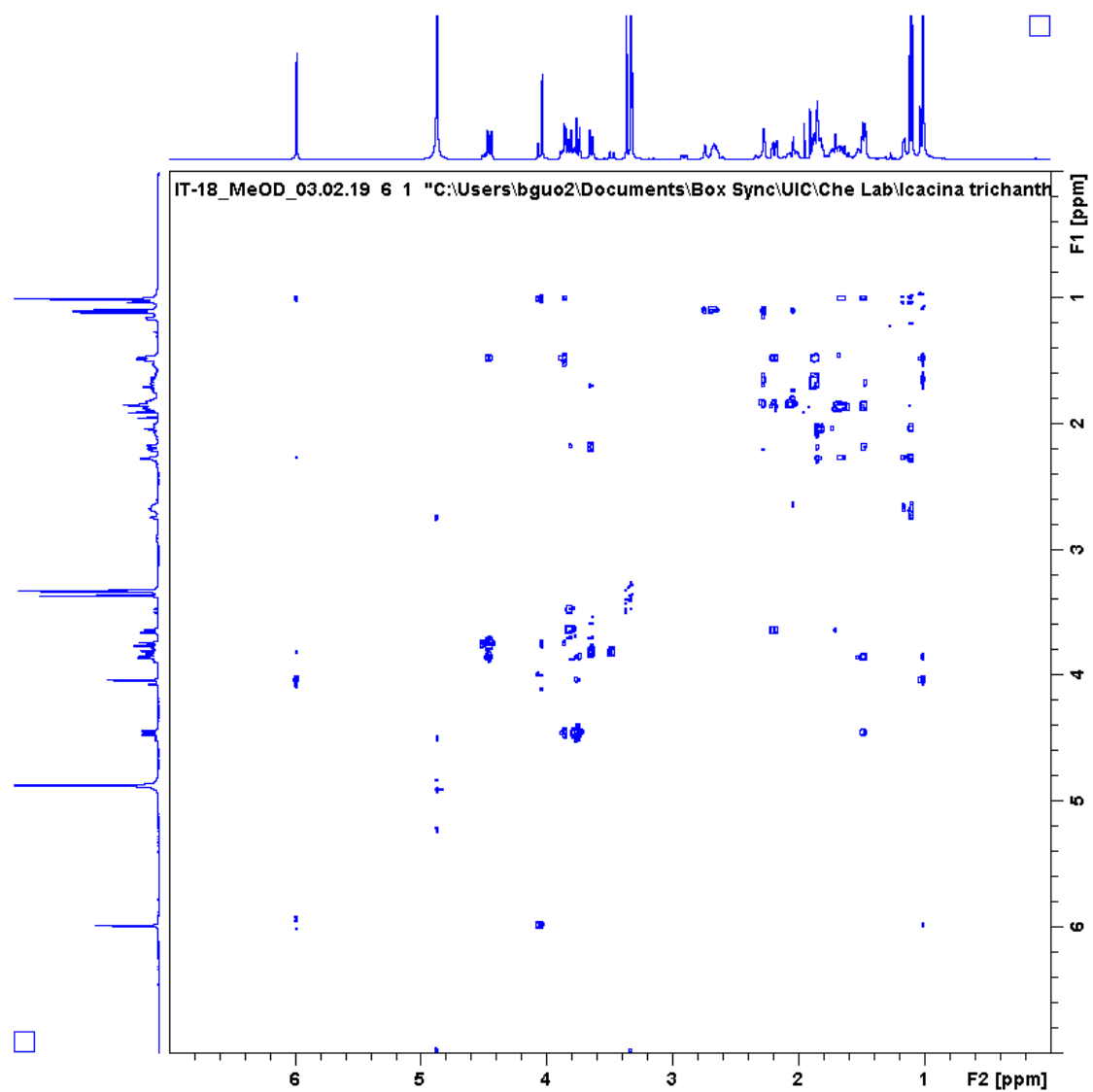
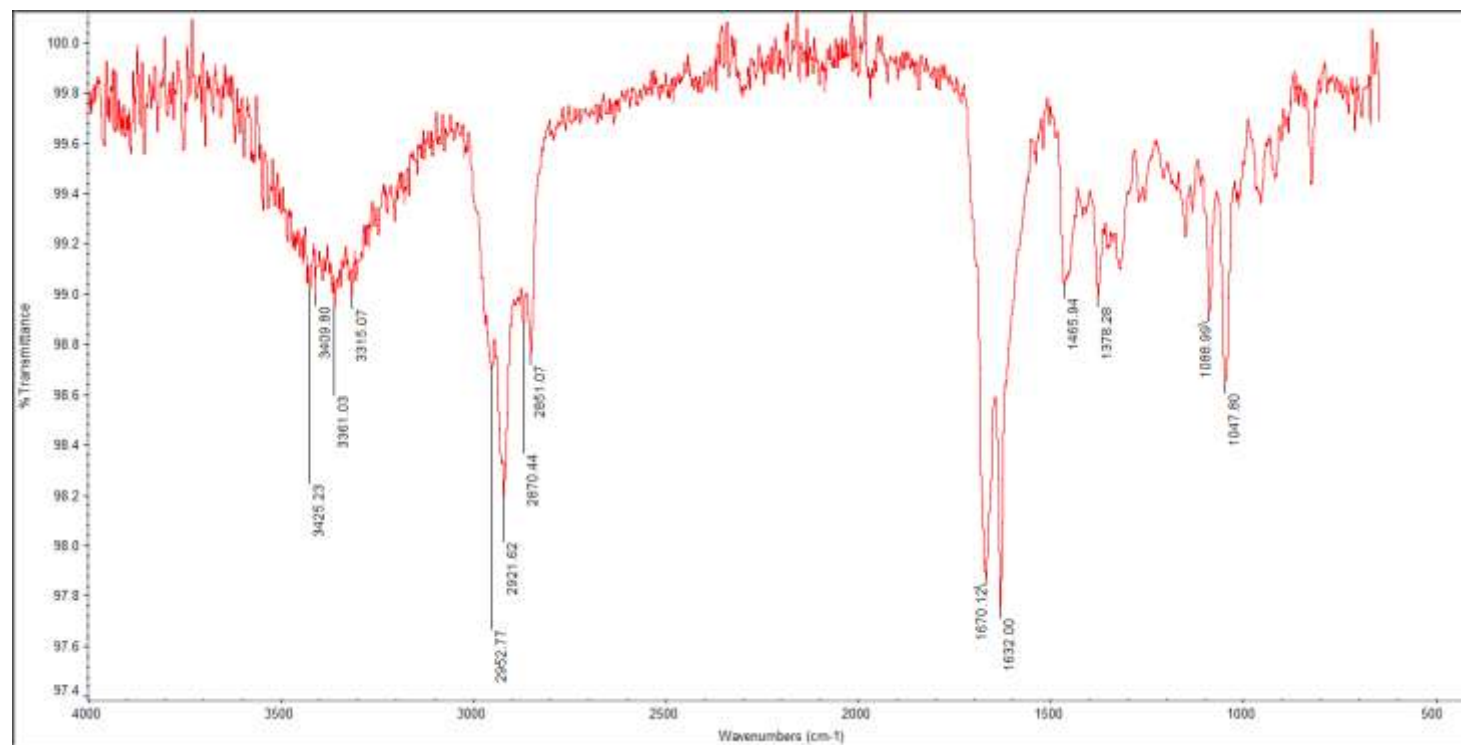
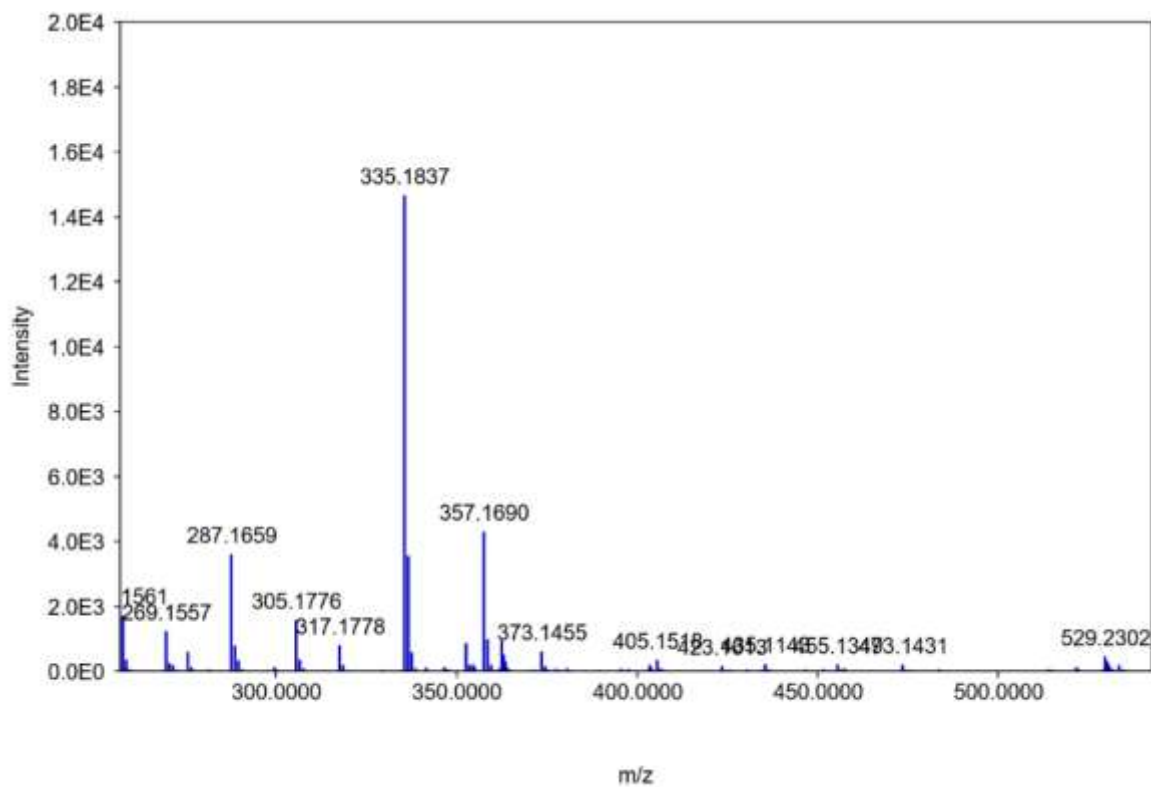


Figure 155. NOESY NMR (400 MHz, CD₃OD) spectrum of icatrichanone

APPENDIX A (continued)

**Figure 156. IR spectrum of icatrichanone**

APPENDIX A (continued)

**Figure 157. HRESIMS (+) spectrum of icatrichanone**

APPENDIX A (continued)

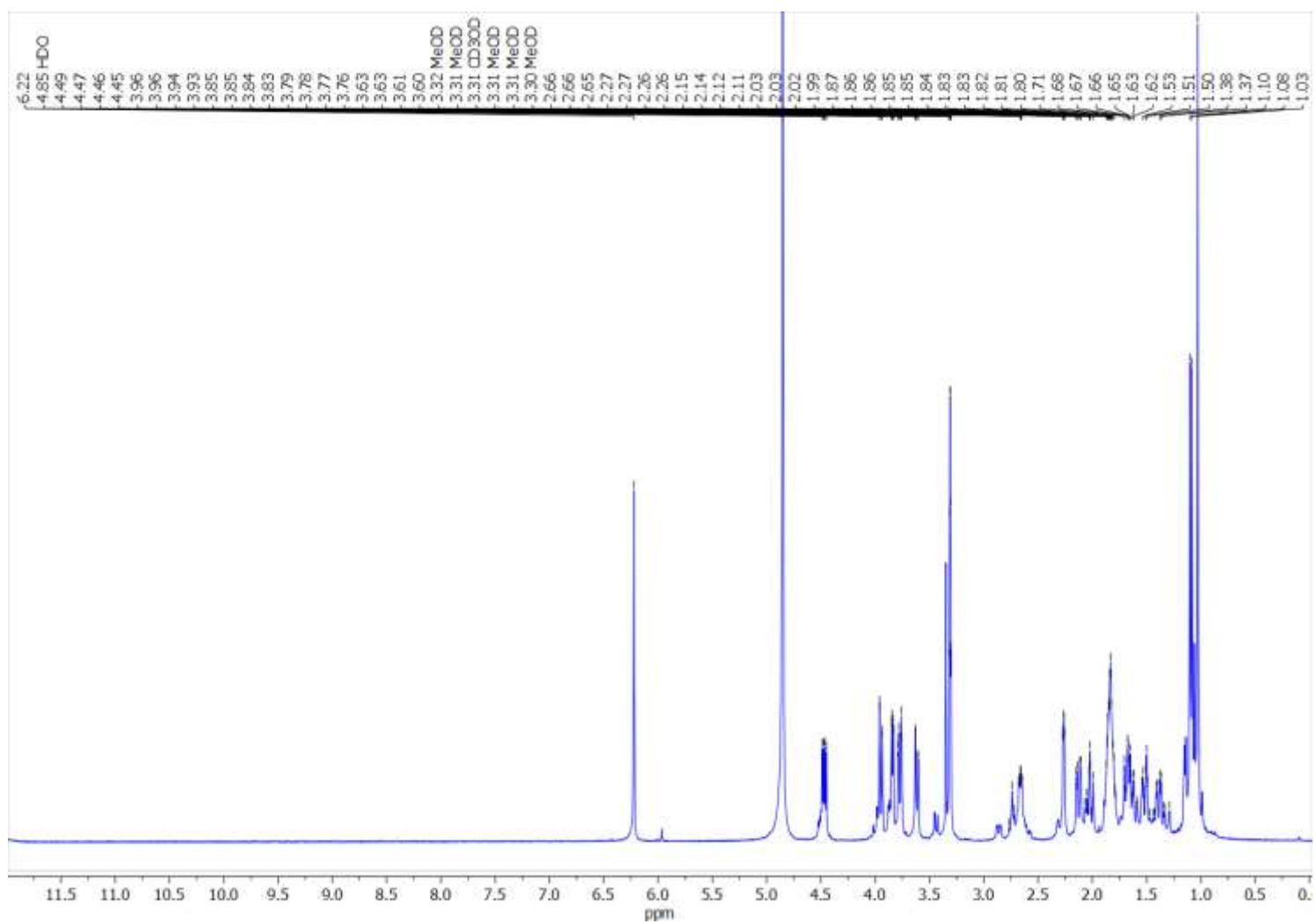


Figure 158. ^1H NMR (400 MHz, CD_3OD) spectrum of 14-hydroxyatricchanone

APPENDIX A (continued)

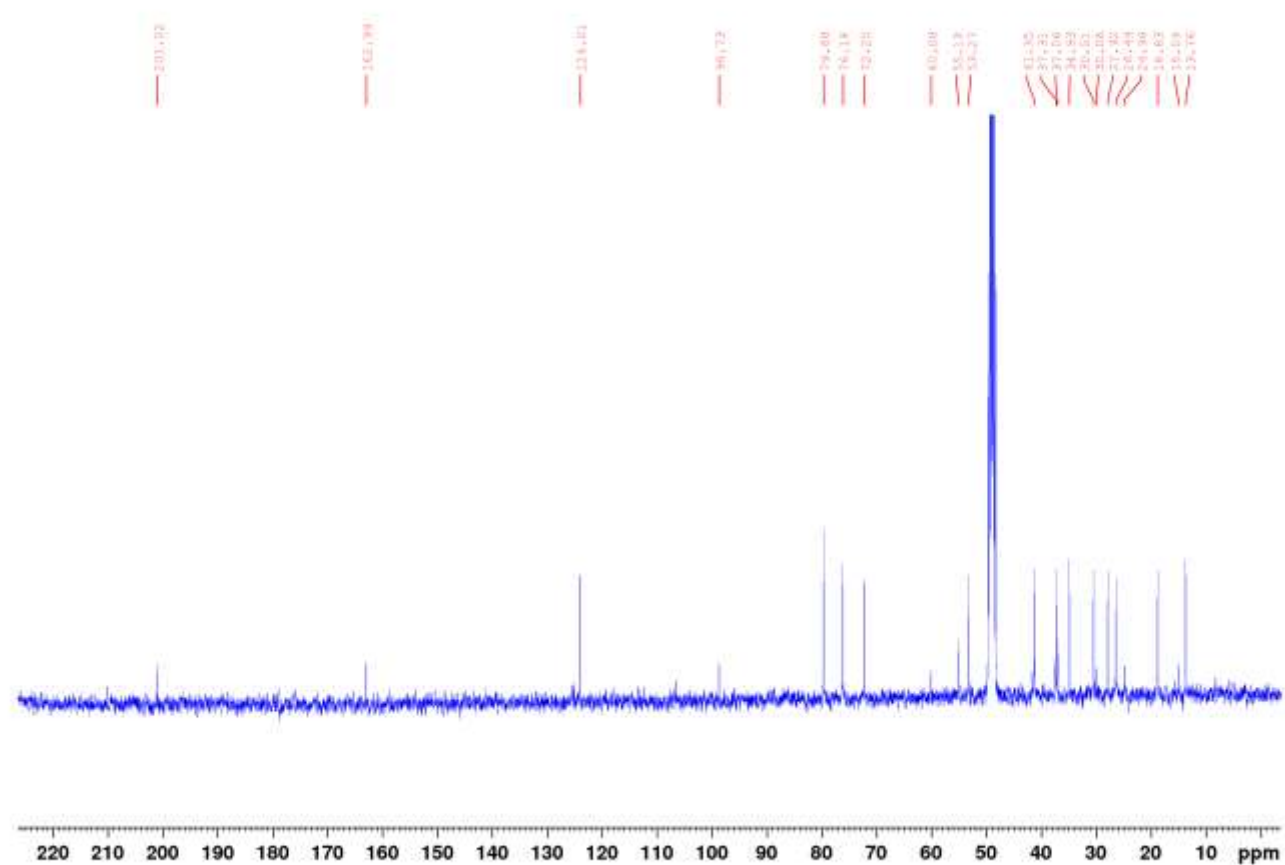


Figure 159. ¹³C NMR (100 MHz, CD₃OD) spectrum of 14-hydroxyatrichanone

APPENDIX A (continued)

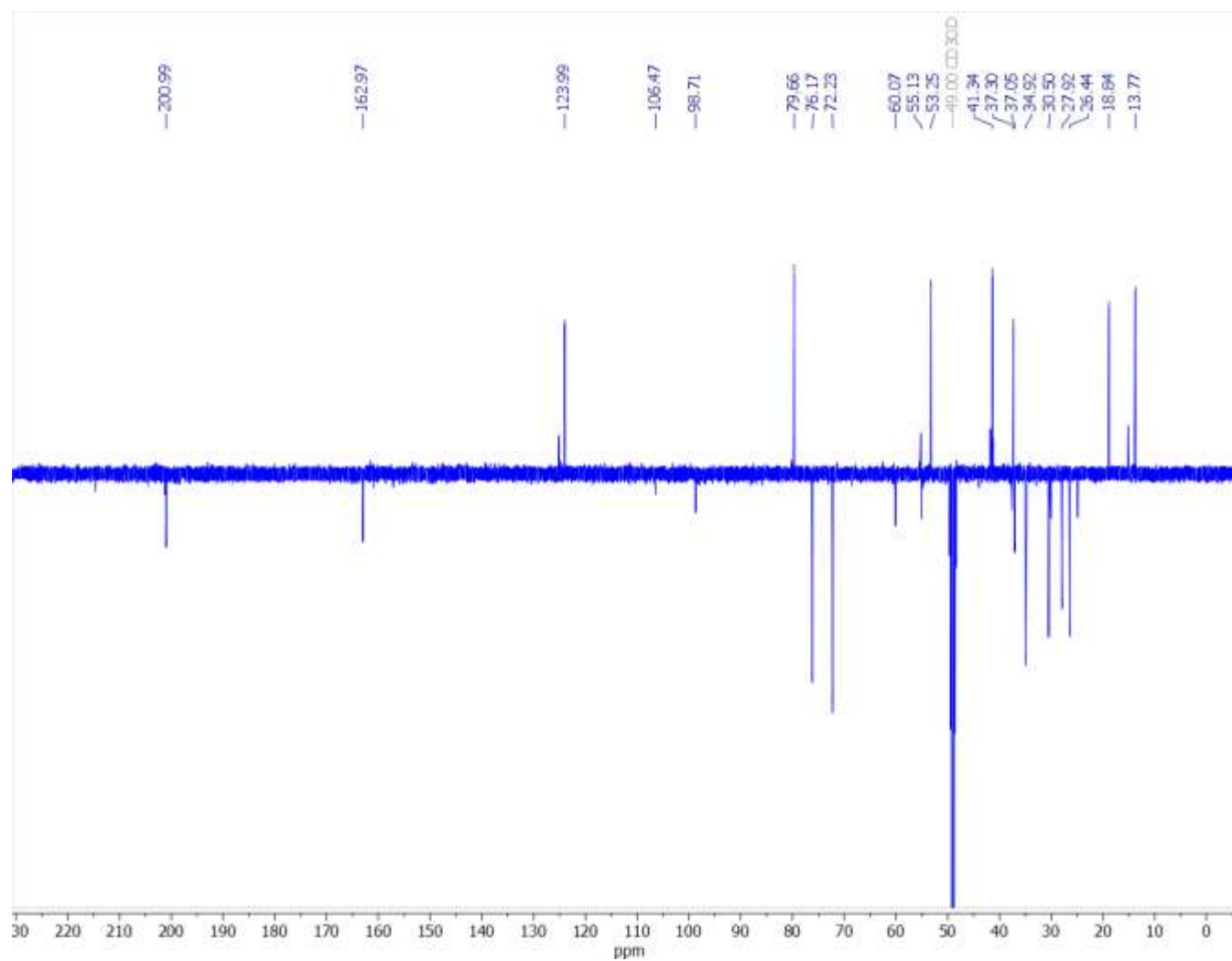


Figure 160. DEPTQ NMR (100 MHz, CD₃OD) spectrum of 14-hydroxyatrichanone

APPENDIX A (continued)

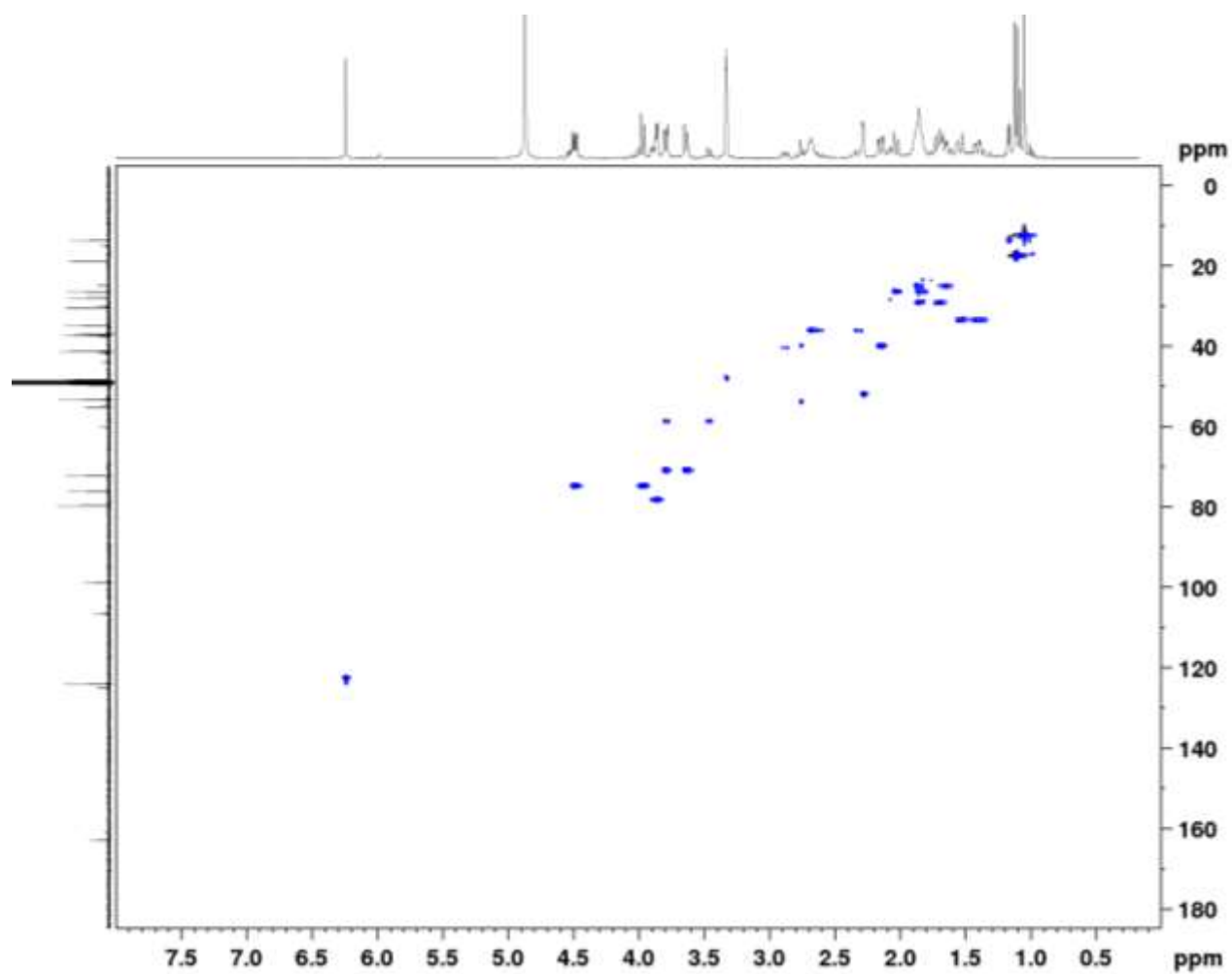


Figure 161. HSQC NMR (400 MHz, CD₃OD) spectrum of 14-hydroxyatrichanone

APPENDIX A (continued)

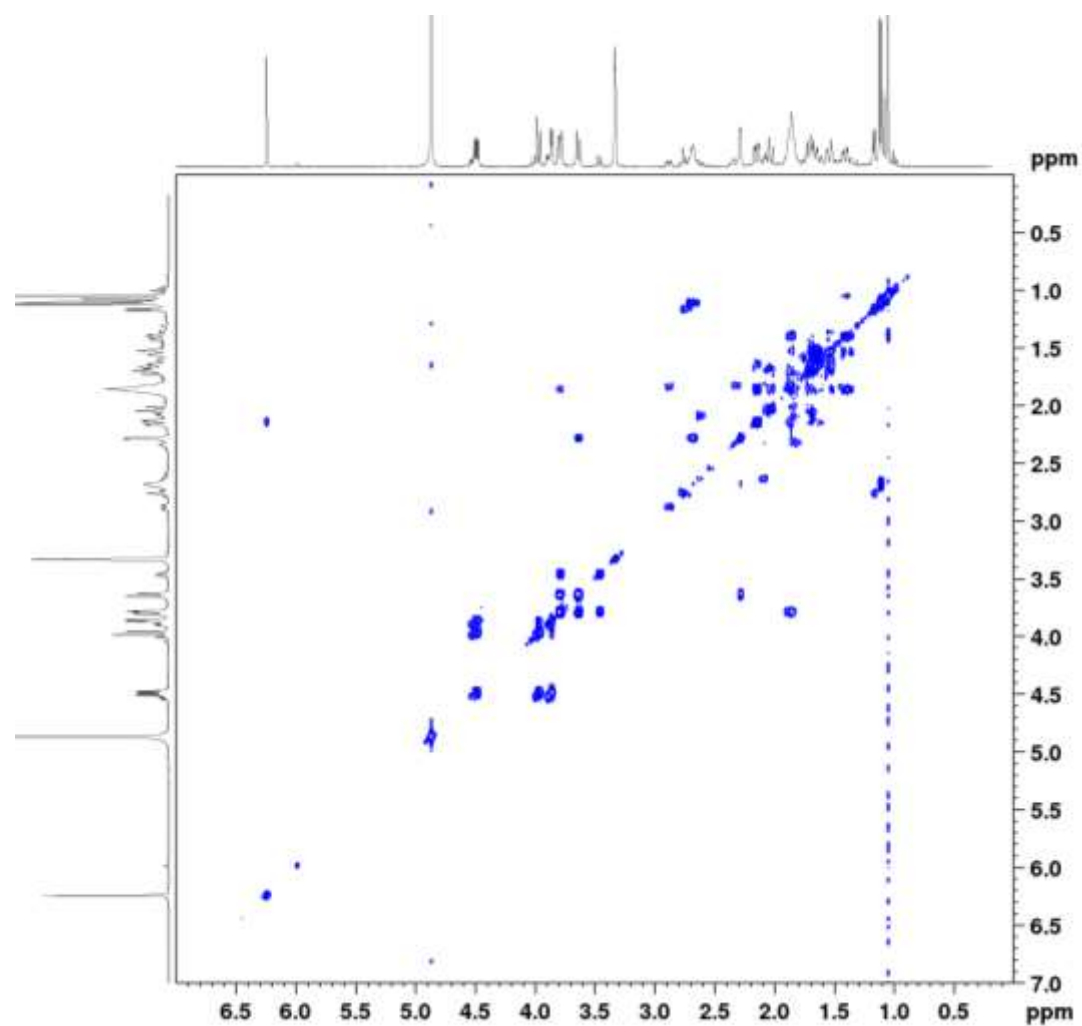


Figure 162. ^1H - ^1H NMR (400 MHz, CD_3OD) spectrum of 14-hydroxyicatrichanone

APPENDIX A (continued)

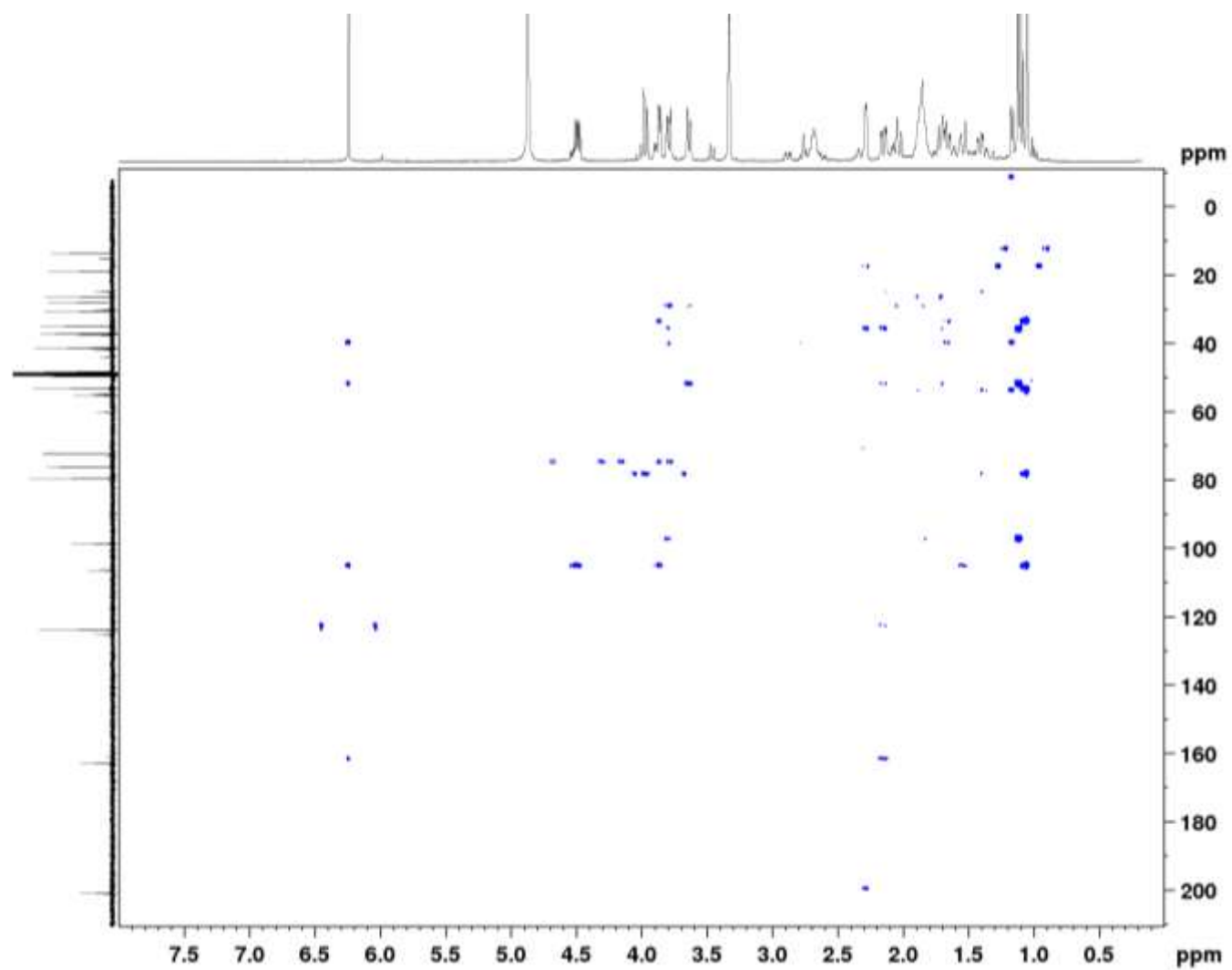


Figure 163. HMBC NMR (400 MHz, CD₃OD) spectrum of 14-hydroxyatrichanone

APPENDIX A (continued)

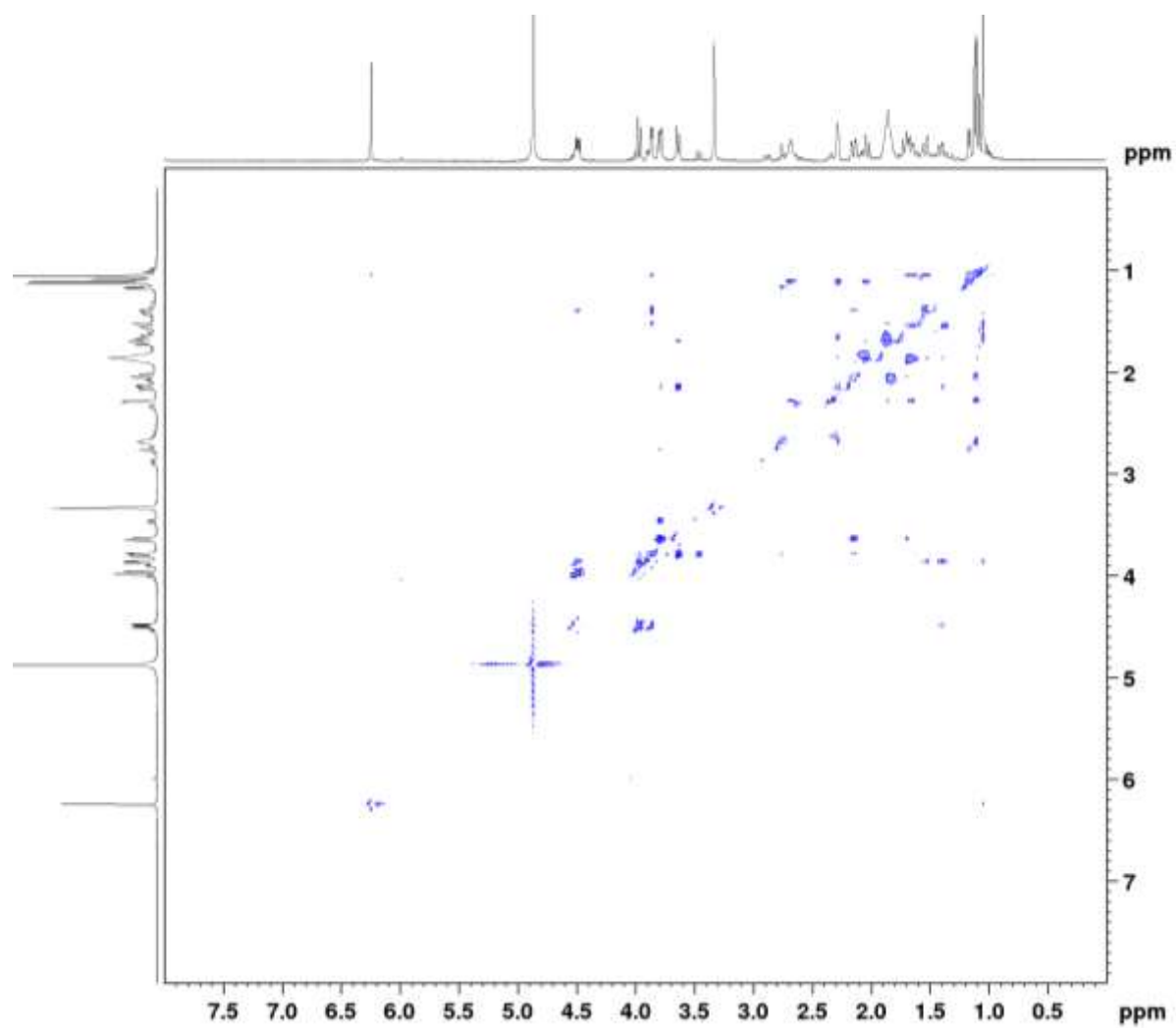


Figure 164. NOESY NMR (400 MHz, CD₃OD) spectrum of 14-hydroxyatrachanone

APPENDIX A (continued)

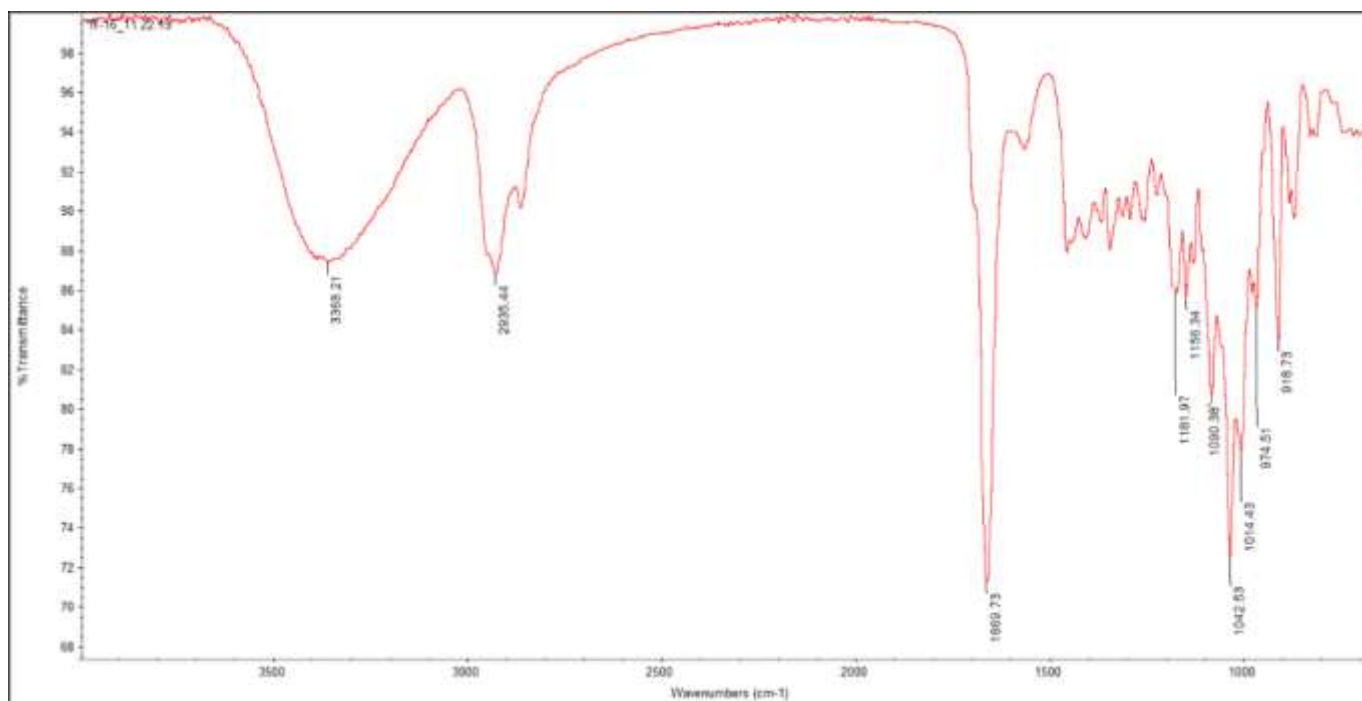


Figure 165. IR spectrum of 14-hydroxycatrachanone

APPENDIX A (continued)

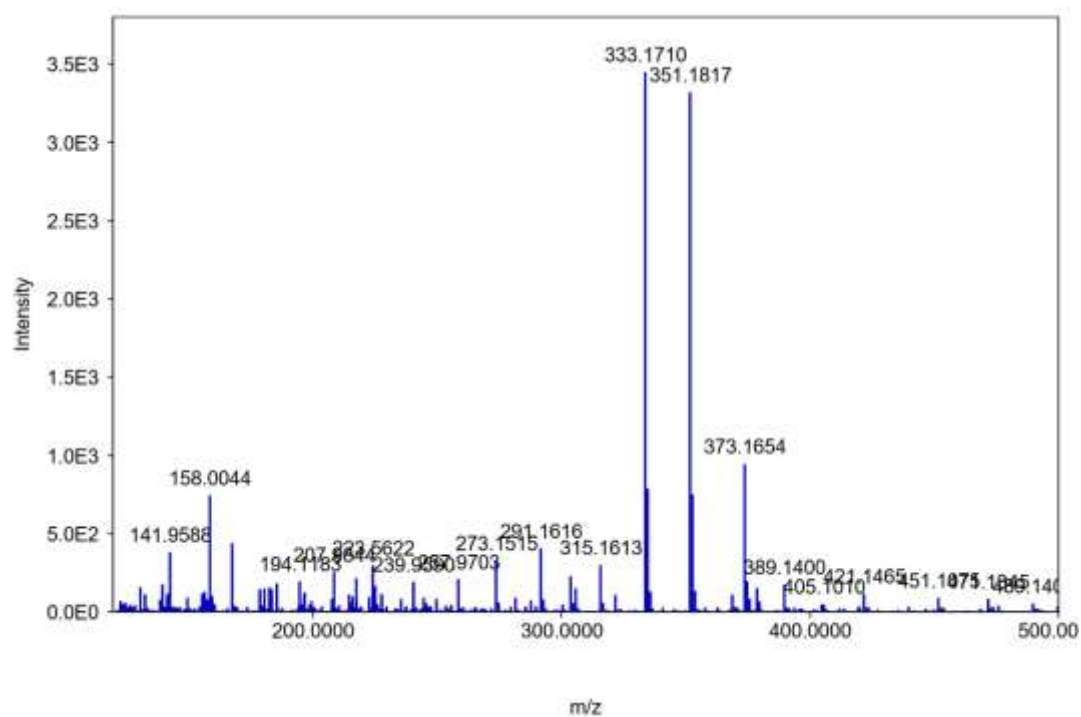


Figure 166. HRESIMS (+) spectrum of 14-hydroxyatrichanone

APPENDIX A (continued)

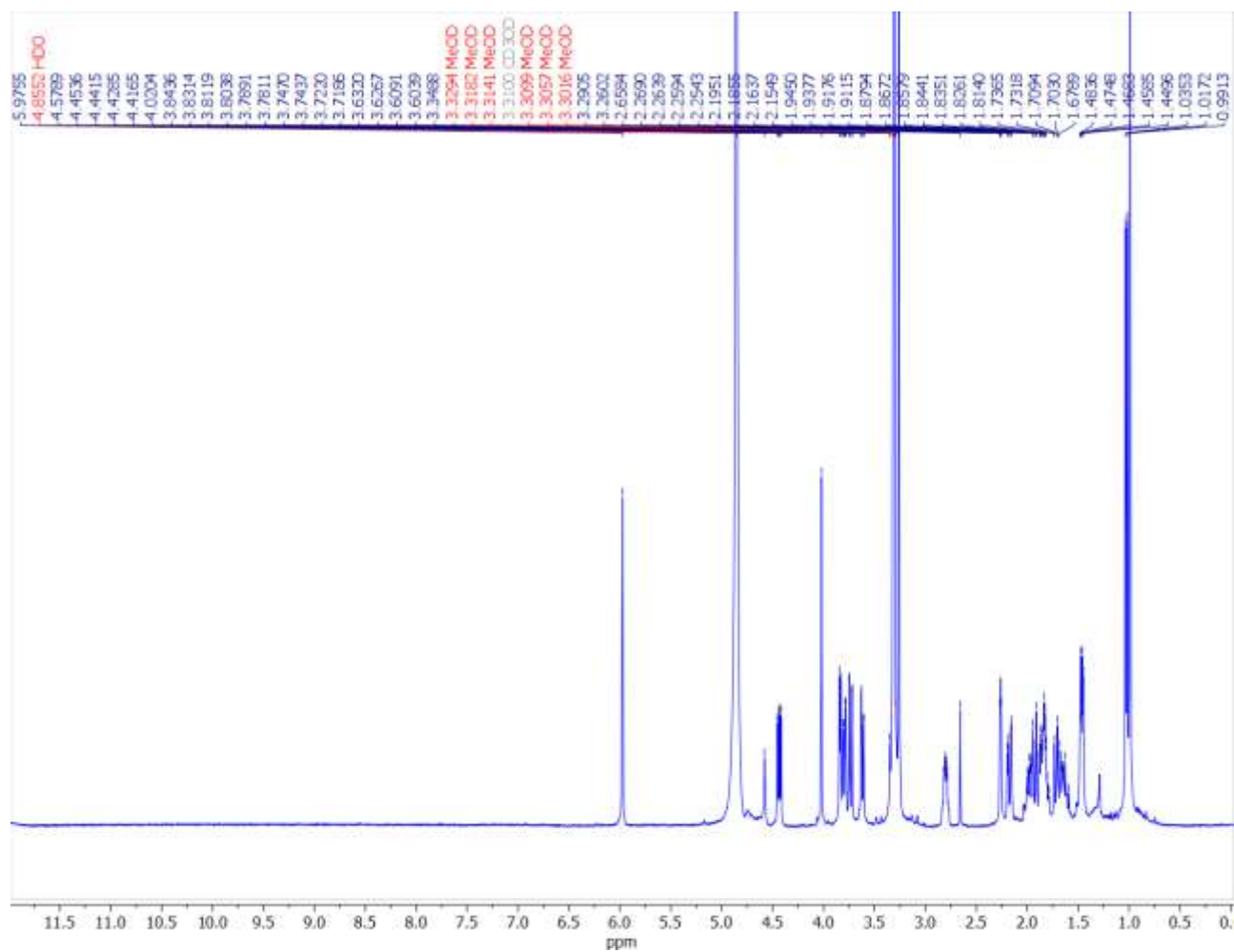


Figure 167. ^1H NMR (400 MHz, CD_3OD) spectrum of 3-methoxycatrichanone

APPENDIX A (continued)

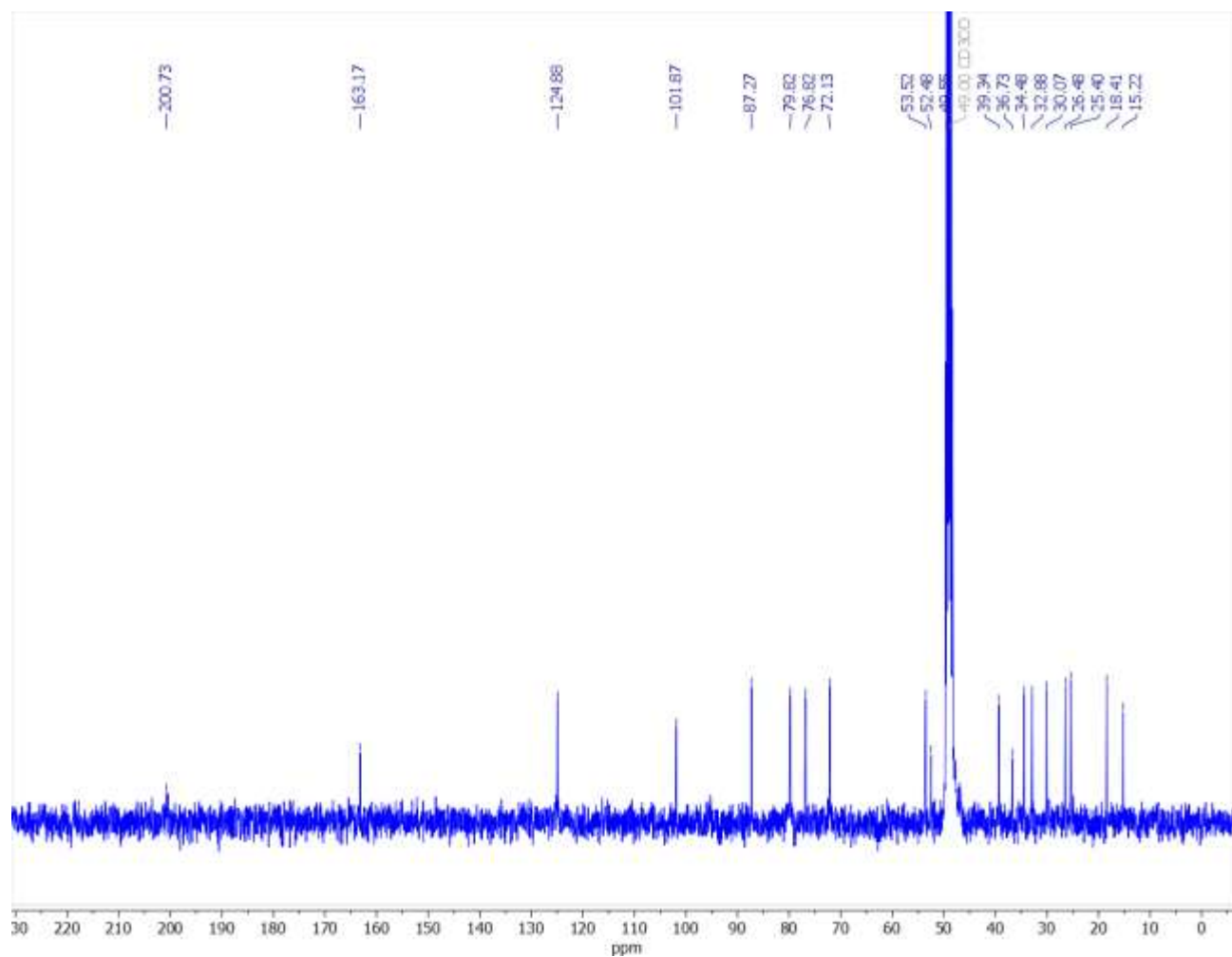


Figure 168. ¹³C (100 MHz, CD₃OD) spectrum of 3-methoxyatrichanone

APPENDIX A (continued)

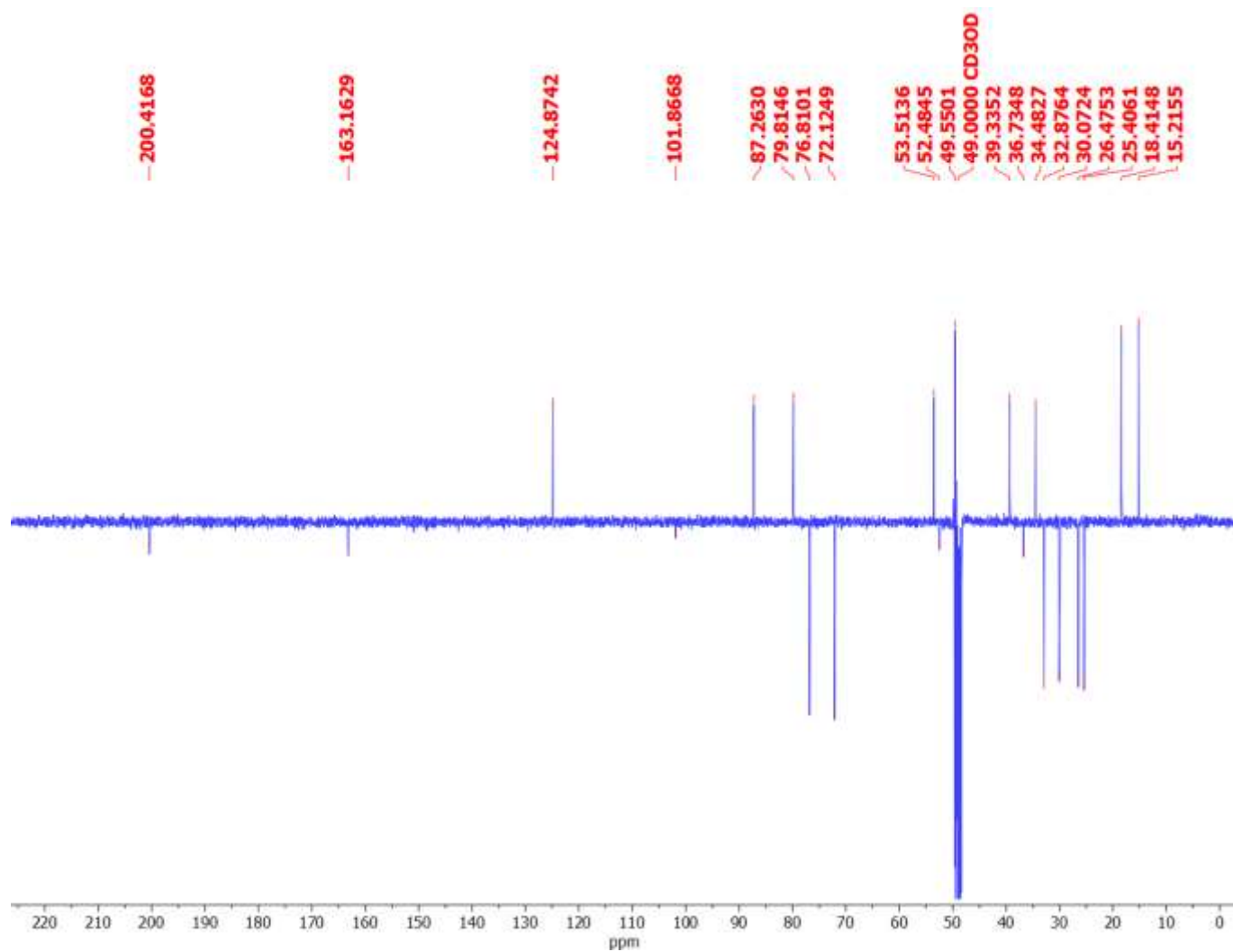


Figure 169. DEPQ (100 MHz, CD₃OD) spectrum of 3-methoxyatrichanone

APPENDIX A (continued)

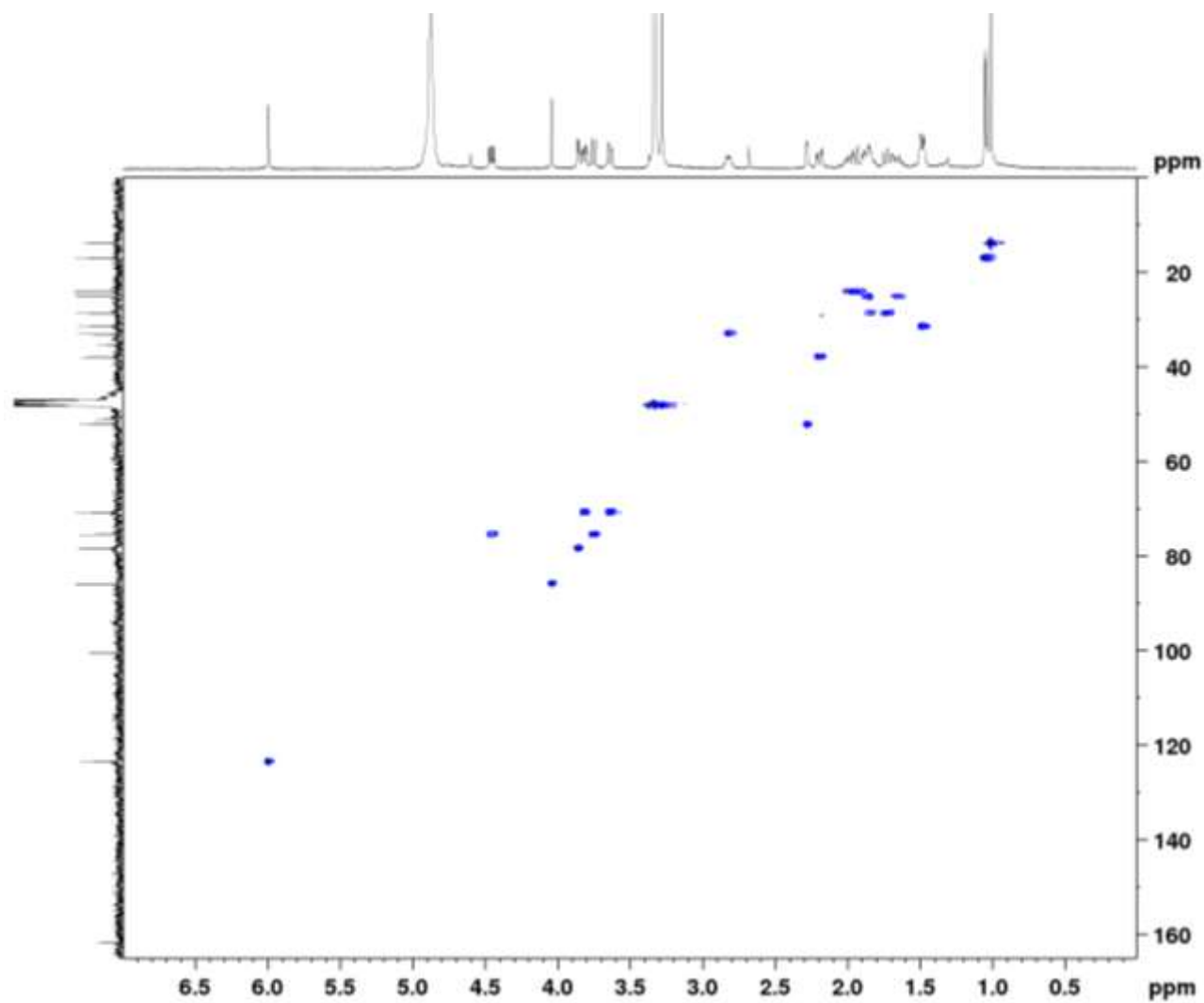


Figure 170. HSQC (400 MHz, CD₃OD) spectrum of 3-methoxyatrichanone

APPENDIX A (continued)

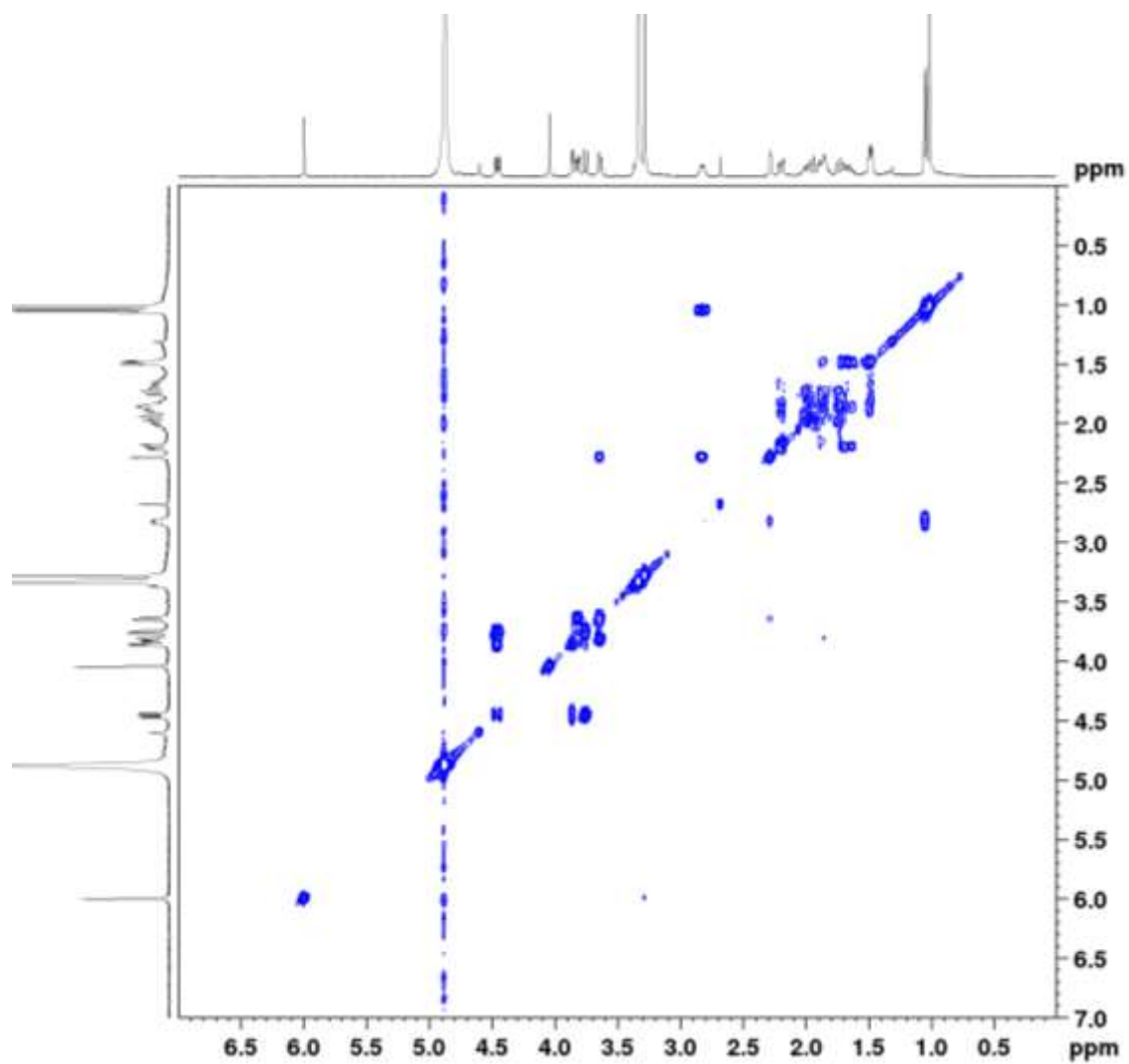


Figure 171. ^1H - ^1H COSY (400 MHz, CD_3OD) spectrum of 3-methoxyatricane

APPENDIX A (continued)

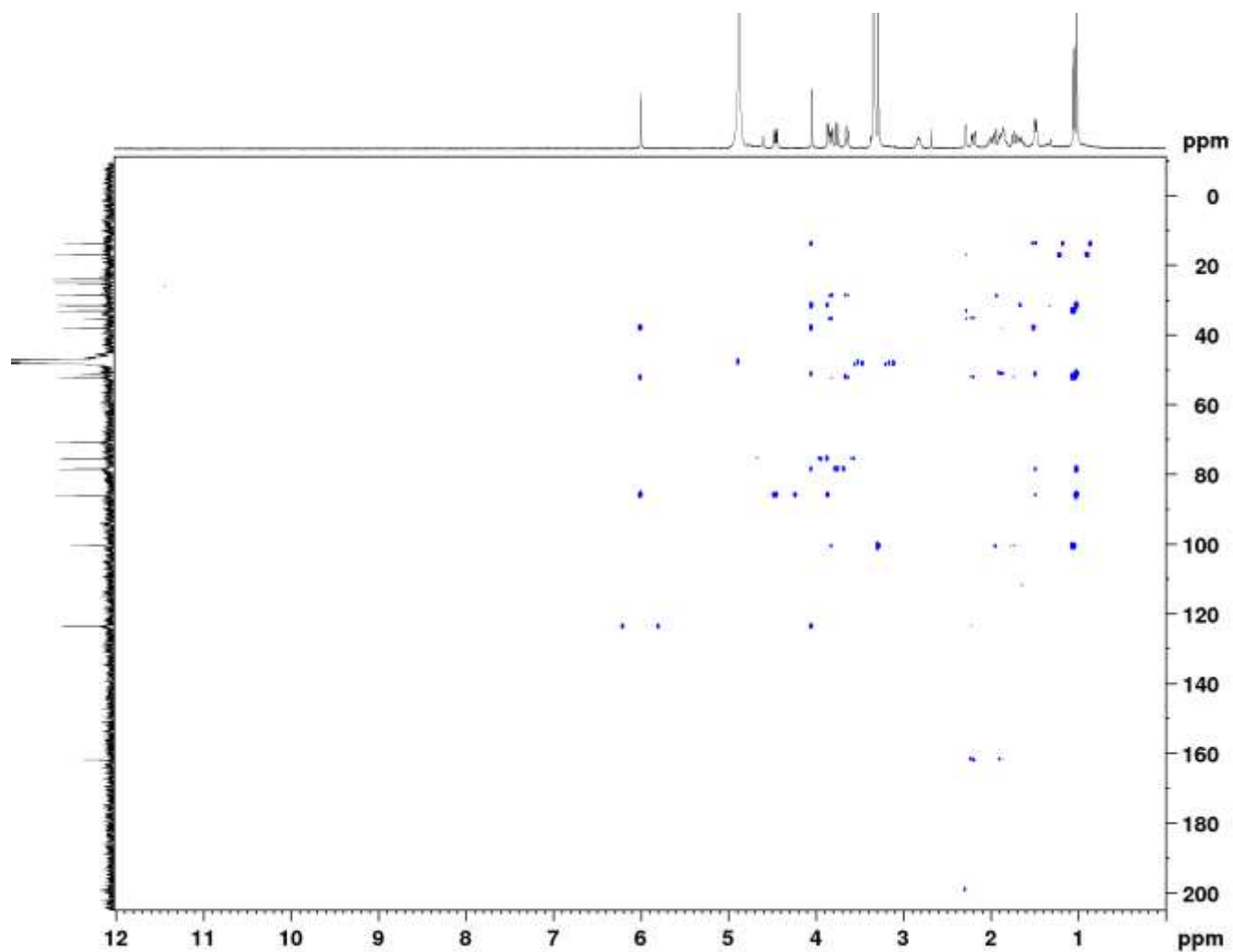


Figure 172. HMBC (400 MHz, CD_3OD) spectrum of 3-methoxyicatrichanone

APPENDIX A (continued)

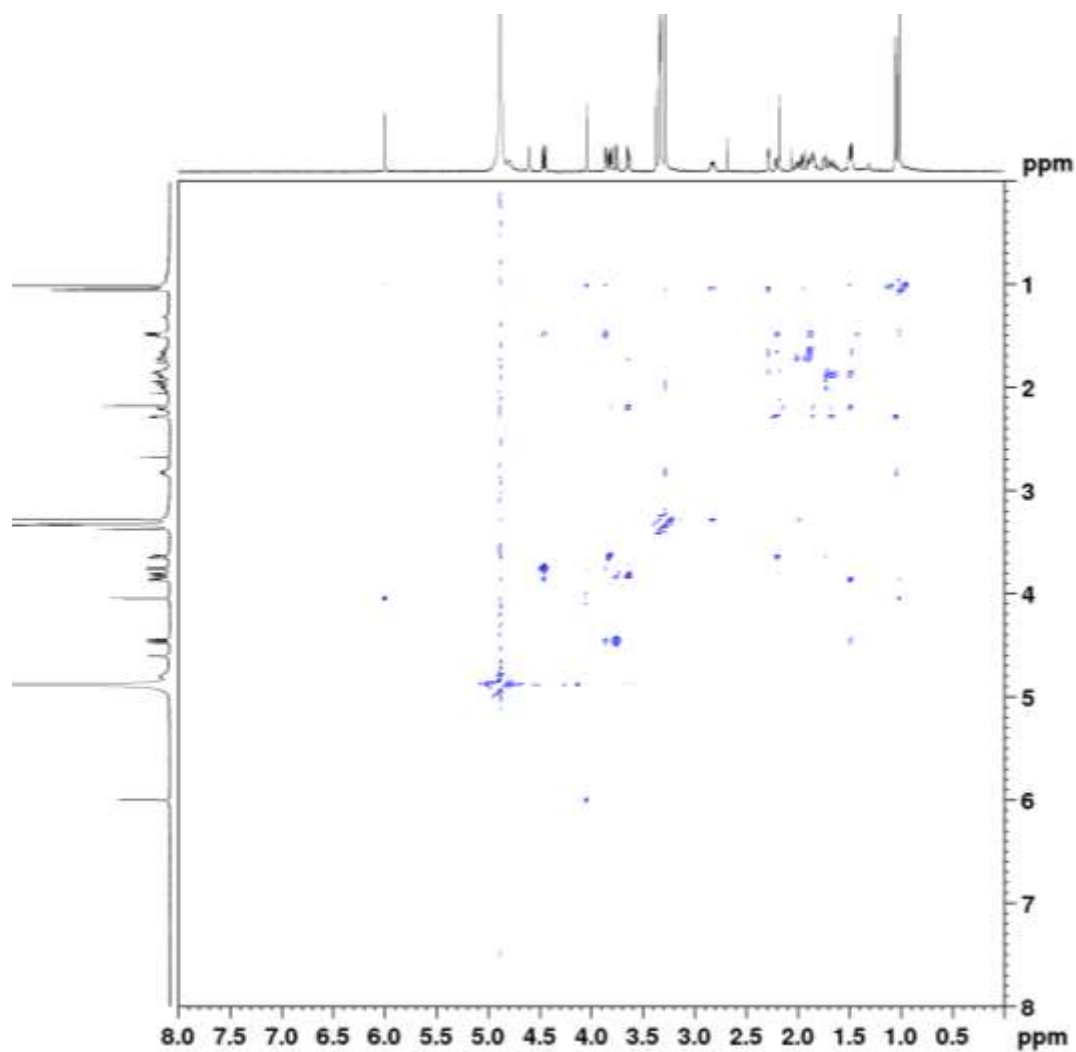
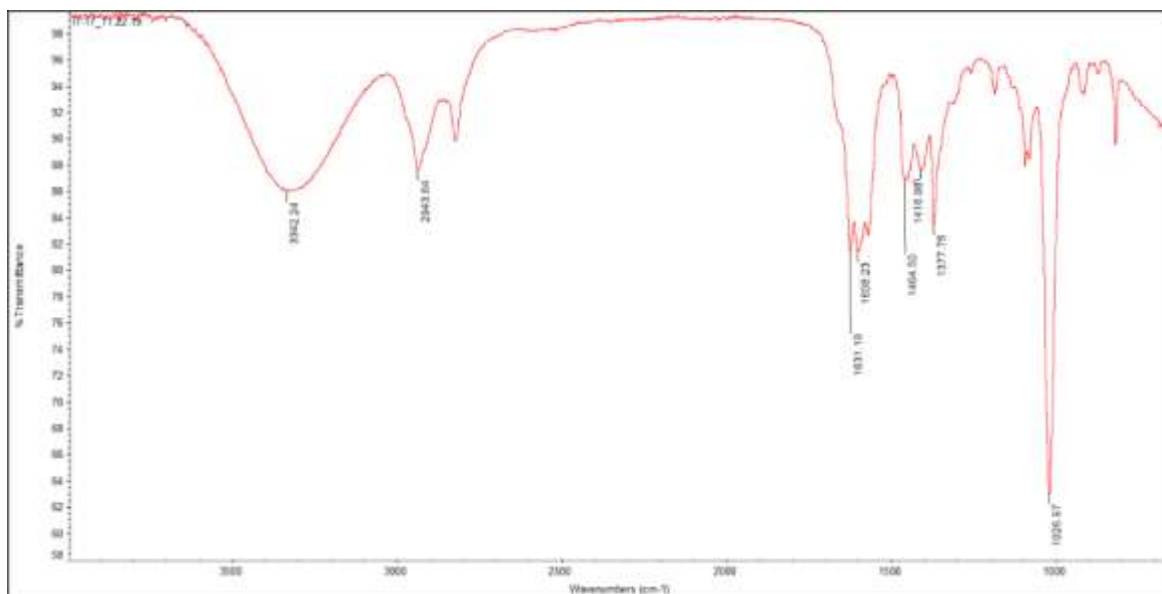
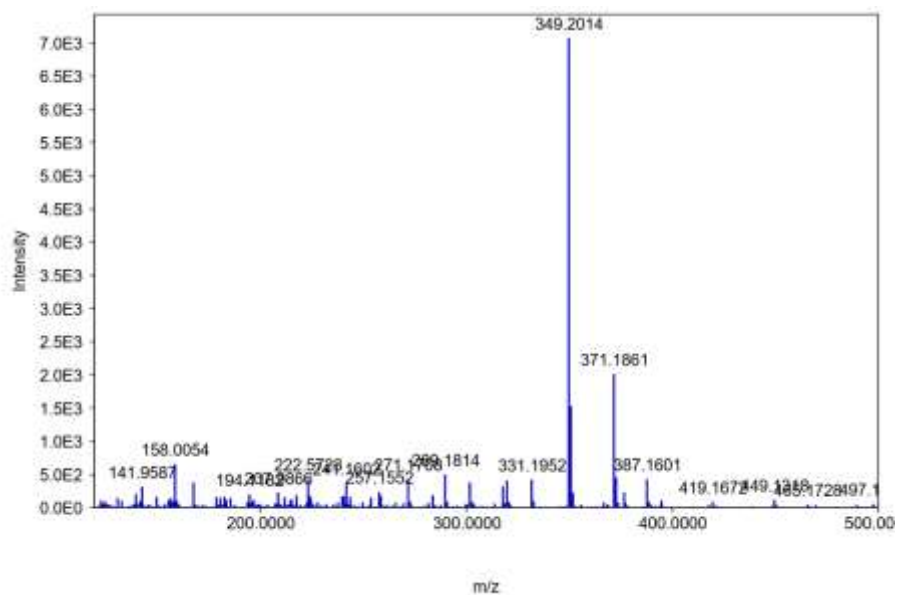


Figure 173. NOESY (400 MHz, CD₃OD) spectrum of 3-methoxyatrichanone

APPENDIX A (continued)

**Figure 174. IR spectrum of 3-methoxyicatrichanone****Figure 175. HRESIMS (+) spectrum of 3-methoxyicatrichanone**

APPENDIX A (continued)

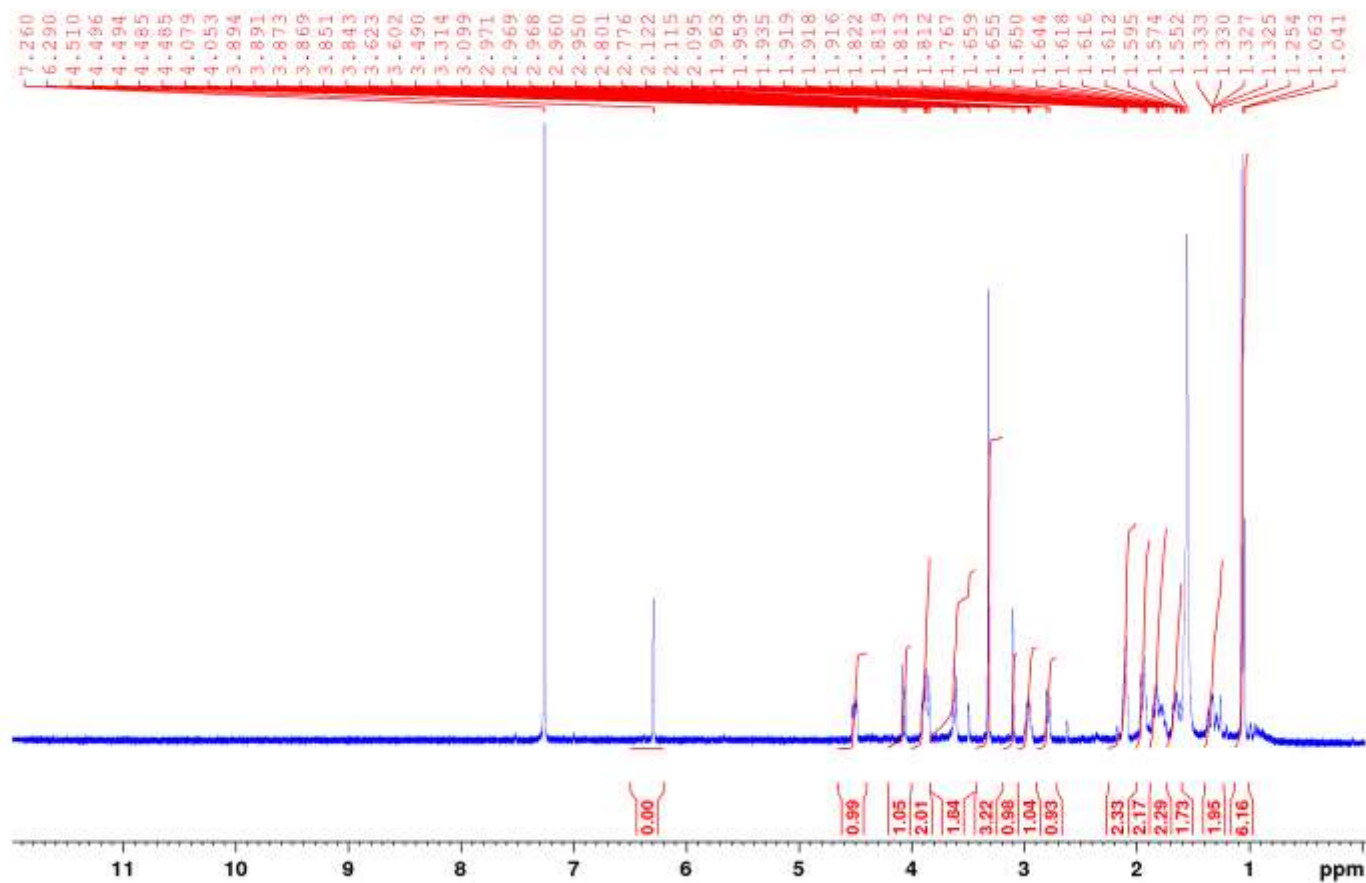


Figure 176. ^1H (400 MHz, CDCl_3) spectrum of 3-methoxy-14-hydroxy-icatrichanone

APPENDIX A (continued)

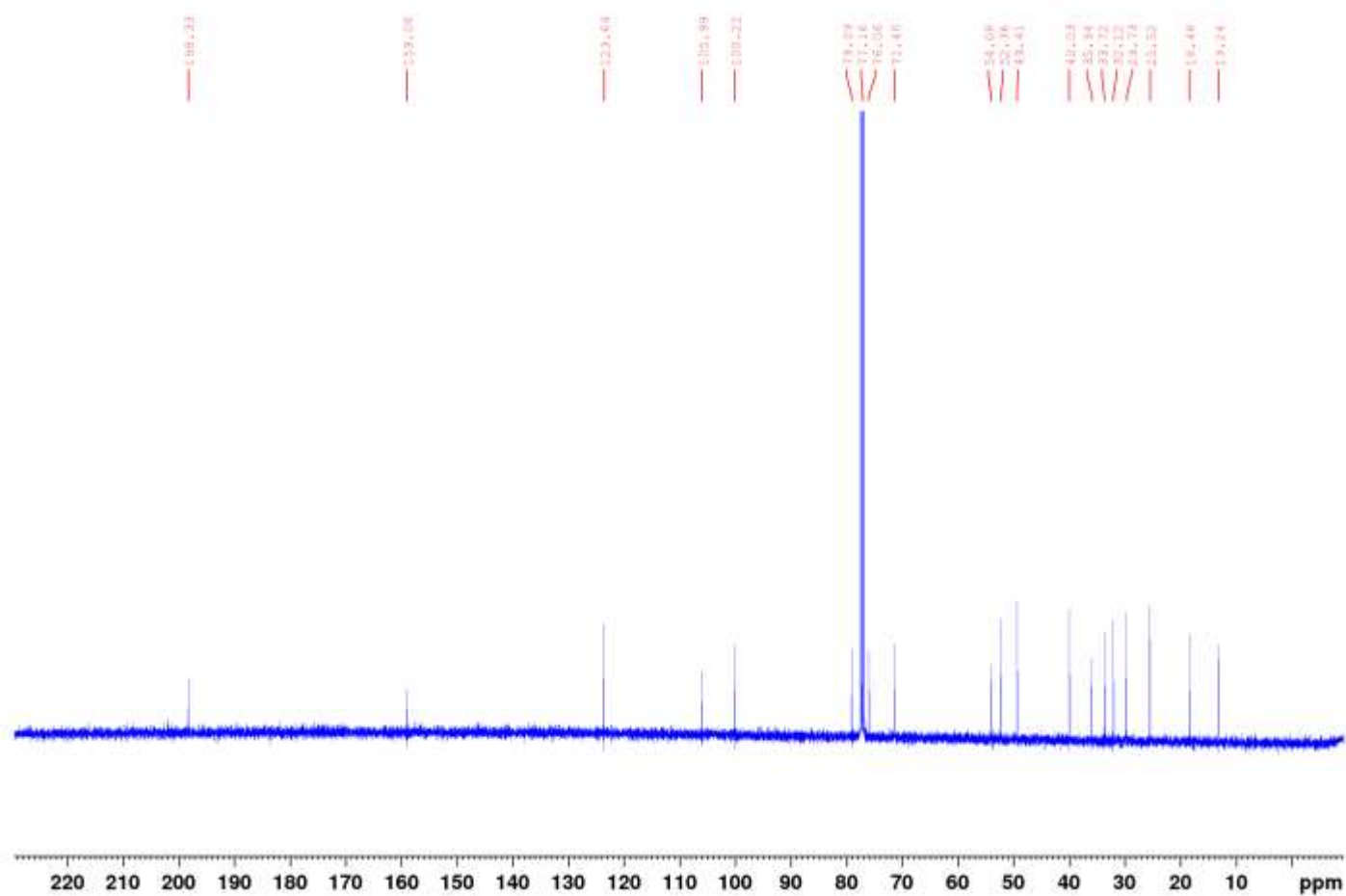


Figure 177. ^{13}C (100 MHz, chloroform-*d*) spectrum of 3-methoxy-14-hydroxy-icatrichanone

APPENDIX A (continued)

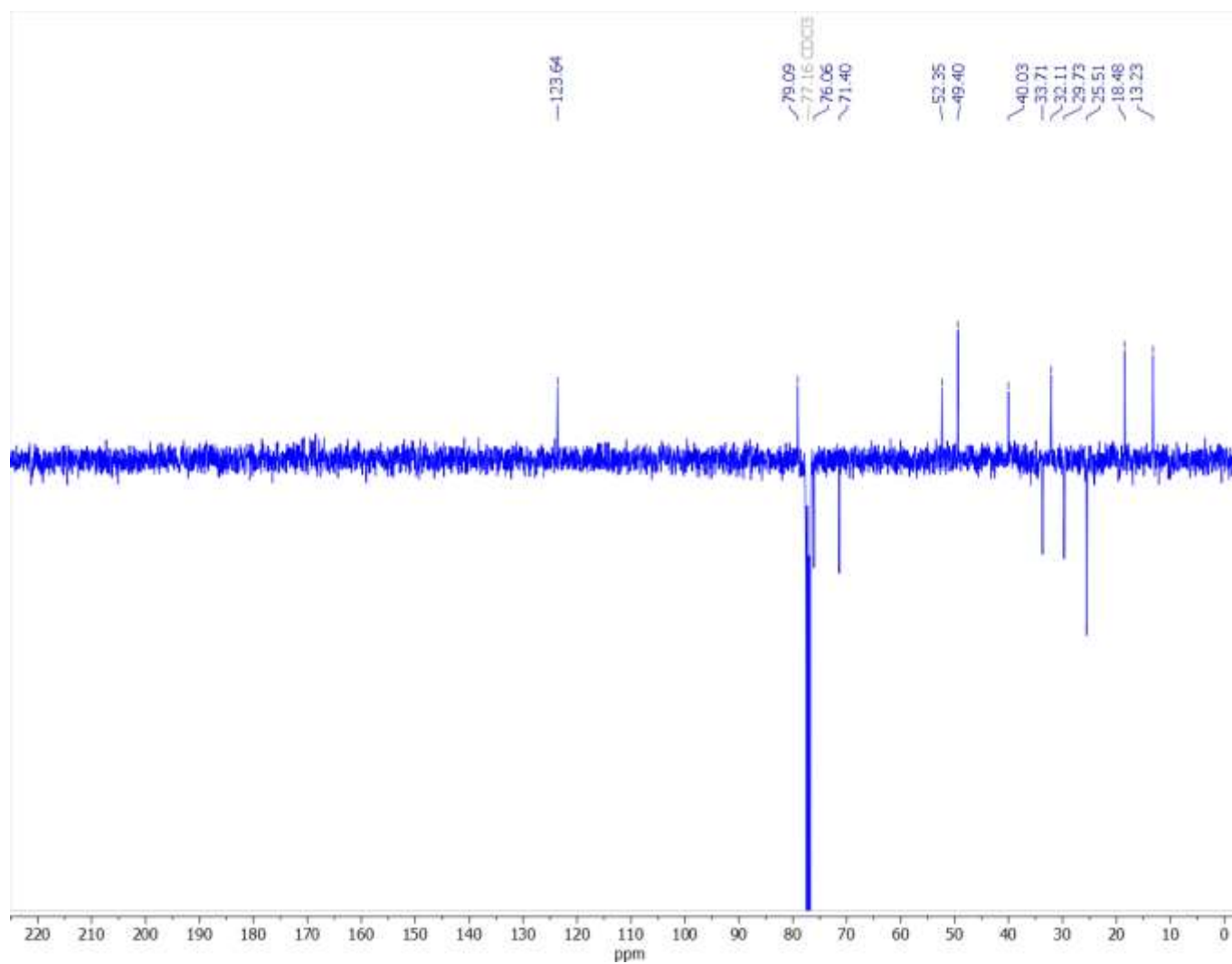


Figure 178. DEPT135 (100 MHz, chloroform-*d*) spectrum of 3-methoxy-14-hydroxy-icatrichanone

APPENDIX A (continued)

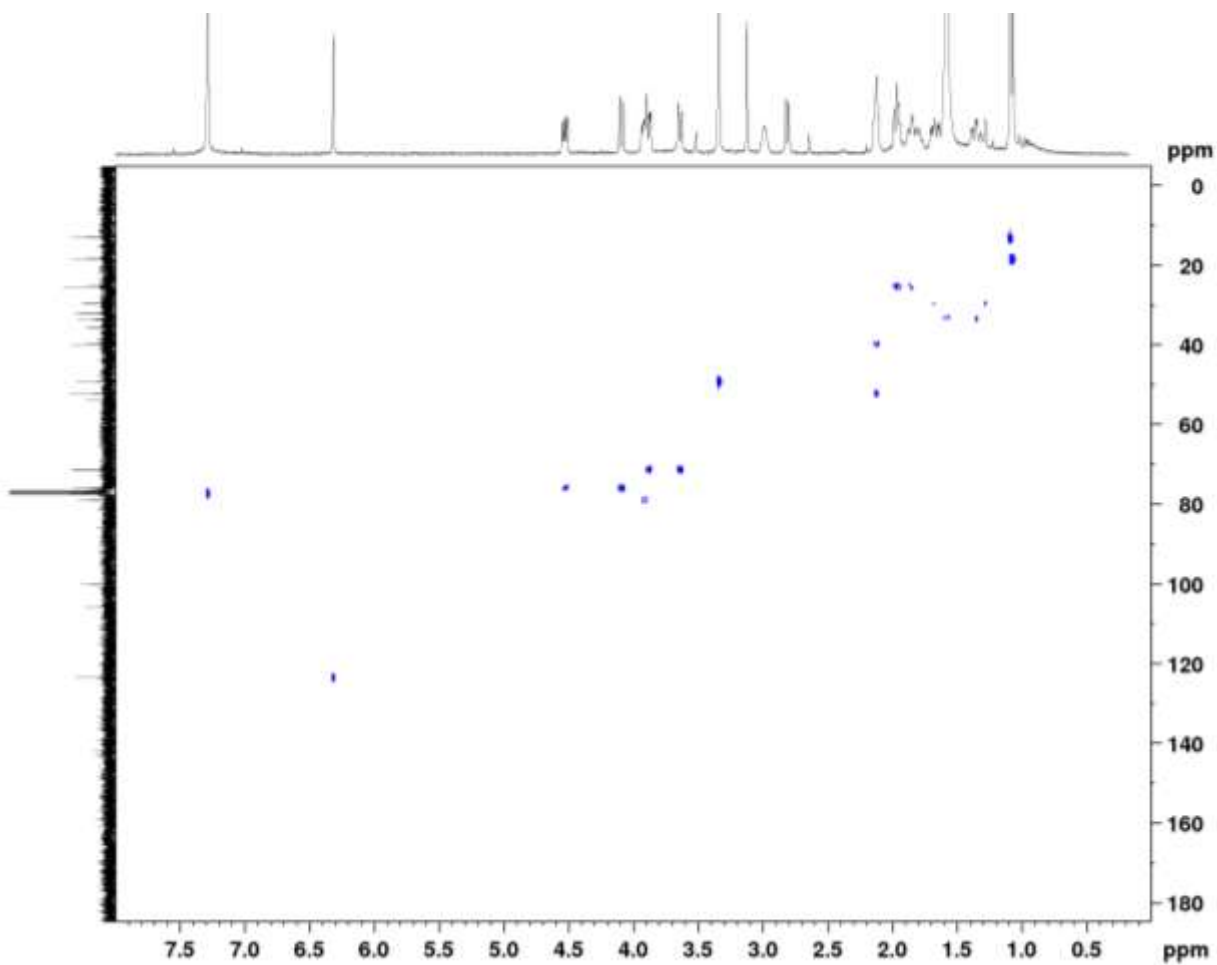


Figure 179. HSQC (400 MHz, chloroform-*d*) spectrum of 3-methoxy-14-hydroxy-icatrichanone

APPENDIX A (continued)

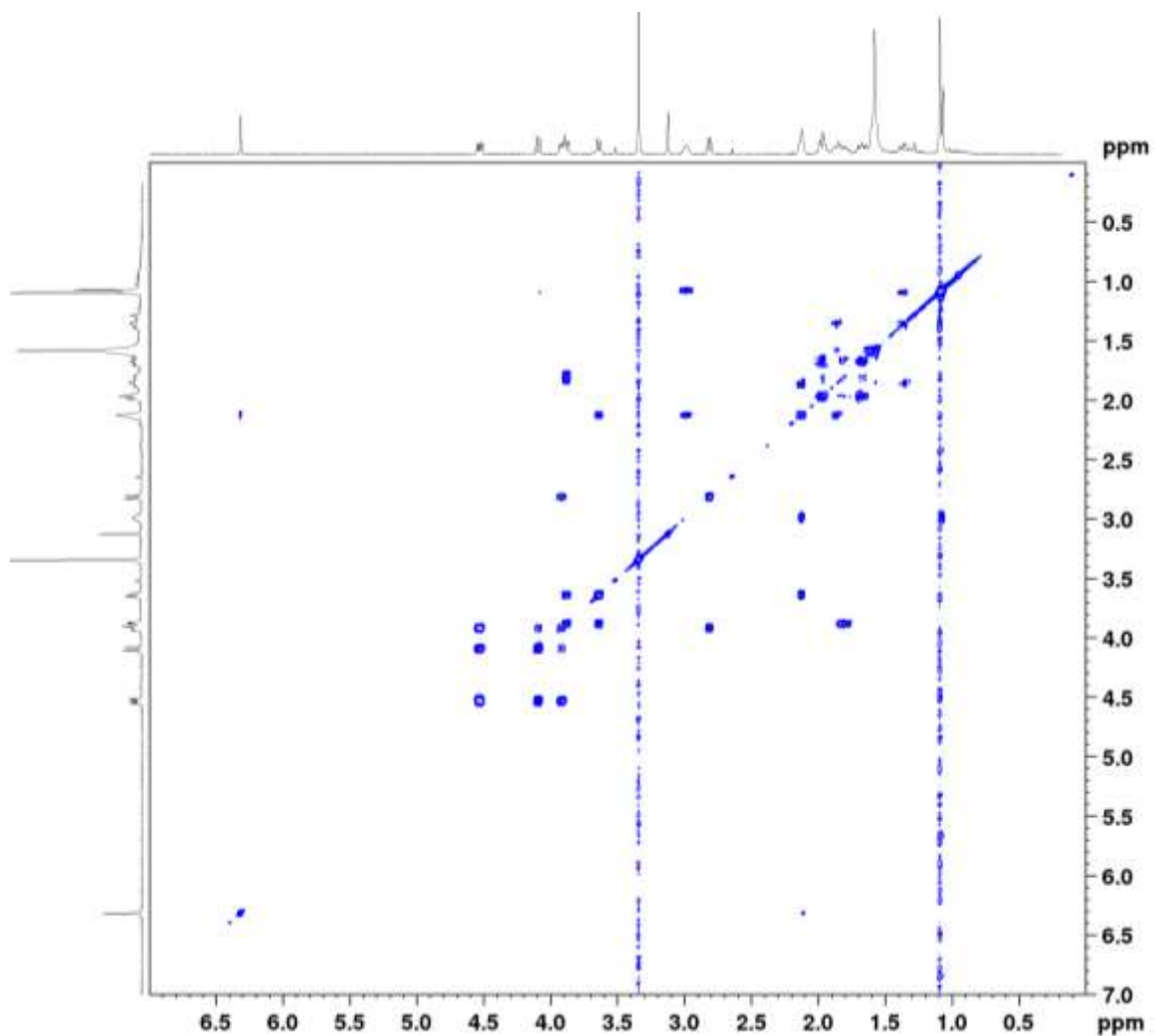


Figure 180. ^1H - ^1H COSY (400 MHz, CDCl_3) spectrum of 3-methoxy-14-hydroxy-icatrichanone

APPENDIX A (continued)

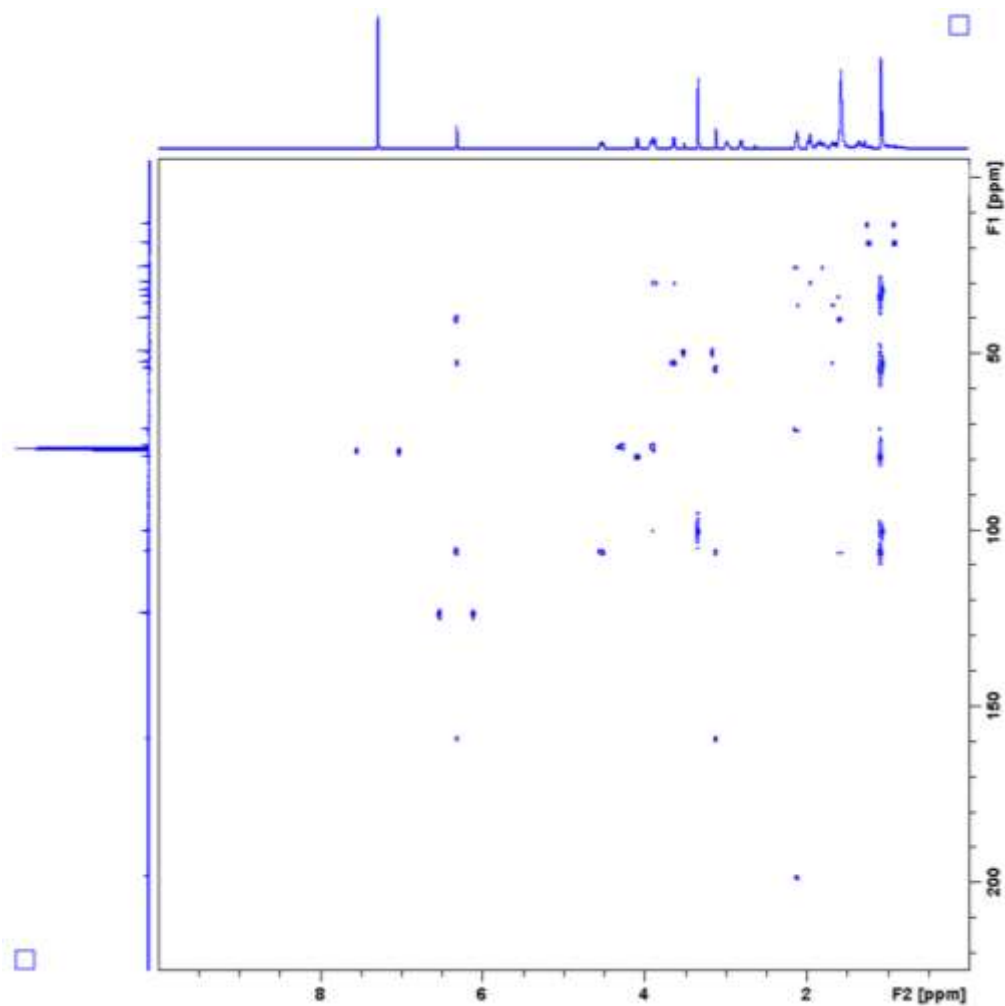


Figure 181. HMBC (400 MHz, chloroform-*d*) spectrum of 3-methoxy-14-hydroxy-icatrichanone

APPENDIX A (continued)

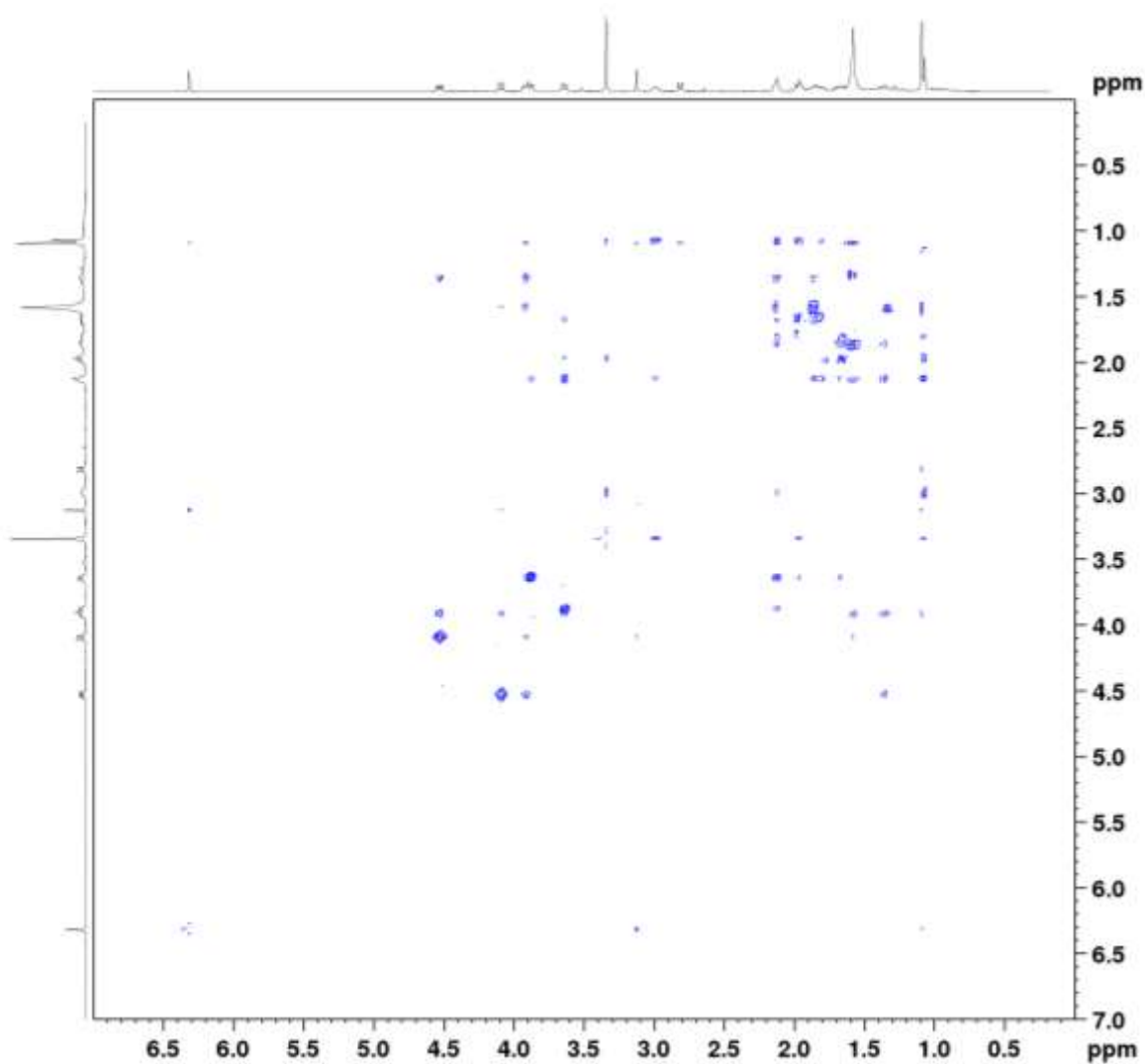


Figure 182. NOESY (400 MHz, chloroform-*d*) spectrum of 3-methoxy-14-hydroxy-icatrichanone

APPENDIX A (continued)

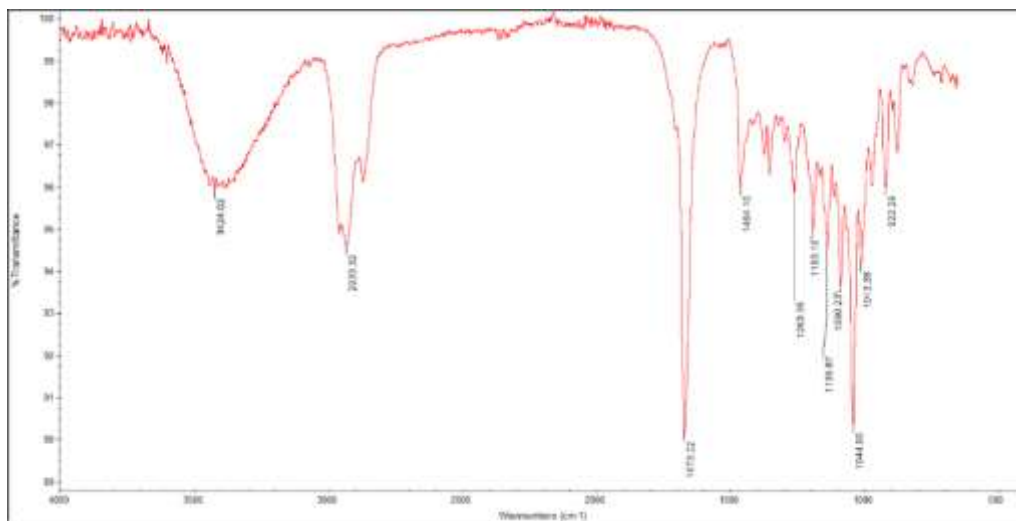


Figure 183. IR spectrum of 3-methoxy-14-hydroxy-icatrichanone

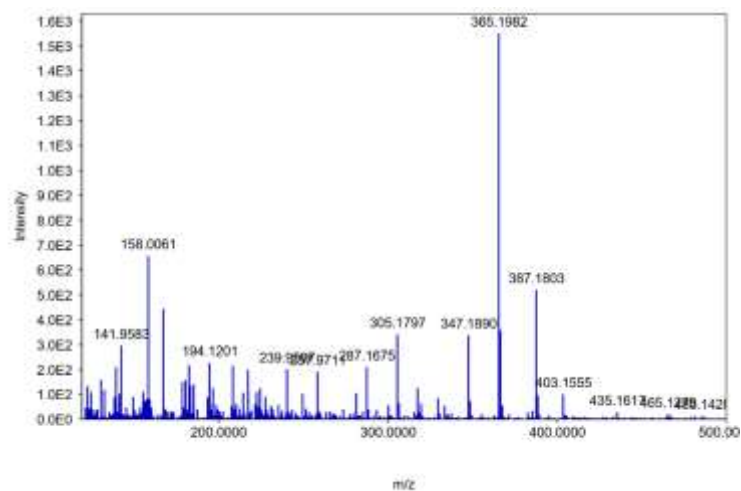
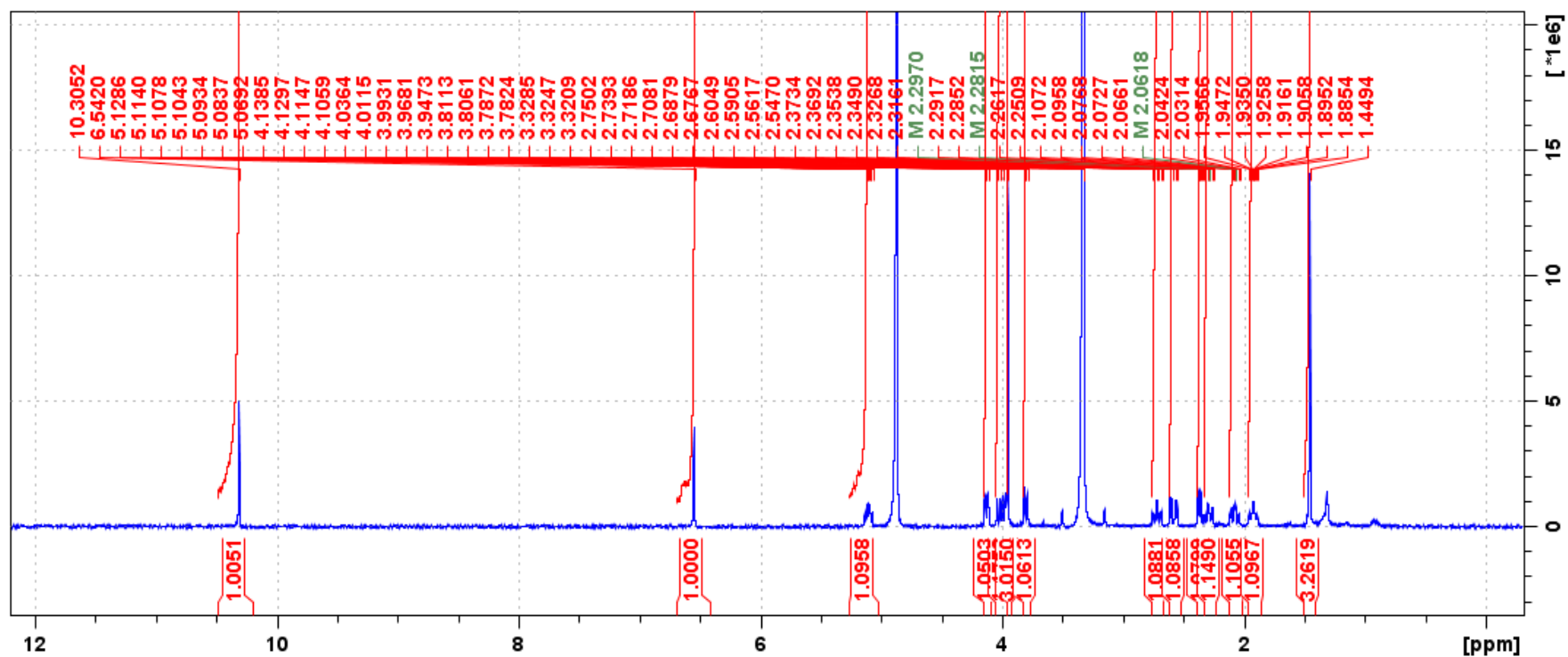
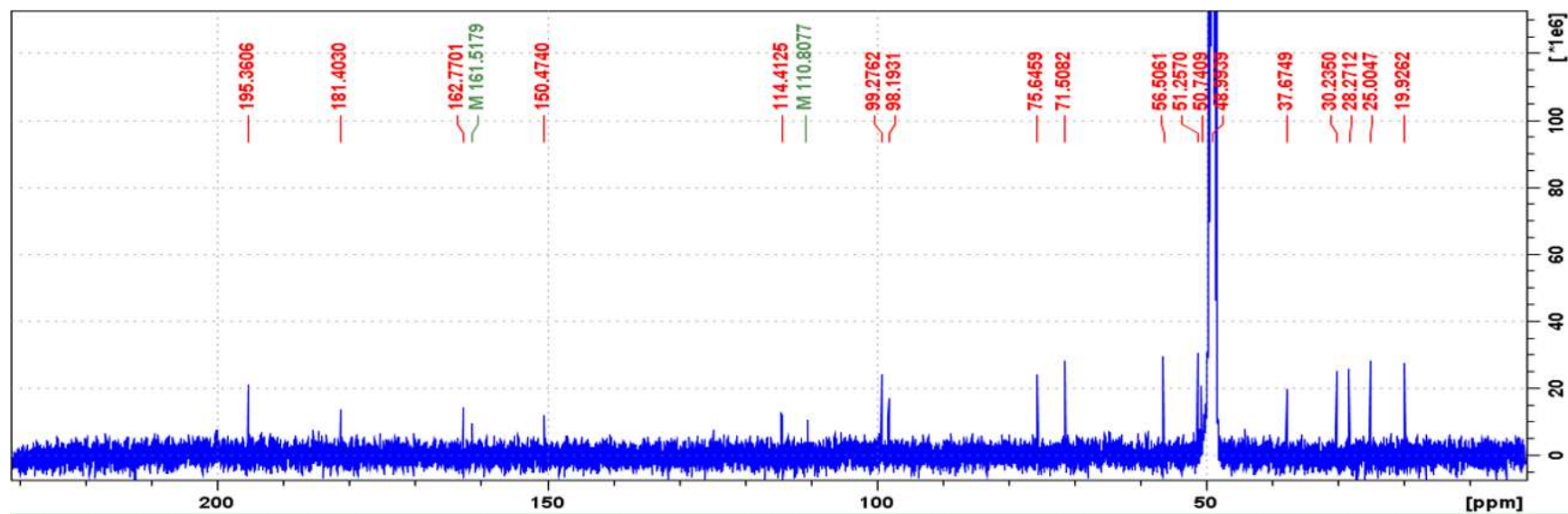


Figure 184. HRESIMS (+) spectrum of 3-methoxy-14-hydroxy-icatrichanone

APPENDIX A (continued)

Figure 185. ¹H (400 MHz, CD₃OD) spectrum of icacinlactone K

APPENDIX A (continued)

Figure 186. ¹³C (100 MHz, CD₃OD) spectrum of icacinlactone K

APPENDIX A (continued)

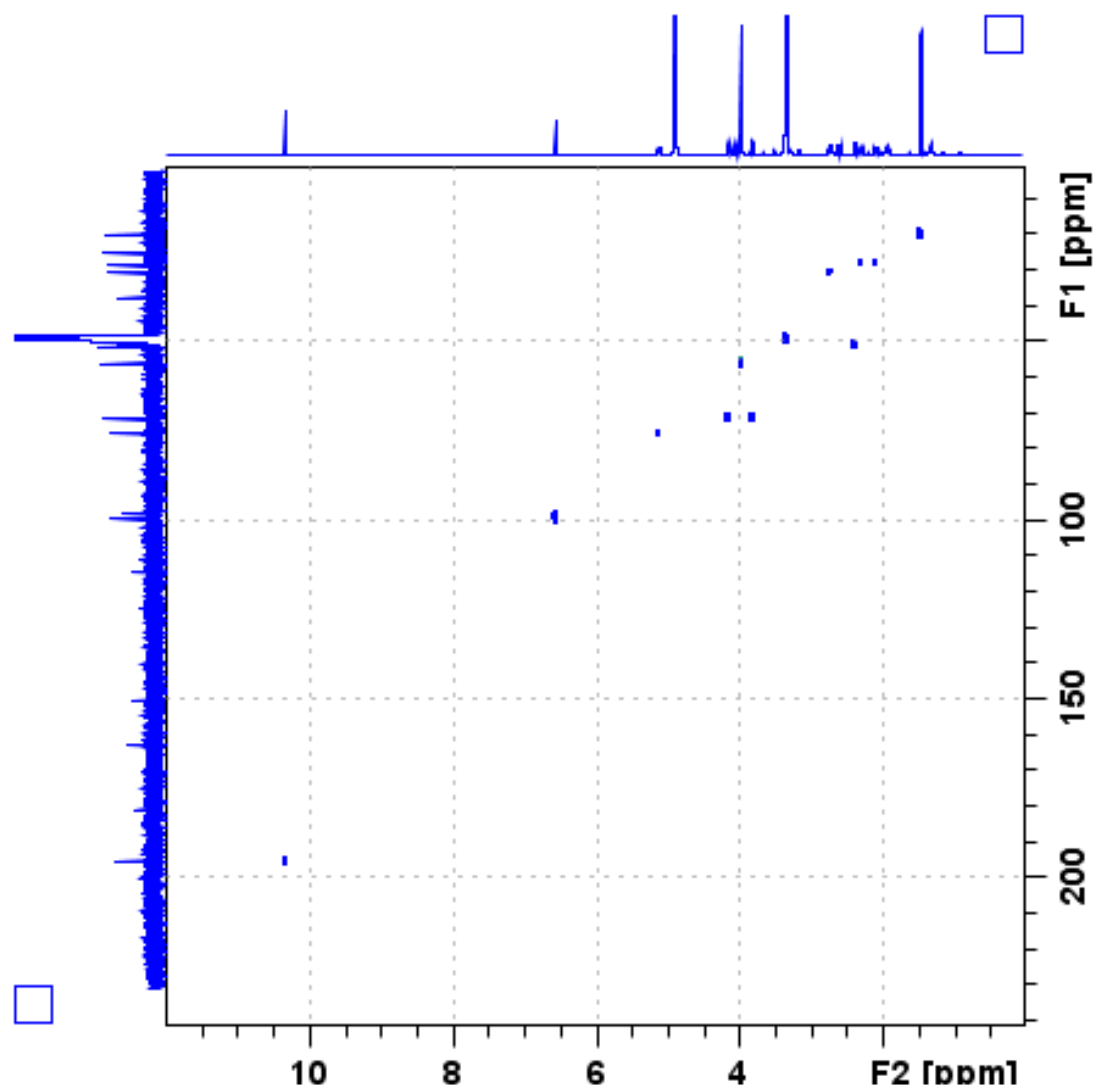


Figure 187. HSQC (400 MHz, CD_3OD) spectrum of icacinlactone K

APPENDIX A (continued)

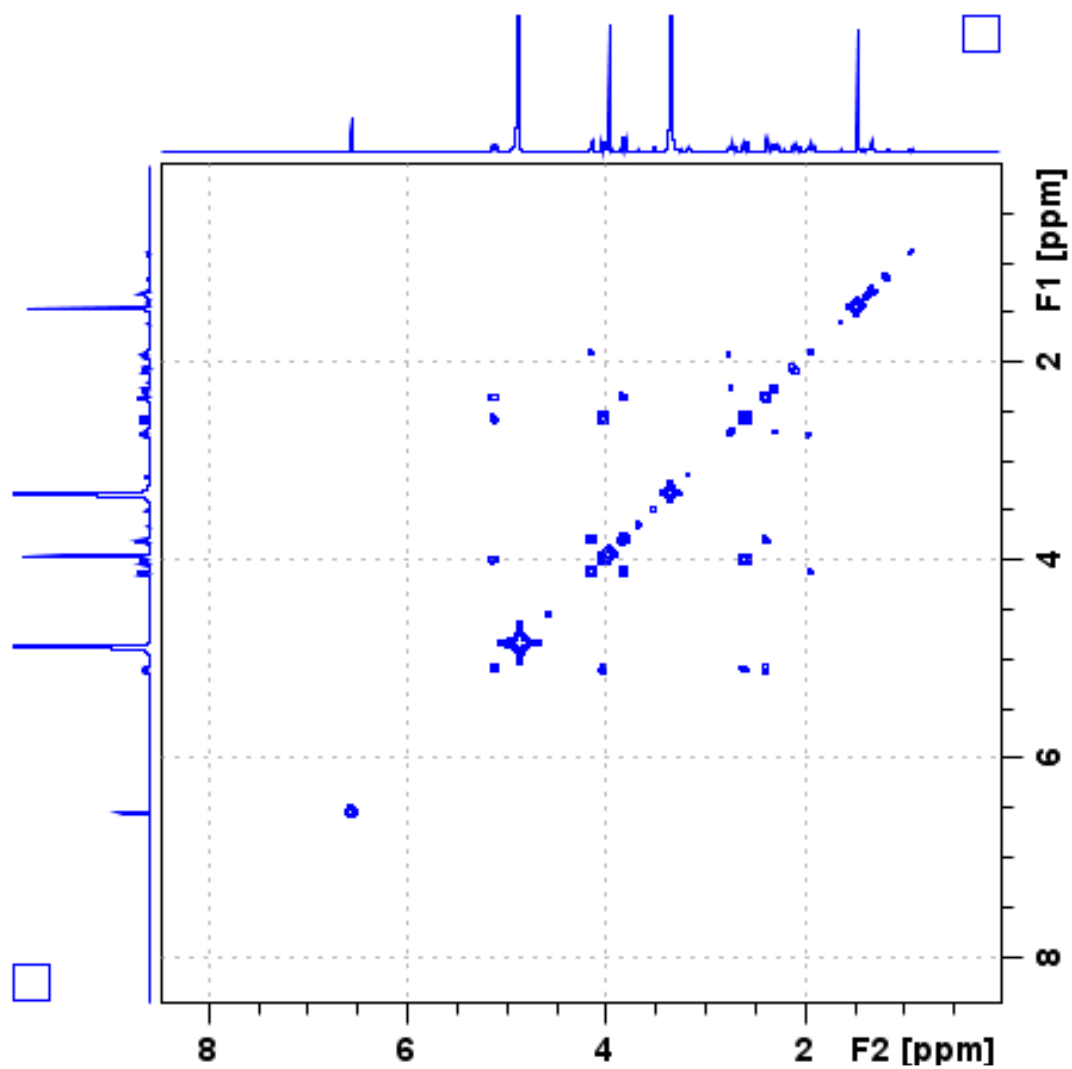


Figure 188. ^1H - ^1H COSY (400 MHz, CD_3OD) spectrum of icacinlactone K

APPENDIX A (continued)

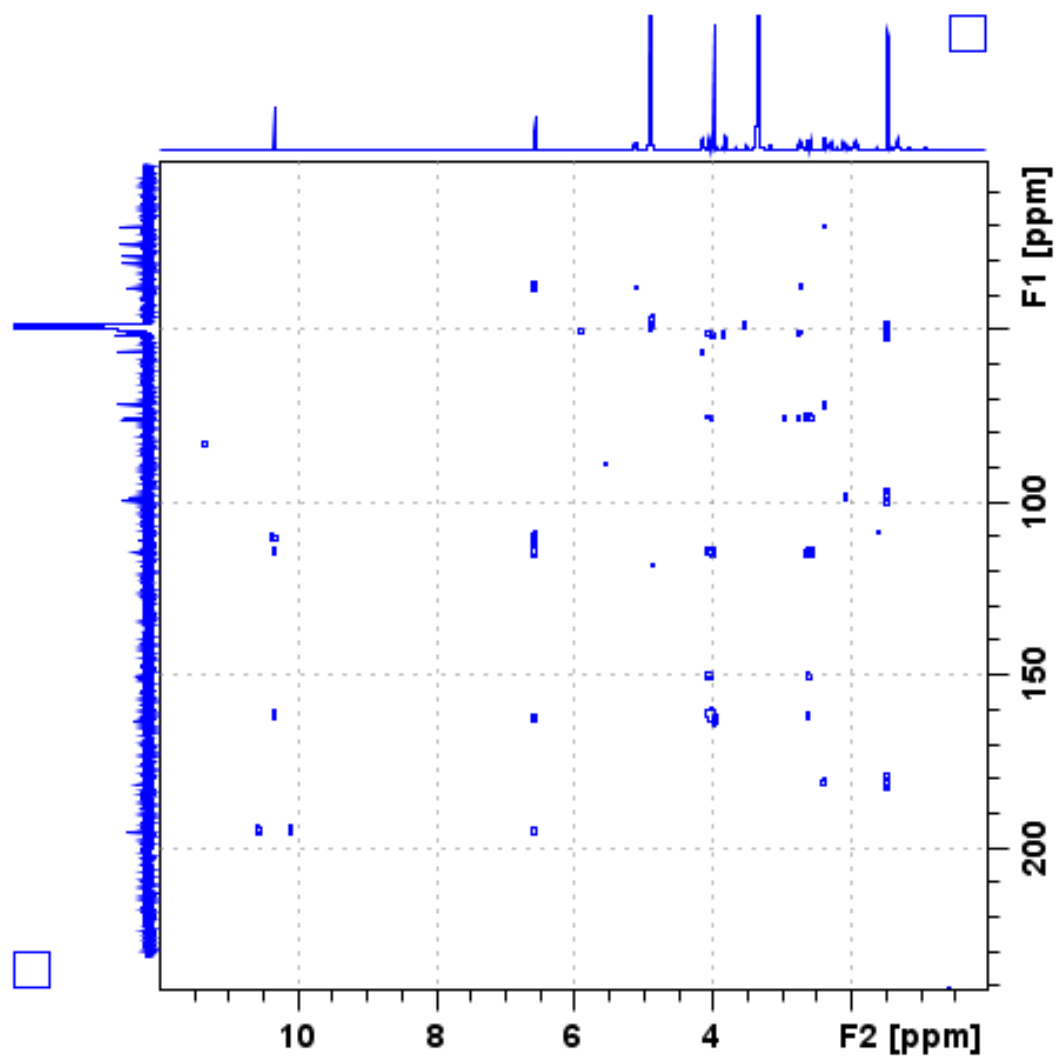


Figure 189. HMBC (400 MHz, CD₃OD) spectrum of icacinlactone K

APPENDIX A (continued)

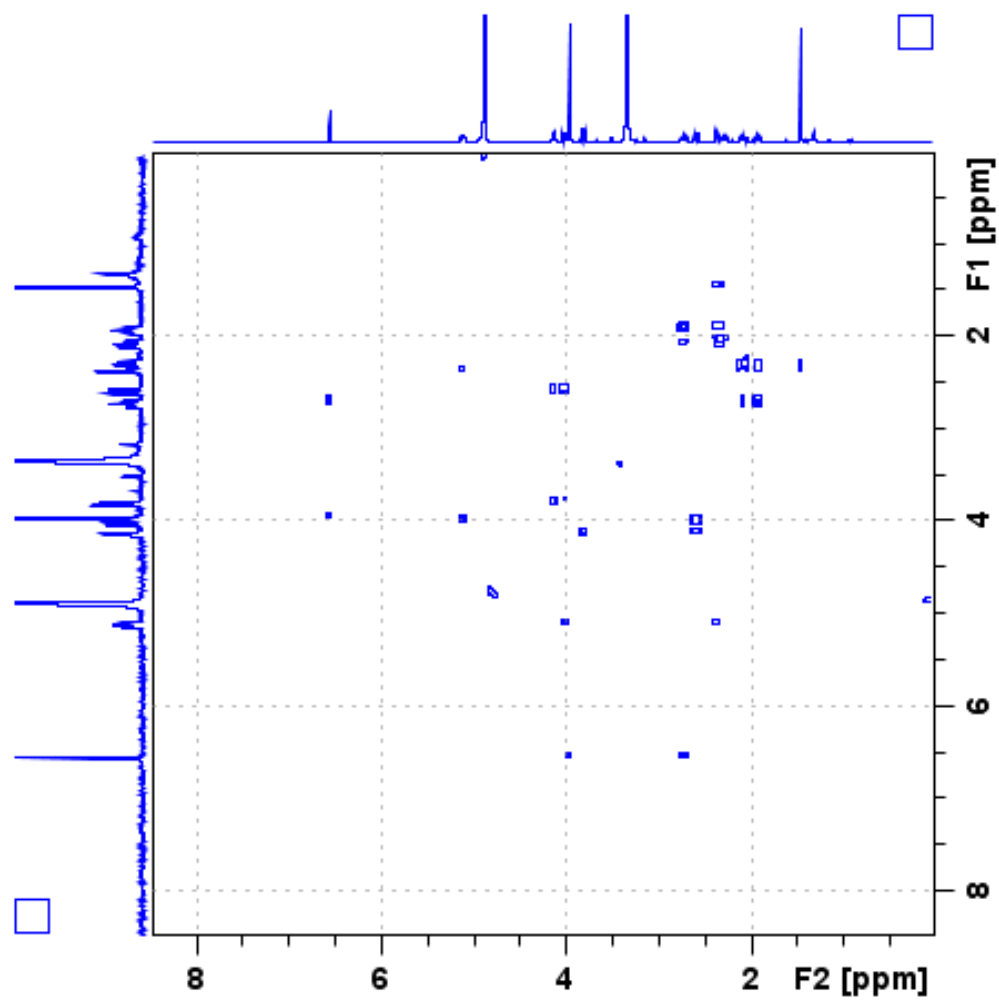
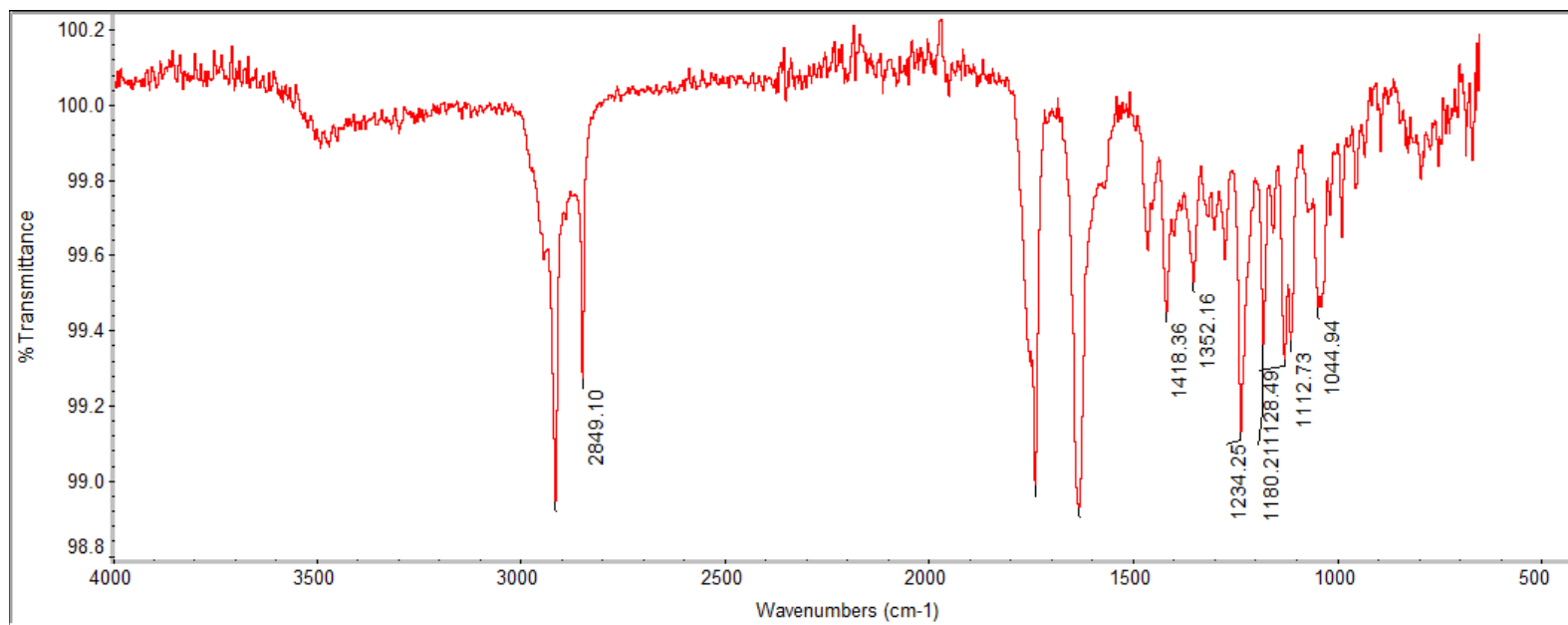
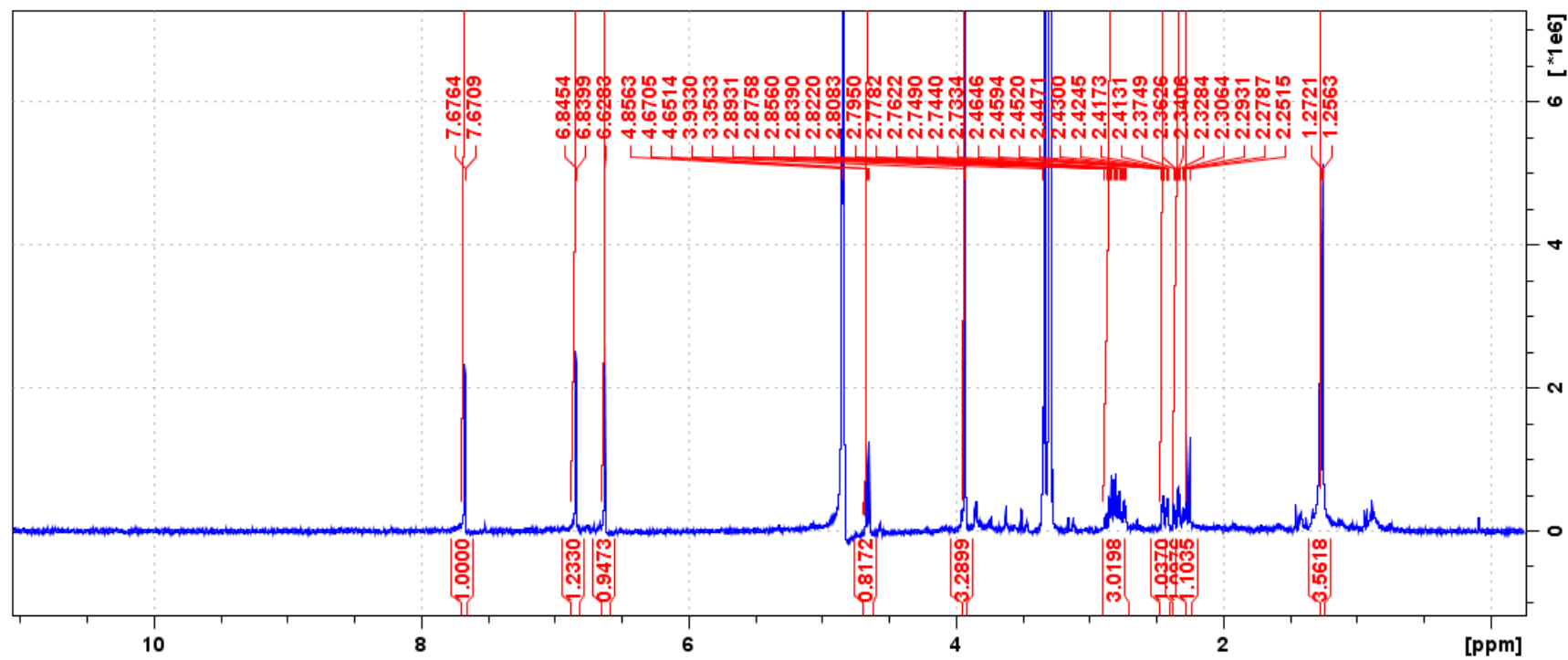


Figure 190. NOESY (400 MHz, CD₃OD) spectrum of icacinlactone K

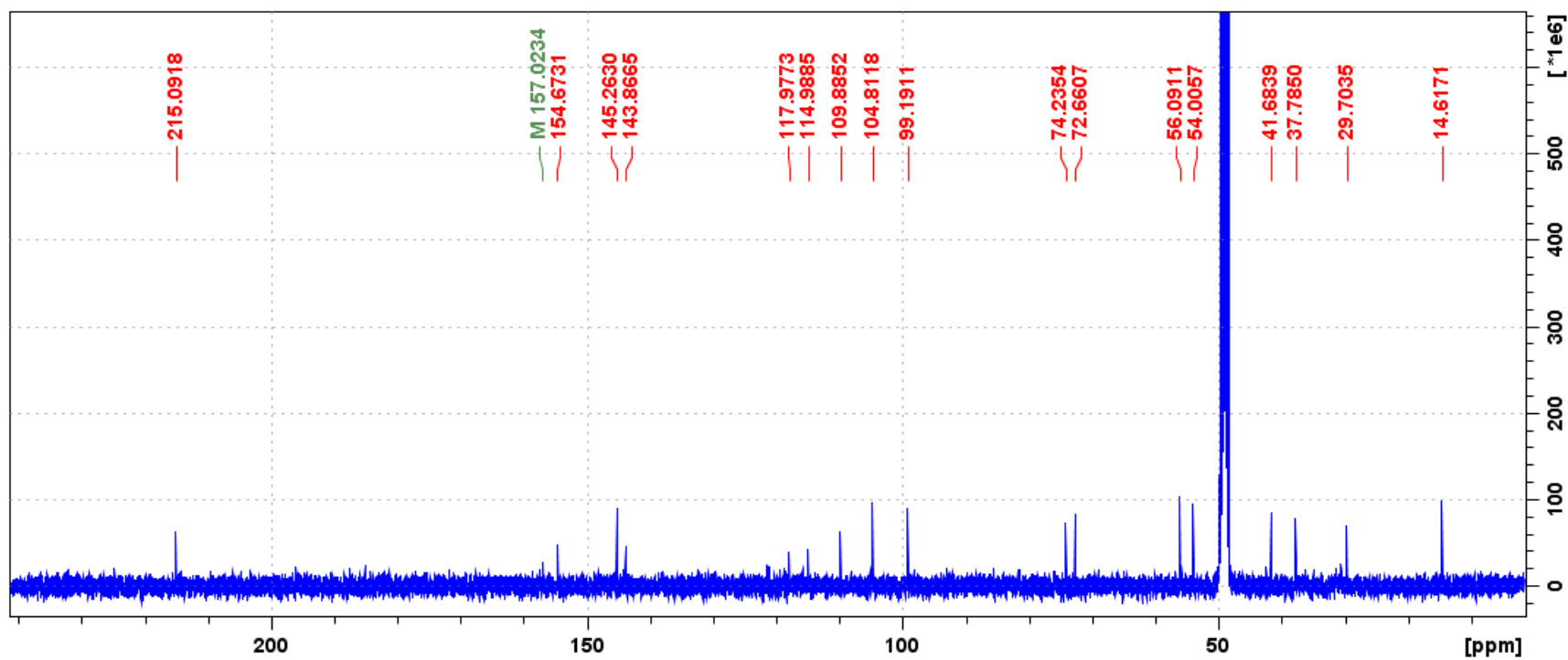
APPENDIX A (continued)

**Figure 191. IR spectrum of icacinlactone K**

APPENDIX A (continued)

Figure 192. ¹H (400 MHz, CD₃OD) spectrum of icacintrichanone

APPENDIX A (continued)

Figure 193. ¹³C (100 MHz, CD₃OD) spectrum of icacintrichanone

APPENDIX A (continued)

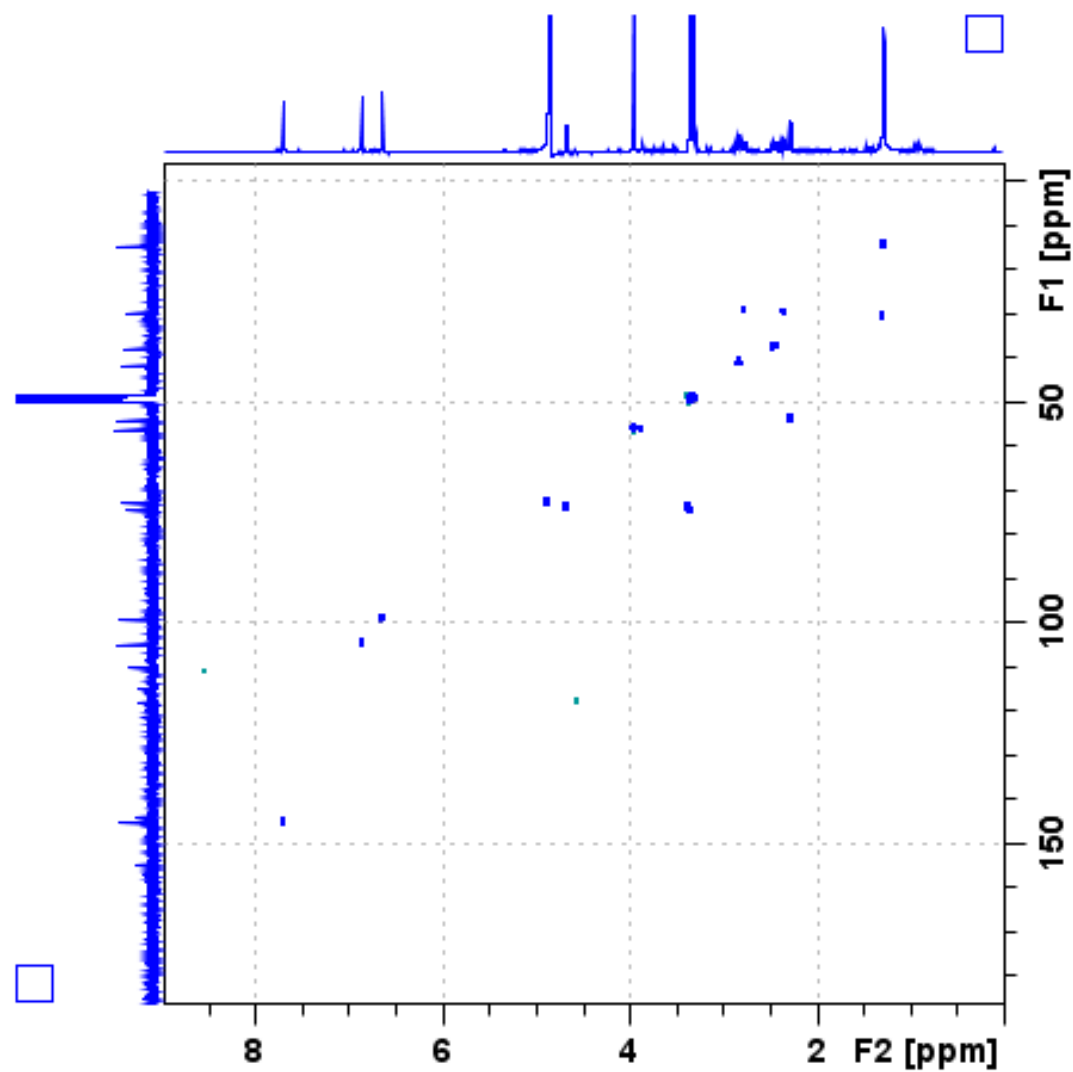


Figure 194. HSQC (400 MHz, CD_3OD) spectrum of icacintrichanone

APPENDIX A (continued)

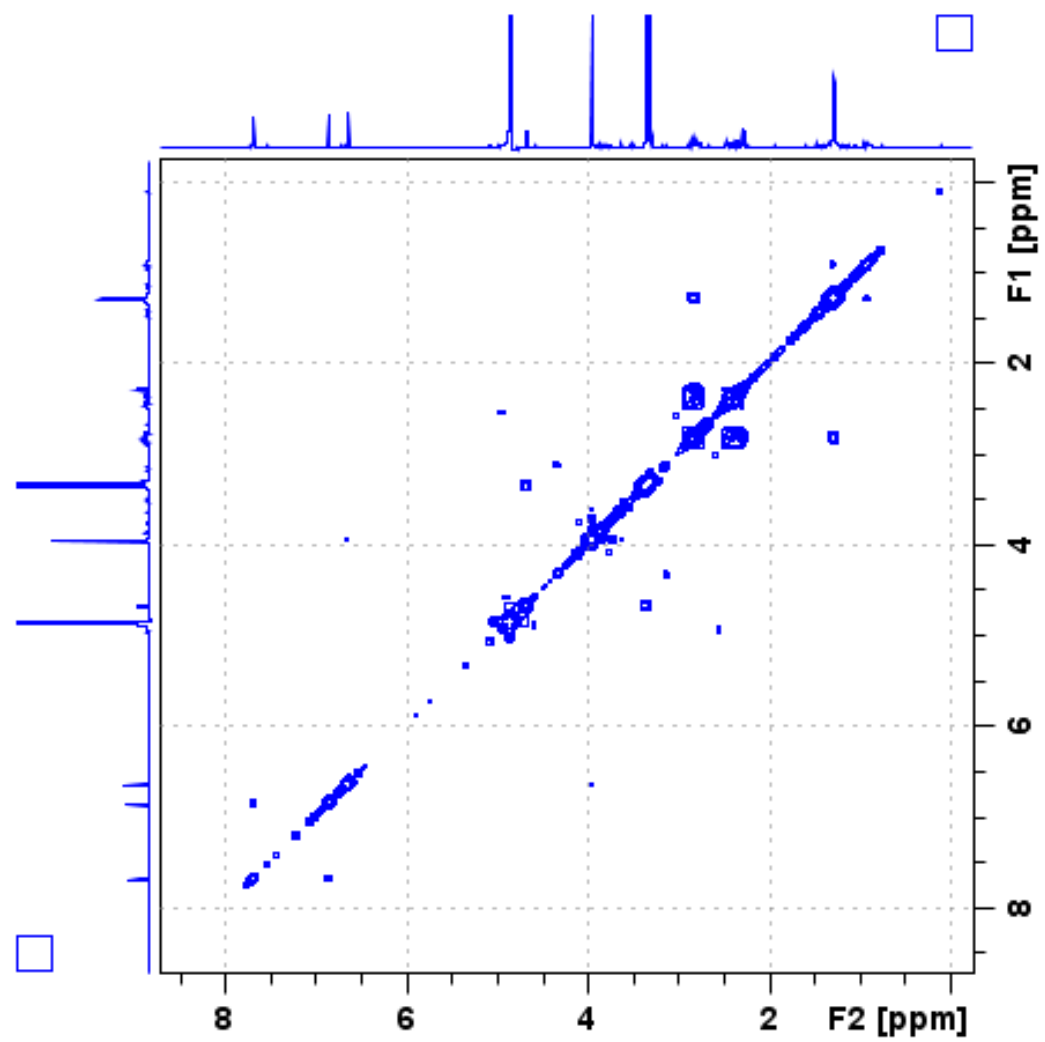


Figure 195. ^1H - ^1H COSY (400 MHz, CD_3OD) spectrum of icacintrichanone

APPENDIX A (continued)

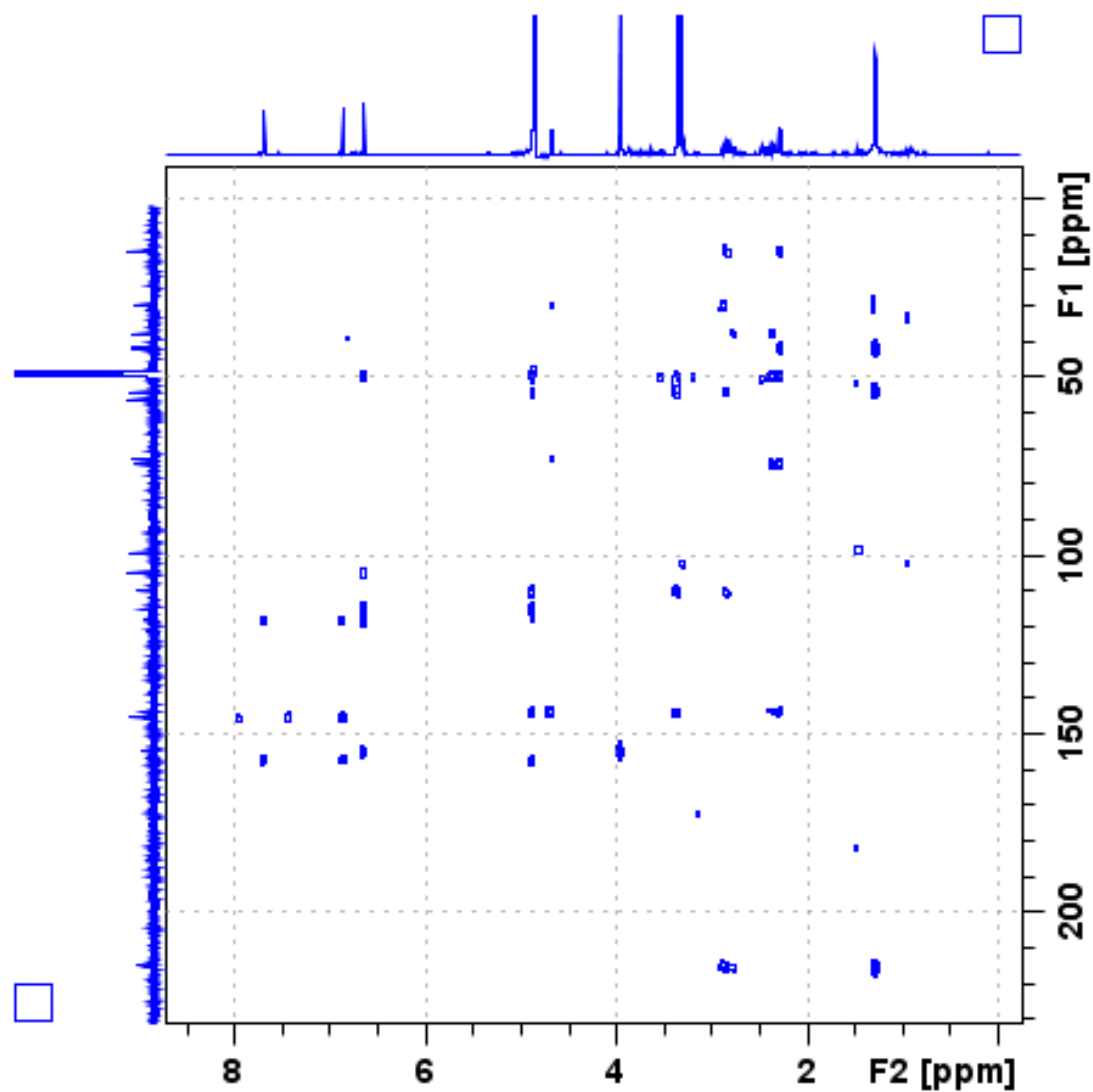


Figure 196. HMBC (400 MHz, CD₃OD) spectrum of icacintrichanone

APPENDIX A (continued)

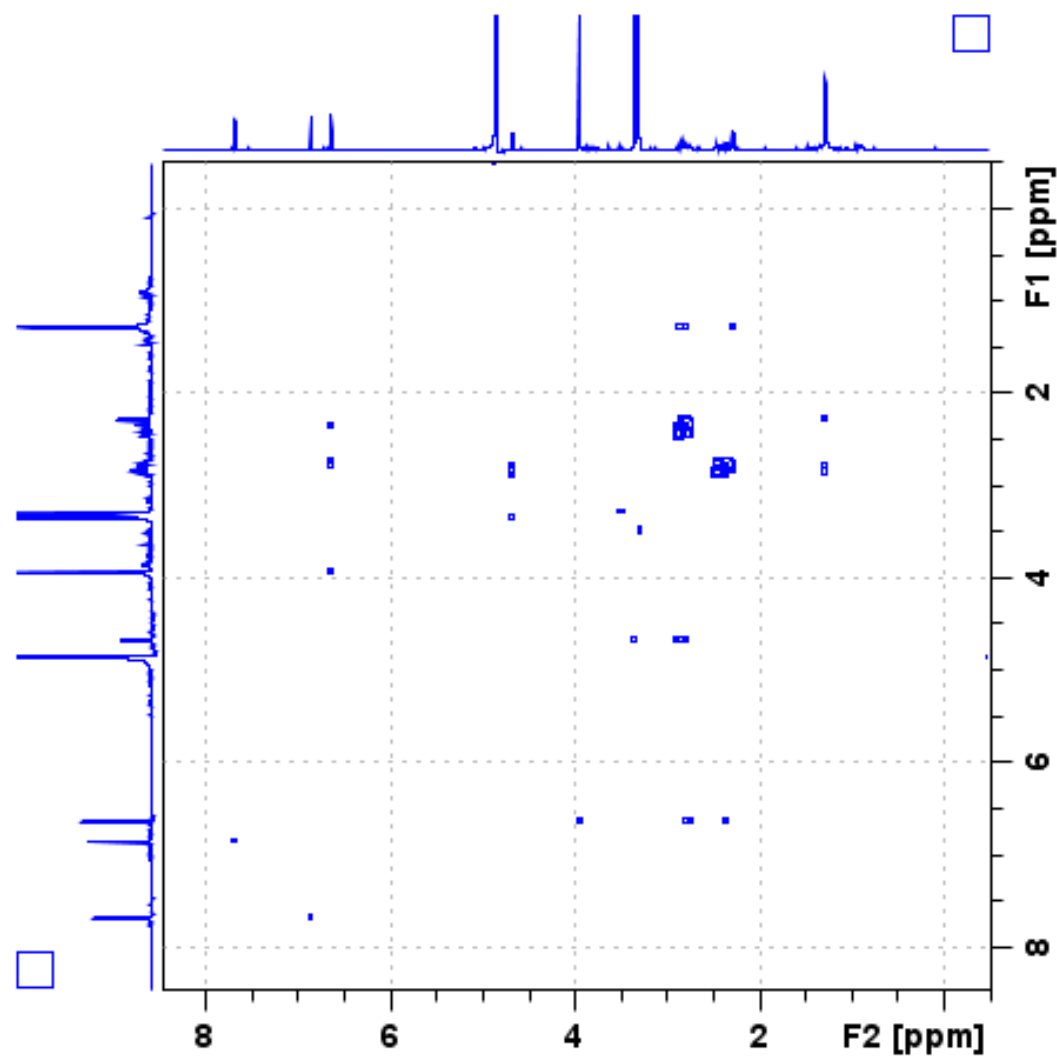
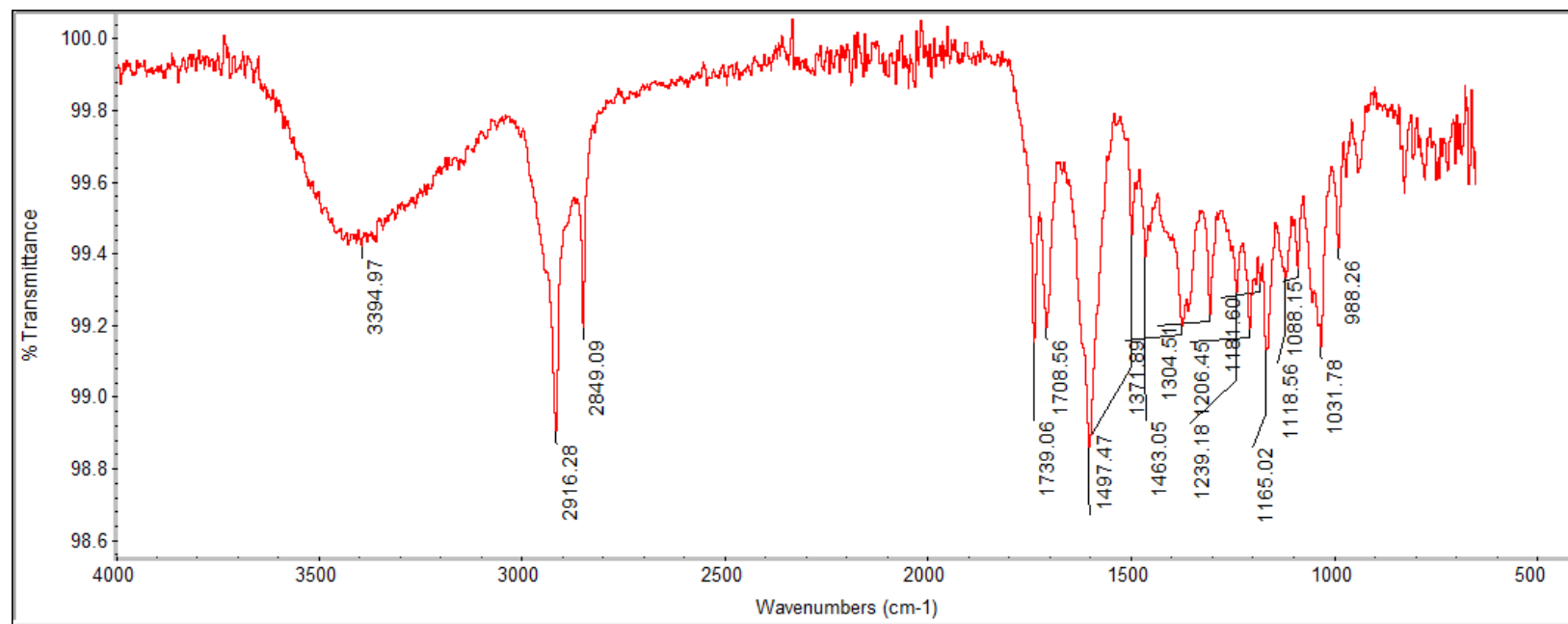


Figure 197. NOESY (400 MHz, CD₃OD) spectrum of icacintrichanone

APPENDIX A (continued)

**Figure 198. IR spectrum of icacintrichanone**

APPENDIX A (continued)

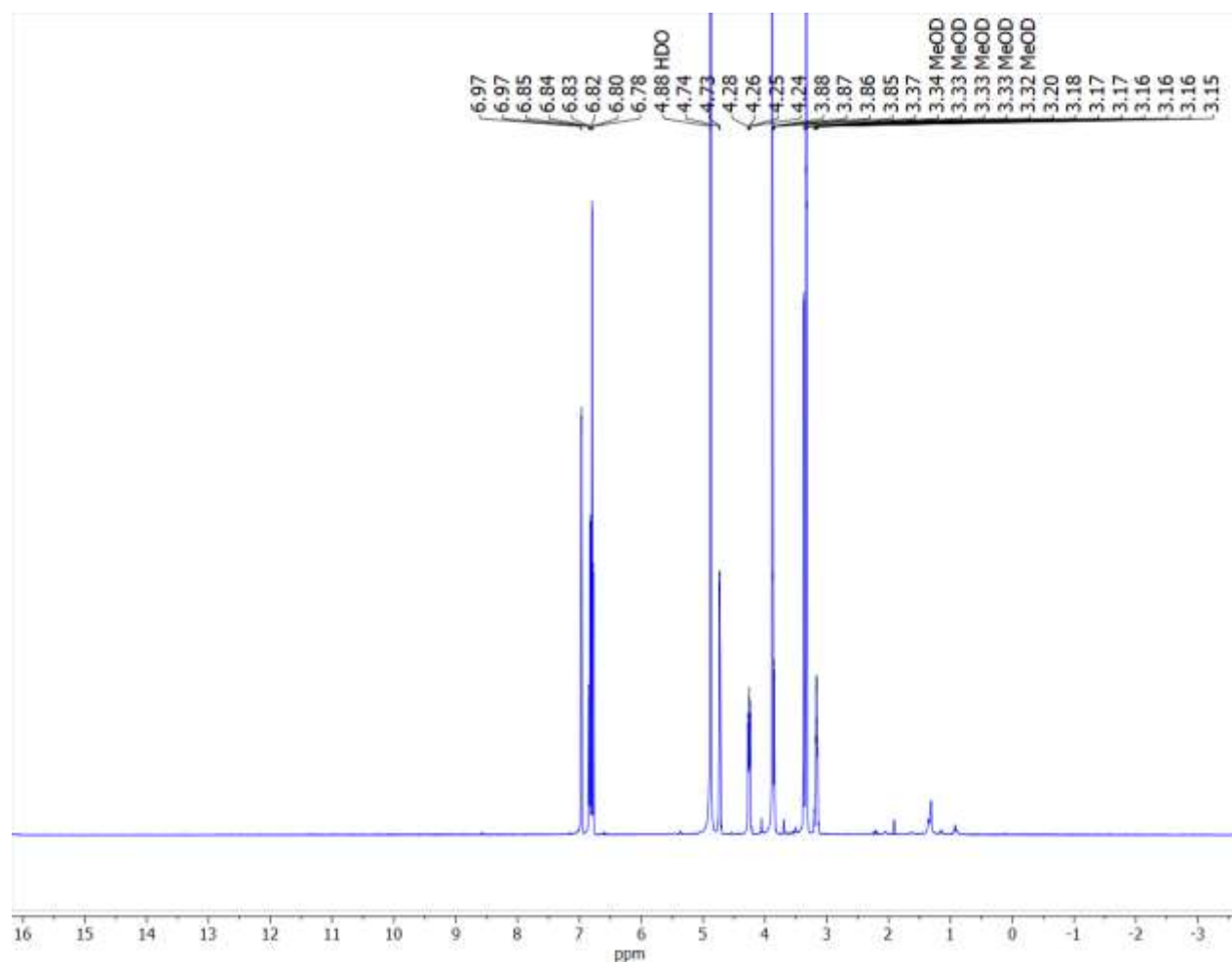


Figure 199. ¹H (400 MHz, CD₃OD) spectrum of (+)-pinoresinol

APPENDIX A (continued)

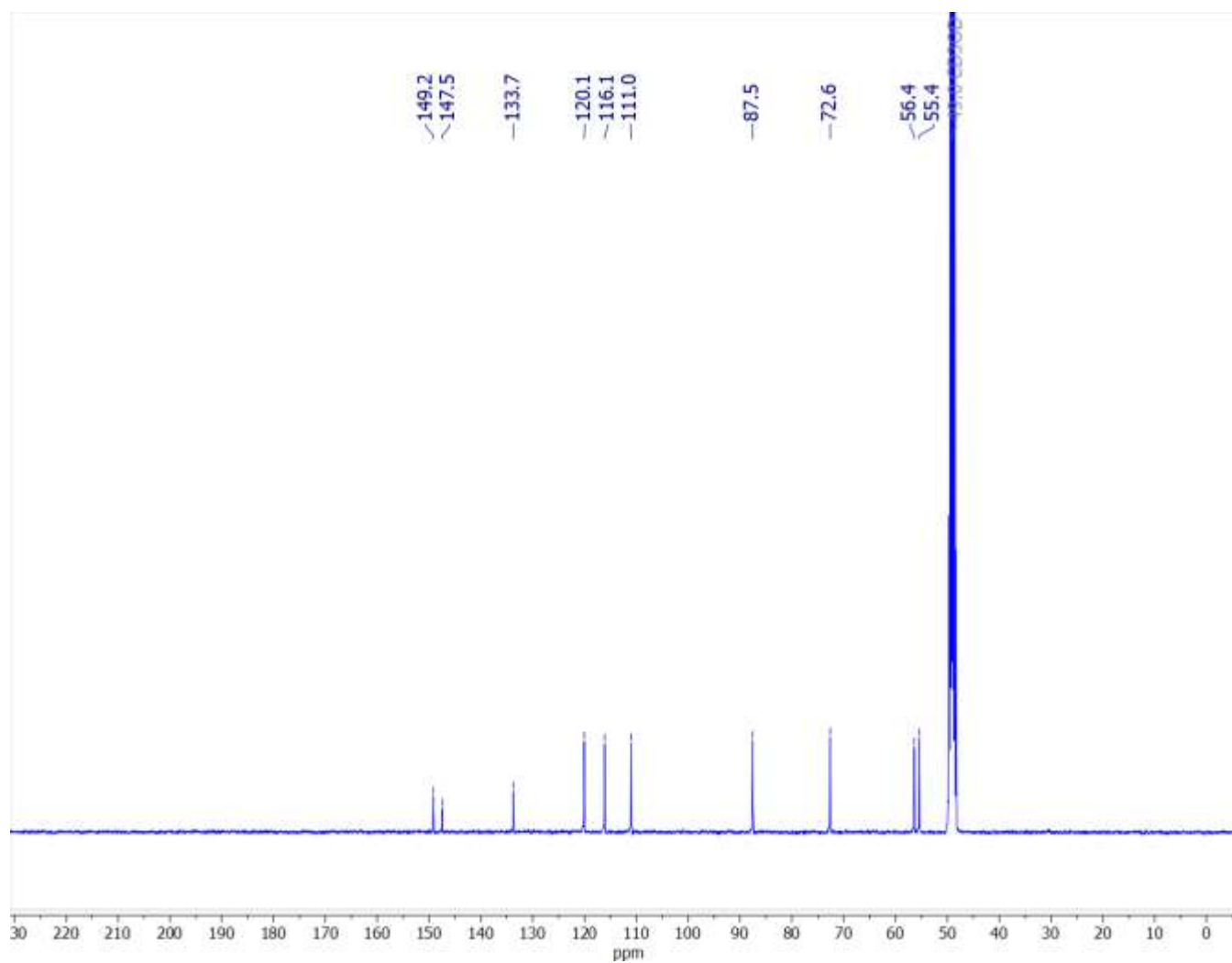


Figure 200. ¹³C (100 MHz, CD₃OD) spectrum of (+)-pinoresinol

APPENDIX A (continued)

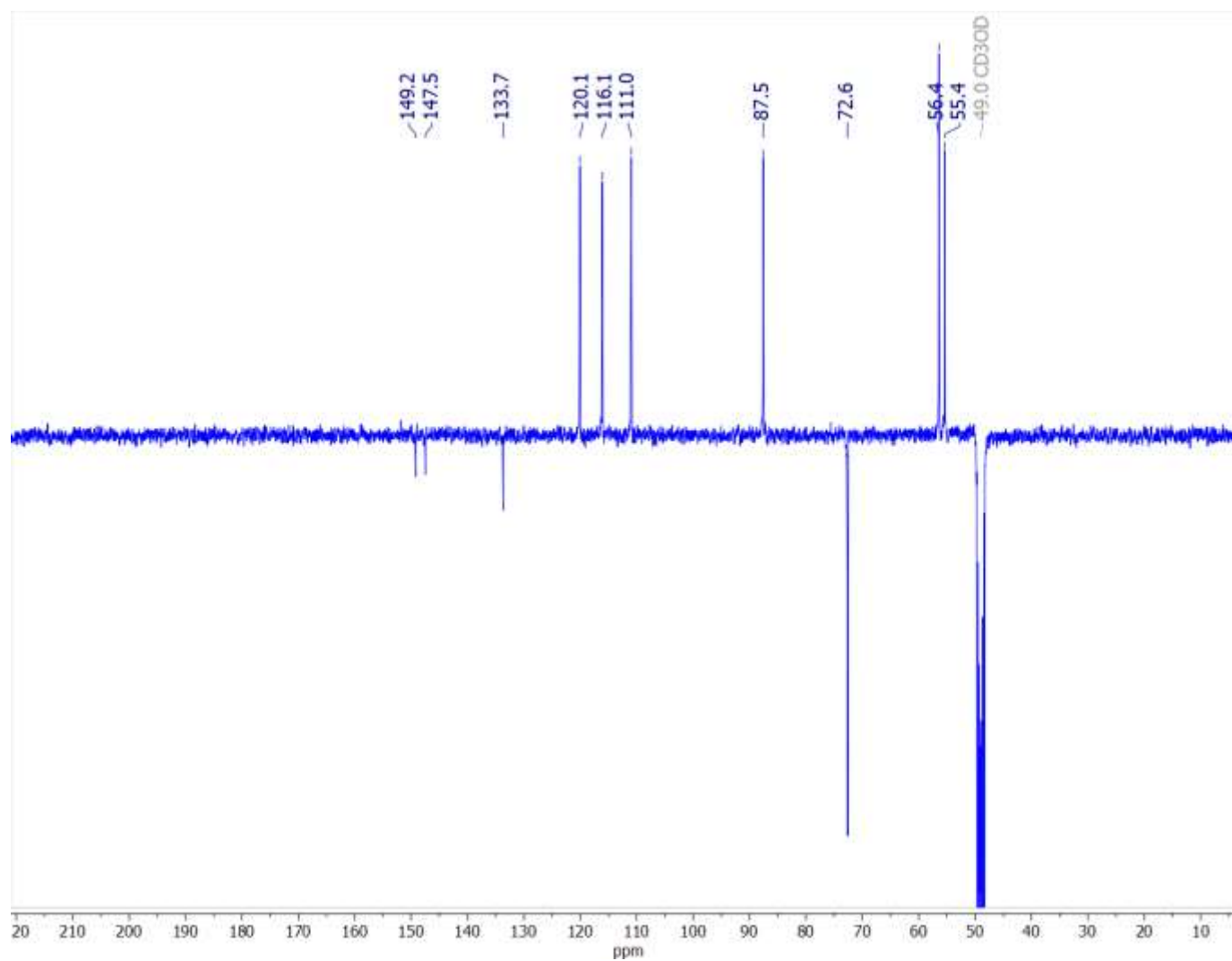


Figure 201. DEPTQ (100 MHz, CD₃OD) spectrum of (+)-pinoresinol

APPENDIX A (continued)

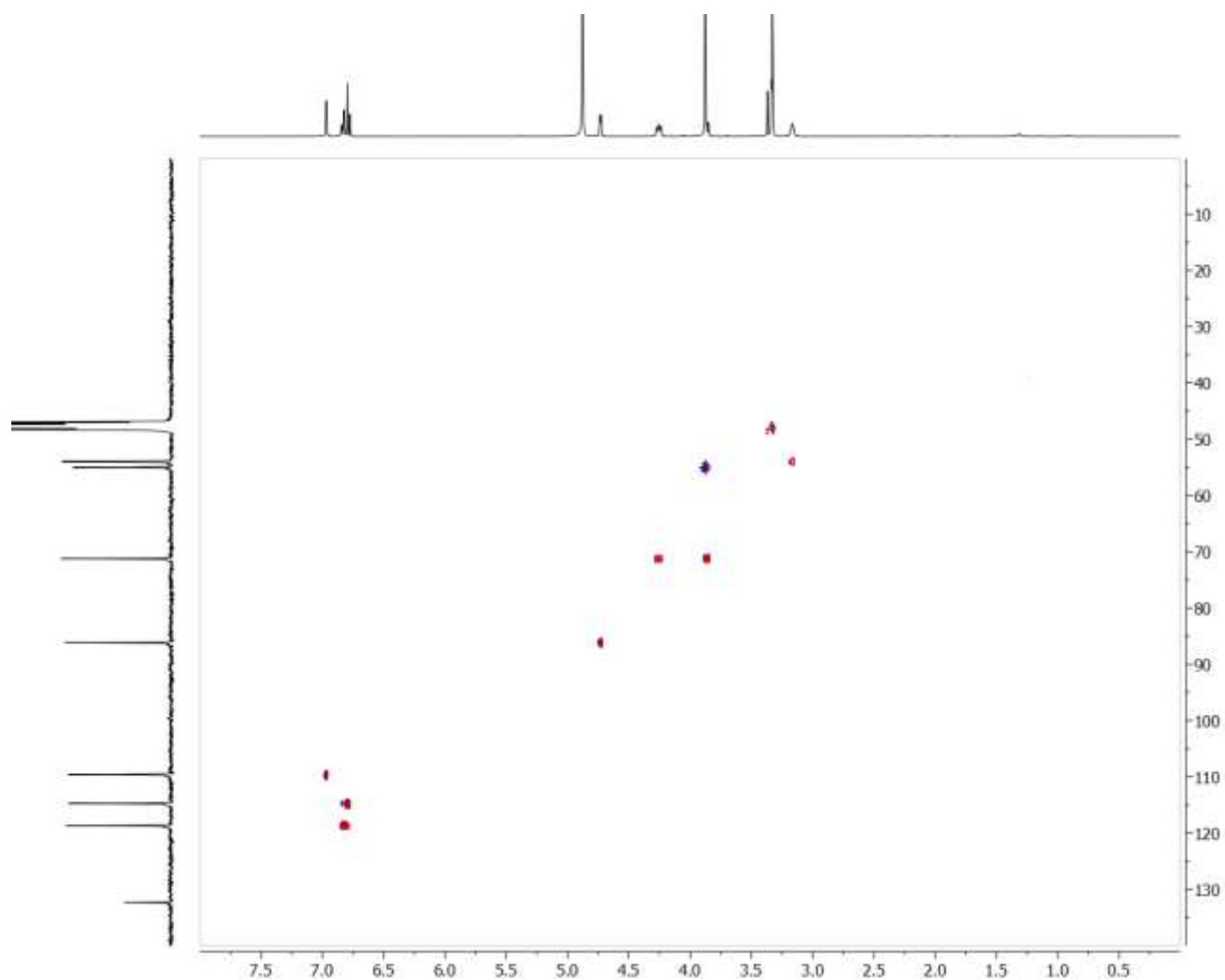


Figure 202. HSQC (400 MHz, CD_3OD) spectrum of (+)-pinoresinol

APPENDIX A (continued)

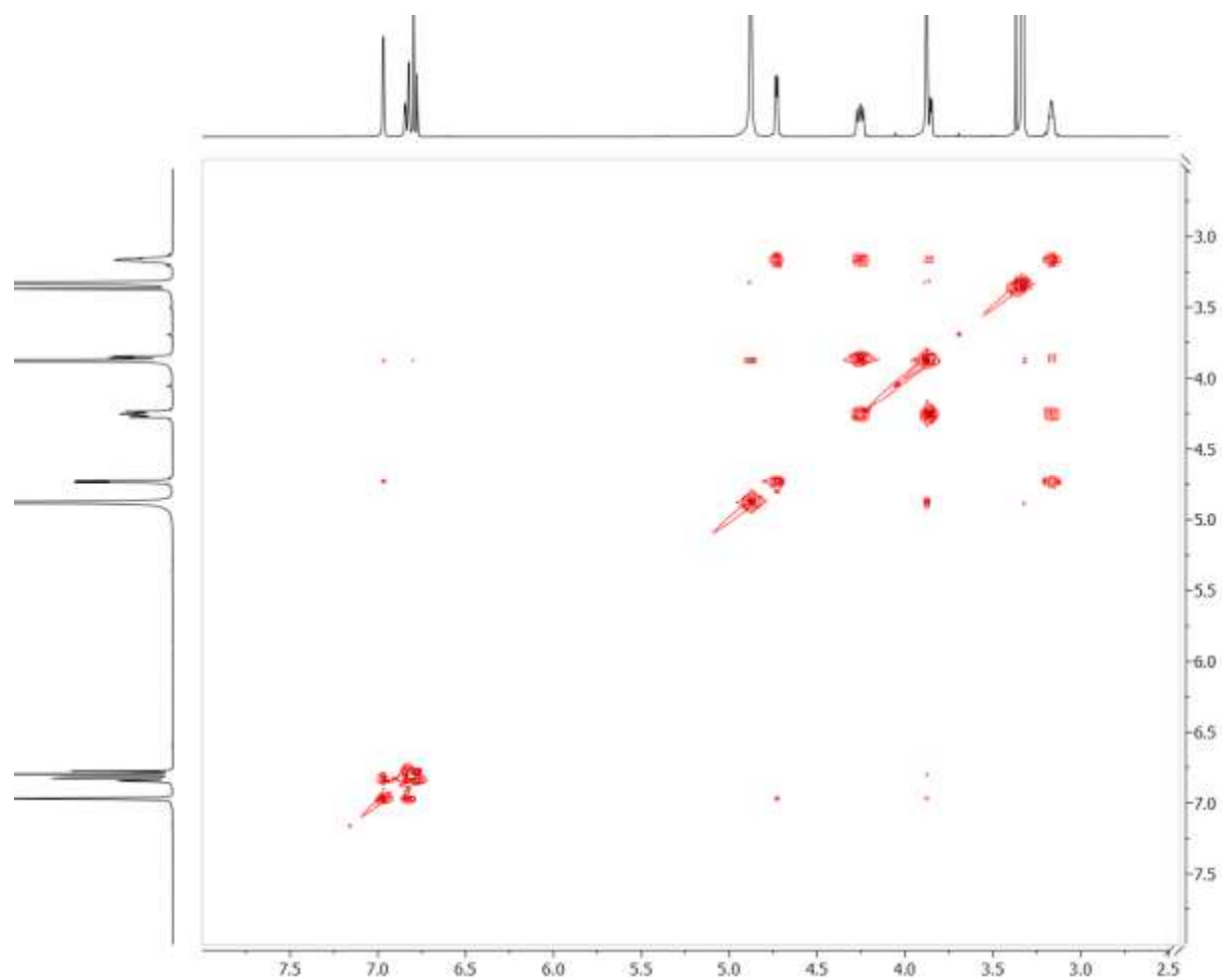


Figure 203. ^1H - ^1H COSY (400 MHz, CD_3OD) spectrum of (+)-pinoresinol

APPENDIX A (continued)

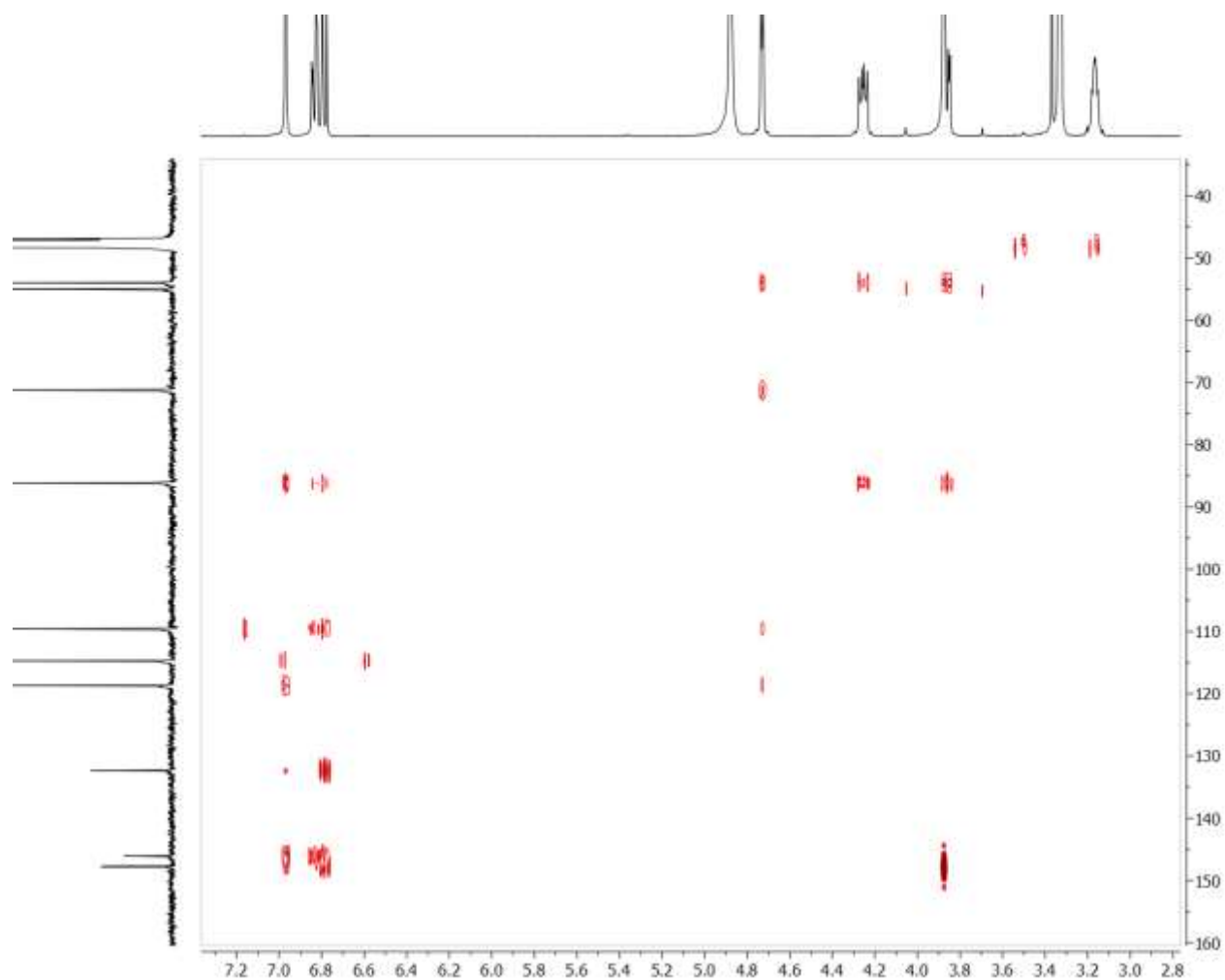


Figure 204. HMBC (400 MHz, CD_3OD) spectrum of (+)-pinoresinol

APPENDIX A (continued)

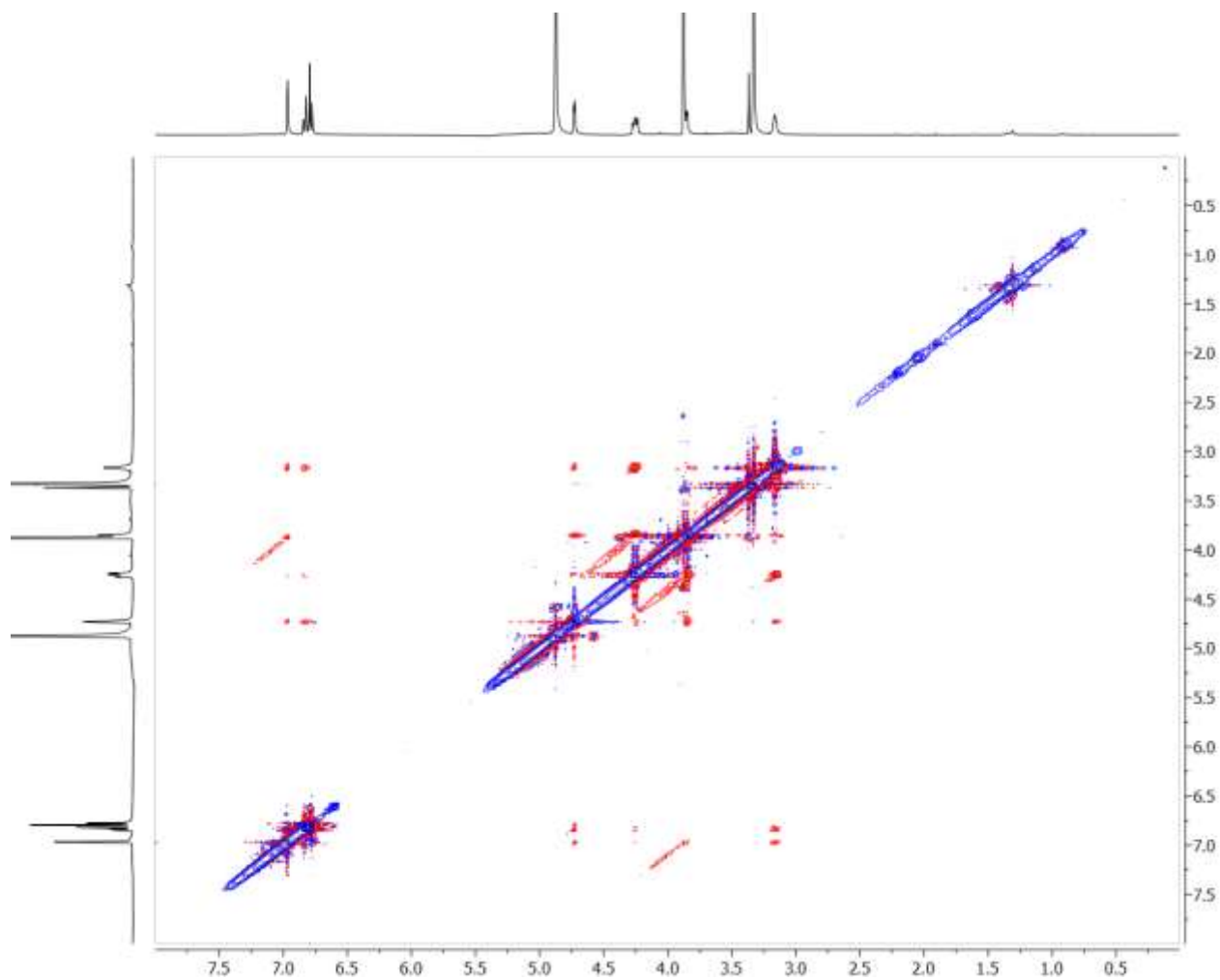
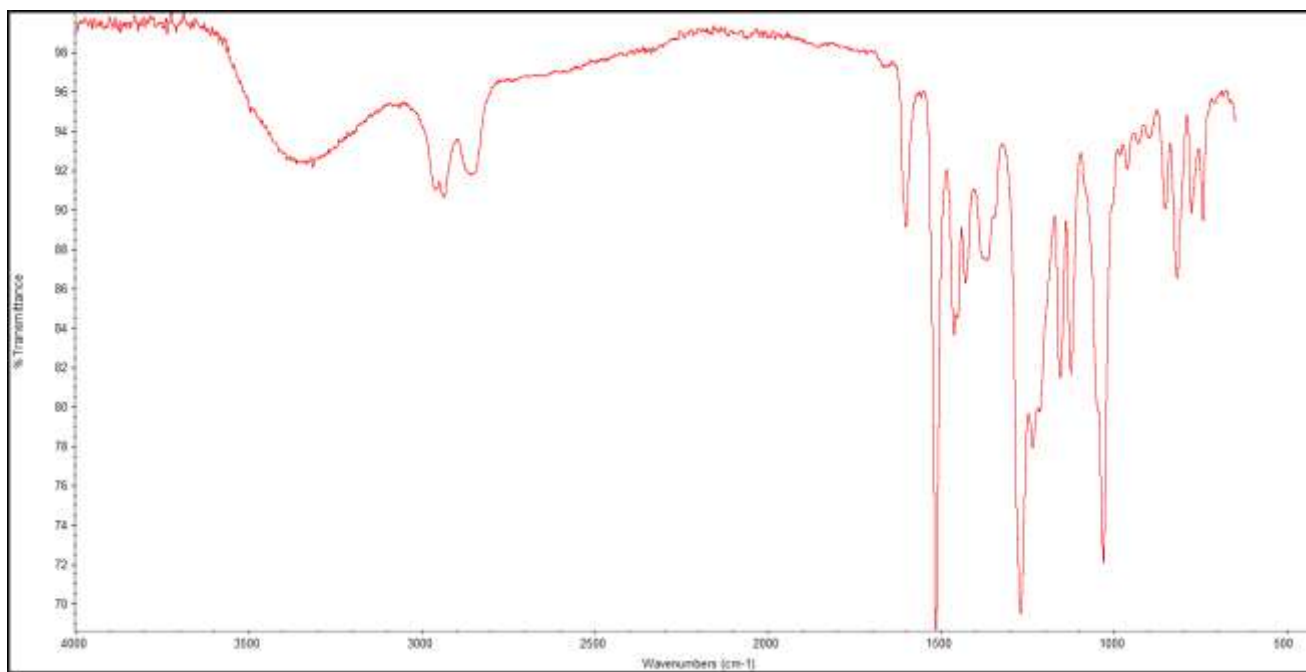


Figure 205. NOESY (400 MHz, CD₃OD) spectrum of (+)-pinoresinol

APPENDIX A (continued)

**Figure 206. IR spectrum of (+)-pinoresinol**

APPENDIX A (continued)

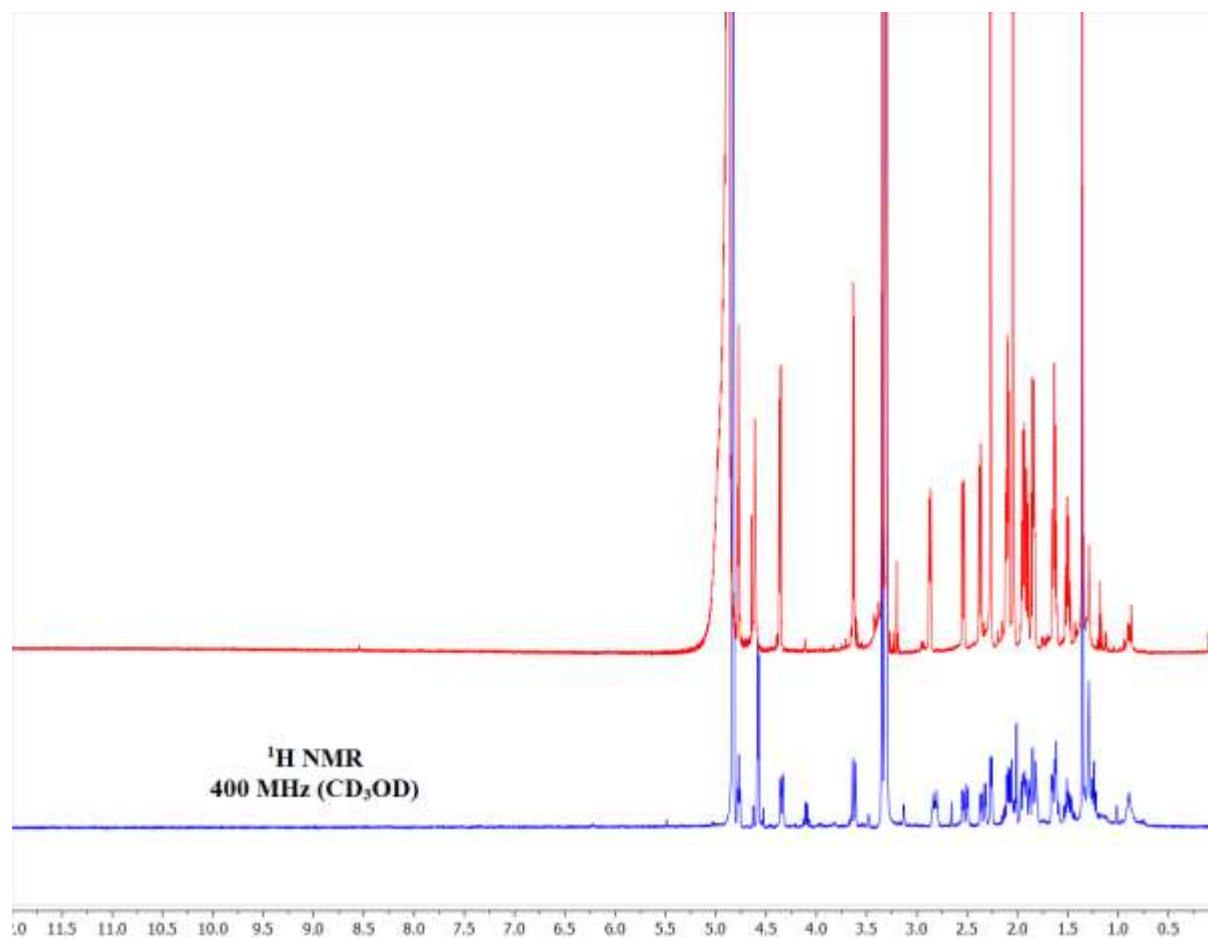


Figure 207. ^1H NMR (400 MHz) spectra of compound 24 (red) and humirianthenolide C standard (blue)

APPENDIX A (continued)

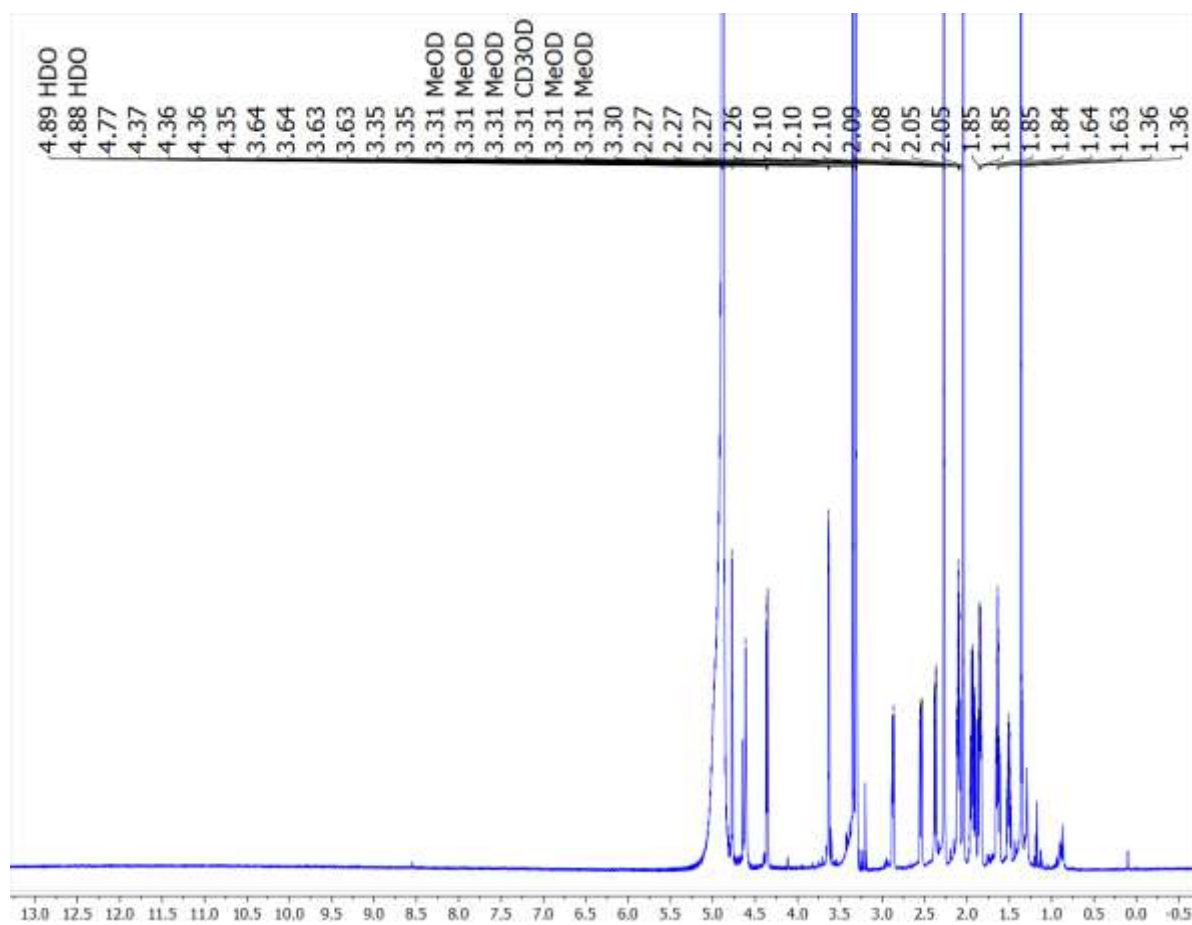
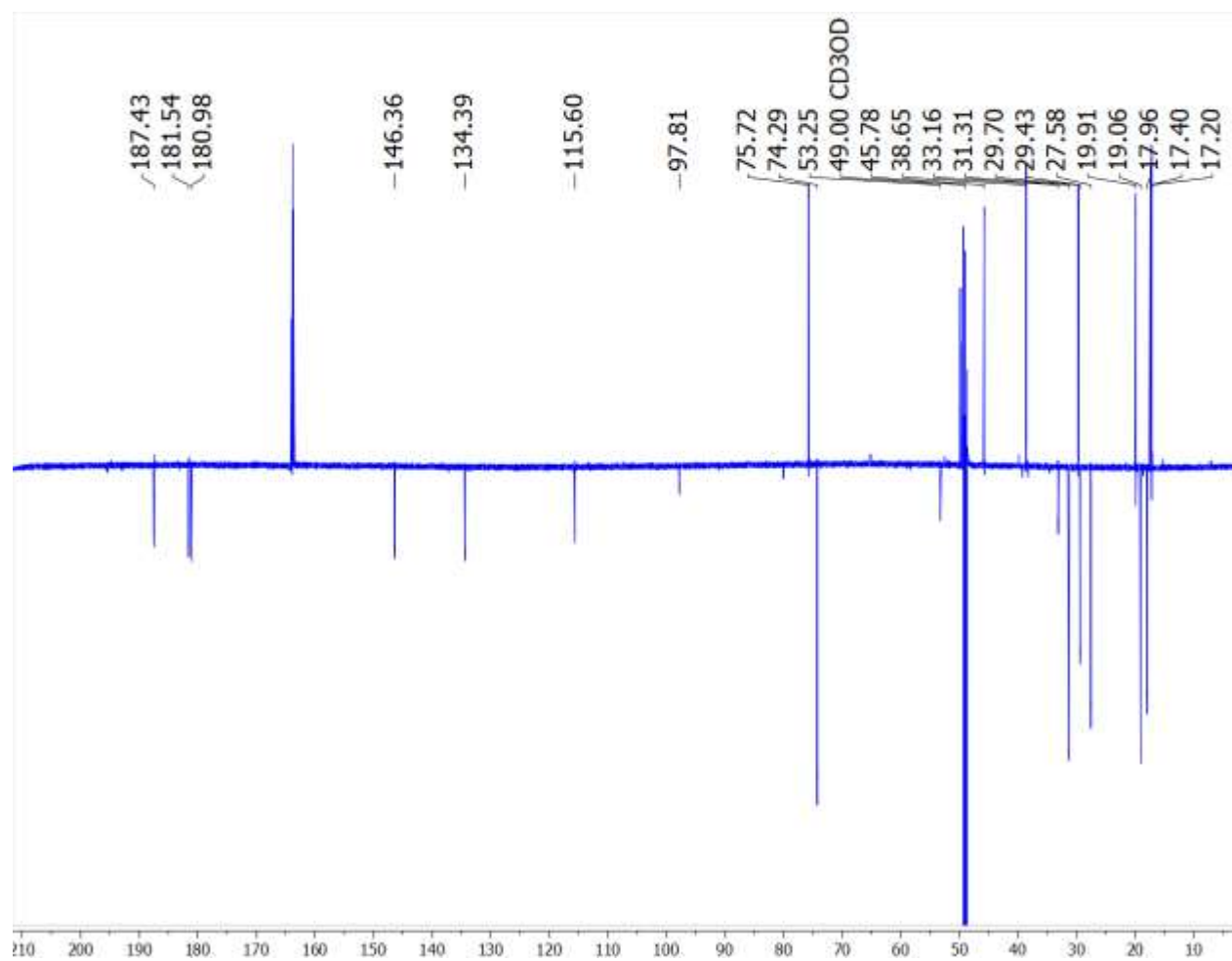


Figure 208. ¹H (900 MHz, CD₃OD) spectrum of compound 24

APPENDIX A (continued)

**Figure 209. DEPTQ (226 MHz, CD₃OD) spectrum of compound 24**

APPENDIX A (continued)

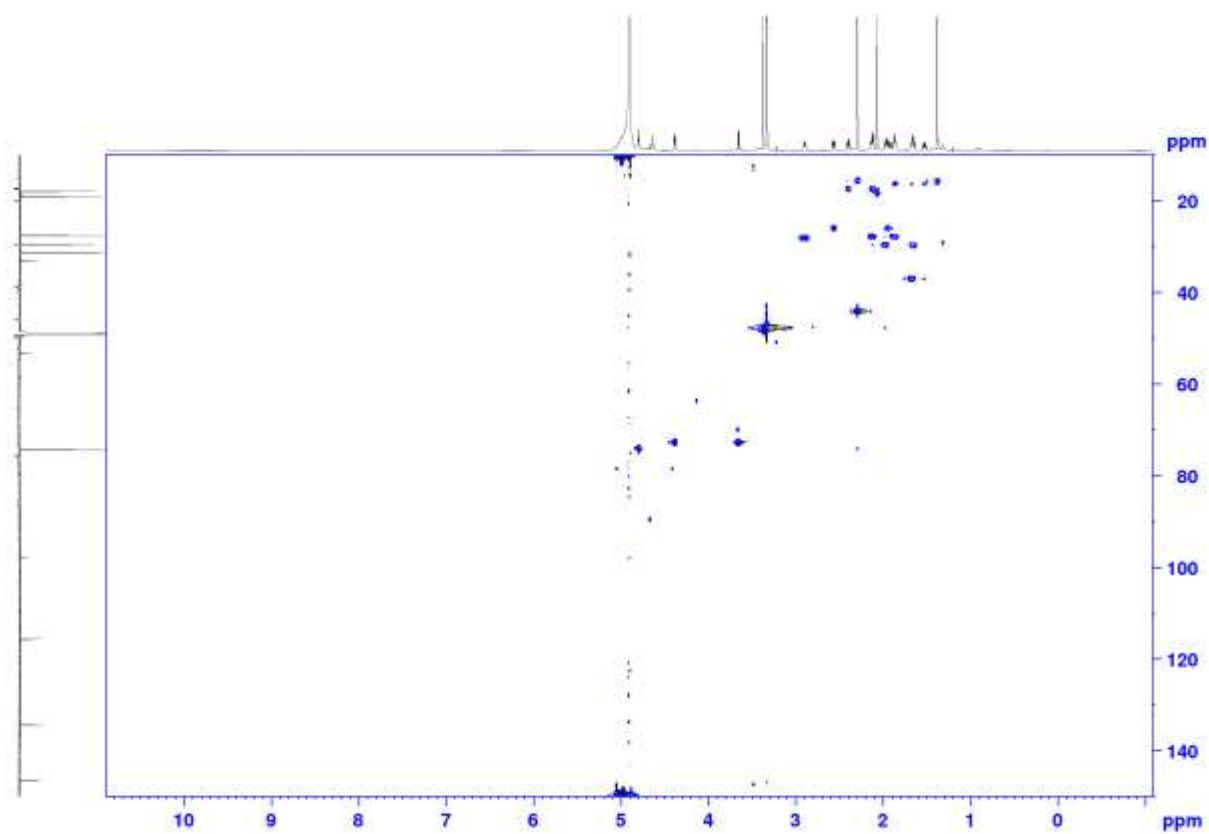


Figure 210. HSQC (900 MHz, CD_3OD) spectrum of compound 24

APPENDIX A (continued)

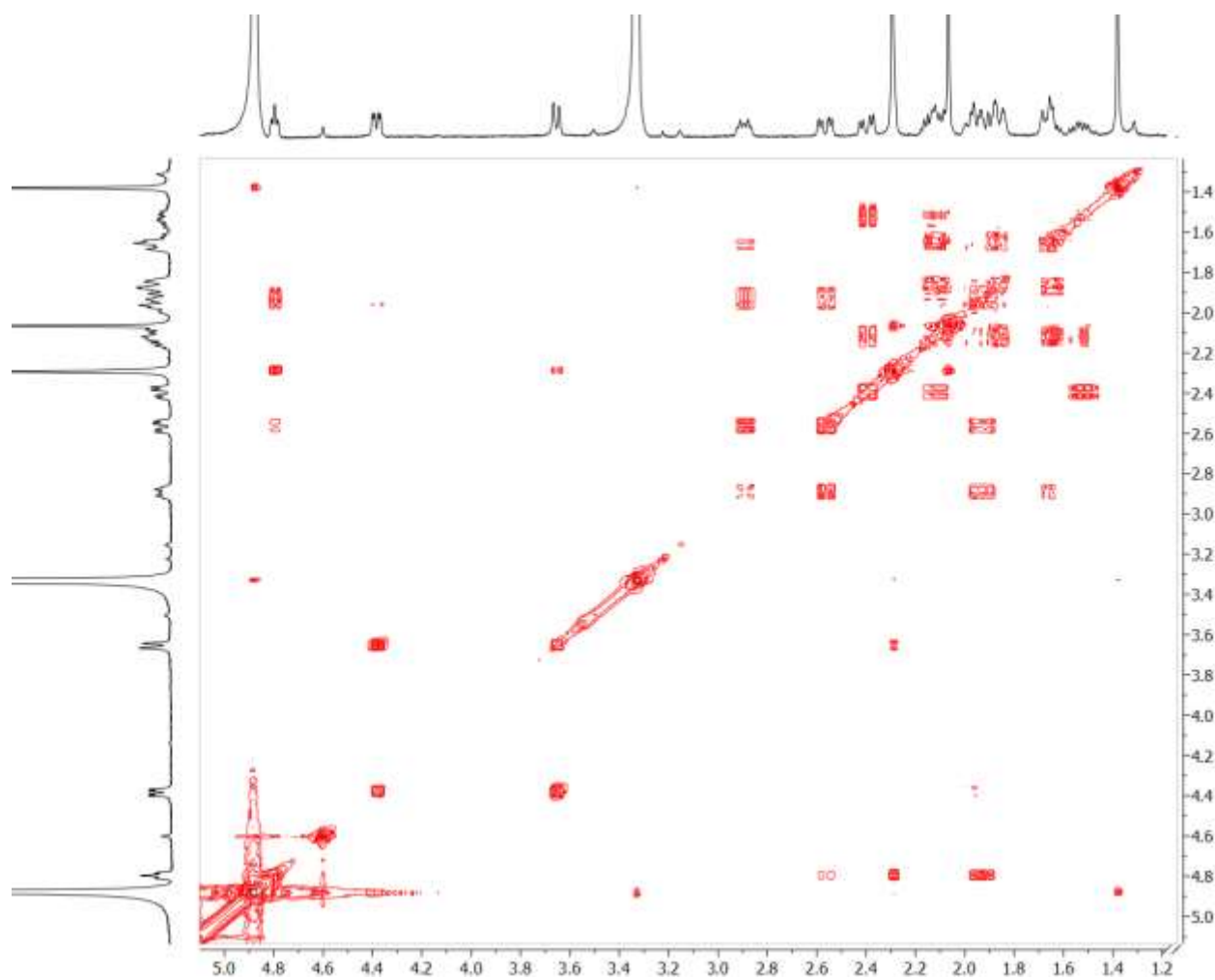


Figure 211. ^1H - ^1H COSY (900 MHz, CD_3OD) spectrum of compound 24

APPENDIX A (continued)

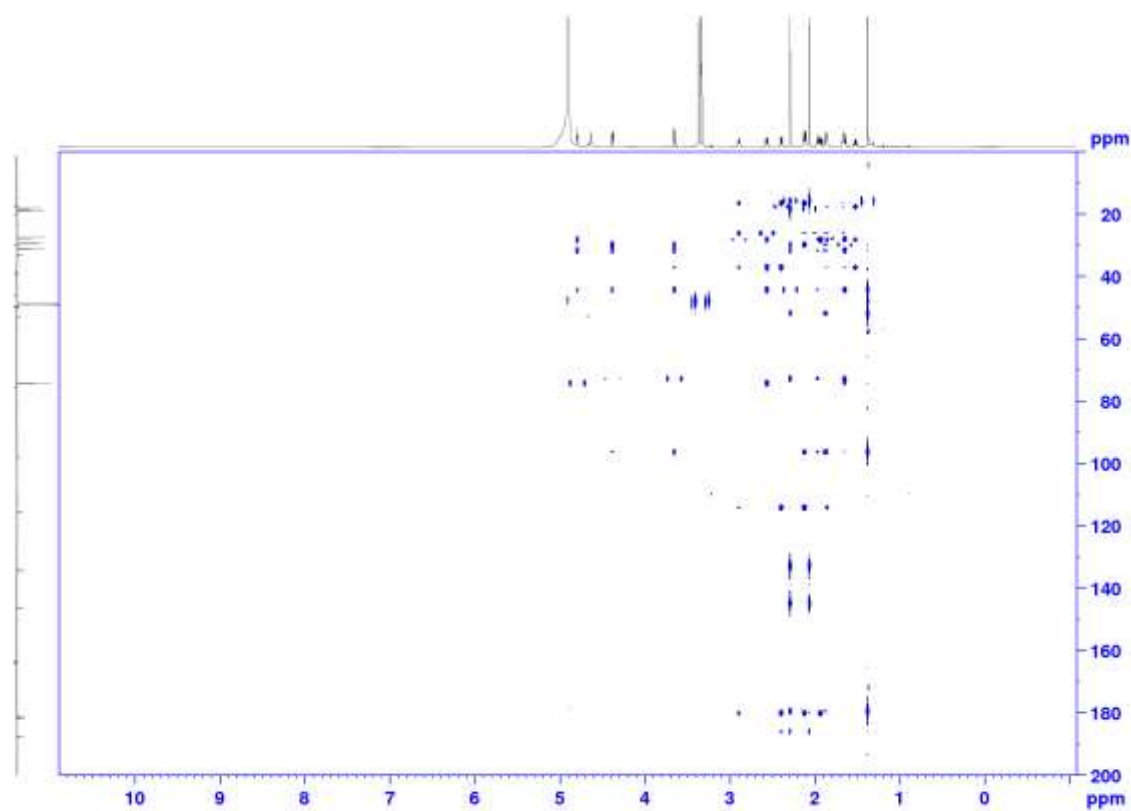


Figure 212. HMBC (900 MHz, CD₃OD) spectrum of compound 24

APPENDIX A (continued)

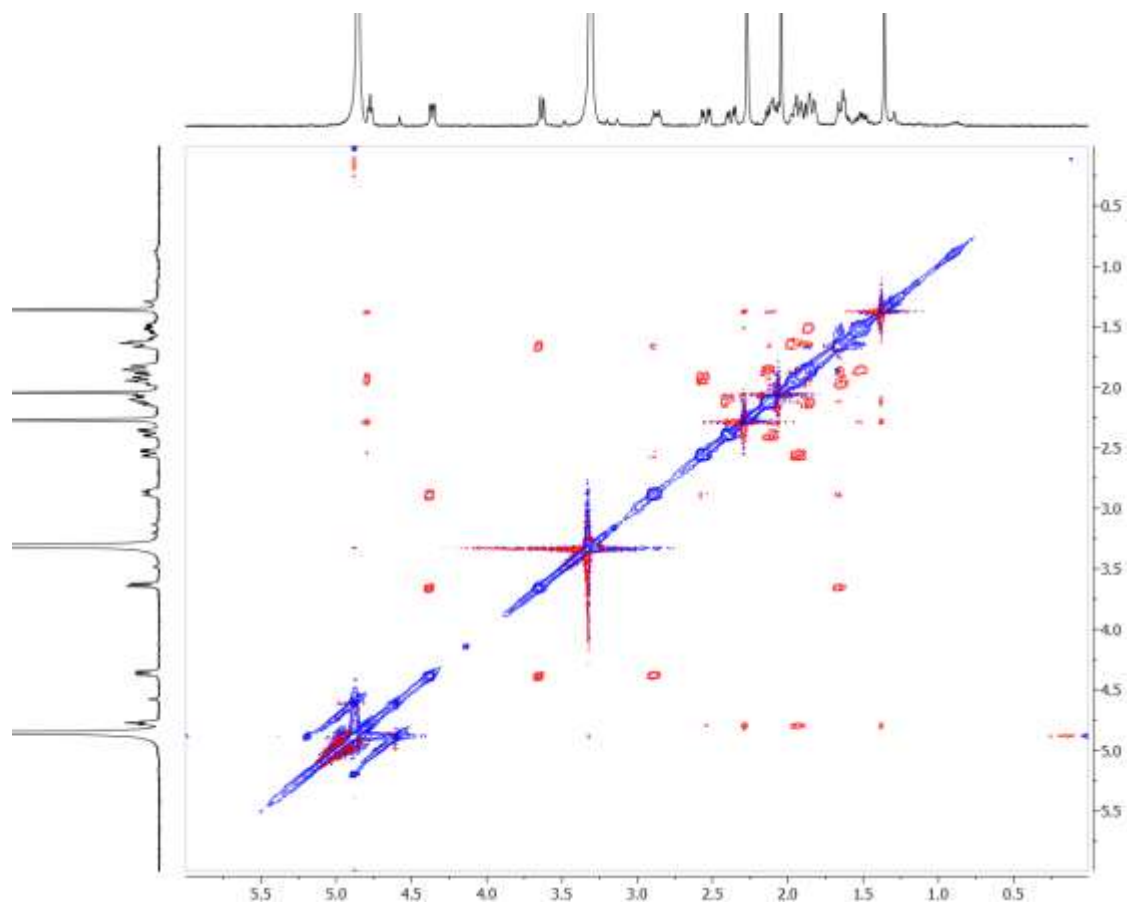


Figure 213. NOESY (900 MHz, CD₃OD) spectrum of compound 24

TABLE XVI. X-RAY CRYSTAL STRUCTURE DETERMINATION FOR COMPOUND 5*Agreement of data as a function of resolution*

RESOLUTION LIMIT	NUMBER OF REFLECTIONS			COMPLETENESS OF DATA	R-FACTOR OBSERVED	I/SIGMA	RMEAS	CC(1/2)
	OBSERVED	UNIQUE	POSSIBLE					
2.38	732	369	406	90.90%	4.30%	20.18	6.10%	98.9*
1.69	1178	593	724	81.90%	3.70%	19.94	5.30%	99.2*
1.38	1541	778	954	81.60%	3.80%	19	5.40%	99.3*
1.2	1861	936	1082	86.50%	4.00%	18.64	5.60%	99.3*
1.07	2156	1086	1248	87.00%	4.10%	18.16	5.70%	99.3*
0.98	2177	1103	1414	78.00%	3.90%	17.17	5.60%	99.3*
0.91	2317	1175	1462	80.40%	4.20%	16.13	5.90%	99.4*
0.85	2678	1359	1644	82.70%	4.40%	14.77	6.20%	99.0*
0.8	2663	1361	1704	79.90%	4.70%	14.11	6.70%	99.1*
TOTAL	17303	8760	10638	82.30%	4.00%	16.94	5.70%	99.3*

APPENDIX A (continued)

TABLE XVII. X-RAY CRYSTAL STRUCTURE DETERMINATION FOR COMPOUND 11*Agreement of data as a function of resolution*

RESOLUTION LIMIT	NUMBER OF REFLECTIONS			COMPLETENESS OF DATA	R-FACTOR OBSERVED	I/SIGMA	RMEAS	CC(1/2)
	OBSERVED	UNIQUE	POSSIBLE					
2.36	525	137	142	96.50%	4.80%	27.45	5.60%	99.8*
1.69	771	215	221	97.30%	4.70%	2570.00%	5.50%	99.6*
1.39	987	287	297	96.60%	5.30%	2294.00%	6.30%	99.2*
1.2	1271	345	350	98.60%	4.60%	2297.00%	5.40%	99.6*
1.08	1385	383	394	97.20%	4.60%	2228.00%	5.50%	99.4*
0.98	1445	434	460	94.30%	5.10%	1935.00%	6.10%	99.3*
0.91	1410	418	434	96.30%	6.00%	1569.00%	7.20%	99.3*
0.85	1591	510	524	97.30%	7.90%	1324.00%	9.70%	98.5*
0.8	1450	496	528	93.90%	9.00%	1002.00%	11.10%	98.8*
TOTAL	10835	3225	3350	96.30%	5.00%	1830.00%	5.90%	99.8*

Definitions

$$\text{R-FACTOR OBSERVED} = (\text{SUM}(\text{ABS}(\text{I}(\text{h}, \text{i}) - \text{I}(\text{h})))) / (\text{SUM}(\text{I}(\text{h}, \text{i})))$$

$$\text{I/SIGMA} = \text{mean of intensity/Sigma(I) of unique reflections after merging symmetry-related observations}$$

$$\text{Sigma(I)} = \text{standard deviation of reflection intensity I estimated from sample statistics}$$

$$\text{RMEAS} = \text{redundancy independent R-factor of I (Diederichs and Karplus, } \textit{Nature Struct Biol}, \textbf{4}, 269-275, 1997)$$

$$\text{CC}(1/2) = \text{percentage of correlation between intensities from random half-datasets. Correlation significant at the 0.1\% level is marked by an asterisk (Karplus and Diederichs, } \textit{Science}, \textbf{336}, 1030-33, 2012)$$

$$\text{ANOM CORR} = \text{percentage of correlation between random half-sets of anomalous intensity differences. Correlation significant at the 0.1\% level is marked.}$$

**TABLE XVIII. CARTESIAN COORDINATE OF PREDOMINANT CONFORMER OF
COMPOUND 17**

Atomic Number	Atomic Type	Conformer 1 coordinates (Angstroms)			Conformer 3 coordinates (Angstroms)		
		X	Y	Z	X	Y	Z
1	6	-3.177983	-1.899655	0.577557	-3.420455	-1.682608	0.679052
2	6	-3.644357	-0.732551	-0.293016	-3.764392	-0.53553	-0.270976
3	6	-3.330605	0.64335	0.338097	-3.294994	0.836842	0.261897
4	6	-1.781744	0.76532	0.465408	-1.741103	0.796674	0.372567
5	6	-1.095193	-0.558406	0.031509	-1.206557	-0.622973	0.03824
6	6	-1.66928	-1.71071	0.893777	-1.900095	-1.629856	0.989654
7	6	-1.209083	1.987404	-0.263355	-1.047363	1.885696	-0.451095
8	6	0.222913	1.943774	-0.618904	0.376383	1.668181	-0.765013
9	6	0.974655	0.83772	-0.466414	1.013323	0.505887	-0.520433
10	6	0.44694	-0.456955	0.103608	0.339519	-0.702286	0.091207
11	6	2.455209	0.82643	-0.747828	2.502735	0.391834	-0.694185
12	6	3.28325	0.319419	0.492902	3.237869	0.070079	0.639944
13	6	2.381434	0.158096	1.735557	2.501007	-1.07709	1.382259
14	6	1.072999	-0.643125	1.525776	0.976529	-0.897555	1.494797
15	8	2.715724	-0.090448	-1.834368	2.824502	-0.715344	-1.54384
16	6	3.909906	-0.811796	-1.542952	4.172237	-1.122568	-1.262575
17	6	3.853013	-1.029909	-0.027317	4.580876	-0.484735	0.080383
18	8	-1.88677	2.982222	-0.495169	-1.617355	2.920515	-0.779086
19	6	4.416765	1.310205	0.813433	3.406104	1.299064	1.538946
20	8	5.107507	-1.320433	0.581438	5.550468	0.522154	-0.218212
21	6	-1.525637	-0.858855	-1.422648	-1.683597	-0.980942	-1.388491
22	8	-2.952167	-0.783518	-1.555459	-3.092242	-0.749567	-1.527148
23	8	-5.00517	-0.902224	-0.577405	-5.137974	-0.573838	-0.541553
24	6	-4.059319	0.902197	1.662839	-3.975027	1.263829	1.569037
25	1	2.788014	1.828549	-1.048152	2.906514	1.321144	-1.12286
26	1	-1.527113	0.939183	1.523813	-1.453568	1.020185	1.413131
27	1	0.851607	-1.258045	-0.531535	0.643629	-1.577124	-0.503923
28	1	-3.781094	-1.948883	1.489148	-4.023596	-1.607518	1.588849
29	1	-3.363647	-2.820793	0.016251	-3.701041	-2.615845	0.18057
30	1	-3.666545	1.397533	-0.383712	-3.554606	1.572806	-0.508559
31	1	-1.115799	-2.635102	0.683409	-1.451151	-2.62389	0.865517
32	1	-1.52518	-1.491678	1.957393	-1.730809	-1.332933	2.031133
33	1	0.639835	2.864008	-1.023807	0.89842	2.516222	-1.203852
34	1	2.121191	1.16662	2.082967	2.68971	-2.025851	0.862557
35	1	2.966737	-0.299337	2.543195	2.936477	-1.184775	2.384932
36	1	1.239834	-1.712159	1.701759	0.55685	-1.786233	1.97836
37	1	0.361528	-0.317933	2.293015	0.733259	-0.041923	2.138956
38	1	3.889833	-1.733718	-2.132749	4.848822	-0.768924	-2.049448
39	1	4.808502	-0.23534	-1.812286	4.188905	-2.21707	-1.240646
40	1	3.142579	-1.839128	0.19228	5.017623	-1.221551	0.769976

APPENDIX A (continued)

41	1	5.098796	1.440183	-0.033946	3.866467	2.133338	0.999401
42	1	3.993297	2.291646	1.058558	2.438913	1.649046	1.915319
43	1	5.008876	0.965979	1.666205	4.028766	1.064759	2.4132
44	1	5.338714	-2.245172	0.406416	5.893022	0.891441	0.610743
45	1	-1.189992	-1.868856	-1.705187	-1.469302	-2.041436	-1.593363
46	1	-1.093647	-0.150257	-2.13689	-1.178388	-0.382845	-2.15438
47	1	-5.229833	-0.302295	-1.309145	-5.301425	-0.006336	-1.31426
48	1	-3.877748	1.93202	1.991806	-3.678633	2.287763	1.825196
49	1	-5.139645	0.764777	1.549657	-5.065184	1.238402	1.470299
50	1	-3.715395	0.231685	2.461083	-3.696862	0.616138	2.410574

TABLE XIX. CARTESIAN COORDINATE OF PREDOMINANT CONFORMER OF COMPOUND 18

Atomic Number	Atomic Type	Conformer 1 coordinates (Angstroms)		
		X	Y	Z
1	6	1.910086	2.368889	-0.186099
1	6	-3.371316	-1.927164	0.331861
2	6	-3.789897	-0.640332	-0.396137
3	6	-3.448719	0.63084	0.400726
4	6	-1.899725	0.666683	0.580099
5	6	-1.242959	-0.608018	-0.017158
6	6	-1.859877	-1.845753	0.678967
7	6	-1.264506	1.956803	0.047913
8	6	0.171965	1.914015	-0.295745
9	6	0.878997	0.770484	-0.310913
10	6	0.300213	-0.567176	0.085765
11	6	2.373719	0.722309	-0.597195
12	6	3.165881	0.073392	0.614643
13	6	2.213898	-0.193911	1.803988
14	6	0.894811	-0.937573	1.484436
15	8	2.553799	-0.152177	-1.718307
16	6	3.74866	-0.91419	-1.519929
17	6	3.715764	-1.245405	-0.03273
18	8	-1.896792	3.002605	-0.038201
19	8	2.919949	1.985069	-0.897314
20	6	4.318372	0.970553	1.094495
21	8	5.011143	-1.651339	0.385231
22	6	-1.656384	-0.708312	-1.503693
23	8	-3.079231	-0.582824	-1.647642
24	8	-5.153889	-0.619401	-0.715079
25	6	-4.208478	0.764473	1.726377
26	1	0.688743	-1.302525	-0.631197
27	1	-1.670769	0.680002	1.658464
28	1	-3.98735	-2.058605	1.226492
29	1	-3.582237	-2.774251	-0.332296

APPENDIX A (continued)

30	1	-3.739626	1.46894	-0.239765
31	1	-1.336479	-2.751979	0.347014
32	1	-1.719776	-1.778833	1.763338
33	1	0.629634	2.871544	-0.52757
34	1	1.969347	0.77837	2.250044
35	1	2.760807	-0.746892	2.580611
36	1	1.035826	-2.023623	1.533324
37	1	0.17866	-0.68889	2.27554
38	1	4.644705	-0.328313	-1.766462
39	1	3.697119	-1.788561	-2.172391
40	1	3.002371	-2.064866	0.135223
41	1	2.592231	2.238982	-1.776615
42	1	3.936927	1.94727	1.405159
43	1	4.817907	0.506453	1.95187
44	1	5.068687	1.133576	0.31816
45	1	4.960751	-2.039519	1.271985
46	1	-1.197923	0.077659	-2.113148
47	1	-1.335936	-1.67978	-1.910651
48	1	-5.293924	-1.246724	-1.444199
49	1	-3.97816	1.731866	2.187464
50	1	-5.289445	0.71388	1.562347
51	1	-3.934424	-0.02095	2.443131

TABLE XX. CARTESIAN COORDINATE OF PREDOMINANT CONFORMER OF COMPOUND 19

Atomic Number	Atomic Type	Conformer 5 coordinates (Angstroms)			Conformer 6 coordinates (Angstroms)		
		X	Y	Z	X	Y	Z
1	6	-1.590091	-1.724494	1.016484	-1.679668	-1.292992	1.317677
2	6	-3.11806	-1.776743	0.754026	-3.204004	-1.34227	1.026011
3	6	-3.519268	-0.577428	-0.10992	-3.534768	-0.318673	-0.075837
4	6	-3.04412	0.765463	0.494805	-2.995286	1.087647	0.251184
5	6	-1.486474	0.735103	0.549426	-1.441754	0.991779	0.323926
6	6	-0.945114	-0.651262	0.106595	-0.971535	-0.483739	0.205505
7	6	-0.835248	1.885215	-0.224623	-0.729983	1.908419	-0.675373
8	6	0.578869	1.708981	-0.602895	0.672724	1.576224	-0.990622
9	6	1.23837	0.543198	-0.456782	1.271137	0.442408	-0.576741
10	6	0.602717	-0.711241	0.098516	0.570286	-0.621235	0.238039
11	6	2.721932	0.46223	-0.692034	2.749243	0.236762	-0.764142
12	6	3.516505	0.054662	0.582137	3.516204	0.090274	0.581898
13	6	2.815021	-1.145227	1.276672	2.751093	-0.88468	1.519341
14	6	1.295579	-0.986882	1.461255	1.240887	-0.614189	1.638879
15	8	3.024549	-0.559564	-1.651974	3.002999	-0.990353	-1.462253
16	6	4.348157	-1.063833	-1.403592	4.298773	-1.487756	-1.086635
17	6	4.835623	-0.45432	-0.070323	4.810341	-0.617584	0.083047
18	6	3.724135	1.215187	1.55967	3.779041	1.430773	1.274551

APPENDIX A (continued)

19	6	-3.680901	1.094391	1.851492	-3.612439	1.724938	1.50279
20	6	-1.471464	-0.927918	-1.320835	-1.503729	-1.047216	-1.13306
21	8	-2.883682	-0.704931	-1.399072	-2.893969	-0.746515	-1.296278
22	8	-1.42712	2.931887	-0.464168	-1.259335	2.911826	-1.138297
23	8	5.832883	0.548842	-0.254674	5.859508	0.267169	-0.306005
24	1	0.893846	-1.541662	-0.563421	0.821426	-1.59328	-0.214484
25	1	3.082996	1.436836	-1.062756	3.162111	1.082513	-1.340251
26	1	-1.165451	0.895525	1.591951	-1.110807	1.36114	1.308719
27	8	-4.902528	-0.660699	-0.307171	-4.90053	-0.185573	-0.34509
28	6	-5.496593	0.272794	-1.211295	-5.605152	-1.35324	-0.763208
29	1	-1.387322	-1.491055	2.068205	-1.489878	-0.831774	2.293797
30	1	-1.134195	-2.70261	0.814573	-1.265748	-2.30899	1.359695
31	1	-3.690952	-1.769678	1.685953	-3.792351	-1.123308	1.922904
32	1	-3.404624	-2.679991	0.206172	-3.496409	-2.33905	0.680823
33	1	-3.323748	1.555134	-0.20878	-3.258394	1.710498	-0.609075
34	1	1.073547	2.592354	-1.00218	1.213683	2.321659	-1.570483
35	1	3.292595	-1.309103	2.251594	3.215585	-0.845892	2.513408
36	1	2.987679	-2.05955	0.693382	2.879171	-1.91494	1.161189
37	1	0.901316	-1.907498	1.904655	0.79736	-1.389345	2.273283
38	1	1.073437	-0.174693	2.166054	1.057684	0.346896	2.137212
39	1	4.291311	-2.157989	-1.374527	4.187586	-2.543381	-0.813491
40	1	5.01822	-0.776756	-2.224244	4.986047	-1.424801	-1.940231
41	1	5.324198	-1.198524	0.565544	5.256458	-1.222055	0.878334
42	1	4.173691	2.085454	1.072133	4.273271	2.145157	0.609287
43	1	2.772771	1.533855	1.99985	2.843665	1.886757	1.617379
44	1	4.393227	0.915868	2.374389	4.429725	1.291981	2.145417
45	1	-3.377295	0.386841	2.633573	-3.351752	1.179854	2.419788
46	1	-4.774285	1.073779	1.79065	-4.70344	1.758762	1.424239
47	1	-3.376338	2.097442	2.172723	-3.246756	2.752718	1.612618
48	1	-0.997497	-0.279727	-2.066406	-0.980345	-0.622288	-1.996298
49	1	-1.252619	-1.971882	-1.59599	-1.35544	-2.13924	-1.155044
50	1	5.52995	1.197987	-0.910337	5.592687	0.768061	-1.094032
51	1	-5.492008	1.293218	-0.806122	-5.097328	-1.844257	-1.599695
52	1	-4.991114	0.260749	-2.181609	-5.737464	-2.065927	0.062353
53	1	-6.531593	-0.05586	-1.331242	-6.588183	-1.003815	-1.087367

APPENDIX A (continued)

TABLE XXI. CARTESIAN COORDINATE OF PREDOMINANT CONFORMERS OF COMPOUND 20

Atomic Number	Atomic Type	Conformer 2 coordinates (Angstroms)			Conformer 3 coordinates (Angstroms)		
		X	Y	Z	X	Y	Z
1	6	-1.769433	-1.907066	0.697408	-1.853972	-1.504605	1.110722
2	6	-3.292497	-1.880131	0.404308	-3.371907	-1.486294	0.784151
3	6	-3.656892	-0.533144	-0.227321	-3.668333	-0.292705	-0.142753
4	6	-3.171742	0.664137	0.624365	-3.123679	1.0344	0.420734
5	6	-1.616271	0.593441	0.698566	-1.573407	0.908491	0.509837
6	6	-1.089531	-0.695581	0.014795	-1.114104	-0.532221	0.161761
7	6	-0.929577	1.851976	0.159563	-0.829132	1.962915	-0.31455
8	6	0.490366	1.726818	-0.21908	0.580832	1.676385	-0.644079
9	6	1.122943	0.540895	-0.286337	1.154798	0.481377	-0.413256
10	6	0.45714	-0.783414	0.0203	0.425402	-0.692481	0.203456
11	6	2.615025	0.454698	-0.534176	2.641043	0.266308	-0.618426
12	6	3.380366	-0.219024	0.66268	3.378892	-0.138898	0.710944
13	6	2.628956	-1.498218	1.125749	2.560635	-1.225159	1.465862
14	6	1.113367	-1.32163	1.319172	1.058836	-0.92401	1.600289
15	8	2.85405	-0.45184	-1.615416	2.827427	-0.888137	-1.453586
16	6	4.15751	-1.041837	-1.472102	4.074828	-1.520887	-1.138712
17	6	4.673327	-0.654021	-0.076838	4.635251	-0.811184	0.110538
18	6	3.620564	0.720301	1.850283	3.681576	1.04378	1.638523
19	6	-3.830454	0.748084	2.007632	-3.763856	1.466729	1.746212
20	6	-1.591188	-0.691355	-1.448015	-1.620187	-0.86251	-1.262157
21	8	-2.998615	-0.432278	-1.506909	-3.004871	-0.524866	-1.402511
22	8	-1.503176	2.934348	0.106902	-1.343887	3.030627	-0.62512
23	8	5.605341	0.427126	-0.270159	5.575447	0.221601	-0.243197
24	1	0.743524	-1.484453	-0.77832	0.673367	-1.582463	-0.395033
25	8	3.109001	1.737577	-0.828742	3.193332	1.411159	-1.212649
26	1	-1.3139	0.551958	1.758099	-1.261248	1.108452	1.548227
27	8	-5.037526	-0.551104	-0.45912	-5.027273	-0.101379	-0.414418
28	6	-5.597832	0.547694	-1.180672	-5.730442	-1.174534	-1.037112
29	1	-1.32528	-2.839491	0.324661	-1.450298	-2.519071	0.993808
30	1	-1.585212	-1.876953	1.777737	-1.682552	-1.212011	2.153174
31	1	-3.883636	-2.035838	1.311598	-3.977851	-1.40835	1.692653
32	1	-3.582237	-2.659625	-0.307459	-3.666074	-2.409718	0.275154
33	1	-3.423376	1.576322	0.075368	-3.360524	1.792866	-0.331501
34	1	1.014883	2.651417	-0.435315	1.15036	2.494172	-1.072394
35	1	3.083893	-1.846701	2.062639	3.003314	-1.356235	2.461897
36	1	2.780465	-2.302192	0.394496	2.660876	-2.191781	0.956158
37	1	0.685391	-2.293431	1.587299	0.581065	-1.773796	2.099785
38	1	0.904636	-0.641217	2.155401	0.894393	-0.04605	2.238584
39	1	4.053769	-2.12491	-1.594925	3.886194	-2.586595	-0.961839
40	1	4.832769	-0.660655	-2.245824	4.76169	-1.429526	-1.990633
41	1	5.179211	-1.486458	0.429831	5.106563	-1.508038	0.815981
42	1	2.678066	0.9604	2.353169	2.75221	1.477491	2.022607

APPENDIX A (continued)

43	1	4.274834	0.242263	2.591922	4.278351	0.706636	2.494517
44	1	4.065019	1.671998	1.547414	4.234599	1.837133	1.134363
45	1	-4.922651	0.760853	1.926008	-4.852466	1.527299	1.651362
46	1	-3.515771	1.66781	2.514739	-3.390814	2.457823	2.030286
47	1	-3.554252	-0.098268	2.649569	-3.529429	0.775891	2.567161
48	1	-1.092699	0.07567	-2.050794	-1.479725	-1.93778	-1.460295
49	1	-1.382916	-1.66962	-1.909701	-1.07467	-0.307049	-2.032313
50	1	5.97965	0.684376	0.587791	6.355532	-0.180131	-0.656809
51	1	4.081296	1.680372	-0.884306	4.164852	1.333031	-1.177128
52	1	-6.633946	0.265978	-1.38275	-6.703597	-0.765289	-1.318479
53	1	-5.589451	1.471834	-0.587909	-5.207568	-1.523959	-1.933328
54	1	-5.069555	0.712205	-2.124568	-5.886394	-2.014384	-0.346031

Conformational searches were performed for the enantiomers of compounds **21** and **22** by Sybyl 8.1 program using Random Searching together with the MMFF94s molecular mechanics force field charged with MMFF94. 2 and 6 conformers for icacinlactone K and icacintrichanone respectively, were obtained. The optimization followed by the ECD calculation of the resulted conformers were performed over the Gaussian09₁ software at B3LYP/6-31+G(d,p)// B3LYP/6-31G(d) level in the gas phase.

TABLE XXII. ECD CALCULATIONS FOR COMPOUND 21

Coordinates and Energy values for icacinlactone K: E(RB3LYP) = -1262.54633367 a.u.

Standard orientation:

Center Number	Atomic Number	Atomic Type	Conformer 1 coordinates (Angstroms)		
			X	Y	Z
1	6	0	2.502307	2.342088	0.214675
2	6	0	3.152304	1.057887	-0.30363
3	6	0	2.880094	-0.13635	0.662772
4	6	0	1.35081	-0.28055	0.843209
5	6	0	0.592449	0.69755	-0.09677
6	6	0	0.966492	2.128123	0.365895
7	6	0	1.073579	-1.77901	0.599584
8	6	0	-0.19333	-2.09409	-0.21171
9	6	0	-1.2403	-1.00525	-0.10262
10	6	0	-0.89057	0.353075	-0.05905
11	6	0	-2.60609	-1.34831	-0.07249
12	6	0	-3.61961	-0.35424	0.004601
13	6	0	-3.22547	1.010033	0.0476

APPENDIX A (continued)

14	6	0	-1.87774	1.355055	0.017423
15	6	0	3.279918	-1.43037	-0.05148
16	8	0	2.242282	-2.2978	-0.09946
17	8	0	4.368494	-1.68577	-0.51669
18	8	0	4.502724	1.272826	-0.52936
19	8	0	2.556807	0.716536	-1.57276
20	6	0	1.130595	0.575156	-1.54534
21	1	0	1.052998	-0.03053	1.867534
22	6	0	3.649196	-0.03545	1.991986
23	6	0	-5.02054	-0.73641	0.038369
24	8	0	-2.93047	-2.6513	-0.12266
25	1	0	-5.75961	0.075429	0.096679
26	8	0	-5.41416	-1.91256	0.005957
27	8	0	-4.23806	1.915004	0.121429
28	6	0	-3.92851	3.305897	0.162422
29	1	0	2.728	3.127799	-0.51253
30	1	0	2.964936	2.638834	1.160553
31	1	0	0.435532	2.868756	-0.24128
32	1	0	0.647947	2.277074	1.40479
33	1	0	1.040104	-2.30757	1.558046
34	1	0	0.102123	-2.23624	-1.25949
35	1	0	-0.6186	-3.04795	0.10725
36	1	0	-1.58344	2.394119	0.057798
37	1	0	4.892773	0.423765	-0.81852
38	1	0	0.884724	-0.38613	-2.00493
39	1	0	0.682112	1.365366	-2.16397
40	1	0	4.72749	-0.00954	1.816406
41	1	0	3.365483	0.87029	2.538286
42	1	0	3.425317	-0.89644	2.63331
43	1	0	-3.9234	-2.71885	-0.08576
44	1	0	-3.39604	3.618591	-0.74391
45	1	0	-4.89064	3.817144	0.215915
46	1	0	-3.33215	3.551543	1.049458

APPENDIX A (continued)

TABLE XXIII. ECD CALCULATIONS FOR COMPOUND 22Coordinates and Energy values for **2**: E(RB3LYP) = -1187.25587820 a.u.



Standard orientation:





Center Number	Atomic Number	Atomic Type	Conformer 1 coordinates (Angstroms)		
			X	Y	Z
1	6	0	-3.00654	2.411116	0.491352
2	6	0	-3.69014	1.5374	-0.54345
3	6	0	-3.401	0.035581	-0.45272
4	6	0	-1.86794	-0.22525	-0.36288
5	6	0	-1.05433	0.736786	0.564991
6	6	0	-1.47987	2.209901	0.452943
7	6	0	-1.48436	-1.55951	0.300454
8	6	0	-0.05053	-1.97692	-0.08592
9	6	0	0.885498	-0.78793	-0.02414
10	6	0	0.441167	0.516076	0.273071
11	6	0	2.245826	-0.91782	-0.30018
12	6	0	3.200801	0.124562	-0.27609
13	6	0	2.72566	1.411777	0.054226
14	6	0	1.361243	1.576452	0.314768
15	8	0	2.846336	-2.0947	-0.65715
16	6	0	4.172218	-1.81482	-0.85764
17	6	0	4.45495	-0.50684	-0.6444
18	8	0	-4.42049	2.011839	-1.39679
19	1	0	-1.46211	-0.18702	-1.38138
20	6	0	-1.36287	0.121466	1.952687
21	8	0	-1.46645	-1.28918	1.72943
22	8	0	-2.37347	-2.60043	0.058648
23	8	0	0.338267	-3.06624	0.757081
24	6	0	-4.05884	-0.72064	-1.61396
25	8	0	3.464856	2.556449	0.143019
26	6	0	4.864845	2.535219	-0.10724
27	1	0	-3.40311	2.155754	1.483801
28	1	0	-3.26366	3.455504	0.291658
29	1	0	-3.85225	-0.29968	0.495092
30	1	0	-1.09782	2.621909	-0.48957
31	1	0	-1.02199	2.799111	1.257361
32	1	0	-0.06284	-2.40444	-1.0952
33	1	0	1.039196	2.58432	0.54852
34	1	0	4.783075	-2.65717	-1.14672
35	1	0	5.432786	-0.06205	-0.7424
36	1	0	-0.56632	0.315684	2.678899
37	1	0	-2.31138	0.484053	2.36883
38	1	0	-1.95055	-3.41366	0.390543
39	1	0	0.259218	-2.74265	1.673449
40	1	0	-5.13414	-0.5209	-1.63766


APPENDIX A (continued)

41	1	0	-3.64796	-0.3857	-2.57356
42	1	0	-3.89662	-1.79436	-1.51264
43	1	0	5.386392	1.879633	0.6001
44	1	0	5.080801	2.227025	-1.13702
45	1	0	5.202099	3.562996	0.03868

APPENDIX B. Permissions to use Copyrighted Material

 Home
  Help
  Email Support
  Brian Guo



Di-nor- and 17-nor-pimaranes from *Icacina trichantha*
 Author: Brian Guo, Monday M. Onakpa, Xiao-Jun Huang, et al
 Publication: Journal of Natural Products
 Publisher: American Chemical Society
 Date: Jul 1, 2016
 Copyright © 2016, American Chemical Society

PERMISSION/LICENSE IS GRANTED FOR YOUR ORDER AT NO CHARGE

This type of permission/license, instead of the standard Terms & Conditions, is sent to you because no fee is being charged for your order. Please note the following:

- Permission is granted for your request in both print and electronic formats, and translations.
- If figures and/or tables were requested, they may be adapted or used in part.
- Please print this page for your records and send a copy of it to your publisher/graduate school.
- Appropriate credit for the requested material should be given as follows: "Reprinted (adapted) with permission from (COMPLETE REFERENCE CITATION). Copyright (YEAR) American Chemical Society." Insert appropriate information in place of the capitalized words.
- One-time permission is granted only for the use specified in your request. No additional uses are granted (such as derivative works or other editions). For any other uses, please submit a new request.

[BACK](#)
[CLOSE WINDOW](#)

© 2019 Copyright - All Rights Reserved |
 [Copyright Clearance Center, Inc.](#) |
 [Privacy statement](#) |
 [Terms and Conditions](#)
 Comments? We would like to hear from you. E-mail us at customercare@copyright.com

APPENDIX B. (continued)



RightsLink®



Home



Help



Email Support



Brian Guo ▾

ACS Publications
Not Found. Not Found. Not Found.**Activity of Icacinol from *Icacina trichantha* on Seedling Growth of *Oryza sativa* and *Arabidopsis thaliana***

Author: Ming Zhao, Brian Guo, Michael M. Onakpa, et al

Publication: Journal of Natural Products

Publisher: American Chemical Society

Date: Dec 1, 2017

Copyright © 2017, American Chemical Society

PERMISSION/LICENSE IS GRANTED FOR YOUR ORDER AT NO CHARGE

This type of permission/license, instead of the standard Terms & Conditions, is sent to you because no fee is being charged for your order. Please note the following:

- Permission is granted for your request in both print and electronic formats, and translations.
- If figures and/or tables were requested, they may be adapted or used in part.
- Please print this page for your records and send a copy of it to your publisher/graduate school.
- Appropriate credit for the requested material should be given as follows: "Reprinted (adapted) with permission from (COMPLETE REFERENCE CITATION). Copyright (YEAR) American Chemical Society." Insert appropriate information in place of the capitalized words.
- One-time permission is granted only for the use specified in your request. No additional uses are granted (such as derivative works or other editions). For any other uses, please submit a new request.

[BACK](#)[CLOSE WINDOW](#)

Vitae

Brian C. Guo

Education

2014 – 2020	University of Illinois at Chicago, Chicago, Illinois NIH/NCCIH T32 Predoctoral Training Fellow and PhD Candidate in Pharmacognosy, Department of Pharmaceutical Sciences, College of Pharmacy
2011 – 2012	Northwestern University, Evanston, Illinois M.S. in Biomedical Engineering
2006 – 2010	Northwestern University, Evanston, Illinois
(2011 with Co-op)	B.S. in Biomedical Engineering

Professional Experience

2014 – Present	Department of Pharmaceutical Sciences, University of Illinois at Chicago, Chicago, Illinois Research Assistant for Dr. C. T. Che
2018	Sirenas Marine Discovery, San Diego, California <i>Research and Development Summer Intern</i>
2014, 2020	College of Pharmacy, University of Illinois at Chicago Graduate Teaching Assistant
2012 – 2013	Medical Devices Quality, Baxter Healthcare, Round Lake, Illinois Quality Technician
2008 – 2010	Renal Division, Baxter Healthcare, Round Lake, Illinois Cooperative Engineering Education Student

Awards and Honors

2019	Oscar Robert Oldberg Prize in Pharmaceutical Chemistry
2018	American Society for Pharmacology and Experimental Therapeutics PIIPS Fellowship

- 2018 American Society of Pharmacognosy Lynn Brady Student Travel Award
 2015 – 2019 NIH/NCCIH T32 Predoctoral Training Fellowship

Publications

- 2020 Guo, B.; Zhao, M.; Wu Z. L.; Onakpa, M. M.; Burdette, J. E.; Che, C.-T. 19-nor-pimaranes from *Icacina trichantha*. *Fitoterapia*. 2020. Forthcoming
- 2018 Zhao, M.; Cheng, J.; Guo, B.; Duan, J.; Che, C.-T. Momilactone and Related Diterpenoids as Potential Agricultural Chemicals. *J. Agric. Food Chem.* 2018, 66 (30), 7859–7872, DOI: 10.1021/acs.jafc.8b02602.
- 2017 Zhao, M.; Guo, B.; Onakpa, M. M.; Wong, T.; Wakasa, K.; Che, C. T.; Warpeha, K. Activity of Icacinol from *Icacina Trichantha* on Seedling Growth of *Oryza Sativa* and *Arabidopsis Thaliana*. *J. Nat. Prod.* 2017, 80 (12), 3314–3318, DOI: 10.1021/acs.jnatprod.7b00668.
- 2016 Guo, B.; Onakpa, M. M.; Huang, X.-J.; Santarsiero, B. D.; Chen, W.-L.; Zhao, M.; Zhang, X.-Q.; Swanson, S. M.; Burdette, J. E.; Che, C.-T. Di -nor - and 17-nor -Pimaranes from *Icacina Trichantha*. *J. Nat. Prod.* 2016, 79 (7), 1815–1821, DOI: 10.1021/acs.jnatprod.6b00289.
- 2016 Che, C.-T.; Zhao, M.; Guo, B.; Onakpa, M. M. *Icacina Trichantha*, a Tropical Medicinal Plant. *Nat. Prod. Commun.* 2016, 11 (7), 1039–1042.

Conference Presentations

- Guo B, Zhao M, Vemu B, Johnson JJ, and Che CT. Further 17-nor-pimaranes from *Icacina trichantha*. American Society of Pharmacognosy Annual Meeting, Madison, WI, July 13-17, 2019.
- Veenstra JP, Vemu B, Nauman M, Guo B, Che CT, Johnson JJ. Evaluating the Effect of Oregano Essential Oil on Sestrin 2 Expression and mTORC1 activity in HCT 116 Colon Cells. American Society of Pharmacognosy Annual Meeting, Madison, WI, July 13-17, 2019.

Guo B, Gurgul A, Johnson JJ, and Che CT. Metabolomics Approach for Evaluation of Bioactive Diterpenes and Other Metabolites in Rosemary Extract. UIC College of Pharmacy Research Day, Chicago, IL February 8, 2019.

Guo B, Zhao M, Onakpa, MM., Che CT . Unusual 19-nor-pimaranes from *Icacina trichantha*. American Society of Pharmacognosy Annual Meeting, Lexington, KY, July 21-25, 2018

Guo B, Zhao M, Onakpa, MM., Czarnecki A, Burdette J, Che CT. Phytochemical Investigation of West African Ethnomedicinal Tuber *Icacina trichantha*. UIC Student Research Forum, Chicago, IL, April 11, 2018.

Guo B, Zhao M, Czarnecki A, Burdette J, Che CT. Phytochemical Exploration of Medicinal Tuber Native to West Africa. UIC College of Pharmacy Research Day, Chicago, IL, February 9, 2018.

Guo B, Zhao M, Onakpa MM, and Che CT. *Icacina trichantha* Revisited for NMR Analysis of 9 β H-Pimaranes. American Society of Pharmacognosy Annual Meeting, Portland, OR, July 29-August 2, 2017.

Guo B, Zhao M, Onakpa MM, Santarsiero BD, Huang X-J, Zhang X-Q, Che CT. Di-nor- and 17-nor-pimaranes from *Icacina trichantha*. 9th Joint Natural Products Conference, Copenhagen, Denmark, July 24-27, 2016.

Memberships

2014 – Present Associate Member of the American Society of Pharmacognosy (ASP)

Institutional Service

2016 – Present UIC Men's Club Ultimate Frisbee Coach and Advisor